



Terms and Conditions of Use of Digitised Theses from Trinity College Library Dublin

Copyright statement

All material supplied by Trinity College Library is protected by copyright (under the Copyright and Related Rights Act, 2000 as amended) and other relevant Intellectual Property Rights. By accessing and using a Digitised Thesis from Trinity College Library you acknowledge that all Intellectual Property Rights in any Works supplied are the sole and exclusive property of the copyright and/or other IPR holder. Specific copyright holders may not be explicitly identified. Use of materials from other sources within a thesis should not be construed as a claim over them.

A non-exclusive, non-transferable licence is hereby granted to those using or reproducing, in whole or in part, the material for valid purposes, providing the copyright owners are acknowledged using the normal conventions. Where specific permission to use material is required, this is identified and such permission must be sought from the copyright holder or agency cited.

Liability statement

By using a Digitised Thesis, I accept that Trinity College Dublin bears no legal responsibility for the accuracy, legality or comprehensiveness of materials contained within the thesis, and that Trinity College Dublin accepts no liability for indirect, consequential, or incidental, damages or losses arising from use of the thesis for whatever reason. Information located in a thesis may be subject to specific use constraints, details of which may not be explicitly described. It is the responsibility of potential and actual users to be aware of such constraints and to abide by them. By making use of material from a digitised thesis, you accept these copyright and disclaimer provisions. Where it is brought to the attention of Trinity College Library that there may be a breach of copyright or other restraint, it is the policy to withdraw or take down access to a thesis while the issue is being resolved.

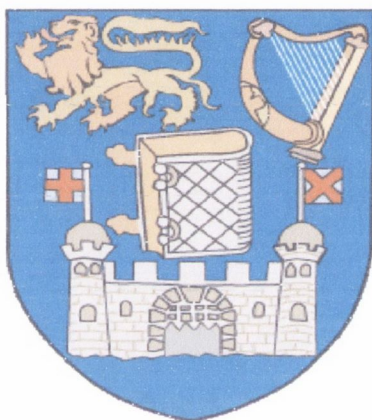
Access Agreement

By using a Digitised Thesis from Trinity College Library you are bound by the following Terms & Conditions. Please read them carefully.

I have read and I understand the following statement: All material supplied via a Digitised Thesis from Trinity College Library is protected by copyright and other intellectual property rights, and duplication or sale of all or part of any of a thesis is not permitted, except that material may be duplicated by you for your research use or for educational purposes in electronic or print form providing the copyright owners are acknowledged using the normal conventions. You must obtain permission for any other use. Electronic or print copies may not be offered, whether for sale or otherwise to anyone. This copy has been supplied on the understanding that it is copyright material and that no quotation from the thesis may be published without proper acknowledgement.

**Highly substituted 2,3,7,8,12,13,17,18-octaethylporphyrins with *meso*
aryl residues for applications in NLO and sensors**

By Julia Richter



**A thesis submitted to the University of Dublin for the degree of Doctor
of Philosophy**

TRINITY COLLEGE DUBLIN

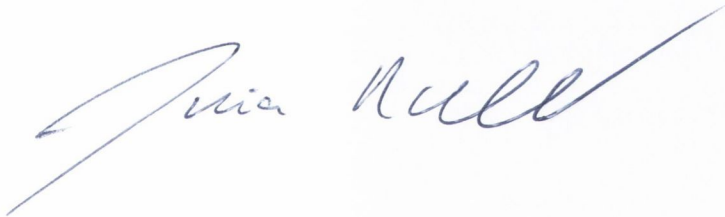
OCTOBER 2008

DECLARATION

This thesis has not been submitted as an exercise for a degree at any other university. Except where stated, the work described therein was carried out by me alone.

I give permission for the Library to lend or copy this thesis upon request.

Signed:

A handwritten signature in blue ink, appearing to read "Julia Hall". The signature is written in a cursive style with a long, sweeping underline that extends to the right.

This thesis has not been submitted as an exercise for a degree at any other university. Except where otherwise stated, the work described herein has been carried out by the author alone.

Mica Rühl

Summary

The synthesis of novel free base *meso* mono- and 5,10-disubstituted (A_2 - and AB-type) 2,3,7,8,12,13,17,18-octaethylporphyrins (OEPs) and of several *meso* trisubstituted ABA- and AAB-type OEPs is reported with optimization details, NMR and UV/vis characterization. Yields for *meso* mono aryl substituted OEPs were excellent (up to 89%) and the subsequent disubstitution step was carried out with ease and also in good yields (maximal 92%) producing *meso* 5,10-AB and 5,10- A_2 -type substituted OEPs. The observed regio selectivity of the disubstitution was furthermore described by M. O. Senge *et al.*¹ and could be also observed for the formation ABA trisubstituted OEPs (287–291), which were obtained directly from the *meso* monosubstituted OEPs 4-8. With 5-(3-trifluoromethylphenyl)-10-(4-dimethylaminophenyl) OEP 253 a novel mini push-pull OEP was prepared in 45% yield and 5,10-bisphenyl OEP 236, which was previously described as not reactive towards phenyllithium,¹ could be used for the preparation of 5,10,15-AAB-type OEPs with *in situ* generated aryllithium reagents and produced the OEPs 292–294 in 17%, 38% and 69% yield. Atropisomers were observed for 9-phenanthrenyl and 1-naphthyl substituted OEPs (chapter 3) and changes in the shape of the UV/vis spectra were encountered for several di- and trisubstituted OEPs (chapter 5) due to the introduced unsymmetry and distortion.

All *meso* substitution was carried out with organolithium reagents as described by I. Bischoff and W. W. Kalisch and was applied repeatedly to prepare higher substituted OEPs.¹ It was found, that the product of the reaction (di-, tri- or tetrasubstitution) depended on the equivalents of *n*-BuLi and bromide used. By variation of those, the synthesis of the *meso* 9-phenanthrenyl series, 5-mono-, 5,10-bis, tris- and tetrakis(9-phenanthrenyl) OEP 8–11, was carried out successfully and the respective palladium (II) complexes could be obtained afterwards in good yields (12–82%). Also 5-(9-phenanthrenyl) Pt(II)OEP 309, 5-phenyl Pt(II)OEP 307 and 5-(1-naphthyl) Pt(II)OEP 308 were prepared in yields between 44–76%.

Furthermore *meso* mono, di- and trisubstituted 1-naphthyl substituted OEPs (7, 235 and 257) were isolated and 5,10-bis(1-naphthyl) Pd(II)OEP 284 was afforded in 61% yield from 5-(1-naphthyl) Pd(II)OEP 282 after optimization.

The *meso* monosubstituted Pd(II) and Pt(II)OEPs were investigated in regard to their triplet state dynamics so as to find a correlation between photophysical properties and the distortion of the molecules. 3D Shapes were calculated and X-ray analysis was carried out and the results were compared to the measured phosphorescence quantum yields and lifetimes and the saddle shaped 5-(9-phenanthrenyl) Pd(II)OEP **12** was reported by Vinogradov *et al.* as a prospect candidate for single molecule experiments, with potential future applications in biomedical probing. 5-(9-Phenanthrenyl) Pd(II)OEP **12** displayed a satisfying phosphorescence quantum yield ($\Phi = 1.1$) and a shortened phosphorescence lifetime ($\tau_0 = 52 \mu\text{s}$), appropriate for sensor applications.²

On the other hand, phenyl substituted OEPs were of no use as they showed extremely shortened phosphorescence lifetimes and low quantum yields, which were attributed to strong annihilation processes due to the rotation of the phenyl substituent.³ However, the introduced distortion of the Pd(II)OEPs decreased the phosphorescence lifetimes and quantum yields in a step wise manner relative to Pd(II)OEP **2**. The resulting phosphorescence could be related to the increased conformational flexibility of the molecules due to the distortion and the respective degree of internal energy conversion and was lower for saddle shaped OEPs than for ruffled OEPs. The 9-phenanthrenyl substituent was furthermore found to be rotationally hindered and atropisomers were identified at ambient temperature. The atropisomerism as well a ruffled conformation e.g. as seen for 5-*n*-butyl Pd(OEP) **17** and to a minor degree being also present in the geometry of the OEP **12**, could be related to moderate annihilation processes, exhibiting phosphorescence most appropriate for biomedical applications. Therefore the synthesis of alkyl-phenanthrenyl-mixed OEPs is suggested for future work.

REFERENCES

- 1) M. O. Senge *Acc. Chem. Res.* **2005**, *38*, 9, 733.
- 2) E. Mei, S. Vinogradov, R. M. Hochstrasser *J. Am. Chem. Soc.* **2003**, *125*, 13198.
- 3) C. M. Muzzi, C. J. Medforth, L. Voss, M. Cancilla, C. Lebrilla, J.-G. Ma, J. A. Shelnutt, K. M. Smith *Tetrahedron Lett.* **1999**, *40*, 6159.

TABLE OF CONTENTS

Aims and Objectives.....	1-9
REFERENCES.....	9

Part I – SYNTHESIS of OEPs

1. Synthesis of OEP and β-substituted porphyrins.....	10-43
1.1 Synthesis of 3,4-diethylpyrrole (38) and other β -substituted pyrroles	10
1.2 Synthesis of β substituted dipyrromethanes.....	16
1.3 Synthesis of tripyrranes and open-chain tetrapyrroles.....	20
1.4 Condensation reactions affording β -substituted porphyrins.....	21
1.4.1 The [4+1] approach.....	21
1.4.2 Synthesis of OEP.....	26
1.4.3 Synthesis of dodecasubstituted porphyrins.....	28
1.4.4 Synthesis of tetrabenzoporphyrins (TBPs)	29
1.4.5 Series of porphyrins.....	32
1.4.6 [2+2] McDonald condensation.....	32
1.5 Synthesis of dodecasubstituted porphyrins <i>via</i> bromination reactions	36
REFERENCES.....	40
2. Synthesis of <i>meso</i> substituted OEPs, palladium(II) and platinum (II) insertion.....	44-115
2.1 Synthesis of <i>meso</i> substituted octaalkylporphyrins reported in literature.....	44
2.1.1 <i>Meso</i> monosubstituted OEPs.....	44
2.1.1.1 Halogenation of OEP.....	44
2.1.1.2 Nitration of OEP.....	45
2.1.1.3 Amines of OEP.....	47
2.1.1.4 5-Methyl OEPs	48
2.1.1.5 Formylation of OEP and derivation reactions	

(Wittig).....	51
2.1.1.6 Ester of OEP <i>via</i> nucleophilic substitution	54
2.1.1.7 <i>Meso</i> monosubstituted OEPs by [2+2] Mc Donald condensation	54
2.1.1.8 Synthesis of OEP dimers, oligomers and sandwich structures.....	55
2.1.2 <i>Meso</i> 5,10- and 5,15-disubstituted OEPs.....	59
2.1.3 <i>Meso</i> tri- and tetrasubstituted OEPs.....	61
REFERENCES.....	63
2.2 <i>Meso</i> substitution of OEPs with organolithium reagents	68
2.2.1. Synthesis of <i>meso</i> monosubstituted OEPs	72
2.2.2 <i>Regio</i> selective synthesis of <i>meso</i> 5,10-disubstituted OEPs.....	78
2.2.3 Synthesis of A_2 and AB Pd(II)OEPs from the respective <i>meso</i> monosubstituted Pd(II)OEPs.....	82
2.2.4 Synthesis of <i>meso</i> trisubstituted OEPs.....	89
2.2.4.1 ABA and A_3 substituted by-products.....	89
2.2.4.2 Synthesis of AAB OEPs	90
2.2.5 Synthesis of the phenanthrenyl series and of members of the naphthyl series.....	91
2.2.5.1 Series described in literature and series attempted during the PhD.....	91
2.2.5.2 The phenanthrenyl series and optimization reactions.....	94
2.2.5.3 The 1-naphthyl series.....	97
REFERENCES.....	98
2.3 Palladium (II) and platinum (II) insertions.....	100
2.3.1 Palladium (II) insertion	100
2.3.2 Platinum (II) insertion.....	105
2.4 Derivation of OEPs	107
2.4.1 Demetallation.....	107

2.4.2 Derivation of introduced methoxyphenyl groups and sulfonation of meso phenyl substituents.....	108
2.4.3 Nitration, amidation and derivation of phenyl substituents	109
2.4.4 β -Meso and β - β fusion reactions (JI extension).....	110
REFERENCES.....	113

3. ^1H NMR spectra of synthesized OEPs: Discussion of atropisomers and assignment of signals and regioisomers 116-153

3.1 Assignment of substituent signals and comparison of the CH_2/CH_3 pattern of OEPs.....	116
3.1.1 Assignment of naphthyl, phenanthrenyl and anthracenyl protons.....	116
3.1.2 CH_2/CH_3 pattern of meso mono-, di-, tri- and tetrasubstituted OEPs.....	123
3.2 5,10 Regioisomers of A_2 - and AB-substituted OEPs and ABA and AAB regioisomers of trisubstituted OEPs.....	127
3.2.1 5,10-AB and -A_2 regioisomers	127
3.2.2 ABA and AAB regioisomers.....	128
3.3 Atropisomerism and ^1H NMR spectra of 9-phenanthrenyl and 1-naphthyl substituted OEPs.....	132
3.3.1 Atropisomers described in literature	132
3.3.2 The atropisomers of 5,10-bis(9-phenanthrenyl)OEP (9)	138
3.3.3 The atropisomers of 5,10-bis(1-naphthyl) OEP (257)	139
3.3.4 The atropisomers of 5,-(1-naphthyl)-10-(9-phenanthrenyl)OEP (259)	140
3.3.5 The atropisomers of 5,15-bis(9-phenanthrenyl)-10-phenyl OEP (287), 5,15-bis(9-phenanthrenyl)-10-(4-n-pentylphenyl) OEP (288), 5,15-bis(9-phenanthrenyl)-10-(1-naphthyl) OEP (289) and 5,15-bis(3-OMe phenyl)-10-phenyl OEP (291).....	141
3.3.6 The atropisomers of 5,10,15-tris(9-phenanthrenyl) OEP (10) ...	145
3.3.7 The atropisomers of 5,10,15,20-tetrakis(9-phenanthrenyl) OEP (11)	146

3.4 <i>Meso</i> proton and NH ¹ H NMR signals of synthesized OEPs.....	147
REFERENCES.....	152
4. Crystal Structure Determinations of Pd(II), Pt(II) and H₂OEPs	154-158
REFERENCES.....	
Results of Part I.....	159-161
Part II – Photophysical Measurements	
5. Ultraviolet/visible spectroscopy (UV/vis).....	162-206
5.1 UV/vis spectra of β -substituted porphyrins.....	162
5.2 UV/vis spectra of prepared <i>meso</i> monosubstituted H ₂ OEPs.....	172
5.3 UV/vis spectra of <i>meso</i> 5,10-disubstituted H ₂ OEPs.....	175
5.4 UV/vis spectra of <i>meso</i> trisubstituted H ₂ OEPs.....	181
5.5 Q band behaviour of <i>meso</i> di- and trisubstituted H ₂ OEPs.....	186
5.6 UV/vis spectra of the phenanthrenyl series (8-11).....	191
5.7 Effect of the Pd(II) and Pt(II) insertion on the UV/vis spectra.....	195
5.7.1 UV/vis spectra of Pd(II) and Pt(II)OEPs.....	195
5.8 Absorption bands of additional chromophores in the UV/vis spectra.....	202
REFERENCES.....	204
6. Phosphorescence and Distortion of Pd(II) and Pt(II)OEPs	207-226
6.1 Phosphorescence and fluorescence of porphyrins.....	207
6.2 The distortion of porphyrins.....	209
6.2.1 Indicators of distortion	209
6.2.2 Calculation of distortions and representation in the NSD model..	210
6.3 Phosphorescence and distortion modes of Pd(II) and Pt(II)OEPs.....	212
6.4 Phosphorescent porphyrins described in literature.....	218
REFERENCES.....	224

Results of Part II.....	227-229
Conclusions and Outlook.....	230-235
Experimental Part	236-279
7. General Methods.....	236
7.1 Synthesis of 2,3,7,8,12,13,17,18-octaethylporphyrin (OEP) (1).....	236
7.2 General synthetic procedure for the preparation of <i>meso</i> mono-, di-, tri- and tetrasubstituted free base 2,3,7,8,12,13,17,18-octaethylporphyrins	236
7.2.1 <i>Octaethylporphyrins with one meso substituent</i>	238
7.2.1.1 2,3,7,8,12,13,17,18-Octaethyl-5-methylporphyrin (227).....	238
7.2.1.2 2,3,7,8,12,13,17,18-Octaethyl-5-(<i>s</i> -butyl)porphyrin (228).....	238
7.2.1.3 2,3,7,8,12,13,17,18-Octaethyl-5-(3-methoxyphenyl)porphyrin (231).....	239
7.2.1.4 2,3,7,8,12,13,17,18-Octaethyl-5-(3-trifluoromethylphenyl)porphyrin (229).....	239
7.2.1.5 2,3,7,8,12,13,17,18-Octaethyl-5-(4- <i>n</i> -pentylphenyl)porphyrin (5).....	240
7.2.1.6 2,3,7,8,12,13,17,18-Octaethyl-5-(4-dimethylamino-phenyl)porphyrin (230).....	241
7.2.1.7 2,3,7,8,12,13,17,18-Octaethyl-5-(3-hydroxyphenyl)porphyrin (232).....	241
7.2.1.8 2,3,7,8,12,13,17,18-Octaethyl-5-(4-methylphenyl)porphyrin (229).....	242
7.2.1.9 2,3,7,8,12,13,17,18-Octaethyl-5-(1-naphthyl)porphyrin (7).....	242
7.2.1.10 2,3,7,8,12,13,17,18-Octaethyl-5-(2-naphthyl)porphyrin (233).....	243

7.2.1.11 2,3,7,8,12,13,17,18-Octaethyl-5-acenaphthyl- porphyrin (234).....	244
7.2.1.12 2,3,7,8,12,13,17,18-Octaethyl-5-(9-phenanthrenyl) porphyrin (8).....	244
7.2.2 <i>Octaethylporphyrins with two meso substituents</i>	245
7.2.2.1 2,3,7,8,12,13,17,18-Octaethyl-5-(9-anthracenyl)-10- phenylporphyrin (246).....	245
7.2.2.2 2,3,7,8,12,13,17,18-Octaethyl-5-(9-phenanthrenyl)-10- phenylporphyrin (247).....	246
7.2.2.3 2,3,7,8,12,13,17,18-Octaethyl-5-(1-naphthyl)-10- phenylporphyrin (248).....	247
7.2.2.4 2,3,7,8,12,13,17,18-Octaethyl-5-(4-dimethylamino- phenyl)-10-phenylporphyrin (249).....	247
7.2.2.5 2,3,7,8,12,13,17,18-Octaethyl-5-(4- <i>n</i> -pentylphenyl)- 10-phenylporphyrin (250).....	248
7.2.2.6 2,3,7,8,12,13,17,18-Octaethyl-5-(4-bromophenyl)-10- phenylporphyrin (251).....	249
7.2.2.7 2,3,7,8,12,13,17,18-Octaethyl-5-(3-methoxyphenyl)- 10-phenylporphyrin (252).....	249
7.2.2.8 2,3,7,8,12,13,17,18-Octaethyl-5-(4-dimethylamino- phenyl)-10-(3-trifluoromethylphenyl)-porphyrin (253).....	250
7.2.2.9 2,3,7,8,12,13,17,18-Octaethyl-5,10-bis(4- <i>n</i> - pentylphenyl)porphyrin (254).....	251
7.2.2.10 2,3,7,8,12,13,17,18-Octaethyl-5-(9-anthracenyl)-10- (4- <i>n</i> -pentylphenyl)porphyrin (255).....	251
7.2.2.11 2,3,7,8,12,13,17,18-Octaethyl-5-(4- <i>n</i> -pentylphenyl)- 10-(9-phenanthrenyl)porphyrin (256).....	252
7.2.2.12 2,3,7,8,12,13,17,18-Octaethyl-5,10-bis(1-naphthyl) porphyrin (257).....	253
7.2.2.13 2,3,7,8,12,13,17,18-Octaethyl-5-(1-naphthyl)-10-(4- <i>n</i> -pentylphenyl)porphyrin (258).....	254
7.2.2.14 2,3,7,8,12,13,17,18-Octaethyl-5,10-bis(9-phenan-	

threnyl)porphyrin (9).....	254
7.2.2.15 2,3,7,8,12,13,17,18-Octaethyl-5-(1-naphthyl)-10-(9-phenanthrenyl)porphyrin (259).....	256
7.2.2.16 2,3,7,8,12,13,17,18-Octaethyl-5-(4-dimethylamino-phenyl)-10-(9-phenanthrenyl)porphyrin (260).....	256
7.2.2.17 (2,3,7,8,12,13,17,18-Octaethyl-5-phenyl-10- <i>s</i> -butylporphyrinato)palladium (II) (276).....	257
7.2.2.18 (2,3,7,8,12,13,17,18-Octaethyl-5-phenyl-15- <i>s</i> -butylporphyrinato)palladium (II) (277).....	258
7.2.2.19 (2,3,7,8,12,13,17,18-Octaethyl-5-phenyl-10- <i>n</i> -butylporphyrinato)palladium (II) (285).....	258
7.2.2.20 (2,3,7,8,12,13,17,18-Octaethyl-5,10-bis- <i>n</i> -butylporphyrinato)palladium (II) (274)	259
7.2.2.21 (2,3,7,8,12,13,17,18-Octaethyl-5,15-bis- <i>n</i> -butylporphyrinato)palladium (II) (275).....	259
7.2.2.22 (2,3,7,8,12,13,17,18-Octaethyl-5-(9-phenanthrenyl)-10- <i>s</i> -butylporphyrinato)palladium (II) (278).....	259
7.2.2.23 (2,3,7,8,12,13,17,18-Octaethyl-5-(9-phenanthrenyl)-15- <i>s</i> -butylporphyrinato)palladium (II) (279).....	260
7.2.2.24 (2,3,7,8,12,13,17,18-Octaethyl-5-(1-naphthyl)-10- <i>n</i> -butylporphyrinato)palladium (II) (286).....	261
7.2.2.25 (2,3,7,8,12,13,17,18-Octaethyl-5,10-bis(1-naphthyl)porphyrinato)palladium (II) (284).....	261
<i>7.2.3 Octaethylporphyrins with three meso substituents</i>	262
7.2.3.1 2,3,7,8,12,13,17,18-Octaethyl-5,15-bis(9-phenanthrenyl)-10-phenylporphyrin (287).....	262
7.2.3.2 2,3,7,8,12,13,17,18-Octaethyl-5-(4-pentylphenyl)-10,20-bis(9-phenanthrenyl)porphyrin (288).....	263
7.2.3.3 2,3,7,8,12,13,17,18-Octaethyl-5,10,15-tris(9-phenanthrenyl)porphyrin (10).....	264
7.2.3.4 2,3,7,8,12,13,17,18-Octaethyl-5-(1-naphthyl)-10,20-bis(9-phenanthrenyl)porphyrin (289).....	264

7.2.3.5	2,3,7,8,12,13,17,18-Octaethyl-5,15-bis(9-anthracenyl)-10-phenylporphyrin (290).....	265
7.2.3.6	2,3,7,8,12,13,17,18-Octaethyl-5,15-bis(3-methoxyphenyl)-10-phenylporphyrin (291).....	266
7.2.3.7	2,3,7,8,12,13,17,18-Octaethyl-5,10-bisphenyl-15-(4-dimethylaminophenyl)porphyrin (292).....	266
7.2.3.8	2,3,7,8,12,13,17,18-Octaethyl-5,10-bisphenyl-15-(4-bromophenyl)porphyrin (293).....	267
7.2.3.9	2,3,7,8,12,13,17,18-Octaethyl-5,10-bisphenyl-15-(4- <i>n</i> -pentylphenyl)porphyrin (294).....	268
7.2.3.10	2,3,7,8,12,13,17,18-Octaethyl-5,10,15-tris(1-naphthyl)porphyrin (235).....	268
7.2.4	<i>Octaethylporphyrins with four meso substituents</i>	269
7.2.4.1	2,3,7,8,12,13,17,18-Octaethyl-5,10,15,20-tetrakis(9-phenanthrenyl)porphyrin (11).....	269
7.3	Palladium(II) insertion	269
7.3.1	<i>Palladium (II) octaethylporphyrins with one meso substituent</i>	270
7.3.1.1	(2,3,7,8,12,13,17,18-Octaethyl-5-methylporphyrinato)palladium(II) (166).....	271
7.3.1.2	(2,3,7,8,12,13,17,18-Octaethyl-5- <i>n</i> -butylporphyrinato)palladium(II) (17).....	271
7.3.1.3	(2,3,7,8,12,13,17,18-Octaethyl-5- <i>s</i> -butylporphyrinato)palladium(II) (299).....	271
7.3.1.4	(2,3,7,8,12,13,17,18-Octaethyl-5-phenylporphyrinato)palladium(II) (273).....	271
7.3.1.5	(2,3,7,8,12,13,17,18-Octaethyl-5-(3-trifluoromethylphenyl)porphyrinato)palladium(II) (300).....	272
7.3.1.6	(2,3,7,8,12,13,17,18-Octaethyl-5-(1-naphthyl)porphyrinato)palladium(II) (301).....	272
7.3.1.7	(2,3,7,8,12,13,17,18-Octaethyl-5-(2-naphthyl)porphyrinato)palladium(II) (302).....	273
7.3.1.8	(2,3,7,8,12,13,17,18-Octaethyl(5-acenaphthyl)	

porphyrinato)palladium(II) (303).....	273
7.3.1.9 (2,3,7,8,12,13,17,18-Octaethyl-5-(9-phenanthrenyl)porphyrinato)palladium(II) (12).....	274
7.3.2 <i>Palladium (II) octaethylporphyrins with two meso substituents</i> ...	274
7.3.2.1 (2,3,7,8,12,13,17,18-Octaethyl-5,10-bis(1-naphthyl)porphyrinato) palladium (II) (284).....	274
7.3.2.2 (2,3,7,8,12,13,17,18-Octaethyl-5,10-bis(9-phenanthrenyl)porphyrinato)palladium (II) (13).....	275
7.3.3 <i>Palladium (II) octaethylporphyrins with three meso substituents</i> .	275
7.3.3.1 (2,3,7,8,12,13,17,18-Octaethyl-5,15-bis(9--)-10-phenylporphyrinato)palladium (II) (304).....	275
7.3.3.2 (2,3,7,8,12,13,17,18-Octaethyl-5,10,15-tris(9-phenanthrenyl)porphyrinato)palladium(II) (14).....	276
7.3.4 <i>Palladium (II) octaethylporphyrins with four meso substituents</i>	
7.3.4.1 (2,3,7,8,12,13,17,18-Octaethyl-5,10,15,20-tetrakis(9-phenanthrenyl)porphyrinato)palladium (II) (15).....	277
7.4 Platinum (II) insertion	277
7.4.1 <i>Platinum (II) octaethylporphyrins with one meso substituent</i>	277
7.4.1.1 (2,3,7,8,12,13,17,18-Octaethyl-5-phenylporphyrinato)platinum (II) (307).....	277
7.4.1.2 (2,3,7,8,12,13,17,18-Octaethyl-5-(1-naphthyl)porphyrinato)platinum (II) (308).....	278
7.4.1.3 (2,3,7,8,12,13,17,18-Octaethyl-5-(9-phenanthrenyl)porphyrinato)platinum (II) (309).....	278

To my mother and in memory of my father



Aims and Objectives

Porphyrins are omnipresent in modern optical technology and biomedical applications due to their light emitting qualities. They are applied in biomedical probing of oxygen or of anions in hydrophilic media such as blood,¹⁻³ in tumour therapy (PDT=photodynamic therapy) and tumour diagnosis,⁴⁻⁶ in LEDs (light emitting diodes),⁷ in light harvesting systems e.g. solar cells for artificial photosynthesis,⁸⁻¹⁰ as optical limiters and in NLO applications (non linear optics).^{11,12} In a similar manner, nature is using them as pigments in various biological processes e.g. most importantly in photosynthesis and their role in biochemistry has been investigated intensely during the past 50 years. However, among the diversity of β -substituted derivatives no *meso* substituted porphyrins are known by nature, but can be prepared in laboratory convenience to fine-tune the physical and chemical properties of porphyrins. This work targeted therefore on the use of 2,3,7,8,12,13,17,18-octaethylporphyrin (OEP) **1**, which is shown in figure 1, as its Pd(II) and Pt(II) complexes **2** and **3** were used in technical applications.¹³⁻¹⁶ OEP **1** can be derived in *meso* position in a nucleophilic substitution reaction with organo lithium reagents^{17,18} and the synthesis of distorted *meso* mono-, di- tri- and tetrasubstituted OEPs was carried out successfully and will be reported as such.

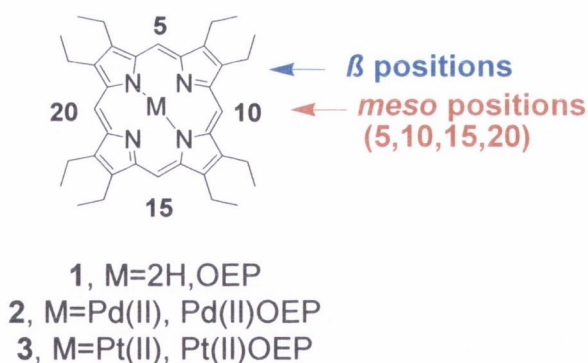


Fig. 1. Chemical structure of OEP **1**, Pd(II)OEP **2** and Pt(II)OEP **3**.

OEP consists of four pyrrole rings bearing ethyl groups in the 3- and 4-positions (β -positions) e.g. in the 2-,3-,7-,8-,12-,13-,17- and 18-positions of the respective porphyrin. The pyrrole units are connected by methylene bridges to form a delocalized 22 π -electron aromatic ring system with $n = 5$ for $(4n + 2)$. *Meso* not substituted OEP is planar and

displays a for flat porphyrins typical UV/vis spectrum with a slim but strong absorption band at 398 nm (B or Soret band) and four less intense absorption bands at 497, 531, 566 and 619 nm (Q bands). The crystals of OEP are dark violet and dissolve red in dichloromethane, absorbing visible light in the violet (Soret band) and the green and yellow portions (Q bands). The spectrum of the respective palladium (II) complex **2** is displayed in figure 5 and shows relative to free base OEP **1** only two Q bands as a result of its increased symmetry. After excitation, Pd(II)OEP **2** is furthermore found to emit phosphorescence from the respective triplet state, which can be used in technical applications, and its phosphorescence lifetime and quantum yield could be determined as $\tau_0=459 \mu\text{s}$ and $\Phi=15.4$. However, OEP **1** and Pd(II)OEP **2** distort with the introduction of substituents in the *meso* positions and physical and chemical changes can be induced. The research carried out, focused therefore on the following tasks:

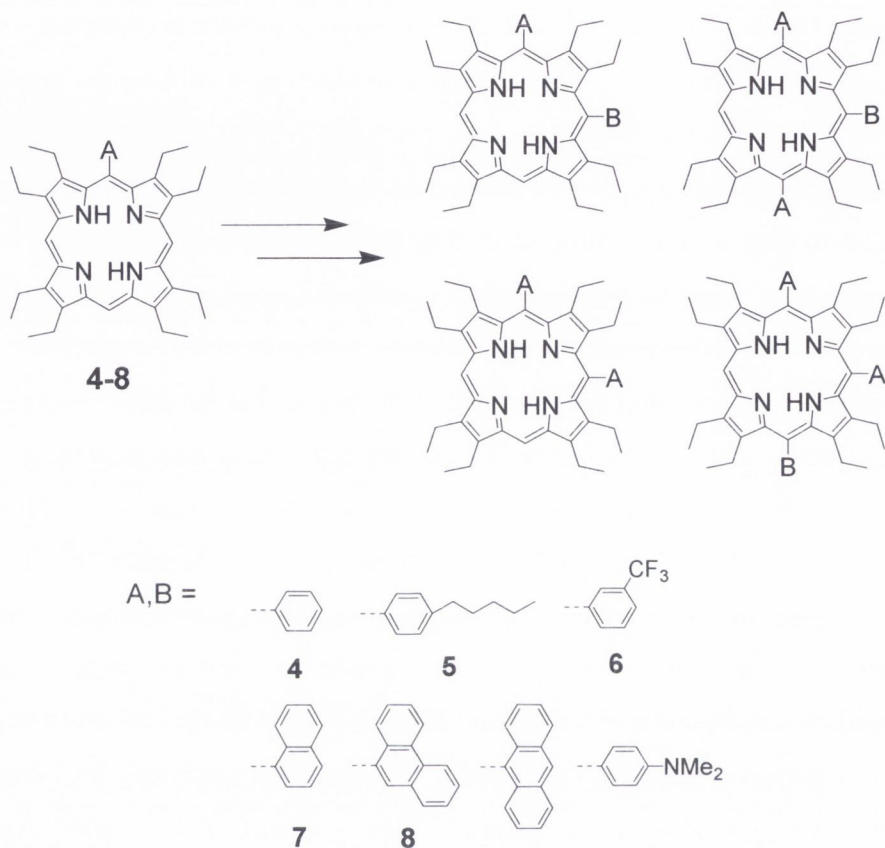
a) To find a reasonable pathway to highly substituted and strongly distorted, symmetric AABB and unsymmetric ABCD octaethylporphyrins with altered physical and chemical properties by the synthesis of appropriate precursors (A-, A₂-, AB-, AAB- and ABA-type OEPs) and to prepare also novel series of octaethylporphyrins using organo lithium reagents (PART I)

b) To elucidate the relationship between conformational and photophysical properties (distortion modes relative to UV/vis absorption and phosphorescence emission) being of high importance for many applications (PART II)

SYNTHESIS. Porphyrins are easily prepared from pyrrole precursors in condensation reactions (see chapter 1) and can be derived in a straightforward manner, when bearing no β substituents, in the *meso* positions by subsequent bromination and coupling reactions such as Suzuki-type or Heck-type coupling to produce a variety of β unsubstituted, *meso* substituted porphyrins for NLO (non linear optics), PDT (photodynamic therapy), sensor and device applications.¹⁹⁻²¹ Unfortunately, β substituted OEP **1** could not be derived in the same manner in the past due to side reactions in the respective media. The controlled access of halogenated derivatives such as *meso* mono- and 5,10- or 5,15-bisbromo OEP remained difficult^{22,23} and no high potential strategy has been found. Nitration on the other hand resulted in the respective *meso* nitro OEPs,

which, by being subsequently transformed into the respective chloro OEPs, may open in future the pathway to novel OEPs, as discussed in chapter 2.1.^{24,25} So far, *meso* substituted OEPs and other *meso-β* substituted porphyrins were most successfully prepared by acid catalyzed condensation reactions, and the recently presented synthesis carried out by Syrbu *et al.*, was the most important, as it allowed the synthesis of highly distorted *β*-substituted porphyrins in a gram scale.²⁶ Alternative methods, consisted in the past in [2+2] McDonald-type condensation reactions, carried out by Y. Chen and co-workers to prepare *meso* mono-octa-*β*-substituted porphyrins,²⁷ by Syrbu *et al.* for the preparation of *meso* 5,15-diaryl-octa-*β*-substituted porphyrins²⁸ and by Banfi *et al.* for the synthesis of a few *meso* ABAB octaethyl- and octamethylporphyrins.²⁹ An overview of obtained *β*-substituted porphyrins and the respective synthetic strategies is given in the chapters 1 and 2.1. However, it is on the other hand also possible to derive OEP 1 directly in the *meso* positions by nucleophilic substitution reactions with organo lithium reagents as reported since 1998 by M. O. Senge *et al.* and as described in chapter 2.1 and 2.2.^{17,18} Due to its simplicity, the possibility to prepare a single OEP selectively, avoiding the separation of mixtures of porphyrins and to introduce also sterically demanding substituents, this method has been chosen during the PhD to produce novel *meso* substituted OEPs. Nucleophilic substitution reactions are considered as a temporary tool, leading to the formation of *meso* altered OEPs in good to excellent yield, while they are limited in scale and can be carried out only with difficulty with “N and O” bearing lithiates. Several novel *meso* monosubstituted octaethylporphyrins with residues of different size and electronic properties could be prepared following previous synthesis reported by I. Bischoff and W. Kalisch and by using *in situ* generated organo lithium reagents for the reactions.^{30,31} *Meso* monosubstitution was furthermore the first step in a sequence of substitution reactions yielding in the synthesis of several novel A₂, AB, ABA and AAB substituted OEPs, as shown in scheme 1 and figure 2. The isolated *meso* di- and trisubstituted OEPs, showed also novel UV/vis features (shoulders, broadenings and changes in the shape of the UV/vis spectra) and additionally particularities in the ¹H NMR spectra due to occurring atropisomers could be observed and are reported in the chapters 3 and 5.³²⁻³⁶ The obtained OEPs are important products on the way to highly distorted, symmetric 5,10-A₂-15,20-B₂ and 5,15-A₂-10,20-B₂ as well as unsymmetric AABC and ABAC OEPs and additionally, also the series of *meso* 9-phenanthrenyl substituted OEPs, shown in figure 2, could be prepared successfully.

The phenanthrenyl series is furthermore an outstanding example for the ease of reaction by using aryl lithium reagents.



Scheme 1. Synthesis of *meso* di- and trisubstituted OEPs

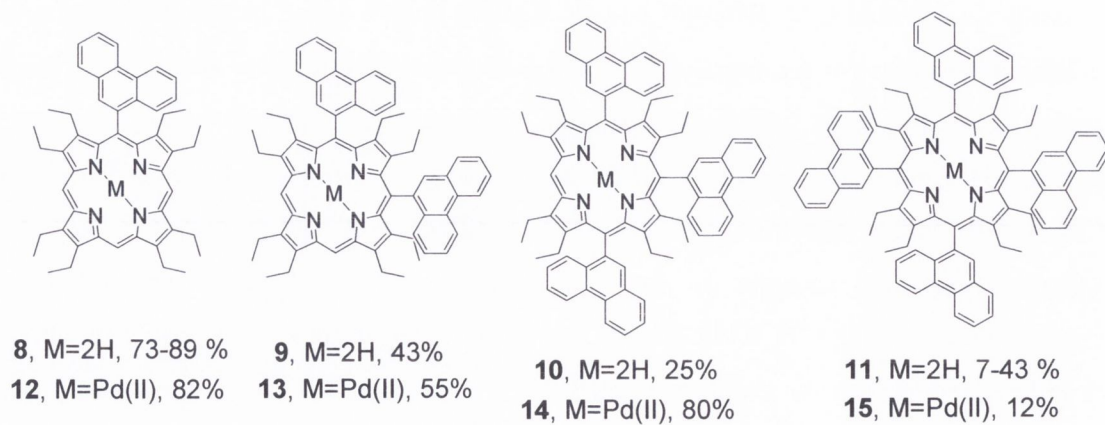


Fig. 2. Prepared *meso* phenanthrenyl series and its palladium (II) complexes

Aiming the investigation of the respective photophysical properties, also several palladium (II) and three platinum (II) complexes were prepared, as it can be seen for example in figure 2. For future derivation, also *meso*- β fusion reactions and direct *meso* linkages were considered during the thesis, but were not carried out as *meso* trisubstituted Pd(II)OEPs were required for the linkage reaction.³⁷⁻⁴⁰ The derivation of methoxy- and dimethylaminophenyl OEPs, as summarized in chapter 2.4, might also be a target for additional derivation, yielding in the formation of NO₂, OH and COOH groups, which are of interest for NLO and sensor applications of porphyrins.

PHOTOPHYSICAL INVESTIGATIONS. With the introduction of substituents in the *meso* positions, OEP **1**, which is in its unsubstituted form planar, distorts as a result of the induced steric strain caused by the hindrance of the ethyl groups in the β -positions and the substituent in the *meso* positions.¹⁷ The introduction of alkyl substituents in *meso* position is furthermore known to cause an overall ruffled conformation of the porphyrin, while aryl substitution induces a mixture of major saddling and minor ruffling, as described in more detail in chapter 6.³³ An example of a solid state structure (see chapter 4) is furthermore displayed in figure 3 showing the newly synthesized 5-(9-phenanthrenyl) OEP **8**. As it can be seen, the introduction of a single aryl substituent had only a small impact on the porphyrin distortion. The deviation from the zero level was minimal and is indicated by the red dashed line in figure 3. Otherwise, for higher substituted OEPs more severe out-of plane and in-plane distortions were reported²² and 3D conformational changes were described to result in changes of the absorption and emission properties (UV/vis absorption, fluorescence and phosphorescence emission), redox-behaviour and other physical and chemical properties of porphyrins.^{26,41,42}

The OEPs **2**, **17**, **18**, Pd(II)OEP, 5-*n*-butyl Pd(II)OEP and Pd(II)OETPP (OETPP= 2,3,7,8,12,13,17,18-octaethyl-5,10,15,20-tetraphenylporphyrin), are for example shown in figure 4, while the recorded absorption spectra are displayed in figure 5 and a detailed discussion can be also found in chapter 5. As it can be seen, the main absorption band e.g. the Soret band shifts with a higher degree of *meso* substitution and the strongest red shift can be found for the *meso* tetrasubstituted OEP **18**, being the strongest distorted. However, the *meso* monosubstituted Pd(II)OEP **17** shows also a relative strong shift

compared to Pd(II)OEP **2** (14nm) and is induced by the substitution with an alkyl substituent.

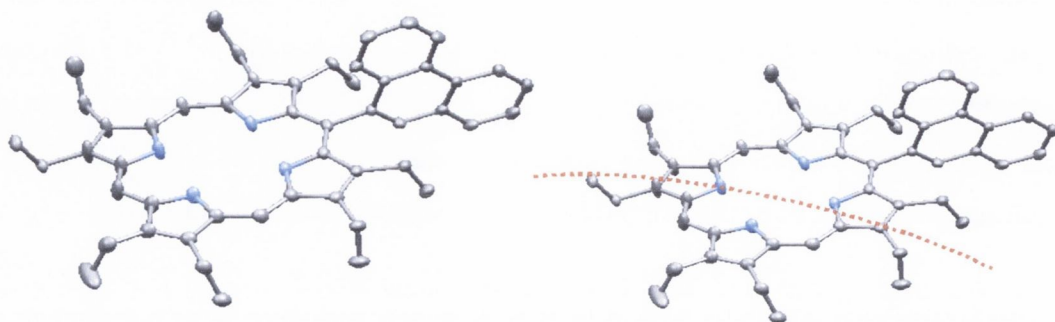


Fig. 3. Crystal structure of 5-(9-phenanthrenyl) OEP **8**. The hydrogen atoms were omitted. The structure is slightly distorted and the β -ethyl groups stick out and are either up or down orientated. The phenanthrenyl substituent is in almost orthogonal position relative to the porphyrin plane.

In theoretical terms, the bathochromic shift can be furthermore explained as the result of the destabilization of the porphyrin HOMO (**h**ighest **o**ccupied **m**olecular **o**rbital), which decreases the HOMO-LUMO gap for the $\pi \rightarrow \pi^*$ excitation and by consequence light of longer, less energetic wavelength is emitted. The effect is especially distinct for porphyrins bearing heavy metal atoms in the porphyrin core and several palladium (II) and platinum (II) complexes were prepared during the PhD for further investigation.

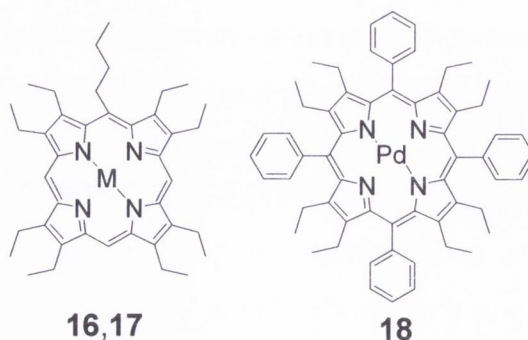


Fig. 4. Chemical structures of 5-*n*-butyl OEP **16** (M=2H), 5-*n*-butyl Pd(II)OEP **17** (M=Pd(II)) and Pd(II)OETPP **18**.

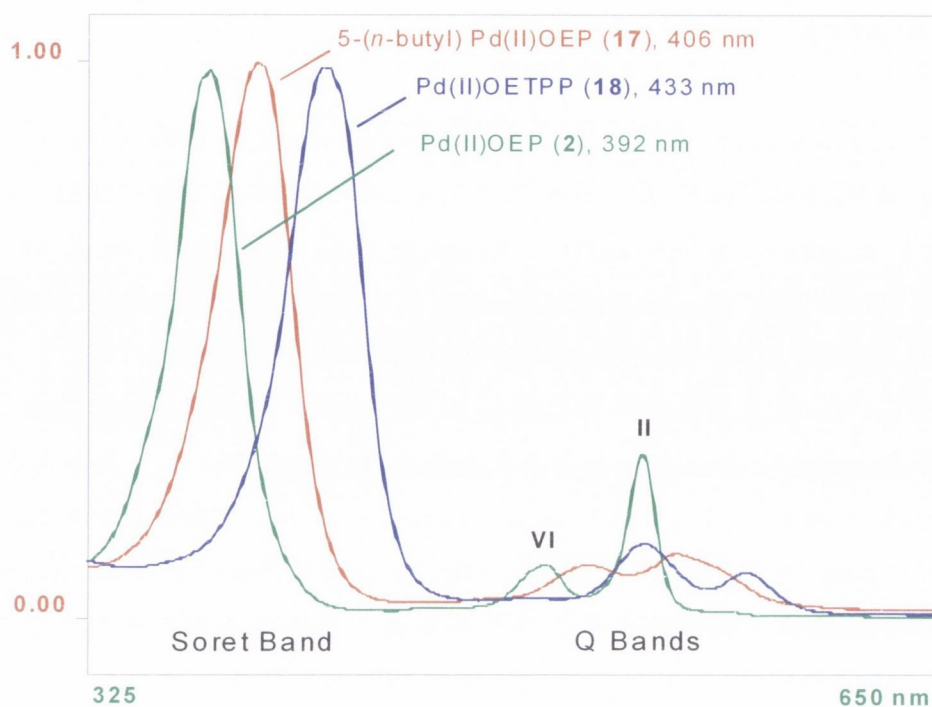


Fig. 5. UV/vis spectra of selected Pd(II)OEPs.

In fact during the *meso* monosubstitution, where planar OEP **1** becomes slightly distorted for the first time, photophysical changes can be directly set in relation to structural changes. The palladium (II) and platinum (II) insertion had furthermore the effect of switching the emission of the triplet state from fluorescence to phosphorescence¹⁻³ and measurements of phosphorescence quantum yields and life times were carried out for synthesized *meso* monosubstituted Pd(II)OEPs by Prof. S. Vinogradov. The collected data was correlated with the observed conformational changes, which could be obtained from the respective crystal structure or which were predicted by model calculations, as described in chapter 6 and defined ruffled conformations as particular useful. However, current applications focus so far on easily available *meso* unsubstituted e.g. flat Pd(II)OEP **2**¹³ and Pt(II)OEP **3**, while distorted Pt(II) and Pd(II)OEPs could enlarge the palette of available compounds, allowing to optimize technology in future.¹⁴⁻¹⁶

REFERENCES

- 1) S. A. Vionogradov, L. W. Lo, D. F. Wilson *Chem. Eur. J.* **1999**, *5*, 1338.
- 2) V. V. Rozhkov, D. F. Wilson, S. A. Vinogradov *Macromolecules* **2002**, *35*, 1991.
- 3) J. E. Rogers, K. A. Nguyen, D. C. Hufnagle, D. G. McLean, W. Su, K. M. Gosset, A. R. Burke, S. A. Vinogradov, R. Prachter, P. A. Fleitz *J. Chem. Phys. A* **2003**, 11331.
- 4) H. Brunner, K.-M. Schellerer *Inorg. Chim. Acta* **2003**, *350*, 39.
- 5) H. Gu, K. Xu, Z. Yang, C. K. Chang, B. Xu *Chem. Commun.* **2005**, 4270.
- 6) H. Brunner, N. Gruber *Inorg. Chim. Acta* **2004**, *357*, 4423.
- 7) Y.-Y. Noh, C.-L. Lee, J.-J. Kim, K. Yase *J. Chem. Phys.* **2003**, *118*, 6, 2853.
- 8) N. Aranti, H. S. Cho, T. K. Ahn, S. Cho, D. Kim, H. Sumi, A. Osuka *J. Am. Chem. Soc.* **2003**, *125*, 9668.
- 9) L. Junzhong, J. S. Lindsey *J. Org. Chem.* **1999**, *64*, 9101.
- 10) J. E. Kroeze, T. J. Savenije, L. P. Candeias, J. M. Warman, L. D. A. Siebbeles *Sol. Energy Mater. Sol. Cells* **2005**, *85*, 189.
- 11) K. Susumu, T. V. Duncan, M. J. Therien *J. Am. Chem. Soc.* **2005**, *127*, 5186.
- 12) M. J. Frampton, H. Akdas, A. R. Cowley, J. E. Rogers, J. E. Slagle, P. A. Fleitz, M. Drobizhev, A. Rebane, H. L. Anderson *Org. Lett.* **2005**, *7*, 24, 5365.
- 13) W. Stampor *Chemical Physics* **2004**, *305*, 77.
- 14) R. C. Kwong, S. Sibley, T. Dubovoy, M. Baldo, S. R. Forest, M. E. Thompson *Chem. Mater.* **1999**, *11*, 3709.
- 15) S. Pan, L. J. Rothberg *J. Am. Chem. Soc.* **2005**, *127*, 6087.
- 16) A. P. Vollmer, R. F. Probst, R. Gilbert, T. Thorsen *Lab Chip* **2005**, *5*, 10.
- 17) M. O. Senge *Chem. Commun.* **2006**, 243.
- 18) M. O. Senge *Acc. Chem. Res.* **2005**, *38*, 9, 733.
- 19) P. Bonifassi, P. C. Ray, J. Leszczynski *Chem. Phys. Lett.* **2006**, *431*, 321.
- 20) M. Pizzotti, R. Ugo, E. Annoni, S. Quici, I. Ledoux-Rak, G. Zerbi, M. Del Zoppo, P. C. Fantucci, I. Invernizzi *Inorg. Chim. Acta* **2002**, *340*, 25, 70.
- 21) I. D. L. Albert, T. J. Marks, M. A. Ratner *Chem. Mater.* **1998**, *10*, 753.
- 22) M. O. Senge. In *The Porphyrin Handbook*; K. M. Kadish, K.M., Smith, R. Guillard (Eds.); Academic Press: San Diego, 2000; Vol. 1, pp 239.
- 23) R. Bonnett, I. H. Champion-Smith, A. N. Kozyrev, A. F. Mironov *J. Chem. Res. (S)* **1990**, 138.

- 24) L.-C. Gong, D. Dolphin *Can. J. Chem.* **1985**, *63*, 406.
- 25) M. J. Crossley, L. G. King, S. M. Pyke, C. W. Tansey *J. Porphyrins Phthalocyanines* **2002**, *6*, 11&12, 685.
- 26) S. A. Syrbu, L. Lyobumova, A. S. Semeikin *Chem. Heterocyclic Comp.* **2004**, *40*, 10, 1262.
- 27) Y. Chen, C. J. Medforth, K. M. Smith, J. Alderfer, T. J. Dougherty, R. K. Pandey *J. Org. Chem.* **2001**, *66*, 3930.
- 28) S. A. Syrbu, T. V. Lyubimova, A.S. Semeikin *Russ. J. Gen. Chem.* **2001**, *71*, 10, 1656.
- 29) S. Banfi, A. Manfredi, G. Pozzi, S. Quici, A. Trebicka *Gazz. Chem. Ital.* **1996**, *126*, 179.
- 30) W. W. Kalisch, M. O. Senge *Angew. Chem.* **1998**, *110*, 8, 1156.
- 31) M. O. Senge, I. Bischoff *Eur. J. Org. Chem.* **2001**, 1735.
- 32) Y. Nakamura, I.- W. Hwang, N. Aranti, T. K. Ahn, D. M. Ko, A. Takagi, T. Kawai, T. Matsumo, D. Kim, A. Osuka *J. Am. Chem. Soc.* **2005**, *127*, 236.
- 33) C. M. Muzzi, C. J. Medforth, L. Voss, M. Cancilla, C. Lebrilla, J.-G. Ma, J. A. Shelnut, K. M. Smith *Tetrahedron Lett.* **1999**, *40*, 6159.
- 34) A. Hoshino, Y. Ohgo, M. Nakamura *Tetrahedron Lett.* **2005**, *46*, 4961.
- 35) A. Osuka, N. Aranti *Org. Lett.* **2001**, *3*, 26, 4213.
- 36) H. Higuchi, T. Maeda, K. Miyabayashi, M. Miyake, K. Yamamoto *Tetrahedron Lett.* **2002**, *43*, 3097.
- 37) A. Tsuda, Y. Nakamura, A. Osuka *Chem. Commun.* **2003**, 1096.
- 38) M. Kamo, A. Tsuda, Y. Nakamura, N. Aratani, K. Furukawa, T. Kato, A. Osuka *Org. Lett.* **2003**, *5*, 12, 2079.
- 39) V. S.-Y. Lin, S. G. DiMagno, M. J. Therien *Science* **1994**, *264*, 1105.
- 40) D. P. Arnold, D. A. James *J. Org. Chem.* **1997**, *62*, 3460.
- 41) J. Takeda, M. Sato *Chem. Lett.* **1994**, 2233.
- 42) X. Z. Song, W. Jentzen, L. Jaquinod, R. G. Khoury, C. J. Medforth, S.-L. Jia; J.-G. Ma, K. M. Smith, J. A. Shelnut *Inorg. Chem.* **1998**, *37*, 2117.

Part I - Synthesis of OEPs

1. Synthesis of OEP and β -substituted porphyrins

In the following chapters the synthesis of OEP **1** and its precursor, 3,4-diethylpyrrole **38**, will be discussed, as those were prepared during this work as starting materials. However, it was also described in the introduction that the synthesis of *meso* substituted OEPs was aimed and that direct nucleophilic substitution reaction was chosen as a tool of derivation, while related nona-, deca-, undeca- and dodecasubstituted porphyrins, can be also obtained by [4+1], [2+2] and open chain condensation reactions.

Therefore the preparation of the required precursors e.g. substituted pyrroles, such as 3,4-diethylpyrrole **38**, dipyrromethanes and tripyrranes will be described in the chapters 1.1 to 1.3, while the respective condensation methods, allowing preparing OEP **1** as well as highly substituted porphyrins, will follow in the chapter 1.4. Additionally, also an alternative pathway to dodecasubstituted porphyrins *via* derivation of *meso* A₄ substituted porphyrins by subsequent bromination and Suzuki-type coupling in β position will be discussed in chapter 1.5.

1.1 Synthesis of 3,4-diethylpyrrole (38) and other β -substituted pyrroles

3,4-Disubstituted pyrroles are the precursors of β -substituted pyrrole dimers e.g. dipyrromethanes and dipyrromethenes, of pyrrole trimers e.g. tripyrranes and β substituted porphyrins. The synthesis of substituted pyrroles will be summarized briefly while a more detailed description was given by K. M. Smith in the porphyrin handbook.¹ The traditional pathway to substituted pyrroles is the synthesis first reported by Knorr, shown in figure 1.1.1.^{2,3} Also hetero aromatics such as furan and thiophen could be obtained similarly by the Paal-Knorr synthesis.³ Possible substituent combinations for pyrroles were described by K. M. Smith and are shown in table 1.1.1.¹

The Knorr pathway was also used by Y. Chen *et al.*² in 2001 for the synthesis of the substituted pyrrole **27**, displayed in scheme 1.1.1 and obtained by the reaction of 2,4-pentadienone **26** with the shown nitrosamine **25**. Subsequent reactions, affording the reactive condensation precursor **28**, were laborious and included the reduction of the β position with diborane and demethylation in 5-position. The disadvantages of the traditional Knorr route were therefore the limited access of the necessary synthons and the required activation of the pyrroles afterwards e.g. by demethylation etc.

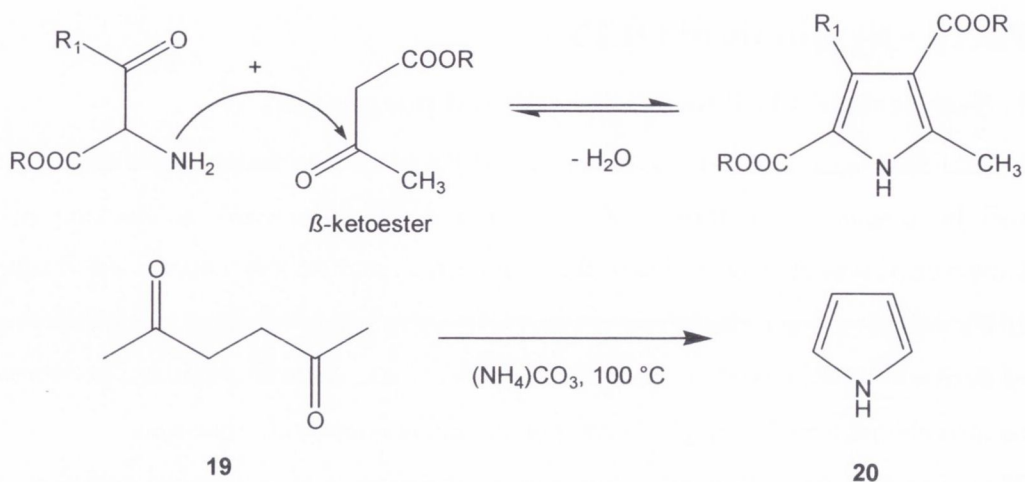
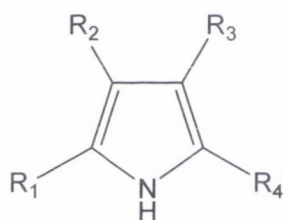


Fig. 1.1.1 Top: Knorr synthesis of a substituted pyrrole using a CH acidic β -ketoester and a protected β -keto aminoacid as “1,3-dicarbonyl synthons”. Bottom: Paal-Knorr synthesis of pyrrole **20**.^{2,3}

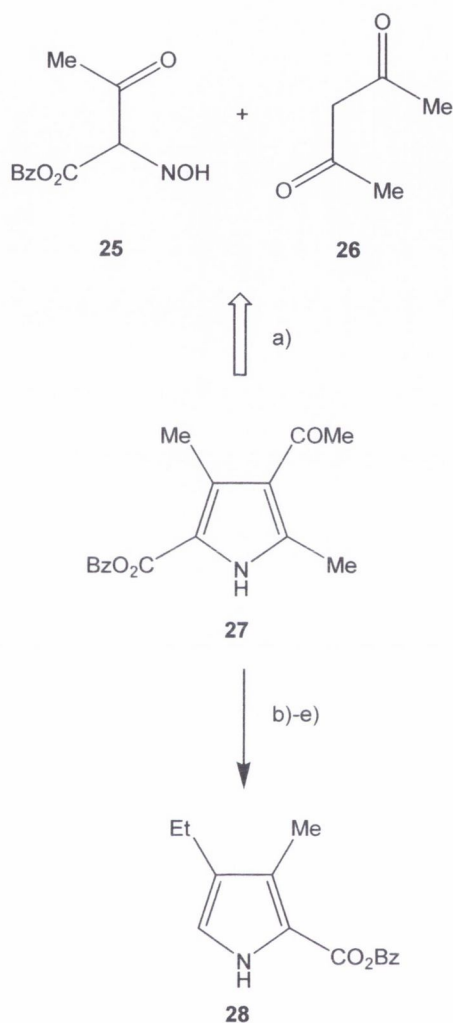


	R₁	R₂	R₃	R₄
21	Me	Me	CO ₂ Et	CO ₂ Et
22	Me	Me	CO ₂ Et	H
23	CO ₂ Et	C ₅ H ₁₁	CO ₂ Et	H
24	H	Ph	Ph	Ph

Table 1.1.1. Substituted pyrroles prepared by Knorr method.¹

More recently the use of the Barton-Zard reaction, investigated by Ono *et al.*,^{4,5} has facilitated the access of substituted pyrroles and was for example used in 1992 by J. L. Sessler for the total synthesis of OEP **1**.⁶ The in scheme 1.1.2 shown diethylpyrrole carboxylate **33** (R_1 - R_3 =Et) is furthermore a possible precursor of OEP **1** and was

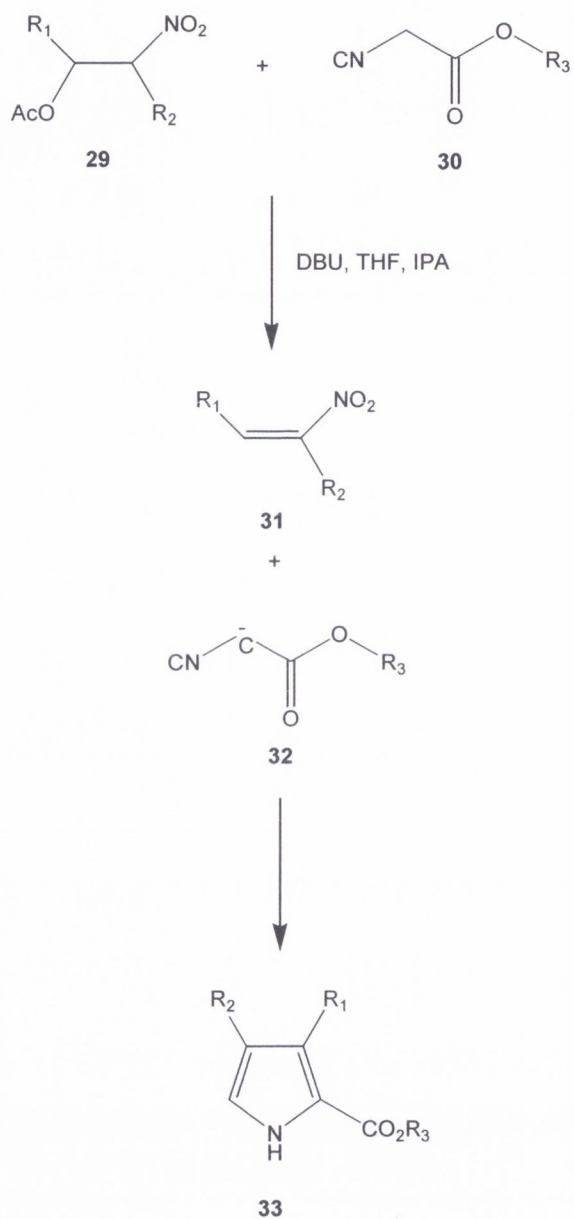
obtained by cyclization of the CH acidic isocyanoester **30** and the acetoxy nitroalkane **29**.



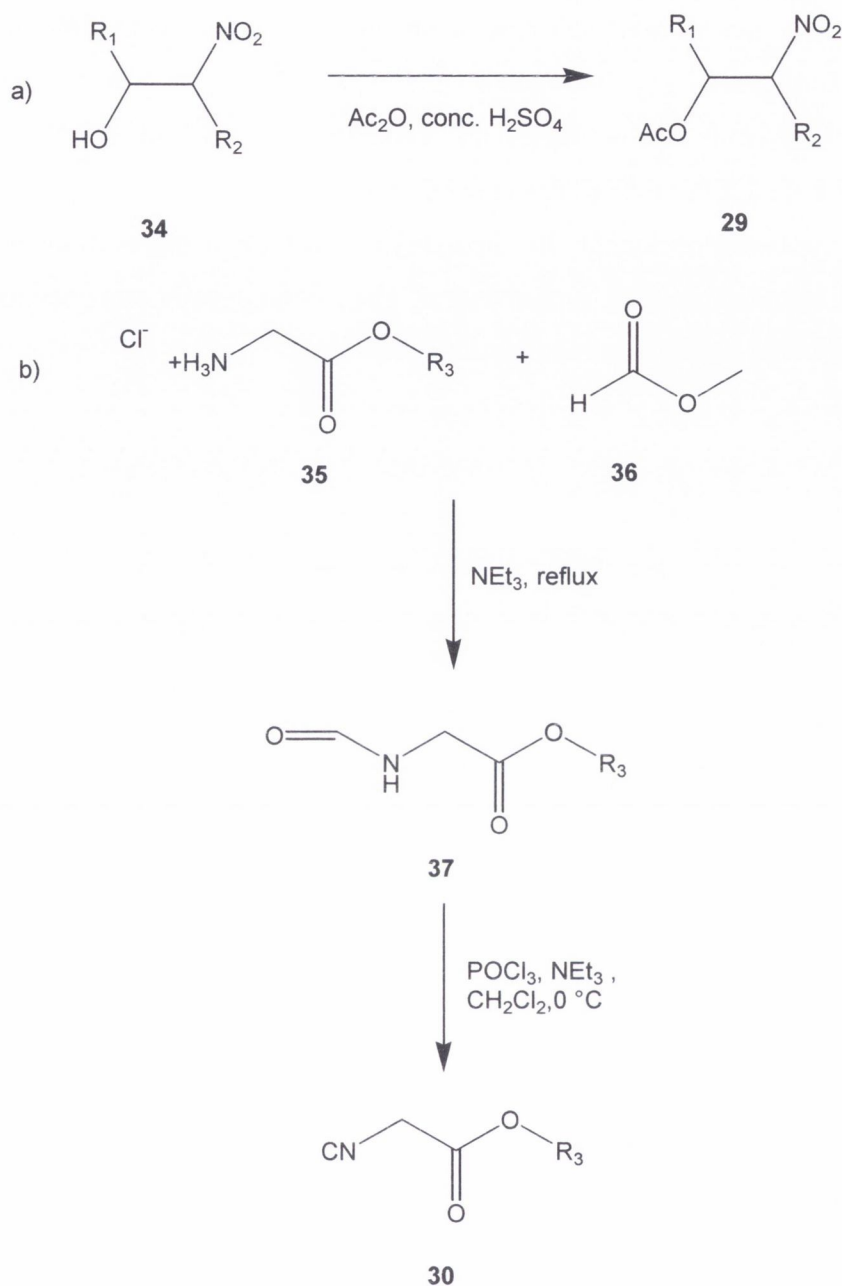
Scheme 1.1.2. Synthesis of the substituted pyrrole **27** and derivation to the condensation synthon **28**; a) Zn/AcOH, CH₃COONa, b) diborane, c) SO₂Cl₂ (3 equiv), d) I₂/KI, e) Zn/AcOH.²

Its formation is due to Michael type addition, induced by deprotonation of the isocyanoester **30** with DBU. The generated anion **32** attacks the electron poor double bond of the precursor **31**, which was also obtained by activation with DBU, and forms the pyrrole carboxylate **33**. The isocyanoester **30** and the acetoxy nitroalkane **29**, were prepared as reported in literature and as shown in scheme 1.1.4.⁷ The access of OEP **1** is

limited by the synthesis of the isocyanoester **30**, which can be bought or prepared and stored frozen for several years. Its odour is unpleasant and traces are easily detected by the characteristic smell.



Scheme 1.1.3. Synthesis of the 3,4-diethylpyrrole carboxylate **33** *via* Barton-Zard reaction; R_{1-3} =ethyl.⁶



Scheme 1.1.4 Synthesis of the Barton-Zard precursors **29** (a.) and **30** (b.); R_{1-3} = ethyl.^{6,7}

Towards OEP, as described in more detail in chapter 1.4.2, the carboxylate **33** was saponified and thermally decarboxylated to afford the reactive diethylpyrrole **38**, shown in figure 1.1.2. The pathway can be also modified by the reduction of the carboxylate to the carbinol **68**, shown in chapter 1.4.2, with LiAlH_4 as carried out by N. Ono *et al.*⁴ and J. Tang and J. G. Verkade.^{8,9} Furthermore also the methyl carboxylate **47**, shown in

figure 1.2.1, can be used and can be obtained by the respective modification of the Barton-Zard precursors. The methyl carboxylate **47** was for example transformed into the diethylpyrrole **38** by Tang and Verkade with LiCl in excellent 100% yield, improving the OEP synthesis presented by Sessler.^{6,8}

Further functionalization of the diethylpyrrole **38** for a more efficient condensation reaction was also reported by Syrbu *et al.* The formyl pyrrole was obtained (not shown) and used in the subsequent condensation reaction.¹⁰⁻¹³

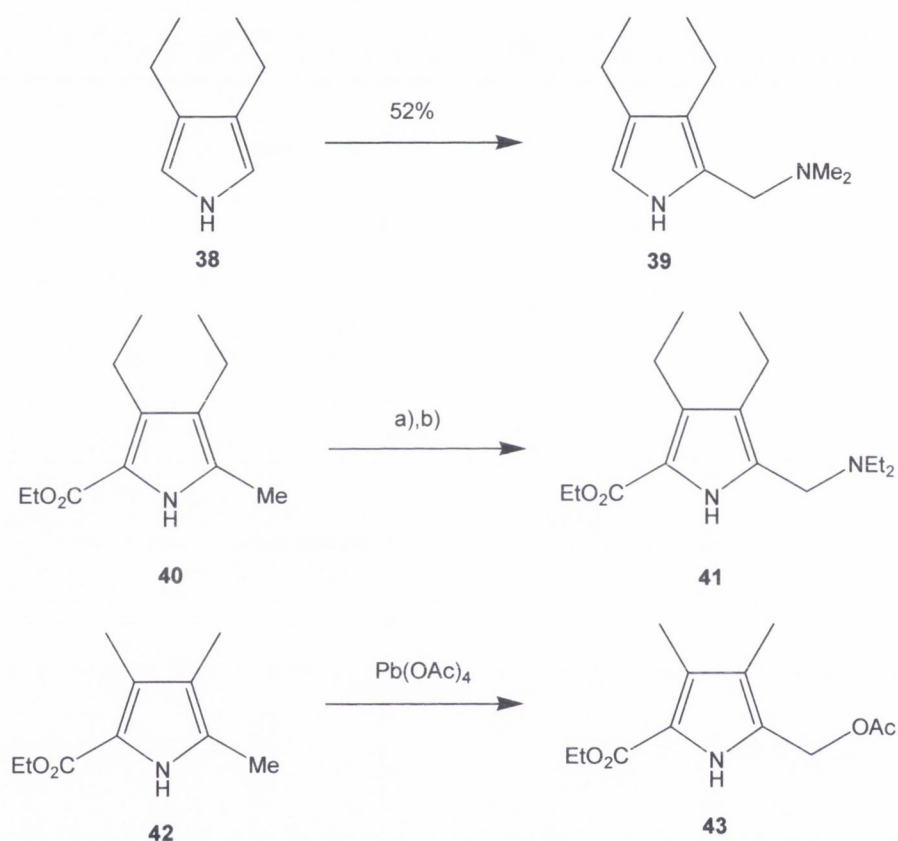
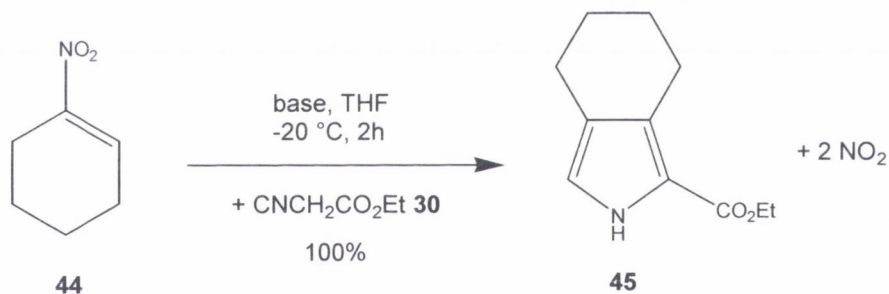


Figure 1.1.2 Activation of diethylpyrrole **38** by Mannich reaction (top, conditions unknown) and of the Knorr type pyrroles **40** and **42** (middle and bottom) by the introduction of a CH_2OAc or CH_2NR_2 substituent in 5-position; a) Br_2 , ether/dichloromethane; b) Et_2NH , ether/dichloromethane.^{14,15}

As it can be seen in figure 1.1.2, also an amino substituent can be introduced in the 5-position of the pyrrole **38** *via* Mannich reaction with dimethylamine and formaldehyde or with Eschenmoser's reagents (N,N-dimethylmethylenammonium iodide)¹⁴ and the

N,N-(dimethylaminomethyl)pyrrole **39** was obtained in 52% yield. Alternatively, also the ethyl ester **41** was prepared as shown in figure 1.1.2,¹⁴ while further synthesis was carried out with the methyl substituted pyrrole **42**, which could be converted to the respective acetate **43** with Pb(OAc)₄.¹⁵ As reported by J. Tang and J. G. Verkade,⁸ more laborious synthesis of substituted pyrroles was also reported in 1981 and 1985 by M. J. Gunter and L. M. Mander¹⁶ as well as by R. Young and C. J. Chang,¹⁷ whereas the Barton-Zard^{4,5} method is the most straightforward and produced a higher variety of novel pyrroles as was shown by Ono *et al.*^{4,18} For example, the synthesis of tetrabenzoporphyrins (TBPs) through Barton-Zard reactions was carried out by S. Vinogradov and co-workers¹⁹ and, as shown in scheme 1.1.5, by Tang and Verkade.^{4,8} As it can be seen, the “TBP pyrrole” **45** was isolated in excellent yield (100%) from the cyclic nitroalkene **44** and the isocyanoester **30**, when the reaction was catalyzed by the a specially designed super base (not shown).⁸



Scheme 1.1.5 Formation of a TBP precursor *via* Barton-Zard reaction.^{4,8,19}

1.2 Synthesis of β substituted dipyrromethanes

Dipyrromethenes were used by Fischer^{20,21} in the 1940th while dipyrromethanes were synthesized more often from the 1980s on. Symmetric dipyrromethanes can be obtained from the dimerization step of a single pyrrole precursor functionalized with a carboxyl group in 5-position by boiling in formic acid and addition of hydrobromic acid.¹ Also bromo pyrroles can be used in hot methanol as shown in figure 1.2.1 and similar was achieved with acetoxymethyl pyrroles when heated in methanol or ethanol with hydrochloric acid or *p*-TsOH as described by Tang and Verkade⁸ and by Chen and co-workers and is shown in figure 1.2.1.² However, the respective bromo pyrroles were obtained from the methyl substituted Knorr pyrroles by addition of Br₂, and reacted

subsequently to the dimers, while the porphyrin formation was avoided as a result of the protective ester group in 5-position.

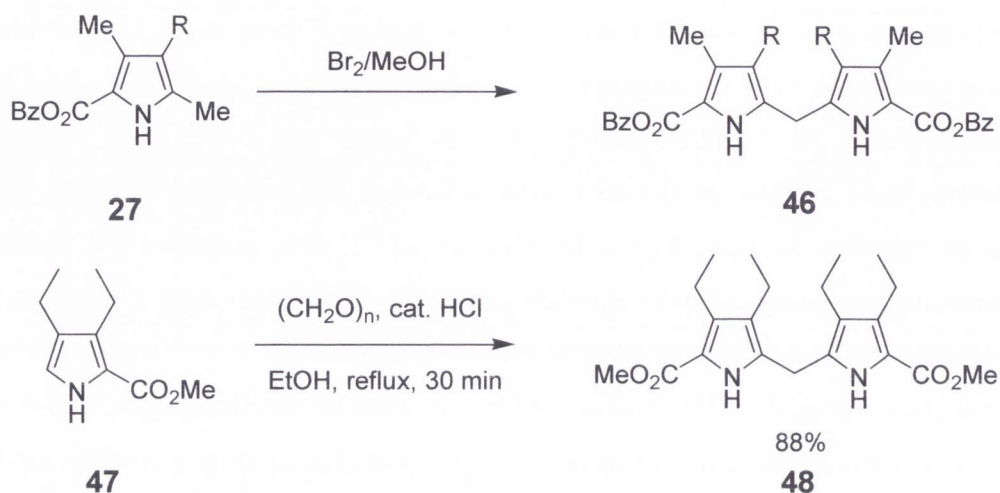
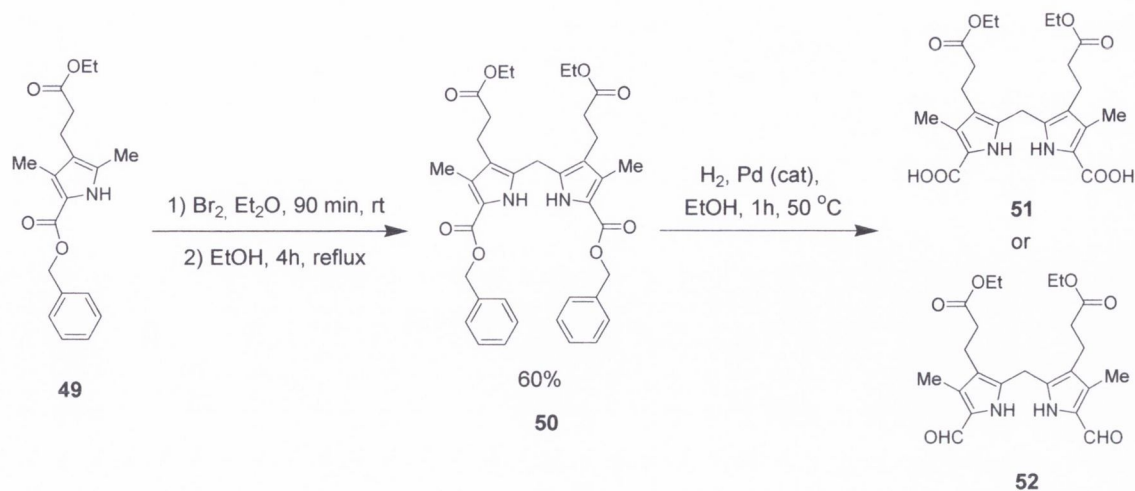
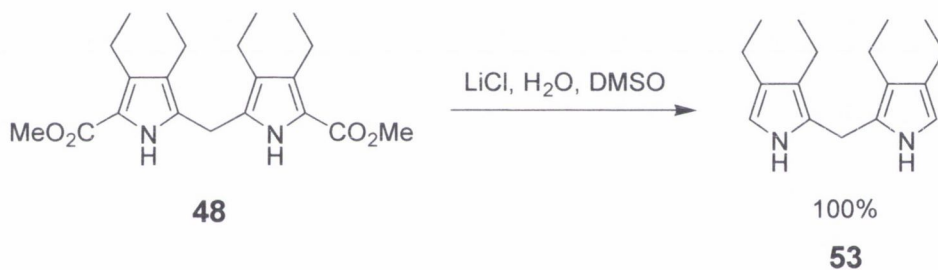


Fig. 1.2.1. Top: Bromination pathway carried out by Chen and co-workers; $\text{R}=\text{COMe}$.²
Bottom: Reaction performed by Tang and Verkade with paraformaldehyde and catalytic HCl .⁸

Another example of the bromination pathway is furthermore displayed in scheme 1.2.1.²² As it can be seen, the benzylic ester of the formed dipyrromethane **50** could be reduced selectively afterwards under a variety of catalytic conditions. The Pd catalyzed hydration yielded in the diacid **51** and by addition of triethylorthoformate (TEOF) the dialdehyde **52** was obtained. The methyl ester **48** shown in scheme 1.2.2, could be on the other hand reduced to 3,4,8,9-tetraethyldipyrromethane **53** with LiCl as described previously for the monopyrrole **38**,⁸ while other alkyl esters have to be subjected to more drastic conditions such as saponification with NaOH and KOH as was carried out by J. L. Sessler using the diethylpyrrole carboxylate **33** and as shown in chapter 1.4.2.^{6,8} An alternative pathway consisted also in the use of the 5-methyl substituted pyrrole **42**¹⁵ or **55**,²³, which could be converted to the acetate with $\text{Pb}(\text{OAc})_4$ ²⁴ and was dimerized as shown in figure 1.2.2. When the benzylic ester (not shown) was prepared, subsequent saponification with NaOH was carried out to yield previously described 3,4,8,9-tetraethyldipyrromethane **53**.²³



Scheme 1.2.1. Pathway *via* bromination of the methyl group in 5-position and dimerization to the dipyrromethane **50**, followed by selective saponification of the benzylester and reduction to the more reactive aldehyde **52** when TEOF was used.²²



Scheme 1.2.2. Pathway by J. Tang and J. G. Verkade for the saponification and reduction of the methyl ester **48** with LiCl.⁸

As furthermore described by Tang and Verkade,⁸ the tetraethylidipyrromethane **53** was not stable and reddened upon exposure to air, but could be kept under nitrogen and in the refrigerator for approximately six month.

However, substituents were also introduced in the bridge position of dipyrromethanes by the addition of aldehydes during the condensation step. The in scheme 1.2.3 shown symmetric *meso* substituted dipyrromethane **56** was obtained by Chen *et al.*² with *p*-TsOH as a catalyst while Tang and Verkade used BF₃ etherate⁸ in analogy to Ono *et al.*⁴ It was also reported by Tang and Verkade that hydrochloric acid couldn't be used while *p*-TsOH slowed the reaction down.

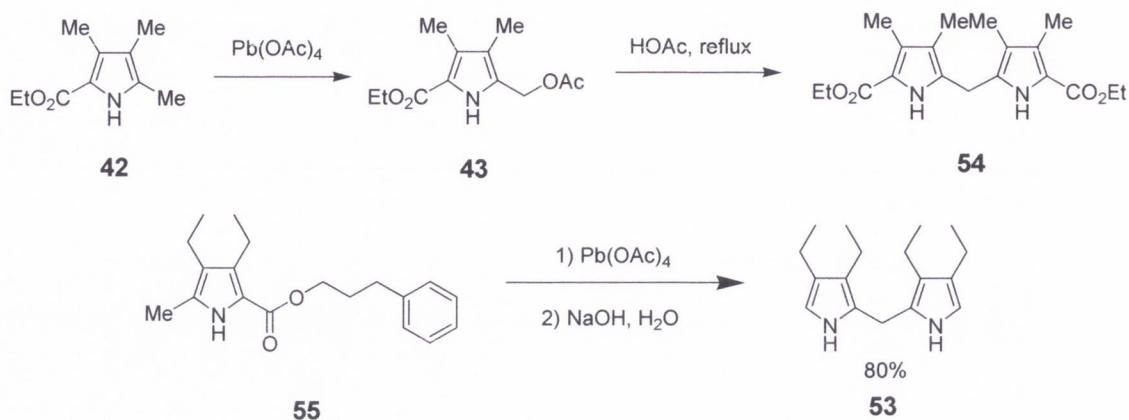


Fig. 1.2.2. Top: $\text{Pb}(\text{OAc})_4$ pathway without saponification.¹⁵ Bottom: $\text{Pb}(\text{OAc})_4$ pathway with subsequent saponification.²³

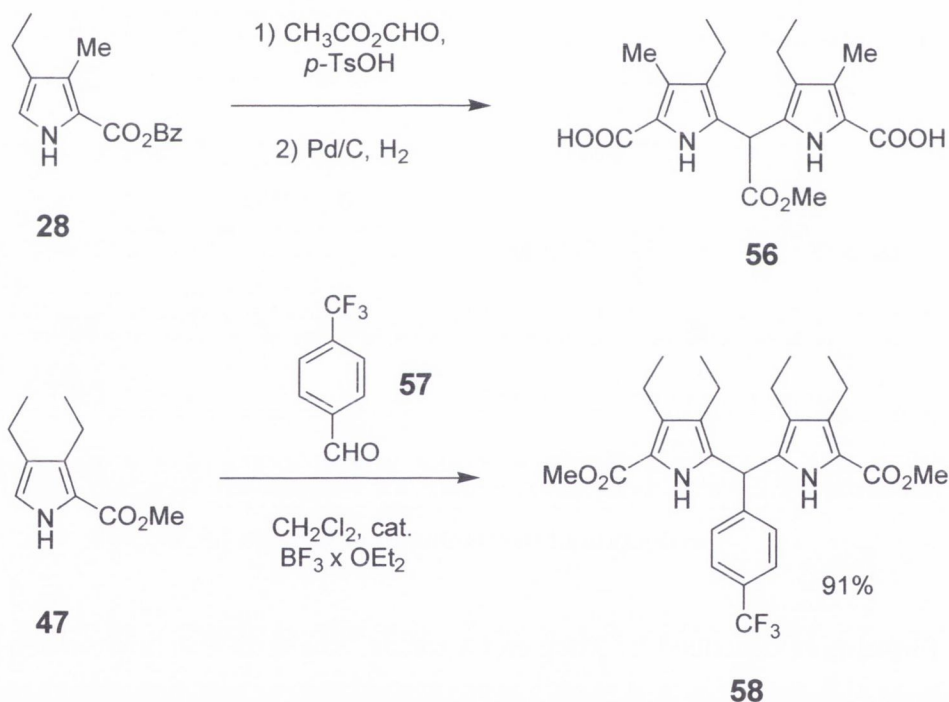


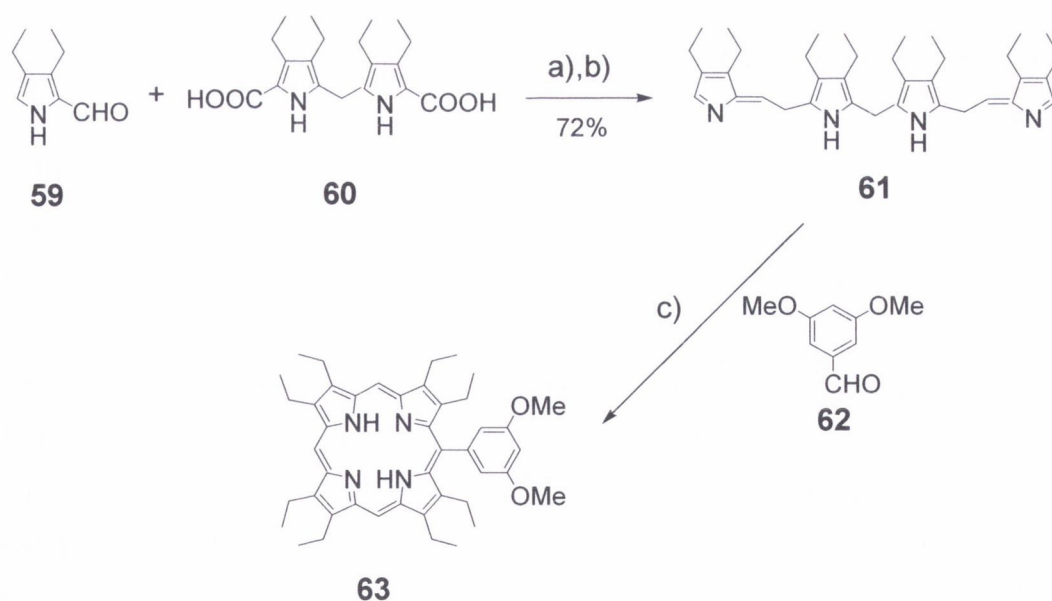
Fig. 1.2.3. Top: Synthesis carried out by Chen *et al.*² Bottom: Reaction performed by Tang and Verkade.⁸

Prolonged reaction times were explained by the hydrogen bond formation between the fluoro atoms of the aldehyde **57** and the pyrrole nitrogen which could be circumvented by using BF_3 etherate, whereas with hydrochloric acid the pyrrole complexation might

have stopped the reaction. For the [2+2] condensation step, the by Chen obtained dipyrromethane (not shown) was, as can be seen in figure 1.2.3, saponified under reductive conditions (Pd/C, H₂) to produce the shown diacid **56**. Several symmetric β -substituted dipyrromethanes with *meso* alkyl and aryl residues (ethyl, *i*-propyl, cyclohexyl, 1-naphthyl and 2,5-dimethoxyphenyl) were also reported by M. O. Senge in 2005,²⁵ summarizing the synthesis carried out by the research groups of K. M. Smith, M. O. Senge, H. K. Hombrecher and G. Horter.²⁶⁻³¹ Some of the described dipyrromethanes were furthermore used in [2+2] McDonald condensation reactions to prepare 5,15-AB, 5,15-AA-type and 5,15-A₂-10,20-B₂-type porphyrins while they were also used for the synthesis of tripyrranes and open-chain tetrapyrroles as will be discussed in the following chapter and chapter 1.4. Unsymmetrical dipyrromethanes are also useful, but most difficult to prepare and an overview was presented by K. M. Smith in the porphyrin handbook.¹

1.3 Synthesis of tripyrranes and open-chain tetrapyrroles

Open chain tri- and tetrapyrroles were seldomly prepared as they are often unstable and only accessible in a laborious step-wise manner.



Scheme 1.3.1. Synthesis of the *meso* monosubstituted OEP **63** via the biladiene **61**; a) MeOH, b) HBr, H₂O, c) HBr, MeOH, AcOH.³²

A more elaborate discussion can be found in the porphyrin handbook,¹ whereas for example the in scheme 1.3.1 shown biladiene **61** in *Z*-conformation could be isolated in 2001 and was, as shown, derived from the monopyrrolic aldehyde **59** and the dipyrromethane **60** under HBr catalyses.³² The biladiene **61** was subsequently condensed with 3,5-dimethoxybenzaldehyde **62** to yield the *meso* monosubstituted OEP **63**. Similar reactions were furthermore carried out by Syrbu *et al.*¹⁰ in 2004.³³

1.4 Condensation reactions affording β -substituted porphyrins

In the following different strategies, mixed and not mixed [4+1] condensation reactions, [2+2] McDonald type condensation reactions and cyclization reactions from the linear tri- and tetrapyrroles, affording β -octaalkyl- and β -octaaryl substituted *meso* free and *meso* partially substituted porphyrins will be presented. The obtained porphyrins could be used as 'starting materials' for *meso* substitution reactions using alkyl- and aryllithium reagents as carried out and reported for OEP **1** in chapter 2.2. A historic discussion e.g. reactions performed before 1999 was provided by K. M. Smith in the porphyrin handbook¹ and the here presented data enlarges the there presented knowledge. Furthermore the synthesis of OEP **1**, which was carried out several times during the thesis, will be reported in chapter 1.4.2.

1.4.1 The [4+1] approach

The most used and best known reaction affording a porphyrin, is the condensation reaction of pyrrole with benzaldehyde reported by Rothmund and Alder/Longo,³⁴ producing TPP **64** (5,10,15,20-tetraphenylporphyrin), shown in figure 1.4.1.1, in 5-10% yield and which was optimized afterwards by Lindsey's group (35%).³⁵ In contrast to that, porphin **67** (P) was only recently available in higher amounts and 74% yield by dealkylation of 5,10,15,20-tetra-*tert*-butyl porphyrin **66** (scheme 1.4.1.1).³⁶ In laboratory convenience, also β -substituted porphyrins, such as OEP **1** or TBP **65** (tetrabenzoporphyrin, compare to chapter 1.4.4) could be isolated in good yields from the reaction of the respective 3,4-substituted pyrroles with dimethoxymethane, formaldehyde or paraformaldehyde. The synthesis of β -phenyl substituted porphyrins will be furthermore described in chapter 1.5.

Condensation reactions, when carried out under N₂ or argon, produce the desired porphyrin in general after oxidation of the porphyrinogen (not shown) by air, DDQ or

chloranil in around 50% yield. Black by-products are typical while not all pyrrole units undergo tetramerization and cyclization, but remain in form of dimers, trimers and oligomers which are quickly destroyed. The pyrrole starting materials can be obtained in various ways as was discussed in chapter 1.1-1.3 and OEP **1** was prepared as shown in scheme 1.4.1.2 from different pyrroles in 50–75% yield depending on scale and the conditions used.¹

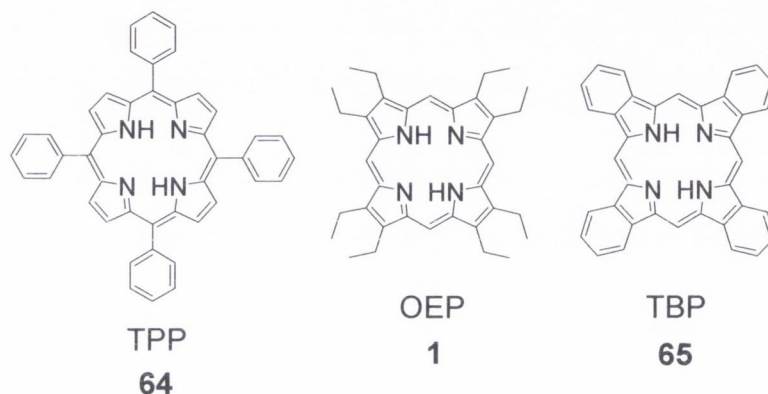
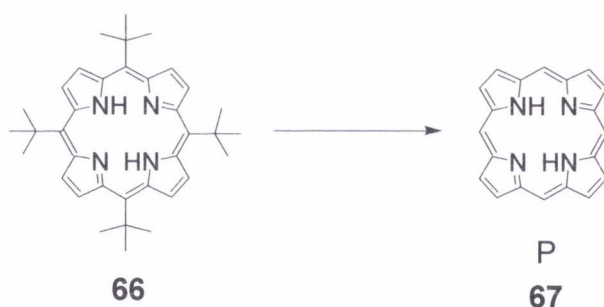


Fig. 1.4.1.1. Often used and easily produced porphyrins.

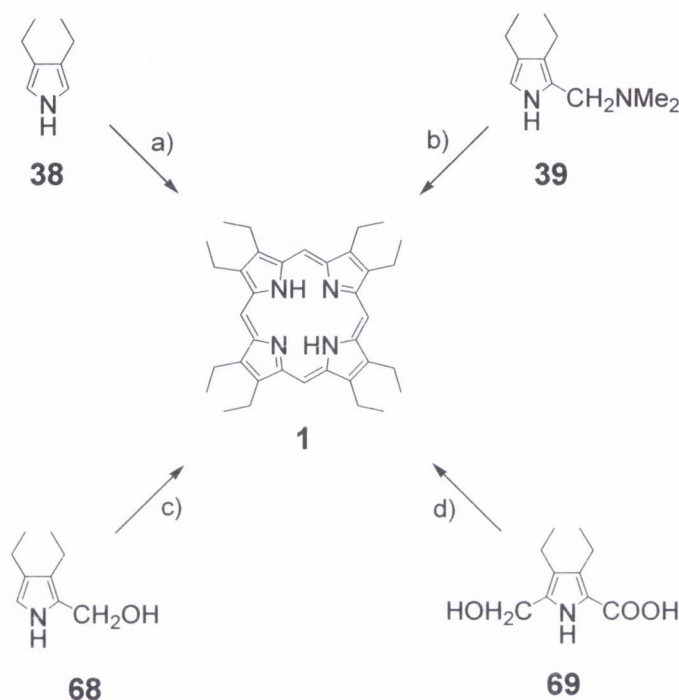


Scheme 1.4.1.1. Porphyrin **67** obtained from the 5,10,15,20-tetra-*tert*-butyl porphyrin **66**; conditions: conc. H₂SO₄, 1-butanol, 90 °C, 15 min.

The polymerisation is usually carried out with on one side functionalized 3,4-substituted diethylpyrroles such as the carbinol **68** and reactive agents that provide the four carbon atoms necessary for the methylene bridges e.g. formaldehyde or dimethoxymethane.

The in scheme 1.4.1.2. shown amino pyrrole **39** was for example obtained with Eschmoser's reagents *via* Mannich reaction from diethylpyrrole **38** and the unstable

carbinol **68** could be prepared from 3,4-diethylpyrrole carboxylate **33** with LiAlH_4 as described in chapter 1.1.^{14,4} The use of diethylpyrrole **38** furthermore required formaldehyde (newer attempts) or formic acid (older attempts) for the reaction, whereas dimethoxymethane could be used for the additionally functionalised carbinol **68**.^{4,6,37}

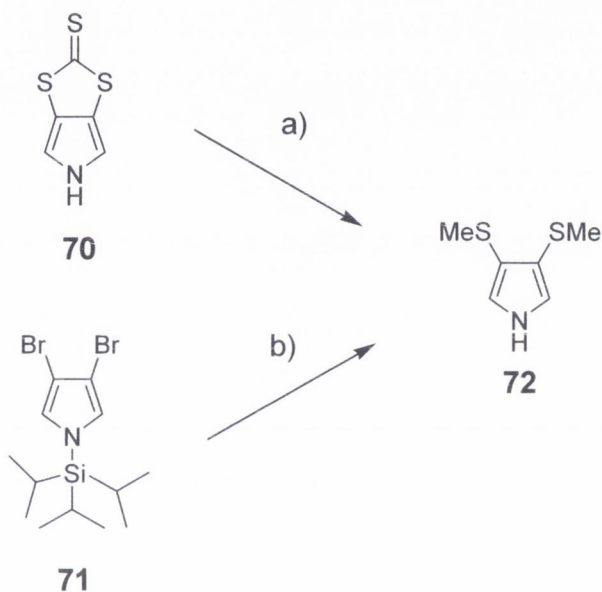


Scheme 1.4.1.2. [4+1] Approach affording OEP **1** by using different pyrroles, a) CH_3COOH or formaldehyde, *p*-TsOH, CH_2Cl_2 , b) ΔT , AcOH, c) H^+ , dimethoxymethane, CH_2Cl_2 and d) ΔT , AcOH, $\text{K}_3\text{Fe}(\text{CN})_6$.¹

The condensation reaction required furthermore an acidic catalyst (*p*-TsOH, TFA or BF_3 etherate) and the methene bridges were, as could be concluded from reactions reported by Syrbu *et al.* in 2004, eventually formed by the substituent in the 5-position of the used pyrrole.¹⁰

Several β -substituted porphyrins with electron donating groups ($-\text{CH}_2\text{CO}_2\text{CH}_3$ and $-\text{CH}_2\text{CH}_2\text{CO}_2\text{CH}_3$) in the β -positions were reported by A. I. Scott *et al.* and some are shown in table 1.4.1.1, while no electron withdrawing substituents could be introduced ($\text{R} = \text{CO}_2\text{Me}$).³⁷

OMTP **75** was also recently investigated by A. Rosa *et al.* and is shown in scheme 1.4.1.3.³⁸ The synthesis of the methylthio precursor **72** was carried out as shown in scheme 1.4.1.4. from the building block **70** in a modified way to K. Seguirra and Y. J. Sakata³⁹ using methyl iodide in the presence of sodium methoxide. Seguirra/Sakata *et al.* used on the other hand the protected bromide **71** and obtained the pyrrole **72** after treatment of **71** with *n*-BuLi and addition of dimethyldisulfide afterwards.

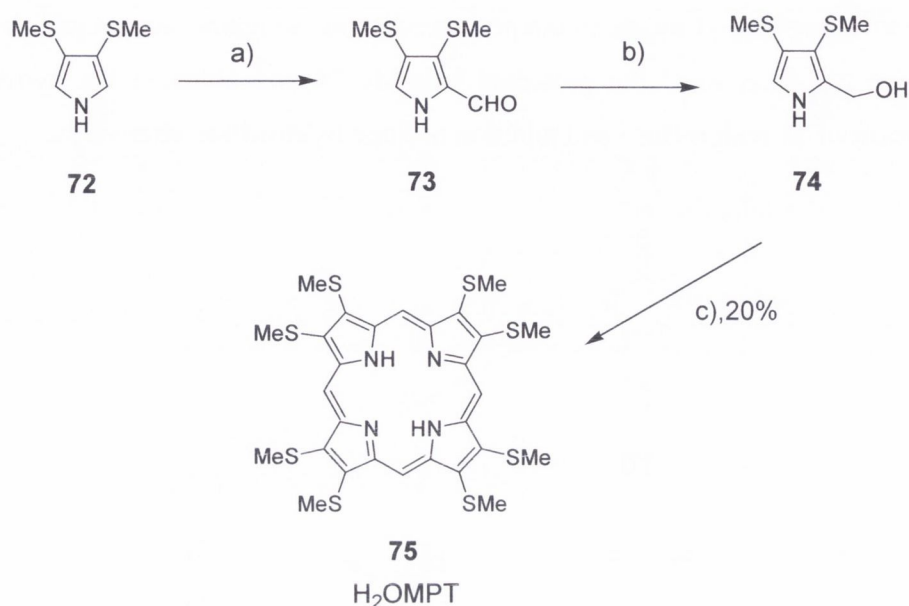


Scheme 1.4.1.3. Synthesis of the methylthio precursor **72** for the preparation of H₂OMTP, a) way by Rosa *et al.*, NaH, MeOH/THF, MeI, 68%,³⁸ b) way by Seguirra/Sakata *et al.*, *n*-BuLi, Me₂S₂.³⁹

For the preparation of H₂OMPT **75**, the precursor **72** was subsequently formylated by Rosa *et al.* yielding the pyrrole **73**, which was then reduced to the reactive carbinol **74**. However, the condensation reaction was carried out with dimethoxymethane under *p*-TsOH catalysis and afforded H₂OMTP **75** in 20% yield in analogy to the synthesis of OEP, which will be presented in the following chapter. The synthesis of the pyrrole thione **70** was furthermore carried out following reported procedures.⁴⁰

Usually, porphyrins with identical β substituents ($R_2=R_3$ such as for OEP **1**) are prepared in higher yield (>50%) than β -mixed porphyrins. The latter are commonly isolated in

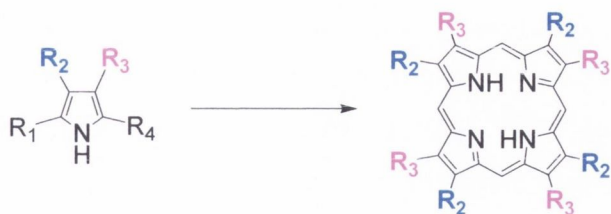
mixtures of four regioisomers due to recombination processes e.g. so-called scrambling of the linear precursors or the porphyrinogen in acidic or basic media.



Scheme 1.4.1.4. Synthesis of H₂OMTP; a) POCl₃, DMF; b) NaBH₄, Et₂O/MeOH; c) CH₂(OMe)₂, *p*-TsOH, dichloromethane.

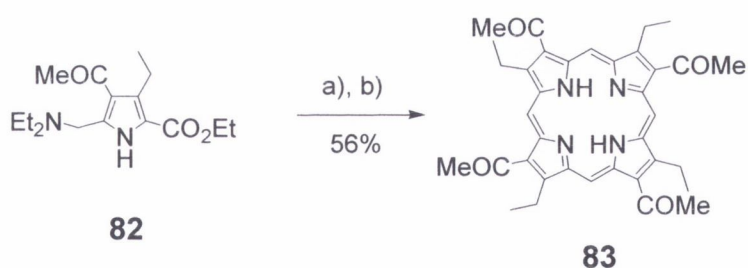
Scrambling was furthermore less observed when the pyrroles used were bulky, when strongly electron withdrawing groups were attached in the future β positions or when acidic or basic media were avoided.⁴¹⁻⁴³ Scott *et al.* prepared for example two novel uro'gen analogues besides other known β -substituted porphyrins investigating the use of TFA (trifluoroacetic acid) and Montmorillonite clay as a catalysts in [4+1] condensation reactions.³⁷ Several porphyrins are displayed in table 1.4.1.1 and highest yields were obtained in CDCl₃ or dichloromethane with TFA. Either the respective carbinol or the diethylamino precursor were used and coproporphyrin I **80** was also obtained by Smith *et al.* in 25% yield and etioporphyrin I **81** in 36% yield with 8% isomer contamination.^{42,44}

On the other hand, a Chinese group reported in 2000 the synthesis of the porphyrin **83** shown in scheme 1.4.1.5 using the dimethylamino precursor **82** after saponification of the ester group.⁴⁵



	R ₂	R ₃	Yield	Porphyrin
76	CH ₂ CO ₂ Me	(CH ₂) ₂ CO ₂ Me	75% of 39% e.g. 29%	uro'gen I
77	CH ₂ CO ₂ Me	(CH ₂) ₃ CO ₂ Me	72% of 60% e.g. 43%	uro'gen analogue
78	(CH ₂) ₂ CO ₂ Me	(CH ₂) ₃ CO ₂ Me	80% of 47% e.g. 37%	uro'gen analogue
79	CO ₂ Me	CH ₂ CO ₂ Me	0%	uro'gen analogue
80	CH ₂ CH ₂ CO ₂ Me	methyl	25%	coproporphyrin I
81	ethyl	methyl	36%	etioporphyrin I

Table 1.4.1.1. Synthesis of porphyrins with mixed β substituents by A. I. Scott *et al.*³⁷ and K. M. Smith *et al.*⁴² For the porphyrins **76-79**³⁷ the yield within the mixtures is displayed besides the overall yield, **80-81**.⁴²

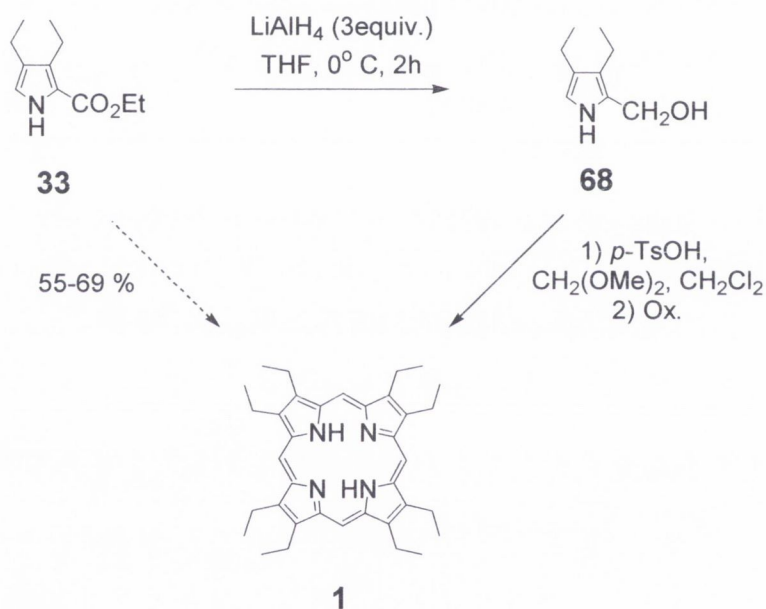


Scheme 1.4.1.5. Condensation reaction yielding the β -mixed porphyrin **83**; a) KOH, H₂O, EtOH, b) AcOH.⁴⁵

1.4.2 Synthesis of OEP

The synthesis of OEP **1** was carried out since 1992 following the general procedure presented by J. Sessler⁶ under variations reported by other groups.^{8,9,14,46} The article published by Sessler summarized the steps towards the diethylpyrrole **38** (compare to

chapter 1.1) and described also the condensation reaction of **38** to OEP **1**, which was achieved in 50% yield using formaldehyde/*p*-TsOH. Instead of the diethylpyrrole **38**, during the PhD, the in scheme 1.4.2.1 shown carbinol **68** was prepared alternatively by reduction of the carboxylate **33** with LiAlH₄ and was used for the condensation reaction in a similar manner (dimethoxymethane/*p*-TsOH).⁸ For the reduction a commercial solution of in THF stabilized LiAlH₄ was used, as no reaction was observed when solid LiAlH₄ was suspended in THF.⁴ In order to obtain a maximum amount of OEP **1**, 1.5 to 2.5 g of the carboxylate **33** were usually treated with LiAlH₄ while two reaction vessels were prepared the same day. The products were combined in the condensation step, which was carried out immediately afterwards, as the carbinol **68** was not stable in an air atmosphere.



Scheme 1.4.2.1. Chosen pathway for the synthesis of OEP **1** from the carboxylate **33** via the unstable carbinol **68**.

The formation of the carbinol **68** was furthermore indicated by its red-brown colour during the evaporation of the solvent or when spilled due to the proceeding degradation. The saponification with LiCl was also described in literature and could have been carried out with the respective methylcarboxylate in 100% yield, circumventing the use of LiAlH₄ and improving the reaction sequence. OEP **1** was furthermore always kept in

solution during the purification due to its low solubility, the solvents were reused and repeated filtration through silica gel with dichloromethane or *n*-hexane/dichloromethane was convenient to afford the pure OEP **1** when precipitation from methanol followed. Approximately 7 g of OEP **1** were prepared in two weeks time from the in the refrigerator stored carboxylate **33**. The carbinol **68** was also recently used by Syrbu *et al.* for reactions producing mixtures of OEPs, but was prepared in an alternative procedure by formylation of 3,4-diethylpyrrole **38** and subsequent reduction with sodium borohydride.¹⁰⁻¹³

1.4.3 Synthesis of dodecasubstituted porphyrins

Several *meso* tetrasubstituted octaethylporphyrins and dodecasubstituted porphyrins have been described in literature and were obtained in [4+1] condensation reactions with different aldehydes.

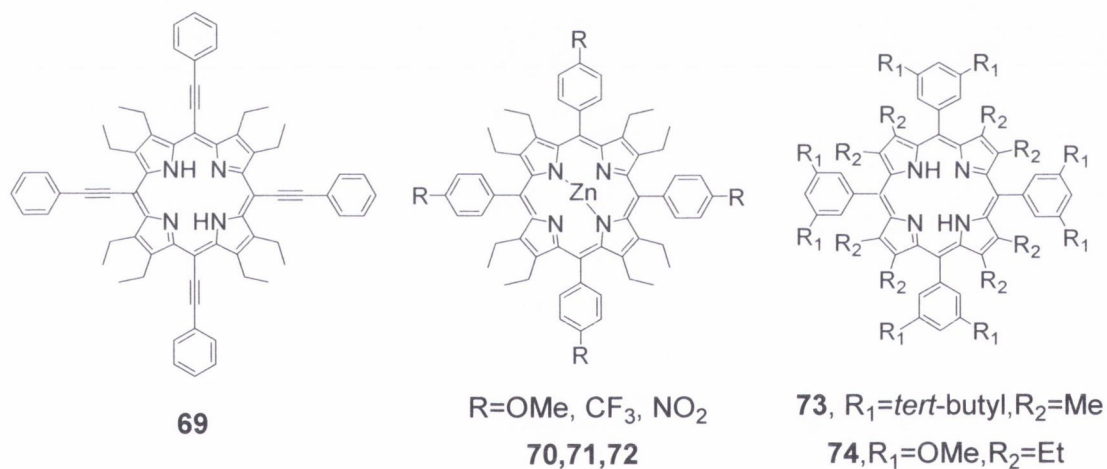


Fig. 1.4.3.1. The porphyrins **69** was prepared from 3,4-diethylpyrrole **38** with the respective aldehyde at -40 °C and BF₃ etherate catalysis in dichloromethane.⁵⁴ The octaethylporphyrins **70-72** were obtained by Nakamura *et al.* and were prepared in dichloromethane under not stated catalyses.⁵⁵ The porphyrin **73** was prepared by Syrbu *et al.* by reacting the respective dimethylpyrrole (not shown) with the corresponding aldehyde using MeOH/HBr¹⁰ and the porphyrin **74** was obtained under F₃CCOOH catalysis in dichloromethane by Barkigia/Renner/Senge/Fajer.⁵⁶

M. O. Senge⁴⁷ reported furthermore that dodecaarylporphyrins were first reported by Tsuchiya *et al.* (e.g. 5,10,15,20-tetrakis(pentafluorophenyl)-2,3,7,8,12,13,17,18-octaphenyl porphyrin)⁴⁸ and were afterwards prepared by Medforth/ Smith *et al.*, by Takeda/Sato and R. Guillard and co-workers.⁴⁹⁻⁵³ The summarized synthesis was carried out before 1998 while afterwards the access to β -substituted porphyrins was facilitated by the use of Barton-Zard precursors as described in chapter 1.1.⁵⁷ Novel dodecasubstituted porphyrins were therefore prepared after 1998 and the in figure 1.4.3.1 shown *meso* tetrasubstituted OEPs were obtained.^{10,54-56} Also the preparation of *meso*-tetrakis(bipyridiniumyl)-octaethylporphyrin was reported *via* electro-synthesis from Zn(II)OEP and pyridine. 100 mg (80%) of the in figure 1.4.3.2 shown OEP **75** were isolated.⁵⁸

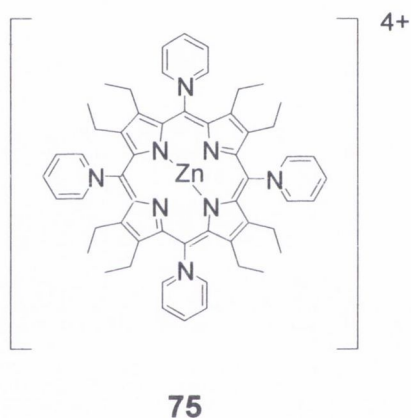


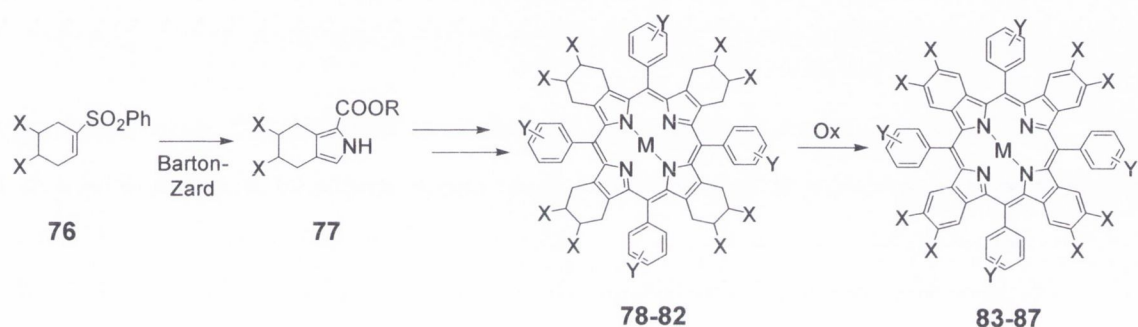
Fig. 1.4.3.2. *Meso*-tetrakis(bipyridiniumyl) OEP **75**.⁵⁸

As described in literature, condensation reactions producing highly substituted porphyrins were furthermore carried out in small flasks and in concentrated reaction mixtures while porphyrins bearing a smaller number of substituents were more solvent demanding.

1.4.4 Synthesis of tetrabenzoporphyrins (TBPs)

In the past years, several articles have been published by S. Vinogradov and co-workers reporting the synthesis of dodecasubstituted and *meso* unsubstituted, Π -extended tetrabenzoporphyrins (TBPs) and tetranaphthoporphyrins (TNPs). TBPs and TNPs are structurally situated between porphyrins and phthalocyanines^{19,59} and the first synthesis

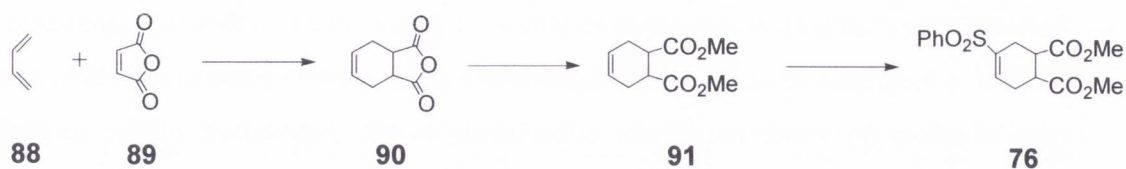
was carried out by J. H. Hellberger in 1937⁶⁰ and by R. P. Linstead in 1940⁶¹ while a lack of general access followed. Novel strategies were only discovered after 1995 by Ono *et al.*^{62,63} T. D. Lash^{64,65} and Cavaleiro and co-workers⁶⁶ due to the newly developed Barton-Zard precursors as described in chapter 1.1 and several TBPs were prepared. In 2003, S. Vinogradov *et al.* presented furthermore an alternative route to Ar₄TBPs, which were obtained by oxidation of the substituents in the β -positions of the respective porphyrin precursors as shown in scheme 1.4.4.1.¹⁹



Scheme 1.4.4.1. Synthesis of TBPs by S. Vinogradov and co-workers with aromatization in the last step, X=CO₂Me, Y=H, 4-CO₂Me, 4-Br, 4-OMe, 4-NO₂.¹⁹

As it can be seen in scheme 1.4.4.1, the Barton-Zard precursor **77** was obtained from 1-phenylsulfonylcyclohexene **76** alternatively to the in scheme 1.1.5 shown activated 1-nitrocyclohexene **44**. The pyrrole **77** was afterwards reduced to the free acid with Perleman catalyst as Pd/C, H₂ failed and the condensation reaction was carried out under Lindsay conditions,³⁵ whereas for some condensation reactions the *tert*-butyl-ester was used and Alder-Longo conditions were applied (“one pot” procedure under reflux with the corresponding aldehyde and *p*-TsOH as a catalyst).³⁴ Furthermore, the sulfonyl approach was reported to be more flexible than the nitro olefine pathway and the shown 3,4-C-anelated pyrrole represented an alternative to the by Ono used “masked” isoindoles,^{62,63,67} which afforded TBPs after condensation and retro Diels-Alder extrusion of ethylene. The vinyl sulfone **76** was furthermore obtained from dimethyl tetrahydrophthalat **91**, which was built from butadiene **88** and maleic anhydride **89**, treated with PhSCl, oxidized and freed from HCl by elimination process as shown in scheme 1.4.4.2.¹⁹ However, the pathway chosen by Cavaleiro and co-workers was similar, while the accessibility of the precursors was limited. β -Tetra-

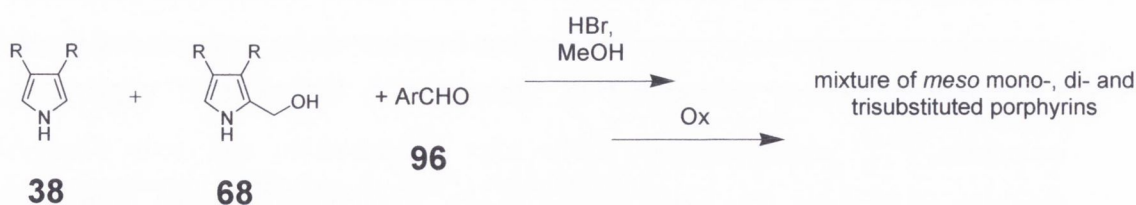
cyclohexenoporphyrins were obtained by Cavaleiro *et al.* and could be transformed into the fully conjugated TBPs by elimination of the attached sulfonyl groups.⁶⁶



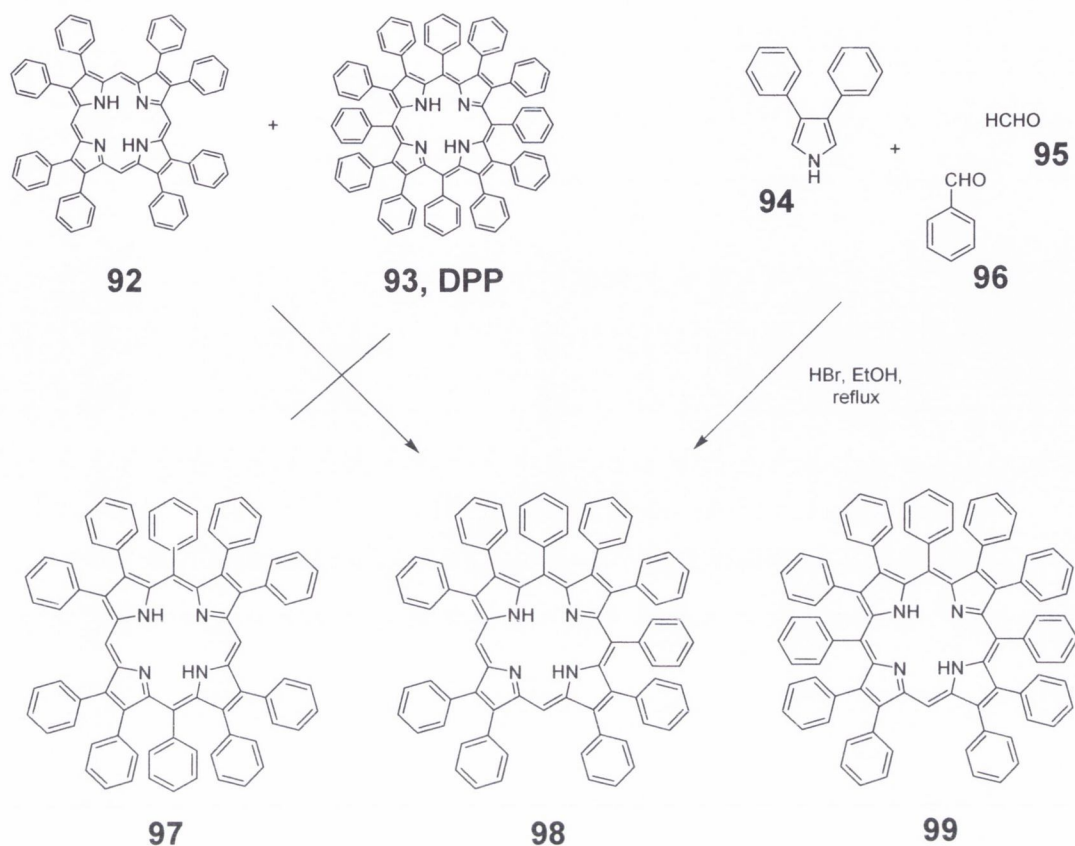
Scheme 1.4.4.2. Synthesis of the vinyl sulfone **76**.¹⁹

1.4.5 Series of porphyrins

A series of porphyrins bearing phenyl substituents in the β and *meso* positions was prepared in 1994 by J. Takeda and M. Sato and is displayed in scheme 1.4.5.2. The condensation reaction was carried out with benz- and formaldehyde (**96** and **95**) in a one pot procedure and a mixture of the shown *meso* di- (5,10 and 5,15), tri- and the tetrasubstituted porphyrin was obtained with an overall yield of 44%.⁶⁸ The *meso* monosubstituted porphyrin was not isolated, while also a scrambling strategy was attempted but failed, as the porphyrins used couldn't be cleaved with acid or base. In 2004, novel series of OEPs and OMPs (octamethylporphyrins) were reported by Syrbu and co-workers by the use of diethylpyrrole **38** and the carbinol **68** in a mixed-condensation reaction as shown in scheme 1.4.5.1.¹⁰ The OMPs and OEPs were obtained in good yield and could be isolated in a gram scale after separation. The UV/vis and ¹H NMR data was displayed and will be discussed in chapter 3 and 5 relative to the prepared OEPs. Furthermore, also OETPP **244** was obtained from 3,4-diethylpyrrole **38** and benzaldehyde **96** and was characterized as described in chapter 3.



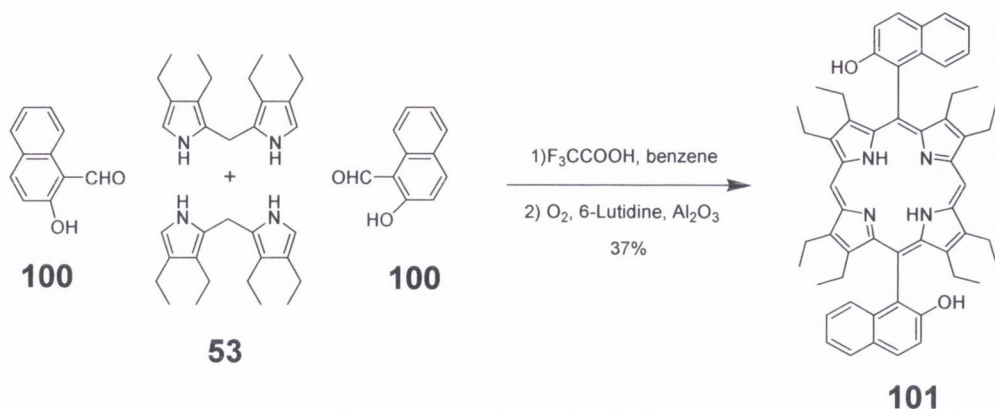
Scheme 1.4.5.1. Mixed condensation performed Syrbu *et al.*; example with R=ethyl and **96**=benzaldehyde.¹⁰



Scheme 1.4.5.2. Synthesis of *meso* substituted octaphenylporphyrins carried out by Takeda *et al.*⁶⁸

1.4.6 [2+2] McDonald condensation

Octa- β -substituted porphyrins such as OEP with additional *meso* substituents could be obtained in the past from the respective dipyrromethanes (compare to chapter 1.2) and aldehydes in a [2+2] McDonald condensation. *Meso* mono- (A-type), 5,10-di- (A_2 - and AB-type) and tetrasubstituted (A_2B_2 -type) porphyrins were isolated as shown in scheme 1.4.6.1., 1.4.6.2. and 1.4.6.3. and figure 1.4.6.1. The OEP **101**, was the earliest reported, e.g. in 1986 and 1988 and was obtained in a mixture with other porphyrins or as a single compound.^{15,69} It was followed by the OEP **103** shown in scheme 1.4.6.2, which could be prepared in 48% yield by Tang and Verkade in 1994.⁸ In the same year, also the *meso* 5,15-AB disubstituted OEP **106** was isolated by Maruyama *et al.* by the use of the respective *meso* substituted dipyrromethanes **104** and **105** as shown in scheme 1.4.6.3.⁷⁰ M. O. Senge reported furthermore in the porphyrin handbook⁴⁷ the synthesis of the β -methyl, *meso* A_2B_2 -substituted porphyrins **112–114**, carried out by Banfi *et al.*⁷¹ in 1996.



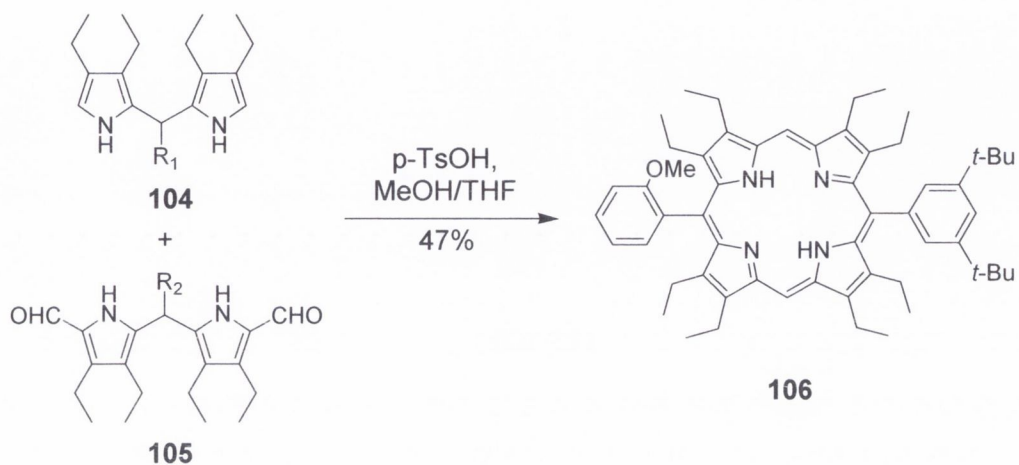
Scheme 1.4.6.1. 5,15- A_2 substituted OEP **101** obtained by a [2+2] McDonald condensation with the dipyrromethane **53** and the naphthoaldehyde **100**¹⁵



Scheme 1.4.6.2. By Tang and Verkade prepared 5,15- A_2 -substituted OEP **103**.⁸

The porphyrins were obtained in moderate to good yield (20–50%) and are shown in figure 1.4.6.1. Further synthesis was also carried out in 2001 by Syrbu *et al.* and β substituted porphyrins with *meso* 5,15-substituents such as hexyl, phenyl, methoxyphenyl and nitrophenyl were obtained (not shown).⁷² The influence of the β -substituent was studied by Syrbu *et al.* and a variety of dipyrromethanes and aldehydes were used. Several *meso* monosubstituted etioporphyrins were also isolated by Chen *et al.* while a systematic investigation of the reaction with osmium tetroxide in β -position followed.² The *meso* 5-*n*-heptyl, 5-(4-methoxyphenyl) and 5-(3,5-dimethoxyphenyl) porphyrins **123-125** were prepared in 35-40% yield from the respectively substituted

dipyrromethanes **116-118** and the dipyrromethane **122** as shown in scheme 1.4.6.4.² Nocera *et al.* obtained furthermore in a similar manner, the *meso* 4-bromophenyl substituted etioporphyrin **379**, shown on page 222, in 51%.⁷³



Scheme 1.4.6.3. Synthesis of the 5,15-AB-substituted OEP **106**, $R_1=2$ -methoxyphenyl, $R_2=3,5$ -di-*tert*-butylphenyl.⁷⁰

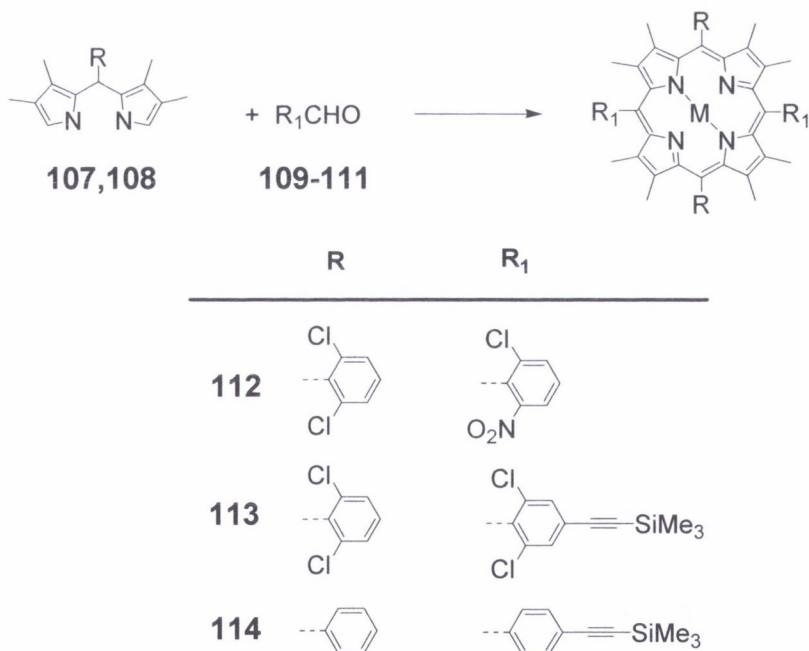
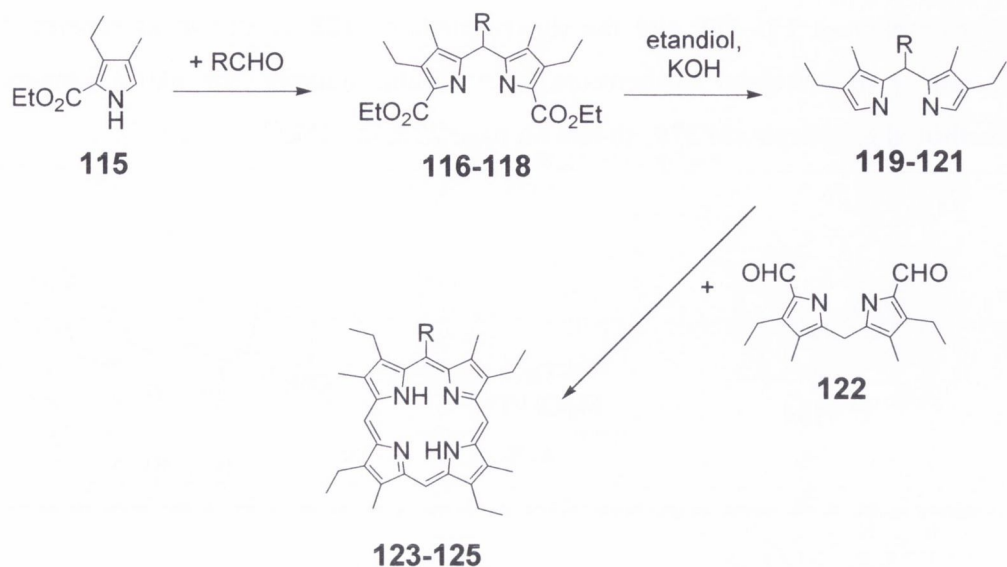
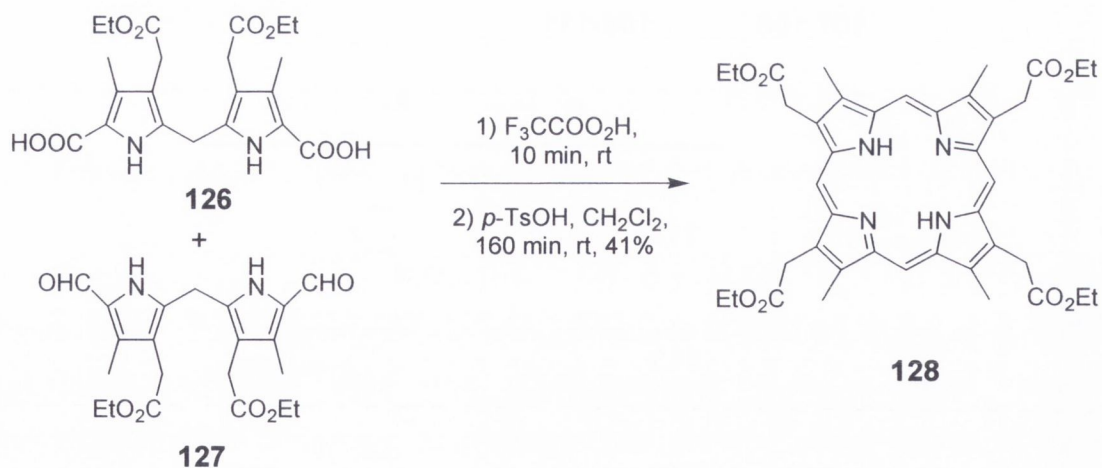


Figure 1.4.6.1. Synthesis of dodecasubstituted octamethylporphyrins carried out by Banfi and co-workers, conditions: BF_3 etherate/dichloromethane.⁷¹



Scheme 1.4.6.4. [2+2] McDonald condensation yielding the *meso* monosubstituted etioporphyrins, R=*n*-heptyl, 4-methoxyphenyl and 3,5-dimethoxyphenyl.²

A single *meso* unsubstituted, β -AB substituted porphyrin, which is similar to the porphyrin **83** shown in chapter 1.4.1, was also obtained in 2002 and is displayed in scheme 1.4.6.5.²²



Scheme 1.4.6.5. Preparation of the porphyrin **128**.²²

1.5 Synthesis of dodecasubstituted porphyrins *via* bromination reactions

Zhou *et al.* presented in 1995/96 the synthesis of β substituted porphyrins *via* bromination and subsequent coupling reactions using Zn(II)TMP **129** (5,10,15,20-tetrakis(2,4,6-trimethylphenyl)porphyrinato zinc(II)), shown in figure 1.5.1., as starting material.⁷⁴ Zn(II)TMP **129** was brominated with NBS in the β positions in 58% yield, demetallated in 95% yield (not shown) and coupled with boronic acids to afford the porphyrins **135-141** shown in table 1.5.1 in high yield (45–88%).⁷⁵⁻⁷⁹

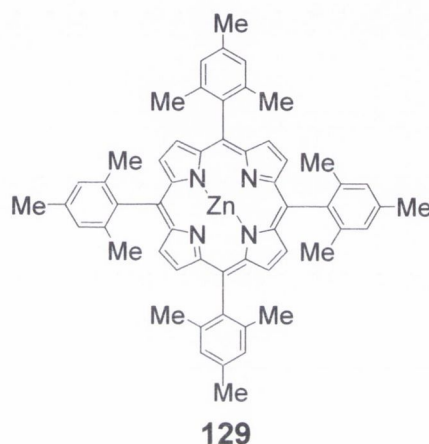
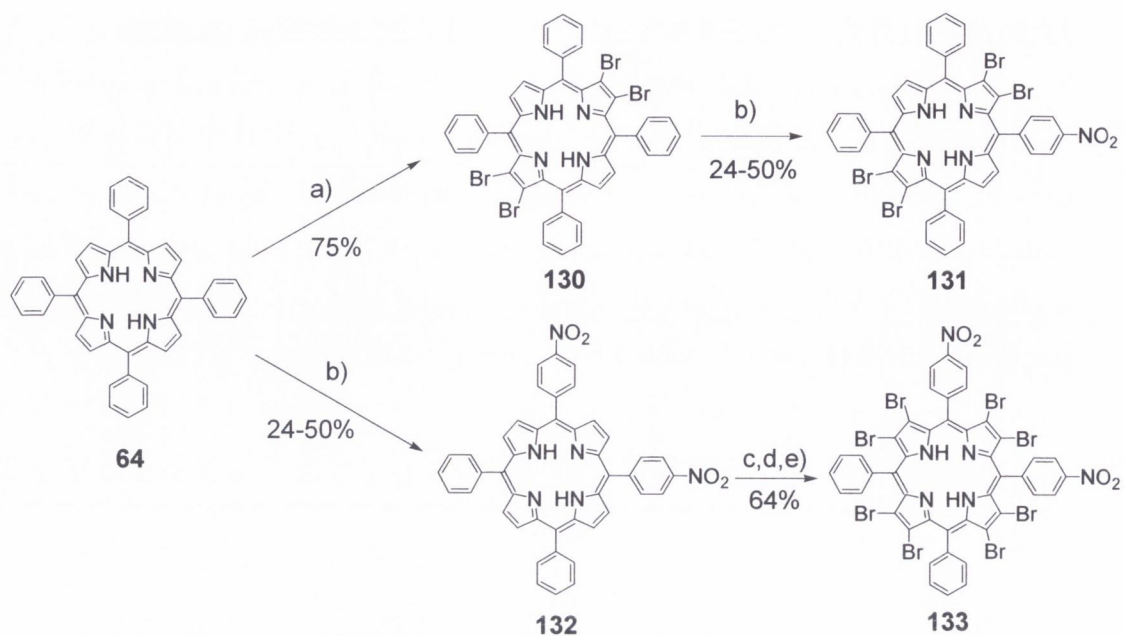


Fig. 1.5.1. Zn(II)TMP⁷⁴

The bromination of free base TMP afforded furthermore pseudo *trans* tetra- β brominated TMPs (6.7 equiv. of NBS) and mono- β brominated TMP (1.7 equiv. of NBS) in 36–52% yield (not shown) and similar synthesis was carried out by Chen *et al.* in 2006.⁷⁷ TPP **64** and 5,10-bis(4-nitrophenyl)-15,20-diphenylporphyrin **132** were brominated as shown in scheme 1.5.2 and the obtained porphyrin **130** was subsequently nitrated to **131** and coupled with MeB(OH)₂ (K₂CO₃/Pd(Ph₃P)₄/toluene, 95–105 °C, 3d) or PhB(OH)₂ (Na₂CO₃/Pd(PPh₃)₄/DMF, 12 h) to produce the respective β methylated and phenylated porphyrins in 87% and 75% yield (not shown).⁸⁰ The *meso* A₂-B₂ substituted octabromoporphyrin **133** was on the other hand coupled with phenylboronic acid only (K₂CO₃/Pd(Ph₃P)₄/toluene, 95–105 °C, 7d) and the respective β phenyl porphyrin was obtained in 55% yield (not shown).^{80,81} Ring opening was also observed elsewhere in literature with NBS and afforded novel β brominated biladienes (not shown), which could be stabilized by zinc insertion for a certain time.⁷⁷



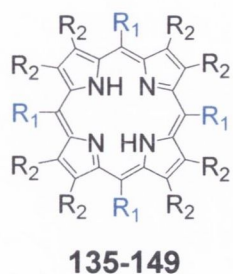
Scheme 1.5.2. Bromination carried out by Chen *et al.*,⁸¹ a) NBS, CH₃Cl, reflux, 3h,⁸² b) fuming HNO₃, 3h, 5 °C,⁸³ c) Cu(OAc)₂, CHCl₃, rt, 1h, d) Br₂, CHCl₃, rt, 1 day, e) HClO₄, CHCl₃, rt, 12h.



Scheme 1.5.1. Suzuki coupling reaction yielding dodecaphenylporphyrin **93** (DDP); PhB(OH)₂ (20 equiv.), K₂CO₃ (40 equiv.), Pd (PPh₃)₄ (15 mol%), toluene, 7 days, 90 °C.⁸⁴

However, in 1999 the product palette was enlarged by Medforth/Smith and Shelnutt and also ¹H NMR temperature experiments were carried out.⁸⁴ TMP **129** and 5,10,15,20-tetrakis(2,3,4,5,6-pentafluorophenyl)porphyrin (not shown) were brominated and coupled with phenyl- and 2-methoxyphenyl boronic acids. The corresponding

porphyrins **142–144** were obtained in 27–52% yield while the reaction carried out with β -brominated TPP **134** and 2,4,6-trimethylphenyl boronic acid didn't proceed (0%).



	R ₁	R ₂	Yield [1/%]
135	2,4,6-trimethylphenyl	phenyl	53
136	2,4,6-trimethylphenyl	4-tolyl	56
137	2,4,6-trimethylphenyl	4-trifluoromethylphenyl	78
138	2,4,6-trimethylphenyl	4-methoxyphenyl	50
139	2,4,6-trimethylphenyl	4-chlorophenyl	88
140	2,4,6-trimethylphenyl	4- <i>tert</i> -butylphenyl	45
141	2,4,6-trimethylphenyl	methyl	74
142	2,4,6-trimethylphenyl	2-methoxyphenyl	27
143	2,4,6-trimethylphenyl	phenyl	31
-	phenyl	2,4,6-trimethylphenyl	0
144	2,3,4,5,6-pentafluorophenyl	phenyl	52
145	phenyl	3-methoxyphenyl	43
146	phenyl	2-methoxyphenyl	14
147	phenyl	4-chlorophenyl	48
148	phenyl	3,5-chlorophenyl	30
149	phenyl	3-thienyl	19

Table 1.5.1. Dodecasubstituted porphyrins obtained after β bromination and Suzuki-type coupling as reported in literature; **135-141**,⁷⁴ **142-149**.⁸⁴

On the other hand, as shown in scheme 1.5.1 and summarized in table 1.5.1, dodecaphenylporphyrin **93** (DPP) was obtained in 58% yield and the TPPs **145–149** in

14–48% yield.^{34,35,84} The synthetic access was difficult when heterocycles such as 2-thienyl, 2-furanyl and 4-pyridinyl had to be introduced (0–19% yield) and when *ortho* substituted 2-methoxyphenyl boronic acid was used (14–27% yield). In all other cases, electronic and steric effects were reported to be moderate and poor yields could be explained as due to competitive side-reactions such as deboronation induced by traces of water.

REFERENCES

- 1) K. M. Smith. In *The Porphyrin Handbook*; K. M. Kadish, K. M. Smith, R. Guilard, Eds. Academic Press: San Diego, CA, 1999; Vol. 1, pp. 1.
- 2) Y. Chen, C. J. Medforth, K. M. Smith, J. Alderfer, T. J. Dougherty, R. K. Pandey *J. Org. Chem.* **2001**, *66*, 3930.
- 3) www.organic-chemistry.org
- 4) H. Kawamura, M. Bougauchi, K. Maruyama, N. Ono *Tetrahedron* **1990**, *46*, 21, 7483
- 5) D. H. R. Barton, J. Kervagore, S. Zard *Tetrahedron* **1990**, *46*, 7587
- 6) J. L. Sessler *Organic Synthesis* **1992**, *70*, 68.
- 7) L. M. Weinstock, G. D. Hartman *Organic Synthesis* **1988**, *VI*, 620.
- 8) J. Tang, J. G. Verkade *J. Org. Chem.* **1994**, *59*, 7793.
- 9) U.S. Patent, 5367084, 22 Nov 1994.
- 10) A. Syrbu, L. Lyobumova, A. S. Semeikin *Chem. Heterocyclic Comp.* **2004**, *40*, 10, 1262.
- 11) K. Ichimura, S. Ichikawa, K. Imamura *Bull. Chem. Soc. Jpn.* **1976**, *4*, 1157.
- 12) H. W. Whitlock, R. J. Hanauer *J. Org. Chem.* **1968**, *33*, 2169..
- 13) A. W. Johnson, I. T. Kay *J. Chem. Soc.* **1965**, 1620.
- 14) U.S. Patent, 5464741, 07 Nov 1995.
- 15) H. Ogoshi, K. Saita, K.-i. Sakurai, T. Watanabe, H. Toi, Y. Aoyama, Y. Okamoto *Tetrahedron Lett.* **1986**, *27*, 52, 6365.
- 16) M. J. Gunter, L. N. Mander *J. Org. Chem.* **1981**, *46*, 4793.
- 17) R. Young, C. J. Chang *J. Am. Chem. Soc.* **1985**, *107*, 898.
- 18) N. Ono, K. Maruyama *Bull. Chem. Soc. Jpn.* **1988**, *61*, 4470.
- 19) O. S. Finikova, A. V. Cheprakov, S. A. Vinogradov *J. Org. Chem.* **2005**, *70*, 9562.
- 20) H. Fischer, W. Klendauer *Liebigs Ann. Chem.* **1941**, *547*, 123.
- 21) H. Fischer, H. Kellermann; F. Balaz *Chem. Ber.* **1942**, *75*, 1178.
- 22) M. M. Koskelin, A. E. Soini, N. J. Meltola, G. V. Ponomarev *J. Porphyrins Phthalocyanines* **2002**, *6*, 7&8, 533.
- 23) A. S. Semeikin, N. G. Kuz'min, O. I. Koifman *Izv. Vyssh. Uchbn. Zaved. Khim. Tekhnol.* **1988**, *31*, 39.
- 24) J. B. Paine, R. B. Woodward *J. Org. Chem.* **1976**, *41*, 2826.

- 25) M. O. Senge *Heterocycles* **2005**, *65*, 4, 797.
- 26) H. Xie, D. A. Lee, M. O. Senge, K. M. Smith *J. Chem. Soc. Chem. Commun.* 1994, 791.
- 27) H. Xie, D. A. Lee, D. M. Wallace, M. O. Senge, K. M. Smith *J. Org. Chem.* 1996, *61*, 8508.
- 28) H. K. Hombrecher, G. Horter, C. Arp *Tetrahedron* 1992, *48*, 9451.
- 29) R. Paolesse, R. K. Pandey, T. P. Forsyth, L. Jaquinod, D. J. Nurco, M. O. Senge, S. Licoccia, T. Boschi, K. M. Smith *J. Am. Chem. Soc.* **1996**, *118*, 3869.
- 30) C. J. Medforth, M. O. Senge, T. P. Forsyth, J. D. Hobbs, J. A. Shelnut, K. M. Smith *Inorg. Chem.* **1994**, *33*, 3865.
- 31) M. O. Senge, C. J. Medforth, T. P. Forsyth, D. A. Lee, M. M. Olmstead, W. Jentzen, R. K. Pandey, J. A. Shelnut, K. M. Smith *Inorg. Chem.* **1997**, *36*, 1149.
- 32) T. Tanaka, K. Endo, Y. Aoyama *Bull. Chem. Soc. Jpn.* **2001**, *74*, 5, 907.
- 33) N. S. Dudkina, E. M. Kuvshinova, A. S. Semeikin *Zh. Obshch. Khim.* **1998**, *68*, 2042.
- 34) A. D. Alder, F. R. Longo, J. D. Finarelli, J. Goldmacher, J. Assour, L. Korsakoff *J. Org. Chem.* **1967**, *32*, 476.
- 35) J. S. Lindsey, I. C. Schreiman, H. C. Hsu, P. C. Kearney, A. M. Marguerettaz *J. Org. Chem.* **1987**, *52*, 827.
- 36) S. Neya, N. Funasaki *Tetrahedron Lett.* **2002**, *43*, 1057.
- 37) C. Pichon-Santander, A. I. Scott *Tetrahedron* **2002**, *43*, 6967.
- 38) A. Rosa, G. Ricciardi, E. J. Baerends, M. Zimin, M. A. J. Rodgers *Inorg. Chem.* **2005**, *44*, 19, 6609.
- 39) K. Sugaira, K. Ushiroda, M. T. Johnson, J. S. Miller, Y. J. Sakata *Mater. Chem.* **2000**, *10*, 2507.
- 40) J. O. Jepperson, K. Takimiya, F. Jensen, T. Brimert, K. Nielsen, N. Throup, J. Becher *J. Org. Chem.* **2000**, *65*, 5794.
- 41) M. G. Vicente, K. M. Smith *Curr. Org. Chem.* **2000**, *4*, 139.
- 42) L. T. Nguyen, M. O. Senge, K. M. Smith *J. Org. Chem.* **1996**, *61*, 998.
- 43) B. J. Littler, Y. Ciringh, J. S. J. Lindsey *J. Org. Chem.* **1999**, *64*, 2864.
- 44) C. Jeandon, H. Callot *J. Bull. Soc. Chim. Fr.* **1993**, *130*, 625.
- 45) Authors not available *Huaxue Shijie/Chem. World* **2000**, *41*, 1, 27.
- 46) N. Ono, K. Maruyama *Chem. Lett.* **1988**, *9*, 1511.

- 47) M. O. Senge (2000). In: The porphyrin Handbook, Vol. 10, p. 264. Ed.: K.M. Kadish; R. Guillard; K. M. Smith. San Diego: Academic Press.
- 48) S. Tsuchiya *Chem. Phys. Lett.* **1990**, 169, 608.
- 49) C. J. Medforth, K. M. Smith *Tetrahedron Lett.* **1990**, 31, 5583.
- 50) J. Takeda, T. Ohya, M. Sato *Chem. Phys. Lett.* **1991**, 183, 384.
- 51) J. Takeda, M. Sato *Chem. Pharm. Bull.* **1994**, 42, 1005.
- 52) K. Perie, J.-M. Barbe, P. Cocolios; R. Guillard *Bull. Soc. Chim. Fr.* **1996**, 133, 697.
- 53) R. Guillard, K. Perie, J.-M. Barbe, D. J. Nurco, K.M. Smith, E. Van Caemelbecke; K.M. Kadish *Inorg. Chem.* **1998**, 37, 973.
- 54) Z. Shen, H. Uno, Y. Shimizu, N. Ono *Org. Biomol. Chem.* **2004**, 2, 3442.
- 55) A. Hoshino, Y. Ohgo, M. Nakamura *Tetrahedron Lett.* **2005**, 46, 4961.
- 56) K. M. Barkigia, M. W. Renner, M. O. Senge, J. Fajer *Heterocycles* **2004**, 63, 3, 505.
- 57) N. Ono, H. Miyagawa, T. Ueta, H. Tani *J. Chem. Soc. Perkin Trans. I* **1998**; 1595.
- 58) A. Giraudeau, S. Lobstein, L. Ruhlmann, D. Melamed, K. M. Barkigia, J. Fajer *J. Porphyrins Pthalocyanines* **2001**, 5, 793.
- 59) O. S. Finikova, S. E. Aleshchenkov, R. P. Brinas, A. V. Cheprakov, P. J. Carroll, S. A. Vinogradov *J. Org. Chem.* **2005**, 70, 4617.
- 60) J. A. Hellberger *Justus Liebigs Ann. Chem.* **1937**, 529, 205.
- 61) P. A. Barret, R. P. Linstead, F. G. Rundall, G. A. P. Tuey *J. Chem. Soc.* **1940**, 1079.
- 62) N. Ono, H. Hironaga, K. Ono; S. Kaneko, T. Murashima, T. Ueda, C. Takamura, T. Ogawa *J. Chem. Soc. Perkin Trans. I*, **1996**, 417.
- 63) H. Uno, N. Ono *J. Synth. Org. Chem. Jpn.* **2002**, 60, 81.
- 64) T. D. Lash *J. Porphyrins Phthalocyanines* **2001**, 5, 267.
- 65) J. D. Spence, T. D. Lash *J. Org. Chem.* **2000**, 65, 1530.
- 66) M. G. H. Vincente, A. C. Tome, A. Walter, J. A. S. Cavaleiro *Tetrahedron Lett.* **1997**, 65, 8020.
- 67) D. Barton, S. Zard *J. Chem. Soc. Chem. Comm.* **1985**, 1098.
- 68) J. Takeda, M. Sato *Chem. Lett.* **1994**, 2233.
- 69) T. Tanaka, K. Endo, Y. Aoyama *Tetrahedron Lett.* **1988**, 29, 41, 5271.
- 70) H. Tamiaki, A. Kiyomori, K. Maruyama *Bull. Chem. Soc. Jpn.* 1994, 67, 2478.
- 71) S. Banfi, A. Manfredi, G. Pozzi, S. Quici, A. Trebicka *Gazz. Chem. Ital.* **1996**, 126, 179.

- 72) S. A. Syrbu, T.V. Lyubimova, A.S. Semeikin *Russ. J. Gen. Chem.* **2001**, *71*, *10*, 1656.
- 73) Z.-H. Loh, S. E. Miller, J. Chang, S. D. Carpenter, D. G. Nocera *J. Phys. Chem. A* **2002**, *106*, 11700.
- 74) X. Zhou, M. K. Tse, T. S. M. Wan, K. S. Chan *J. Org. Chem.* **1996**, *61*, 3590.
- 75) C.-J Liu, W.-Y. Yu, S.-M. Peng, T. C. W. Mak, C.-M. Che *Chem. Soc. Dalton Trans.* **1998**, 1805.
- 76) K. S. Chan, X. Zhou, M. T. Au, C. Y. Tam *Tetrahedron* **1995**, *51*, 3129.
- 77) C. Liu, D.-M. Shen, Q.-Y. Chen *Chem. Commun.* **2006**, 770.
- 78) K. S. Chan, X. Zhou, B.-S. Luo, T. C. W. J. Mak *J. Chem. Soc. Chem. Commun.* **1994**, 271.
- 79) K. S. Chan, X. Zhou, M. T. Au, C. Y. Tam *Tetrahedron* **1995**, *51*, 3129.
- 80) N. Miyaura, A. Suzuki *Chem. Rev.* **1995**, *95*, 2457.
- 81) B. Chen, W. Song, L. Aixiao, L. Feng, Z. Xiang, C. Xiaoping, H. Zhike *Tetrahedron* **2006**, *62*, 5487.
- 82) P. Hoffman, A. Robert, B. Meunier *Bull. Soc. Chim. Fr.* **1992**, *129*, 85.
- 83) W. J. Kruper, T. A. Chamberlain, M. Kochanny *J. Org. Chem.* **1989**, *54*, 2753.
- 84) C. M. Muzzi, C. J. Medforth, L. Voss, M. Cancilla, C. Lebrilla, J.-G. Ma, J. A. Shelnutt, K. M. Smith *Tetrahedron Lett.* **1999**, *40*, 6159.

2. Synthesis of *meso* substituted OEPs, palladium (II) and platinum (II) insertion

2.1 Synthesis of *meso* substituted octaalkylporphyrins reported in literature

In this section the synthesis of *meso* mono-, di-, tri- and tetrasubstituted OEPs reported in literature will be summarized. The number of existing derivatives is small and a few compounds were already discussed in chapter 1. Condensation methods will be therefore only briefly mentioned, while the synthesis of *meso* substituted octaalkylporphyrins by the means of electrophilic substitution reactions, such as formylation and nitration, Wittig reaction, and by nucleophilic substitution reactions will be of major interest. Additionally, dimerization products will be shortly introduced, as they were considered as equivalents to *meso* monosubstituted OEPs, whereas the synthesis carried out during the PhD will follow in chapter 2.2.

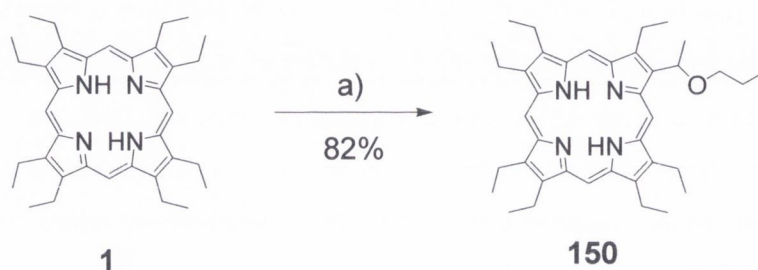
2.1.1 *Meso* monosubstituted OEPs

In the porphyrin handbook several *meso* monosubstituted octaethyl- and octamethylporphyrins as well as dimers and dimer sandwich structures as special cases of *meso* monosubstitution have been described by M. O. Senge and were added to the presented data.¹ Dimers will be discussed in the following subchapter and *via* nucleophilic substitution reaction obtained OEPs will be described in chapter 2.2. Reactions affording *meso* monosubstituted octaalkylporphyrins will be in the following section sorted in reaction categories. For condensation methods see additionally the previous chapter. Also, octaalkylsubstituted porphyrins bearing a *p*-benzoquinone-2-yl,² N-succinimidyl,³ 8-((bis-2-picolino)amine-methyl)naphthyl⁴ and 8-((bis-2-picolyl)-amine-methyl)naphthyl⁵ substituent in 5-position were reported by M. O. Senge.¹

2.1.1.1 Halogenation of OEP

Meso bromination is widely used for porphyrins bearing no β substituents and is highly effective as Suzuki-type coupling reactions can be performed afterwards in an easy manner and in good yields. Unfortunately, the bromination of octaethylporphyrin is difficult and couldn't be used so far for its functionalization as the yields are low and as inseparable mixtures were obtained. *Meso* chlorination and bromination were attempted initially by Nencki and Zaleske^{1,6} and were further investigated by Hans Fischer.^{7,8,9}

More recent studies were carried out by Bonnett *et al.* and it was reported that the bromination proceeded predominantly at the CH₃ groups of the β -ethyl substituents while also dealkylation occurred^{10,11,12} and only small amounts of *meso* monobrominated OEP were isolated by the use of Br₂. On the other hand, the addition of NBS and AIBN resulted in the formation of the in scheme 2.1.1.1 shown ether when propanol was used as a solvent. However, without AIBN, an inseparable mixture of 5,10 and 5,15-dibromo OEP was obtained in low yield.¹³



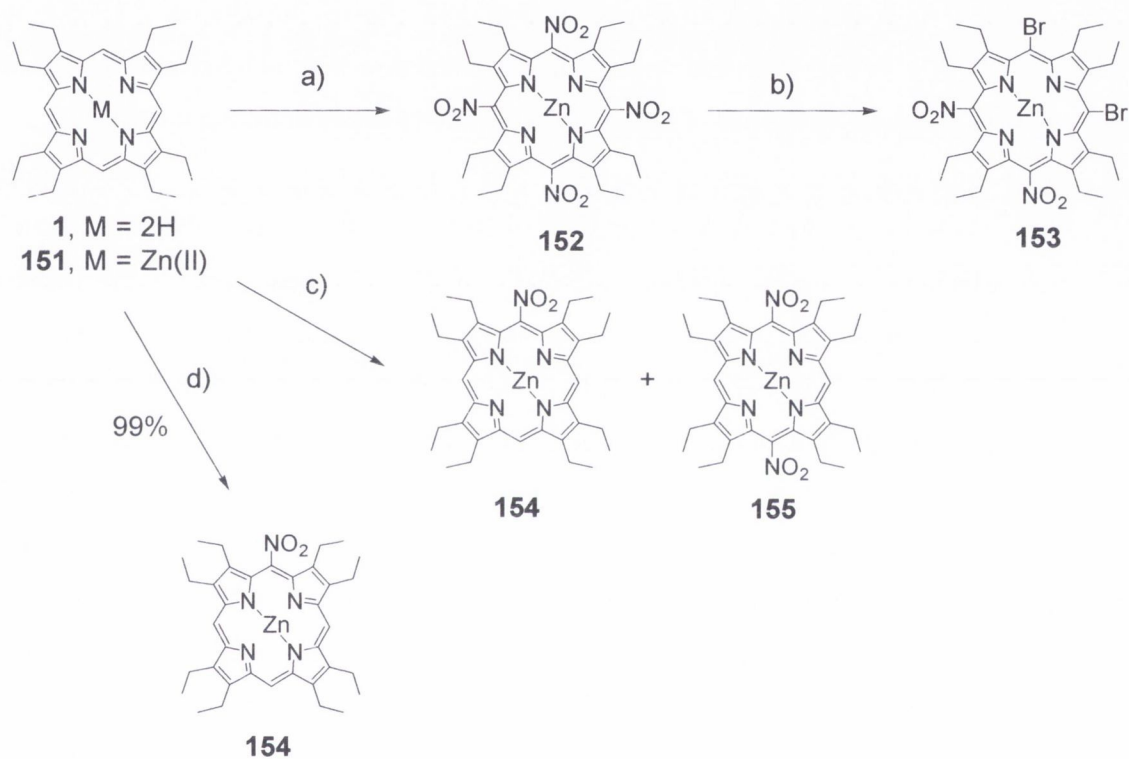
Scheme 2.1.1.1. Attempted bromination of OEP affording the shown ether **150** with a) NBS/AIBN in *n*-propanol/dichloromethane.¹³

Chlorination of OEP, carried out by Bonnett *et al.* produced furthermore 5,15-bischloro OEP in 20% yield and in a mixture with 5-chloro OEP in 25% yield using THF and 0.3% H₂O₂ in 0.5 N HCl (not shown). When the reaction was performed in glacial acetic acid with concentrated HCl and 3% H₂O₂ in 0.5N HCl, 5,10,15,20-tetrakischloro OEP was obtained in 43% yield.^{10,11,12} Fluorination was also attempted the respective *meso* monofluorinated OEP could be isolated in 5% yield (Balz-Schiemann reaction)¹⁴ or in a mixture of *meso* fluorinated OEPs when caesium fluoroxysulfate (FOSO₂OCs) in dioxane was used e.g. the following products were isolated: 5-fluoro OEP in 29% yield, 5,15-bisfluoro OEP in 9% yield and 5,10-bisfluoro OEP in 11% yield.¹⁵ 5,10,15,20-Tetrakisfluoro OEP was also isolated in 20% yield by addition of N-fluoropentachloropyridinium triflate (20% yield).¹⁶

2.1.1.2 Nitration of OEP

Electrophilic substitution reactions introducing formyl and nitro groups were the first reactions reported for OEP and produced the respective *meso* substituted products. Nitration was carried out between 1930 and 1940 by H. Fischer,^{17,18} and afterwards by

R. Bonnett and G. F. Stevenson¹⁰ in the 1960s. During the 1970s furthermore, D. Dolphin and co-workers¹⁹ as well as E. Watanabe *et al.* investigated the nitration of OEP,^{1,20,21} while recent attempts are reported for Zn(II)OEP **151** using AgNO₃ in MeCN/dichloromethane, which led to the formation of 5-nitro Zn(II)OEP **154** in 99% yield after ten hours of stirring at ambient temperature as shown in scheme 2.1.1.2.1.²² Demetallation furthermore yielded in the respective free base 5-nitro OEP (not shown) in 80% yield with HCL.²²



Scheme 2.1.1.2.1. A), b) Nitration and Zn(II) insertion of H₂OEP **1**²⁰ and subsequent substitution with HBr²⁴, c) electrolytic pathway affording 5-nitro Zn(II)OEP **154** and 5,15-bisnitro Zn(II)OEP **155**,²³ d) *meso* mononitration carried out with AgNO₃ in MeCN/dichloromethane.²²

In the 1970s Bonnett¹⁰ reported also the step wise nitration with N₂O₄ in dichloromethane, which produced the whole series of *meso* nitrated OEPs while Watanabe²⁰ obtained *meso* 5,10,15,20-tetrakisnitro Zn(II)OEP from free base OEP **1** with zinc insertion during the nitration. Also an electrolytic pathway, yielding in the formation of 5-nitro and 5,15-bisnitro Zn(II)OEP **154** and **155**, was reported by Wu and

Leung and is displayed in scheme 2.1.1.2.1.²³ However, nitration of OEP is interesting as the nitro groups can be exchanged afterwards by bromo or chloro groups using HCl or HBr as shown by D. Dolphin and co-workers and allowing subsequent coupling reactions (scheme 2.1.1.2.1 and not shown).²⁴

2.1.1.3 Amines of OEP

The reduction of 5-nitro OEP (not shown) to the amine was achieved in phenol by adding sodium phenolat and was accomplished in 29% yield. Furthermore, also OEP and the *meso* monosubstituted OEP phenoether **187** shown in scheme 2.1.1.6.1 were obtained in 15% and 9% yield during the same reaction step as by-products.²¹ Another pathway consisted in the use of Raney nickel in EtOH with 5-nitro Pd(II)OEP.²¹

5-N-Aryl amino and 5-N-aryl amido OEPs (aryl=phenyl, 1-pyrenyl and 3-fluoroanthenyl) have also been prepared by A. Gold *et al.* in 2000.²⁵ In some cases also azaryl chlorins were obtained through oxidative cycloaddition of the substituents to the nearest β position as shown in scheme 2.1.1.3.1. During the cycloaddition, a β ethyl group migrated from its original β position to the neighbouring β position. Similar fused systems e.g. naphthylchlorins were also reported previously (consult references 1-9 in reference 25). However, the initial synthesis of the 5-N-aryl amino and amido OEPs started with procedures for pyridine and imidazole OEPs²⁶ whereas the reactivity could be enhanced with anionic nitrogen species generated from the corresponding N-acetamido precursors by treatment with NaH. Nucleophilic attack of the JI-cation radical of Zn(II)OEP **151** afforded then the in figure 2.1.1.3.1 shown *meso* substituted OEPs **156-158**. Deacylation of the synthesized amido OEPs **156-158** was furthermore not possible and strong conditions such as *n*-BuLi in THF destroyed the macrocycle rapidly. Therefore the trifluoroacetamides were prepared (not shown) using trifluoroacetanilide and N-(3-fluoroanthenyl)trifluoroacetamid and deacylation followed with 20 fold molar excess of sodium methoxide in refluxing THF/methanol resulting in the formation of the corresponding amino complexes together with small amounts of the fused chlorins when the anthenyl OEP **157** was deacylated. Also, subsequent metal removal produced small amounts of the *meso*- β fused chlorin as a by-product.

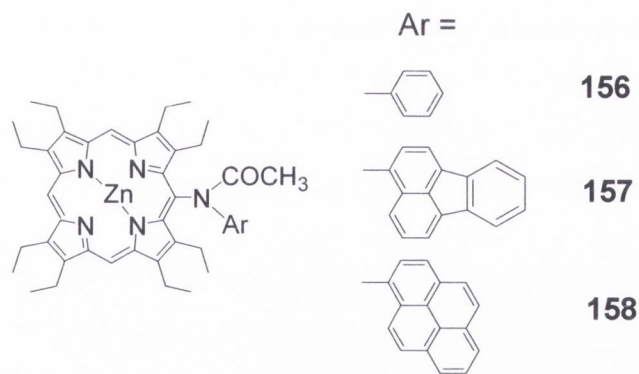
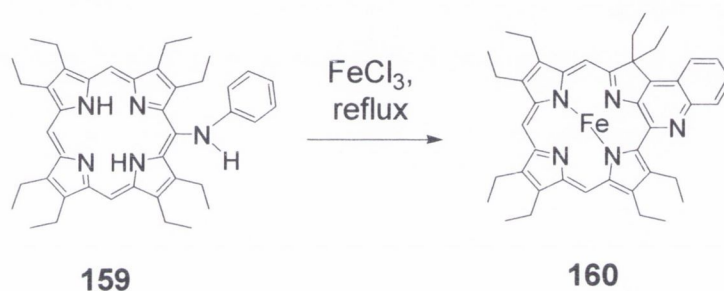


Fig. 2.1.1.3.1. Amido OEPs **156-158** synthesized by A. Gold *et al.* in 2000.²⁵



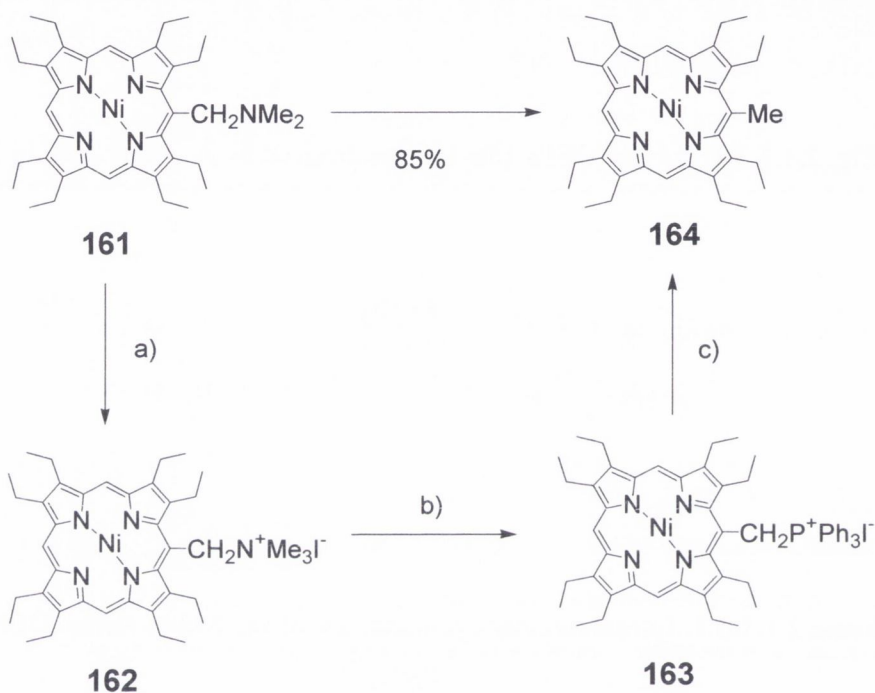
Scheme 2.1.1.3.1. Intramolecular cycloaddition of the N-aryl amino OEP **159** with FeCl₃.²⁵

Furthermore, when the phenyl substituted amine **159** was refluxed for a short time with ferrous chloride (FeCl₃) the fused Fe(III) chlorin **160** was obtained exclusively, while only metal insertion occurred when the temperature was kept at 25 °C.

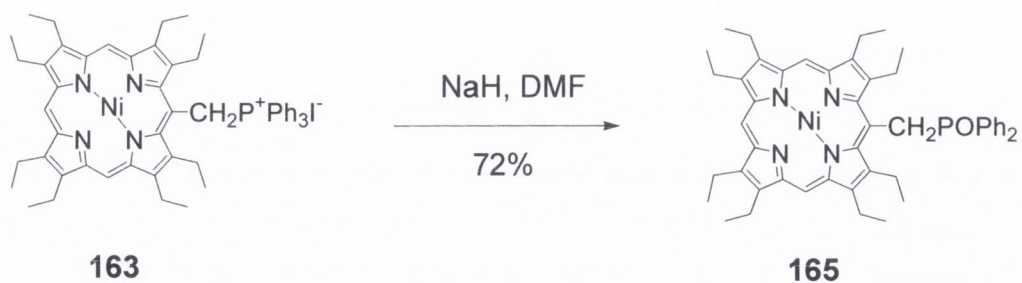
2.1.1.4 5-Methyl OEPs

5-Methyl Ni(II)OEP **164** was obtained in 1996 in 85% yield from 5-dimethylaminomethyl Ni(II)OEP **161** by G. V. Ponomarev and D. P. Arnold.^{27,28} The corresponding article for the preparation of 5-dimethylaminomethyl Ni(II)OEP was unfortunately not available. 5-Dimethylaminomethyl Ni(II)OEP **161** was probably obtained by Mannich reaction with Eschenmoser's reagent. To afford 5-methyl Ni(II) OEP **164**, 5-dimethylaminomethyl Ni(II)OEP **161** was N-methylated with methyl iodide in dichloromethane and the trimethylporphyrinyl ammonium salt was formed *in situ* as shown in scheme 2.1.1.4.1. Trisphenylphosphine was added to result in the formation of

the stable *meso* porphyrinylphosphonium iodide and treatment with methanol in the presence of NEt_3 produced smoothly 5-methyl Ni(II)OEP **164** with an overall yield of 85%. Additionally, the ylid formation was attempted with NaH in DMF but resulted only in the formation of diphenylphospin oxide **165** in 72% yield, which is shown in scheme 2.1.1.4.2.²⁷

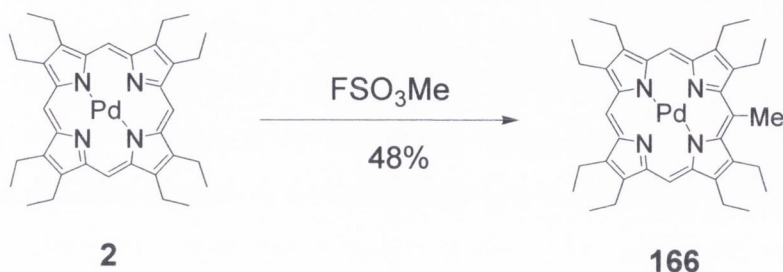


Scheme 2.1.1.4.1. Formation of 5-methyl Ni(II)OEP **164**, a) MeI , dichloromethane, b) PPh_3 , dichloromethane, c) MeOH , Et_3N , dichloromethane.²⁷



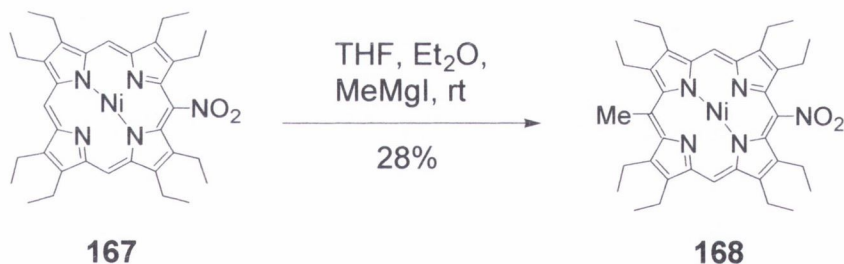
Scheme 2.1.1.4.2. Attempted ylid formation producing the diphenylphospin oxide **165**.²⁷

In 1972, 5-methyl Pd(II)OEP **166** was also obtained in 48% yield in an electrophilic reaction by refluxing Pd(II)OEP **2** for 48 hours in dichloromethane in the presence of an excess of methylfluorosulfonate, as shown in scheme 2.1.1.4.3, and was carried out by Grigg *et al.*²⁹



Scheme 2.1.1.4.3. 5-Methyl Pd(II)OEP **166** obtained by Grigg and co-workers with electrophilic methylfluorosulfonate.²⁹

A nucleophilic methylation pathway has also been reported by addition of the respective Grignard reagent and produced the in scheme 2.1.1.4.4. shown *meso* 5,15-AB disubstituted OEP **168** in 28% yield, starting with activated 5-nitro Ni(II)OEP **167**.²²

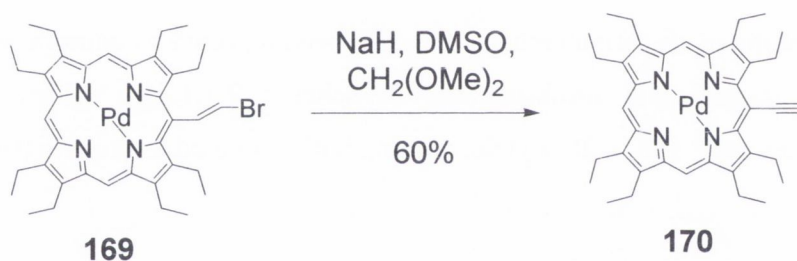


Scheme 2.1.1.4.4. Methylation of 5-nitro Ni(II)OEP **167** with Grignard reagent²²

A quick and straight forward pathway towards 5-methyl OEP **227** will be furthermore presented in chapter 2.2 by using methyl lithium (MeLi) and not activated OEP **1** and was carried out during the PhD.

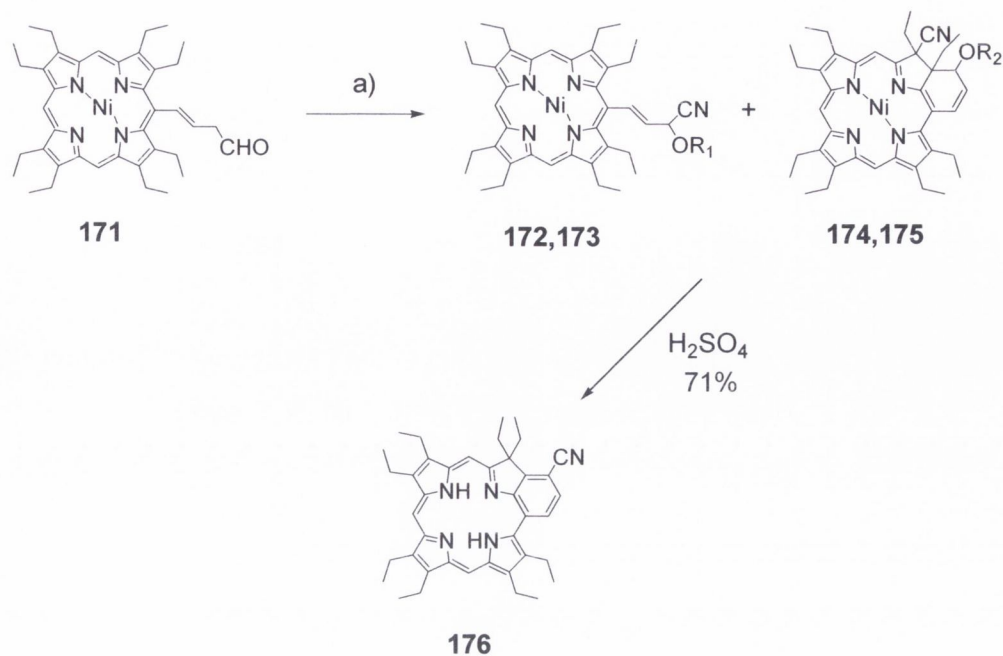
2.1.1.5 Formylation of OEP and derivation reactions (Wittig)

Vilsmeier formylation has been carried out on Pd(II) and Pt(II)OEP **2** and **3** to result for example when carried out in a mixture of DMF/1,2-dichloroethane with POCl₃ in the formation of 5-formyl Pt(II)OEP in 74% yield.³⁰ Formylation of Ni(II)OEP was furthermore reported in 2002 in 91% yield using Me₂N⁺=CHCl Cl⁻ in 1,2-dichloroethane and addition of NaOAc in H₂O.³¹ 5-Formyl Ni(II)OEP was also obtained by K. M. Smith *et al.* in 1977 in 70% yield and by Y. Chen *et al.* in 2001.^{32,33,34} It can be demetallated under strong acidic conditions in quantitative yield³³ and can be also derived with Wittig reagent e.g. Ph₃P=CHCO₂Et, which produced the corresponding alkene (not shown) in 90% yield.³⁴ Also 5-bromovinyl OEP **169**, shown in scheme 2.1.1.5.1, was obtained by Wittig reaction and was transformed into the acetylene in 60% yield.³⁵ A similar reaction was carried out as described in chapter 2.1.1.8 and the transmetallated Pd(II) porphyrin **195** was obtained in a one pot reaction.³⁵

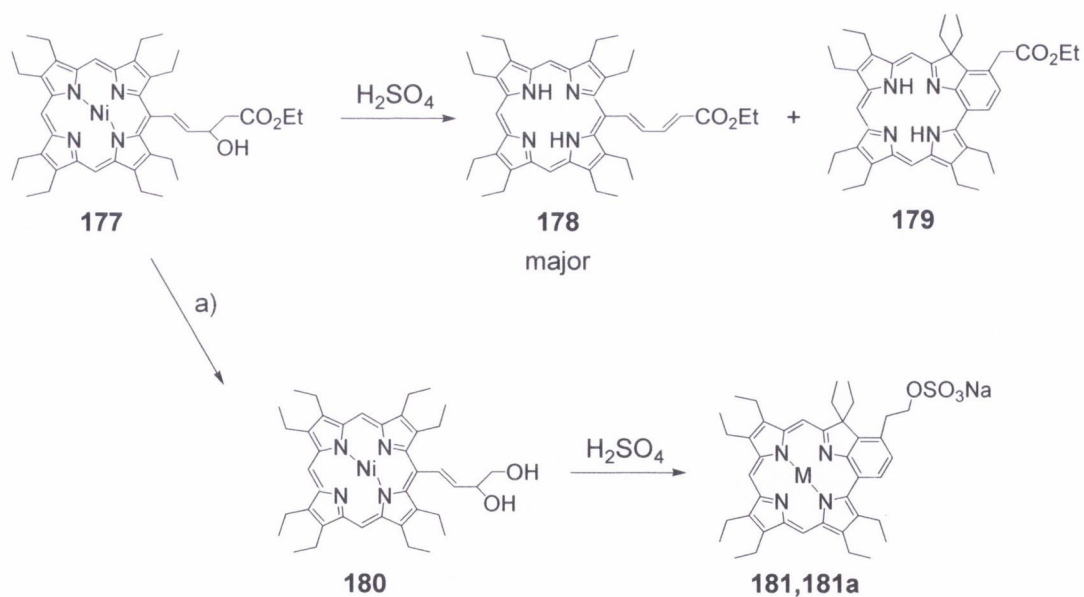


Scheme 2.1.1.5.1. Formation of 5-acetylene Pd(II)OEP **170**.³⁵

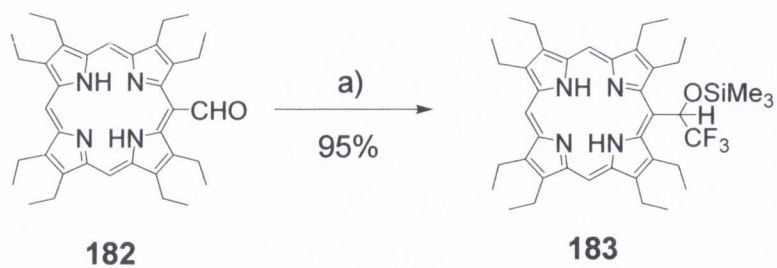
Also the in scheme 2.1.1.5.2 shown vinyl formyl OEP **171** was derived from 5-formyl OEP and was used for the preparation of *meso*- β fused OEP chlorins in 2003 by R. K. Pandey and co-workers.³⁶ The fused chlorins **174** and **175** were obtained as the major products when copper (II) triflate was used, whereas with indium (III) triflate the unstable open chain porphyrins **172/173** were isolated together with minor amounts of the fused chlorins as shown in scheme 2.1.1.5.2. Furthermore, when the crude mixtures of the porphyrins **172/174** and **173/175** were stirred with concentrated H₂SO₄ the 3-cyanobenzochlorine **176** was obtained in 71% yield in a mixture with three other benzochlorins in low yields (2%, 5% and 1%, not shown).



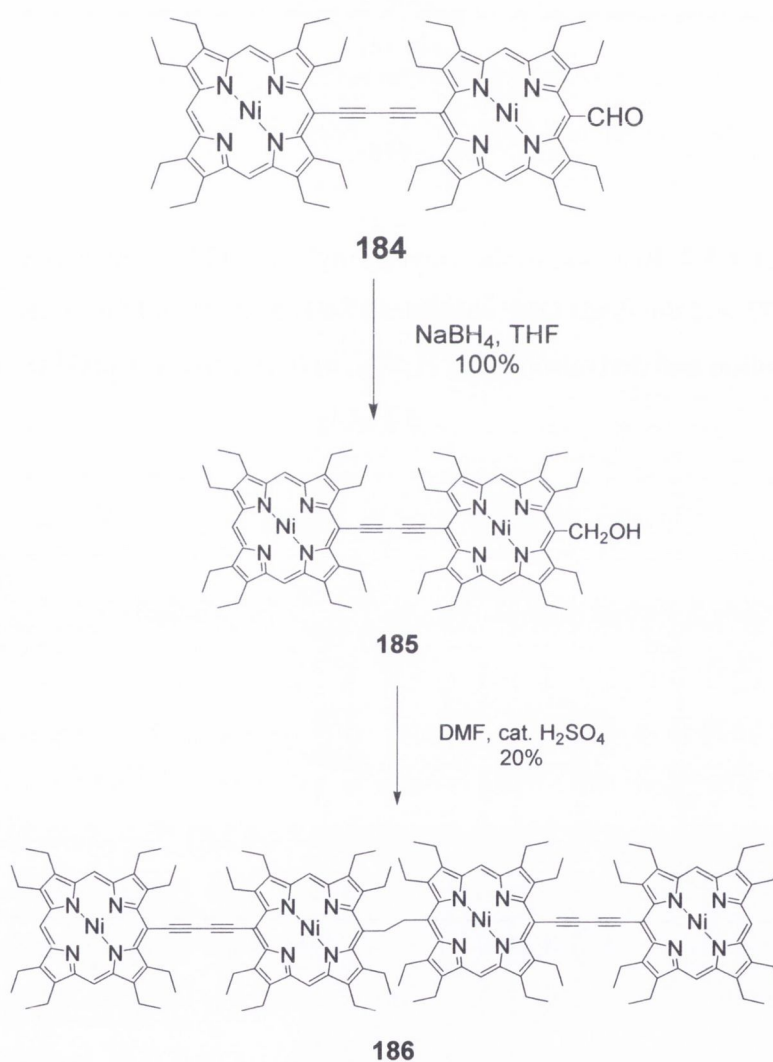
Scheme 2.1.1.5.2. Reaction of the vinyl formyl OEP **171** to the open chain cyanoethers **172/ 173** and the fused OEP chlorines **174/175** (R=H and Si(CH₃)₃) followed by cyclization and derivation using H₂SO₄, a) (CH₃)₃SiCN, Cu(OTf)₂ or In(OTf)₃, CH₂Cl₂.³⁶



Scheme 2.1.1.5.3. Cyclization of the *meso* substituted OEPs **177** and **180** producing the benzochlorins **179** and **181/181a**; a) DIBAL-H/NaBH₄; M=2H and Ni (II).



Scheme 2.1.1.5.4. Protection and prolongation of the CHO group of 5-formyl OEP **182** with a silyl reagent; a) CF_3SiMe_3 , $\text{Bu}_4\text{N}^+\text{F}^-$ (cat.).³⁷



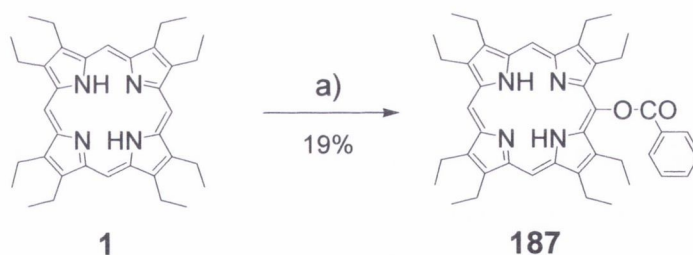
Scheme 2.1.1.5.5. Reduction of the formyl OEP **184** and formation of the ethyl-linked tetramer **186** via homo-coupling.³⁷

The formation of two other benzochlorins (**179/181**) by adding H₂SO₄ for the cyclization of the precursors **177/180** is furthermore shown in scheme 2.1.1.5.3.

The vinyl OEP **177** was also derived from 5-formyl OEP **182**. However, when the dialcohol **180** was prepared, no elimination occurred during the cyclization step and only the OEP adduct **181** was obtained. Furthermore, the use of H₂SO₄ induced also the demetallation of the respective porphyrin and the bezochlorin **181a** was obtained. Further derivation of 5-formyl OEP **182** with trimethylsilyltrifluoromethane and tetrabutylammonium fluorid as a catalyst produced as reported in 1999 the protected and chain prolongedated silyl OEP **183** shown in scheme 2.1.1.5.4.³⁷ The CHO group of the in scheme 2.1.1.5.5 shown formyl OEP dimer **184** was furthermore reduced quantitatively to the alcohol **185** with NaBH₄ in THF and in the presence of traces of H₂O. Additionally, the obtained carbinol **185** was subsequently homo-coupled to the ethyl bridged tetramer **186** in 20% yield³⁸ and similar reactions were carried out as described in chapter 2.1.1.8.

2.1.1.6 Ester of OEP via nucleophilic substitution

The OEP benzyl ester **187** was obtained in a nucleophilic reaction with the corresponding peroxide as shown in scheme 2.1.1.6.1.³⁹



Scheme 2.1.1.6.1. Formation of the benzyl ester **187** using (PhCO₂)₂ in PhCl.³⁹

2.1.1.7 Meso monosubstituted OEPs by [2+2] Mc Donald condensation

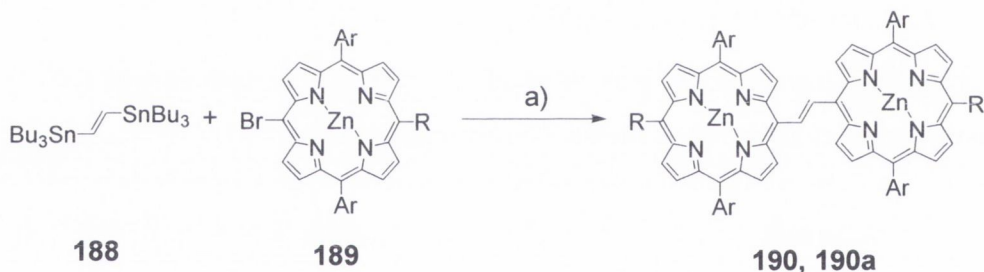
Meso monosubstituted etioporphyrins bearing *n*-heptyl, 4-methoxyphenyl, 3,5-dimethoxyphenyl and 4-bromophenyl residues were prepared by *Chen et al.* and Nocera and co-workers as discussed in chapter 1.4.6.^{33,40,41} The obtained yields were competitive to yields obtained by *meso* monosubstitution with organo lithium reagents

which will be described in chapter 2.2. Also 5-(3,5-dimethoxyphenyl) OEP **63** was obtained by cyclization of the biladiene *Z*-conformer as reported in chapter 1.3.³⁴

2.1.1.8 Synthesis of OEP dimers, oligomers and sandwich structures

OEP dimers are a class of *meso* monosubstitution OEPs and were in the recent years synthesized by several research groups.^{42,43,44,45,46,47,48,49,50} Furthermore their UV/vis and photophysical properties will be discussed in chapter 5 and chapter 6 in comparison to the measured absorption and emission of synthesized OEPs and Pd(II)OEPs.

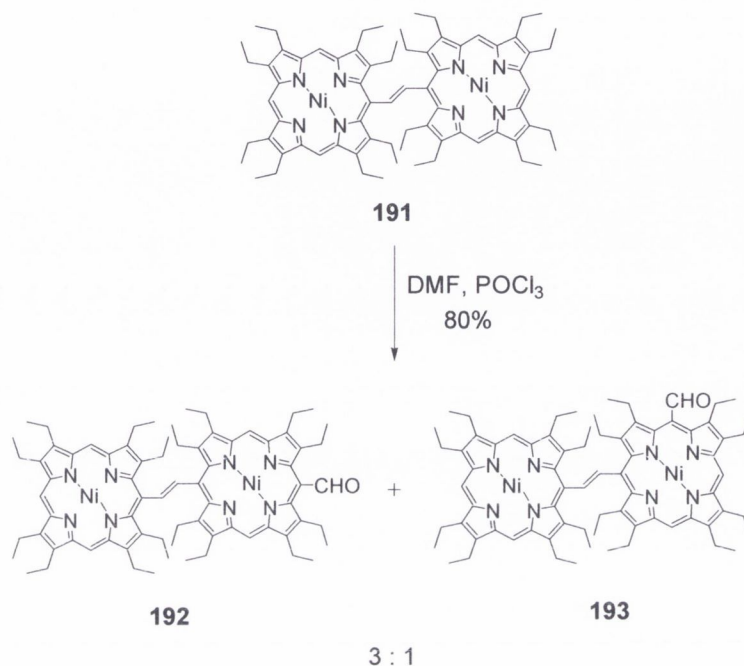
Compared to OEP dimers, β not substituted dimers were prepared with relative ease by H. L. Anderson using *meso* bromo functionalised porphyrins in coupling reactions.⁴⁷ Initial attempts to obtain the porphyrin dimer by McMurry and Wittig couplings failed,⁵¹ while Stille coupling with bis(tributylstannyl)ethene and Baldwin's conditions (addition of CuI, CuF) produced the porphyrin dimer **190** successfully as shown in scheme 2.1.1.8.1.^{52,53,54,55}



Scheme 2.1.1.8.1. Synthesis of the β free porphyrin dimer **190/190a** via Stille coupling using Baldwin's conditions ($\text{Pd}(\text{PPh}_3)_4$, CuI, CsF, R=phenyl or H); Ar=3,5-di-*tert*-butylphenyl.⁴⁷

Meso monobromination was unfortunately as described in chapter 2.1.1.1 not possible for OEPs and dimerization is therefore usually carried out through formylation in *meso* position and subsequent functionalization. The vinylene bridged Ni(II)OEP dimer **191** shown in scheme 2.1.1.8.2 was obtained by D. P. Arnold, G. V. Ponomarev and A. M. Shul'ga through formylation followed by Wittig reaction.^{44,48} Higuchi *et al.* furthermore used the dimer **191** in 2002 for further functionalization.⁵⁶ The formylation resulted in the shown regioisomers **192** and **193** in an 3:1, ratio while the *trans* linkage between the

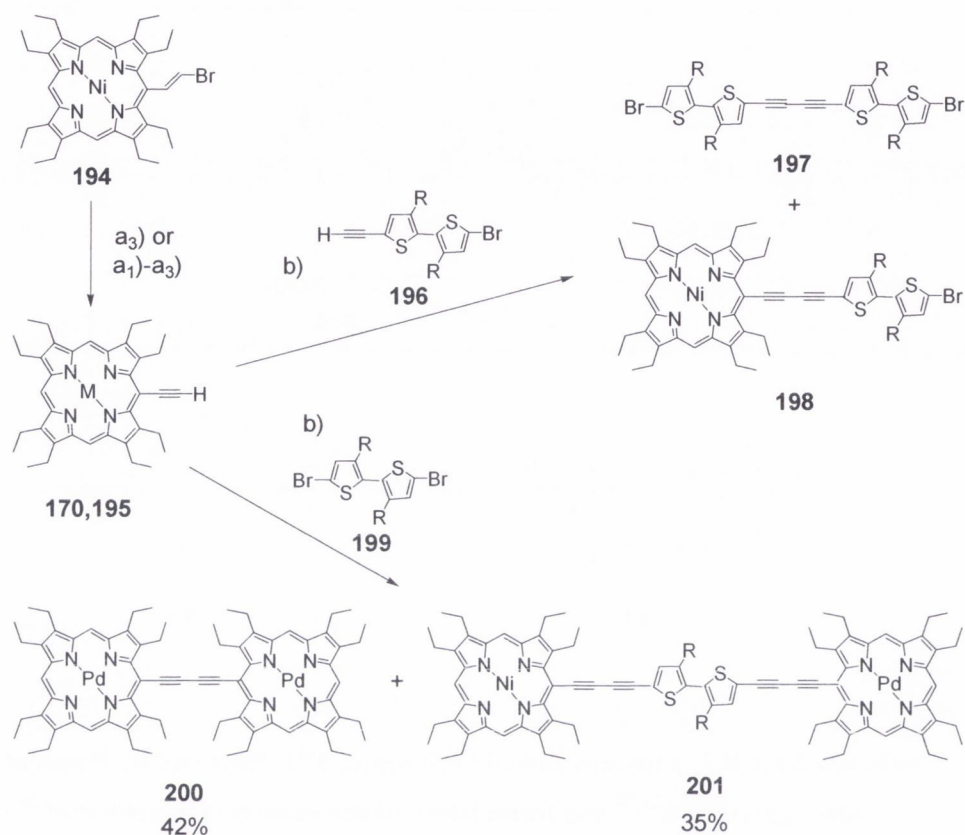
porphyrin subunits remained unchanged. Wittig reaction and acetylene formation followed (not shown) as described in chapter 2.1.1.5.



Scheme 2.1.1.8.2. Vinylene linked OEP dimer **191** described by Ponomarev and Shul'ga in 1986^{44,48} and formylation of the same by Higuchi *et al.*⁵⁶

OEP dimers were also obtained in 2003 by H. Higuchi *et al.* 5-Bromovinyl Ni(II)OEP **194** was derived as described in chapter 2.1.1.5 from 5-formyl Ni(II)OEP and was transformed into the acetylene **170** or under transmetallation conditions into the respective Pd(II) complex **195**. Oxidative coupling was carried out as shown in scheme 2.1.1.8.3 with the dibromo synthon **199** and resulting in the homo-coupled OEP dimer **200** in 42% yield in a mixture with the bridge prolonged dimer **201** in 35% yield.⁵⁷ The dibromothiophen **199** was also transformed to the mono acetylenic synthon **196** by Sonogashira treatment using trimethylsilylacetylen and followed by alkaline hydrolyses.^{59,60,61} With the synthon **196** the *meso* monosubstituted Ni(II)OEP **198** was obtained together with the homo-coupling product **197** as shown in scheme 2.1.1.8.3. OEP dimers were also obtained from 5-dimethylaminomethyl OEP **161** (compare to chapter 2.1.1.3), which was homo-coupled in the presence of ethyl iodide to afford the ethyl bridged dimer **202** in 87% yield as shown in figure 2.1.1.8.1.⁶² Similar couplings

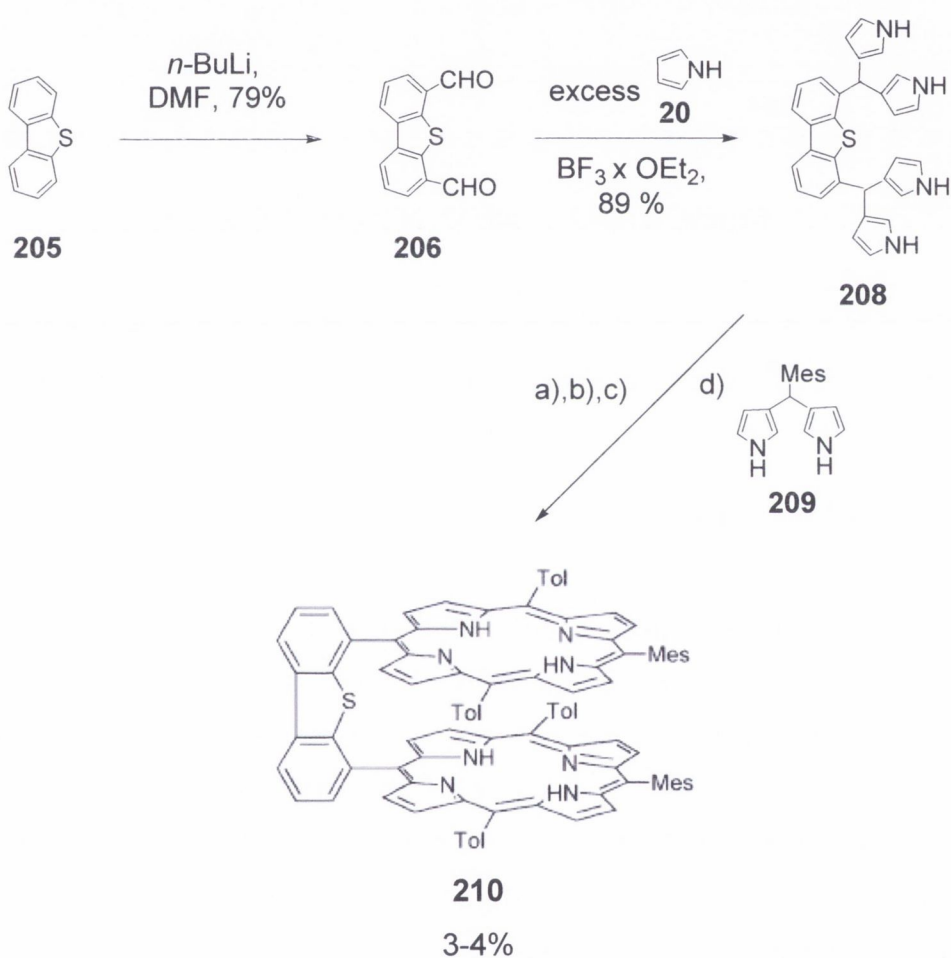
could be performed with the *meso* methylalcohol **204**, which was derived from 5-formyl OEP **182**, as shown in figure 2.1.1.8.1.⁶³



Scheme 2.1.1.8.3. Oxidative cross couplings performed by H. Higuchi *et al.* using 5-acetylene Ni(II) or 5-acetylene Pd(II)OEP **170/195**; M=Pd(II) or Ni(II);⁵⁷ a₁) H₂SO₄, CHCl₃, a₂) Pd(OAc)₂, CHCl₃/MeOH, a₃) DMSO, CH₂(OMe)₂, NaH, b) Cu(OAc)₂, Py-MeOH, 40 °C.⁵⁸

Furthermore, during the dimerization with trifluoroacetic acid also the copper was removed as can be seen in the respective reaction scheme. The synthesis of etio-type pacman porphyrins was furthermore most laborious and was reported by R. Guillard and co-workers and by D. G. Nocera *et al.* For example H₄DPS (compare to chapter 6), was prepared in a fourteen step synthesis with an overall yield of 0.3%.⁶⁴⁻⁷³ Else wise, the β not substituted pacman porphyrin H₄DPSN **210** could be obtained by R. Guillard in 2005 in only five steps in 3-4% yield as shown in scheme 2.1.1.8.4. The reaction sequence was furthermore optimized by conditions described by Lindsey *et al.*^{74,75} and

three strategies towards the porphyrin dimer **210** were possible: a) A spacer with two protected functional groups was used in which two porphyrin units were introduced step by step as chosen by Collman and co-workers,⁷⁶⁻⁷⁹ b) the formation of a linked porphyrin dimer was attempted in which the linker could be modified afterwards to obtain the desired angle, which was followed by Therien^{80,81} and Kobuke *et al.*^{82,83} and c) the coupling of a difunctionalized spacer with a porphyrin, dipyrromethane or pyrrole by condensation reaction or Sonogashira or Suzuki type coupling was carried out by Nocera⁸⁴, Collman⁷⁷ and Guillard *et al.*⁶⁵



Scheme 2.1.1.8.4. Synthesis of the in β -position not substituted sandwich porphyrin H_4DPSN **210**; a) EtMgBr , b) ClCOTol , c) NaBH_4 , (THF/MeOH, 30%), d) TFA, **209**, then DDQ/ NEt_3 , Mes=mesityl. The porphyrin structure was taken from the article due to special needs in the drawing, which could not be performed with Chem Draw Ultra.⁶⁵

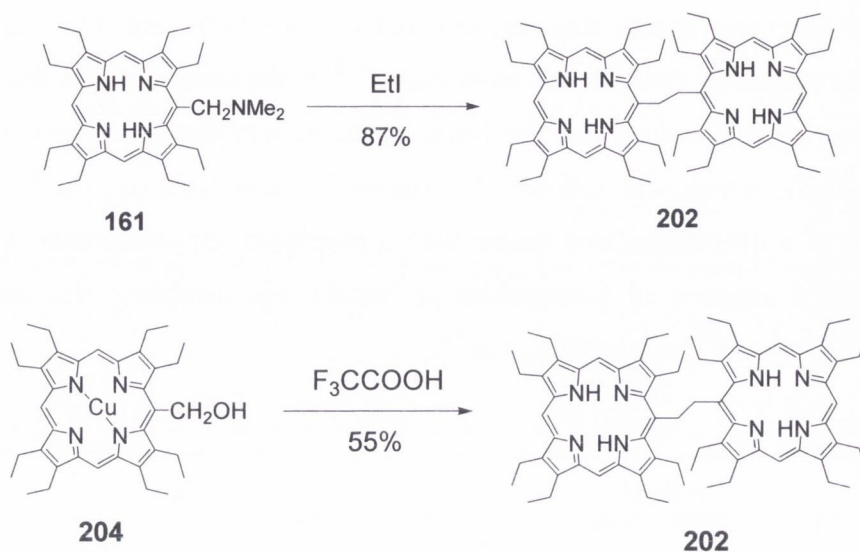


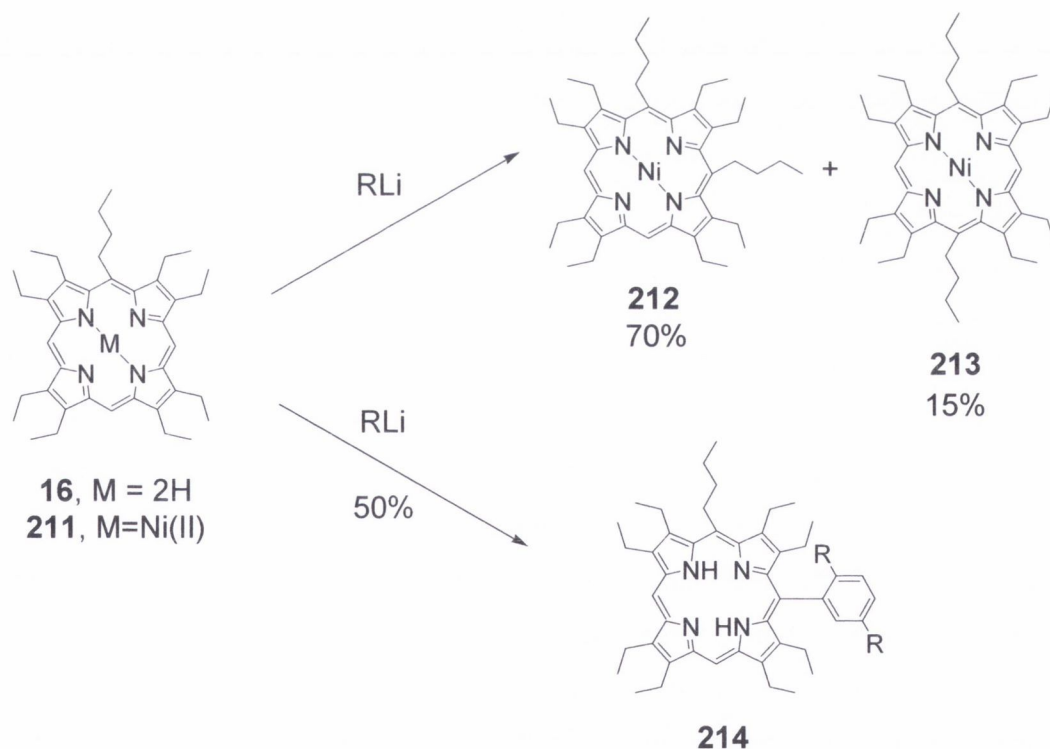
Figure 2.1.1.8.1. Synthesis of the OEP dimer **202**.^{62,63}

As it can be seen in scheme 2.1.1.8.4, following strategy c), the spacer **208**, was derived several times in order to produce finally by reaction with the dipyrromethane **209** H_4DPSN **210**.⁶⁵ Further synthesis was also described by Chang *et al.* in the 1980th.⁸⁴⁻⁸⁷

2.1.2 *Meso* 5,10- and 5,15-disubstituted OEPs

Almost all in literature described *meso* disubstituted OEPs are 5,15-disubstituted OEPs due to their straightforward synthesis *via* [2+2] condensation reactions as described in chapter 1.4.6. Furthermore, several novel 5,10 regio isomers could be obtained during the thesis and were derived from the *meso* monosubstituted OEPs with organo lithium reagents as will be described in chapter 2.2 and what increased the number of known 5,10 regio isomers considerably. Only recently also another, more elaborate pathway for the synthesis of *meso* 5,10- and 5,15-disubstituted OEPs in mixtures together with higher substituted OEPs was published by A. Syrbu and co-workers.⁸⁸ Mixtures of highly substituted OEPs were obtained by reaction of diethylpyrrole **38** with its more reactive carbinol **68** and aldehydes in a “[4+1]” manner under BF_3 catalysis in methanol and have been separated from each other by column chromatography using subsequently a column filled with silica gel and aluminum oxide.⁸⁸ However, the synthesis of those was discussed in chapter 1.4.5. Else wise, the *meso* 5,15-disubstituted OEPs reported in

the porphyrin handbook were substituted with methyl, ethyl, nitro and formyl groups and nitration and formylation of OEP was described in the chapters 2.1.1.2 and 2.1.1.5. Methyl groups were furthermore introduced by Buchler's reductive methylation^{89,90} and other alkyl residues were also derived from the formyl precursors.^{91,92} Furthermore a few strapped and caged OEPs have been described¹ while the first considerable synthesis of *meso* 5,15-A₂ substituted octaethylporphyrins was published in 1986 and 1988 by Y. Okamoto *et al.* ("Novel chiral C₂ symmetric octaethylporphyrins")^{93,94} followed in 1994 by J. Tang and J. G. Verkade⁹⁵ using tetra-ethyl dipyrromethane **53** as starting material for [2+2] condensation reactions under acid catalysis with CF₃COOH or *p*-TsOH in benzene or methanol as described in chapter 1.4.6. Also in 1994 a single 5,15-AB substituted OEP was synthesized in the same manner (see page 34).⁹⁶ In 2001 also Syrbu *et al.* investigated the formation of *meso* 5,15-disubstituted, β -substituted porphyrins using a variety of tetra-alkyl dipyrromethanes.⁹⁷



Scheme 2.1.2.1. Ni(II)OEPs **212** and **214** prepared by W.W. Kalisch; R=OMe.⁹⁹

5,10-disubstituted OEPs on the other hand were obtained from 1998 on with organo lithium reagents by M. O. Senge *et al.*⁹⁸ and the “RLi method” was followed during the PhD while previously for example, W. W. Kalisch prepared 5,10-bis(*n*-butyl) Ni(II)OEP **212** and 5-*n*-butyl-10-(2,5-dimethoxyphenyl) OEP **214** as shown in scheme 2.1.2.1. 5,10-Bis(*n*-butyl) Ni(II)OEP **212** was obtained from 5-*n*-butyl Ni(II)OEP **211** in 70% yield and also the regioisomer **213** was isolated in 15% yield and both could be separated. Also 5-*n*-butyl-10-(2,5-dimethoxyphenyl) OEP **214** was prepared from 5-*n*-butyl OEP **16** in 50% yield.⁹⁹ The 5,15-AB substituted OEP **168** was furthermore obtained in 28% yield from activated 5-nitro Ni(II)OEP **167** with the respective Grignard reagent and was shown in scheme 2.1.4.4 on page 50. However, an inversed regio selectivity was observed in contrast to the use of organo lithium reagents, and was explained by the electron withdrawing character of the nitro substituent.²²

2.1.3 *Meso* tri- and tetrasubstituted OEPs

Only a few *meso* trisubstituted octaethylporphyrins were reported in literature and were mostly obtained from condensation pathways within the whole series of the respectively substituted porphyrins (compare to chapter 1.4.5).^{88,100} Apparently, undecasubstituted OEPs are still very rare and only 5,10,15-tris-*n*-butyl Ni(II)OEP **215** and two other etioporphyrins were described by M. O. Senge in 2000.¹ Most access was laborious and seldomly done. However, 5,10,15-trisphenyl Ni(II)OEP **217** and 5,10-bis(*n*-butyl)-15-(2,5-dimethoxyphenyl) Ni(II) OEP **215** were obtained, as shown in figure 2.1.3.1, from a sequence of nucleophilic substitution reactions by I. Bischoff and W. Kalisch, as will be described in more detail in chapter 2.2.^{101,102} Therefore, nine novel, during the PhD synthesized undecasubstituted OEPs enlarge the variety of compounds immensely and might lead to further interesting insights.¹ On the other hand, several *meso*-A₄ substituted OEPs were reported in literature and were described in the chapter 1.4.1. The synthesis of symmetric *meso*-A₄ substituted octaethylporphyrins was compared to the synthesis of nona-, deca- and undecasubstituted OEPs and was carried out with relative ease in a typical [4+1] condensation. [4+1] condensation reactions yielding in dodecasubstituted porphyrins have been furthermore intensely investigated by C. J. Medforth, K. A. Smith, J. A. Shelnutt and other research groups during the 1990s.^{100,103-105} The condensation

was also optimized by H. L. Anderson in 2003 using BF_3 etherate catalysis¹⁰⁶ and was followed by various other groups in 2004 and 2005.¹⁰⁷⁻¹¹⁰

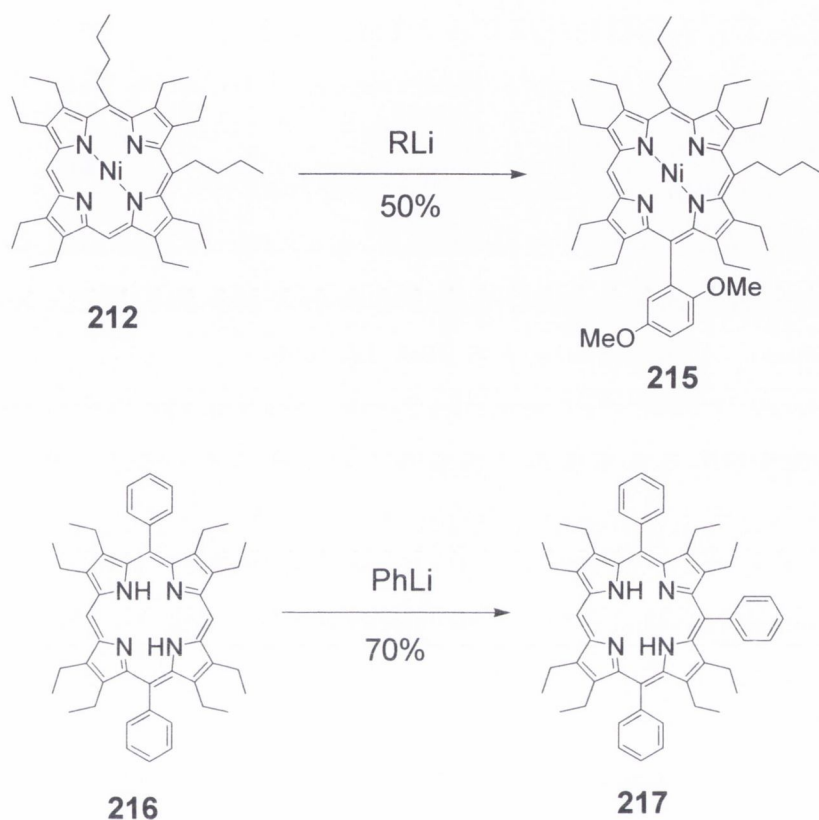


Fig. 2.1.3.1. OEPs obtained by I. Bischoff and W. Kalisch by substitution reactions using organo lithium reagents.^{101,102}

M. O. Senge reported for dodecaarylporphyrins first synthesis performed by Tsuchiya e.g. 5,10,15,20-tetrakis(pentafluorophenyl)-2,3,7,8,12,13,17,18-octaphenylporphyrin was prepared¹ and dodecasubstituted porphyrins were also afterwards obtained by Takeda/Sato and R. Guillard *et al.*¹¹¹⁻¹¹⁶ *Meso* A_4 -substituted porphyrins have been furthermore often used and tested in PDT applications, as they were the easiest accessible, and they were especially interesting when hydrophilic substituents were attached targeting the use of in body fluids.¹¹⁷

REFERENCES

- 1) M. O. Senge (2000). In: The porphyrin Handbook, Vol. 10, 280ff. Ed.: K.M. Kadish, R. Guillard, K. M. Smith. San Diego: Academic Press.
- 2) E. Hoffmann, P. M. Wrench, F. P. Sharples, R. G. Hiller, W. Welte, K. Diederichs *Science* **1996**, 272, 1788.
- 3) P. Hildebrandt *Biochim. Biophys. Acta* **1990**, 1040, 175.
- 4) E. Gudowska-Nowak, M. D. Newton, J. Fajer *J. Phys. Chem.* **1990**, 94, 9795.
- 5) D. E. Tronrud, M. F. Schmid, B. W. Matthews *J. Mol. Biol.* **1986**, 188, 443.
- 6) M. Nencki, J. Zaleski *Chem. Ber.* **1901**, 34, 1000.
- 7) H. Fischer, H. Orth. Die Chemie des Pyrrols. Akademische Verlagsgesellschaft. Leipzig, 1937.
- 8) H. Fischer, W. Klendauer *Liebigs Ann. Chem.* **1941**, 547, 123.
- 9) H. Fischer, H. Kellermann; F. Balaz *Chem. Ber.* **1942**, 75, 1178.
- 10) R. Bonnett, I. A. D. Gale, G. F. Stephenson *J. Chem. Soc. (C)* **1966**, 1600.
- 11) R. Bonnett, I. H. Champion-Smith, A. N. Kkozyrev, A. F. Mironov *Chem. Res. (S)* **1990**, 138.
- 12) R. Bonnett, I. H. Champion-Smith, A. N. Kkozyrev, A. F. Mironov *J. Chem. Res (M)* **1990**, 1015
- 13) M. Graça, H. Vicente, K. M. Smith *Tetrahedron* **1991**, 47, 34, 6887.
- 14) M. J. Billig, E. W. Baker *Chem. Ind.* **1969**, 654.
- 15) L. E. Andrews, R. Bonnett, A. N. Kozyrev, A. F. Mironov *J. Chem. Soc. Perkin Trans. 1* **1988**, 1735.
- 16) Y. Narutam, F. Tani, K. Maruyama *Tetrahedron Lett.* **1992**, 33, 1069.
- 17) H. Fischer, A. Treibs *Liebigs Ann. Chem.* **1928**, 466, 188.
- 18) H. Fischer, W. Neumann *Liebigs Ann. Chem.* **1932**, 494, 255.
- 19) L. C. Gong, D. Dolphin *Tetrahedron Lett.* **1976**, 2197.
- 20) E. Watanabe, S. Nishimura, H. Ogoshi, Z. Yoshida *Tetrahedron* **1975**, 31, 1385.
- 21) U.S. Patent, 5464741, 07 Nov 1995.
- 22) M. J. Crossley, L. G. King, S. M. Pyke, C. W. Tansey *J. Porphyrins Phthalocyanines* **2002**, 6, 685.
- 23) G.-Z. Wu, H.-K. Leung, W.-X. Gan *Tetrahedron* **1990**, 46, 3223.
- 24) L.-C. Gong, D. Dolphin *Can. J. Chem.* **1985**, 63, 406.

- 25) K. Jayaraj, A. Gold, L. M. Ball, P. S. White *Inorg. Chem.* **2000**, *39*, 3652.
- 26) K. M. Smith, G. H. Barnett, B. Evans, Z. Martynenko *J. Am. Chem. Soc.* **1979**, *101*, 5953.
- 27) D. V. Yashunski, G. V. Ponomarev, D. P. Arnold *Tetrahedron Lett.* **1996**, *37*, 39, 7147.
- 28) G. V. Ponomarev *Khim. Geterocycl. Soed.* 1980, 943.
- 29) R. Grigg, G. Shelton, A. Sweeney *J. Chem. Soc. Perkin I* **1972**, 1789.
- 30) No authors available online *Liebigs Ann. Chem.* **1988**, *1*, 43.
- 31) U. S. Pat. Appl. Publ. 2002137924, 26. Sep 2002.
- 32) M. J. Bushell, B. Evans, G. W. Kenner, K. M. Smith *Heterocycles* **1977**, *7*, 67.
- 33) Y. Chen, C. J. Medforth, K. M. Smith, J. Alderfer, T. J. Dougherty, R. K. Pandey *J. Org. Chem.* **2001**, *66*, 3930.
- 34) T. Tanaka, K. Endo, Y. Aoyama *Bull. Chem. Soc. Jpn.* **2001**, *74*, 5, 907.
- 35) N. Hayashi, M. Murayama, K. Mori, A. Matsuda, E. Chikamatsu, K. Tani, K. Miyabayashi, M. Miyake, H. Higuchi *Tetrahedron* **2004**, *60*, 30, 6363.
- 36) G. Li, S. K. Pandey, A. Graham, M. P. Dobhal, R. Mehta, Y. Chen, A. Gryshuk, K. Rittenhouse-Olson, A. Oseroff, R. K. Pandey *J. Org. Chem.* **2004**, *69*, 158.
- 37) G. Li, Y. Chen, J. R. Missert, A. Rungta, T. J. Dougherty, Z. D. Grossman, R. K. Pandey *J. Chem. Soc. Perkin Trans. I* **1999**, *13*, 1785.
- 38) N. Hayashi, A. Naoe, K. Miyabayashi, M. Yamada, M. Miyake, H. Higuchi *Tetrahedron Lett.* **2004**, *45*, 8215.
- 39) A. H. Jackson, K. R. N. Rao, M. Wilkins *J. Chem. Soc. Perkin Trans. I* **1987**, *2*, 307.
- 40) M. Walker, T. P. Forsyth, K. M. Smith. Unpublished results.
- 41) Z.-H. Loh, S. E. Miller, J. Chang, S. D. Carpenter, D. G. Nocera *J. Phys. Chem. A* **2002**, *106*, 11700.
- 42) H. L. Anderson *Inorg. Chem.* **1994**, *33*, 972.
- 43) T. E. O. Screen, I. M. Blake, L. H. Rees, W. Clegg, S. J. Borwick, H. L. Anderson *J. Chem. Soc. Perkin Trans. I* **2002**, 320.
- 44) D. P. Arnold, D. A. James *J. Org. Chem.* **1997**, *62*, 3460.
- 45) V. S.-Y. Lin, S. G. DiMagno, M. J. Therien *Science* **1994**, *264*, 1105.
- 46) K. Susumu, T. V. Duncan, M. J. Therien *J. Am. Chem. Soc.* **2005**, *127*, 5186.
- 47) M. J. Frampton, H. Akdas, A. R. Cowley, J. E. Rogers, J. E. Slagle, P. A. Fleitz, M. Drobizhev, A. Rebane, H. L. Anderson *Org. Lett.* **2005**, *7*, 24, 5365.

- 48) G. V. Ponomarev, A. M. Shul'ga *Chem. Heterocycl. Compd.* **1986**, *22*, 228.
- 49) D. V. Yashunsky, G. V. Ponomarev, D. P. Arnold *Tetrahedron Lett.* **1995**, *36*, 8485.
- 50) M. G. H. Vicenta, K. M. Smith *J. Org. Chem.* **1991**, *56*, 4407.
- 51) T. E. O. D. Screen *Phil. Thesis*, Oxford University, Oxford, **2002**.
- 52) S. G. DiMagno, V. S.-Y Lin, M. J. Therien *J. Am. Chem. Soc.* **1993**, *115*, 2513.
- 53) X. Shi, S. R. Amin, L. S. Liebeskind *J. Org. Chem.* **2000**, *65*, 1650.
- 54) S. P. Mee, V. Lee, J. E. Baldwin *Angew. Chem. Int. Ed.* **2004**, *43*, 1132.
- 55) S. P. Mee, V. Lee, J. E. Baldwin *J. E. Chem. – Eur. J.* **2005**, *11*, 3294.
- 56) H. Higuchi, T. Maeda, K. Miyabayashi, M. Miyake, K. Yamamoto *Tetrahedron Lett.* **2002**, *43*, 3097.
- 57) N. Hayashi, A. Matsuda, E. Chikamatsu, K. Mori, H. Higuchi *Tetrahedron Lett.* **2003**, *44*, 7155.
- 58) G. Ellington, A. R. Galbraith *Chem. Ind.* **1956**, 737.
- 59) H. Higuchi, T. Nakayama, H. Koyama, J. Ojima, T. Wada, H. Sasabe *Bull. Chem. Soc. Jpn.* **1995**, *68*, 2363.
- 60) H. Higuchi, S. Yoshida, Y. Uraki, J. Ojima *Bull. Chem. Soc. Jpn.* **1998**, *71*, 2229.
- 61) K. Sonogashira, Y. Tohda, N. Hagihara *Tetrahedron Lett.* **1975**, *16*, 4467.
- 62) No authors available online *Khim. Geterocycl. Soed.* **1993**, *12*, 1692.
- 63) No authors available online *Khim. Geterocycl. Soed.* **1988**, *3*, 339.
- 64) F. Bolze, C. P. Gros, M. Drouin, E. Espinosa, P. D. Harvey, R. Guilard *J. Organometal. Chem.* **2002**, *89*, 643.
- 65) S. Faure, C. Stern, R. Guilard, P. D. Harvey *Inorg. Chem.* **2005**, *44*, 9232.
- 66) Z.-H. Loh, S. E. Miller, C. J. Chang, S. D. Carpenter, D. G. Nocera *J. Phys. Chem. A* **2002**, *106*, 11700.
- 67) Y. Deng, C. J. Chang, D. G. Nocera *J. Am. Chem. Soc.* **2000**, *122*, 410.
- 68) C. J. Chang, E. A. Baker, B. J. Pistorio, Y. Deng, Z.-H. Loh, S. E. Miller, S. D. Carpenter, D. G. Nocera *Inorg. Chem.* **2002**, *41*, 3102.
- 69) B. J. Pistorio, C. J. Chang, D. G. Nocera *J. Am. Chem. Soc.* **2002**, *124*, 7884.
- 70) C. J. Chang, Y. Deng, A. F. Heyduk, C. K. Chang, D. G. Nocera *Inorg. Chem.* **2000**, *39*, 959.
- 71) C. J. Chang, C.-Y. Yeh, D. G. Nocera *J. Org. Chem.* **2002**, *67*, 403.
- 72) C. J. Chang, Y. Deng, C. Shi, C. K. Chang, F. C. Anson, D. G. Nocera *Inorg. Chem. Commun.* **2000**, 1355.

- 73) C. J. Chang, Y. Deng, G.-H. Lee, S. M. Peng, C.-Y. Yeh, D. G. Nocera *Inorg. Chem.* **2002**, *41*, 3008.
- 74) P. D. Rao, S. Danalekshmi, B. J. Littler, J. S. Lindsey *J. Org. Chem.* **2000**, *65*, 7323.
- 75) S.-I. Tamaru, L. Yu, W. Youngblood, K. Muthukumaran, M. Taniguchi, J. S. Lindsey *J. Org. Chem.* **2004**, *69*, 765.
- 76) J. P. Collman, D. A. Tyvoll, L. L. Chng, H. T. Fish *J. Org. Chem.* **1995**, *60*, 1926.
- 77) J. P. Collman, L. L. Chng, D. A. Tyvoll *Inorg. Chem.* **1995**, *34*, 1311.
- 78) J. P. Collman, H. T. Fish, P. S. Wagenknecht, D. A. Tyvoll, L. L. Chng, T. A. Eberspacher, J. I. Braumann, J. W. Bacon, L. H. Pignolet *Inorg. Chem.* **1996**, *35*, 6746.
- 79) J. E. Hutchison, T. A. Poslethwaite, C. H. Chen, K. W. Hathcock, R. S. Ingram, W. Ou, R. W. Linton, R. W. Murray, D. A. Tyvoll, L. L. Chng, J. P. Collman *Langmuir* **1997**, *13*, 2143.
- 80) J. T. Fletcher, M. J. Therien *J. Am. Chem. Soc.* **2002**, *124*, 4298.
- 81) J. T. Fletcher, M. J. Therien *Inorg. Chem.* **2002**, *41*, 331.
- 82) H. Meier, Y. Kobuke, S.-I. Kugimiya *J. Chem. Soc., Chem. Commun.* **1989**, 923.
- 83) Y. Tomohiro, A. Satake, Y. Kobuke, *J. Org. Chem.* **2001**, *66*, 8442.
- 84) L. L. Chng, C. J. Chang, D. G. Nocera *J. Org. Chem.* **2003**, *68*, 4075.
- 85) C. K. Chang, I. Abdalmuhdi *J. Org. Chem.* **1983**, *48*, 5388.
- 86) C. K. Chang, I. Abdalmuhdi *Angew. Chem. Int. Ed.* **1984**, *23*, 164.
- 87) S. S. Eaton, G. R. Eaton, C. K. Chang *J. Am. Chem. Soc.* **1985**, *107*, 3177.
- 88) S. A. Syrbu, T.V. Lyubimova, A. S. Semeikin *Chem. Heterocyclic Comp.* **2004**, *40*, 10, 1262.
- 89) A. Botulinski, J. W. Buchler, K.-L. Lay, H. Stoppa *Liebigs Ann. Chemie* **1984**, 1259.
- 90) J. W. Buchler, L. W. Puppe *Liebigs Ann. Chem.* **1970**, *740*, 142.
- 91) X. Jiang, D. Nurco, K. M. Smith *Chem. Commun.* **1996**, 175.
- 92) H. Vicente, M. da Graca. In *The Porphyrin Handbook*; Kadish, K. M.; Smith, K. M.; Guillard, R. Eds. Academic Press: San Diego, CA, 1999; Vol. 1, pp. 149.
- 93) H. Ogoshi, K. Saita, K.-I. Sakurai, T. Watanabe, H. Toi, Y. Aoyama, Y. Okamoto *Tetrahedron Lett.* **1986**, *27*, 52, 6365.
- 94) Y. Aoyama, T. Uzawa, K. Saita, Y. Tanaka, H. Toi, H. Ogoshi, Y. Okamoto *Tetrahedron Lett.* **1988**, *29*, 41, 5271.
- 95) J. Tang, J. G. Verkade *J. Org. Chem.* **1994**, *59*, 7793.

- 96) H. Tamiaki, A. Kiyomori, K. Maruyama *Bull. Chem. Soc. Jpn.* **1994**, *67*, 2478.
- 97) S. A. Syrbu, T.V. Lyubimova, A.S. Semeikin *Russ. J. Gen. Chem.* **2001**, *71*, *10*, 1656.
- 98) M. O. Senge, I. Bischoff *Tetrahedron Lett.* **2004**, *45*, 1647.
- 99) W. W. Kalisch, M. O. Senge *Angew. Chem.* **1998**, *110*, *8*, 1156.
- 100) J. Takeda, M. Sato *Chem. Lett.* **1994**, *12*, 2233.
- 101) M. O. Senge, I. Bischoff *Eur. J. Org. Chem.* **2001**, 1735.
- 102) M. O. Senge, W. W. Kalisch, I. Bischoff *Chem. Eur. J.* **2000**, *6*, 2721.
- 103) C. J. Medforth, K. M. Barkigia, M. D. Berber, J. Fajer, M. W. Renner, K. M. Smith *J. Am. Chem. Soc.* **1990**, *112*, 8851.
- 104) C. J. Medforth; M. D. Berber; K. M. Smith; J. A. Shelnut *Tetrahedron Lett.* **1990**, *31*, 3719.
- 105) M. R.-J. Cheng, P.-Y. Chen, P.-R. Gau, C.-C. Chen, S.-M. Peng *J. Am. Chem. Soc.* **1997**, *119*, 2563.
- 106) A. Krivokapic, A. R. Cowley, H. L. Anderson *J. Org. Chem.* **2003**, *68*, 1089.
- 107) K. M. Barkigia, M. W. Renner, M. O. Senge, J. Fajer *Heterocycles* **2004**, *63*, *3*, 505.
- 108) Z. Shen, H. Uno, Y. Shimizu, N. Ono *Organic & Biomolecular Chemistry* **2004**, *2*, 3442.
- 109) A. Hoshino, Y. Ohgo, M. Nakamura *Tetrahedron Lett.* **2005**, *46*, 4961.
- 110) L. A. Yatsunyk, H. Ogura, F. A. Walker *Inorg. Chem.* **2005**, *44*, 2867.
- 111) S. Tsuchiya *Chem. Phys. Lett.* **1990**, *169*, 608.
- 112) C. J. Medforth, K. M. Smith *Tetrahedron Lett.* **1990**, *31*, 5583.
- 113) J. Takeda, T. Ohya, M. Sato *Chem. Phys. Lett.* **1991**, *183*, 384.
- 114) J. Takeda, M. Sato *Chem. Pharm. Bull.* **1994**, *42*, 1005.
- 115) K. Perie, J.-M. Barbe, P. Cocolios, R. Guillard *Bull. Soc. Chim. Fr.* **1996**, *133*, 697.
- 116) R. Guillard, K. Perie, J.-M. Barbe, D. J. Nurco, K.M. Smith, E. Van Caemelbecke, K.M. Kadish *Inorg. Chem.* **1998**, *37*, 973.
- 117) Y.-J. Ko, K.-J. Yun, M.-S. Kang, J. Park, K.-T. Lee, S. Bum Park, J.-H. Shin *Bioorg. Med. Chem. Lett.* **2007**, *17*, *10*, 2789.

2.2 Meso substitution of OEPs with organolithium reagents

The discussion of in literature reported *meso* mono-, 5,15-di-, tri- and tetrasubstituted OEPs obtained by condensation methods was summarized in chapter 1. Electrophilic substitution reactions such as formylation and nitration as well as Wittig reactions were described in the previous chapter (2.1) and were used to derive OEP **1** in its *meso* positions. This chapter presents the synthesis carried out during the PhD and introduces the pathway of nucleophilic *meso* substitution with organolithium reagents, which was elaborated from 1998 on in the research group of Prof. M. O. Senge.¹⁻¹⁰ The nucleophilic substitution pathway is known to be unique, straightforward and competitive with condensation reactions. I. Bischoff obtained for example the in figure 2.2.1 shown 5-(4-bromophenyl) OEP **221** in 56% yield directly from OEP **1**,⁴ whereas Nocera and co-workers prepared 5-(4-bromophenyl) etioporphyrin (the Pd(II) complex **379** is shown in chapter 6.4) in 51% yield in a [2+2] condensation reaction.¹¹ On the other hand, the *meso* substitution with organo lithium reagents is limited in scale and the *meso* monosubstituted OEPs could be only obtained in 30-200 mg, whereas Nocera *et al.* isolated 3.25 g of the respective etioporphyrin.

However, not activated porphyrins can be used for nucleophilic substitution reactions and *meso* substitution can be carried out with ease on OEP and other porphyrins with commercially available phenyl lithium (PhLi), methyl lithium (MeLi), *n*-, *sec*- and *tert*-butyl lithium (BuLi) or with so-called translithiates, which are generated *in situ* from the respective halogeno compound, preferentially from the bromide, with *n*-BuLi, *s*-BuLi or PhLi in ether, petrol ether or THF at low temperatures.¹² Series of *meso n*-butyl and *meso* phenyl Ni(II)OEPs were obtained in the past years by W. W. Kalisch⁸ and by I. Bischoff⁴ as shown for example in table 2.2.1 and W. W. Kalisch investigated also the *n*-butylation of nickel (II) (40%), copper (II) (75-87%) and cobalt (II) OEP (40%).⁸ Kalisch and Bischoff attempted else wise first nucleophilic substitution reactions on Ni(II)OEPs and H₂OEP **1** with translithiates e.g. 4-bromophenyllithium, 2,5-dimethoxyphenyllithium, 4-ethynylphenyllithium etc.^{3,8} and prepared the in figure 2.2.1 shown *meso* monosubstituted OEPs in good to excellent yields. It was furthermore reported,^{1,3,4,8} that the yields of nucleophilic substitution reactions carried out on metal e.g. nickel (II) OEPs were good to excellent and that 4 to 8 equivalents of *n*-BuLi or PhLi were used to perform the reactions.

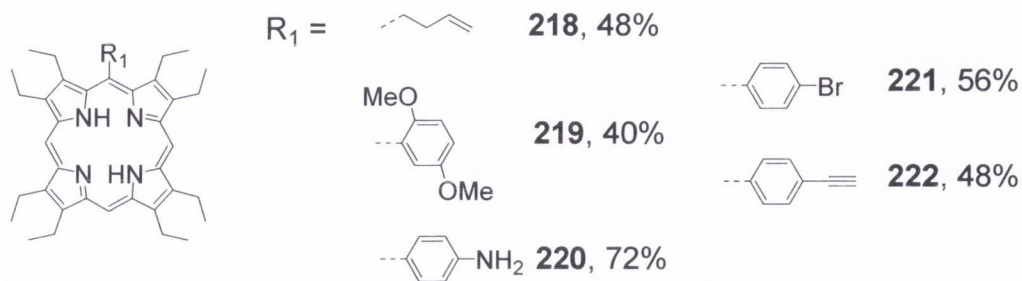


Fig. 2.2.1. *Meso* monosubstituted OEPs prepared by I. Bischoff and W. W. Kalisch.^{3,8}



	R ₁	R ₂	R ₃	R ₄
223a	<i>n</i> -butyl	<i>n</i> -butyl	phenyl	phenyl
223b	<i>n</i> -butyl	phenyl	<i>n</i> -butyl	phenyl
223c	<i>n</i> -butyl	<i>n</i> -butyl	<i>n</i> -butyl	phenyl
223d	<i>n</i> -butyl	phenyl	phenyl	phenyl

Table 2.2.1. By I. Bischoff synthesized *n*-butyl-phenyl serie.⁴

On the other hand, with H₂OEP **1** higher amounts of the reagent were necessary due to the lithiation of the inner NH groups and approximately 6 to 10 equivalents were added. *N*-Butylation of H₂OEP **1** was furthermore performed in lower yield, while arylation was usually achieved in higher and excellent yields and *vice versa* for the respective metal OEPs. For example, 5-*n*-butyl Cu(II)OEP (not shown) was prepared from Cu(II)OEP in 75–87% yield, whereas 5-*n*-butyl OEP **16** was only isolated in 50% yield from H₂OEP **1**. On the other hand, 5-phenyl OEP **4** was obtained from H₂OEP **1** in 90–99% yield and 5-phenyl Ni(II)OEP **242** was afforded from Ni(II)OEP **226** in only 65% yield.

Following those results, the synthesis of several novel *meso* monosubstituted H₂OEPs as well as di- and trisubstituted OEPs was carried out during the PhD and will be presented

in the following sections. Additionally, the respective palladium (II) and platinum (II) complexes were prepared and will be discussed in chapter 2.3, while the investigation of their photophysical properties will be summarized in chapter 6. Else wise, it was attempted, to introduce electron donating and withdrawing groups such as OMe, NMe₂ and CF₃ as it will be described in section 2.2.2 to 2.2.4. For example the OEP **253**, possessing an unsymmetric substitution pattern and push-pull properties could be obtained in good yield (30%) by the repeated use of organo lithium reagents as shown in scheme 2.2.1 from OEP **1** and the respective *meso* monosubstituted OEP **6** in two reaction steps.

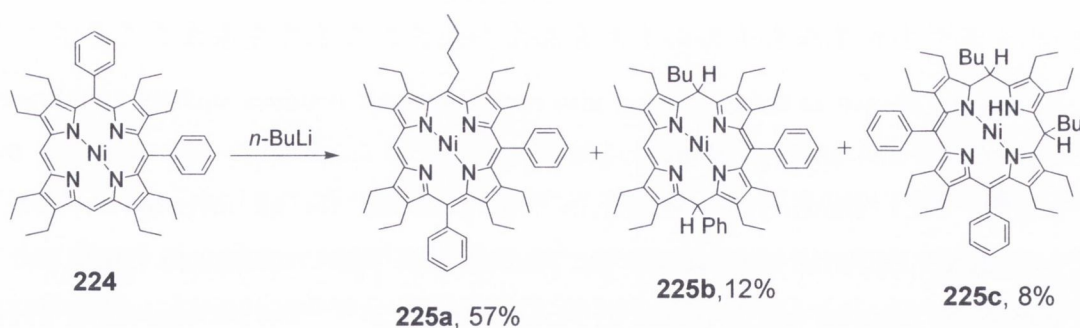


Scheme 2.2.1. Synthesis of the *meso* AB-substituted OEP **253**, 1a) 3-bromobenzotrifluoride/*n*-BuLi in ether, $-30\text{ }^{\circ}\text{C}$ to rt for 3h, 1b) addition of OEP **1**/THF, $-30\text{ }^{\circ}\text{C}$ to $+50\text{ }^{\circ}\text{C}$, 40 min, 1c) H₂O, then DDQ/CH₂Cl₂, $-10\text{ }^{\circ}\text{C}$; 2a to 2c) in similarity to 1a) to 1c).

As will be shown in the following, also novel aromatic residues such as 9-anthracenyl, 9-phenanthrenyl and 1-naphthyl could be introduced successfully. Furthermore, the in scheme 2.2.1 shown regio selectivity was observed for all prepared A₂ and AB substituted OEPs as well as for the formation of ABA substituted OEPs and was previously reported and discussed by M. O. Senge *et al.*^{5,6,8} The corresponding ¹H NMR data and identification of the regio isomers, will be furthermore described in chapter 3. However, when the substitution with alkyl residues was attempted on Pd(II)OEPs, also the pathway to 5,15-disubstituted OEPs was opened as will be reported in chapter 2.2.3 and was previously observed for *n*-butylation and phenylation by Bischoff and Kalisch with Ni(II)- and free base OEPs in some cases.^{4,8}

Finally, in chapter 2.2.5 the synthesis and optimization carried out for the preparation of the phenanthrenyl series, which was shown in the introduction, will be reported. Mixtures of atropisomers were also obtained for several of the prepared di-, tri- and tetrasubstituted OEPs and will be discussed with the corresponding ^1H NMR and UV/vis data in the chapters 3 and 5.

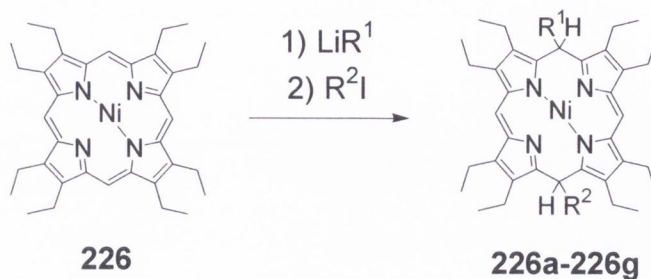
During former works, I. Bischoff described also the isolation of stable porphodimethenes as end-points in synthetic access when *n*-butyl or other alkyl residues were attempted to be introduced into Ni(II)OEPs. Porphodimethenes were generally formed, when the introduction of a residue opposite to already existing substituents was aimed as it can be seen in scheme 2.2.2. However, also when trapping reactions with iodates were attempted, 5,15-substitution could be observed and resulted in several porphodimethenes with Ni(II)OEPs as shown in scheme 2.2.3. The 5,15-substitution was furthermore explained by being the result of a preferred, roof-type conformation during the reaction, which facilitated the income of the second substituent in the 15-position according to Buchler.¹³⁻¹⁵ On the other hand, no porphodimethenes were observed during the PhD as the 10-position was in all cases accessible. However, it also seemed that the formation of porphodimethenes was prone to the use of alkyl reagents and Ni(II)OEPs. Senge *et al.* described additionally, that stirring times and oxidation before quenching could have influenced the formation of porphodimethenes.⁶



Scheme 2.2.2. Porphodimethene formation observed by I. Bischoff during the trisubstitution step.⁴

The stirring time was therefore always kept short (1 to 4 hours) during the PhD and also the oxidation of the porphyrinogen was carried out quickly e.g. approximately five

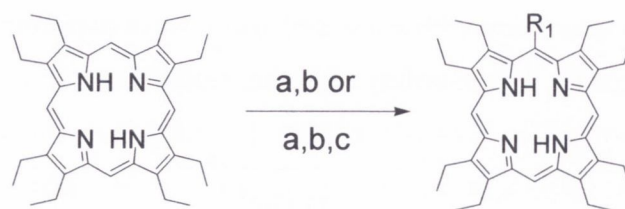
minutes after the quenching with water and was always performed at low temperatures (e.g. - 40 °C) to reduce the possibility of further reactions.



Scheme. 2.2.3. Porphodimethenes obtained by I. Bischoff; R₁= *n*-butyl, *n*-hexyl or phenyl, R₂= *n*-hexyl, *n*-butyl, (CH₂)₃CH₂ I, (CH₂)₃CN, (CH₂)₄CO₂Et, (CH₂)₂CH₂I.⁶

2.2.1 Synthesis of *meso* monosubstituted OEPs

Meso monosubstituted free base and metallo OEPs have been synthesized previously by W. W. Kalisch and I. Bischoff using organo lithium reagents.^{1,3,4,8} Additionally, the in table 2.2.1.1 shown *meso* monosubstituted OEPs **227-234** and **4-8**, were prepared during this work and the OEP **228**, was for the first time obtained from free base OEP **1**. The OEPs **4**, **16**, **227** and **228** were prepared by addition of commercial lithium reagents (MeLi, *n*-BuLi, *s*-BuLi and PhLi) to OEP **1** in dry THF at low temperatures and under an argon atmosphere. The *n*-butylation was carried out as described by W. Kalisch and produced the OEP **16** quickly in 50% yield,^{9,16} whereas methylation proceeded only slowly and in low yield (27%) and was attempted for the first time. The use of reactive *s*-BuLi, on the other hand, resulted in the formation of the OEP **228** in poor yield (11%), accompanied by a bigger amount of black polymerization by-products, which made the purification difficult and explained the low yield. However, it was reported by I. Bischoff that the use of *iso*-propyllithium didn't produce the respective *meso* monosubstituted OEP, while it remained unknown if OEP **1** could be recovered.³ An alternative pathway towards 5-*s*-butyl OEP **228** was furthermore presented by I. Bischoff, using Ni(II)OEP **226** as starting material, which reacted smoothly with *s*-BuLi, affording the respective *meso* monosubstituted Ni(II)OEP (not shown) in excellent 82% yield.¹⁷ The OEP **4** was furthermore prepared by gentle heating of the reaction mixture to 40 °C as described by Kalisch.⁹



	R_1	Yield [1/%]
227	methyl	27
16	<i>n</i> -butyl	50
228	<i>s</i> -butyl	11
4	phenyl	68–90
229	4-tolyl	20
230	4-dimethylaminophenyl	17
231	3-methoxyphenyl	3
232	3-hydroxyphenyl	26
5	4- <i>n</i> -pentylphenyl	83
6	3-trifluoromethylphenyl	64
7	1-naphthyl	49
233	2-naphthyl	31
234	acenaphthyl	26
8	9-phenanthrenyl	73–89

Table 2.2.1.1 Novel *meso* monosubstituted OEPs prepared during the PhD and OEPs **4** and **16**, which were also previously prepared by W. W. Kalisch and I. Bischoff;^{3,9} a) ether, RBr/*n*-BuLi, low temperatures to rt, b) OEP **1**/THF, low temperatures to rt, 1h–4h, c) H₂O, DDQ/CH₂Cl₂ or a) THF/MeLi or *n*-Buli or PhLi, –75 °C, –50 °C or 0 °C to rt/40 °C, b) H₂O, DDQ/CH₂Cl₂.

However, the OEPs **229-234** were derived from *in situ* generated translithiates and could be successfully obtained by applying conditions similar to those used by Kalisch and Bischoff.^{3,8} The translithiates were prepared first, while afterwards a solution of OEP **1** in THF was added. TLC control during the reactions showed that the formation of the desired *meso* monosubstituted OEP proceeded generally slowly and indicated also, that room temperature was needed to start and to complete the reaction in difference to the in chapter 2.2.3 described disubstitution, which occurred faster and easier.

Best results for *meso* monosubstitution, were obtained for the OEPs **6, 7** and **8**, which could be isolated in good to excellent yield (49-89%). Usually 20/40 and after further optimization 31/40 or in some cases 20/60 equivalents of bromide/*n*-BuLi (OEP **233**) were used for the preparation of the OEP. During the translithiation, the reaction mixture was allowed to warm up to room temperature to destroy remaining *n*-BuLi and to circumvent the butylation of OEP **1**. However, an overall excess of at least 9 equivalents of *n*-BuLi relative to the equivalents of the bromide was in most cases to perform the reaction and might have been needed for the core lithiation during the substitution. I. Bischoff and W. Kalisch used furthermore 1/28/42 equivalents of H₂OEP **1**/bromide and *n*-BuLi for the preparation of 5-(4-ethynylphenyl) OEP **222**, 1/22/22 equivalents for the synthesis of 5-(4-bromophenyl) OEP **221** and 1/42/78 equivalents for the introduction of an 1-*n*-butenyl substituent.¹ In contrast to that, the preparation of related nickel (II) OEPs proceeded with lower *n*-BuLi amounts and could be explained by the fact that a metal was already inserted in the porphyrin core. 5-(2,5-Dimethoxyphenyl) Ni(II)OEP **243** was for example obtained in 65% yield with 1/27/28 equivalents of Ni(II)OEP/bromide and *n*-BuLi¹ and the respective free base OEP **219** was obtained from OEP **1** in 27% with the same equivalents by W. Kalisch and indicating that methoxyphenyl lithiates might require lower equivalents of *n*-BuLi than other translithiates. However, I. Bischoff used for the synthesis of 5-(4-aminophenyl)OEP **220** 1/26/75 equivalents of OEP **1**/bromide/*n*-BuLi and 1/29/88 equivalents when she started with the respective Ni(II)OEP due to the additional NH₂ group of the bromide and also the respective hydroxyphenyl lithiates required higher equivalents of *n*-BuLi.

As it can be seen in table 2.2.1.1, the substitution with phenyl lithiates bearing OH, OMe and methyl groups was also more difficult than with others and resulted in the formation of the respective *meso* monosubstituted OEPs, **229, 230, 231** and **232** in low to average yields only (3% to 26%). During the formation of the OEPs **229, 230, 231** and **232** high

amounts of yellow and black derivatives as a result of the destruction and polymerization of OEP **1** were observed and explained the diminished yields. However, as it will be described in the following section, the use of 4-dimethylphenyllithium was facilitated during the disubstitution step and high yields of the respective OEPs were obtained (48-79%), while the addition of 3-methoxyphenyllithium was still observed to result in the respective di- and trisubstituted OEPs in low yield, competing with the total loss of the starting material. The enhanced reactivity during the disubstitution was furthermore explained by the increased solubility of the *meso* monosubstituted OEPs in THF.

OEP **1** was on the other hand destroyed when added to prepared 4-hydroxy-, 2- and 4-methoxyphenyl lithium during the *meso* monosubstitution, whereas no reaction occurred when 4-trifluoromethylphenyl lithium was used. The latter is only stable at -40 °C and the lack of reaction was explained by the low solubility of OEP **1** in THF at low temperatures. When on the other hand 3-trifluoromethylphenyl lithium was used, which is stable at room temperature, the OEP **6** could be prepared in good yield (64%) and the difference in reactivity was explained by a) the better solubility of OEP at room temperature and b) as due to the altered reactivity of the lithiate.¹²

However, W. Kalisch prepared successfully 5-(2,5-dimethoxyphenyl) OEP **219** in 40% yield⁹ and 5-(4-NH₂-phenyl) OEP **220** was obtained by I. Bischoff in 72% yield⁴ as shown in figure 2.2.1 and the success of the reactions might be due to better adjusted equivalents of the reagent and different temperature conditions. Low yields were also observed with acenaphthyl and 2-naphtyl lithium as reagents and the respective OEPs **233** and **234** were isolated in 31% and 26% yield only.

However, the introduction of an anthracenyl residue was also attempted several times. The respective translithiate was generated in ether, THF or petrol ether with low and high equivalents of *n*-BuLi and 9-bromoanthracene, but showed in all cases no reaction with OEP **1**, while a mixture of OEP **1** and a silver, shiny anthracene derivative was obtained. Geometric factors such as *meso*- β hindrance and the low solubility of the lithiate in THF were related to the lack in reaction. However, difficulties occurred also when temperature sensitive translithiates e.g. nitrophenyl-, pyridinyl-, quinolinyl- and thiazolyl lithiates were used. The translithiates had to be kept all times at low temperatures and OEP **1** was destroyed quickly, when added, due to the remaining

excess of *n*-BuLi. In those cases also traces of the butylated OEP **16** could be isolated afterwards.

The OEPs **4–8** were furthermore used subsequently in the disubstitution step as they were isolated in highest yields and the respective synthesis will be reported in the chapters 2.2.3 and 2.2.4. Additionally, also the in figure 2.2.1.1 shown tri- and tetrasubstituted OEPs **235** and **11** could be isolated in traces during the *meso* monosubstitution, reflecting the affinity of the respective translithiates to OEP **1**.

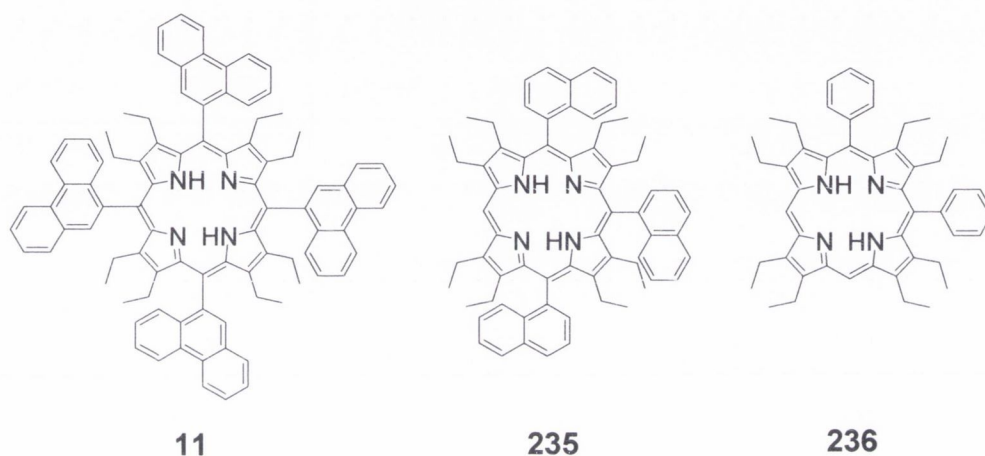


Fig. 2.2.1.1. Formed by-products during the *meso* monosubstitution.

The OEPs **11** and **235** were obtained as polar, dark green fractions and could be identified after accumulation by repeating the reaction. A similar green by-product was also observed during the formation of 5-(4-*n*-pentylphenyl) OEP **5**, but couldn't be characterized afterwards. The elution of the green by-products was carried out by adding EtOH or MeOH to the eluent. Else wise, when 12 instead of 6 equivalents of phenyllithium were used, also the in figure 2.2.1.1 shown disubstituted 5,10-bisphenyl OEP **236** could be obtained. The yield was high (77%) and smaller amounts of the *meso* monosubstituted 5-phenyl OEP **4** could be separated easily. 5,10-Bisphenyl OEP **236** dissolves with a brown-orange colour in dichloromethane and can be eluted from silica gel by adding acetone or ethylacetate to the solvent.

In order to classify the reactivity of OEP **1** towards organo lithium reagents, reactions carried out with OEP **1** can be furthermore compared to reactions performed with porphyrin **67**. Porphyrin **67** was only recently obtained from tetrakis-*tert*-butylporphyrin¹⁸

in an easy manner and was derived in *meso* position afterwards by nucleophilic substitution as shown in table 2.2.1.2. As it can be seen, both porphyrins show similar trends, whereas the yields for porphyn were usually lower and could be explained by its decreased solubility.

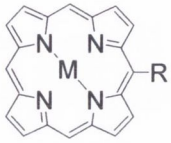
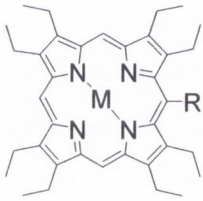
R =	 237-240		 	
	M=2H	M=Ni	M=2H	M=Ni
<i>n</i> -butyl	237 , 48%	-	16 , 50%	211 , >95%
<i>s</i> -butyl	-	-	228 , 11%	241 , 82%
<i>tert</i> -butyl	238 , 4%	-	-	-
phenyl	239 , 65%	-	4 , 90–99%	242 , 65%
2-methoxyphenyl	240 , 17%	-	-	-
3-methoxyphenyl	-	-	230 , 3%	-
(2,5-bis-methoxyphenyl)	-	-	218 , 27% ¹³	243 , 60%

Table 2.2.1.2. Nucleophilic substitution with organo lithium reagents on OEP **1** and on porphyn **67**.^{1,16}

The butylation of H₂OEP **1** and free base porphyn **67** proceeded furthermore in 48% and 50% yield, whereas a phenyl residue was introduced into porphyrin with lower yield (65%) relative to OEP **1** (90-99% yield). For both porphyrins, the introduction of a methoxyphenyl substituent was difficult and was achieved in higher yield when Ni(II)OEP **226** was used and indicated again the difference in reactivity of methoxy lithiates compared to other aryl lithiates. However, *s*-butylation wasn't carried out with porphyn, but is expected to proceed easier than with OEP as the steric repulsion between the β -positions and the incoming *meso* substituent decreases. Furthermore, also a *tert*-butyl group could be introduced in the *meso* position of porphyn (4% yield) suggesting that it could be also derived with *s*-BuLi.

2.2.2 Regio selective synthesis of *meso* 5,10-disubstituted OEPs

First synthesis of *meso* 5,10-disubstituted OEPs with organo lithium reagents was reported by W. W. Kalisch.⁹ He prepared the in figure 2.1.2.1 and 2.1.3.1 shown 5-(*n*-butyl)-10-(2,5-dimethoxyphenyl) Ni(II)OEP **214** and 5,10-bis(*n*-butyl)OEP-15-(2,5-dimethoxyphenyl) OEP **215** in 50% yield each with *in situ* generated 2,5-dimethoxyphenyllithium.⁹ He used 1/27/28 equivalents of 5-*n*-butyl Ni(II)OEP **211**/bromide and *n*-BuLi for the synthesis and applied those equivalents also to the trisubstitution step, while starting with 5,10-bis(*n*-butyl) Ni(II)OEP **212**. Afterwards I. Bischoff obtained also the in figure 2.2.2.1 shown disubstituted free base OEPs **244** and **245** in 61% and 65% yield.³

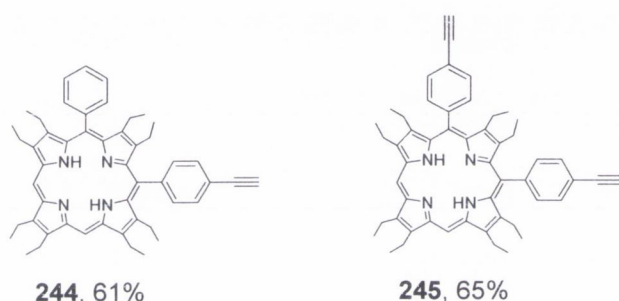
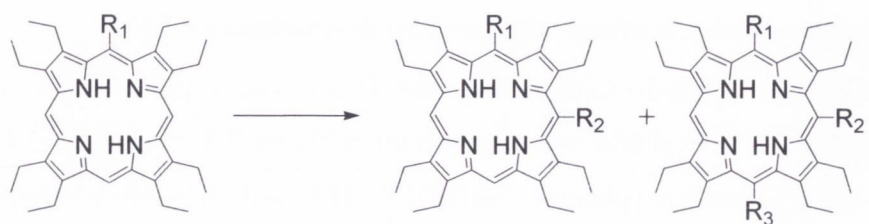


Fig. 2.2.2.1. 5,10-AB- and 5,10-A₂-type OEPs obtained by I. Bischoff.³

Unfortunately, I. Bischoff didn't describe the reaction conditions in her thesis, while vague information could be obtained from the corresponding article.³ She probably used 1/28/53 equivalents of the respective *meso* monosubstituted OEP, the corresponding bromide and *n*-BuLi. However, I. Bischoff could show that both, nickel (II) and free base OEPs worked conveniently well in the di- and trisubstitution step. During the disubstitution furthermore, exclusively 5,10 regio selectivity, as shown in figure 2.2.2.1, was observed and was discussed by M. O. Senge, I. Bischoff and X. Feng in the respective articles.^{5,6,8}

With the aim to continue I. Bischoff's work and to prepare useful novel OEPs, it was decided to use the in chapter 2.2.1 shown OEPs **5** to **8** for further synthesis as well as 5-phenyl OEP **4** due to its easy accessibility.



	R ₁	R ₂	Yield (1/%)
246	phenyl	9-anthracenyl	16*
247	phenyl	9-phenanthrenyl	13*-92
248	phenyl	1-naphthyl	47
249	phenyl	4-dimethylaminophenyl	79
250	phenyl	4- <i>n</i> -pentylphenyl	45
251	phenyl	4-bromophenyl	46
252	phenyl	3-methoxyphenyl	4*
253	3-trifluoromethylphenyl	4-dimethylaminophenyl	48
254	4- <i>n</i> -pentylphenyl	4- <i>n</i> -pentylphenyl	47
255	4- <i>n</i> -pentylphenyl	9-anthracenyl	38
256	4- <i>n</i> -pentylphenyl	9-phenanthrenyl	16*
257	1-naphthyl	1-naphthyl	47
258	1-naphthyl	4- <i>n</i> -pentylphenyl	36
9	9-phenanthrenyl	9-phenanthrenyl	43
259	9-phenanthrenyl	1-naphthyl	46
260	9-phenanthrenyl	4-dimethylaminophenyl	71

Table 2.2.2.1. Synthesis of *meso* 5,10-disubstituted octaethylporphyrins. * = Also the respective *meso* ABA trisubstituted OEP was obtained as shown in chapter 2.2.4.

The in table 2.2.2.1 shown novel *meso* 5,10- A_2 and AB disubstituted OEPs were derived from those successfully during the PhD and in some cases, also the respective ABA (R_1 and $R_3=A$) trisubstituted OEPs were obtained in the same reaction step. When this was the case, the yield of the respective disubstituted OEP decreased drastically as will be discussed in section 2.2.4. However, the separation of di- and trisubstituted OEPs was carried out with ease and *meso* trisubstituted OEPs were obtained for all reactions displaying a star besides the yield as shown in table 2.2.2.1. The ABA OEPs were furthermore obtained when 9-phenanthrenyllithium, 3-methoxyphenyllithium or 9-anthracenyllithium were used, while the exception was formed by the reaction affording the disubstituted OEP **255**, which could be isolated as a single compound in 38% yield, using high equivalents of 9-bromoanthracene and *n*-BuLi.

The in table 2.2.2.1 displayed 5,10 *meso* AB disubstituted OEPs were obtained in good to excellent yield (36% to 98%), they were produced exclusively, while the yields decreased to 13% to 16% for the OEPs **246**, **247** and **256**, when the respective trisubstituted OEP was formed in the same reaction step. The highest yields were furthermore obtained for the OEP **260**, **247** and **249**, which proceeded most smoothly (71% to 98% yield). In contrast to the *meso* monosubstitution, also all reactions with 4-dimethylaminophenyl lithium could be carried out with ease and in good yields (48% to 79%), which was related to the better solubility of the starting material relative to OEP **1**. However, individually adjusted equivalents of *n*-BuLi and bromide were used for all reactions; while a ratio of 40/50 equivalents of the respective bromide relative to *n*-BuLi seemed convenient to start with for most reactions as it can be seen in the experimental part and as it will be discussed in chapter 2.2.5. For the reaction resulting in the formation of the OEP **247**, the equivalents were furthermore altered in a second attempt to 43/34 equivalents of bromide/*n*-BuLi and the yield could be increased from 13% to excellent 92%, avoiding the formation of the respective *meso* trisubstituted OEP **287**, while the latter was obtained exclusively with high equivalents of *n*-BuLi as will be described in chapter 2.2.5.2. However, only when 9-phenanthrenyl lithium was used, no excess of *n*-BuLi relative to the bromide was necessary and the OEP **9** could be obtained in 43% yield by the use of 40/40 equivalents of 9-bromophenanthrene/*n*-BuLi besides the *meso* tri- and tetrasubstituted OEPs **10** and **11** in 25% and 7% yield. On the other hand, the use of 30/30 equivalents when started with the OEP **4**, resulted in the formation of the OEP **247** in 13% together with its trisubstituted counterpart, the OEP

287, in 10% yield. Several attempts and the addition of very high equivalents of *n*-BuLi and bromide were furthermore necessary for the preparation of 5,10-bis(1-naphthyl) OEP **257** (bromide/*n*-BuLi = 60/75 equivalents) and could be explained by the low solubility of the starting material in THF. However, the synthesis of *meso* 5,10- A_2 disubstituted OEPs was also followed with high interest as those OEPs were direct precursors of the desired *meso* 5,10- A_2 -15,20- B_2 tetrasubstituted OEPs. The OEPs **9**, **254** and **257** could be prepared successfully in good yield (43%-47%) as shown in table 2.2.2.1. Unfortunately, the synthesis of the in figure 2.2.2.2 shown 5,10-bis(3-trifluoromethylphenyl) OEP failed, what was again explained by the low solubility of the starting material. Even the addition of 60/75 equivalents of bromide/*n*-BuLi, showed no reaction, while the starting material was left intact. On the other hand, the OEP **253** could be obtained successfully and represented an important step towards NLO applications. The OEP **253** was obtained in lower, but good yield (48%) relative to the OEPs **260** and **249**, and was indeed a first mini-push-pull OEP due to its substitution with an electron withdrawing CF_3 group and an electron pushing NMe_2 group as could be shown in chapter 5.

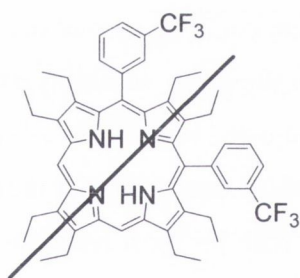


Fig. 2.2.2.2. Not obtained 5,10-bis(3-trifluoromethylphenyl) OEP.

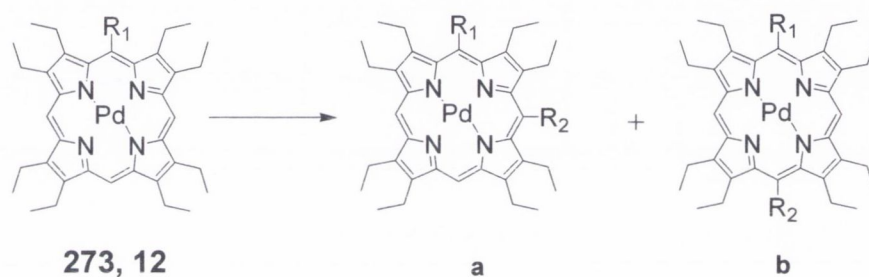
1H NMR investigations showed furthermore that the OEPs **9** and **259** were obtained as mixtures of atropisomers and a detailed discussion will be given in chapter 3.

However, the disubstitution proceeded generally, quicker, easier and in better yield than the *meso* monosubstitution, even it remained still difficult to introduce methoxyphenyl substituents as the starting material got destroyed, when added to the respective lithiate. On the other hand, 9-anthracenyllithium could be successfully used during the disubstitution in contrast to the lack of reactivity during the *meso* monosubstitution (see

chapter 2.2.1) and the respective *meso* disubstituted OEPs **246** and **255** were isolated in low to good yields (16% to 38% yield). The introduction of heteroaromatic residues such as pyridinyl and hydroxynaphthyl was also not possible, while attempts were carried out with easy accessible 5-phenyl OEP **4**. The temperatures had to be held low for those lithiates at all times and when OEP **4** was added, its quick destruction was observed due to the use of excess *n*-BuLi, which was necessary for other reactions.

2.2.3 Synthesis of A₂ and AB substituted Pd(II)OEPs from the respective *meso* monosubstituted Pd(II)OEPs

Meso monosubstituted Pd(II)OEPs showed an increased reactivity towards organo lithium reagents in comparison to Pd(II)OEP **2**, which didn't react neither with *n*-BuLi nor with *s*-BuLi and for which a pink-red product was indicated in TLC when phenyl lithium was added, while it couldn't be isolated.



A	B	R ₁	R ₂	Yield* [1/%]
274	275	<i>n</i> -butyl	<i>n</i> -butyl	82 [#]
276	277	phenyl	<i>s</i> -butyl	37
278	279	9-phenanthrenyl	<i>s</i> -butyl	11

Table 2.2.3.1. Substitution reactions carried out on *meso* monosubstituted Pd(II)OEPs with *n*- and *s*-BuLi; 10 equivalents, -60 °C, THF; *overall yield, [#]the mixture contained also smaller amounts of 5-*n*-butyl Pd(II)OEP **17**.

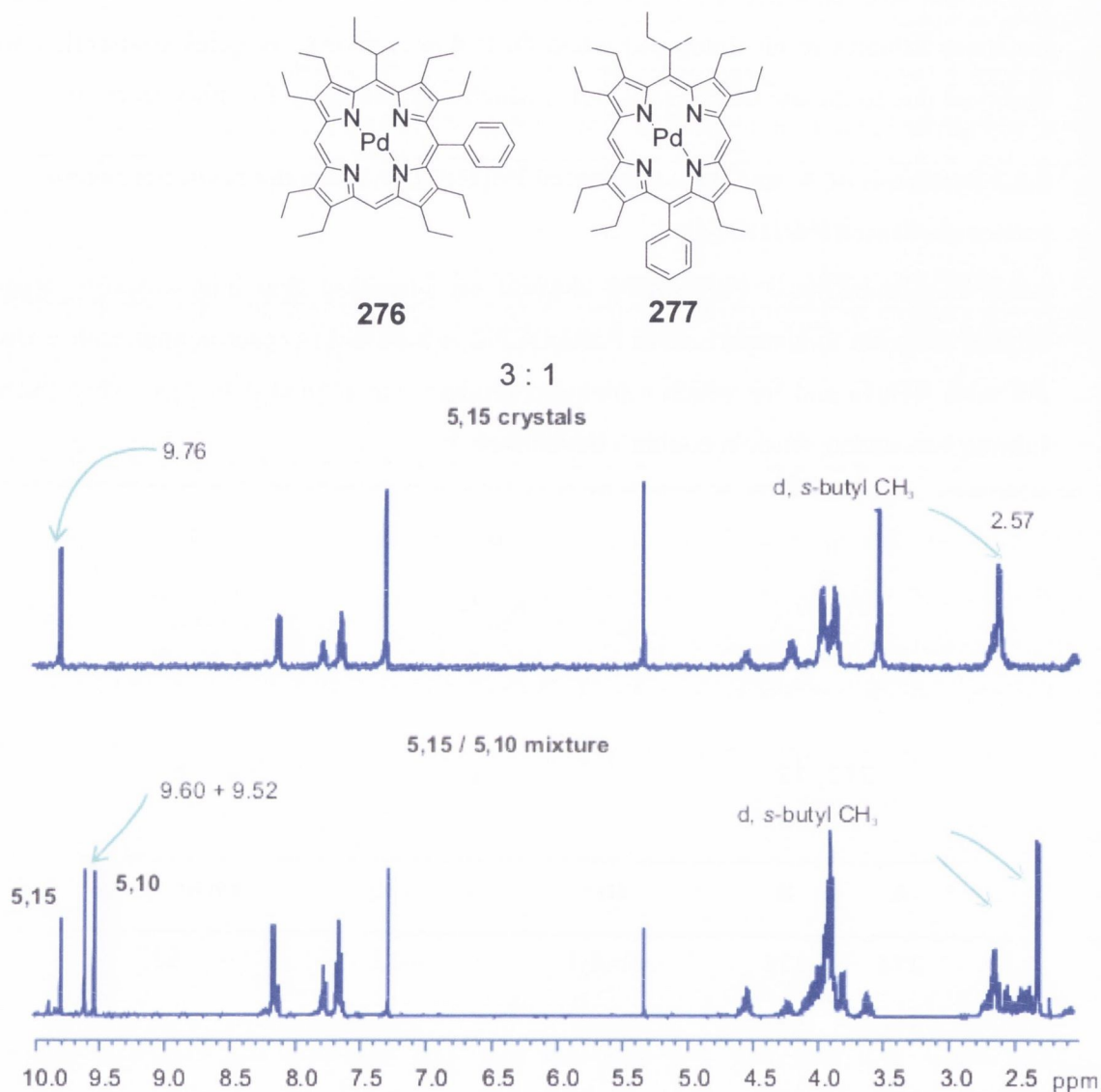


Fig. 2.2.3.1. Structure and ¹H NMR spectrum (10-2.5 ppm) of 5-phenyl-15-*s*-butyl Pd(II)OEP **277** (top) and of the mixture with its regio isomer **276** (bottom, 5,10/5,15 = 3/1).

However, Pd(II)OEP derivatives were also described to be accessible with electrophiles and 5-methyl Pd(II)OEP **166** was prepared accidentally in 1972 by Grigg *et al.* with trifluoromethyl sulfonate and Pd(II)OEP **2** (not shown).¹⁹

During this work, chromatographically inseparable mixtures of 5,10- and 5,15 disubstituted Pd(II)OEPs were obtained when *n*- or *s*-BuLi was added to 5-phenyl Pd(II) **273**, 5-*n*-butyl Pd(II)OEP **17** and 5-(9-phenanthrenyl) Pd(II)OEP **12** as shown in table 2.2.3.1. This result was in contrast to the observed high regio selectivity described in the

previous chapter for the disubstitution of free base OEPs and the loss of regio selectivity was accorded to the influence of the newly introduced heavy metal atom, which disfavoured a nucleophilic attack of the porphyrin, making both reaction sites, the 10- and the 15-position, more attractive, while also the strength of the reagent and the fastness of the reaction were related to the loss of selectivity. However, the yields were observed to be higher, the smoother the reaction was e.g. when *n*-BuLi was used instead of *s*-BuLi. Additionally, the in table 2.2.3.1 displayed regioisomers **276** and **277** could be separated by precipitation from MeOH/dichloromethane, yielding 9% of the *meso* 5,15 disubstituted Pd(II)OEP **277**, while the *meso* 5,10 disubstituted Pd(II)OEP **276** remained in solution. The ratio of the regioisomers was furthermore determined from the intensities of the singlets displayed for the *meso* protons in the ^1H NMR spectrum as shown in figure 2.2.3.1.

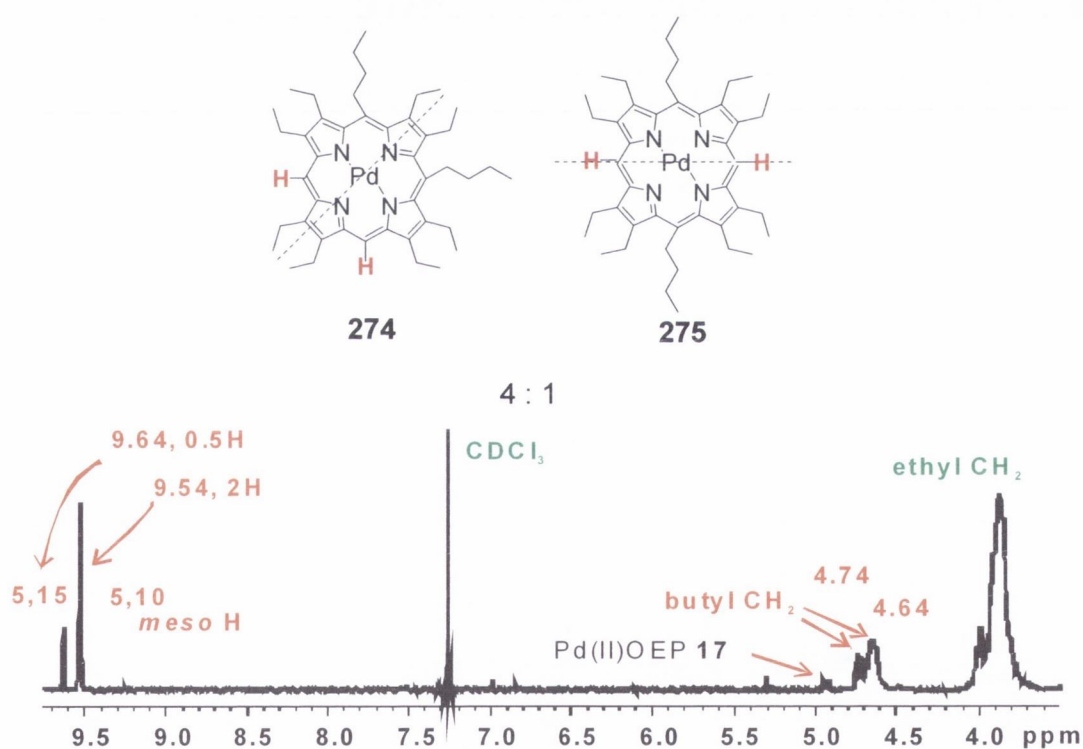


Fig. 2.2.3.2. Downfield ^1H NMR spectrum of the mixture of 5,10- and 5,15-bis(*n*-butyl) Pd(II)OEP **274** and **275** (4/1 ratio); the *meso* proton peaks of the contamination with 5-*n*-butyl Pd(II)OEP **17** are not displayed, while the respective *n*-butyl CH_2 signal can be seen at 4.93 ppm.

The ^1H NMR spectrum of the mixture of 5,10- and 5,15-bis(*n*-butyl) porphyrinato palladium **274** and **275** is furthermore shown in figure 2.2.3.2. Both were isolated in a 4/1 ratio (5,10/5,15), containing also impurities of the starting material and were prepared by addition of *n*-BuLi to 5-*n*-butyl Pd(II)OEP **17**. The ^1H NMR spectrum of the mixture of 5-(9-phenanthrenyl)-10-*s*-butyl Pd(II)OEP **278** and 5-(9-phenanthrenyl)-15-*s*-butyl Pd(II)OEP **279** is shown in figure 2.2.3.3.

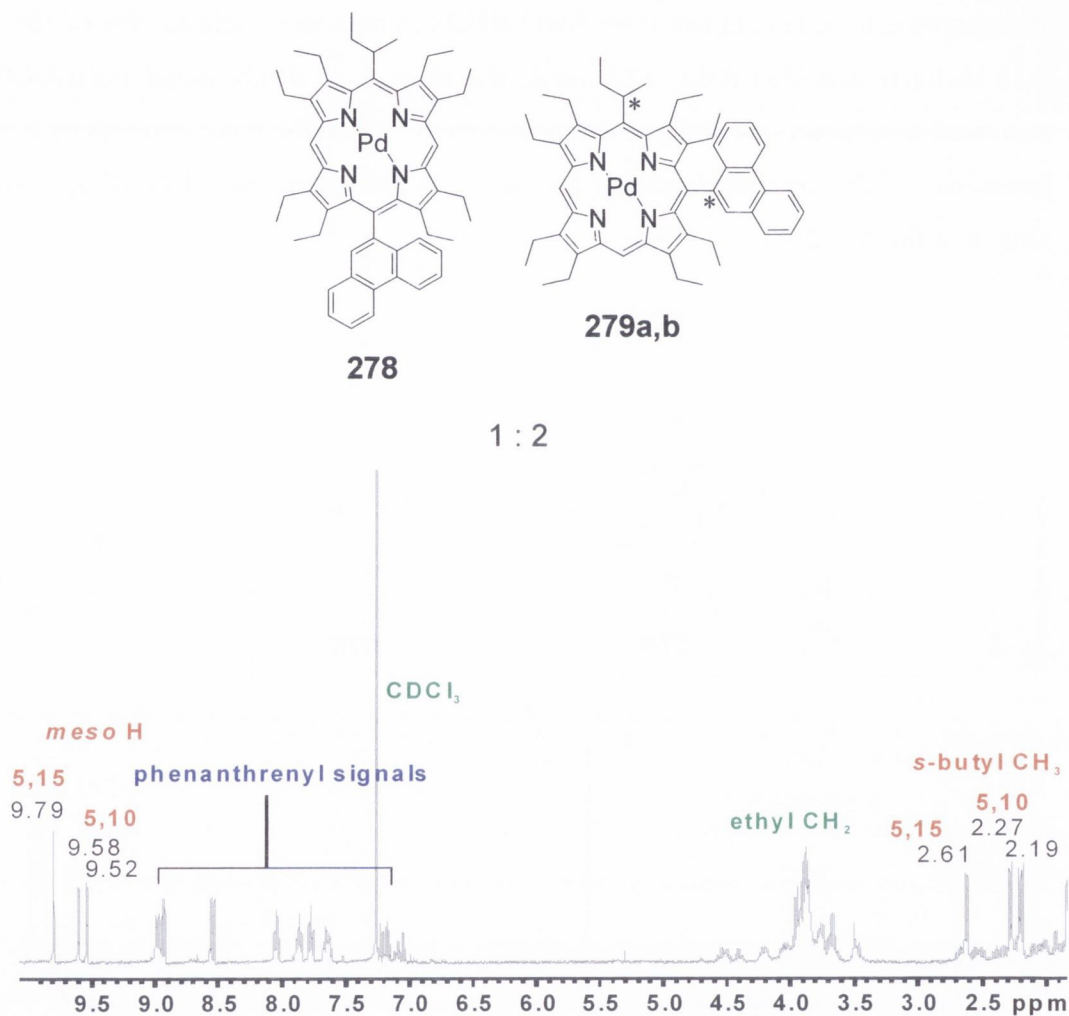
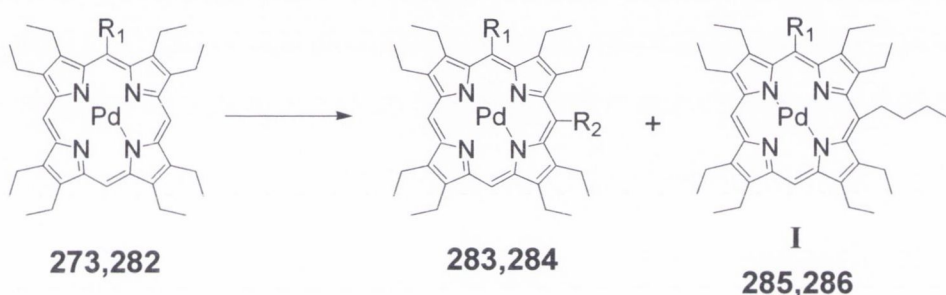


Fig. 2.2.3.3. Structures and ^1H NMR spectrum of the mixture of the 5,10 and 5,15-regioisomers **278/279a,b**.

The 5,10/5,15 ratio was determined as 2/1 (statistical ratio). The *meso* proton signal of the 5,15 substituted OEP **279** appeared downfield shifted at 9.79 ppm, while two split

singlets were displayed at 9.58/9.59 and 9.52/9.53 ppm for the 5,10 regioisomer **278**, which was obtained in a 1/1 ratio of the two possible diastereoisomers **278a,b** as shown in figure 2.2.3.3. Additionally, also other signals appeared double, corresponding to **278a,b**. For example three singlets were displayed for the 8'-phenanthrenyl proton as well as three *s*-butyl CH₃ doublets at 2.61, 2.27 and 2.19 ppm, which belonged to the OEPs **278** and **279a,b**.

In contrast to the substitution with *n*- and *s*-BuLi, the substitution carried out with 1-naphthyl lithium on 5-phenyl Pd(II)OEP **273** or 5-(1-naphthyl) Pd(II)OEP **282** proceeded slowly and with re-established 5,10 regio selectivity as shown in table 2.2.3.2.



	R ₁	R ₂	<i>n</i> -BuLi (equiv)	bromide (equiv)	Yield (1/%)	I (1/%)
-	phenyl	1-naphthyl	42	38	-	-
283	phenyl	1-naphthyl	40	31	+*	-
283	phenyl	1-naphthyl	66	22	+*	-
285	phenyl	1-naphthyl	95	25	-	44
286	1-naphthyl	1-naphthyl	80	30	-	+~
284	1-naphthyl	1-naphthyl	75	60	61 [#]	-

Table 2.2.3.2. Optimization reactions carried out using *meso* monosubstituted Pd(II)OEPs in the disubstitution step; * a not separable mixture of 5-(1-naphthyl)-10-phenyl Pd(II)OEP **283** and the respective starting material was obtained; ~ an exact yield could not be obtained due to a high amount of impurities; [#] the OEP **284** could be separated from traces of starting material and was afforded as a mixture of the respective atropisomers as will be described in chapter 3.

Furthermore, full conversion was only achieved, when high equivalents of the reagents were used e.g. 60/75 equivalents of 1-bromonaphthalene and *n*-BuLi resulting in the formation of 5,10-bis(1-naphthyl) Pd(II)OEP **284** in excellent 61% yield. However, previous attempts were also carried out with easier accessible 5-phenyl Pd(II)OEP **273** as shown in table 2.2.3.2 and produced inseparable mixtures of starting material and product or when the *n*-BuLi equivalents were largely increased, 5-(1-naphthyl)-10-*n*-butyl Pd(II)OEP **286** was obtained in a mixture with naphthalene after precipitation from MeOH/dichloromethane and 5-*n*-butyl-10-phenyl Pd(II)OEP **285** could be isolated in 44% yield respectively from 5-phenyl Pd(II)OEP **273**. 5-*N*-Butyl-10-phenyl Pd(II)OEP **285** could be furthermore identified by its ¹H NMR spectrum in comparison to the respective free base OEP and also a crystal structure was obtained (not shown).

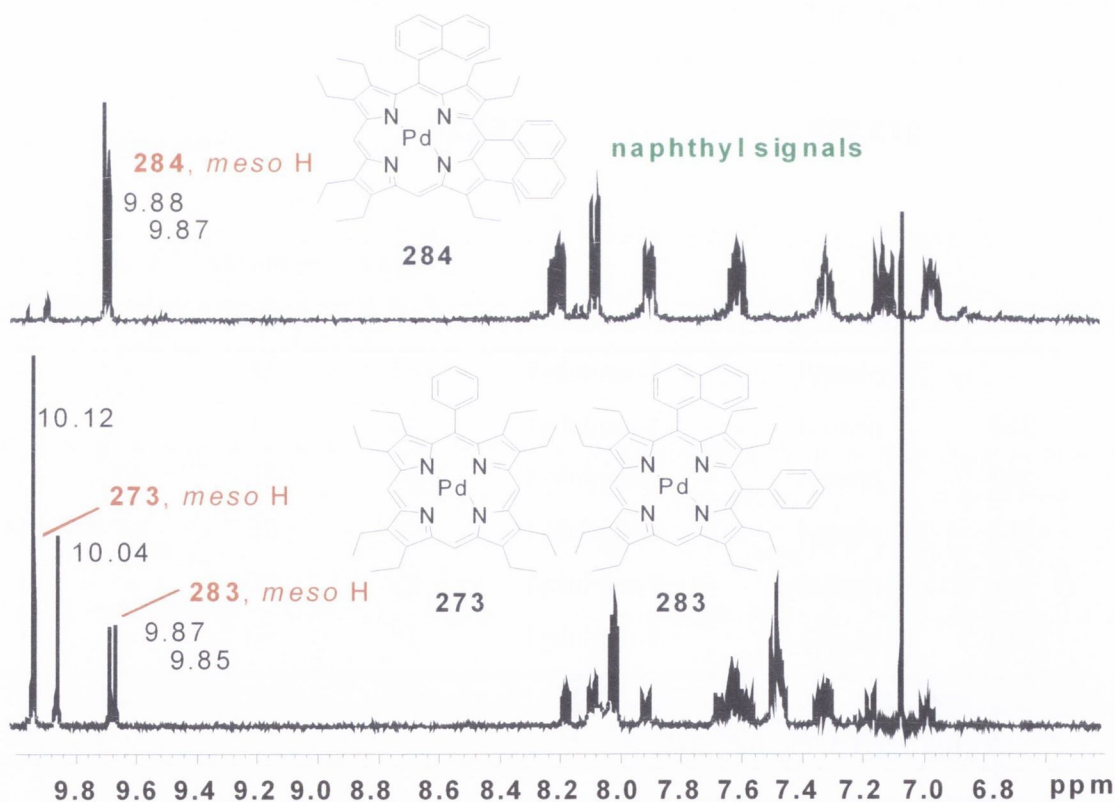


Fig. 2.2.3.4. Downfield ¹H NMR spectrum of 5,10-bis(1-naphthyl) Pd(II)OEP **284** (top, two atropisomers) and the mixture of 5-phenyl Pd(II)OEP **273** and 5-(1-naphthyl)-10-phenyl Pd(II)OEP **283** obtained with 40/31 or 66/22 equivalents of *n*-BuLi and bromide (bottom).

The ^1H NMR spectrum of the mixture of 5-phenyl Pd(II)OEP **273** and 5-(1-naphthyl)-10-phenyl Pd(II)OEP **283** is shown in figure 2.2.3.4 together with the ^1H NMR spectrum of the successfully obtained 5,10-bis(1-naphthyl) Pd(II)OEP **284**. However, as it can be seen in table 2.2.3.2, no reaction occurred with a low *n*-BuLi excess (4 equivalents) as it was also described for the substitution of free base OEPs, while the role of excess *n*-BuLi couldn't be elucidated.

5-(1-Naphthyl)-10-*n*-butyl Pd(II)OEP **286** and 5-*n*-butyl-phenyl Pd(II) OEP **285** were furthermore surprisingly obtained 5,10 regio selective, which was related to the presence of 1-naphthyllithium. The spectrum of 5-(*n*-butyl)-10-naphthyl Pd(II)OEP **286** is displayed in figure 2.2.3.5 and the structure could be determined due to the obtained crystals (not shown). However, the ^1H NMR signals were particularly broadened, which was typical for the substitution with butyl residues due to an enhanced floppiness of the molecule and the increased steric interaction. As a result of the 5,10-AB substitution, two *meso* signals were displayed at 9.79 and 9.73 ppm and are upfield shifted compared to the above shown aryl substituted Pd(II)OEPs. The naphthyl signals appeared as broadened signals between 8.30 ppm and 6.81 ppm and only the doublet at 8.29 ppm could be clearly identified. The blurry signal at 4.76 ppm furthermore, represented the to the porphyrin attached butyl CH₂ group and the CH₂ signals of the ethyl groups as well as the signals of the 2'-butyl CH₂ protons were located between 4.0 and 2.0 ppm e.g. at 3.80 ppm for the butyl signal. The ethyl CH₃ protons as well as the 3'-butyl CH₂ protons appeared at 1.8–2.0 ppm and the broad signal at 0.64 ppm belongs to the butyl CH₃ group.

As the equivalents of 60/75=bromide/*n*-BuLi worked furthermore well, they were also applied to the trisubstitution of free base OEPs as will be reported in chapter 2.2.4 and 2.2.5.2. However, 5,10-bis(1-naphthyl) Pd(II) OEP **284** could be also obtained from the palladium insertion of the respective free base OEP in an overall yield of 15% for the subsequent *meso* substitution with two naphthyl residues and the introduction of palladium (II). On the other hand, the sequence of substitution, palladium insertion and substitution resulted, as described above, in the formation of 5,10-bis(1-naphthyl) Pd(II) OEP **284** in an overall yield of 26% and was therefore more effective than the palladium (II) insertion at the end of the sequence.

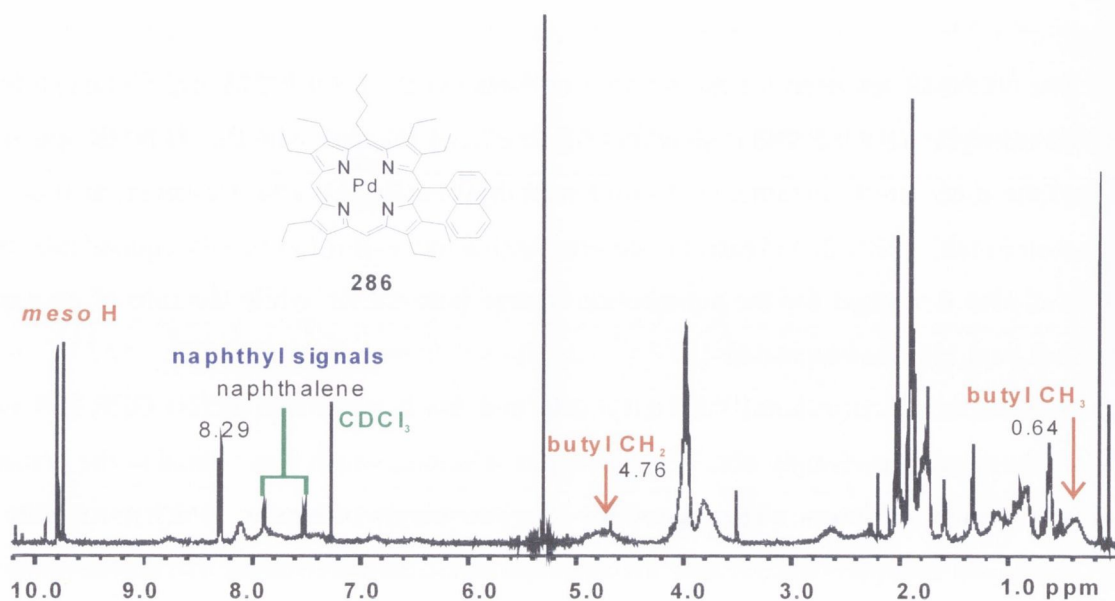
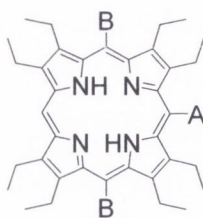


Fig. 2.2.3.5. ^1H NMR spectrum of 5-(1-naphthyl)-10-*n*-butyl Pd(II)OEP **286**.

2.2.4 Synthesis of *meso* trisubstituted OEPs

2.2.4.1 *Meso* ABA and A_3 substituted by-products

During the synthesis of the in table 2.2.2.1 shown *meso* AB and A_2 substituted OEPs, also ABA trisubstituted by-products were obtained and are displayed in table 2.2.4.1.1. The trisubstituted OEPs could be easily separated from the disubstituted OEPs as they eluted only when acetone or ethylacetate were added to the mobile phase. They were furthermore obtained when 9-phenanthrenyllithium, 9-anthracenyllithium or 3-methoxyphenyllithium were used during the disubstitution step. The *meso* trisubstituted OEPs **287** and **288** were obtained in good yield (25-33%), accompanied by the respective disubstituted OEPs **247** and **256** in lower yield (13-16%) and as discussed in chapter 2.2.2. However, the yield remained low (4%) when a methoxyphenyl rest was introduced (OEP **291**), which could be explained by the destruction of the starting material during the reaction due to excess *n*-BuLi at low temperature conditions. The use of anthracenyl lithium resulted in the formation of the trisubstituted ABA OEP **290** in 7% only, while the respective disubstituted OEP **246** was obtained in 16% yield during the same reaction step and the low yields might be also due to low temperature conditions and remaining excess *n*-BuLi.



	A	B	Yield [1/%]
287	phenyl	9-phenanthrenyl	3-33
288	4- <i>n</i> -pentylphenyl	9-phenanthrenyl	25
10	9-phenanthrenyl	9-phenanthrenyl	9-25
289	1-naphthyl	9-phenanthrenyl	14
290	phenyl	9-anthracenyl	7
291	phenyl	3-methoxyphenyl	3

Table 2.2.4.1.1. Trisubstituted ABA by-products, obtained as shown in table 2.2.2.1.

The OEPs **10** and **287** were isolated in variable yields, depending on the equivalents of bromide and *n*-BuLi used as will be discussed in more detail in chapter 2.2.5.2.

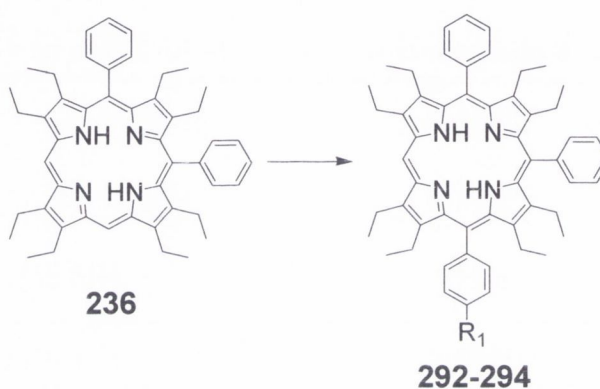
However, the ABA OEPs were symmetrical substituted and could be identified due to a reduced number of signals in the ^1H NMR spectrum relative to AAB substituted OEPs. Except of the OEP **290**, they were else wise obtained as mixtures of atropisomers as will be described in chapter 3. The regio selectivity of the reaction, could be furthermore explained in similarity to the formation of the *meso* 5,10-AB and A_2 substituted OEPs by an attack of the anion in 10- and 20-position at the same time.^{5,6,8}

Additionally, also 5,10,15-tris(1-naphthyl) OEP **235**, shown in figure 2.2.1.1, was obtained during the *meso* monosubstitution. The respective reaction was repeated several times and the OEP **235** could be successfully accumulated and identified.

2.2.4.2 Synthesis of *meso* AAB substituted OEPs

On the way to *meso* 5,10- A_2 -15,20- B_2 substituted OEPs, three novel AAB substituted OEPs could be prepared starting with 5,10-bisphenyl OEP **236**. The prepared OEPs **292** to **294** are shown in table 2.2.4.2.1 and were isolated in low to good yields (17-69%)

against earlier predictions that 5,10-bisphenyl OEP **236** would not be reactive towards organo lithium reagents.³ 5,10-Bisphenyl OEP **236** could be furthermore directly obtained from OEP **1** in 77% yield as described in chapter 2.2.1. However, several attempts were required to produce the shown OEPs **292-294** successfully and complete conversion was only achieved when 60/75 equivalents of the respective bromide and *n*-BuLi were used. The AAB constitution was confirmed as described in chapter 3 by the high number of signals observed in the ¹H NMR and ¹³C NMR spectra.



	R ₁	Yield [1/%]
292	4-dimethylaminophenyl	69
293	4-bromophenyl	38
294	4- <i>n</i> -pentylphenyl	17

Table 2.2.4.2.1. Synthesis of AAB type trisubstituted octaethylporphyrins.

2.2.5 Synthesis of the phenanthrenyl series and of members of the naphthyl series

2.2.5.1 Series described in literature and series attempted during the PhD

Several highly distorted, dodecasubstituted porphyrins were obtained from [4+1] condensation reactions during the past 50 year as described in chapter 1.²⁰⁻²⁸ However, the preparation of so-called series of porphyrins was the most demanding and was also attempted during the PhD. Takeda *et al.* obtained for example series of octaphenylporphyrins^{24,25} and Syrbu and co-workers presented recently the preparation of novel series of OEPs as summarized in chapter 1.^{27,28} Else wise, a novel hybrid-series

situated between planar OEP **1**, flat tetraphenylporphyrin (TPP) **64** and highly distorted OETPP (octaethyltetraphenylporphyrin; Pd(II)OETPP **18**, page 6) could be prepared by W. W. Kalisch in 1996²⁹ by mixed condensation reactions as shown in figure 2.2.5.1.1. He introduced successfully two, four or six ethyl substituents in the β -positions of TPP **64**. Series of *meso* *n*-butyl and phenyl substituted Ni(II)OEPs were furthermore prepared as described in chapter 2.2 by I. Bischoff and W. W. Kalisch^{1,2-6,8-10} using *n*-BuLi and PhLi in a step by step synthesis and producing the respective *meso* mono-, di-, tri- and tetrasubstituted OEPs.

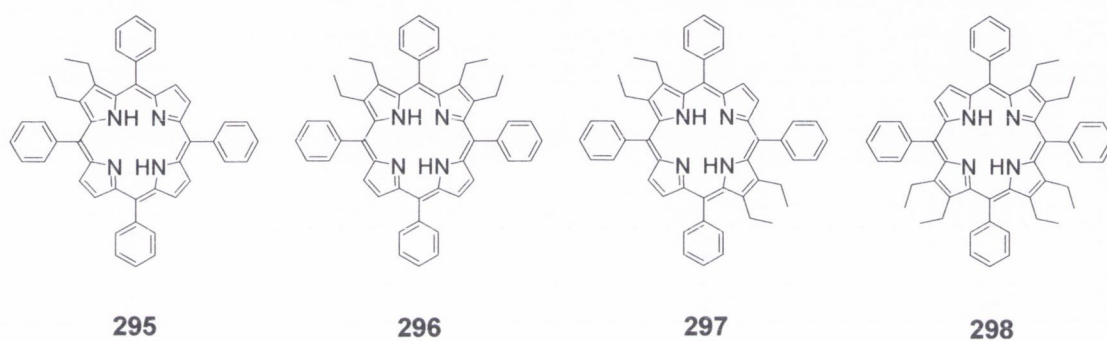


Fig. 2.2.5.1.1. Series of β -ethylsubstituted tetraphenylporphyrins.²⁹

The respective *meso* mono- and disubstituted Ni(II)OEPs were furthermore obtained in 60% to 99% yield for each step, while tri- and tetrasubstitution proceeded with more difficulty in 50% to 70% yield. As shown in scheme 2.2.2 for example 5,10-bisphenyl OEP **236** could be butylated to prepare the OEP **225a** in 57% yield. 5,10,15-Trisphenyl OEP **217** could be prepared from 5,15-bisphenyl OEP **216** in 70% yield as shown in figure 2.1.3.1, while it could not be derived from 5,10-bisphenyl OEP **236** as explained in chapter 2.2. The use of *n*-butyl and *n*-hexyl lithium resulted furthermore during the trisubstitution in some cases in the formation of porphodimethenes, decreasing the yield of the desired porphyrin as described in chapter 2.2 and as shown in scheme 2.2.2, while the in figure 2.2.5.2 shown *meso* A₂B₂ and A₃B OEPs **223** and **225** could be obtained successfully from the step by step substitution in an overall yield of 22% and 26% by I. Bischoff.⁴ However, with the synthesis of series of porphyrins in the past continuous changes in structural, chemical and physical properties could be obtained and it was described that newly incoming *meso* substituents increased the distortion of the OEP,

which on the other hand changed the UV/vis and ^1H NMR properties e.g. a red shift appeared and the shape of the Q bands changed (compare to chapter 4) in the UV/vis spectra and the ^1H NMR NH signals were downfield shifted.

As the investigation of phosphorescence quantum yields and lifetimes was furthermore targeted during this work, the preparation of novel series of OEP was also suggested and it was planned to elucidate the relation of photophysical properties and changes in the 3D shape within a continuing series of OEPs. The synthesis of novel alkyl-series e.g. methyl, *n*-butyl and *s*-butyl Pd(II)OEPs, was aimed and measurements of phosphorescence lifetimes and quantum yields were planned.

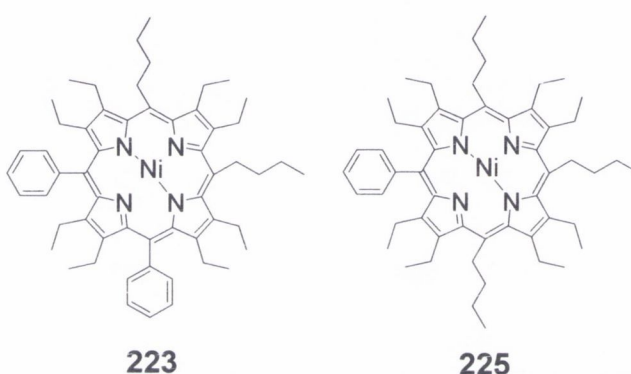


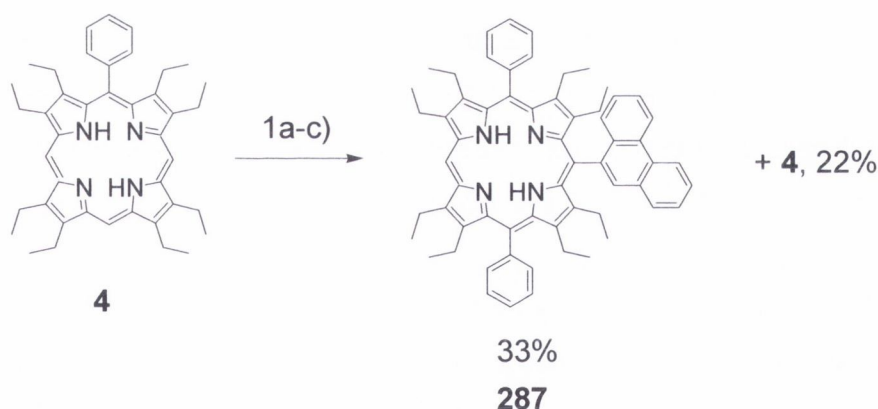
Fig. 2.2.5.1.2. By I. Bischoff synthesized A_3B and A_2B_2 OEPs **223** and **225**.⁴

Unfortunately, those series could not be prepared during the PhD due to the lack of synthetic access when *n*-BuLi, *s*-BuLi and MeLi were added to H_2OEP **1** or the respective *meso* monosubstituted H_2OEPs **16**, **227** and **228** and **17**. For example the synthesis of 5,10-bismethyl OEP failed several times. No product could be isolated and the starting material was destroyed in all cases. The attempted butylation of 5-*n*-butyl OEP **16** produced furthermore an inseparable mixture of 5,10- and 5,15-bis(*n*-butyl) OEP (not shown) in low yield as described previously by W. W. Kalisch,^{9,13} and the switch to 5-*n*-butyl Pd(II)OEP **17** showed similar results as described in chapter 2.2.3. Therefore it was suggested to carry out the synthesis of the butyl and methyl series by using the respective nickel (II) or copper (II) complexes as for example the disubstitution of 5-*n*-butyl Ni(II)OEP yielded in a separable mixture of 5,10-bis(*n*-butyl) Ni(II)OEP and 5,15-bis(*n*-butyl) Ni(II)OEP in 70% and 15% yield as described by W.

W. Kalisch.⁹ However, this way was found to be too laborious and the synthetic target was swapped towards the phenanthrenyl and the 1-naphthyl series, which were prepared alternatively as described in the following sections due to the observed favourable triplet state behaviour of 5-(9-phenanthrenyl) OEP **8** (compare to chapter 5).

2.2.5.2 The phenanthrenyl series and optimization reactions

Optimization reactions were carried out with quickly accessible 5-phenyl OEP **4** to facilitate the preparation of the 9-phenanthrenyl and 1-naphthyl series afterwards. For all reactions a commercially available solution of *n*-BuLi was used, which was stored in the refrigerator for short periods of time and which was added without previous determination of the concentration to the respective bromides. From previous experience, it was assumed that the concentration will vary between 2.5 to 2.3 mol/l, resulting in repeatable and trend setting results. In first attempts, surprisingly, only the trisubstituted 5,15-bis(9-phenanthrenyl)-10-phenyl OEP **287** was obtained exclusively in 33% yield by addition of 9-phenanthrenyl lithium to 5-phenyl OEP **4** as shown in figure 2.2.5.2.1 and table 2.2.5.2.1 and it was also accompanied by 22% of the starting material.

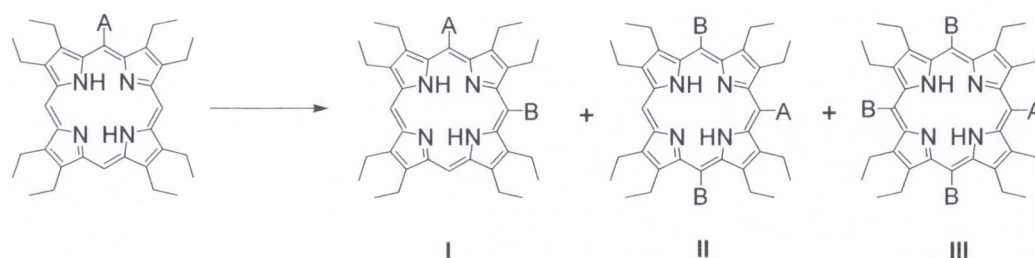


Scheme 2.2.5.2.1. One-pot trisubstitution of the OEP **4**, 1a) 9-bromophenanthrene/*n*-BuLi in ether, $-70\text{ }^{\circ}\text{C}$ to rt for 1h, 1b) addition of the OEP **4** in THF, $-40\text{ }^{\circ}\text{C}$ to rt, 45 min, 1c) H_2O and after 5 minutes DDQ/ CH_2Cl_2 , $-35\text{ }^{\circ}\text{C}$.

For the reaction 37/24 equivalents of *n*-BuLi and 9-bromophenanthrene were used, while with 20/10 equivalents only traces of the green, trisubstituted OEP **287** were

indicated in TLC, but couldn't be isolated afterwards. However, the use of 40/20 equivalents of *n*-BuLi/bromide produced the *n*-butylated OEP (not shown) which was previously described by I. Bischoff.³ With 30/30 equivalents on the other hand, the disubstituted OEP 5-(9-phenanthrenyl)-10-phenyl OEP **247** could be isolated in 13% yield and was separated easily from the also formed trisubstituted OEP **287** (10% yield) besides 5-phenyl OEP **4** in 22% yield. With the aim to obtain a full conversion, 43/34 equivalents of *n*-BuLi/bromide were used afterwards and allowed to prepare 5-(9-phenanthrenyl)-phenyl OEP **247** in excellent 92% yield. Apparently, *n*-BuLi or its derivatives played a role in the further substitution of 5-phenyl OEP **4**, while a detailed investigation was not carried out. As it can be seen in table 2.2.5.2.1, an excess of *n*-BuLi relative to the bromide was found to be needed for all reactions with exception of reactions, which were performed with 9-phenanthrenyl lithium. However, the ratio of *n*-BuLi to bromide was defined for a farther understanding of the outcome of the reaction: With 9-phenanthrenyl lithium a 1/1=1 ratio could be used for most reactions, while a ratio of 1.2 to 1.3 was needed for all other lithiates and ratios >1.3 as well as <1.2 were found to be less likely to produce the desired reaction products. However, a minimum of 32 equivalents of *n*-BuLi were necessary for each substitution. Table 2.2.5.2.1 displays furthermore the reaction details of the synthesis of the anthracenyl substituted AB OEPs **246** and **255**. Several attempts were carried out to prepare 5-(9-anthracenyl) OEP and failed as described in chapter 2.2.1. Due to the increased solubility of *meso* monosubstituted OEPs in THF, the introduction of an anthracenyl residue was then attempted with 5-phenyl OEP **4** and was found to be successful, when high amounts of 9-bromoanthracene and *n*-BuLi were used (50/60 equivalents) as shown in table 2.2.5.2.1. With 5-phenyl OEP **4** furthermore both, the respective di- and trisubstituted OEPs **246** and **290** were obtained in one step in low yield (16% and 7%). When on the other hand the sterical more demanding 5-(4-*n*-pentylphenyl) OEP **5** was used, the disubstituted OEP **255** was obtained exclusively in good yield (38%), whereas also the equivalents of *n*-BuLi and bromide had to be increased (75/60). In regard to prepare the phenanthrenyl series, it was furthermore decided after first reactions, to use a ratio of 1.29 and to increase the amount of *n*-BuLi/bromide to 40/31 equivalents relative to the results obtained from the synthesis of 5-(9-phenanthrenyl)-10-phenyl OEP **247** (reaction with 8% yield). In a first attempt, 5,10-bis(9-phenanthrenyl) OEP **9** was obtained

successfully in 12% yield and was accompanied by the tri- and tetrasubstituted OEPs **10** and **11** in 9% and 11% yield as displayed in table 2.2.5.2.1.



A	B	a*	b [#]	a/b	I	II	III
					Yield [1/%]	Yield [1%]	Yield [1/%]
phenyl	9-phenanthrenyl	20	10	2	-	traces	-
phenyl ^{a)}	9-phenanthrenyl	40	20	2	-	-	-
phenyl	9-phenanthrenyl	37	24	1.54	-	287 , 33	-
phenyl ^{b)}	9-phenanthrenyl	30	30	1.00	247 , 13	287 , 10	-
phenyl ^{c)}	9-phenanthrenyl	32	25	1.28	247 , 8	287 , 8	-
phenyl	9-phenanthrenyl	43	34	1.26	247 , 92	-	-
9-phenanthrenyl	9-phenanthrenyl	40	31	1.29	9 , 12	10 , 9	11 , 11
9-phenanthrenyl	9-phenanthrenyl	40	40	1	9 , 43	10 , 25	11 , 7
9-phenanthrenyl	9-phenanthrenyl	60	60	1	9 , ^{d)}	10 , ^{e)}	11 , 42
4- <i>n</i> -pentylphenyl	9-phenanthrenyl	40	40	1.00	256 , 16	288 , 25	-
phenyl	9-anthracenyl	60	50	1.20	246 , 16	290 , 7	-
4- <i>n</i> -pentylphenyl	9-anthracenyl	75	60	1.25	255 , 38	-	-

Table 2.2.5.2.1. Optimization carried out for the disubstitution and the phenanthrenyl series; *equivalents of *n*-BuLi, [#]equivalents of the respective bromide, a) the starting material was butylated, b) 22% of the starting material were recovered, c) 51% of the starting material were recovered, d) and e) not measured, minor amounts.

Targeting to shift the yield towards the OEP **9**, 40/40 equivalents of *n*-BuLi/bromide were applied afterwards and the yield could be increased to 43%, while 5,10,15-tris(9-phenanthrenyl) and 5,10,15,20-tetrakis(9-phenanthrenyl) OEP **10** and **11** were also

isolated in 25% and 7% yield respectively. However, the use of 60/60 equivalents resulted in the formation of the tetrasubstituted OEP **11** in high yield (42%), accompanied by minor amounts of the di- and trisubstituted OEP **9** and **10**. In this way, each member of the in figure 2 shown phenanthrenyl series could be obtained successfully and palladium (II) insertion was carried out subsequently as will be described in chapter 2.3.

2.2.5.3 The 1-naphthyl series

During the *meso* monosubstitution as described in chapter 2.2.2, also 5,10,15-tris(1-naphthyl) OEP **235** could be isolated and accumulated during repeated reactions. A second green fraction was furthermore obtained and was suggested to be 5,10,15,20-tetrakis(1-naphthyl) OEP, whereas no mass spectrum could be obtained. However, the signals in the respective ^1H NMR spectrum were broadened and weren't sufficient to prove that the green compound was 5,10,15,20-tetrakis(1-naphthyl) OEP. 5,10-Bis(1-naphthyl) OEP **257** and the respective Pd(II)OEP **284** were on the other hand obtained from 5-(1-naphthyl) OEP **7** or the respective *meso* monosubstituted Pd(II)OEP **282** in 65% and 61% yield as reported in chapter 2.2.3 and 2.3 and all prepared members of the 1-naphthyl series are shown in figure 2.2.5.3.1.

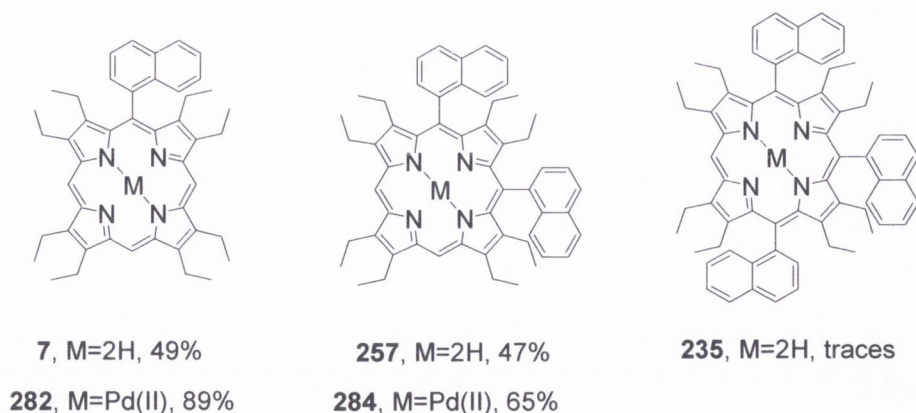


Fig. 2.2.5.3.1. Prepared members of the 1-naphthyl series.

REFERENCES

- 1) M. O. Senge *Acc. Chem. Res.* **2005**, *38*, 9, 733.
- 2) M. O. Senge *Chem. Commun.* **2006**, 243.
- 3) M. O. Senge, I. Bischoff *Tetrahedron Lett.* **2004**, *45*, 1647.
- 4) M. O. Senge, I. Bischoff *Eur. J. Org. Chem.* **2001**, 1735.
- 5) M. O. Senge, I. Bischoff, X. Feng *J. Org. Chem.* **2001**, *66*,26, 8693.
- 6) M. O. Senge, I. Bischoff, X. Feng *Tetrahedron* **2001**, *57*, 5573.
- 7) M. O. Senge, X. Feng *J. Chem. Soc. Perkin Trans. 1* **2001**, 1030.
- 8) M. O. Senge, W.W. Kalisch, I. Bischoff *Chem. Eur. J.* **2000**, *6*,15, 2721.
- 9) M. O. Senge, W. W. Kalisch *Angew. Chem.* **1998**, *110*, 8, 1156.
- 10) M. O. Senge, W. W. Kalisch *Angew. Chem. Int. Ed.* **1998**, *37*, 8, 1107.
- 11) Z.-H. Loh, S. E. Miller, J. Chang, S. D. Carpenter, D. G. Nocera *J. Phys. Chem. A* **2002**, *106*, 11700.
- 12) M. Schlosser (2002): „Organometallics in Synthesis. A Manual“ John Wiley & Sons Ltd.: England, West Sussex.
- 13) A. Botulinski, J. W. Buchler, K. L. Lay, H. Stoppa *Liebigs Ann. Chem.* **1984**, *7*, 1259.
- 14) J. W. Buchler, L. Puppe *Liebigs Ann. Chem.* **1974**, 1046.
- 15) J. W. Buchler, L. Puppe *Liebigs Ann. Chem.* **1970**, *740*, 142.
- 16) W. W. Kalisch, Dissertation 1997 (Freie Universität Berlin):„Synthese, Modifizierung und Strukturuntersuchung neuer Tetrapyrrolysysteme mit variabler Konformation als Modelverbindungen natürlicher Pigmente.“, p. 110, 157ff.
- 17) T. E. O. Screen, I. M. Blake, L. H. Rees, W. Clegg, S. J. Borwick, H. L. Anderson *J. Chem. Soc. Perkin Trans. 1* **2002**, 320.
- 18) S. Neya, N. Funasaki *Tetrahedron Lett.* **2002**, *43*, 1057.
- 19) R. Grigg, G. Shelton, A. Sweeney *J. Chem. Soc. Perkin I* **1972**, 1789.
- 20) M. O. Senge (2000). In: The porphyrin Handbook, Vol. 10, p. 264. Ed.: K.M. Kadish; R. Guillard; K. M. Smith. San Diego: Academic Press.
- 21) S. Tsuchiya *Chem. Phys. Lett.* **1990**, *169*, 608.
- 22) R. Guillard, K. Perie, J.-M. Barbe, D. J. Nurco, K. M. Smith, E. Van Caemelbecke, K. M. Kadish *Inorg. Chem.* **1998**, *37*, 973.
- 23) K. Perie, J.-M. Barbe, P. Cocolios, R. Guillard *Bull. Soc. Chim. Fr.* **1996**, *133*, 697.

- 24) J. Takeda, T. Ohya, M. Sato *Chem. Phys. Lett.* **1991**, 183, 384.
- 25) J. Takeda, M. Sato *Chem. Pharm. Bull.* **1994**, 42, 1005.
- 26) J. Takeda, M. Sato *Chem. Lett.* **1994**, 2233.
- 27) A. Syrbu, L. Lyobumova, A. S. Semeikin *Chem. Heterocyclic Comp.* **2004**, 40, 10, 1262.
- 28) S. A. Syrbu, T. V. Lyubimova, A. S. Semeikin *Russ. J. Gen. Chem.* **2001**, 71, 10, 1656.
- 29) M. O. Senge, W. W. Kalisch *Tetrahedron Lett.* **1996**, 37, 8, 1183.

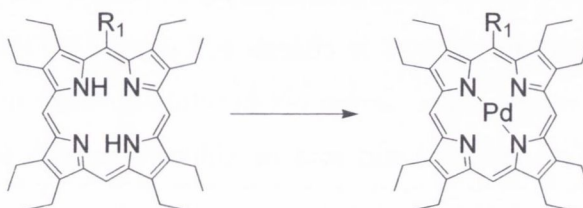
2.3 Palladium (II) and platinum (II) insertion

2.3.1 Palladium (II) insertion

For photophysical measurements palladium (II) was inserted into several *meso* monosubstituted OEPs and the respective triplet state dynamics of 5-methyl-, 5-*n*-butyl, 5-phenyl, 5-(4-trifluoromethylphenyl), 5-(4-*n*-pentylphenyl)-, 5-(1-naphthyl)-, 5-(9-phenanthrenyl) and 5,15-bis(9-phenanthrenyl)-10-phenyl Pd(II)OEP **12/16/166/273/283/300/301/304** will be reported in chapter 6. Common Pd (II) sources are PdCl₂ and Pd(OAc)₂ and the reactions are carried out in refluxing DMF or acetonitrile with PdCl₂ and in a mixture of MeOH/acetic acid or chloroform with Pd(OAc)₂. Additionally, K₂CO₃, Na₂CO₃ or NaCH₃COO can be added as bases to increase the reaction rate.¹ Yields vary between 60% and 99%.^{1,2,3}

The in table 2.3.1.1 shown, palladium (II) complexes were obtained in good to excellent yield (37% to 98%) and the synthesis was carried out with palladium acetate, first in DMF and later in chloroform/methanol. Two equivalents of palladium (II) acetate were added and the reaction was performed in an air atmosphere. The stirring times varied between five minutes to twelve hours at ambient temperature or under gentle heating at 40 °C depending on the *meso* substituent. Initially, the palladium insertions were performed by adding 10 to 20 equivalents of base e.g. NaCH₃COO in accordance to literature.¹ Unfortunately, low yields were obtained relative to the palladium (II) insertion without base and for further reactions the base was avoided.³ When for example, palladium (II) was introduced into 5-phenyl OEP **4**, the yield was increased from 58% to 92% without base and similar was observed for the palladium (II) insertion into 5-(9-phenanthrenyl) OEP **8** (60% with base and 82% without base). However, the palladium insertion was not repeated for 5-methyl Pd(II)OEP **166** and the displayed yield of 37% was obtained by adding 10 equivalents of sodium acetate. Furthermore, when the palladium (II) insertion of 5-*s*-butyl OEP **228** was performed with 10 equivalents of base in DMF, an inseparable mixture of Pd(II)OEP **2** and 5-*s*-butyl Pd(II)OEP **299** was isolated in an 1/4 ratio (measured by the comparison of the *meso* signal intensities) and with calculated yields of 53% for 5-*s*-butyl Pd(II)OEP **299** and 22% for Pd(II)OEP **2**. The combination of base and palladium acetate corresponded furthermore to Suzuki type coupling reaction conditions and seemed to have activated the *meso* monosubstituted OEPs, resulting in either, the elimination of the substituent or

the destruction of the porphyrin. The palladium (II) insertion of 5-(2-naphthyl) OEP **233** was also only achieved in low yield (20%) whereas no base was added. Relative to that, 5-(2-naphthyl) OEP **233** was also obtained only with difficulties (31%) from OEP **1** as described in chapter 2.2.2 and might have been unstable under the conditions used for the palladium (II) insertion.



Pd(II)OEP	R ₁	Yield (1/%)
166	methyl	37
17	<i>n</i> -butyl	100
299	<i>s</i> -butyl	53*
273	phenyl	58–92
300	3-trifluoromethylphenyl	93
301	4- <i>n</i> -pentylphenyl	82
282	1-naphthyl	89
302	2-naphthyl	20
303	acenaphthyl	98
12	9-phenanthrenyl	60–82

Table 2.3.1.1. Palladium (II) insertion in *meso* monosubstituted OEPs; *an inseparable mixture with 22% Pd(II)OEP **2** was obtained.

However, S. Vinogradov and co-workers carried out the palladium insertion into basic and strongly distorted TBPs and in opposition to the palladium (II) insertion into nearly

planar and therefore less basic *meso* monosubstituted OEPs, the palladium insertion into TBPs was slow and usually not complete without addition of base (NEt_3 or K_2CO_3). In more difficult cases, S. Vinogradov and co-worker changed also to reaction conditions, using PdCl_2 in refluxing benzonitrile.⁴ Under these conditions, first the formation of a palladium (II) benzonitrile complex could be observed due to the high affinity of palladium (II) to the aromatic π system. Gaseous HCl was leaving and the newly formed palladium (II) complex reacts subsequently smoothly with the porphyrin. Similar conditions were furthermore needed for the platinum (II) insertion described in the following chapter. In accordance to literature furthermore Pd(II)OEP **2** was obtained from H_2OEP **1** in 77% yield at room temperature in $\text{MeOH}/\text{chloroform}$ (no base) and Pd(II)OETPP **18** from H_2OETPP in 55% yield by refluxing the highly distorted porphyrin for two hours at 50°C in DMF with 20 folds of NaOAc . The UV/vis spectrum of Pd(II)OETPP **18** was displayed in the introduction (aims and objectives) and will be compared to the spectrum of 5,10,15,20-tetrakis(9-phenanthrenyl) Pd(II)OEP **15** in chapter 5, whereas phosphorescence quantum yields and lifetimes were measured for Pd(II)OEP **2** and are reported in chapter 6.

Palladium (II) was also introduced into a few higher substituted OEPs e.g. 5,10-bis(1-naphthyl) OEP **257** and 5,15-bis(9-phenanthrenyl)-10-phenyl OEP **287**, which are shown in figure 2.3.1.1 as well as into the phenanthrenyl series which was displayed in the introduction and was discussed in chapter 2.2.6.3.

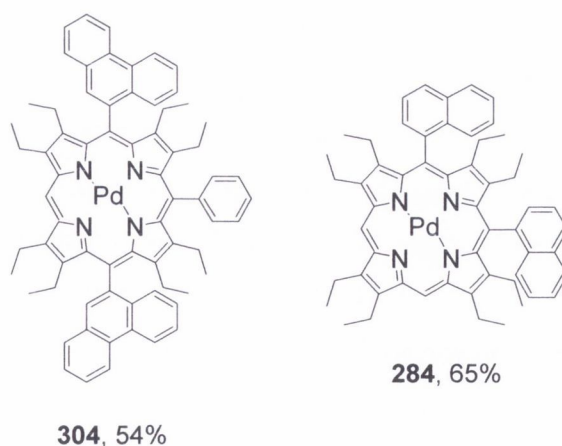


Fig. 2.3.1.1. Synthesized higher substituted Pd(II)OEPs **304** and **284**.

The synthesis of *meso* disubstituted palladium (II) complexes required slightly longer reaction times than the synthesis of *meso* monosubstituted palladium (II) OEPs but proceeded also without base. 5,10-Bis(1-naphthyl) Pd(II)OEP **284** was formed after 2 hours of stirring in MeOH/chloroform in 65% yield and 5,10-bis(9-phenanthrenyl) Pd(II)OEP **13** was afforded in 55% yield after 5 hours of stirring. Showing a higher degree of distortion and therefore an increased basicity, furthermore the palladium (II) insertion into 5,15-bis(9-phenanthrenyl)-10-phenyl OEP **287** and 5,10,15-tris(9-phenanthrenyl) OEP **10** was carried out within 30 minutes under gentle heating to 40–50 °C and argon was applied in the case of **10**. 5,10,15,20-Tetrakis(9-phenanthrenyl) OEP **11** shown in figure 2.2.2.1 and in figure 2 was furthermore treated at room temperature only and was stirred for three days for complete conversion. The palladium (II) insertion of 5,10,15-tris(9-phenanthrenyl) Pd(II)OEP **14** from **10** was achieved in high yield (80%), whereas 5,10,15,20-tetrakis(9-phenanthrenyl) Pd(II)OEP **15** was only obtained in low yield (12%). Additionally, the increased basicity of 5,10,15-tris(9-phenanthrenyl) OEP **14** and 5,10,15,20-tetrakis(9-phenanthrenyl) OEP **15** made it necessary to deprotonate the by elution with MeOH/CH₂Cl₂ from silica gel obtained dications as otherwise the palladium (II) insertion didn't proceed in previous attempts. Deprotonation was carried out by passing the dark green solutions through a short column filled with aluminum oxide and eluting the brown-green free base OEPs with dichloromethane. On the other hand, also the addition of base to the reaction mixture might have achieved the neutralization, but might have also decreased the yields and was therefore avoided. The in chapter 5 displayed UV/vis spectra of the free base porphyrins were furthermore measured after the deprotonation step. Vinogradov *et al.* described also similar for highly distorted, strongly basic *meso* tetrasubstituted TBPs.⁴ The easily formed dications could be only deprotonated with strong base such as DBU or triethylamine and even solutions of dichloromethane/pyridine = 3/1 still contained 50% of the dication whereas in pure pyridine 10% of the TBPs stayed protonated.⁴ However, the basicity of porphyrins was well documented between 1990 and 1992^{5,6,7} and the formation of dications was also described as due to the addition of oxidizing agents circumventing for example the aromatization step towards TBPs (compare to chapter 1).⁴ Furthermore, especially electro active metals e.g. Fe, Mn and Co tend to protonate porphyrins, whereas bivalent metals such as Zn(II), Cu(II), Pd(II) and Ni(II) are less basic. The basicity of the obtained OEPs was furthermore reflected in the downfield shift of the ¹H

NMR NH signals. The respective ppm values will be displayed in chapter 3 and can be explained by the degree of distortion, which increased with each substituent, pushing the NH groups out of the aromatic porphyrin plane and reinforcing therefore their aliphatic character e.g. their basicity. The basic character of the NH groups can be also affected by extended π -conjugation as observed for TBPs, which are weaker bases than comparable not extended porphyrins as shown by Vinogradov and co-workers.⁸ The extended π -system absorbs the electron density from the core nitrogens and makes the porphyrin more electron deficient (decreased basicity), which favors the metal insertion. On the other hand, the metal extrusion for example the removal of palladium (II) or nickel (II), resulted for TBPs in the destruction of the macrocycle.⁸

With PdCl₂, Bhyrappa and Krishnan introduced furthermore palladium (II) into the electron withdrawing groups bearing octabromotetraphenylporphyrin.⁹ The palladium (II) insertion proceeded quickly within 30 minutes by refluxing the porphyrin in a mixture of chloroform and acetic acid and was achieved in high yield (85%) as shown in figure 2.3.1.2.

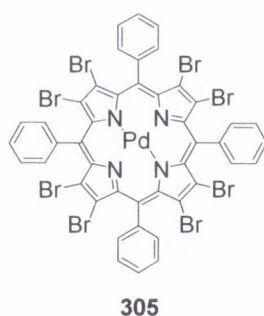
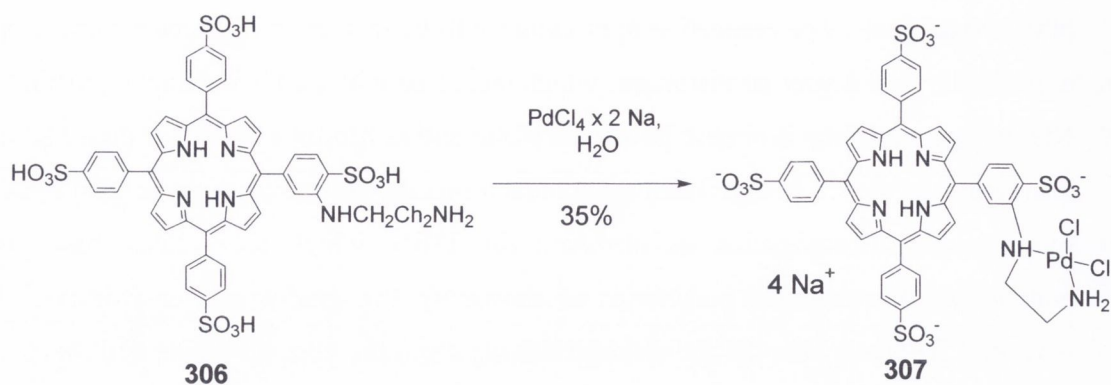


Fig. 2.3.1.2. Palladium (II) porphyrin **305** with electron withdrawing bromo groups obtained by Bhyrappa and Krishnan.⁹

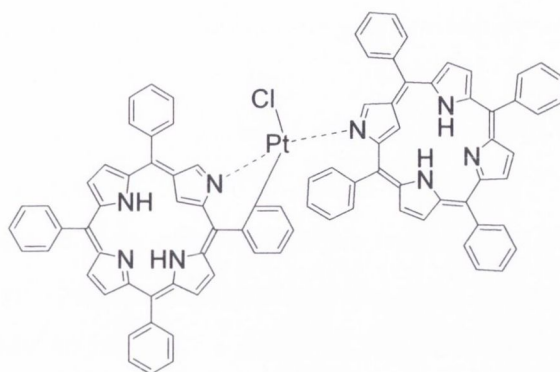
More recently but in an increasing number, palladium (II) and platinum (II) were also introduced in the periphery of NH functionalized porphyrins or in the *meso* position of porphyrins as shown in scheme 2.3.1.1 and applications in cancer therapy were targeted.¹⁰⁻¹⁴



Scheme 2.3.1.1. Synthesis of the peripheral palladium (II) complex **307**.¹²

2.3.2 Platinum (II) insertion

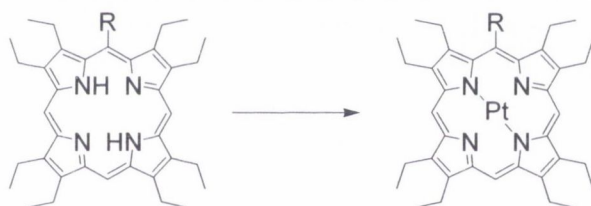
Pt(II)OEP **3** is commercially available from Porphyrin Products Inc.¹⁵ Platinum (II) insertion was furthermore described for octabromotetraphenylporphyrin by Bhyrappa and Krishnan in 1991.⁹ The platinum (II) complex was obtained in not displayed yield by refluxing the porphyrin for 24 hours in DMF with Pt(COD)₃, dichloro-(cyclooctadiene) platinum (II). The application of the same conditions for OEP on the other hand, did not result in the formation of the desired product during the PhD. However, in N-confused or inverted porphyrins platinum (II) was inserted by P. J. Chmielewski and I. Schmidt using five equivalents of Pt(PhCN)₂Cl₂, which was obtained by refluxing PtCl₂ under an argon atmosphere in benzonitrile.¹⁶ The platinum (II) insertion was completed within six hours and produce the respective azaporphyrins in 60% and 70% yield (not shown). Chmielewski and Schmidt also described that the effectiveness of the insertion of platinum(II) into the inverted porphyrins depended on the solvent used. With chloroform, the asymmetric dimer **308** was isolated as shown in figure 2.3.2.1 instead of the desired inner platinum (II) complex. Similar was observed by H. Furuta *et al.*¹⁷ The formation of the peripheral complex was furthermore described to be due to the high affinity of platinum (II) to the phenyl substituent but could be circumvented when aromatic solvents such as benzonitrile or chlorobenzene were used. During the PhD, three platinum (II) complexes, 5-phenyl, 5-(1-naphthyl) and 5-(9-phenanthrenyl) Pt(II)OEP **309-311**, were prepared to investigate their photophysical properties. The yields were good to high (44-76%) and are displayed in table 2.3.2.1.



306

Fig. 2.3.2.1. Peripheral platinum (II) complex obtained by Chmielewski and Schmidt.¹⁶

The reactions were carried out under an argon atmosphere using PtCl_2 in refluxing benzonitrile. The formation of the platinum complexes was slow and was completed within one to three days.



	R	Yield [1/%]
307	phenyl	76
308	1-naphthyl	44
309	9-phenanthrenyl	54

Table 2.3.2.1. Platinum (II) insertion into *meso* monosubstituted octaethylporphyrins using PtCl_2 in refluxing benzonitrile.

2.4 Derivation of OEPs

During the PhD and by former group members, methoxyphenyl substituents as well as dimethylamino groups were introduced successfully in the *meso* position of OEP 1.

However, electron withdrawing NO₂ groups are required for applications in NLO as well as water-soluble porphyrins for sensor applications (NO₂ is here furthermore not stable). Unfortunately, the direct introduction of nitrophenyl groups in the *meso* positions of OEP **1** was so far not possible with organo lithium reagents and also the introduction of hydroxyphenyl residues remained difficult or impossible as discussed in chapter 2.2. An alternative on the other hand are condensation reactions as described in chapter 1 whereas also the deprotection and oxidation of introduced NMe₂ and OMe groups was reported to be successful as will be summarized in the following sections. Furthermore *β-meso* fusion reactions, performed in the past years by Osuka *et al.* will be discussed as similar reactions were planned during the thesis as will be reported in the outlook.¹⁸⁻²¹ However, Diels-Alder reactions will not be included in the following section even if they constitute an alternative functionalization pathway for the introduced anthracenyl residues. Also coupling reactions with boronic acids and esters are not summarized as OEP **1** can't be brominated adequately as was described in chapter 2.1. On the other hand, demetallation would have been an alternative pathway to obtain the desired methyl and *s*-butyl series as was described in chapter 2.2 and therefore also a few features will be reported briefly.

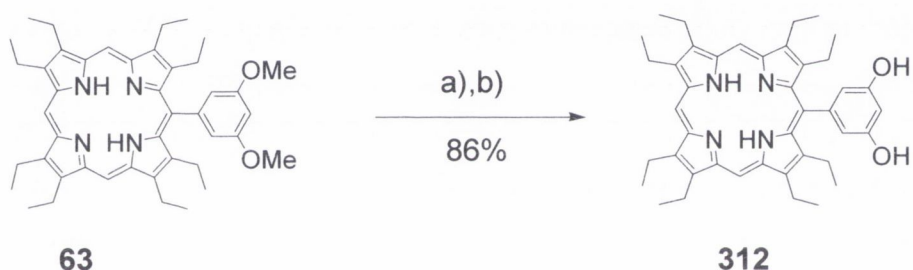
2.4.1 Demetallation

Nonplanar porphyrins exhibit a stronger basicity than planar porphyrins.^{4,22} Distorted zinc (II) complexes for example can be demetalated by TFA in chloroform.²³⁻²⁴ Nickel (II) and palladium (II) in contrast are difficult to remove and in *meso* tetrasubstituted benzoporphyrins demetallation conditions destroy the porphyrin macrocycle. On the other hand, copper (II) can be also removed from highly distorted porphyrins. Strongly acidic conditions e.g. conc. H₂SO₄ resulted in the formation of the free base porphyrins, while also ester groups can be cleaved during the reaction. From less distorted porphyrins, copper (II) can be removed with glacial acetic acid according to Falk's, Phillip's and Buchler's scale (e.g. middle to low-stable complexes, class II-IV).^{4,22} Furthermore, it was described by S. Vinogradov that electron rich *meso* aryl groups can facilitate side-reactions e.g. sulfonation during the metal removal. In those cases, the yields for the free base porphyrin were drastically lowered (5%). Alternatively and avoiding side-reactions, poly phosphoric acid can be used. Aryl substituents with

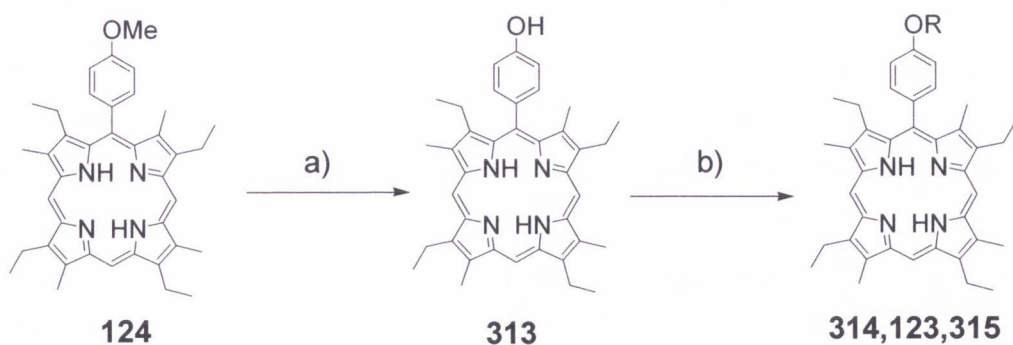
strongly electron withdrawing substituents such as NO₂ circumvented on the other hand in certain cases the metal extrusion.⁴

2.4.2 Derivation of introduced methoxyphenyl groups and sulfonation of *meso* phenyl substituents

When phenyl residues with methoxy groups were introduced in the *meso* position of OEP, the deprotection, resulting in hydroxyl porphyrins was carried out for example as shown in figure 2.4.2.1.²⁵ However, hydroxyl groups are important as they change the polarity and solubility of the respective porphyrin relative to the needs for applications in hydrophilic media (e.g. PDT, photodynamic therapy/tumor treatment). On the other hand, OH groups are also interesting for further derivation, and the formation of strapped, caged or basket handle porphyrins as was described in chapter 2.1.^{26,27}



Scheme 2.4.2.1. Deprotection of methoxy groups of OEPs; a) BBr₃, dichloromethane, b) NaHCO₃, H₂O.²⁵



Scheme 2.4.2.1. Deprotection and transformation of the *p*-methoxyphenyl substituent; a) BBr₃, MeCN, b) RBr/K₂CO₃/MeCN with R = *n*-hexyl, *n*-heptyl and *n*-decyl.²⁸

Also ethers were obtained subsequently with etioporphyrin as shown in scheme 2.4.2.1 as well as esters (not shown).^{28,29}

2.4.3 Nitration, amidation and derivation of phenyl substituents

Nitration of phenyl substituents in porphyrins was described by Chen *et al.* and details were given in chapter 2.1.³⁰ Yields vary from 24% to 50% for the introduction of one to two nitro groups in the *para* positions of the phenyl substituents of TPP **64**. 5,10-bis(4-nitrophenyl)-15,20-diphenylporphyrin was for example obtained in 46% yield (not shown). Conditions used were CF₃COOH and NaNO₂ for 90 seconds at rt.³⁰ Furthermore, the nitro groups of dodecaarylsubstituted porphyrins were reduced with SnCl₂ x 2 H₂O and conc. HCl at 80 °C within two hours in up to 60% yield. Protective methylation by the introduction of cationic N⁺(CH₃)₃ groups at the phenyl substituents was carried out with methyl iodide (CH₃I) in DMF at 40-45 °C in five hours to one day and 60% to 85% yield, depending on the porphyrin. Phenyl-COOME and COOH groups were also easily transformed into the respective amides with amines.³¹ The derivation of aryl attached NH₂ groups in porphyrins producing highly polar e.g. water soluble isothiocyano (NCS) Pd(II) and Pt(II) coproporphyrins was carried out by A. E. Soini and co-workers with CSCl₂, NaHCO₃ in acetone and five minutes of stirring at ambient temperature in order to obtain porphyrins which can be used as labels.^{32,33} Furthermore perylene porphyrin arrays were presented by M. R. Wasielewski and co-workers in 1992³⁴ and also by J. S. Lindsay *et al.* in 2001.³⁵ For example, the dimer shown in figure 2.4.3.1 was obtained from 5-(4-aminophenyl)-10,15,20-tris-*n*-pentylporphyrin (not shown) in low yield in a mixed [4+1]-condensation reaction by addition of perylen and with an overall yield of >1%. Another approach was therefore presented in 2003 by M. Wang *et al.*²⁶ TPP **64** was prepared in 35% from the respective condensation step by refluxing pyrrole and benzaldehyde in chloroacetic acid/xylol and was derived under conditions described by Kruper *et al.*³⁷ yielding in 5-(4-nitrophenyl)-10,15,20-triphenylporphyrin (not shown), which was subsequently reduced to the amine **317**, and reacted with perylen to the in figure 2.4.3.1 shown array **318**. The overall yield for **318**, starting with pyrrole **20** was calculated as 14%. On the other hand, the sulfonation of the TPP derivative **319** was performed as shown in scheme 2.4.3.1 in 50% yield.¹²

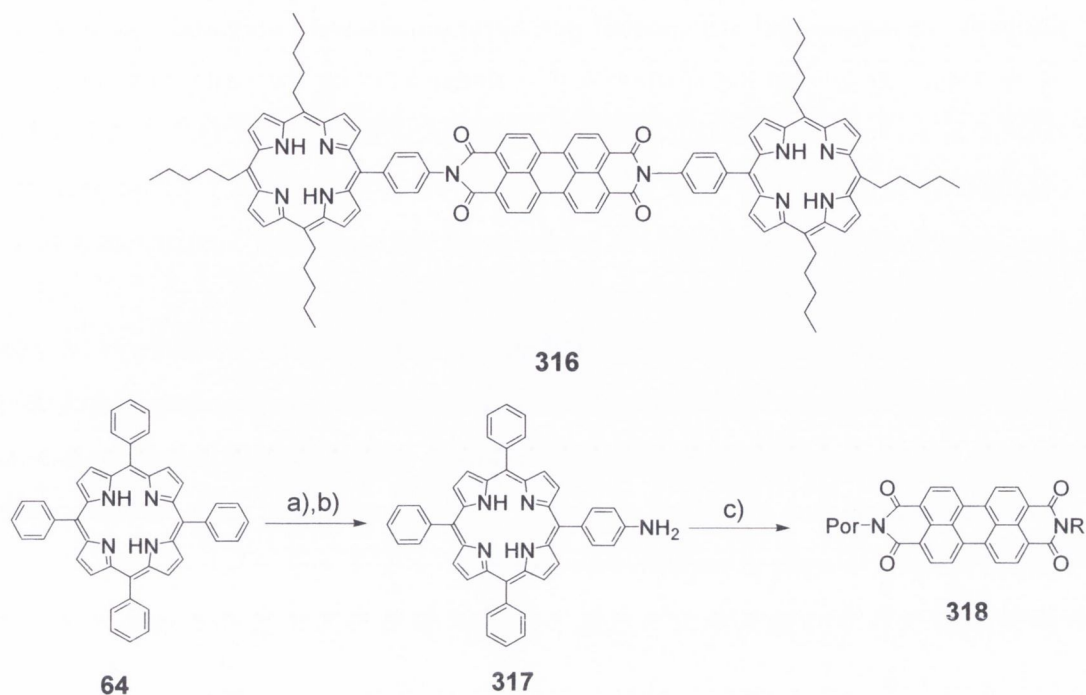
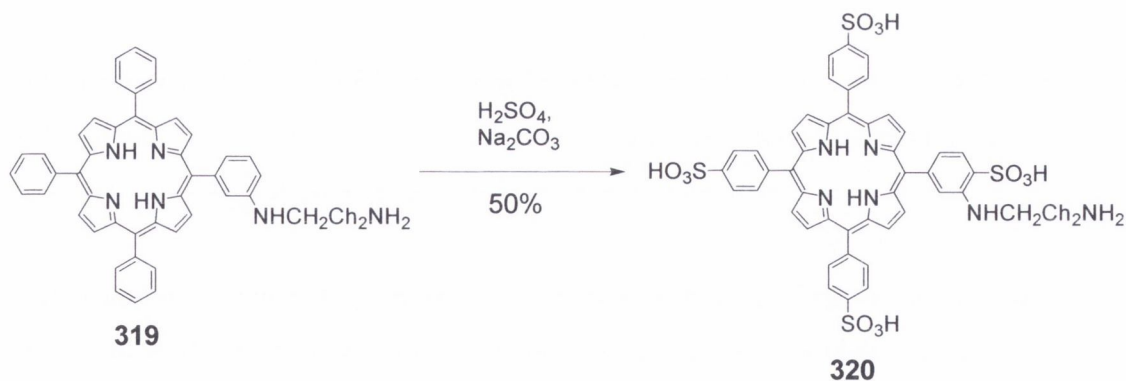


Fig. 2.4.3.1. By Wasilewski and co-workers synthesized array (top) and short cut through TPP by Wang *et al.* (bottom); a) fuming nitric acid, chloroform, 0–5 °C, 58% b) $\text{SnCl}_2 \times 2 \text{H}_2\text{O}$, HCl, 65–70 °C, 89%, c) perylene, imidazole, *m*-cresol, 170–175 °C, por = TPP, 76%, $\text{R}=(\text{CH}_2)_{11}\text{CH}_3$.^{36,37}



Scheme 2.4.3.1. Sulfonation of the TPP 319.¹²

2.4.4 β -Meso and β - β fusion reactions (JI-extension)

After 2000 β -meso fusion reactions were carried out using aromatic residues or functionalized substituents in the *meso* and β -position of the porphyrin and JI-extended, β -meso fused chlorins were obtained for example by Bergman cycloaromatization.³⁸⁻⁴²

Furthermore β -*meso* and β - β coupled porphyrin dimers were prepared and investigated by A. Osuka *et al.* and the reaction was optimized during the past years starting with BAHA as a reagent and using later more successfully Sc(OTf)₃/DDQ.¹⁸⁻²¹ A fused OEP, obtained by A. Gold *et al.*, was for example shown in scheme 2.1.1.3.1 on page 48 and the respective UV/vis spectrum will be discussed in chapter 5.³⁸ Similar reactions using FeCl₃ were furthermore reported recently in literature.⁴³

To obtain the linked porphyrins **324-327** shown in figure 2.4.4.1, Osuka *et al.* used in 1999 “phenyl-capped” 5,10,15-tris(3,5-bis-*tert*-butylphenyl)porphyrinato nickel (II) (not shown) or the respective palladium (II) complex adding tris(4-bromophenyl)aminium hexachloroantimonate (BAHA), a typical electron oxidizing agent, which produced cation radicals in order to perform the reaction.¹⁹

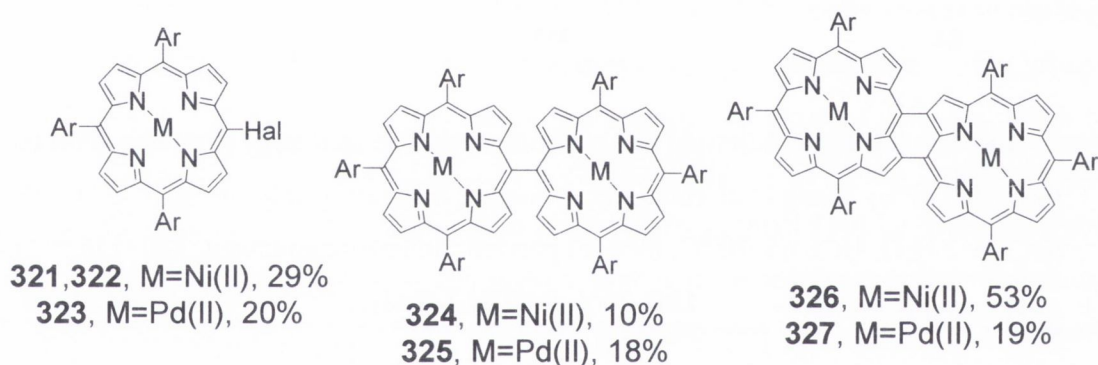


Fig. 2.4.4.1. Obtained porphyrins **321-327** from 5,10,15-trisphenylporphyrinato nickel (II) and palladium (II) with BAHA by Osuka *et al.*; Ar = 3,5-di-*tert*-butylphenyl, **321/322** were obtained in a mixture (Hal=Br and Cl), **323** with Hal=Br.¹⁹

However, when 5,15 disubstituted porphyrins were used, complex product mixtures were obtained and the product ratio depended for all reactions on the time of stirring and the amounts of BAHA added. Three equivalents of BAHA yielded in the formation of a β -chlorinated, *meso*- β doubly linked porphyrin dimer in 49% yield (not shown), together with the respective *meso* brominated monomer. However, the use of BAHA is thought to produce also β -halogenated derivatives of OEP instead of diporphyrins and only singly linked dimers were obtained with zinc (II) and free base porphyrins.¹⁸ The doubly linked porphyrins displayed furthermore strongly broadened and low intense UV/vis spectra as

will be described in chapter 5. Osuka *et al.* applied the oxidative fusion reactions also to already *meso-meso* linked porphyrin arrays and obtained with Sc(OTf)₃/DDQ triply linked tapes in yields between 50% and 90%.²⁰⁻²¹ First attempts were made using (*p*-BrC₆H₄)₃NSbCl₆ in C₆F₆ but yielded also in β -chlorination for longer chains. Similar fusion reactions were furthermore performed by K.-i. Seguirra and M. Yamashita *et al.* in 2003 using *meso*-pyrenyl porphyrins and PhI(OTf)₂ and BF₃ etherate in dichloromethane or Sc(OTf)₃/DDQ in toluene as reagents.⁴⁴ JI-Extended TBPs and TNPs were additionally described by S. Vinogradov *et al.* and will be discussed in chapter 6 due to their particular emission and absorption properties.⁴⁵⁻⁴⁷

REFERENCES

1. M. Pawlicki, L. Latos-Grazynski *Chem. Eur. J.* **2003**, *9*, 4650.
2. I. B. Rietveld, E. Kim and S. A. Vinogradov *Tetrahedron* **59** **2003**, 3821.
3. I. Scalise, E. N. Durantini, *J. Photochem. Photobiol. A: Chem.* **2004**, *162*, 105.
4. O.S. Finikova, A. V. Cheprakov, I. P. Beletskaya, P. J. Carroll, S. A. Vinogradov *J. Org. Chem.* **2004**, *69*, *2*, 522.
5. C. J. Medforth, M. D. Berber, K. M. Smith, J. A. Shelnut *Tetrahedron Lett.* **1990**, *31*, 3719.
6. K. M. Barkigia, M. D. Berber, J. Fajer, C. J. Medforth, M. W. Renner, K. M. Smith *J. Am. Chem. Soc.* **1990**, *112*, 8851.
7. J. Takeda, T. Ohya, M. Sato *Inorg. Chem.* **1992**, *31*, 2877.
8. O. Finikova, A. Galkin, V. Rozhkov, M. Cordero, C. Hagerhall, S. Vinogradov *J. Am. Chem. Soc.* **2003**, *125*, 4882.
9. P. Bhyrappa, V. Krishnan *Inorganic Chemistry* **1991**, *30*, *2*, 239.
10. R. D. Hartnell, D. P. Arnold *Organometallics* **2004**, *23*, 391.
11. R. D. Hartnell, D. P. Arnold *Eur. J. Inorg. Chem.* **2004**, 1262.
12. No authors available online *J. Heterocycl. Chem.* **1986**, *23*, *5*, 1565.
13. M. C. Lensen, M. Castriciano, R. G. E. Coumans, J. Foekema, A. E. Rowan, L. M. Scolaro, R. J. M. Nolte *Tetrahedron Lett.* **2002**, *43*, 9351.
14. C. Monnereau, J. Gomez, E. Blart, F. Odobel, S. Wallin, A. Fallberg, L. Hammarström *Inorg. Chem.* **2005**, *44*, 4806.
15. L. Campbell, S. Tanaka, S. Mukamel *Chemical Physics* **2004**, *299*, 11.
16. P. J. Chmielewski, I. Schmidt *Inorganic Chemistry* **2004**, *43*, *6*, 2004, 1885.
17. H. Furuta, K. Youfu, H. Maeda, A. Osuka *Angew. Chem., Int. Ed.* **2003**, *42*, 2186.
18. A. Tsuda, A. Nakano, H. Furuta, H. Yamochi, A. Osuka *Angew. Chem. Int. Ed.* **2000**, *393*, 558.
19. A. Tsuda, H. Furuta, A. Osuka *J. Am. Chem. Soc.* **2001**, *123*, 10304.
20. A. Tsuda, A. Osuka *Adv. Mater.* **2002**, *14*, *1*, 75.
21. M. Kamo, A. Tsuda, Y. Nakamura, N. Aratani, K. Furukawa, T. Kato, A. Osuka *Org. Lett.* **2003**, *5*, *12*, 2079.
22. O. S. Finikova, A. V. Cheprakov, J. C. Carroll, S. Dalosto, S. A. Vinogradov, *Inorg. Chem.* **2002**, *41*, *26*, 6944.

23. R. J. Cheng, Y. R. Chen, C. E. Chuang *Heterocycles* **1992**, *34*, 1.
24. V. N. Koprnenkov, E. A. Makarova, E. A. Lukyanets *Zh. Obshch. Khim.* **1981**, *51*, 2727.
25. T. Tanaka, K. Endo, Y. Aoyama *Bull. Chem. Soc. Jpn.* **2001**, *74*, 5, 907.
26. No authors available online *Khim. Geterocycl. Soed.* **1988**, *3*, 339.
27. H. Ogoshi, K. Saita, K.-i. Sakurai, T. Watanabe, H. Toi, Y. Aoyama, Y. Okamoto *Tetrahedron Lett.* **1986**, *27*, 52, 6365.
28. Y. Chen, C. J. Medforth, K. M. Smith, J. Alderfer, T. J. Dougherty, R. K. Pandey *J. Org. Chem.* **2001**, *66*, 3930.
29. H. Tamiaki, A. Kiyomori, K. Maruyama *Bull. Chem. Soc. Jpn.* **1994**, *67*, 2478.
30. B. Chen, W. Song, L. Aixiao, L. Feng, Z. Xiang, C. Xiaoping, H. Zhike *Tetrahedron* **2006**, *62*, 5487.
31. V. Rozhkov, D. Wilson, S. Vinogradov *Macromolecules* **2002**, *35*, 1991.
32. M. M. Koskelin, A. E. Soini, N. J. Meltola, G. V. Ponomarev *J. Porph. Phthal.* **2002**, *6*, 533.
33. E. A. Soini, D. Y. Yashunsky, N. J. Metola, G. V. Ponomarev *J. Porph. Phthal.* **2001**, *5*, 385.
34. M. P. O. Neil, M. P. Niemczyk, W. A. Svec, D. Gosztola, G. L. Gaines, M. R. Wasielewski *Science* **1992**, *257*, 63.
35. S. Prathapan, S. I. Yang, M. A. Miller, D. F. Bocian, D. Holten, J. S. Lindsey *J. Phys. Chem. B* **2001**, *105*, 8237.
36. X. G. Yang, J. Z. Sun, M. Wang, H. Z. Chen *Chin. Chem. Lett.* **2003**, *14*, 11, 1105.
37. W. J. Kruper, T. A. Chamberlin, M. Kochanny *J. Org. Chem.* **1989**, *54*, 11, 2753.
38. K. Jayaraj, A. Gold, L. M. Ball, P. S. White *Inorg. Chem.* **2000**, *39*, 3652.
39. G. Li, S. K. Pandey, A. Graham, M. P. Dobhal, R. Mehta, Y. Chen, A. Gryshuk, K. Rittenhouse-Olson, A. Oseroff, R. K. Pandey *J. Org. Chem.* **2004**, *69*, 158.
40. D. Sengupta, B. C. Robinson *Tetrahedron* **2002**, *58*, 5497.
41. M. Nath, J. C. Huffman, J. M. Zaleski *J. Am. Chem. Soc.* **2003**, *125*, 11487.
42. J. Fouchet, C. Jeandon, R. Ruppert, H. J. Callot *Org. Lett.* **2005**, *7*, 23, 5257.
43. K. Tsuchiya, Y. Shibasaki, M. Aoyagi, M. Ueda *Macromolecules* **2006**, *39*, 3964.
44. O. Yumane, K.-i. Seguirra, H. Miyasaka, K. Nakamura, T. Fujimoto, K. Nakamura, T. Kaneda, Y. Sakata, M. Yamashita *Chem. Lett.* **2004**, *33*, 1, 40.

45. O. S. Finikova, S. E. Aleshchenkov, R. P. Brinas, A. V. Cheprakov, P. J. Carroll, S. A. Vinogradov *J. Org. Chem.* **2005**, *70*, *12*, 4617.
46. J. E. Rogers, K. A. Nguyen, D. C. Hufnagle, D. G. McLean, W. Su, K. M. Gosset, A. R. Burke, S. A. Vinogradov, R. Prachter, P. A. Fleitz *J. Phys. Chem. A* **2003**, *107*, 11331.
47. V. V. Rozhkov, M. Khajehpour, S. A. Vinogradov *Inorg. Chem.* **2003**, *42*, 4253.

3. ^1H NMR spectra of synthesized OEPs: Discussion of atropisomers and assignment of signals and regioisomers

3.1 Assignment of substituent signals and comparison of the CH_2/CH_3 pattern of OEPs

3.1.1 Assignment of naphthyl, phenanthrenyl and anthracenyl protons

The ^1H NMR spectra of symmetric anthracene, phenanthrene and naphthalene **328-330** display only a few signals, as it can be seen in figure 3.1.1.1 and table 3.1.1.1,¹ and are different to anthracenyl, phenanthrenyl and naphthyl residues attached to porphyrins. Due to the unilateral bonding, the protons of the anthracenyl, phenanthrenyl and naphthyl substituents in porphyrins become non equivalent and various signals have been observed in the ^1H NMR and ^{13}C NMR spectra of OEPs.

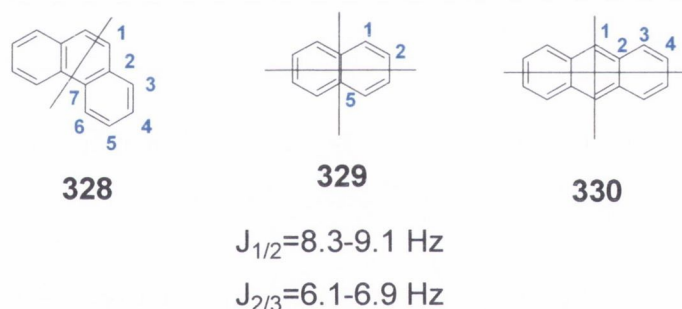


Fig. 3.1.1.1 Numbering of non equivalent protons and carbon atoms in phenanthrene, naphthalene and anthracene **328/330**.¹

However, in 5-(1-naphthyl) OEP **7** all naphthyl protons were found to be non equivalent due to the bond to the porphyrin and the unsymmetry induced. Six signals were observed in the respective ^1H NMR region as two proton signals merged into each other at 6.96 ppm as it can be seen in figure 3.1.1.8. The measured coupling constants (compare to the experimental part) were furthermore similar to the coupling constants displayed for naphthalene **329** and due to the deshielding effect of the porphyrin several signals of 5-(1-naphthyl) OEP **7** were downfield shifted, appearing above 8.0 ppm.

	Compound	Position	¹ H NMR signal, [1/ppm]	¹³ C NMR signal, [1/ppm]
328	phenanthrene	1	7.71	127.3
		2	-	132.3
		3	8.12	128.9
		4	7.82	126.7
		5	7.88	126.7
		6	8.93	123.0
		7	-	130.0
329	naphthalene	1	7.81	128
		2	7.46	125.9
		5	-	133.6
330	anthracene	1	8.31	132.5
		2	-	132.2
		3	7.91	130.1
		4	7.39	125.6

Table 3.1.1.1 ¹H NMR and ¹³C NMR shifts of phenanthrene, naphthalene and anthracene **328/330**.¹

Furthermore, the ¹³C NMR signals observed at 125.9, 128.4 or 127.7 and 132.6 ppm were attributed to the naphthyl substituent by comparison to the data displayed in table 3.1.1.1. In analogy to 5-(1-naphthyl) OEP **7**, 5-(9-phenanthrenyl) OEP **8** displayed eight signals in the ¹H NMR spectrum, while the signal at 7.09 ppm covered two protons. The phenanthrenyl proton signals were located between 9.03 and 7.09 ppm with coupling constants of 8.56, 7.54, 7.89 and 7.27 Hz for the doublets (compare to figure 3.1.1.8). As for 5-(1-naphthyl) OEP **7**, the multiplet at 7.09 ppm was upfield shifted relative to the signals of phenanthrene **328**. The ¹³C NMR signals at 123.4, 126.9, 127.8, 129.4 and 131.2 ppm were referred to the phenanthrenyl substituent and the full ¹H NMR spectrum is shown figure 3.1.1.2, representing a typical spectrum of *meso* monosubstituted OEPs with an 2/1 intensity for the *meso* protons and two NH signal due to the inner core

unsymmetry und slow tautomerisation at ambient temperature relative to the ^1H NMR time scale.²

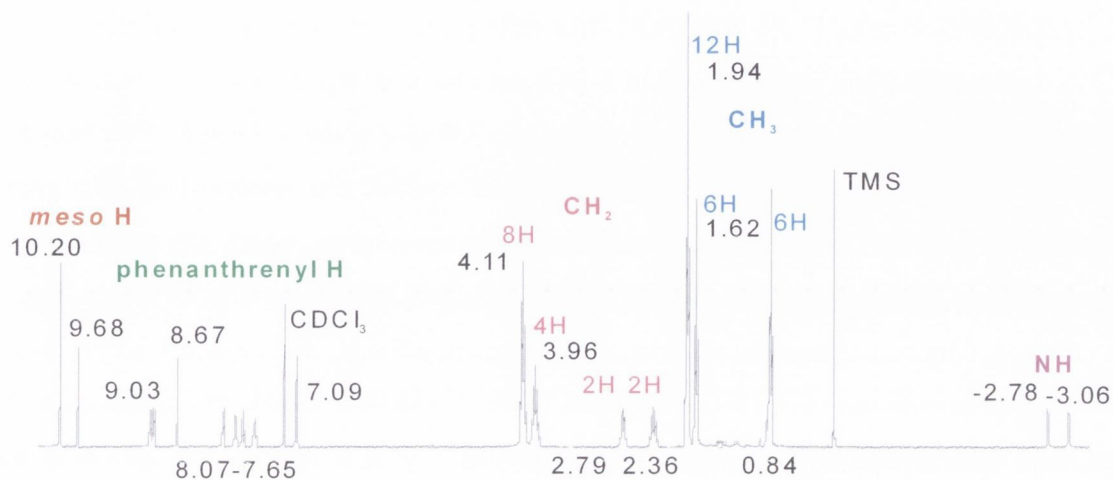


Fig 3.1.1.2. Typical ^1H NMR spectrum of a *meso* monosubstituted OEPs e.g. of 5-(9-phenanthrenyl) OEP **8**; [ppm].

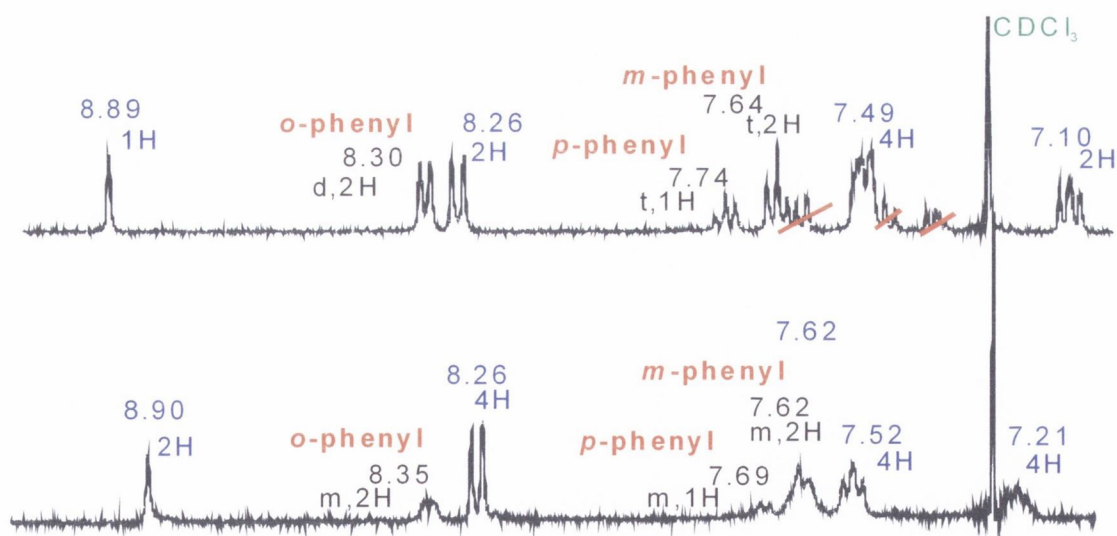


Fig. 3.1.1.3. Aromatic ^1H NMR region of 5-(9-anthracenyl)-10-phenyl OEP **246** (top) and 5,15-bis(9-anthracenyl)-10-phenyl OEP **290** (bottom), anthracenyl signals=blue; [ppm]; impurities are marked.

However, for 5-(9-anthracenyl)-10-phenyl OEP **246** four anthracenyl signals were observed in the ^1H NMR spectrum, which is shown in figure 3.1.1.3. Indeed, as observed for the OEPs **7** and **8**, two signals merged into each other at 7.49 ppm (the *quasi-para*-protons/4',-6',-12'- and 14'-position), forming an intense multiplet. A characteristic singlet appeared at 8.89 ppm and was significantly downfield shifted (approximately 0.5 ppm) relative to anthracene **330** due to the influence of the porphyrin ring current. Furthermore, a downfield shifted doublet was observed at 8.26 ppm in similarity to the OEPs **7** and **8** and representing the protons, which are attached on the side next to the porphyrin in the *quasi-ortho*-positions (7',11'-positions). The strength of the coupling constant of the doublet at 8.26 ppm was 8.6 Hz and typically larger than for phenyl substituents (6.6 Hz). As for the OEPs **7** and **8**, a signal was observed at 7.10 ppm, upfield from CDCl_3 (*quasi-meta*-positions, 5',13'-positions) and for comparison also the spectrum of 5,15-bis(9-anthracenyl)-10-phenyl OEP **290** is displayed in figure 3.1.1.3.

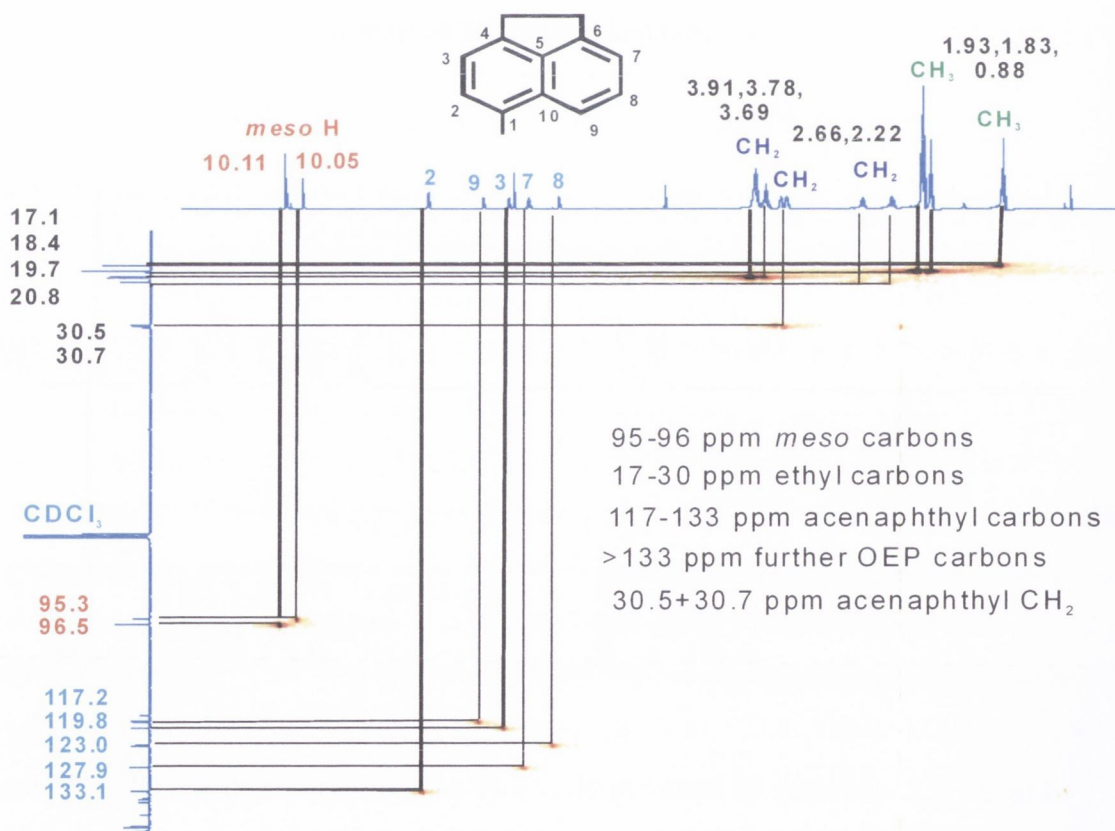
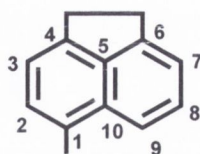


Fig. 3.1.1.4. HMQC spectrum of 5-acenaphthyl Pd(II)OEP **303**.



Position	^1H NMR shift [1/ppm]	^{13}C NMR shift [1/ppm]
2	8.35	133.1
3	7.29	127.9
7	7.01	119.8
8	6.52	117.2
9	7.62	127.9

Table 3.1.1.2. ^1H NMR and ^{13}C NMR correlations and position assignment for 5-acenaphthyl Pd(II)OEP **303**.

As it can be seen in figure 3.1.1.3, the proton signal of the phenyl substituents appeared typically in the order *ortho*, *para* and *meta* from down to upfield shifts.

The downfield ^1H NMR and ^{13}C NMR signals of 5-acenaphthyl Pd(II)OEP **303** were also correlated as shown in figure 3.1.1.4 and table 3.1.1.2. The signals of the *meso* carbon atoms that carry protons, were displayed in the ^{13}C NMR spectrum at 95.3 and 96.5 ppm and could be correlated to the respective *meso* proton singlets at 10.11 and 10.05 ppm. The proton assignment was carried out relative to 5-(1-naphthyl) OEP **7** and naphthalene **329**. The ethyl signals of 5-acenaphthyl Pd(II)OEP **303** occurred commonly around 20 ppm in the carbon spectrum while the acenaphthyl CH_2 bridge signals were downfield shifted to 30.5 and 30.7 ppm due to the heavy metal influence, while all signals appeared below 21 ppm for the respective free base OEP **234**. Also the ^{13}C NMR DEPT spectrum is shown in figure 3.1.1.5 relative to the common carbon spectrum and allowed the bridge CH_2 signal assignment due to the orientation of the signals and in comparison to the HMQC spectrum. In order to assign the proton signals of 5-(2-naphthyl) porphyrinato palladium (II) **302** a H,H COSY spectrum was recorded and is shown in figure 3.1.1.7 with assignment in figure 3.1.1.6. Additionally, the respective coupling constants were considered (compare to experimental part) and the assignment of the

signals of all introduced aryl residues can be found in figure 3.1.1.8, while the downfield spectra are displayed in figure 3.1.1.9.

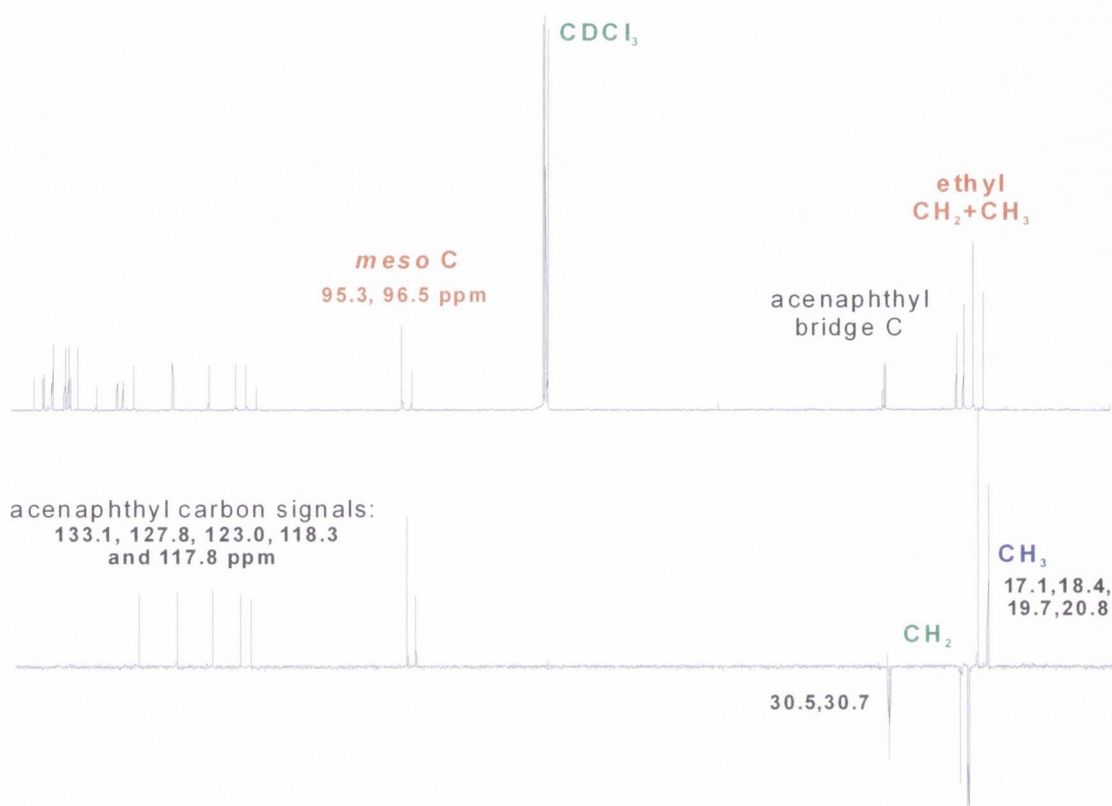


Fig. 3.1.1.5. ^{13}C NMR (top) and DEPT ^{13}C NMR (bottom) spectra of 5-acenaphthyl Pd(II)OEP **234**.

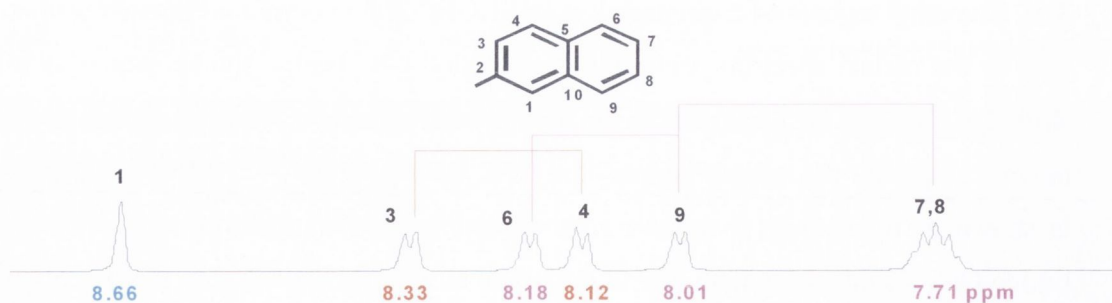


Fig. 3.1.1.6. Observed H,H coupling for 5-(2-naphthyl) Pd(II)OEP **302** and signal assignment.

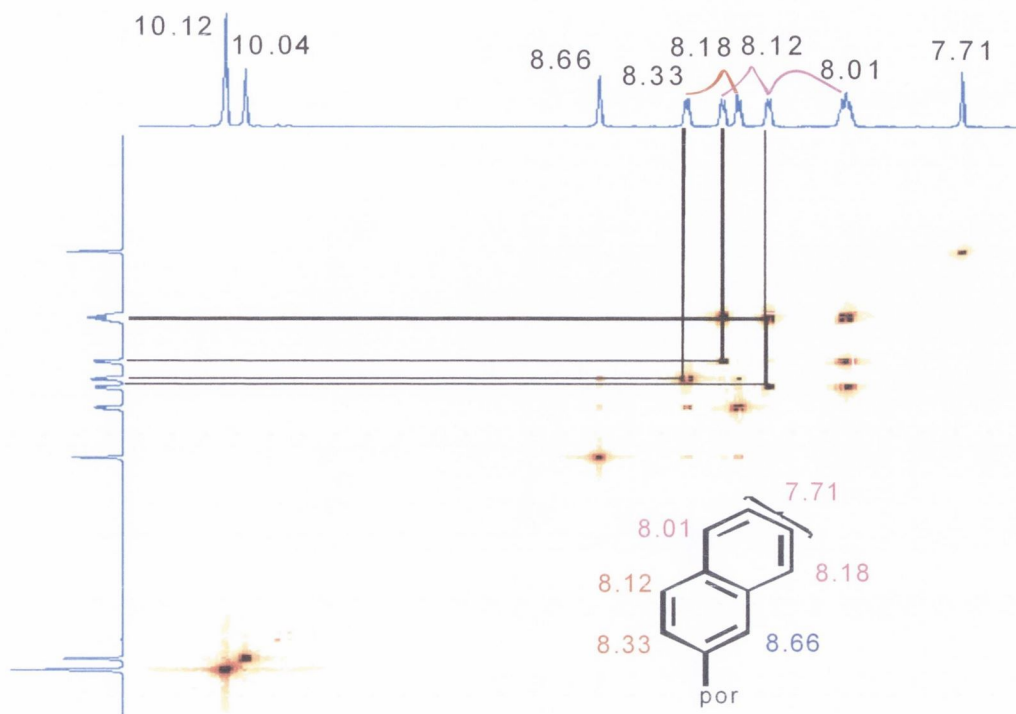


Fig. 3.1.1.7. H,H COSY downfield couplings of 5-(2-naphthyl) Pd(II)OEP **302**;
por=Pd(II)OEP.

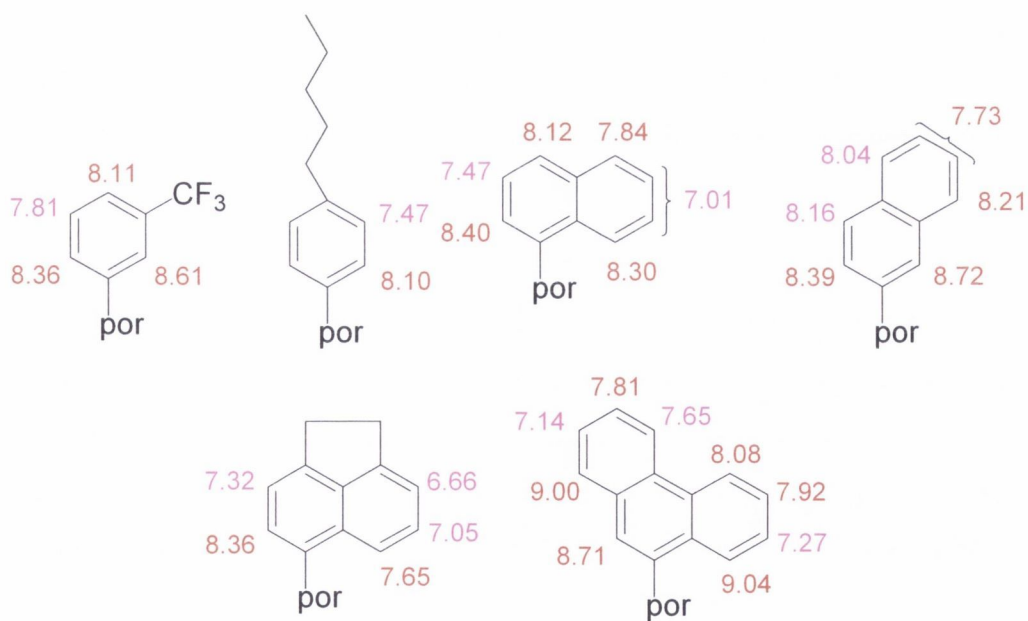


Fig. 3.1.1.8. ^1H NMR signal assignment of the *meso* monosubstituted H₂OEP **5-8** and **233-234**; por=H₂OEP.

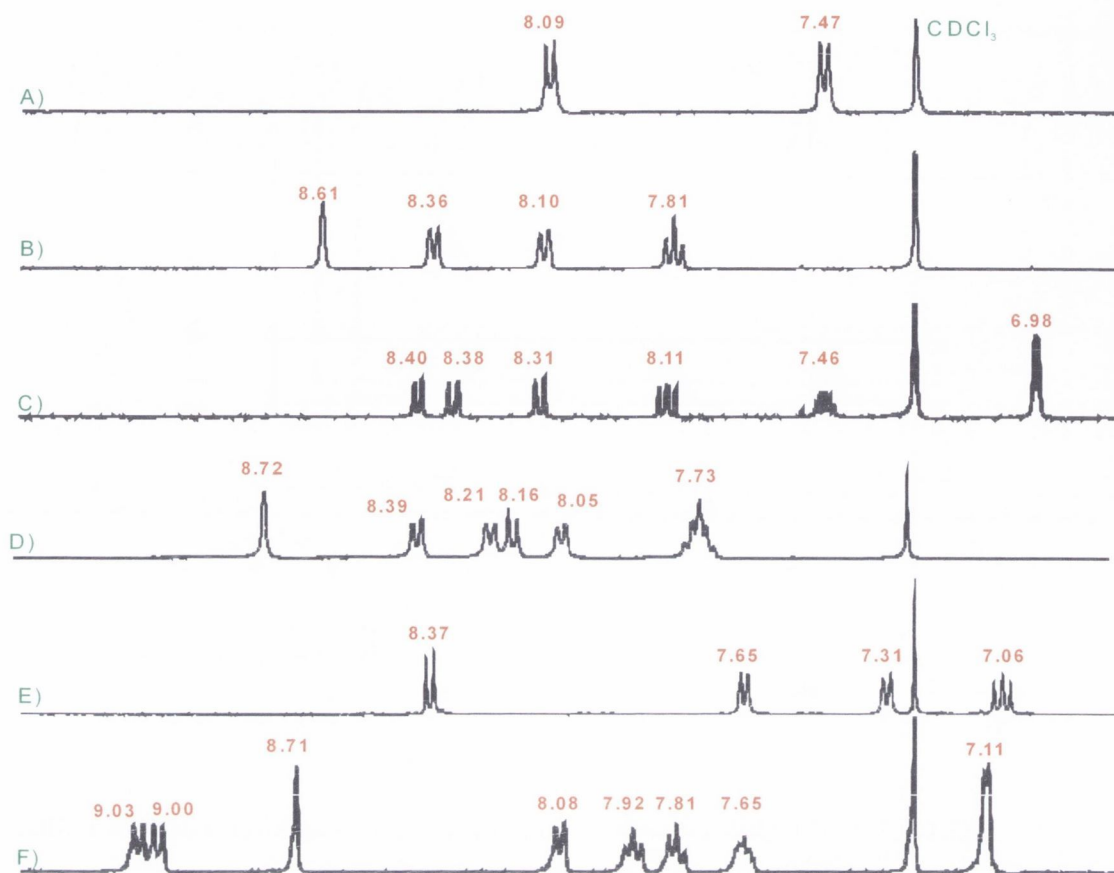


Fig. 3.1.1.9. Downfield aryl proton signals of the *meso* monosubstituted OEPs 5-(4-*n*-pentylphenyl) OEP **5** (A), 5-(3-trifluoromethylphenyl) OEP **6** (B), 5-(1-naphthyl) OEP **7** (C), 5-(2-naphthyl) OEP **233** (D), 5-acenaphthyl OEP **234** (E) and 5-(9-phenanthryl) OEP **8** (F); [ppm].

3.1.2 CH₂/CH₃ pattern of *meso* mono-, di-, tri- and tetrasubstituted OEPs

While OEP **1** displayed only two signals for the respective ethyl CH₂ and CH₃ protons e.g. a quartet at 4.12 ppm for 16 protons and a triplet at 1.93 ppm for 24 protons, the CH₂/CH₃ signals of the β -ethyl groups “split” in the case of *meso* substitution. The substituent causes nonequivalence due to the induced 2D unsymmetry and alters the chemical environment as well as the 3D geometry (different ring current influence), causing signal “splits” and resulting in the observed upfield shifts. As it can be seen for 5-(2-naphthyl) Pd(II)OEP **302** in figure 3.1.2.1, relative to the signal observed at 4.05 ppm for eight CH₂ protons, an additional ethyl CH₂ signal appeared at 3.95 ppm for two

of the eight ethyl groups (4 protons) and two further CH₂ signals, each for a single CH₂ group, were displayed at 2.70 and 2.45 ppm. The protons of the signals at 4.05 and 3.95 coupled furthermore with the respective protons of the neighboring CH₃ groups e.g. with the signals at 1.94 and 1.85 ppm and respective intensities were observed (8+4=12 CH₂ protons to 12+6=18 CH₃ protons), while the protons of the CH₂ signals at 2.70 and 2,45 ppm coupled with a single signal at 1.03 ppm, which represented the remaining six CH₃ protons.

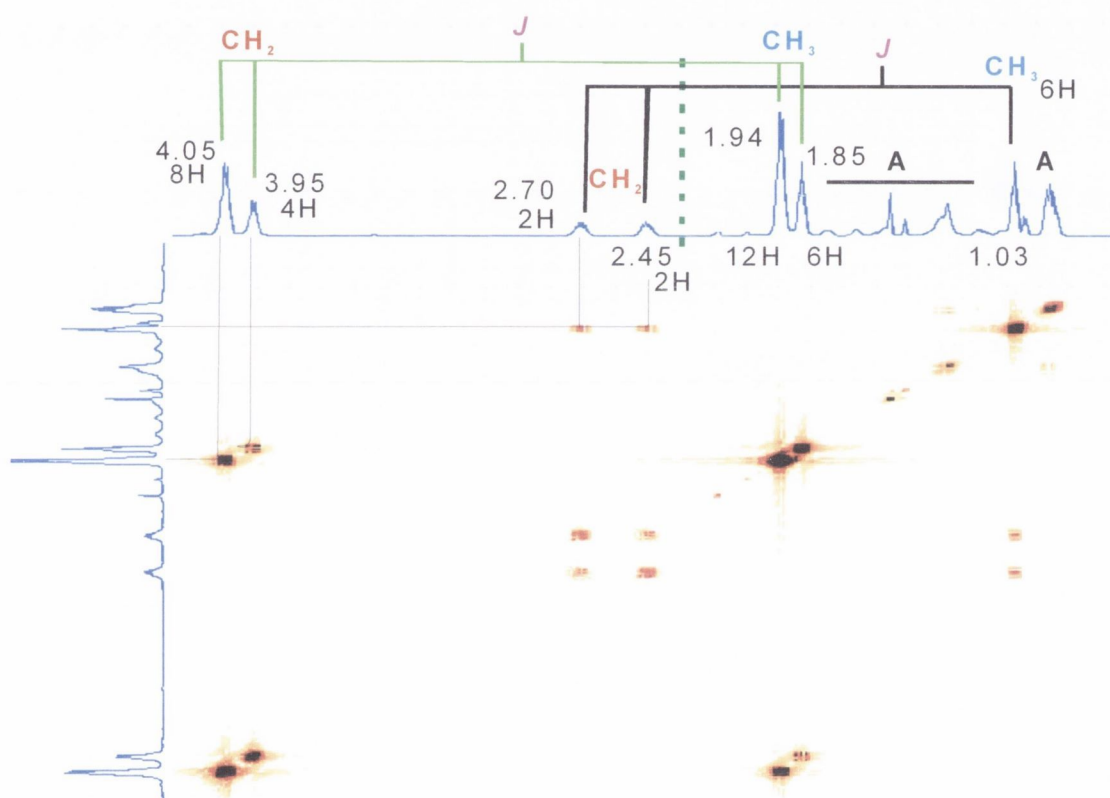


Fig. 3.1.2.1. H,H COSY CH₂/CH₃ coupling of 5-(2-naphthyl) Pd(II)OEP **302**,
A=impurities.

Additionally, an upfield shift of all signals was found with each newly incoming substituent for the phenanthrenyl series as shown in figure 3.1.2.2 and also further splits appeared. 5,10,15,20-Tetrakis(9-phenanthrenyl) OEP **11** displayed in the end only CH₂/CH₃ ethyl signals below 2.37 ppm and the proton assignment was restricted due to

the broadening of the signals, which was caused by the increased conformational flexibility of the porphyrin.^{2,3,4}

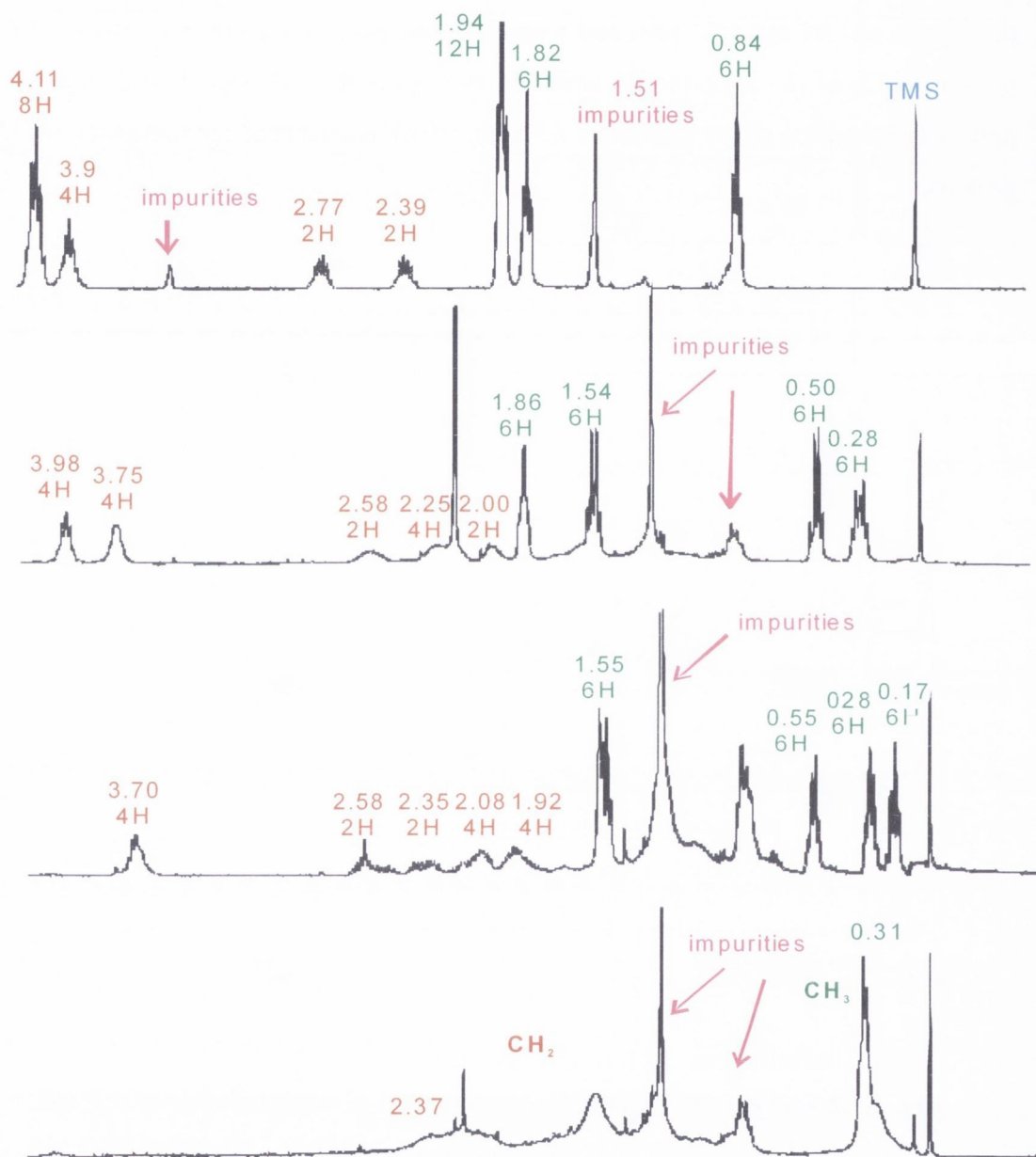


Fig 3.1.2.2. Upfield shift of the ethyl CH₂ and CH₃ signals of 5-(9-phenanthrenyl) OEP **8**, 5,10-bis(9-phenanthrenyl) OEP **9**, 5,10,15-tris(9-phenanthrenyl) OEP **10** and 5,10,15,20- tetrakis(9-phenanthrenyl) OEP **11** (top to bottom), [ppm].

Blurry methylen signals were for example also observed by Nakamura *et al.*⁵ They observed that the methylen signals in the *meso* tetrasubstituted OEP **332**, shown in figure 3.1.2.3, appeared broadened at room temperature and higher temperature, while at lower temperature the signals were well defined (“frozen”). Else wise, the *meso* tetra- (*para*-phenyl) substituted porphyrin **331** showed the same trend while the signals sharpened at higher temperatures (288 K for **331** and 244 K for **332**). As a result of the destabilization of the minimal energy conformer, an increased flexibility was attributed to the *ortho*-phenyl substituted OEP **332**, explaining the blur in the spectrum due to permanent conformational changes at room temperature.⁵

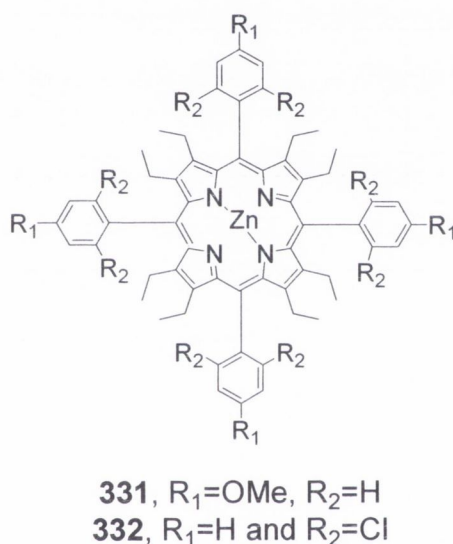


Fig. 3.1.2.3. Prepared and investigated OEPs by M. Nakamura *et al.*⁵

However, 5-methyl OEP **227** and 5-*n*-butyl OEP **16** displayed no additional CH₂/CH₃ signals, while a higher multiplicity occurred for both and a blurry CH₂ signal for 5-*n*-butyl OEP **16** relative to OEP **1**. 5-Phenyl OEP **4** displayed furthermore an 8/4/4 split of the ethyl CH₂ protons and a 12/6/6 proton pattern for the CH₃ signals, indicating the increased steric interaction between the β- and *meso* positions and different chemical environments, while for 5-(3-trifluoromethylphenyl) OEP **6** further splits were observed (CH₂: 8/4/2/2 protons) as a result of the *meta*-phenyl substituent. The same signal split was also encountered for 5-(1-naphthyl), 5-acenaphthyl and 5-(9-phenanthrenyl) OEP

7/8/234 while also increased multiplicities were observed. The signal split was additionally enforced for 5,10-bis(1-naphthyl) porphyrinato palladium (II) **284**, which displayed a 2/2/2/2 pattern for the CH₂ signals and a 6/6/6/6 pattern for the CH₃ signals in accordance to the 5,10 substitution and influence of the heavy metal atom.

3.2 5,10 Regioisomers of A₂- and AB-substituted OEPs and ABA and AAB regioisomers of trisubstituted OEPs

3.2.1 5,10-AB and -A₂ regioisomers

The assignment of the 5,10 arrangement of the A₂ substituted OEPs **9**, **254** and **257** was carried out by comparison of the *meso* proton and NH ¹H NMR signals relative to those of the known 5,10-bisphenyl OEP **236** and its counterpart the 5,15-substituted regioisomer **216**.^{6,7} Additionally also the ¹H NMR data of 5,15-bis(4-trifluoromethylphenyl)- and 5,15-bis-(7-naphtholyl) OEP **101/103** could be consulted and the respective *meso* proton and NH signal shifts can be found in table 3.4.1.^{8,9} For 5,10 substituted OEPs the *meso* proton signal appeared around 9.6 ppm, while for 5,15 substituted OEPs the signal was downfield shifted to above 10.0 ppm. Indeed, 5,10-bis(4-*n*-pentylphenyl) OEP **254** showed a *meso* proton singlet with an intensity of two protons at 9.63 ppm while 5,10-bis(1-naphthyl) OEP **257** and 5,10-bis(9-phenanthrenyl) OEP **9** displayed two *meso* singlets at 9.88/9.87 and 9.73/9.70 ppm. The doubled *meso* signals could be attributed as described in chapter 3.3 to the existence of two atropisomers in an 1/1 mixture, while the downfield shift could be related to the influence of the phenanthrenyl and naphthyl substituents as also discussed in chapter 4, where in the respective UV/vis spectra additional red shifts of the Soret bands were observed. Furthermore, due to the unsymmetric substitution, two ¹H NMR *meso* signals were encountered for the respective 5,10-AB substituted OEPs, with exception of the OEPs **249** and **254**, which displayed a single *meso* proton signal at 9.63 and 9.68 ppm. The ppm shifts of the AB substituted OEPs **246/247/253/255/258** were furthermore located between 9.61 and 9.73 ppm and with highest downfield shifts for the anthracenyl AB-substituted OEPs **246/255**.

Another indicator for 5,10 or 5,15 substitution was furthermore the ¹H NMR CH₂/CH₃ pattern. For 5,15 substituted OEPs the proton signals of the CH₃ groups are downfield shifted relative to the signals of 5,10 substituted OEPs and the most upfield shifted

signal appeared at 1.18 ppm compared to 5,10-substituted OEPs with the farthest upfield shifted CH₃ signal at 0.26 ppm for anthracenyl substitution (**246**). Additionally, the following ¹H NMR CH₂/CH₃ pattern were observed: 5,10 disubstituted OEPs displayed a 4/4/4/4 proton CH₂ split while the CH₃ groups appeared as four signals, ideally triplets of 6/6/6/6 protons and often furthermore the CH₂ signals around 2 ppm were blurry. The more symmetric 5,15-substituted OEPs^{8,9} on the other hand showed less signals e.g. two times twelve protons for the CH₃ groups and two times eight protons for the CH₂ groups. Additional splits were observed for 5,10-disubstituted OEPs when *meta*-substituted phenyl substituents were attached or for substitution with 3-trifluoromethylphenyl residues, and the respective CH₃ pattern was 6/6/6/3/3 and 6/6/3/3/3/3. *Para*-substitution had furthermore no effect on the CH₂/CH₃ pattern, while the introduction of naphthyl and phenanthrenyl substituents had a strong effect and signal splits of 4/2/2/2/2/2 protons for the CH₂ groups and of 6/3/3/3/3/3 protons for the CH₃ groups were observed due to the increased meso-β interactions and introduced unsymmetry.

3.2.2 ABA and AAB regioisomers

The trisubstituted OEPs **287-291** could be isolated during the disubstitution step as described in chapter 2.2 and were expected to be the ABA substituted regioisomers due to the preferred attack of the 10- e.g. the 20-position during the substitution reaction as was discussed for the formation of *meso* 5,10-disubstituted OEPs.^{7,10,11} The ABA substituted OEPs were furthermore compared to the AAB substituted OEP **292-294**, which were derived from 5,10-bisphenyl OEP **236**. The prepared AAB substituted OEPs **292-294**, showed compared to the obtained ABA substituted OEPs **287-290** upfield shifted *meso* protons and NH signals. The NH signals were located around -2.1 ppm while the *meso* proton signals were displayed in the ¹H NMR spectrum at 9.40-9.43 ppm as it can be seen in table 3.4.1. The shift differences were explained as due to the additional phenanthrenyl and anthracenyl substituents for the ABA substituted OEPs and similar was observed in chapter 3.2.1. Furthermore the *meso* proton and NH signals of the OEPs **292-294** were relative to the ABA substituted OEP **291** downfield shifted, due to the influence of the additional methoxy groups attached to the OEP **291**. However, the AAB substituted OEPs **292-294** were unsymmetrical substituted, while besides of the possibility of the formation of atropisomers, which will be discussed in the following chapter, the ABA OEPs **287-291** were symmetrical substituted. Therefore ABA and

AAB substitution could be identified due to the number of signals for the *meso* substituents appearing in the ^1H NMR and ^{13}C NMR spectra (the less signals, the more symmetric the OEP).

Figure 3.2.2.1 for example displays the HMQC spectrum of the AAB substituted OEP 5,10-bisphenyl-15-(4-*n*-pentylphenyl) OEP **294**, while the ^1H MMR profiles of all AAB substituted OEPs are shown in figure 3.2.2.2. As it can be seen, several signals were displayed in the aromatic area for the OEPs **294** and a quick overview of the number of signals could be obtained from the HMQC spectrum. The six ^1H NMR signals between 8.35 and 7.46 ppm were attributed to the OEP **294** by comparison of the in the experimental part gathered ^1H NMR data, while the signals at 7.15 and 7.09 ppm were identified as impurities.

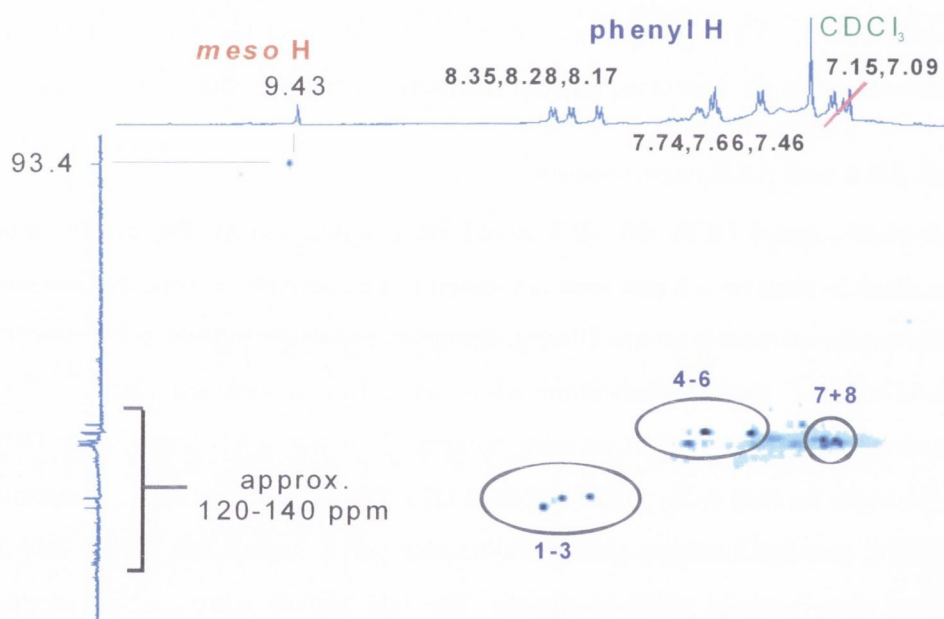


Fig. 3.2.2.1. HMQC downfield spectrum of the AAB substituted 5,10-bisphenyl-15-(4-*n*-pentylphenyl) OEP **294**; [ppm].

Due to the AAB substitution the *ortho*-phenyl protons appeared as three well separated doublets at 8.35, 8.28 and 8.17 ppm (2 protons each) while the *para*- and *meta*-signals of the phenyl substituents merged slightly into each other and could be located at 7.74 ppm (2H, *para*-phenyl H) and at 7.66 ppm (4H, *meta*-phenyl H). The *meta*-phenyl doublet of the 4-*n*-pentylphenyl substituents was furthermore displayed at 7.46 ppm (2H).

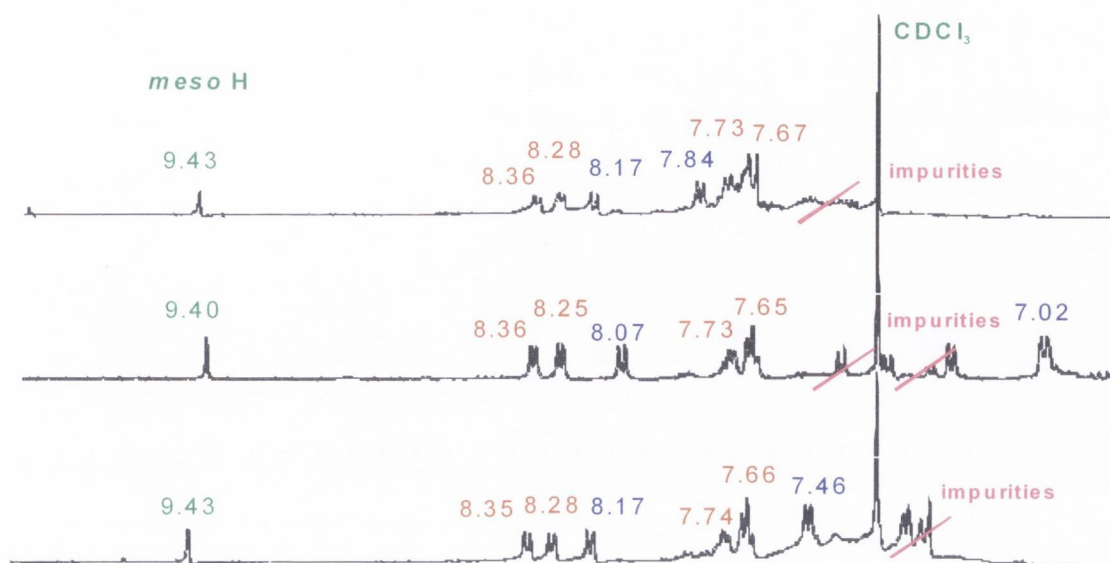


Fig. 3.2.2.2. *Meso* proton and aryl proton signals of the synthesized, unsymmetric AAB substituted OEPs **292-294**; 5,10-bisphenyl-15-(4-bromophenyl) OEP **293** (top), 5,10-bisphenyl-15-(4-dimethylaminophenyl) OEP **292** (middle) and 5,10-bisphenyl-15-(4-*n*-pentylphenyl) OEP **294** (bottom); [ppm], blue=bromophenyl, dimethylaminophenyl and *n*-pentylphenyl signals.

Additionally, the in figure 3.2.2.2 shown downfield profiles, displayed the same trends in respect to the AAB substitution. As was shown in figure 3.1.1.6, on the other hand, that 5,15-bis(9-anthracenyl)-10-phenyl OEP **246** displayed only a single “*ortho*-anthracenyl” doublet at 8.26 ppm with an intensity of four protons due to the ABA substitution. In figure 3.2.2.3 furthermore the spectrum of 5,15-bis(9-phenanthrenyl)-10-phenyl OEP **287** is compared to 5,10-bis-(9-phenanthrenyl) OEP **9**. 5,10-Bis-(9-phenanthrenyl) OEP **9** occurred as a 1/1 mixture of two atropisomers as will be described in chapter 3.3 and therefore several signals appeared double while the effect was less obvious for the ABA substituted OEP **287**, as the signals at 8.44, 8.39 and 8.30 ppm of the *ortho*-phenyl protons and the slight split of the 8'-phenanthrenyl singlet were the only indicators. No additional *quasi-ortho*-signals (6',11'-position) were observed and proved also the ABA substitution pattern.

Furthermore the blurry ^1H NMR spectrum of 5,15-bis(3-methoxyphenyl)-10-phenyl OEP **291** is shown in figure 3.2.2.4.

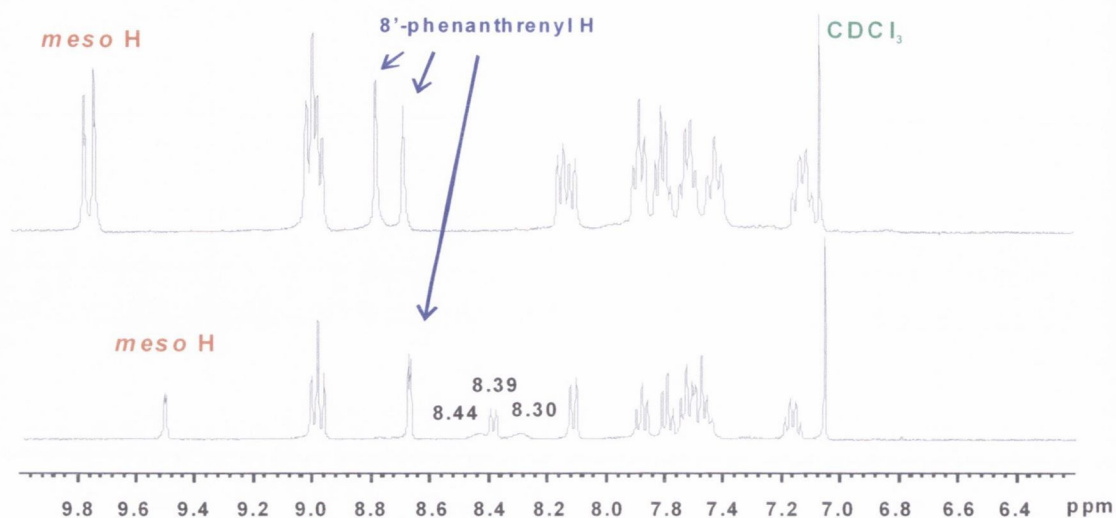


Fig. 3.2.2.3. Comparison of the phenanthrenyl signals of 5,10-bis(9-phenanthrenyl) OEP **9** (top) and 5,15-bis(9-phenanthrenyl)-10-phenyl Pd(II)OEP **304** (bottom).

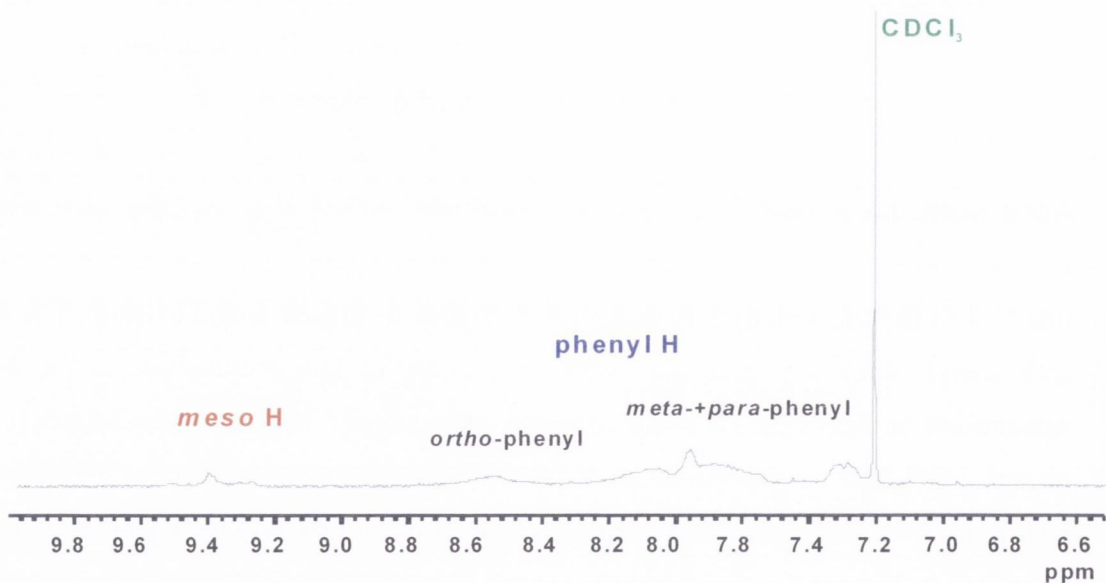


Fig. 3.2.2.4. Downfield ^1H NMR spectrum of 5,15-bis(3-methoxyphenyl)-10-phenyl OEP **291**.

However, the spectrum of OETPP (not shown, compare to Pd(II)OETPP **18**) was also observed to display strongly broadened signals as well as the spectrum of 5,10,15,20-tetrakis-(9-phenanthrenyl) OEP **11** of which the upfield spectrum was shown in figure

3.1.2.2. The broadened signals were explained by the conformational flexibility at room temperature due to the methoxyphenyl and tetrasubstitution of the OEPs **291** and **11**.^{2,3,4} As it can be seen in figure 3.2.2.4, the signal assignment was difficult for the OEP **287**, while the respective mass, UV/vis and ¹³C NMR spectra were obtained. On the other hand, the spectrum of the respective *meso* disubstituted OEP **252** was sharp (not shown). Strongly broadened ¹H NMR spectra were also described by Syrbu *et al.* for *meso* tetrasubstituted octaethyl- and octamethylporphyrins.^{13,14} Protonation of the core nitrogens by addition of acid furthermore reduced the broadening due the enhanced core rigidity induced by the additional protons.¹³ Variable temperature experiments were carried out in 1995 by Smith/Medforth/Shelnutt³ using dodecaarylsubstituted porphyrins and in 2005 by Nakamura and co-workers as discussed previously.⁵ Temperature experiments and protonation (addition of trifluoroacetic acid) were also attempted for the prepared 5,10,15,20-tetrakis(9-phenanthrenyl) OEP **11** but didn't show significant changes and were therefore not presented in this work.

3.3 Atropisomerism and ¹H NMR spectra of 9-phenanthrenyl and 1-naphthyl substituted OEPs

Due to the unsymmetry of the 9-phenanthrenyl and 1-naphthyl substituents, OEPs with at least two 9-phenanthrenyl or 1-naphthyl substituents were observed to appear as mixtures of stable atropisomers (α,β and α,α conformers) due to the hindered rotation of the aryl substituents and an orthogonal orientation of the substituents relative to the porphyrin plane. Doubled ¹H NMR signals were observed and the respective OEPs were compared to previously reported atropisomers.^{14-18,20}

3.3.1 Atropisomers described in literature

C. J. Medforth *et al.* described atropisomerism for synthesized and investigated peripherally crowded porphyrins. They investigated β and *meso* phenyl rotation barriers in TPPs, dodecaarylporphyrins (DARPs) and tetraaryloctaphenylporphyrins (TArOPPs) in dependency of the core substitution and the induced macrocycle deformation.¹⁴ They used variable temperature ¹H NMR spectroscopy (VT) to determine aryl-porphyrin rotational barriers for β and *meso* substituents and investigated dynamic processes in porphyrins e.g. the NH tautomerism and the inversion of the macrocycle. For the experiments they induced asymmetry in the porphyrins by using respective substituents

or ligands and a 3-methoxyphenyl residue was chosen as a standard substituent, as it could be readily introduced. Usually atropisomers were observed in the corresponding crystals with multiple orientations of the phenyl substituent due to steric repulsion. The relative orientation of the methoxyl group was furthermore observed to have a minimal effect on the calculated rotational barriers and also the effect on the macrocycle distortion was small. Additionally, an unsymmetric 3-thienyl group was introduced and octa-(3-thienyl)-tetrakisphenylporphyrin **233** was prepared. Two nonplanar atropisomers could be isolated in solid state and the structures are shown in fig. 3.3.1.1.

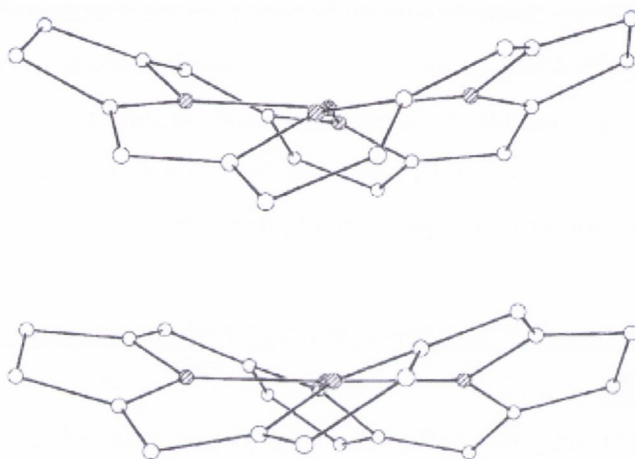


Fig. 3.3.1.1. Crystal structures of octa-(3-thienyl)-tetrakisphenyl porphyrin **233a,b**. The aryl substituents and protons have been omitted and the shown atropisomers were obtained.¹⁴

The overall conformation of the atropisomers **233a,b** contained saddling and ruffling deformations and similar was reported for Ni(II)OETNP by M. O. Senge in 1993.¹⁵ The ¹H NMR spectrum of octa-(3-thienyl)-tetrakisphenyl porphyrin **233a,b** displayed furthermore three signals at 6.64, 6.57 and 6.40 ppm with an intensity of eight protons for each of the eight thienyl substituents. Instead of two clear doublets, broadened signals were observed and the broadening was attributed to the increased molecular flexibility.¹⁴ However, in 2003 Burell and co-workers¹⁶ prepared stable β -substituted α,β and β,β porphyrin atropisomer in solution by [2+2] condensation reaction as shown in figure 3.3.1.2 and also the respective copper (II) complexes were obtained.

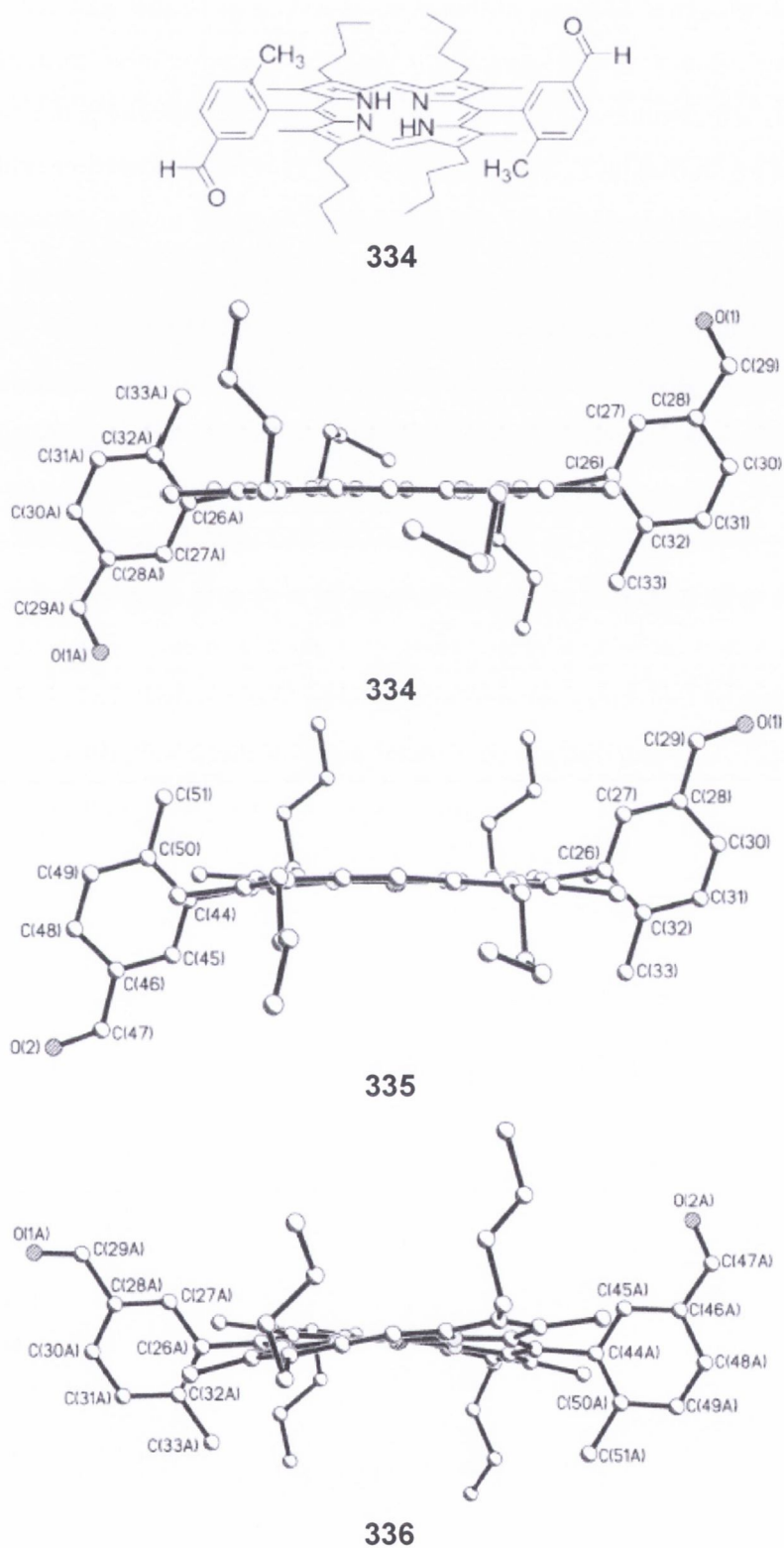


Fig. 3.3.1.2. Chemical structure of the α,β atropisomer **334**, the respective solid state structure, the bent α,β copper (II) complex **335** and the twisted α,α copper (II) complex **336**; the hydrogen atoms were omitted for clarity.¹⁶

The α,β atropisomer **334** was furthermore observed to be the least polar and was eluted first during column chromatography. It was flat shaped relative to the bent and twisted copper (II) atropisomers **235/236**. For crystal growth, especially the copper complexes were used by Burrell and co-workers, and the ^1H NMR assignment could be carried out due to the nonequivalence of the CH_2 butyl signals in the stronger perturbed α,β atropisomer **234**.¹⁶ The authors provided additionally a brief overview of the history of atropisomerism of porphyrins and reported that first atropisomers were described by Gottwald and Ullman while mostly *meso* mono-, di- and tetrasubstituted, β -substituted porphyrins were reported afterwards by different authors. Atropisomerism was furthermore observed when additional groups were attached in *ortho*-position of the *meso* substituents due to the hindered rotation and as a result of the *meso*- β interactions. The *meso* substituents remained in orthogonal positions relative to the porphyrin plane, which allowed atropisomerism. However, atropisomers were often of interest in applications of molecular recognition, as selective binding was achieved due to their “two faces”. The introduction of a metal atom in the porphyrin core, was furthermore observed to result in either, an increase or an restricted rotation, depending on the porphyrin.¹⁶

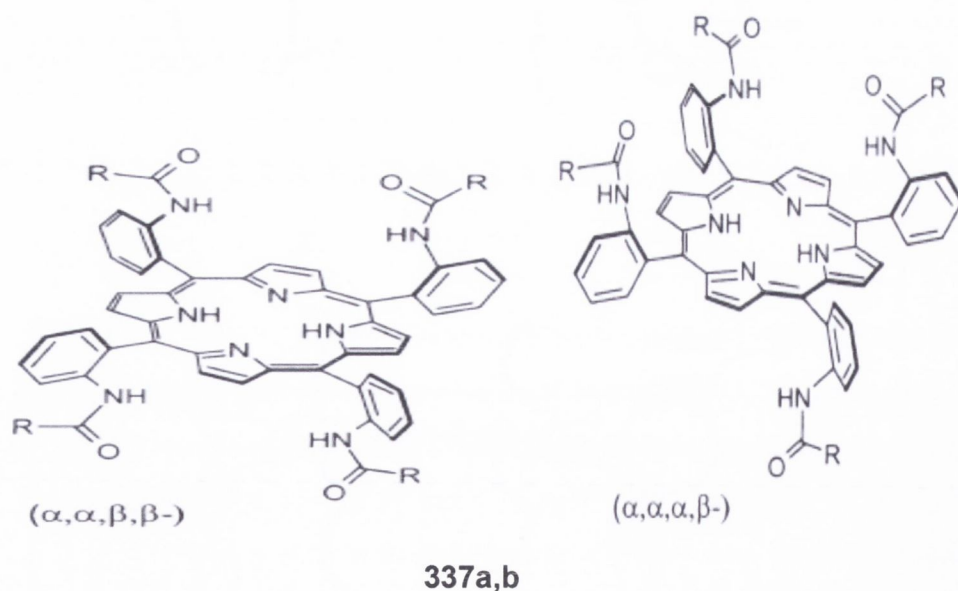


Fig. 3.3.1.3. Prepared atropisomers by Paleta *et al.*¹⁷

Furthermore in 2002, Paleta *et al.* obtained the in figure 3.3.1.3 shown $\alpha,\alpha,\beta,\beta$ and $\alpha,\alpha,\alpha,\beta$ atropisomers **337a,b**¹⁷ and Cammidge/Öztürk prepared the naphthol atropisomers **339a,b** shown in figure 3.3.1.4.¹⁸ The naphthol atropisomers **339a,b** were also observed to be stable in solution at room temperature and the synthesis had to be carried out with the protected methoxynaphthyl precursors (not shown) as the use of the respective 1,8-dialdehyde failed. In order to obtain a small number of atropisomers and atropisomers that were separable furthermore a [2+2] strategy was applied (compare to chapter 1) and the shown pentafluorophenyl dipyrromethanes were chosen in order to prevent side reactions by scrambling due to the destabilizing of the respective carbocations. Sets of methyl and naphthyl signals in the ¹H NMR spectrum indicated the existence of atropisomers in the crude mixture and subsequent separation by column chromatography afforded the single atropisomers.

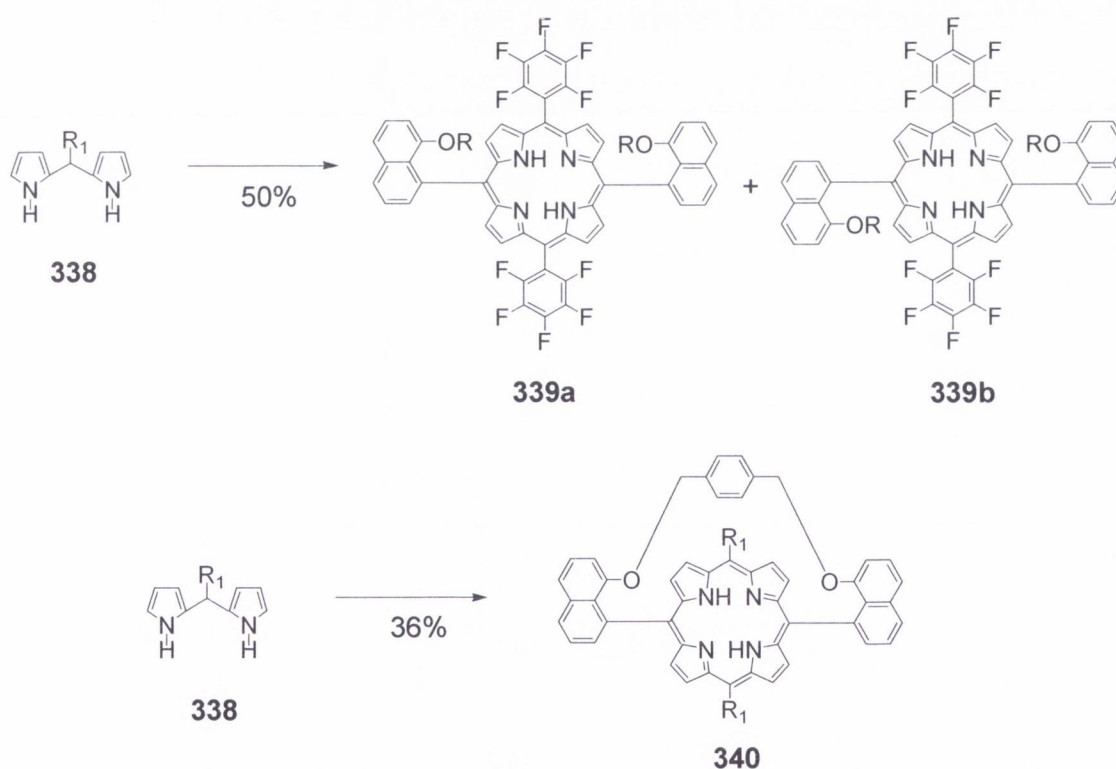
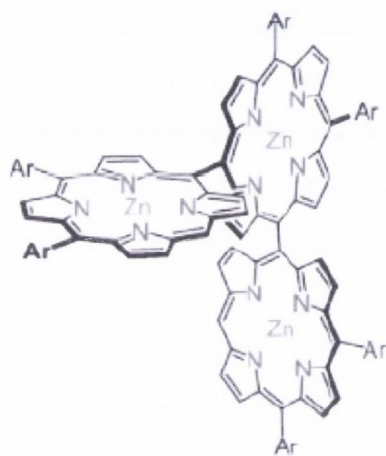
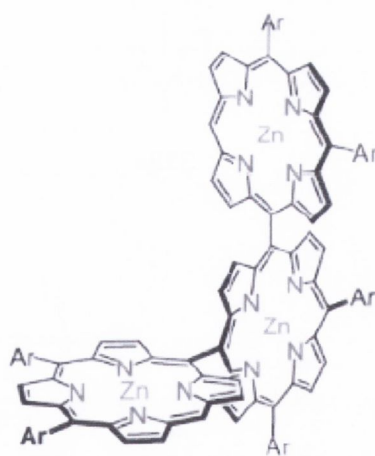


Fig. 3.3.1.4. Synthesized α,α -5,15 and α,β -5,15 atropisomers **339a,b** (top) and preparation of the single α,α -5,15-bridged atropisomer **340** (bottom); R=methyl, R_1 =pentafluorophenyl.^{18,19}

The α,α -5,15 atropisomer displayed a single methyl proton singlet at 2.22 ppm while it appeared for the α,β -5,15 atropisomer at 2.04 ppm and only a shift difference of 0.03 ppm was observed for certain naphthyl protons. As it can be seen in figure 3.3.1.4, also the α,α -bridged 5,15 atropisomer **341** was obtained in 36% yield, while additional scrambling prevention had to be applied and a similar OEP was already obtained in 1986.^{18,19} The enantiomers **341/342**, shown in figure 3.3.15, were furthermore isolated by Osuka *et al.*²⁰



341



342

Fig. 3.3.1.5. Enantiomers **341** and **342** obtained by Osuka *et al.*;²⁰ Ar=3,5-di-*tert*-butylphenyl.

3.3.2 The atropisomers of 5,10-bis(9-phenanthrenyl) OEP (9)

In figure 3.3.2.1 the downfield ^1H NMR regions of 5-(9-phenanthrenyl) OEP **8** and 5,10-bis(9-phenanthrenyl) OEP **9** are shown. As it can be seen, the signals observed for the 4'- and 12'-phenanthrenyl protons shift with the disubstitution from 7.14 (the signal is not displayed) and 7.27 ppm to 7.31 ppm. Furthermore, the two singlets displayed at 8.75 and 8.65 ppm could be attributed to an 1/1 mixture of the α,α and α,β atropisomers, which resulted from at ambient temperature up and down conformations of the phenanthrenyl substituents, remaining in an 90 degree angle relative to the porphyrin plane. The shift difference of those is relative strong (signals at 8.74 and 8.65 ppm) due to proximity of the 8'-phenanthrenyl proton to the porphyrin ring (*quasi-ortho*-position). The *meso* monosubstituted OEP **9** displayed furthermore a single singlet at 8.71 ppm and two doublets can be seen around 8.08 ppm for the 14'-position of the OEP **10**, which indicated also two atropisomers. Furthermore, also two *meso* proton signals were displayed at 9.73 and 9.70 ppm (not shown), as well as two slim NH signals at -2.40 and -2.49 ppm due the atropisomers.

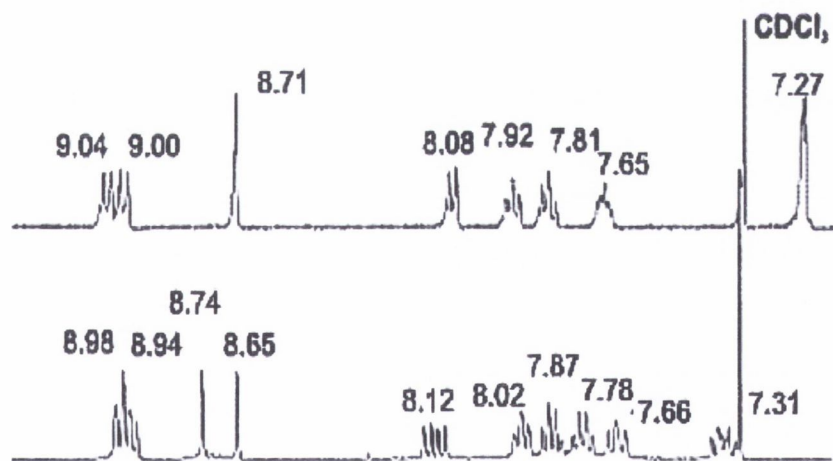


Fig. 3.3.2.1. Downfield ^1H NMR spectrum of 5-(9-phenanthrenyl) OEP **8** (top) and 5,10-bis(9-phenanthrenyl) OEP **9** (bottom).

The spectrum of the respective palladium (II) complex **13** was similar to the spectrum of the free base OEP **9**. However, only three instead of four signals were observed between 7.6 and 8.1 ppm and the gap between the 8'-phenanthrenyl singlets decreased slightly

(signals at 8.64 and 8.58 ppm) due to the heavy metal influence. Further splitting occurred also for the ethyl CH₂ signals between 2.00 and 2.60 ppm.

3.3.3 The atropisomers of 5,10-bis(1-naphthyl) OEP (257)

5,10-Bis(1-naphthyl) OEP **257** showed similar features in the ¹H NMR spectrum as the previously discussed 5,10-bis(9-phenanthrenyl) OEP **9**. Double sets of signals (doublets at 8.47 and 8.40 ppm for the 2'-naphthyl proton), as it can be seen in figure 3.3.3.1, indicated also an 1/1 mixture of two atropisomers. The CH₂ signals were broadened and blurry due to the overlaid signals and two *meso* proton signals (9.67 and 9.69 ppm) were displayed as well as two slim NH signals in the upfield. As observed for 5,10-bis(9-phenanthrenyl) OEP **9**, a strong downfield shift was found for the 7'- and 8'-naphthyl protons (6.98 to 7.20 ppm) relative to the *meso* monosubstituted OEP **7**.

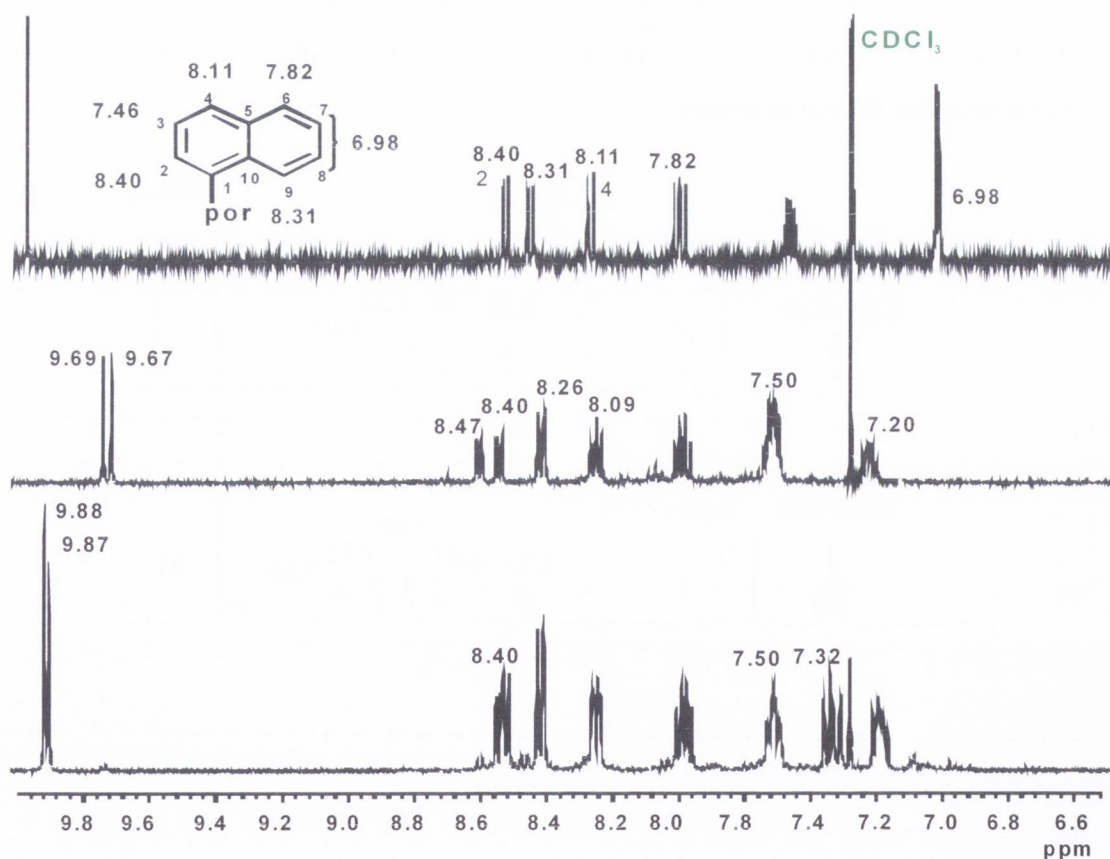


Fig. 3.3.3.1. Comparison of the downfield ¹H NMR spectra of 5-(1-naphthyl) OEP **7** (top), the mixture of atropisomers of 5,10-bis(1-naphthyl) OEP **257** (middle) and of 5,10-bis(1-naphthyl) Pd(II)OEP **284** (bottom).

The *meso* proton signals were furthermore strongly upfield shifted for the OEP **257** relative to the OEP **7** and with the incorporation of palladium (II), as can be seen in figure 3.3.3.1, a downfield shift was observed and also the doublets of the 2'-naphthyl protons of the respective atropisomers merged into each other at 8.40 ppm. The palladium (II) OEP **284** displayed sharp CH₂/CH₃ signals, while the signals of the free base were blurry. Atropisomers can be therefore easier identified in the respective free base porphyrins as the shift differences are increased.

3.3.4 The atropisomers of 5-(1-naphthyl)-10-(9-phenanthrenyl)OEP (**259**)

In analogy to the previously discussed OEPs **9** and **257**, 5-(1-naphthyl)-10-(9-phenanthrenyl) OEP **259** formed at ambient temperature two stable atropisomers in an 1/1 mixture.

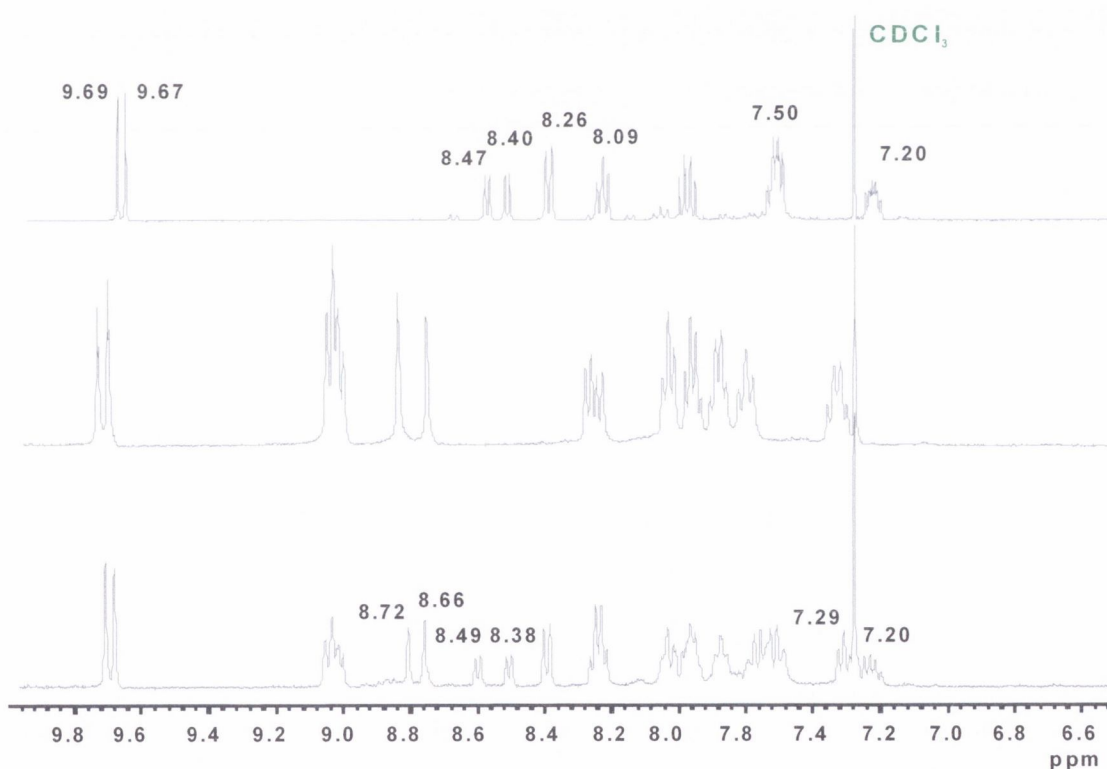


Fig. 3.3.4.1. Comparison of the downfield ¹H NMR regions of 5,10-bis(1-naphthyl) OEP **257** (top), 5,10-bis(9-phenanthrenyl) OEP **9** (middle) and 5-(1-naphthyl)-10-(9-phenanthrenyl) OEP **259**.

Due to the AB substitution two *meso* proton signals were displayed and were observed to be slightly doubled due to the mixture of atropisomers. Additionally two NH signals (not shown) were displayed and the ethyl CH₂ signals were blurry as described previously. As it can be seen in figure 3.3.4.1, also double 8'-phenanthrenyl singlets and doubled 2'-naphthyl doublets were displayed.

3.3.5 The atropisomers of 5,15-bis(9-phenanthrenyl)-10-phenyl OEP (287), 5,15-bis(9-phenanthrenyl)-10-(4-*n*-pentylphenyl) OEP (288), 5,15-bis(9-phenanthrenyl)-10-(1-naphthyl) OEP (289) and 5,15-bis(3-methoxyphenyl)-10-phenyl OEP (291)

5,15-Bis(9-phenanthrenyl)-10-phenyl OEP **287** was obtained in analogy to the disubstituted OEPs **9/257/259** in a 1/1 mixture of two atropisomers, which could be identified due to double signal sets in the ¹H NMR spectrum. Two close *meso* signals were displayed at 9.51 and 9.52 ppm with an intensity of one proton each and could be attributed to the α,α and α,β atropisomer shown in figure 3.3.5.1 and also two 8'-phenanthrenyl singlets were observed at 8.67 and 8.68 ppm as it can be seen in figure 3.3.5.2.

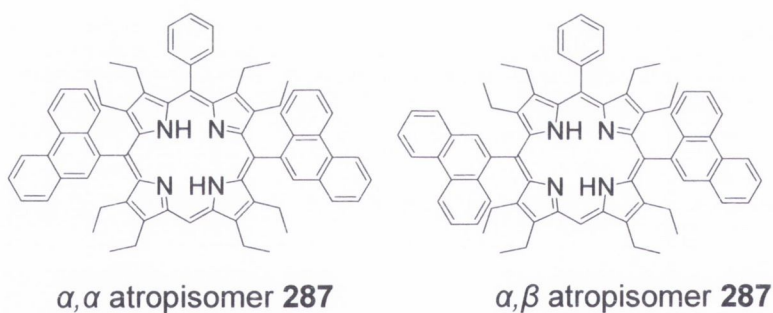


Fig. 3.3.5.1. Atropisomers of 5,15-bis(9-phenanthrenyl)-10-phenyl OEP **287**.

An unusual split could be furthermore observed for the *ortho*-phenyl protons, which appeared as a doublet at 8.39 ppm (1H) and as two broad “singlets” at 8.44 and 8.30 ppm (each 0.5H) and similar was reported in literature.⁴ The same behaviour was furthermore observed for *ortho*-phenyl protons of 5,15-bis(9-phenanthrenyl)-10-(4-*n*-pentylphenyl) OEP **288** (not shown). Furthermore, as observed for the disubstituted OEPs **9/257/259**, the palladium(II) incorporation into 5,15-bis(9-phenanthrenyl)-10-phenyl OEP **287** sharpened all signals, including the *ortho*-phenyl signals due to the

equalizing effect of the heavy metal atom (higher core rigidity), while the distance between the 8'-phenanthrenyl singlets increased surprisingly, as shown in figure 3.3.5.3. A single singlet also observed for the *meso* protons of the two atropisomers of the palladium (II) complex **304**.

However, the spectrum of 5,15-bis(9-phenanthrenyl)-10-(1-naphthyl) OEP **289** was more complex and three atropisomers were observed as shown in figure 3.3.5.5 and as illustrated in figure 3.3.5.4. The statistical ratio for the appearance of the three atropisomers was $\alpha,\alpha',\beta/\alpha,\beta',\alpha/\alpha,\alpha',\alpha = 1/0.5/0.5$ and the intensities of the *meso* proton signals (1/3) were explained by identical shifts of the α,α atropisomers **289a,b** relative to the α,β atropisomer **289c**.

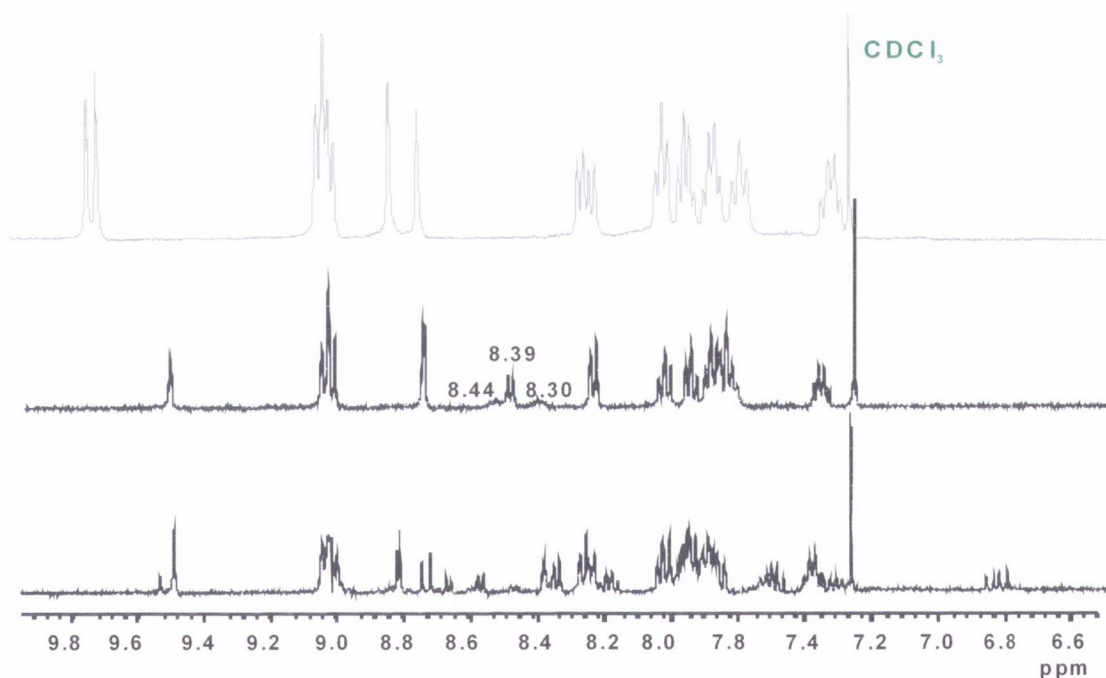


Fig. 3.3.5.2. Comparison of the downfield ^1H NMR region of 5,10-bis(9-phenanthrenyl) OEP **9** (top), 5,10-bis(9-phenanthrenyl)-10-phenyl OEP **287** (middle) and 5,15-bis(9-phenanthrenyl)-10-(1-naphthyl) OEP **289** (bottom). The signals at 8.44 and 8.30 nm are due to the line withdraw, which was necessary for the print difficult to recognize. A slightly better print could be furthermore achieved for the corresponding palladium (II) complex **304**, shown in figure 3.2.2.4.

Two 8'-phenanthrenyl singlets (the close singlets at 8.74 and 8.75 ppm) could be furthermore attributed to the α,α',β atropisomer **289c**, while the singlets at 8.67 and 8.64 ppm, with equal intensities belonged to the atropisomers **289a,b**.

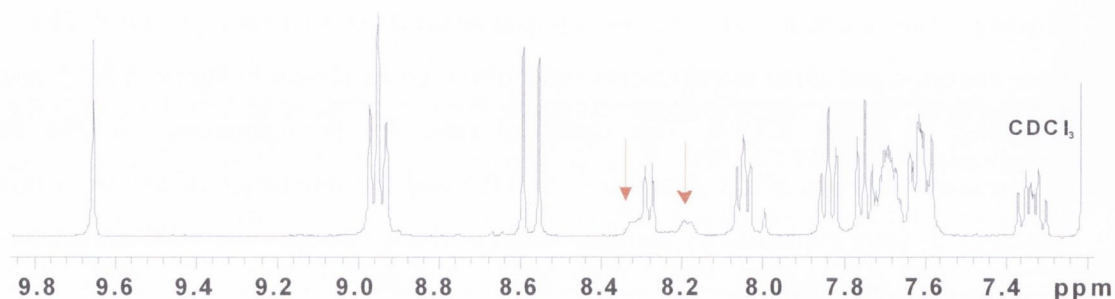


Fig. 3.3.5.3. Aromatic ^1H NMR area of 5,15-bis(9-phenanthrenyl)-10-phenyl Pd(II)OEP **304**. The sharpened *ortho*-phenyl signals are indicated by the red arrows.

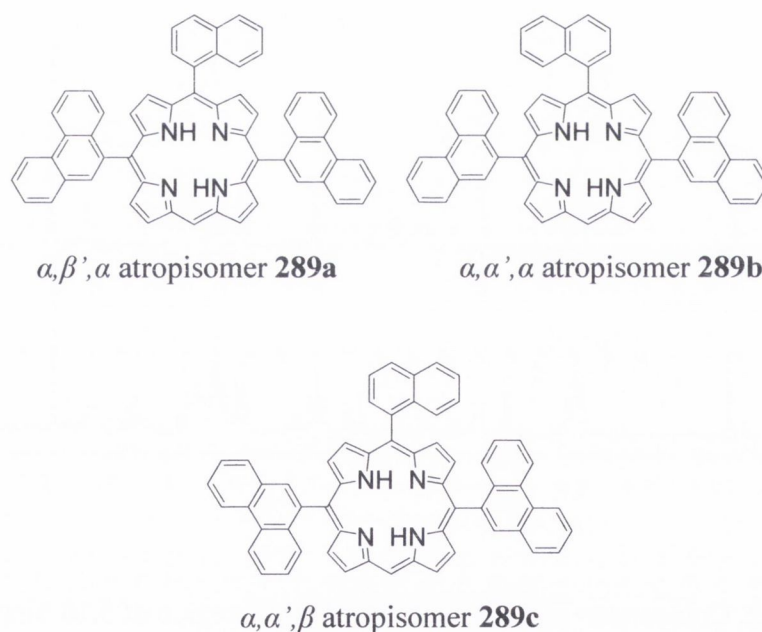


Fig. 3.3.5.4. Atropisomers of 5,15-bis(9-phenanthrenyl)-10-(1-naphthyl) OEP **289**.

The doublet at 8.48 ppm, representing a 2'-naphthyl proton, was again attributed to the α,α',β atropisomer **289c**, while the doublets at 8.37 and 8.57 ppm belonged to the atropisomers **289a,b** and were only displayed with half intensity compared to the doublet at 8.48 ppm following the statistical ratio. Overall seven signals were displayed

in the ^1H NMR spectrum for the 8'-phenanthrenyl and 2'-naphthyl protons and followed the ratio of 1/1/2 (figure 3.3.5.5). Furthermore the downfield ^1H NMR region of the OEP **289** is shown in figure 3.3.5.6 relative to the respective disubstituted OEP **259**.

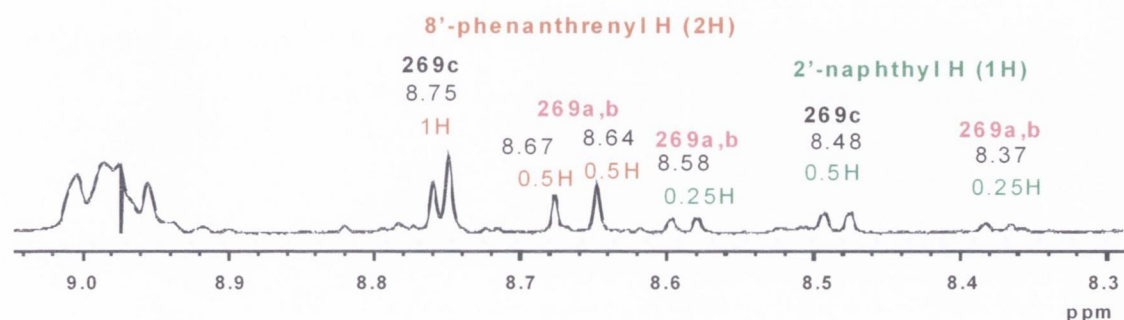


Fig. 3.3.5.5. ^1H NMR 8'-phenanthrenyl singlets and 2'-naphthyl doublets of the three atropisomers in a 2/1/1 ratio for **229c/229a/229b**.

The spectrum of 5,15-bis(3-dimethoxyphenyl) OEP **291** also wise shown in figure 3.2.2.4 and didn't allow a signal assignment due to its blurry appearance, whereas in analogy to 5,15-bis(9-phenanthrenyl)-10-phenyl OEP **287** two atropisomers were expected.

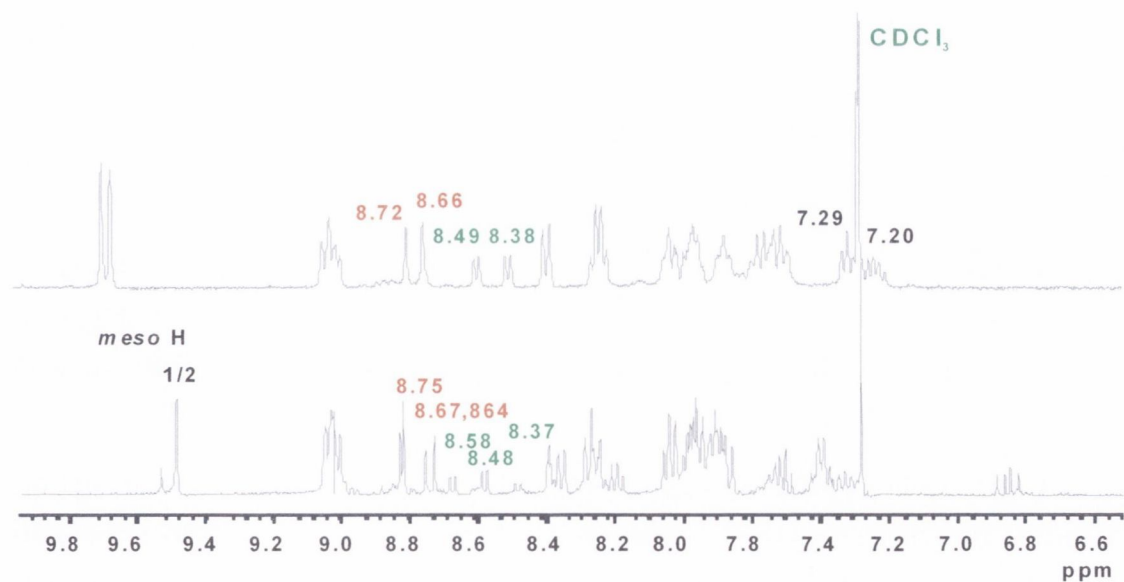


Fig. 3.3.5.6. Downfield ^1H NMR spectrum of 5-(1-naphthyl)-10-(9-phenanthrenyl) OEP **259** (top) and 5,15-bis(9-phenanthrenyl)-10-(1-naphthyl) OEP **289** (bottom).

3.3.6 The atropisomers of 5,10,15-tris(9-phenanthrenyl) OEP (10)

The ethyl CH₂ and CH₃ signals of 5,10,15-tris(9-phenanthrenyl) OEP **10** appeared with an increased multiplicity due to the overlay of the signals of three atropisomers, whereas the signals of the respective Pd(II) complex **14** were sharp, indicating chemical equivalence. The ¹H NMR downfield region of OEP **10** is shown in figure 3.3.6.1 in comparison to the *meso* mono- and disubstituted OEPs **8** and **9**.

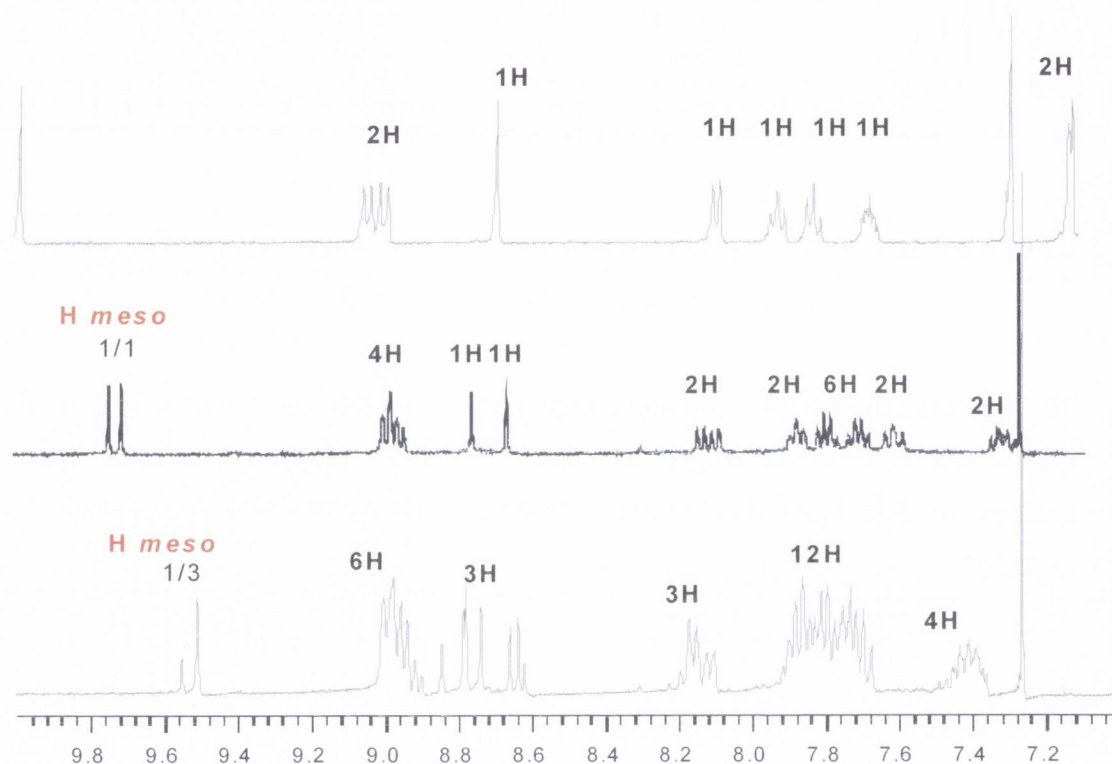


Fig. 3.3.6.1. Comparison of the downfield ¹H NMR region of 5-(9-phenanthrenyl) OEP **8** (top), the mixture of two atropisomers of 5,10-bis(9-phenanthrenyl) OEP **9** (middle) and the mixture of three atropisomers of 5,10,15-tris(9-phenanthrenyl) OEP **10** (bottom).

As for 5,15-bis(9-phenanthrenyl)-10-(1-naphthyl) OEP **289**, two *meso* proton signals with 1/3 intensities were observed. Furthermore several doublets with variable intensities were displayed between 9.00 and 8.90 ppm belonging to the 6' and 11'-phenanthrenyl protons of three atropisomers. As it can be seen in figure 3.3.6.2 and figure 3.3.6.3, the 8'-phenanthrenyl proton intensities corresponded to the statistical ratio of 2/1/1 for the atropisomers $\alpha,\alpha,\beta/\alpha,\beta,\alpha/\alpha,\alpha,\alpha$.

As twice two of nine 8'-phenanthrenyl protons were equivalent, seven singlets were observed in the respective ^1H NMR downfield region. The non equivalent 8'-phenanthrenyl protons of the α,α,β atropisomer were displayed at 8.78, 8.77 and 8.73 ppm with intensities of 0.66/0.66/0.66 protons, while the mixture of atropisomers followed the statistical ratio and intensities of 0.34/0.17/0.34/0.17/0.66/0.66/0.66 protons were observed.

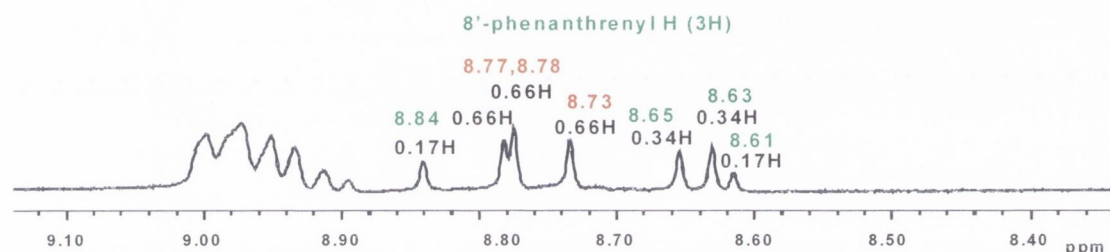


Fig. 3.3.6.2. Signal intensities and ppm shift of the 8'-phenanthrenyl protons represented in seven singlets for the α,α,β , α,β,α and α,α,α atropisomers of OEP **10**.

The palladium (II) complex of **10**, showed furthermore sharpened signals and three singlets were displayed for the *meso* protons at 9.70, 9.69 and 9.68 ppm with an 1/2/1 intensity corresponding to the α,α,β , α,α,α , and α,β,α atropisomers. The 8'-phenanthrenyl singlets were furthermore observed to be clearly separated from each other due to increased shift differences.

3.3.7 The atropisomers of 5,10,15,20-tetrakis(9-phenanthrenyl) OEP (**11**)

5,10,15,20-Tetrakis(9-phenanthrenyl) OEP **11** was obtained in a statistical mixture of four atropisomers e.g. with intensities of $(0.5/0.5/1/2)=4$ protons for $\alpha,\beta,\alpha,\beta$, $\alpha,\alpha,\alpha,\alpha/\alpha,\alpha,\alpha,\beta/\alpha,\alpha,\beta,\beta$ as it can be seen in figure 3.3.7.1. Two 8'-phenanthrenyl singlets had to be displayed for the $\alpha,\beta,\alpha,\beta$ atropisomer, a single singlet for the $\alpha,\alpha,\alpha,\alpha$ atropisomer, three singlets for the $\alpha,\alpha,\alpha,\beta$ atropisomer and two singlets for the $\alpha,\alpha,\beta,\beta$ atropisomer (overall eight singlets) with intensities of $2 \times 0.25/1 \times 0.5/3 \times 0.33$ and $2 \times 1=0.5/0.5/1/2=4$ protons. Indeed, the palladium (II) complex **15** displayed six 8'-phenanthrenyl singlets, as it can be seen in figure 3.3.7.1, while two times two singlets merged into each other at 8.79 and 8.72 ppm. On the other hand, the free base OEP **10**

displayed seven signals, as three instead of two signals appeared now between 8.75 and 8.90 ppm relative to the palladium (II) complex **15**.

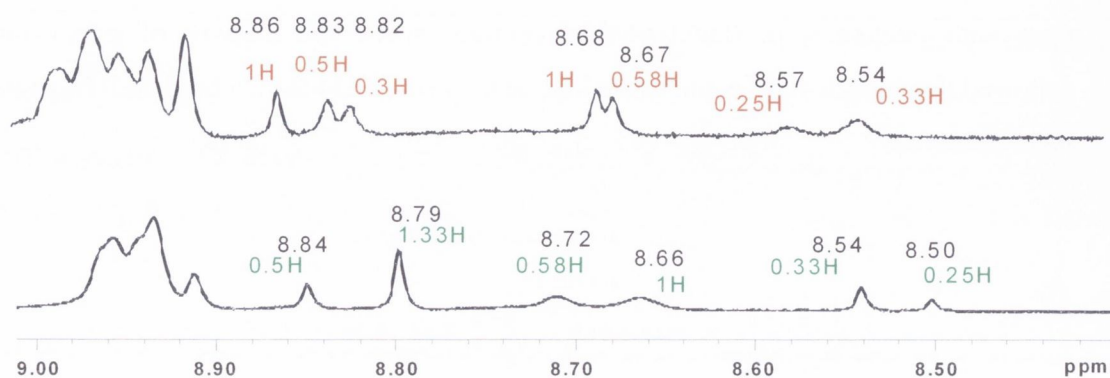


Fig. 3.3.7.1. 8'-Phenanthrenyl signals of the OEP **11** (top) and its Pd(II) complex **15** (bottom).

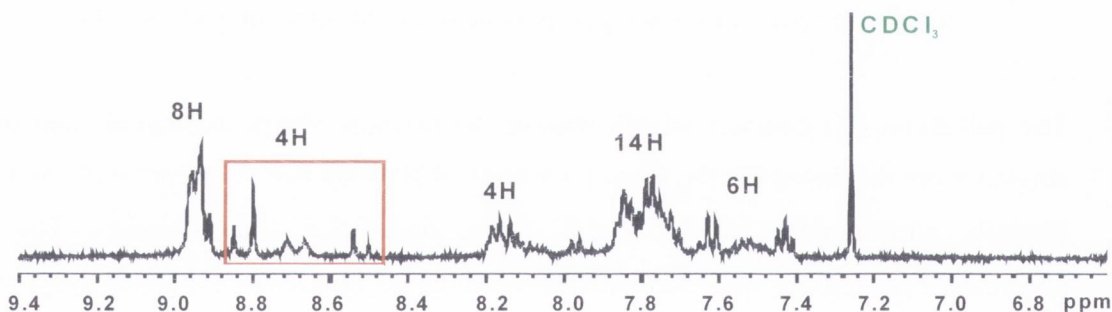


Fig. 3.3.7.2. Downfield ^1H NMR region of 5,10,15,20-tetrakis(9-phenanthrenyl) Pd(II)OEP **15**.

3.4 Meso proton and NH ^1H NMR signals of synthesized OEPs

Mono-, di-, tri- and tetrasubstituted OEPs could be readily differentiated and identified by their characteristic *meso* proton and NH signals in the ^1H NMR spectrum. Two *meso* proton singlets (9.75–10.25 ppm) with intensities of 2/1, were displayed for *meso* monosubstituted OEPs, a single singlet for 5,10 (9.63–9.73 ppm) or 5,15- A_2 disubstituted OEPs (10.2 ppm), representing two equivalent protons, two singlets with 1/1 intensity for 5,10-AB substituted OEPs (9.63–9.73 ppm) and a single *meso* proton signal for *meso* trisubstituted OEPs (9.39–9.54 ppm). As it can be seen in table 3.4.1, the

meso proton signals shifted upfield from OEP **1** to *meso* trisubstituted OEPs due to the weakening ring current,²¹ while the NH signals shifted downfield from -3.7 ppm (OEP **1**) to $+0.26$ ppm for the OEP **69** as displayed in table 3.4.1, while the trisubstituted methoxyphenyl and anthracenyl OEPs **291/290** showed also strongly downfield shifted NH signals at -0.08 and -0.25 ppm. The NH signals of *meso* monosubstituted OEPs were furthermore displayed between -3.24 and -2.30 ppm, for 5,10-disubstituted OEPs between -2.74 and -2.40 ppm, for 5,15-disubstituted OEPs between -2.96 and -2.10 ppm, for trisubstituted OEPs between -2.11 and -0.08 ppm. Due to mixtures of atropisomers, the unsymmetric A or AB substitution and slow NH tautomerisation at room temperature as described in the chapters 3.3.2ff and 3.2.1, often two NH signal were observed. The spectrum of the OEP tetramer **343** (figure 3.4.2), prepared by Higuchi *et al.* is additionally shown in figure 3.4.1 and displayed two *meso* proton signals in analogy to *meso* monosubstituted OEPs.²²

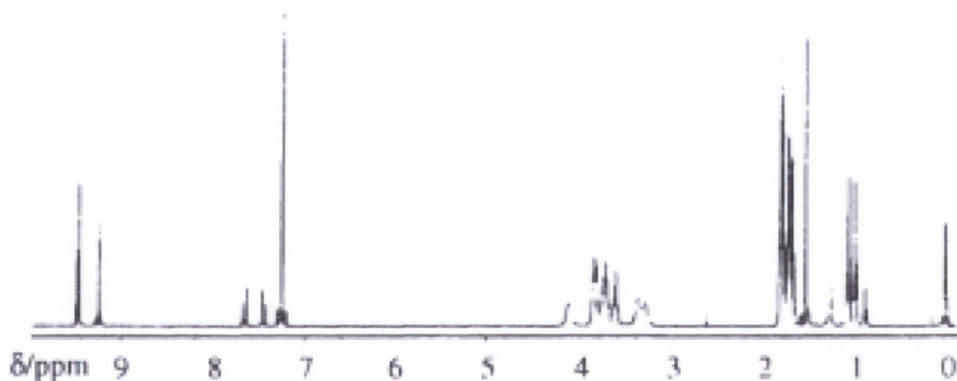


Fig. 3.4.1. ^1H NMR spectrum of the tetramer **343**.²²

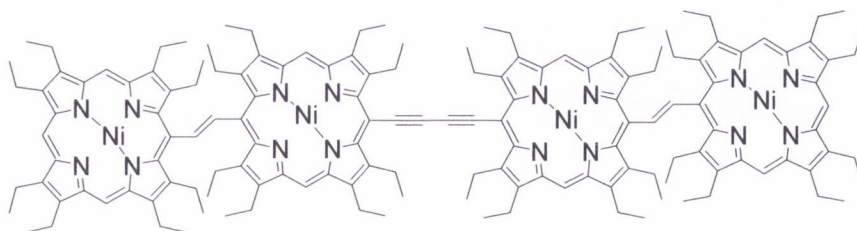


Fig. 3.4.2. OEP tetramer **343**, prepared by Higuchi *et al.*²²

During the synthesis it was furthermore observed, that certain reactions were carried out with ease, while others were only achieved with difficulty. A factor that influences furthermore the reaction is the change of geometry or distortion from starting material to product. A growing distortion was furthermore indicated roughly by downfield shifted NH signals as described in chapter 6 for series of porphyrins.^{13,23,24} An example for the ease of substitution was furthermore the reaction described by I. Bischoff of 5,15-bisphenyl OEP **216** to 5,10,15-trisphenyl OEP **217**, while 5,10-bisphenyl OEP **236** did not react with PhLi. In contrast to that, the OEPs **292-294** could be successfully derived from the OEP **236** during the PhD by addition of high equivalents and due to the increased reactivity of the chosen lithiates. A comparison of the NH values displayed in table 3.4.1, showed $\Delta(\text{NH})= 0.62$ ppm from OEP **236** to OEP **217**, while only $\Delta= -0.02$ ppm was observed for the OEP **216** to OEP **217**. Therefore the reaction of 5,15-bisphenyl OEP **216** to the OEP **217** was favored, while the reaction of **236** to **217** had to climb a distortional barrier, which could not be overcome by the use of phenyllithium.

OEPs	<i>meso</i> H [ppm ⁻¹]	NH [ppm ⁻¹]
1 OEP	10.28	- 3.75
221 ²⁵ 5-(4-bromophenyl) OEP	10.10, 9.85	- 3.24, - 3.11
233 5-(2-naphthyl) OEP	10.22, 9.98	- 3.09 - 2.92
231 5-(3-methoxyphenyl) OEP	10.17, 9.92	-3.07
7 5-(1-naphthyl) OEP	10.20, 9.98	- 3.04, - 2.79
234 5-acenaphthyl OEP	10.21, 9.98	- 3.04, - 2.80
5 5-(4- <i>n</i> -pentylphenyl) OEP	10.16, 9.92	- 3.02, - 3.15
6 5-(3-trifluoromethylphenyl) OEP	10.20, 9.67	- 3.02, - 3.17
4 5-phenyl OEP	10.17, 9.93	- 3.01, - 3.15
8 5-(9-phenanthrenyl) OEP	10.20, 9.98	- 3.00, - 2.73
232 5-(3-hydroxyphenyl) OEP	10.16, 9.92	-
229 5-(4-tolyl) OEP	10.23, 9.98	- 2.94
230 5-(4-dimethylaminophenyl) OEP	10.20, 9.95	- 2.91
227 5-methyl OEP	10.01, 9.81	- 2.88
16 5- <i>n</i> -butyl OEP	10.07, 9.83	- 2.75, - 2.81
228 5- <i>s</i> -butyl OEP	10.03, 9.77	- 2.30

Table 3.4.1. ¹H NMR NH and *meso* proton shifts of OEPs.

<i>OEPs</i>	<i>meso</i> H [ppm ⁻¹]	NH [ppm ⁻¹]
<i>Meso disubstituted OEPs</i>		
<i>5,10 regio isomers</i>		
249	5-(3-methoxyphenyl)-10-phenyl OEP	9.63 -2.74
236	5,10-bisphenyl OEP	9.63 -2.72
254	5,10-bis(4- <i>n</i> -pentylphenyl) OEP	9.62 -2.71
250	5-(4- <i>n</i> -pentylphenyl)-10-phenyl OEP	9.68 -2.70
253	5-(3-trifluoromethylphenyl)-10-(4-dimethylaminophenyl) OEP	9.64, 9.61 -2.68
258	5-(1-naphthyl)-10-(4- <i>n</i> -pentylphenyl) OEP	9.67, 9.66 -2.61
247	5-(9-phenanthrenyl)-10-phenyl OEP	9.69, 9.67 -2.58
257	5,10-bis(1-naphthyl) OEP	9.69, 9.67 -2.52, -2.44
246	5-(9-anthracenyl)-10-phenyl OEP	9.70, 9.67 -2.50 (br)
255	5-(9-anthracenyl)-10-(4- <i>n</i> -pentylphenyl) OEP	9.70, 9.68 -2.48
9	5,10-bis(9-phenanthrenyl) OEP	9.73, 9.70 -2.40, -2.49
<i>5,15 regio isomers</i>		
103 ⁸	5,15-bis(4-trifluoromethylphenyl) OEP	10.26 -2.10
216 ¹²	5,15-bisphenyl OEP	10.23 -2.08
101 ⁹	5,15-bis(naphtolyl) OEP	- -
106 ²¹	5-(3,5-di- <i>tert</i> -butylphenyl)-10-(2-methoxyphenyl) OEP	- -1.96
<i>Meso trisubstituted OEPs</i>		
<i>AAA type</i>		
217 ^{6,7}	5,10,15-trisphenyl OEP	9.39 -2.11
235	5,10,15-tris(1-naphthyl) OEP	9.51, 9.47 -1.64
10	5,10,15-tris(9-phenanthrenyl) OEP	9.54, 9.49 -1.53
<i>AAB type</i>		
294	5,10-bisphenyl-15-(4- <i>n</i> -pentylphenyl) OEP	9.43 -2.12
293	5,10-bisphenyl-15-(4-bromophenyl) OEP	9.43 -2.11
292	5,10-bisphenyl-15-(4-dimethylaminophenyl) OEP	9.40 -2.05
<i>ABA-type</i>		
287	5,15-bis(9-phenanthrenyl)-10-(4-phenyl) OEP	9.52 -1.78
288	5,15-bis(9-phenanthrenyl)-10-(4- <i>n</i> -pentylphenyl) OEP	9.50 -1.73
289	5,15-di-(9-phenanthrenyl)-10-(1-naphthyl) OEP	9.48 -1.51
290	5,15-bis(9-anthracenyl)-10-phenyl OEP	9.52 -0.25
291	5,15-bis(4-dimethoxyphenyl)-phenyl OEP	9.38, 9.26 -0.08

Table 3.4.1. ¹H NMR NH and *meso* proton shifts of OEPs.

<i>OEPs</i>		<i>meso</i> H [ppm ⁻¹]	NH [ppm ⁻¹]
<i>Meso</i> tetrasubstituted OEPs			
15	5,10,15,20-tetrakis(9-phenanthrenyl) OEP	-	- 1.14
69 ¹²	5,10,15,20-tetrakis(phenylethynyl) OEP	-	+ 0.26
344	OETPP (dication)	-	- 0.19

Table 3.4.1. ¹H NMR NH and *meso* proton shifts of OEPs.

REFERENCES

- 1) L. D. Field, S. Sternhell, J. R. Kalmann (2002): "Organic structures from spectra." John Wiley & sons (West Sussex, England).
- 2) J. E. Rogers, K. A. Nguyen, D. C. Hufnagle, D. G. McLean, W. Su, K. M. Gossett, A. R. Burke, S. A. Vinogradov, R. Pachter, P. A. Fleitz *J. Phys. Chem. A* **2003**, *107*, 51, 11331.
- 3) C. M. Muzzi, C. J. Medforth, L. Voss, M. Cancilla, C. Lebrilla, J.-G. Ma, J. A. Shelnut, K. M. Smith *Tetrahedron Lett.* **1999**, *40*, 6159.
- 4) K. Jayarai, A. Gold, L. M. Ball, P. S. White *Inorg. Chem.* **2000**, *39*, 3652.
- 5) A. Hoshino, Y. Ohgo, M. Nakamura *Tetrahedron Lett.* **2005**, *46*, 4961.
- 6) M. O. Senge, I. Bischoff *Eur. J. Org. Chem.* **2001**, 1735.
- 7) M. O. Senge, W. W. Kalisch, I. Bischoff *Chem. Eur. J.* **2000**, *6*, 2721.
- 8) J. Tang, J. G. Verkade *J. Org. Chem.* **1994**, *59*, 7793.
- 9) H. Ogoshi, K. Saita, K.-i. Sakurai, T. Watanabe, H. Toi, Y. Aoyama, Y. Okamoto *Tetrahedron Lett.* **1986**, *27*, 52, 6365.
- 10) M. O. Senge, I. Bischoff, X. Feng *J. Org. Chem.* **2001**, *66*, 26, 8693.
- 11) M. O. Senge, I. Bischoff, X. Feng *Tetrahedron* **2001**, *57*, 5573.
- 12) S. A. Syrбу, T.V. Lyubimova; A. S. Semeikin *Chem. Heterocyclic Comp.* **2004**, *40*, 10, 1262.
- 13) S. A. Syrбу, T. V. Lyubimova, A.S. Semeikin *Russ. J. Gen. Chem.* **2001**, *71*, 10, 1656.
- 14) C. J. Medforth, R. E. Haddad, C. M. Muzzi, N. R. Dooley, L. Jaquinod, D. C. Shyr, D. J. Nurco, M. M. Olmstead, K. M. Smith, J.-G. Ma, J. A. Shenut *Inorg. Chem.* **2003**, *42*, 2227.
- 15) M. O. Senge *J. Chem. Soc. Dalton Trans.* **1993**, 3539.
- 16) P. G. Plieger, A. K. Burrell, G. B. Jameson, D. L. Officer *Dalton Trans.* **2004**, 319.
- 17) O. Paleta, M. Benes, J. Koutnikova, V. Kral *Tetrahedron Lett.* **2002**, *43*, 6827.
- 18) A. N. Cammidge, O. Ozturk *J. Org. Chem.* **2002**, *67*, 7457.
- 19) Ogoshi, K. Saita, K.-i. Sakurai, T. Watanabe, H. Toi, Y. Aoyama, Y. Okamoto *Tetrahedron Lett.* **1986**, *27*, 52, 6365.

- 20) Y. Nakamura, I.- W. Hwang, N. Aranti, T. K. Ahn, D. M. Ko, A. Takagi, T. Kawai, T. Matsumo, D. Kim, A. Osuka *J. Am. Chem. Soc.* **2005**, *127*, 236.
- 21) H. Tamiaki, A. Kiyomori, K. Maruyama *Bull. Chem. Soc. Jpn.* **1994**, *67*, 2478.
- 22) H. Higuchi, T. Maeda, K. Miyabayashi, M. Miyake, K. Yamamoto *Tetrahedron Lett.* **2002**, *43*, 3097.
- 23) J. Takeda, M. Sato *Chem. Lett.* **1994**, 2233.
- 24) X. Z. Song, W. Jentzen, L. Jaquinod, R. G. Khoury, C. J. Medforth, S.-L. Jia; J.-G. Ma, K. M. Smith, J. A. Shelnut *Inorg. Chem.* **1998**, *37*, 2117.
- 25) M. O. Senge, I. Bischoff *Tetrahedron Lett.* **2004**, *45*, 1647.
- 26) Z. Shen, H. Uno, Y. Shimizu, N. Ono *Org. Biomol. Chem.* **2004**, *2*, 3442.

4. Crystal Structure Determinations of Pd(II), Pt(II) and H₂OEPs

The structural features of 5-*n*-butyl Pd(II) OEP **17** shown in figure 4.1 are similar to those of other *meso* monosubstituted metallo OEPs reported in literature.^{1,2,3,4} The butyl group is folded back towards one side of the molecule and in the crystal closely intersected layers of molecules are formed.

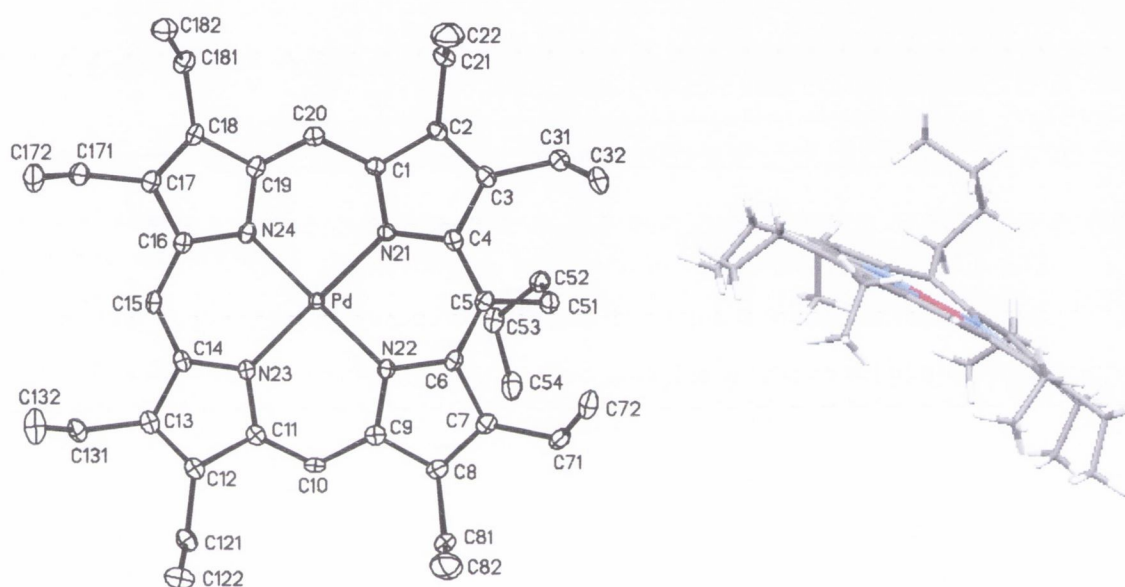


Fig. 4.1. Left side: Molecular structure and numbering of 5-(*n*-butyl) Pd(II) OEP **17** in solid state. The ellipsoids are drawn for 50% occupancy and the hydrogen atoms have been omitted for clarity. Right side: Stick model of 5-(*n*-butyl) Pd(II) OEP **17** in a side view. The hydrogen atoms are displayed.

The degree of π overlap among the molecules was small. The closest contact was the H18B \cdots Pd contact of 3.222 Å and for 5-phenyl Pd(II) OEP **273**, which is shown in figure 4.2, a Pd \cdots H53 contact of 3.287 Å and a Pd \cdots H17B contact of 3.094 Å. In 5-phenyl Pd(II) OEP **273** the phenyl ring is orthogonal orientated to the porphyrin plane with a phenyl tilt angle of 91.9° to the 4N-plane.

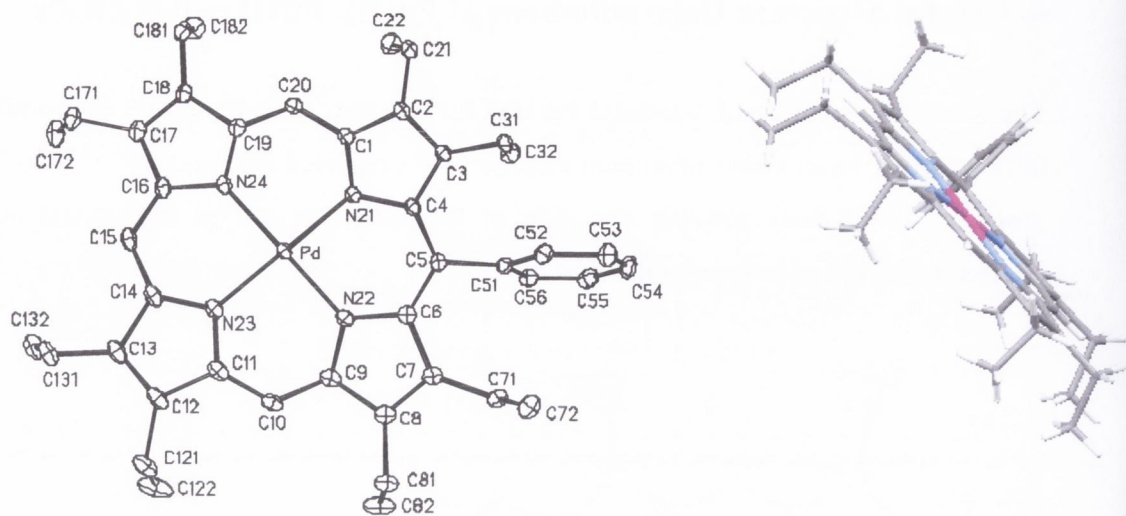


Fig. 4.2. Left side: Molecular structure and numbering of 5-phenyl Pd(II) OEP **273** in solid state. The ellipsoids are drawn for 50% occupancy and the hydrogen atoms have been omitted for clarity. Right side: Stick model of 5-phenyl Pd(II) OEP **273** in a side view. The hydrogen atoms are displayed.

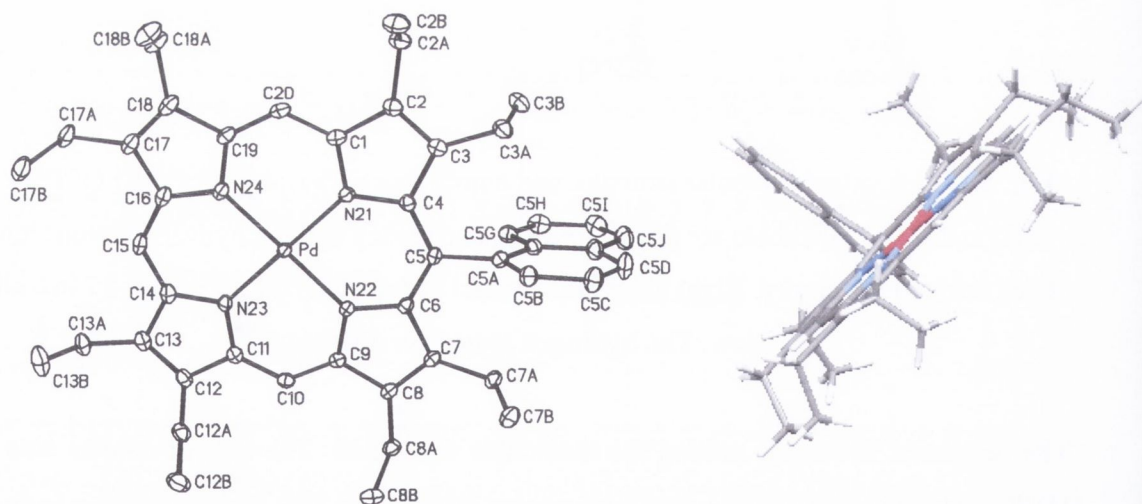


Fig. 4.3. Left side: Molecular structure and numbering of 5-(1-naphthyl) Pd(II) OEP **282** in solid state. The ellipsoids are drawn for 50% occupancy and the hydrogen atoms have been omitted for clarity. Right side: Stick model of 5-(1-naphthyl) Pd(II) OEP **282** in a side view. The hydrogen atoms are displayed.

The solid state structure of 5-phenyl Pt(II) OEP **307** (not shown) is furthermore isostructural to the corresponding palladium (II) complex **273**. The closest intermolecular contact is $\text{Pt} \cdots \text{H13A}$ with 3.085 Å and the phenyl ring is tilted by 91.7° against the 4N-plane. However, the tilt angle for 5-(1-naphthyl) Pd(II) OEP **282** is 84.1° and the structure is shown in 4.3. The crystal packing is characterized by the formation of weak π -stacked dimers. The separation of the 4N-planes is 3.405 Å, the center-to-center separation 4.711 Å, and the slip angle is 43.8°. The closest intermolecular contact is the contact between the C7 ethyl group and the Pd ion ($\text{H7B} \cdots \text{Pd} = 3.257$ Å).

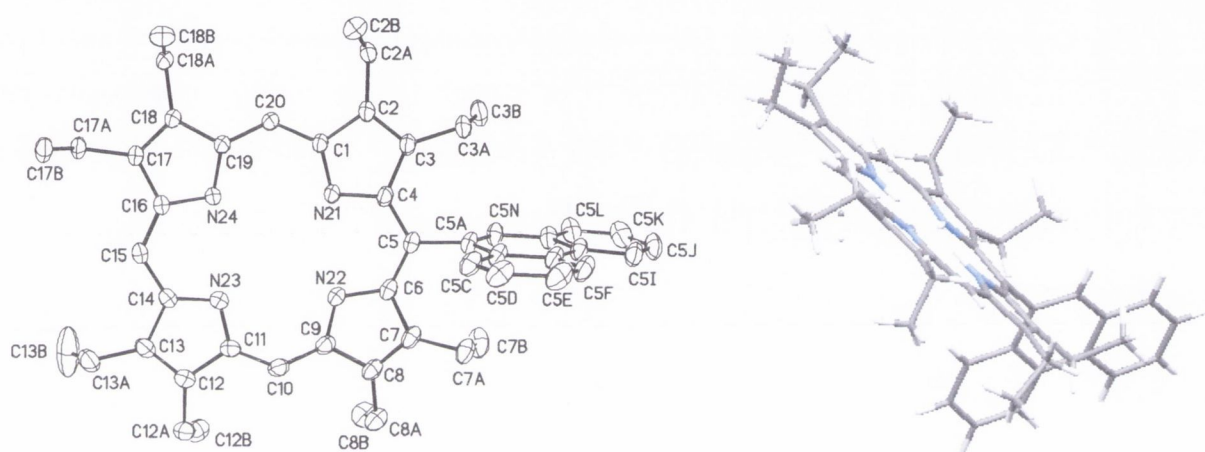


Fig. 4.4. Left side: Molecular structure and numbering of 5-(9-phenanthrenyl) OEP **8** in solid state. The ellipsoids are drawn for 50% occupancy and the hydrogen atoms have been omitted for clarity. Right side: Stick model of 5-(9-phenanthrenyl) OEP **8** in a side view. The hydrogen atoms are displayed.

Similar to the phenyl substituted OEP **307**, the 5-(1-naphthyl) Pt(II)OEP **309** (not shown) and the respective Pd(II)OEP **282** are isostructural and the tilt angle of 5-(1-naphthyl) Pt (II) OEP **309** is 83.9°. The structural parameters of the palladium(II) porphyrin cores are similar to those of symmetric Pd(II) porphyrins (table II in the appendix). The average Pd-N bond lengths of around 2.02 Å are only slightly elongated compared to planar Pd(II)OEP **2** [$\text{Pd}-\text{N}_{\text{av}} = 2.014(3)$ Å]⁶ or other S_4 symmetric Pd(II) porphyrins such as the ruffled 5,10,15,20-tetraphenyl- and -tetraisopropylporphyrins.^{7,8} Furthermore, the *meso* aryl substituted metallo OEPs show no significant degree of macrocycle distortion^{1,3} and the average deviation of the 24 macrocycle atoms from their

least-squares-plane (Δ_{24}) is similar to that of Pd(II) OEP **2** ($\Delta_{24}=0.05$ Å). In contrast, the 5-*n*-butyl Pd(II) OEP **17** exhibits a moderate but significant deviations from planarity and shows differences in displacements of the substituted and unsubstituted C_m atoms which is in agreement with earlier observations for *meso* sp^3 hybridized substituents.¹ None of the Pd(II) or Pt(II) structures showed any in-plane distortion as can be seen by the minute core elongation parameter values Ξ . In-plane distortions are more typically found in nona- and decasubstituted free base porphyrins⁹ and the obtained crystal structure of 5-(9-phenanthrenyl) OEP **8**, shown in figure 4.4, is an example for in-plane distortions. 5-(9-Phenanthrenyl) OEP **8** exhibits a significant degree of core elongation ($\Xi = 0.325$ Å), while the overall degree of out-of-plane macrocycle distortion is negligible ($\Delta_{24} = 0.06$ Å). Like in the other metallo OEPs described above the phenanthrenyl unit is orthogonal orientated to the mean plane and forms an angle of 91.8° with the 4N-plane.

REFERENCES

- 1) M. O. Senge. In *The Porphyrin Handbook*; K. M. Kadish, K. M. Smith, R. Guilard, Eds.; Academic Press: San Diego, 2000; Vol. 1, pp 239-347.
- 2) M. O. Senge *Chem. Commun.* **2006**, 243.
- 3) M. O. Senge, W. W. Kalisch, I. Bischoff. *Chem. Eur. J.* **2000**, *6*, 2721.
- 4) M. O. Senge, T. P. Forsyth, K. M. Smith *Z. Kristallogr.* **1996**, *211*, 176.
- 5) W. R. Scheidt, Y.-J. Lee *Struct. Bonding* **1987**, *64*, 1.
- 6) A. M. Stolzenberg, L. J. Schussel, J. S. Summers, B. M. Foxman, J. L. Petersen *Inorg. Chem.* **1992**, *31*, 1678.
- 7) E. B. Fleischer, C. K. Miller, L. E. Webb *J. Am. Chem. Soc.* **1964**, *86*, 2342.
- 8) M. O. Senge, I. Bischoff, N. Y. Nelson, K. M. Smith *J. Porphyrins Phthalocyanines* **1999**, *3*, 99.
- 9) M. O. Senge, C. J. Medforth, T. P. Forsyth, D. A. Lee, M. M. Olmstead, W. Jentzen, R. K. Pandey, J. A. Shelnut, K. M. Smith *Inorg. Chem.* **1997**, *36*, 1149.

Results of Part I

Several novel *meso* monosubstituted free base OEPs with aromatic residues such as 1-naphthyl, 2-naphthyl, acenaphthyl and 9-phenanthrenyl were prepared in good to excellent yields (26–89%) by nucleophilic substitution reactions carried out with organolithium reagents as described in chapter 2.2.1. Methylation with MeLi proceeded compared to the facile *n*-butylation slowly and in low yield (27%), while *s*-butylation was only achieved with difficulty in 11% yield. Also phenyl residues with different substituents, could be introduced and 5-(4-dimethylaminophenyl), 5-(3-hydroxyphenyl), 5-(3-methoxyphenyl), 5-(4-tolyl), 5-(4-*n*-pentylphenyl) and 5-(trifluoromethylphenyl) OEP **5**, **6** and **229-232** were obtained in 17% to 83% yield. The introduction of the methoxyphenyl substituent (OEP **231**) was difficult (3% yield) and the use of methoxylithiates was observed to destroy OEP quickly. Low yields were furthermore obtained with 4-tolylolithium and 4-dimethylaminolithium (20% and 17%) and were attributed to the reactive methyl groups. Furthermore, neither anthracenyllithium, nor heteroaromatic lithiates such as benzothiazolyl-, methylpyridinyl- and quinolinylithium resulted in the formation of the respective *meso* monosubstituted OEPs while the starting material was in some cases recovered. The *meso* monosubstituted OEPs, obtained in best yields e.g. 5-phenyl-, 5-(4-*n*-pentylphenyl), 5-(3-trifluoromethylphenyl), 5-(1-naphthyl) and 5-(9-phenanthrenyl) OEP **4-8** were furthermore used in the disubstitution step, producing 5,10-A₂ and AB substituted OEPs in 4–52% yield (chapter 2.2.2). The for further synthesis (5,10-A₂-15,20-B₂ OEPs) desired 5,10-A₂ OEPs **9**, **254** and **257**, bearing 4-*n*-pentylphenyl, 1-naphthyl and 9-phenanthrenyl substituents, were obtained in 47%, 47% and 43% yield. Furthermore, with 5-(4-dimethylaminophenyl)-10-(3-trifluoromethylphenyl) OEP **253**, a 5,10-mini-push-pull OEP was obtained in good yield (48%) and also two anthracenyl substituted AB OEPs could be prepared in 16% and 38% yield. In contrast to the *meso* monosubstitution, especially the disubstitution carried out with 4-dimethylphenyllithium produced the respective OEPs **249** and **260** in high yields (79% and 71%) and proceeded quickly due to the enhanced solubility of the starting materials. 5,10-Bis(9-phenanthrenyl) OEP **9** as well as 5,10-bis(1-naphthyl) OEP **257** were furthermore identified as 1/1 mixtures of atropisomers due to the hindered

rotation and the unsymmetry of the 9-phenanthrenyl and 1-naphthyl units. The respective ^1H NMR data was be discussed in chapter 3.

Additionally, during the disubstitution, also a few trisubstituted ABA OEPs were obtained when 9-phenanthrenyl-, 9-anthracenyl- and 4-methoxyphenyllithium were used (chapter 2.2.4). 5,10-Bis(9-phenanthrenyl)-10-phenyl OEP **287** was isolated in 3–33% yield relative to the equivalents of *n*-BuLi and bromide used (compare to chapter 2.2.5.2) and palladium (II) could be introduced in the subsequent substitution step in 54% yield (OEP **304**, chapter 2.3). The ABA-regioisomers occurred also as mixtures of atropisomers when at least two 1-naphthyl, 9-phenanthrenyl or 3-methoxyphenyl substituents were attached and the ^1H NMR spectra were discussed in chapter 3. A further step towards 5,10-A₂-15,20-B₂ push-pull OEPs was achieved by using towards PhLi as not reactive described 5,10-bisphenyl OEP **236** in the trisubstitution step. The OEP **236** could be obtained directly from OEP **1** in 77% yield and was converted into the respective 5,10-A₂-15-B substituted OEPs **292-294** in average to good yields (17%-69%). However, the synthesis of 5,10-bis(9-phenanthrenyl), 5,10,15-tris(9-phenanthrenyl) and 5,10,15,20-tetrakis(9-phenanthrenyl) OEP **9-11**, shown in figure 2, could be also achieved in one step from 5-(9-phenanthrenyl) OEP **8** in good yields (43%, 25% and 7–43%). The yield of 43% for the OEP **11** was furthermore obtained by increasing the equivalents of *n*-BuLi and bromide, which shifted the product ratio in favour of the tetrasubstituted OEP. Palladium (II) was also inserted into the phenanthrenyl OEPs and the respective palladium (II) complexes **12-15** were obtained in 82%, 55%, 80% and 12% yield as discussed in chapter 2.3. On the other hand, series of methyl, *n*-butyl and *s*-butyl Pd(II)OEPs couldn't be prepared during the PhD as described in chapter 2.2.5.1.

With the aim to modulate the photophysical properties of the porphyrins, platinum (II) and platinum(II) incorporation was carried out with several *meso* monosubstituted OEPs and for example 5-phenyl Pt(II)OEP **307**, 5-(1-naphthyl) Pt(II)OEP **308** and 5-(9-phenanthrenyl) Pt(II)OEP **309**, were prepared in 76%, 44% and 54% yield (chapter 2.3), while the *meso* monosubstituted palladium (II) complexes **12**, **17**, **166**, **273**, **282** and **300-303** were obtained in average to excellent yields (20%-100%) in accordance to literature and were used for measurements of phosphorescence quantum yields and lifetimes as will be described in chapter 6. Pd(II)OEP **2** was furthermore found to be not reactive towards *n*- and *s*-BuLi and the reactivity was only slightly enhanced with PhLi.

On the other hand, *meso* monosubstituted Pd(II)OEPs could be substituted with lithium reagents as shown in chapter 2.2.3, producing inseparable mixtures of the respective 5,10- and 5,15-disubstituted Pd(II)OEPs (**274-279**) when *n*-BuLi or *s*-BuLi were used. However, with aryllithium reagents e.g. 1-naphthyllithium, 5,10-bis-(1-naphthyl) Pd(II)OEP **284** could be obtained regioselectively and in good yield (61%) and was also obtained from the palladium insertion using the respective free base OEP **257**. The overall yield of the subsequent introduction of two 1-naphthyl residues and the incorporation of palladium (II) afterwards was furthermore 15%, while the sequence of substitution, palladium insertion and substitution, afforded 5,10-bis(1-naphthyl) Pd(II)OEP **284** in an overall yield of 26% and was therefore more effective.

Part II - Photophysical Measurements

5. Ultraviolet/visible spectroscopy (UV/vis)

5.1 UV/vis spectra of β -substituted porphyrins

A limited number of β - and dodecasubstituted porphyrins are described in literature. In relation to the appearance of the UV/vis spectra, two trends are obvious: A red shift of the absorption bands can be achieved by substituents, which induce a polar character to the porphyrin or which exhibit a mesomeric effect as was for example shown by Padmanabhan and George.^{1,2} Additionally, a from the usual planarity deviating distortion of the porphyrin, achieved by bulky *meso* substituents or overcrowding and which might induce unsymmetry to the macrocycle, was related to observed bathochromic shifts and was recently investigated by Zhou *et al.*³ and Syrbu and co-workers.^{4,5} Earlier on such effects on UV/vis spectra were also described by Medforth, Smith and Shelnut⁶ as well as Takeda *et al.*⁷

K. M. Smith, C. J. Medforth and J. A. Shelnut investigated the UV/vis spectra of a series of distorted *meso tert*-butyl metalloporphyrins.⁶ They observed that compared to porphyrin, the absorption bands of the UV/vis spectra of the *tert*-butyl metalloporphyrins were red shifted with an increasing number of *meso* substituents. Furthermore, the absorption bands broadened and the intensities of the Q₀ band and the vibrational side band (Q_v) became weaker. The obtained data was attributed to the increasing degree of distortion with the introduction of the *meso* substituents and the OOPs (out-of-plane displacements) were correlated to the UV/vis red shifts as shown in figure 5.2.1.⁶

In 1994, J. Takeda *et al.* reported the synthesis of a series of overcrowded, β and *meso* phenyl substituted porphyrins as described in chapter 1.4.5.⁷ Dodecaphenylporphyrin **93** (H₂DPP) was furthermore described previously by Smith/Takeda and co-workers and was characterized as saddle shaped.⁸⁻¹¹ The non-planarity of the members of the 'dodecaphenyl'-series increased with each substituent and the UV/vis absorption bands were consequently red shifted. The Q band behavior was observed to be irregular e.g. certain absorption bands were designated as shoulders of others while the intensities were not given.

Also the ^1H NMR NH and *meso* proton shifts were reported and could be correlated to the UV/vis red shifts as shown in table 5.1.1 and displayed a typical upfield shift due to the higher degree of distortion, which moved the NH groups out of the porphyrin plane.

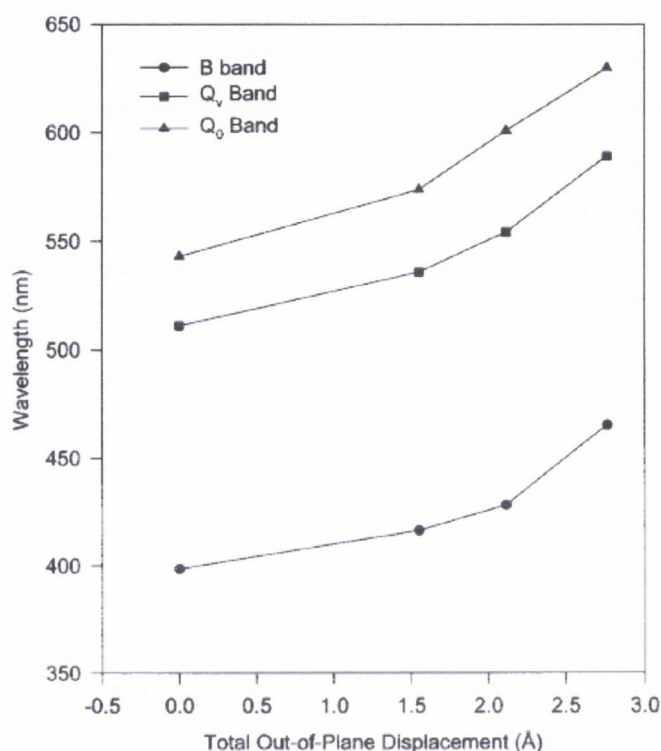


Fig. 5.1.1. Correlation of the out-of-plane displacements (OOPs) and the UV/vis absorption maxima of the *meso tert-butyl* series.⁶

		^1H NMR (1/ppm)		UV/vis in CH_2Cl_2
		<i>meso</i> H	NH	λ_{max} (1/nm)
92	H_2OPP	10.32	-3.03	423, 515, 551, 583, 635
97	$\text{H}_2(\text{trans-DecPP})$	10.16	-	429, 521, 553, 588, 640 (sh)
98	$\text{H}_2(\text{cis-DecPP})$	9.91	-1.99	439, 531, 568 (sh), 606, 668
99	H_2UPP	9.63	-1.10	452, 546, 574, 618 (sh), 686
93	H_2DPP	-	-0.90	468, 564, 617, 722

Table 5.1.1. ^1H NMR NH and *meso* proton shifts and UV/vis absorption of the members of the 'dodecaphenyl'-series.⁷

A hybrid-series, situated between planar OEP **1** / TPP **64** and OETPP **18** was also prepared by W. W. Kalisch in 1996.¹² Common mixed-condensation reactions were used, to prepare a mixture of tetraphenylporphyrins bearing two, four and six ethyl groups in the β -positions as shown in figure 2.2.5.1 (OEPs **295-298**). The UV/vis spectra displayed a typical combination of Soret and four Q bands with exception of the pseudo-*cis* OEP **296**, for which no QIII band was displayed. However, the absorption bands were red shifted in the shown order and X-ray analysis confirmed the increased overall-distortion ($\Delta 24=10 \text{ \AA}$, 0.29 \AA , 0.38 \AA and 0.46 \AA) and saddle-type displacement. Except of the distortion of the pseudo-*cis* porphyrin **296**, all distortions were symmetric and therefore the unsymmetric distortion of the porphyrin **296** might be related to the changed Q band shape.

Padmanabhan and George reported in 2003 the synthesis of *meso* tetra- and dodecasubstituted porphyrins bearing 1-, 2-naphthyl, *o*-, *m*- and *p*-tolyl and bromo groups in β and *meso* positions. The bromo porphyrins were obtained from the *meso* tetrasubstituted precursors after copper (II) insertion, bromination and subsequent metal removal. An example is shown in table 5.1.2.^{1,2}

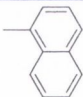
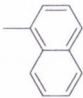
	R	X
345		H
346		Br

Table 5.1.2. By Padmanabhan and George prepared β -bromo and β unsubstituted *meso* naphthyl porphyrins **345** and **346**.^{1,2}

The brominated porphyrins displayed due to the bulky bromo groups, the induced distortion and the electronic withdrawing effect, which lowered the LUMO relative to the HOMO, strongly red shifted Q bands compared to β unsubstituted porphyrins as shown in table 5.1.3.^{1,2} Additionally, the solvent dependency increased with the polarity of the porphyrins as it can be seen in table 5.1.3.

For example, the porphyrin **346** displayed a Q band shift of 12 nm to the blue when the solvent was switched from CH₂Cl₂ to DMF, while the Q band of the porphyrin **345** was considerably less blue shifted, e.g. 4 nm only, when the solvent was changed.^{8,13-16} Furthermore, it was found that the Soret bands of naphthyl porphyrins were stronger red shifted than those of tolyl substituted porphyrins (not shown) and the authors explained the additional Soret shift by the mesomeric effect of the naphthyl groups as well as due to an increased degree of distortion.

porphyrin	Toluene	benzene	CHCl ₃	CH ₂ Cl ₂	DMF
345	515	516	515	515	511
	552	551	550	550	551
	589	589	589	589	596
346	564	568	567	567	655 (br)
	622	625	623	623	765 (br)
	733	733	734	736	

Table 5.1.3. Q band absorptions ($\lambda = [1/\text{nm}]$) of the porphyrins **345** and **346**.^{1,2}

It can be also seen in table 5.1.3, that the porphyrins **345** and **346** displayed only three instead of four Q bands and that the number of Q bands was even reduced to two when the porphyrin **346** was dissolved in DMF.

Also Ni(II)OMTP **75a** was recently investigated by DFT studies and red shifts of 40 nm to 50 nm were observed in the UV/vis spectrum relative to Ni(II)P.^{17,18}

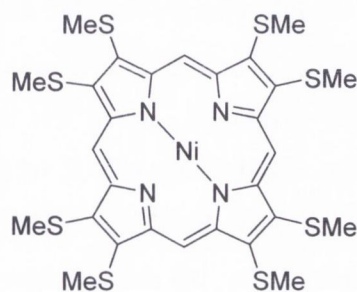


Fig. 5.1.2. Ni(II)OMTP **75a**.^{17,18}

Ni(II)OMTP **75a** is shown in figure 5.1.2 and the strong red shift of the Soret band, which was located between 400 and 450nm, was attributed to the electronic effects of the β substituents and was to a minor degree seen as due to the induced ruffling.^{17,18}

UV/vis spectra of dodecasubstituted porphyrins with $R_\beta = 3,5\text{-tert-butylphenyl}$, methyl or ethyl and $R_{meso} = \text{phenyl}$ were also recently described by Syrbu and co-workers.^{4,5}

Typically a reduced number of Q bands (less than four) and Q band shoulders were found. The changed Q band shape was explained by the induced distortion and was presented as a tool for the fine-tuning of photo-physical properties.⁵ Else wise, Syrbu and co-workers investigated the effect of acid and base addition on the UV/vis spectra. When for example NEt_3 was added to OETPP **18** (the during the PhD recorded spectrum is shown in figure 5.1.3), the shape of the UV/vis spectrum changed and two Q bands with a preceding shoulder were observed relative to the single, shouldered Q band of **18** and as it can be seen in table 5.1.4. Compared to OETPP **18**, the formed porphyrin anion **18a** ($[\text{por}]^- \text{HN}^+\text{Et}_3$) was expected to be unsymmetric, which could have resulted in the changed Q band shape. It was also described that addition of acid (CF_3COOH) to $\text{H}_2\text{OETPP } \mathbf{18}$ had a similar effect. The Q band of **18b** was slightly blue shifted relative to **18** and was located at 687nm instead of 691 nm and also the formation of a second Q band shoulder was observed preceding the QI and QII absorption bands (compare to table 5.1.4).⁴

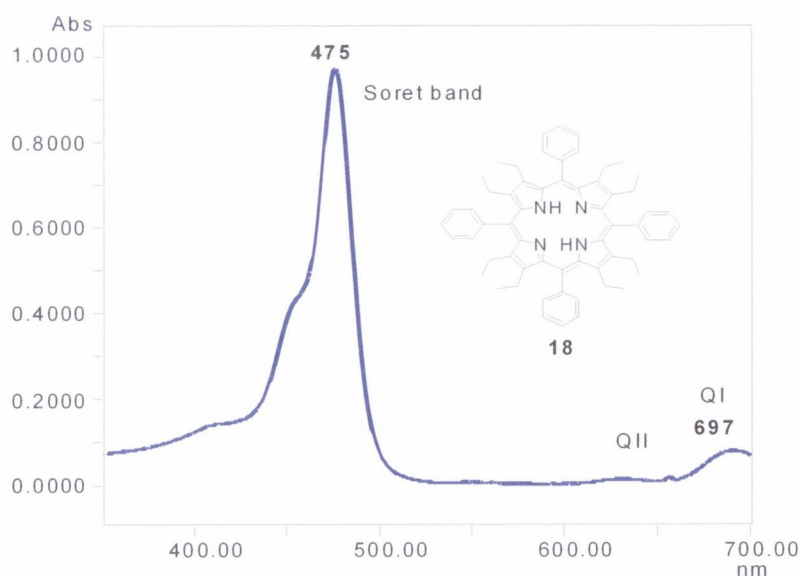
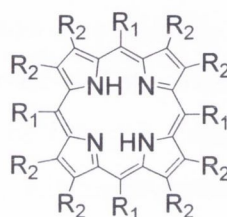


Fig. 5.1.3. UV/vis spectrum of OETPP **18**, recorded during the PhD in CH_2Cl_2 .

The different appearance of the spectra of **18** and **18b** showed else wise that traces of HCl in chloroform or dichloromethane have a minor effect on the shape of the UV/vis spectrum and that their presence can be neglected compared to the effect obtained by the addition of CF₃COOH. Also Zhou *al.* investigated dodecasubstituted porphyrins in 1996 and the UV/vis data is summarized in table 5.1.4 together with the data presented by Syrbu *et al.*^{4,5,19} while the intensities of the absorption bands can be obtained from the published articles.



	R ₁	R ₂	Soret	QIV	QIII	QII	QI
135	phenyl	mesityl	461	557	601	-	703
136	4-tolyl	mesityl	457	551		635	696
137	4-CF ₃ -phenyl	mesityl	458	556	598	-	720
138	4-OMe-phenyl	mesityl	457	551	-	635	696
139	4-chlorophenyl	mesityl	460	555	600	-	-
140	4- <i>t</i> -butylphenyl	mesityl	464	558	-	-	706
141	methyl	mesityl	458	-	614	666	-
347a	methyl [#]	phenyl	454	553	-	602	694
347b	methyl*	phenyl	466	-	sh	sh	687
73a	methyl [#]	3,5-di- <i>t</i> -bu-phenyl	450	549	sh	595	693
73b	methyl*	3,5-di- <i>t</i> -bu-phenyl	473	-	sh	sh	700
18	ethyl	phenyl	475	-	-	sh	697
18a	ethyl [#]	phenyl	452	551	sh	598	696
18b	ethyl*	phenyl	471	-	sh	sh	691

Table 5.1.4. UV/vis data of dodecasubstituted porphyrins described in literature; [#]=base addition; * =acid addition/dication; **135-141,**¹⁹ **347ab, 73ab, 18ab.**⁴

As it can be seen in table 5.1.4, different substituents in β and *meso* positions have different influences on the Q bands of dodecasubstituted porphyrins. All porphyrins

were expected to be highly distorted, which resulted in the shown Q band perturbations. The by Zhou and co-workers obtained porphyrins (**135-141**) displayed QIV and QIII bands resembling to dodecasubstituted porphyrin dications prepared by Syrbu *et al.*⁴ However, the intense QIV, QIII and QII bands could be related to the aryl substitution of the β positions, whereas the porphyrin **141** with R_{β} =alkyl is most similar to OETPP **18**. The most deviant Q band behavior relative to OETPP **18** was furthermore found for the porphyrin **139**, bearing additional chloro groups and displaying no QI band. The addition of base to the porphyrins **347**, **73** and **18**, resulted furthermore in a blue shift of the Soret band (11 nm to 23 nm) as well as in the appearance of QIV bands, in similarity to β -aryl substituted porphyrins. In comparison to this, the Soret shift induced by acid was much smaller (only 4 nm from **18** to **18b**) relative to the addition of base. Acid and base addition had furthermore an opposite effect on the QI bands. The shift of the QI band of **18b** was 6 nm, while the QI band shift of **18a** was only 1 nm relative to OETPP **18**, when acid or base was added. The QI band of the CF₃ substituted porphyrin **137** was furthermore the farthest shifted and was found at 720 nm relative to 697 nm of **18**. Additionally, the QII band shifts varied stronger than others and the highest red shift was displayed by the methyl-mesityl substituted porphyrin **141** with the Q band at 666 nm. The by Syrbu *et al.* presented porphyrins **18a**, **73a** and **347a** to which base was added, showed furthermore QIV>QIII>QI Q band intensities (not displayed) as did also the by Zhou and co-workers obtained octaarylporphyrins (QIV>QII>QI, QIV>QIII and QIII>QII), while the tolyl and methoxyphenyl substituted porphyrins **136** and **138** displayed irregular Q band intensities (QII>QIV>QI).^{4,19} For the trifluoromethylphenylporphyrin **132** also equal Q band intensities were found. Other *meso* A₃B and 5,10-A₂-15,20-B₂ dodecasubstituted porphyrins, obtained by Zhou *et al.* are furthermore shown in figure 5.1.4 and the respective UV/vis data is given in table 5.1.5.³ The unsymmetric dodecasubstituted porphyrins **133**, **409-413** displayed all QIII bands together with QII bands in difference to the symmetric dodecasubstituted porphyrins, which showed only a QIII or a QII band (porphyrins **135-141**) as was shown in table 5.1.4 or which displayed shoulders for the QIII band when β -alkyl substituents were attached and acid or base was added (**18a/b**, **73a/b**, **347a/b**). This effect was else wise attributed to the additional functional groups in the *meso* positions of the porphyrins **133** and **348** to **352**. The Soret band shifts of the porphyrins **133**, **348-352** were furthermore comparable to the Soret band shifts observed for β -alkyl substituted

porphyrins (**11**, **18**, **73** and **347**), while the strong red shifts of the porphyrins **350-352** were related to the influence of the additional NH₂ and NO₂ chromophores. A competitive red shift to those porphyrins was furthermore only displayed by 5,10,15,20-tetrakis(9-phenanthrenyl) OEP **11** as will be described in chapter 5.6. Else wise, the Soret band of the porphyrin **410** was displayed at the same wavelength as the Soret band of H₂DPP **93**.⁷

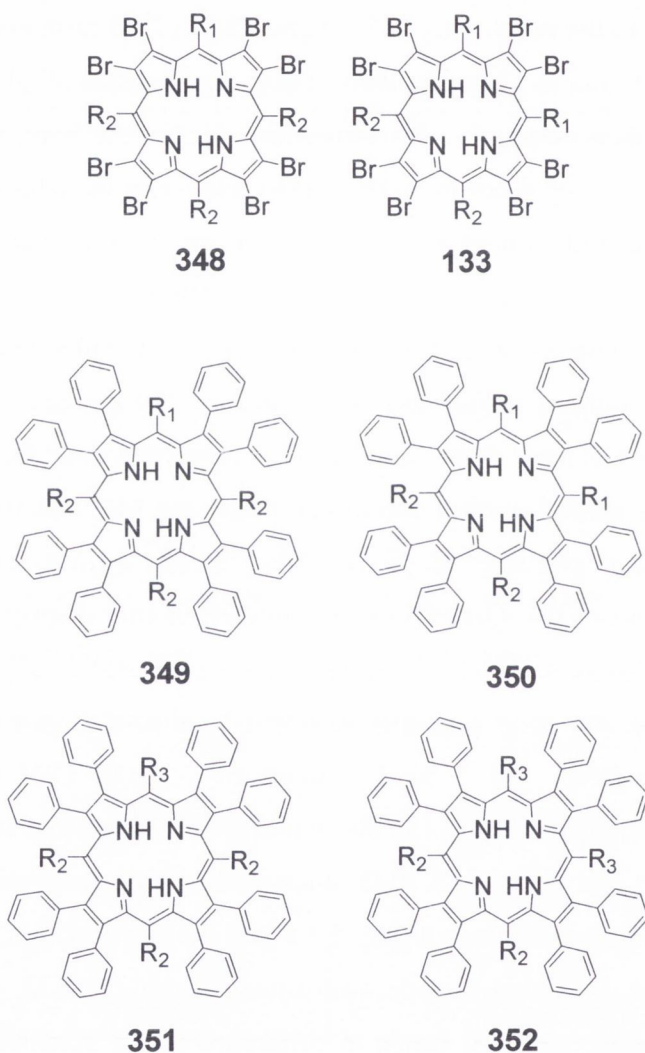
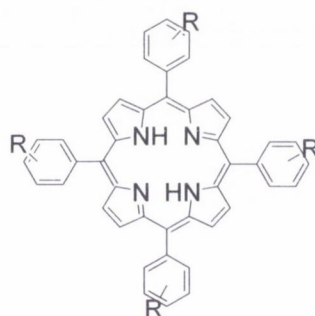


Fig. 5.1.4. Unsymmetric dodecasubstituted porphyrins prepared by Zhou and co-workers, R₁= 4-nitrophenyl, R₂= phenyl, R₃= 4-aminophenyl.³

	Soret	QIV	QIII	QII	QI
348	473 (5.17)	-	574 (3.84)	626 (4.00)	-
133	465 (5.10)	-	573 (3.84)	625 (3.92)	-
349	469 (4.99)	-	562 (3.83)	617 (3.81)	-
350	493 (4.89)	-	586 (3.15)	642 (3.56)	-
351	490 (4.88)	-	576 (3.11)	642 (3.51)	-
352	501 (4.89)	-	-	-	-

Table 5.1.5. UV/vis data of the porphyrins **133**, **348-352**³

An unusual observation was also made by Cornejo and co-workers. They described the in table 5.1.6 shown TPPs **405-407** and found a reduced number of Q bands for the TPP **407** (see figure 5.1.5), and classified it as a phyllo-type porphyrin with an additional loss of the QI band.²⁰



	R	Name
405	2-NH ₂	(2-aminophenyl) ₄ TPP
406	3-NH ₂	(3-aminophenyl) ₄ TPP
407	4-NH ₂	(4-aminophenyl) ₄ TPP

Table 5.1.6 Synthesized amino-TPPs **405-407**.²⁰

Furthermore, also the by Zhou *et al.* prepared porphyrin **356**, shown in figure 5.1.6, displayed only three Q bands, situated at 525 nm (4.23), 605 nm (3.71) and 660 nm (3.94) and.¹⁹

Another observation, which was recently made, was the appearance of split or shouldered Soret bands of *meso* unsubstituted TBPs and TNPs with additional chromophores in the β positions as described by Vinogradov *et al.*²¹ and the observed effect was explained by the author as due to the additionally induced distortion or as due to the newly introduced chromophores but wasn't investigated any further.²²

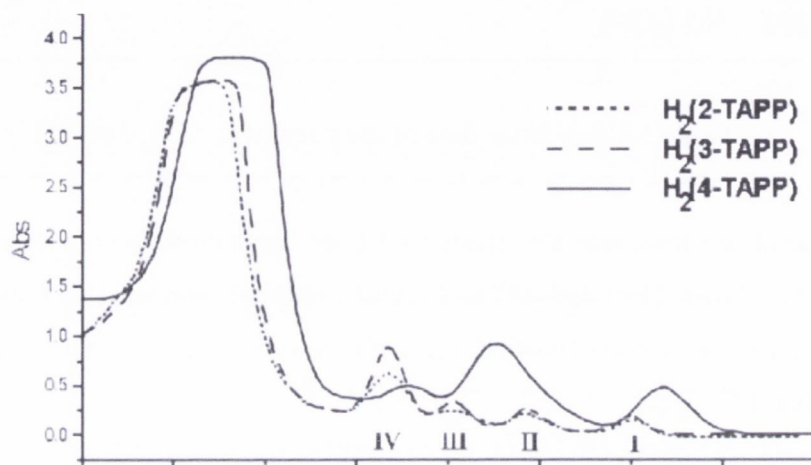


Fig. 5.1.5. UV/vis spectra of the TPPs 405-407 in DMF under addition of tetrabutylammonium perchlorate, TBAP.²¹



Fig. 5.1.6 Porphyrin 356, obtained by Zhou *et al.*, R_1 =mesityl.¹⁹

In the following chapter in relation to the above described deviances in UV/vis behavior, the UV/vis spectra of the during the PhD prepared OEPs will be discussed, while the respective data is also gathered in the appendix. The discussion of the free base OEPs will be followed by the discussion of the respective Pd(II) and Pt(II)OEP complexes.

5.2 UV/vis spectra of prepared *meso* monosubstituted H₂OEPs

Planar H₂OEP is D_{2h} symmetric and displayed an UV/vis spectrum with a strong Soret band and four less intense Q bands, which is typical for flat porphyrins. The Q band intensities decreased towards longer wavelength (QVI>QIII>QII>QI) and the spectrum belongs to so-called 'etio-type' spectra according to the Stern definition.^{21,24} The intense Soret or B band near 400 nm results from the allowed $^1A_{1g}-^1E_u$ transition and the four Q bands correspond to quasi-forbidden transitions and are illustrated in figure 5.2.1. The Q bands I and III can be attributed to the $A_{1g}-B_{3u}$ and $A_{1g}-B_{2u}$ transitions, whereas the Q bands II and IV are vibrational satellite bands or overtones of those at higher, more energetic wavelengths.

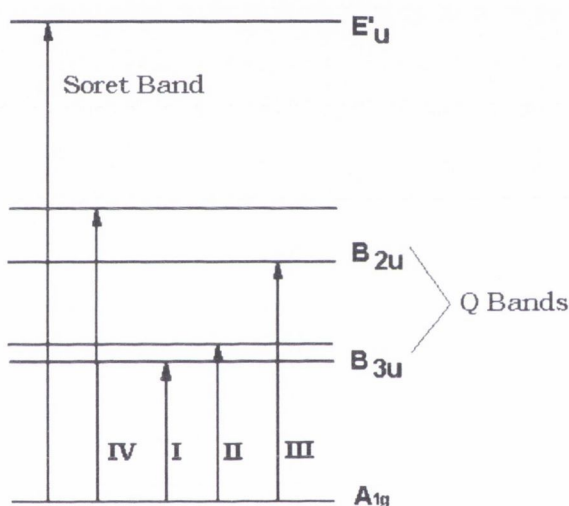
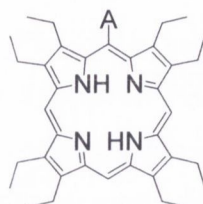


Fig. 5.2.1. Schematic diagram of the electronic transitions of etio-type porphyrins with D_{2h} symmetry.^{21,24}

The recorded UV/vis data of prepared *meso* monosubstituted OEPs is furthermore assembled in table 5.2.1. The spectra of 5-methyl OEP **227** and 5-(9-phenanthrenyl) OEP **8** are shown in figure 5.2.2 and are clearly etio-type spectra.

Similar spectra are displayed by 5-(4-tolyl), 5-(4-pentyl), 5-(3-hydroxyphenyl), 5-(3-trifluoromethylphenyl) and 5-acenaphthyl OEP **229**, **5**, **232**, **6** and **234**. However, two trends were observed for those OEPs: a) the intensities of the QIII and QII bands became

similar and b) the intensity of the QI band decreased and the band remained in a few cases undetected.



OEP	A	Soret	QIV	QIII	QII	QI
1	-	398	497	531	566	619
227	methyl	406 (5.53)	506 (4.39)	541 (4.07)	575 (3.96)	624 (3.16)
16	<i>n</i> -butyl	407 (5.48)	506 (4.26)	541 (3.71)	576 (3.75)	622 (2.86)
229	4-tolyl	406 (5.09)	505 (3.95)	538 (3.67)	571 (3.66)	624 (3.16)
5	4- <i>n</i> -pentylphenyl	404 (5.12)	503 (4.99)	537 (4.69)	571 (4.64)	n. d.
230	4-NMe ₂ -phenyl	406 (5.26)	505 (4.33)	538 (3.97)	572 (3.97)	624 (3.59)
232	3-OH-phenyl	404 (5.03)	503 (4.02)	537 (3.79)	571 (3.76)	623 (3.45)
6	3-CF ₃ -phenyl	404 (6.68)	503 (5.44)	537 (4.93)	571 (4.76)	n. d.
231	3-OMe-phenyl	405 (5.32)	503 (4.26)	537 (3.95)	571 (3.92)	623 (3.41)
7	1-naphthyl	406 (4.13)	504 (4.02)	538 (3.84)	572 (3.85)	625 (n. d.)
233	2-naphthyl	406 (5.61)	505 (4.48)	538 (4.20)	572 (4.20)	624 (3.71)
234	acenaphthyl	407 (5.02)	505 (3.92)	538 (3.66)	574 (3.64)	625 (3.26)
8	9-phenanthrenyl	406 (5.13)	504 (4.13)	538 (3.86)	571 (3.83)	624 (3.52)

Table 5.2.1. UV/vis absorption of *meso* monosubstituted OEPs (CH₂Cl₂, λ_{\max} (lg ϵ), $\lambda = [1/\text{nm}]$); n. d. = no data obtained.

The weakening of the QI band could be furthermore explained as a result of the energy loss to the vibrational overtone, the QII band, due to the higher degree of unsymmetry compared to OEP **1**. As it can be seen in table 5.2.1, the lowest QI intensities were found for 5-(4-tolyl) OEP **229** and 5-methyl OEP **227**, which displayed both an oscillator strength of 3.16 for the QI band, whereas also 5-(*n*-butyl) OEP **16** displayed a QI band intensity of 2.86 as described earlier on in literature.^{5,23}

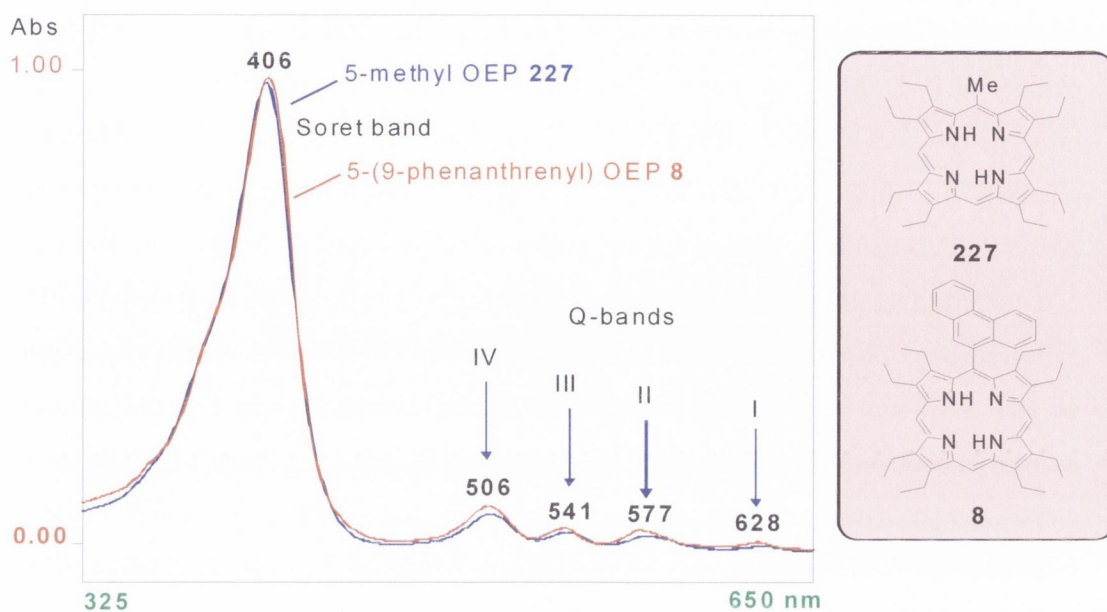


Fig. 5.2.2. UV/vis spectra of 5-methyl OEP **227** and 5-(9-phenanthrenyl) OEP **8**. The intensities are scaled to 1.

For 5-(4-dimethylaminophenyl) OEP **230** and 5-(2-naphthyl) OEP **233** the QIII and QII band intensities were furthermore equal and for 5-*n*-butyl OEP **16** and 5-(1-naphthyl) OEP **7** the QII band became stronger than the QIII band and the respective Q band area of 5-*n*-butyl OEP **16** is shown in figure 5.2.3.

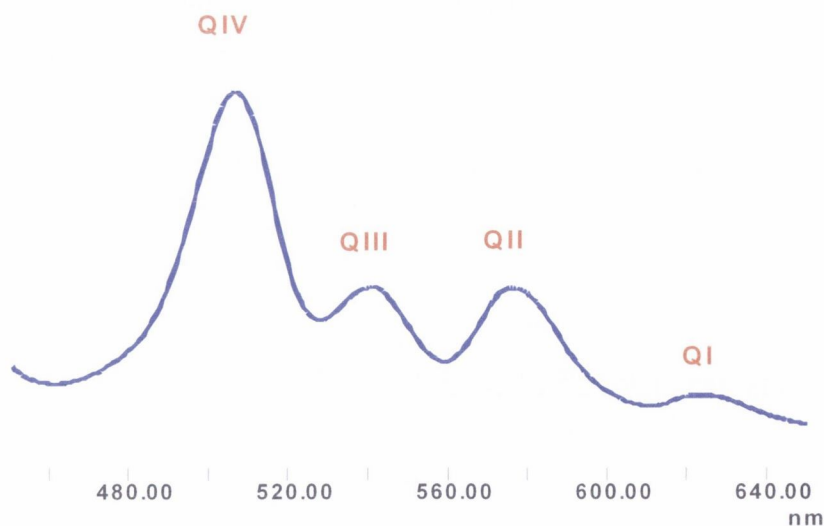
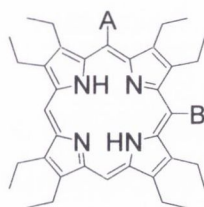


Fig. 5.2.3. Q band area of 5-*n*-butyl OEP **16**

The Q band changes were attributed to the altered 2D- and 3D-symmetry respective to planar OEP **1**. Low QI band intensities were also displayed by *meso* 5,15-bis(2-nitrophenyl), 5,15-bis(3-nitrophenyl), 5,15-bis(4-nitrophenyl), 5,15-bis(4-methoxyphenyl), 5,15-bisphenyl and 5,15-bis(*n*-hexyl) β -substituted porphyrins reported by Syrbu and co-workers.⁵ When the intensities of all absorptions bands were furthermore considered, overall high values were obtained for 5-(3-trifluoromethylphenyl) OEP **231**, followed by 5-(2-naphthyl) OEP **233** and 5-methyl OEP **227** and couldn't be explained so far. As it can be also seen in figure 5.2.2, the absorption bands of the synthesized *meso* monosubstituted OEPs are relative slim and typical for porphyrin monomers with electronically not communicating, single-bonded and orthogonal orientated substituents.²⁴ Furthermore, they displayed a red shift of 7 to 10 nm relative to planar OEP **1**, which was explained as due to the induced distortion by the substituents, with a major impact of the *n*-butyl substituent and which is in accordance to series of porphyrins described in literature^{4,7,25} as well as to previous observations that alkyl substituents shift the absorption bands stronger to the red than aryl substituents.²⁶ 5-*N*-butyl OEP **16** was followed in its strong red shift by 5-acenaphthyl OEP **234** and enhanced *meso*- β interactions might be the reason for the intense red shift of **234**. However, the mesomeric effect of the naphthyl and phenanthrenyl substituents was translated into a higher red shift when compared to phenyl substituted OEPs, while a slight blue shift was found for OH, OMe and CF₃ substituted OEPs (**231**, **232**, **6**) within the members of *meso* monosubstituted OEPs and could be related to the electron withdrawing effect of those groups. On the other hand, the NMe₂ group induced a shift, which is similar to the 9-phenanthrenyl residue and the same trends will be observed in the following chapters. However, all observed shift differences were small as the degree of induced distortion was minimal (compare to chapter 4), but will drastically increase with further substitution.

5.3 UV/vis spectra of *meso* 5,10-disubstituted H₂OEPs

Table 5.3.1 summarizes the recorded UV/vis data for the prepared 5,10-disubstituted OEPs. Irregularities in the Q band behaviour will be discussed in chapter 5.5 while this section focuses on the shift of the absorption bands (including Q bands) and the Soret band shape relative to OEP **1** and *meso* monosubstituted OEPs and in regard to the by the substituents induced unsymmetry and polarity.



OEP	A,B	Soret	sh	QIV	QIII	QII	QI
1	-	398		497	531	566	619
236	Ph,Ph	413 (5.39)		510 (4.25)	sh	578 (3.89)	sh
254	2 <i>xn</i> PP	425 (5.17)		521 (4.00)	552 (sh)	592 (3.78)	639 (sh)
257	2 <i>x</i> 1-naph	426 (4.89)		521 (3.79)	552 (sh)	592 (3.53)	639 (sh)
9	2 <i>x</i> phen	426 (5.45)	455 (sh)	519 (4.56)	sh	592 (4.35)	sh
250	<i>n</i> PP,Ph	425 (5.50)		521 (4.29)	sh	592 (4.13)	sh
251	BrPh,Ph	425 (3.99)		521 (3.81)	sh	592 (3.61)	sh
248	1-naph,Ph	425 (3.22)		520 (3.01)	sh	592 (sh)	650 (sh)
246	anth,Ph	425 (4.54)		520 (3.54)	sh	592 (3.92)	sh
255	anth, <i>n</i> PP	425 (4.68)		520 (3.63)	sh	592 (3.34)	644 (2.78)
253	3-CF ₃ Ph, 4-NM ₂ Ph	429 (4.72)		514 (sh)		595 (3.67)	663 (3.74)
249	4-NM ₂ Ph,Ph	427 (4.40)		522 (sh)	sh	593 (3.27)	667 (3.30)
260	NM ₂ Ph,phen	433 (4.93)		521 (4.09)		596 (3.63)	664 (3.45)
258	naph, <i>n</i> PP	426 (4.88)	sh	519 (3.74)	555 (3.61)	592 (3.72)	643 (3.48)
252	3-OMePh,Ph	425 (4.59)	448 (4.36)	521 (3.48)	sh	592 (3.37)	636 (3.57)
259	naph,phen	430 (5.01)	455 (5.01)	519 (3.90)	559 (sh)	591 (4.04)	643 (3.81)
247	phen,Ph	430 (sh)	454 (4.76)			587 (3.63)	638 (3.42)
256	<i>n</i> PP,phen		460 (5.25)	sh	589 (4.19)	639 (4.07)	sh

Table 5.3.1. UV/vis absorption of 5,10-disubstituted OEPs (CH₂Cl₂, λ_{max} (lg ε), λ = [1/nm]); sh=shoulder; *n*PP=*n*-pentylphenyl, phen=9-phenanthrenyl, BrPh=4-bromophenyl, anth=9-anthracenyl, 3-CF₃Ph=3-trifluoromethylphenyl, 4-NMe₂Ph= 4-dimethylaminophenyl, 3-OMePh=3-methoxyphenyl.

The Soret and Q band shift of the prepared *meso* 5,10-disubstituted OEPs relative to the *meso* monosubstituted OEPs was 20 nm and was in accordance with comparable data in literature and the observed shift from OEP **1** to *meso* monosubstituted OEPs.^{4,7} The *meso* 5,10-A₂ disubstituted OEPs, 5,10-bis(1-naphthyl) OEP **257**, 5,10-bis(4-*n*-pentylphenyl) OEP **254** and 5,10-bis(9-phenanthrenyl) OEP **9**, displayed a Soret band at

425–426 nm as well as the 5,10-AB substituted OEPs **246**, **248**, **250**, **251**, **258**, **252** and **255** bearing phenyl or 4-*n*-pentylphenyl residues and regardless if the second substituent was 1-naphthyl, anthracenyl, bromophenyl or methoxyphenyl. Stronger Soret band red shifts were only encountered for the dimethylaminophenyl substituted OEPs e.g. 5-(4-dimethylaminophenyl)-10-phenyl OEP **249**, 5-(4-dimethylaminophenyl)-10-(3-trifluoromethylphenyl) OEP **253** and 5-(4-dimethylaminophenyl)-10-(9-phenanthrenyl) OEP **260** (427 nm, 429 nm and 433 nm)²⁷ as well as for 5-(1-naphthyl)-10-(9-phenanthrenyl) OEP **259** and 5-(9-phenanthrenyl)-10-phenyl OEP **247** (both 430 nm) and were related to the influence of the NMe₂ chromophore as well as to the effects induced by the 9-phenanthrenyl substituent. Furthermore, 5-(4-*n*-pentylphenyl)-10-(9-phenanthrenyl) OEP **258** showed a Soret band, which was among the prepared disubstituted OEPs the most red shifted. Its Soret band was found at 460 nm as shown in figure 5.3.1 and could be related to the later described observed Soret splits of *meso* disubstituted OEPs (the split became in this case probably the actual Soret band). 5-(4-*N*-pentylphenyl)-10-(9-phenanthrenyl) OEP **258** might be therefore the most distorted porphyrin in the group of the *meso* disubstituted OEPs, showing the strongest Soret red shifted.

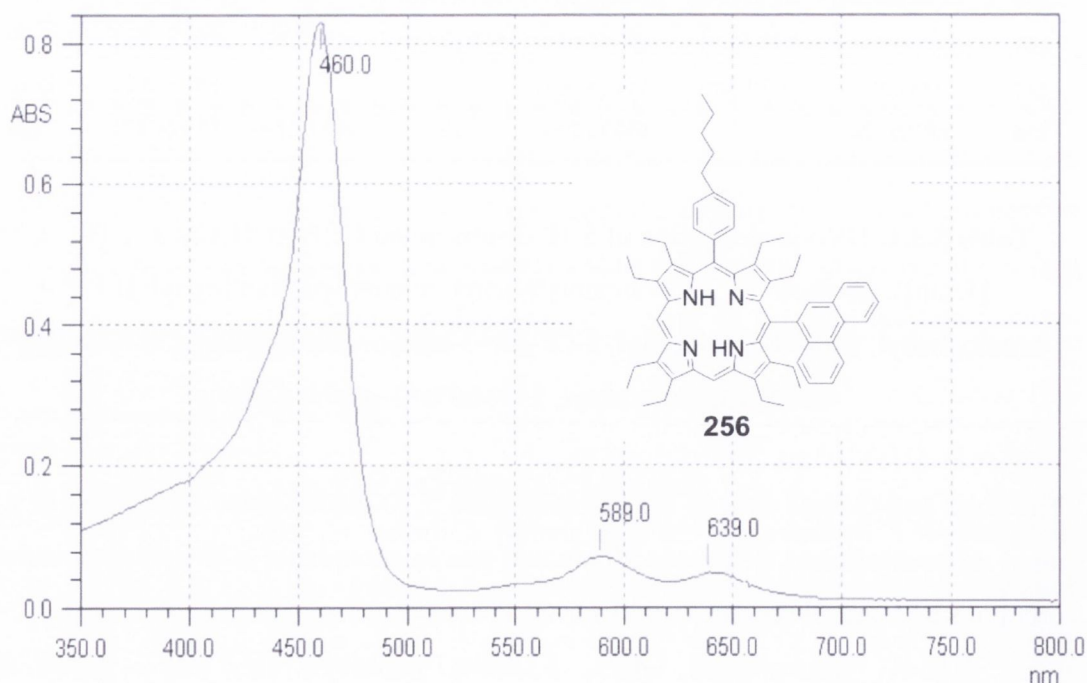


Fig. 5.3.1. UV/vis spectrum of 5-(4-*n*-pentylphenyl)-10-(9-phenanthrenyl) OEP **256**

The observed red shifts of the OEPs **249**, **253** and **260** are furthermore in accordance with strong red shifts for porphyrins bearing aryloxy, alkoxy, arylamino and alkylamino groups, described in literature, and which possess an increased polarity.²⁸⁻³⁵ The shifts, observed for the AB OEPs (**259** and **247**) with naphthyl- or phenanthrenyl substituents were also seen in relation to the porphyrins described by Padmanabhan and George^{1,2} and might show increased *meso*- β interaction as was described by Vinogradov *et al.*^{214,21} while π -extension as described by Osuka *et al.* and Anderson and co-workers^{22,36-48} could be excluded as the substituents are attached by a single bond to OEP and were found to be in an orthogonal orientation relative to the porphyrin plane (see chapter 4). On the other hand, the symmetric substituted OEP **257** and the AB-OEP **248** bearing one or two 1-naphthyl substituents did not display a particular shift of the Soret band and therefore the influence of the 1-naphthyl substituents was classified as minor relative to the 9-phenanthrenyl substituent. As described in the chapter 3, 4 and 6, phenanthrenyl substituents were furthermore found to be responsible for strong ¹H NMR CH₂/CH₃ “splits” and were also found to induce a certain amount of ruffling and in-plane distortions to the porphyrin. No particular effect was surprisingly encountered for the 9-anthracenyl substituted OEPs **246** and **255**, whereas its symmetric connectivity might be the reason.

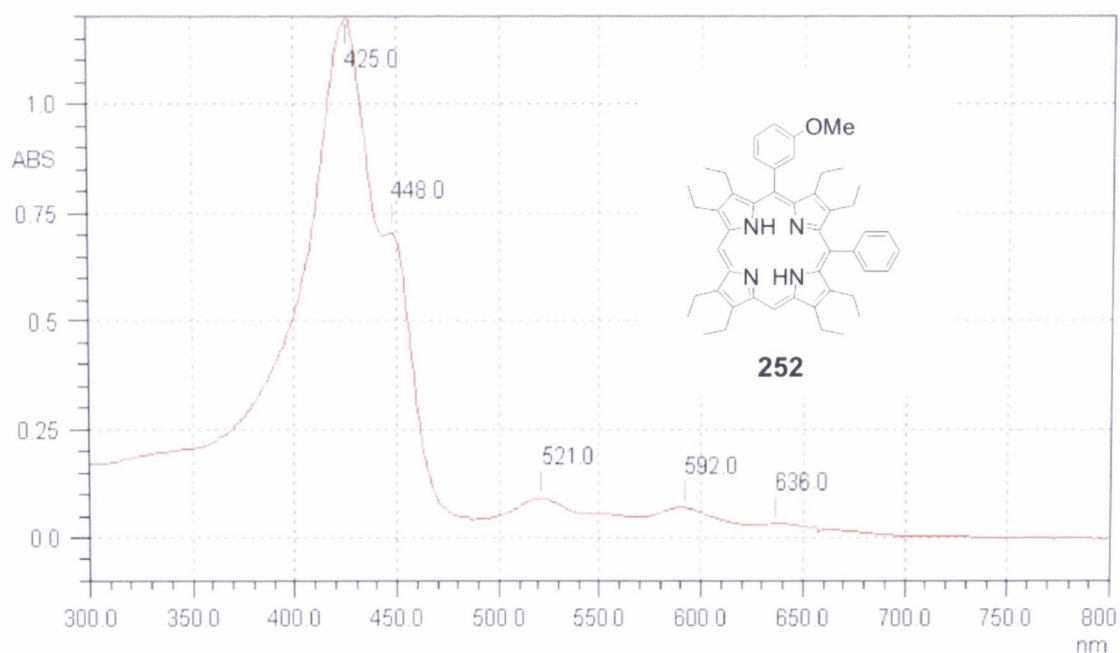


Fig. 5.3.2. UV/vis spectrum of 5-(3-methoxyphenyl)-10-(phenyl) OEP **252**

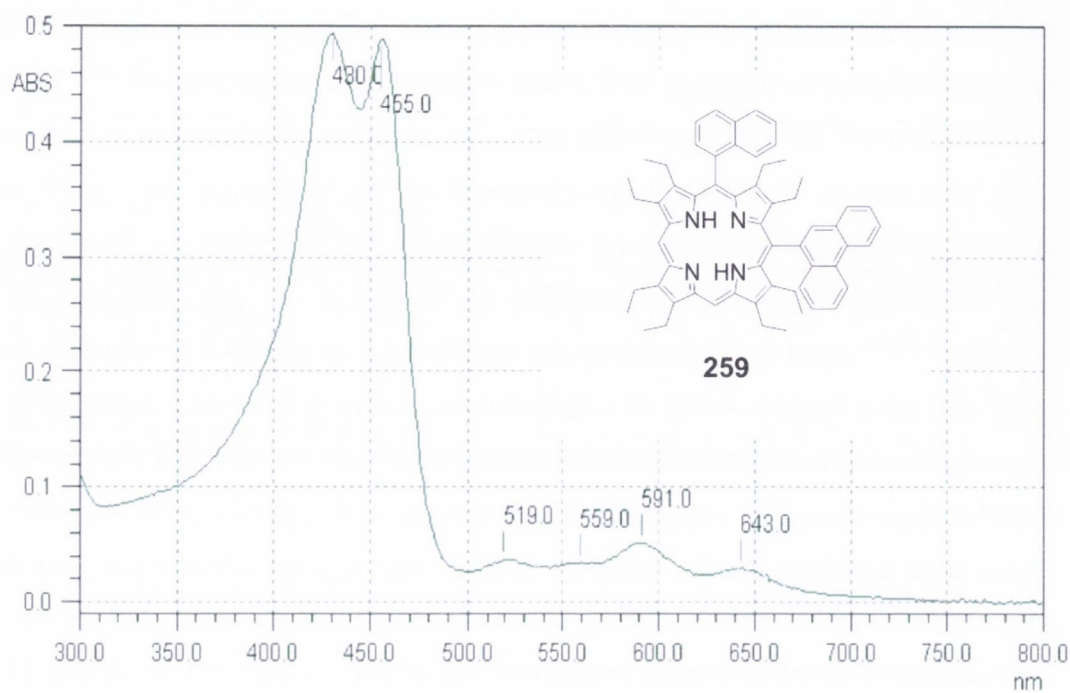


Fig. 5.3.3 UV/vis spectrum of 5-(1-naphthyl)-10-(9-phenanthrenyl) OEP **259**

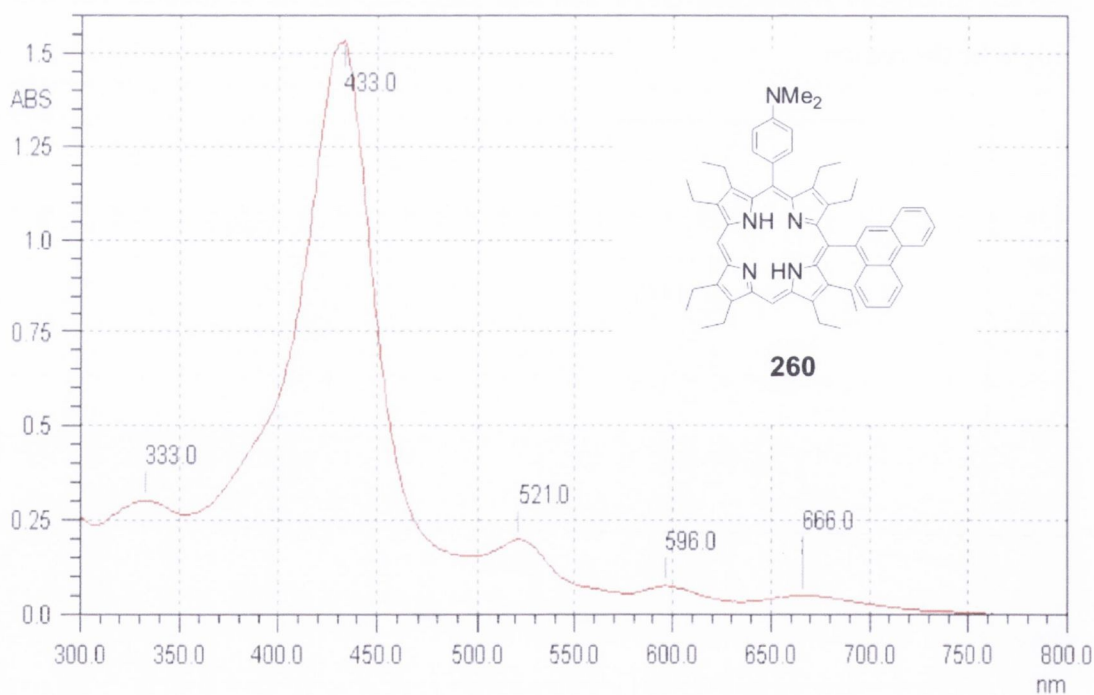


Fig. 5.3.4. UV/vis spectrum of 5-(4-dimethylaminophenyl)-10-(9-phenanthrenyl) OEP

260

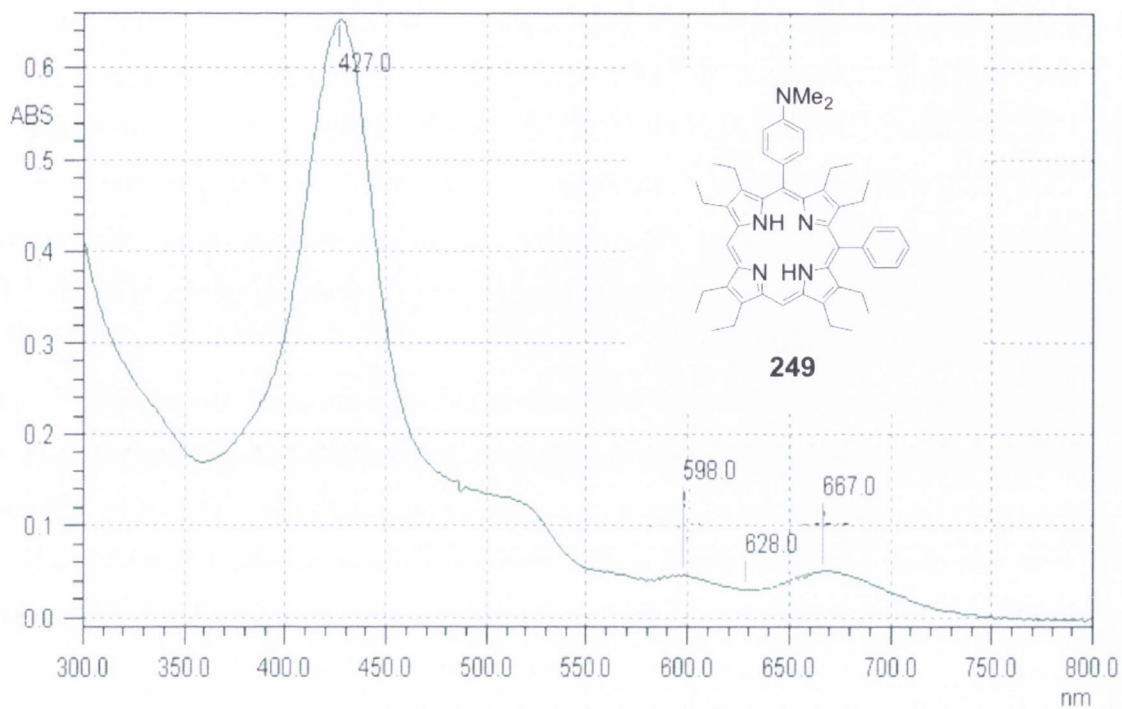


Fig. 5.3.5. UV/vis spectrum of 5-(4-dimethylaminophenyl)-10-phenyl OEP **249**

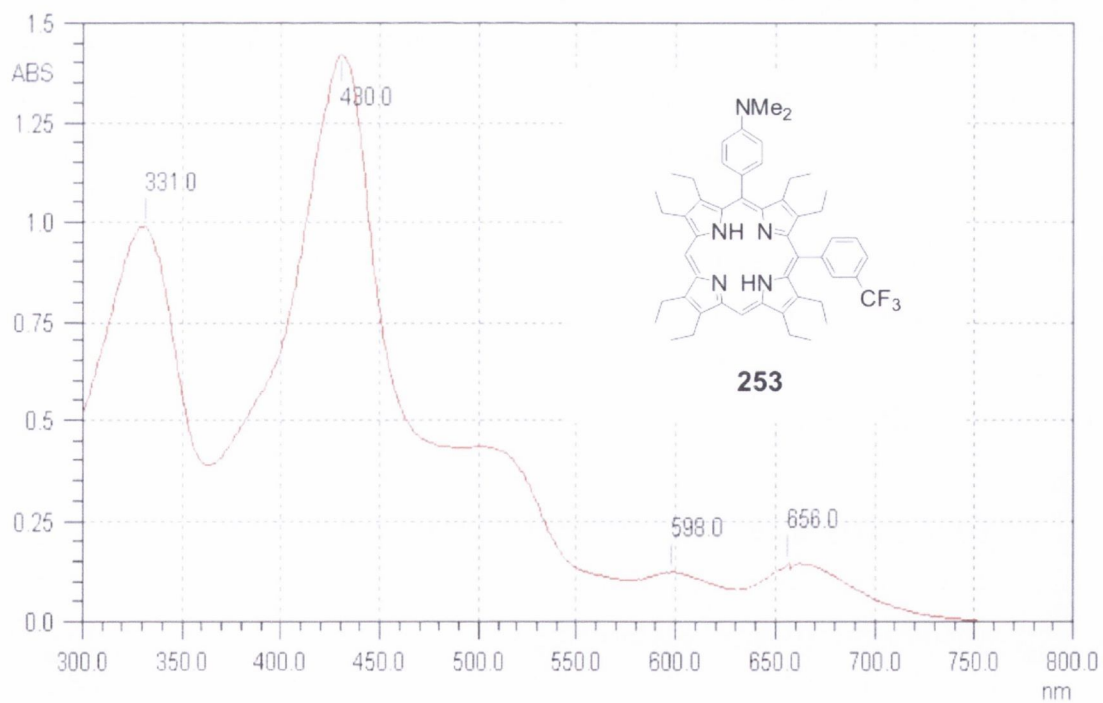


Fig. 5.3.6. UV/vis spectrum of 5-(4-dimethylaminophenyl)-10-(3-trifluoromethylphenyl) OEP **253**

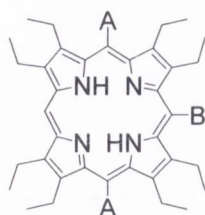
5,10-Bis(9-phenanthrenyl) OEP **9**, 5-(1-naphthyl)-10-(4-pentylphenyl) OEP **258**, 5-(3-methoxyphenyl)-10-phenyl OEP **252**, 5-(1-naphthyl)-10-(9-phenanthrenyl) OEP **259** and 5-(9-phenanthrenyl)-10-phenyl OEP **247** displayed furthermore a split or shouldered Soret band, with the shoulder located between 448 and 455 nm. The Soret shoulder of 5-(3-methoxyphenyl)-10-phenyl OEP **258** was in accordance with the electron withdrawing substituent slightly blue shifted (Soret at 448 nm as shown in figure 5.3.2) relative to the other OEPs.

Soret splits might be attributed in regard to Vinogradov and co-workers^{21,49-52} and Higuchi *et al.*⁵³⁻⁵⁵ as due to the newly introduced polarity, the increased unsymmetry and the higher flexibility of the molecule as a result of the substitution. The OEPs **259** and **9** were also described in chapter 3 as 1/1 mixtures of the respective atropisomers, which might also explain the observed Soret splits and the spectrum of the OEP **259** is shown in figure 5.3.3. On the other hand, 5,10-bis(1-naphthyl) OEP **257** was also obtained as a mixture of two atropisomers but did not display a split Soret band as discussed earlier on. However, no Soret splits occurred also for the dimethylaminophenyl substituted OEPs **249**, **253** and **260** and the respective spectra are shown in figure 5.3.4, 5.3.5 and 5.3.6. On the other hand the trisubstituted AAB OEP **292**, which will be described in chapter 5.4, displayed a Soret split, which could be therefore attributed to the unsymmetric substitution pattern (see figure 5.4.2). Especially the Q band area of the NMe₂ substituted OEPs changed (enhanced QIV band intensities and a smaller Soret-Q band distance) and will be discussed in section 5.5. The overall broadening of the spectra was accorded to an increased polarity (NMe₂ and CF₃ substituents) and the higher floppiness of the molecules and was observed to be the strongest for the mini-push-pull OEP **253**.

5.4 UV/vis spectra of *meso* trisubstituted H₂OEPs

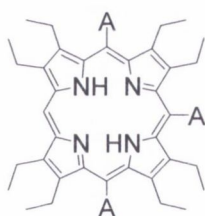
The Soret bands of *meso* trisubstituted OEPs are located between 438 nm and 446 nm and are compared to *meso* disubstituted OEPs 8 nm to 21 nm red shifted. 5,10,15-Trisphenyl OEP **217**⁵⁶ and 5,10-bisphenyl-15-(4-*n*-pentylphenyl) OEP **294** displayed the smallest shifts and their Soret bands were located at 338 nm (see table 5.4.1 and 5.4.2). They are furthermore followed by 5,10-bisphenyl-15-(4-bromophenyl) OEP **293**, displayed in table 5.4.3, and 5,10,15-tris(1-naphthyl) OEP **235**, which displayed both a Soret band at 441 nm due to the bromo group and the slight impact of the 1-naphthyl

substituent. On the other hand, the trisubstituted OEPs bearing methoxyphenyl, anthracenyl and phenanthrenyl residues displayed stronger Soret shifts (445 nm and 446 nm) as a result of the increased *meso*- β interaction, which should induce a higher degree of overall distortion compared to other trisubstituted OEPs.



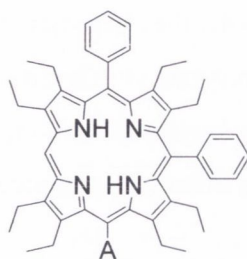
OEP	A,B	Soret	sh	QIV	QIII	QII	QI
1	-	398		497	531	566	619
288	phen,nPP	442 (5.06)	470 (4.76)	537 (3.95)	sh	609 (3.75)	665 (3.73)
290	anth,Ph	446 (4.59)		538 (3.59)	sh	609 (3.42)	666 (3.31)
235	3-OMePh,Ph	442 (4.80)		537 (3.78)		609 (3.51)	673 (3.23)
291	phen,naph		465 (5.32)	569 (3.56)	608 (3.86)	663 (4.01)	sh
287	phen,Ph		472 (5.14)		564 (sh)	608 (3.38)	663 (3.70)

Table 5.4.1. UV/vis absorption of ABA *meso* trisubstituted OEPs (CH_2Cl_2 , λ_{max} (lg ϵ), $\lambda = [1/\text{nm}]$)); sh=shoulder; nPP=*n*-pentylphenyl, phen=9-phenanthrenyl, anth=9-anthracenyl, 3-OMePh=3-methoxyphenyl.



OEP	A	Soret	sh	QIV	QIII	QII	QI
1	-	398		497	531	566	619
217	phenyl ⁵³	438 (5.28)		534 (4.14)	sh	608 (3.91)	667 (3.79)
235	naphthyl	442 (4.80)		537 (3.78)		609 (3.51)	673 (3.23)
289	phenanthrenyl	445 (4.89)	472 (3.65)	538 (3.78)	sh	611 (3.64)	665 (3.51)

Table 5.4.2. UV/vis absorption of A₃ *meso* trisubstituted OEPs (CH_2Cl_2 , λ_{max} (lg ϵ), $\lambda = [1/\text{nm}]$)); sh=shoulder.



OEP	A	Soret	sh	QIV	QIII	QII	QI
1	-	398		497	531	566	619
292	4-NMe ₂ -phenyl	446 (4.10)		480 (4.02)	sh	623 (3.09)	682 (3.47)
293	4-bromophenyl	441 (4.35)	465 (4.46)	533 (3.30)	sh	610 (3.20)	676 (3.31)
294	4-pentylphenyl	438 (4.65)	sh	533 (3.72)	sh	605 (3.43)	673 (3.24)

Table 5.4.3. UV/vis absorption of AAB *meso* trisubstituted OEPs (CH₂Cl₂, λ_{\max} (lg ϵ), $\lambda = [1/\text{nm}]$); sh=shoulder.

A strongly red shifted Soret band was also displayed by 5,10-bisphenyl-15-(4-dimethylaminophenyl) OEP **292** and can be related to the dimethylaminophenyl chromophore, which adds a shift of approximately 6 nm.²⁷⁻³⁵

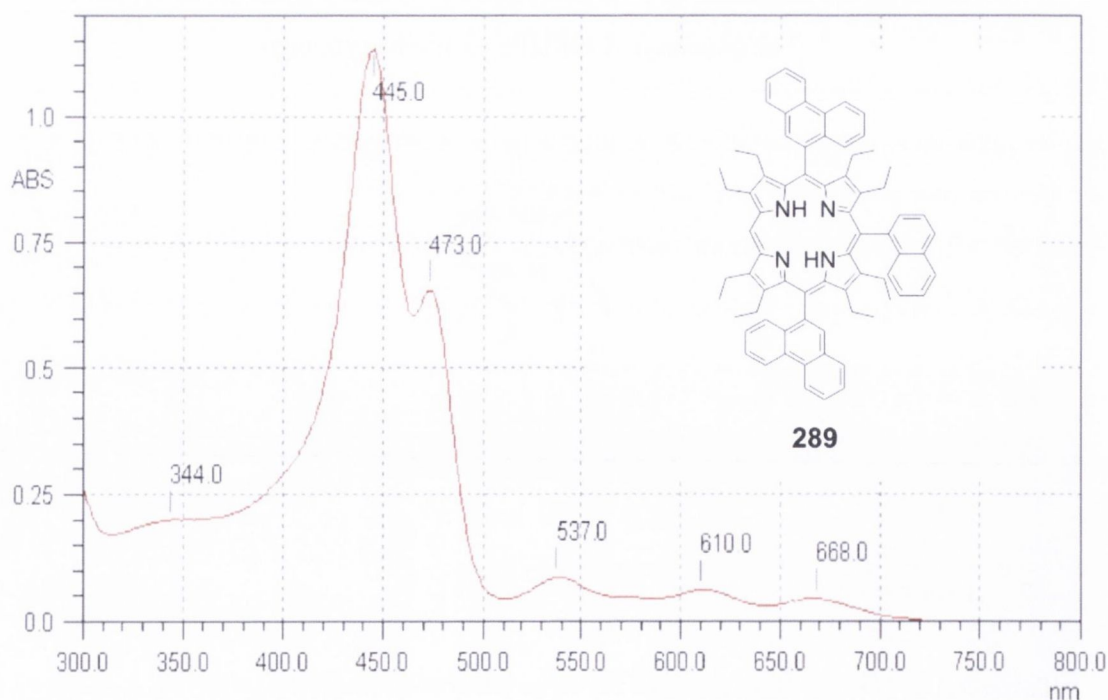


Fig. 5.4.1 UV/vis spectrum of 5,15-bis(9-phenanthrenyl)-10-(1-naphthyl) OEP **289**

Soret splits appear furthermore for the unsymmetric substituted AAB OEPs e.g. for 5,10-bisphenyl-15-(4-bromophenyl) OEP **293**, for 5,10-bisphenyl-15-(4-*n*-pentylphenyl) OEP **294**, and for the OEPs **288**, **289** and **10** (470-473 nm), which were isolated as mixtures of atropisomers, while for 5,10,15-tris(1-naphthyl) OEP **235** no Soret split was observed. As for the in section 5.3 described disubstituted OEP **256**, also for the trisubstituted OEPs **291** and **287**, the Soret split mutates to the actual Soret band and was displayed at 465 nm and 472 nm.

The blue shift of the Soret band, which was observed for the OEP **235** relative to the OEP **287** and **291**, was else wise related to the electron withdrawing effect of the methoxy chromophore. Strong Soret shifts and the encountered Soret band splits were attributed to an unsymmetric or severe distortion, which resulted in an increased molecular flexibility.²¹ For the OEPs **289**, **291** and **10** also the existence of stable atropisomers could have resulted in the observed effects.

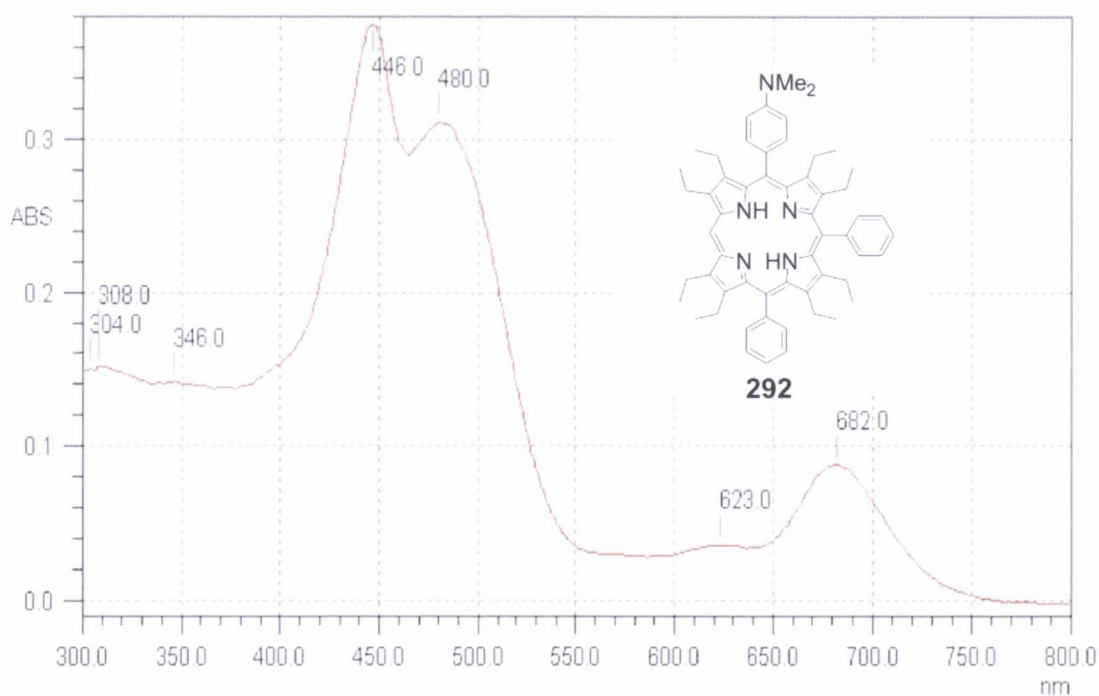


Fig. 5.4.2. UV/vis spectrum of 5,10-bisphenyl-15-(4-dimethylaminophenyl) OEP **292**

The spectra of 5,10,15-tris(9-phenanthrenyl) OEP **10** and 5,15-bis(9-phenanthrenyl)-10-(1-naphthyl) OEP **289** are furthermore shown in figure 5.4.1 and 5.6.3 and displayed a

similar UV/vis shape, whereas the absorption bands of 5,10,15-tris(9-phenanthrenyl) OEP **10** were slightly broadened. The broadening could be explained by the existence of atropisomers and the unsymmetry induced by the phenanthrenyl substituents.^{23,48,49} The spectrum of 5,10-bisphenyl-15-(4-dimethylaminophenyl) OEP **292**, shown in figure 5.4.2, was also strongly broadened and displayed a distinctive Soret split. The broadening was attributed to the additional chromophore e.g. the NMe₂ group in combination with the unsymmetric substitution pattern.

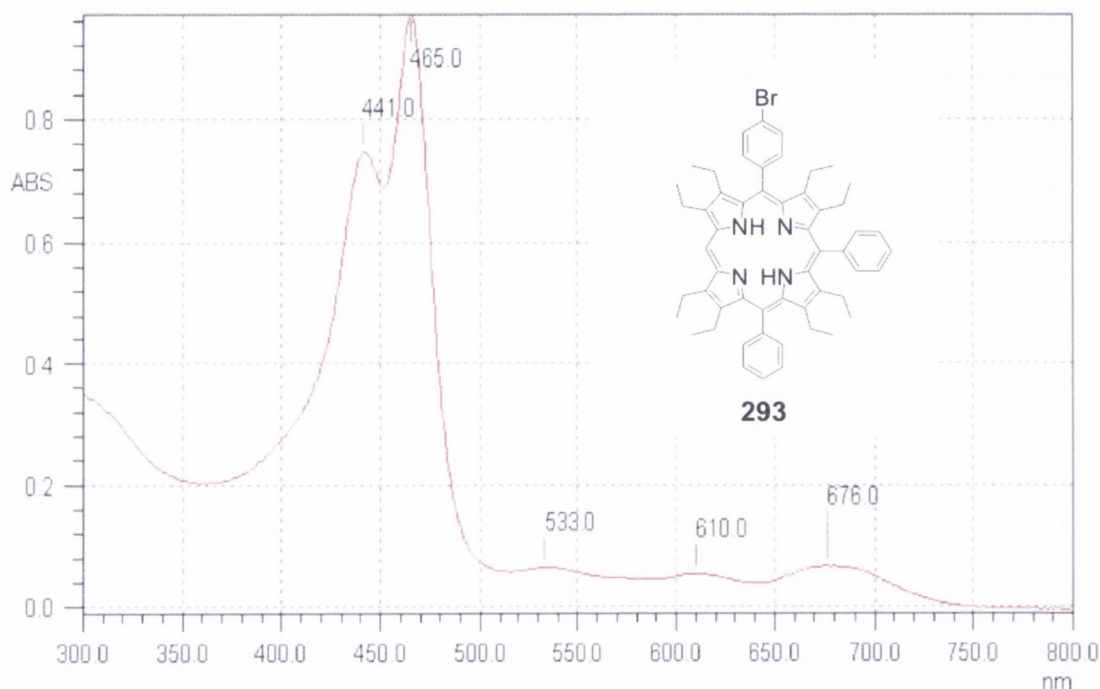


Fig. 5.4.3. UV/vis spectrum of 5,10-bisphenyl-15-(4-bromophenyl) OEP **293**

Obviously, the introduction of unsymmetry had the strongest effect on the UV/vis absorption, while the shape of the spectrum can be also influenced by additional chromophores such as NMe₂ and CF₃. 9-Phenanthrenyl and *n*-pentylphenyl substituents seem to have a major influence on the symmetry as well as *meso* AAB substitution. NMe₂ and phenanthrenyl substituents induce particular red shifts, while CF₃, bromo and OMe groups shift blue. In comparison to the OEP **292**, the spectrum of 5,10-bisphenyl-15-(4-bromophenyl) OEP **293** was slim shaped. It displayed a blue shifted Soret split, situated at the same wavelength as the Soret band of 5,15-bis(3-methoxyphenyl)-10-phenyl OEP **291** (465 nm), which was again attributed to the AAB substitution pattern.

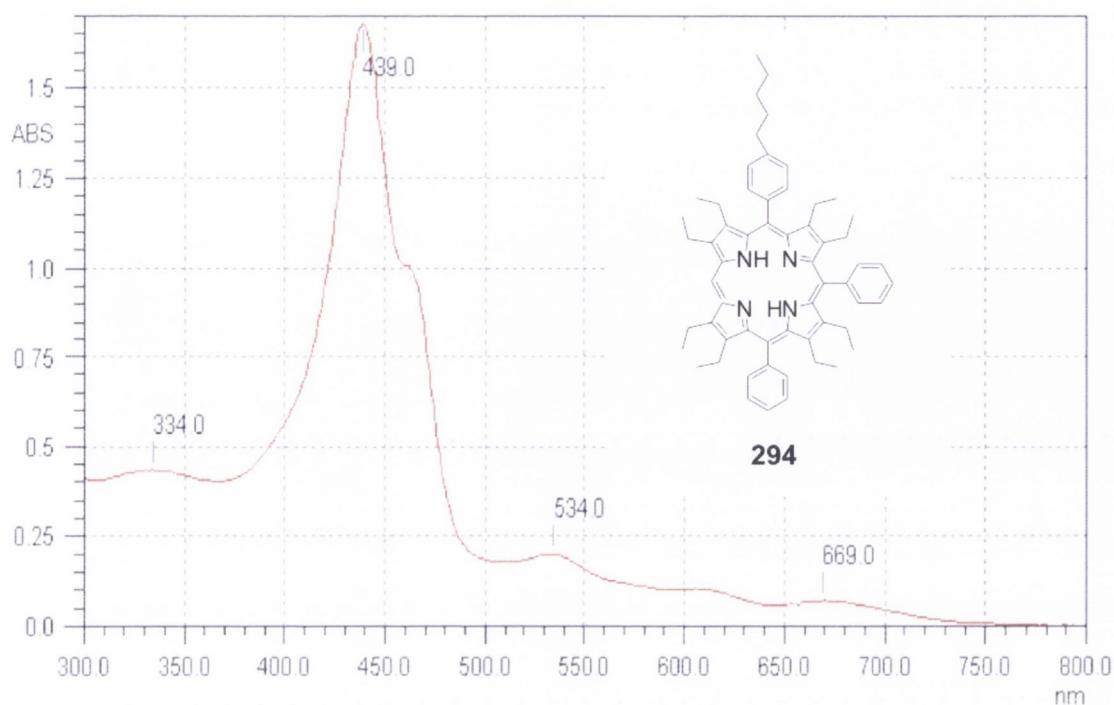


Fig. 5.4.4. UV/vis spectrum of 5,10-bisphenyl-15-(4-*n*-pentylphenyl) OEP **294**

However, the Soret band of 5,10-bisphenyl-15-(4-*n*-pentylphenyl) OEP **294** was only slightly shouldered relative to the minor influence of the pentyl group on the overall polarity of the molecule as shown in figure 5.4.4. Exceptional Soret shifts and observed splits of the Soret bands of di- and trisubstituted OEPs vanished for the corresponding palladium (II) complexes **13**, **14**, **284** and **304** due to the heavy metal effect and the higher core symmetry (see chapter 5.7.1).

5.5 Q band behaviour of *meso* di- and trisubstituted substituted H₂OEPs

Q bands with ‘phyllo-type’ behaviour (QIV>QII>QIII>QI) were described in literature for 5,15-A₂ substituted OEPs, for porphyrins with additional electron donating (NH₂) and withdrawing groups and were also observed for the prepared *meso* 5,10-disubstituted OEPs.^{4,20} Furthermore also chlorins displayed and altered Q-band shape due to the reduced β -position as shown in figure 5.5.1, but which is different to the observed Q band shape of the prepared OEPs.^{24,57}

During the PhD, Q band irregularities were observed e.g. deviations from for OEP **1** typical four Q bands with intensities of QIV>QIII>QII>QI. Those deviations were found

to depend less on the number of substituents, but more on the kind of substituents and the substitution pattern in combination with a 3D deviation from the zero plane.

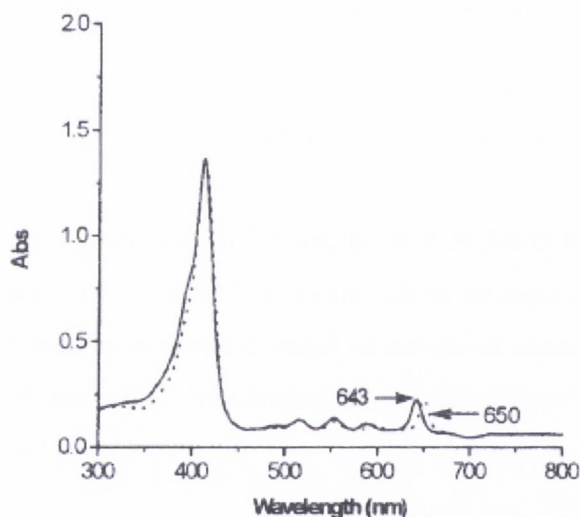
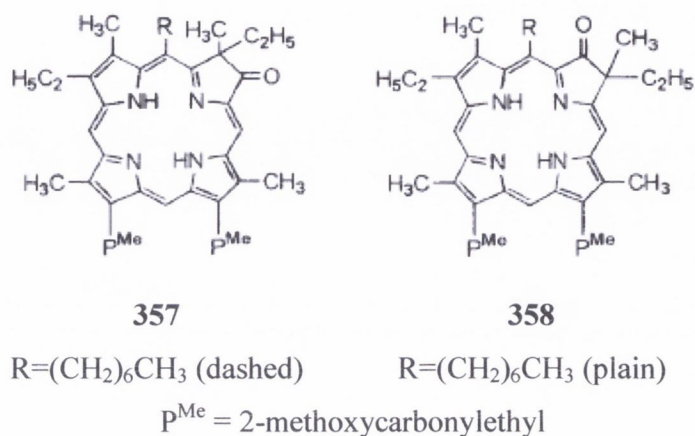
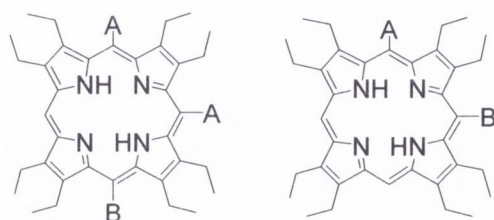


Fig. 5.5.1. Structures and UV/vis spectra of the chlorins **357** (dashed line) and **358** (plain line) displaying a typical high QI band in the long wavelength range.⁵⁷

Most of the *meso* monosubstituted OEPs showed regular behavior relative to OEP **1** while smaller deviances appeared as discussed in chapter 5.2 e.g. a changed Q band intensity (QII>QIII). The so-called distortion of the *meso* monosubstituted OEPs was furthermore described to be small and could be related to the limited effects on the UV/vis spectra (see chapter 4). More explicit changes were only observed with a higher degree of distortion and unsymmetry for *meso* 5,10-di- and ABA/AAB trisubstituted OEPs. Especially the OEPs with an unsymmetric substitution pattern (AB or AAB, see

figure 5.5.1) and substituents that induced by nature a higher degree of unsymmetry or polarity e.g. 9-phenanthrenyl residues and NMe₂ groups showed more deviances.



unsymmetric

Fig. 5.5.1. Symmetry of synthesized octaethylporphyrins

The prepared *meso* 5,10-A₂ and 5,10-AB substituted OEPs **246**, **248**, **250**, **252** and **255** bearing at least one phenyl or 4-*n*-pentylphenyl substituent besides others as well as 5,10-bis(1-naphthyl) OEP **257** displayed similar Q band perturbations. The Q band area of 5-(4-*n*-pentylphenyl)-10-phenyl OEP **250** is shown in figure 5.5.2 and showed an intense QIV and QII band as well as shoulders for the QIII and QI bands in similarity to *meso* monosubstituted OEPs and 5,15 disubstituted OEPs.⁴ The *meso* monosubstituted OEPs, displayed furthermore equal intense QIII and QII bands while for 5-(4-*n*-pentylphenyl)-10-phenyl OEP **250** and other AB and ABA substituted OEPs QII>QIII was observed (phyllo-type Q band shape) due to the higher degree of distortion and unsymmetry.

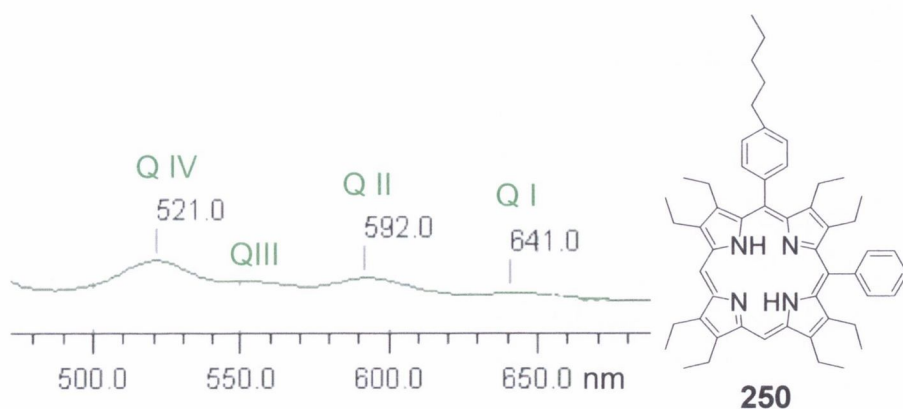


Fig. 5.5.2. Q band area of 5-(4-*n*-pentylphenyl)-10-phenyl OEP **250**

5-(1-Naphthyl)-10-(4-*n*-pentylphenyl) OEP **258** (not shown) displayed additionally a broadened Q band area relative to 5-(4-*n*-pentylphenyl)-10-phenyl OEP **250**, which could be related to the influence of both substituents. Also three of the trisubstituted OEPs, the symmetric ABA and A₃ substituted OEPs **288**, **10** and **289** displayed a Q band shape as shown in figure 5.5.2, while similarities must arise from equal degrees of unsymmetry.

A slightly different Q band shape was also observed for 5-(4-*n*-pentylphenyl)-10-(9-phenanthrenyl) OEP **256**, showing a particularly weak QIV and QI band as it can be seen in figure 5.5.3.

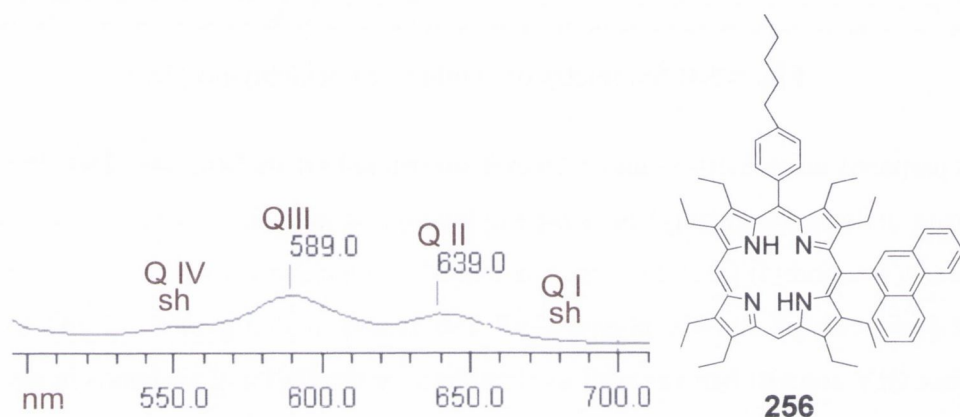


Fig. 5.5.3. Q band area of 5-(4-*n*-pentylphenyl)-10-(9-phenanthrenyl) OEP **256**

Obviously the combination of the pentyl substituent and the unsymmetrical connected phenanthrenyl substituent induced a higher degree of unsymmetry, which had the shown impact on the Q band intensities.

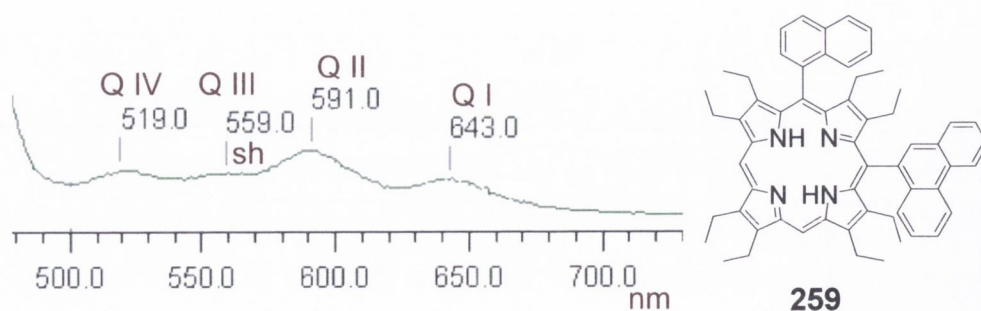


Fig. 5.5.4. Q band area of 5-(1-naphthyl)-10-(9-phenanthrenyl) OEP **259**

Another variation could be also found for the Q band area of 5-(1-naphthyl)-10-(9-phenanthrenyl) OEP **259** and the trisubstituted 5,15-bis(3-methoxyphenyl)-10-phenyl OEP **291**, displaying a strong QII band relative to weaker QIV and QIII bands as shown in figure 5.5.4. A small Q–Soret band distance and a merging of the QIV band into the Soret band was furthermore found for the NMe₂ bearing di- and AAB trisubstituted OEPs **249**, **260**, **253**, **292** and **293**. The merging was also accompanied by an altered (broadened) Q band shape and was explained by the increased polarity of the molecule due to the NMe₂ chromophore in addition to the unsymmetry induced by the substitution pattern. The Q band area of 5-(4-dimethylaminophenyl)-10-phenyl OEP **249**, which displayed decreased Q band intensities as for etio-type porphyrins (QIV>sh>QII>QI), is shown in figure 5.5.5.

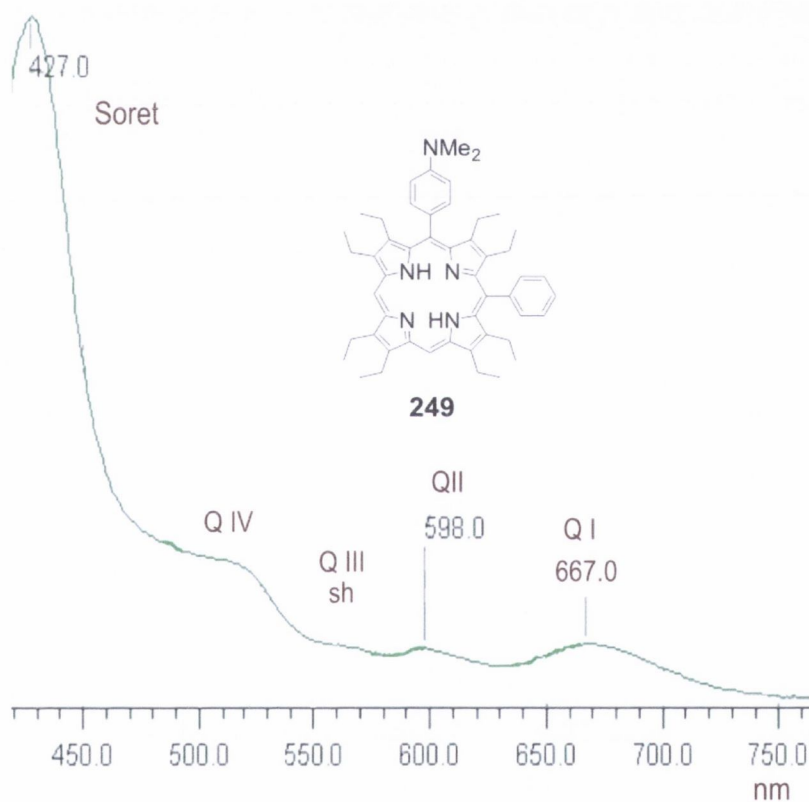


Fig. 5.5.5. Q band area of 5-(4-dimethylaminophenyl)-10-(phenyl) OEP **249**

Also the ABA trisubstituted 5,15-bis(9-anthracenyl)-10-phenyl OEP **287** showed surprisingly a merging of the QIV band into the Soret band as did the OEP **249** as well

as 5,10-bis(9-phenanthrenyl) OEP **9** (see chapter 5.6), which must rely in an unsymmetric distortion of the molecule or for the OEP **9** in the existence of atropisomers as was described in chapter 3. As it can be seen in the figures 5.3.4-5.3.6, the OEPs **249**, **253** and **260** displayed also broadened absorption bands with the strongest broadening for 5-(3-trifluoromethylphenyl)-10-(4-dimethylaminophenyl) OEP **253** and the effect was explained by the polarity induced by the NMe₂ chromophore and by the CF₃ substituent.²¹

5.6 UV/vis spectra of the phenanthrenyl series (8-11)

OEP	Soret	sh	QIV	QIII	QII	QI
8	406 (5.13)		504 (4.13)	538 (3.86)	571 (3.83)	624 (3.52)
9	426 (5.45)	455 (sh)	519 (4.56)	sh	592 (4.35)	sh
10	445 (4.38)	473 (4.14)	539 (3.14)	sh	608 (3.09)	665 (2.95)
11	493 (5.37)		sh	640 (3.11)	697 (4.13)	

Table 5.6.1. UV/vis absorption of the members of the phenanthrenyl series, CH₂Cl₂, λ_{\max} (lg ϵ), λ = [1/nm]); sh=shoulder.

The figures 5.6.1 to 5.6.4 show the UV/vis spectra of 5-(9-phenanthrenyl) OEP **8**, 5,10-bis(9-phenanthrenyl) OEP **9**, 5,10,15-tris(9-phenanthrenyl) OEP **10** and 5,10,15,20-tetrakis(9-phenanthrenyl) OEP **11**. As it can be seen in figure 5.6.1, the Q band behavior of the OEP **8** was analogous to the in chapter 5.2 described phyllo-type porphyrins displaying QIV>QIII≈QII>>QI. Compared to 5,10,15,20-tetrakis(9-phenanthrenyl) OEP **10**, a broader Soret band was observed and might be the result of the reduced symmetry. The spectrum of 5,10-bis(9-phenanthrenyl) OEP **9** on the other hand was slightly broadened relative to the OEP **9** and showed a shouldered Soret band, etio-type Q band behavior, a merging of the Q bands into each other and of the QIV band into the Soret band. The Q band behavior of 5,10-bisphenyl OEP **236** is furthermore similar, while for the regioisomer, 5,15-bisphenyl OEP **216**, no formation of Q band shoulders was observed and the intensities were phyllo-type like (QIV>QII>QIII>QI) due to a higher degree of symmetry.⁴ The additional red shift induced by the phenanthrenyl substituents is 12 nm relative to 5,10-bisphenyl OEP **236**. The broadening and the Soret band split of 5,10-bis(9-phenanthrenyl) OEP **9** were attributed to the mixture of two atropisomers.

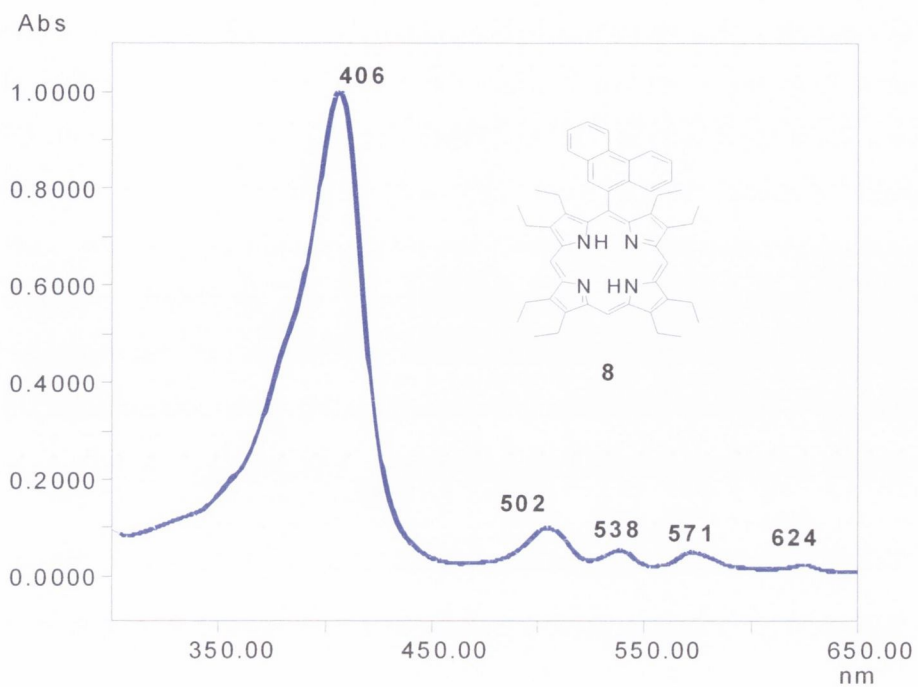


Fig. 5.6.1. UV/vis spectrum of 5-(9-phenanthrenyl) OEP 8

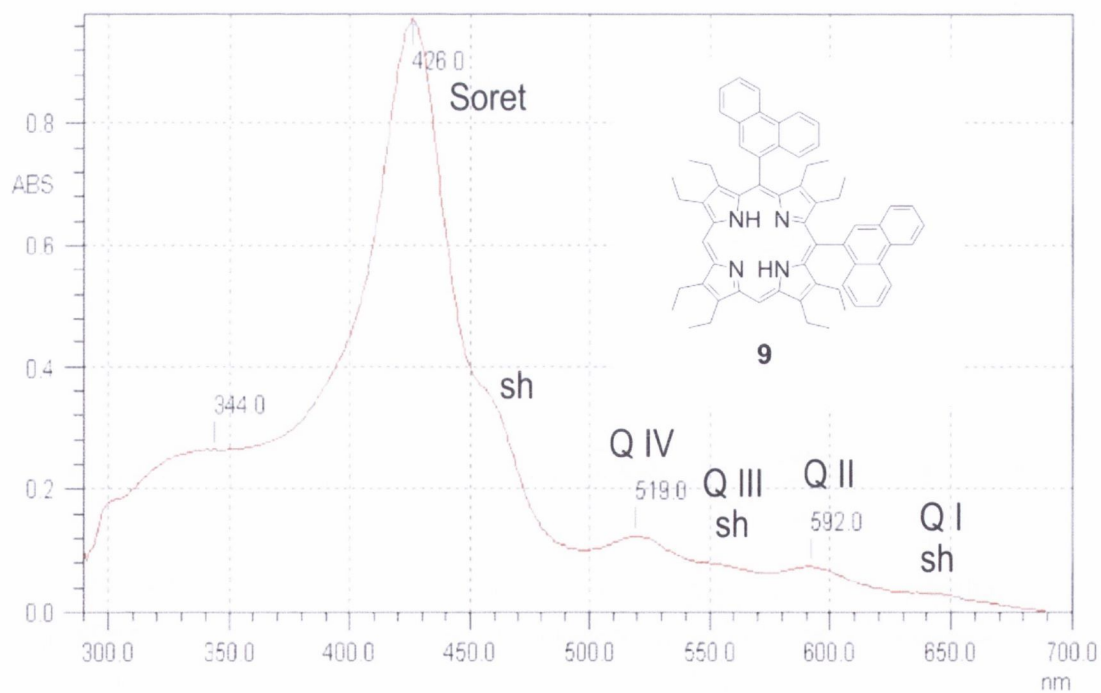


Fig. 5.6.2. UV/vis spectrum of 5,10-bis(9-phenanthrenyl) OEP 9

The Q band area of 5,10,15-tris(9-phenanthrenyl) OEP **10** on the other hand is clearly separated from the Soret band, while the Soret band becomes slightly slimmer and shows a Soret band split at 473 nm. Phyllo-type Q band behavior with $Q_{III} < Q_{II}$ was observed, whereas the QI band increased in intensity. Three atropisomers were encountered as described in chapter 3 and might be the reason for the Soret band split. As it can be seen in the shown figures and table 5.6.1, the absorption bands shifted red within the phenanthrenyl series, which indicated a continuously increasing distortion.^{4,7,57} The red shift was relative small for the *meso* monosubstitution (6 nm) and stronger for the di- and trisubstitution (20 nm).

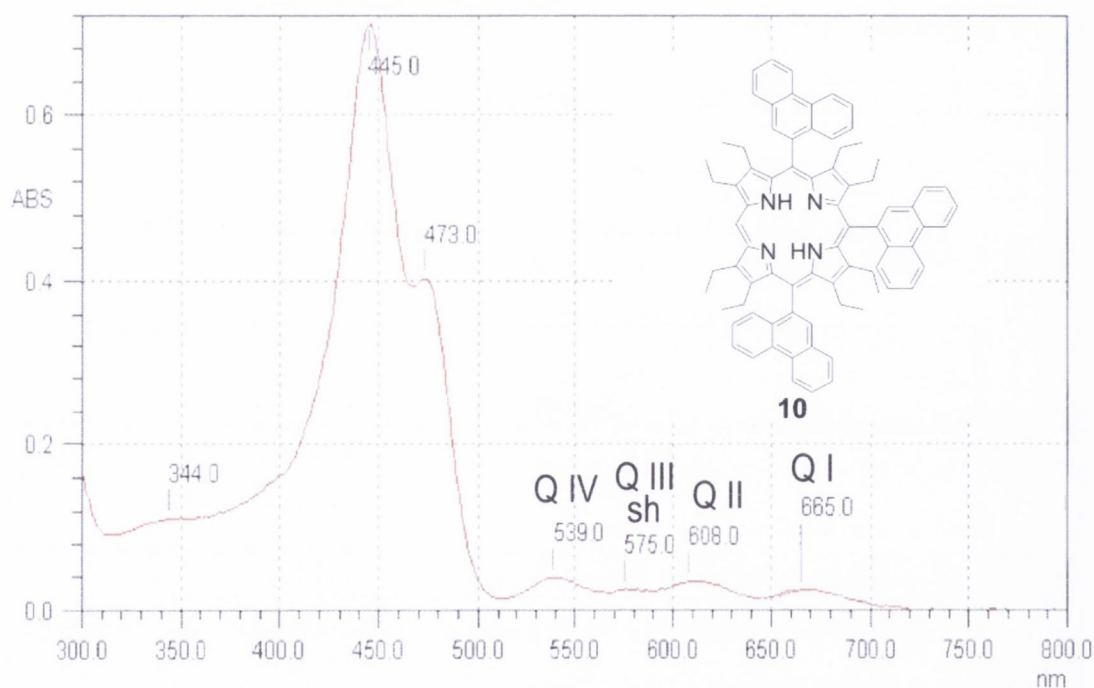


Fig. 5.6.3. UV/vis spectrum of 5,10,15-tris(9-phenanthrenyl) OEP **10**

From the tri- to the tetrasubstituted OEP (**10** to **11**), the red shift increased by 48 nm and was higher than the relative shift observed within the phenyl series ($\Delta=37$ nm). The phenanthrenyl series could be furthermore compared to members of the 1-naphthyl series. The spectra of 5-(1-naphthyl) OEP **7** and 5-(9-phenanthrenyl) OEP **8** were similar and both displayed equal oscillator strengths for the QIII and the QII bands ($Q_{III}=Q_{II}$).

On the other hand, no Soret split was observed in the UV/vis spectrum of 5,10-bis(1-naphthyl) OEP **257** relative to 5,10-bis(9-phenanthrenyl) OEP **9**, whereas both were obtained as mixture of two atropisomers.

5,10,15,20-Tetrakis(9-phenanthrenyl) OEP **11** displayed furthermore only two Q bands as was described in literature for the OETPP **18**^{4,5} and as shown in figure 5.6.4. Relative to the results of Padmanabhan and George, the Soret band of 5,10,15,20-tetrakis(9-phenanthrenyl) OEP **11** was far red shifted indicating a strong influence of the phenanthrenyl substituent compared to the weaker influence of the phenyl substituents in OETPP **18**.

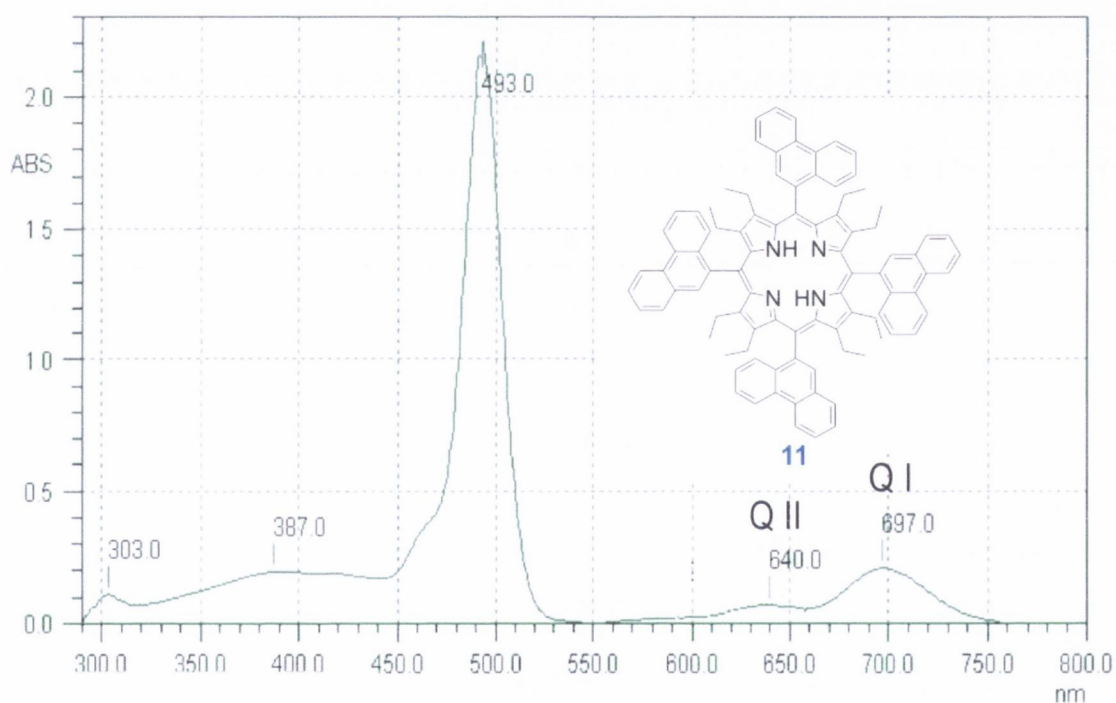


Fig. 5.6.4. UV/vis spectrum 5,10,15,20-tetrakis(9-phenanthrenyl)OEP **11**

The phenanthrenyl substituent induced furthermore a mixture of saddling and ruffling deformations to the porphyrin macrocycle as described in chapter 3 and 6 and similar effects on the Q band shape and the amount of red shift were also observed for related di- and trisubstituted OEPs as was described in chapter 5.3 and 5.4.

5.7 Effect of Pd(II) and Pt(II) insertion on the UV/vis spectra

Figure 5.7.1 shows the excitation energies of D_{4h} symmetric, metal inserted porphyrins. The spectra display a strong and slim Soret band in combination with two further red shifted Q bands. Due to the metal insertion, the energy levels B_{2u} and B_{3u} combine and form a single, degenerated Q band (Q_x), which is displayed with its vibrational overtone (Q_y).

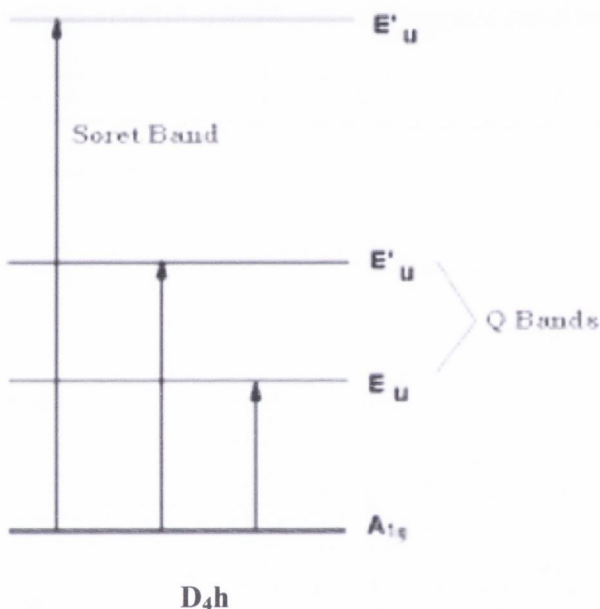
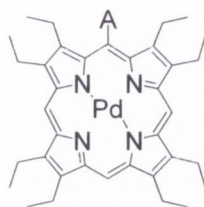


Fig. 5.7.1. Schematic diagram of the electronic transitions of D_{4h} symmetric bivalent metal inserted porphyrins.

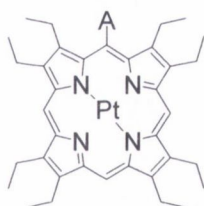
5.7.1 UV/vis spectra of Pd(II) and Pt(II)OEPs

Several *meso* monosubstituted Pd(II) and Pt(II)OEPs were obtained as described in chapter 2 and the respective UV/vis data is displayed in table 5.7.1.1 and 5.7.1.2. The di- and trisubstituted Pd(II)OEPs **284** and **304** and the Pd(II)OEPs of the phenanthrenyl series (**13-15**) were additionally prepared and the Soret band perturbations of the respective free base OEPs reported in the chapters 5.2 to 5.4 were not observed (compare to table 5.7.1.3) due to the higher degree of symmetry effected by the core metal insertion.



OEP	A	Soret	Q _x	Q _y
2	-	392 (5.41)	511 (4.36)	545 (4.87)
166	methyl	405 (5.18)	520 (4.15)	552 (5.92)
17	<i>n</i> -butyl	406 (5.79)	521 (4.64)	555 (4.78)
299	<i>s</i> -butyl	409 (6.01)	526 (4.94)	557 (5.04)
273	phenyl	399 (5.14)	515 (3.98)	549 (4.35)
301	4-pentylphenyl	402 (4.47)	516 (3.89)	549 (4.00)
300	3-CF ₃ -phenyl	400 (5.41)	516 (3.89)	550 (4.53)
282	1-naphthyl	401 (5.00)	516 (3.79)	551 (4.18)
302	2-naphthyl	400 (4.90)	516 (3.80)	550 (4.14)
303	acenaphthyl	399 (5.11)	515 (4.03)	548 (4.36)
12	9-phenanthrenyl	400 (5.86)	516 (4.79)	550 (5.12)

Table 5.7.1.1. UV/vis absorption of *meso* monosubstituted Pd(II)OEPs (CH₂Cl₂, λ_{max} (lg ε), λ = [1/nm])

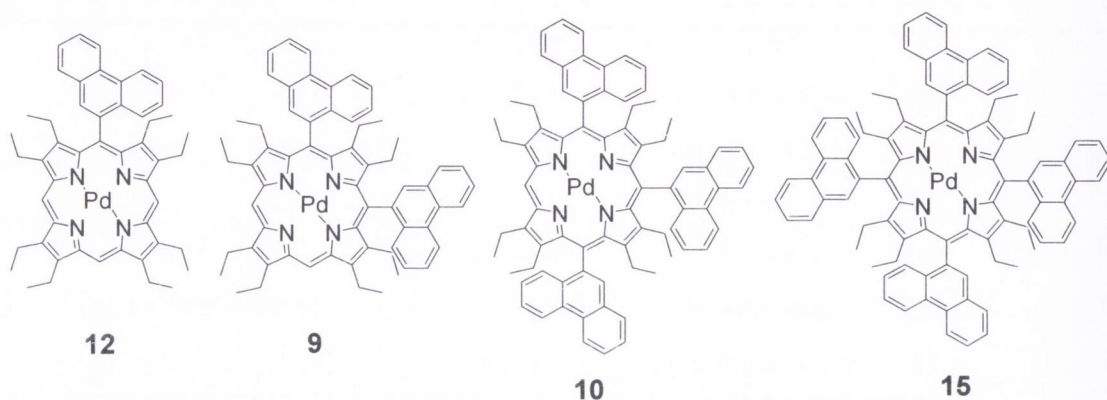


OEP	A	Soret	Q _x	Q _y
3	-	380 (5.30)	500 (4.22)	535 (4.62)
307	phenyl	386 (6.60)	504 (5.28)	539 (5.78)
308	naphthyl	387 (5.79)	504 (4.51)	538 (4.99)
309	9-phenanthrenyl	387 (6.04)	504 (4.71)	538 (6.20)

Table 5.7.1.2. UV/vis absorption of *meso* monosubstituted Pt(II)OEPs (CH₂Cl₂, λ_{max} (lg ε), λ = [1/nm])

On the other hand a shoulder was now surprisingly encountered for 5,10-bis(1-naphthyl) Pd(II)OEP **284** (not shown) and might be the result of two atropisomers as described in chapter 3. Spectral changes were else wise described for metal inserted porphyrin dimers in literature,⁵³⁻⁵⁵ while only a slight variation of the Q band intensities was found for the prepared Pd(II)OEPs as shown in figure 5.7.1.1.

The effect of the palladium(II) and platinum(II) insertion into the prepared OEPs is a blue or hypsochromic shift of the Soret band and the Q bands, whereas the shift for the platinum(II) insertion is stronger.

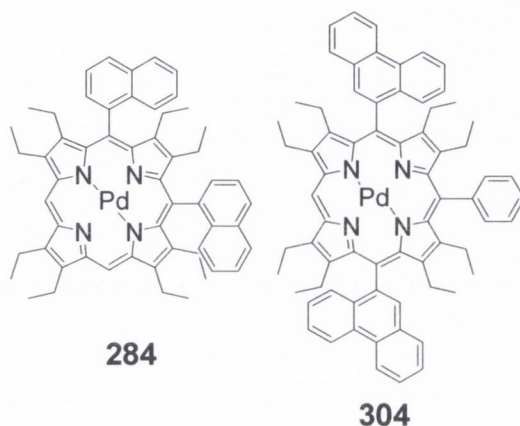


OEP	Soret	Q _x	Q _y
12	400 (5.86)	516 (4.79)	550 (5.12)
9	414 (5.15)	527 (4.09)	562 (4.24)
10	429 (4.11)	539 (4.04)	573 (4.06)
15	443 (4.43)	553 (3.89)	590 (3.75)

Table 5.7.1.3. UV/vis absorption of the Pd(II) inserted members of the phenanthrenyl series, CH₂Cl₂, λ_{max} (lg ε), λ = [1/nm].

For example the Soret band of 5-methyl OEP **227** was displayed at 406 nm, while the respective Pd(II) complex **166** displayed a Soret band at 405 nm (Δ=1nm to the blue) and the Soret band of 5-naphthyl OEP **7** was located at 406 nm, while the Pd(II) complex **282** displayed a Soret band at 401 nm (Δ=5nm to the blue) and 5-(1-naphthyl) Pt(II) OEP **309** at 387 nm (Δ=19 nm to the blue). Also a 8 nm shift of the Soret band

was observed from Pd(II)OEP **2** to 5-(1-naphthyl) Pd(II)OEP **282** and from Pd(II)OEP **2** to 5-methyl Pd(II)OEP **166** a shift of 14 nm was observed.⁵⁸



OEP	Soret	sh	Q _x	Q _y
284	412 (498)	486 (sh)	527 (3.95)	561 (4.08)
304	427 (4.87)		539 (3.78)	573 (3.72)

Table 5.7.1.4. UV/vis absorption of the Pd(II)OEPs **284** and **304**, CH₂Cl₂, λ_{max} (lg ε), λ = [1/nm]); sh=shoulder.

Furthermore, the red shifts within the phenanthrenyl series, decreased for the respective palladium(II) complexes **12-15**. The red shift from OEP **1** to 5-(9-phenanthrenyl) OEP **8** was 8 nm, to 5,10-bis(9-phenanthrenyl) OEP **9** 28 nm, to 5,10,15-tris(9-phenanthrenyl) OEP **10** 44 nm and to 5,10,15,20-tetrakis(9-phenanthrenyl) OEP **11** 95 nm, while it was 8 nm from Pd(II)OEP **2** to 5-(9-phenanthrenyl) Pd(II)OEP **12**, 22 nm to 5,10-bis(9-phenanthrenyl) Pd(II)OEP **13**, 37 nm to 5,10,15-tris(9-phenanthrenyl) Pd(II)OEP **14** and 51 nm to 5,10,15,20-tetrakis(9-phenanthrenyl) Pd(II)OEP **15**. The amount of red shift for the Soret band from Pt(II)OEP **3** to *meso* monosubstituted 5-(1-naphthyl) Pt(II)OEP **309** was 7 nm. However, the Q band intensities of Pd(II)OEP **2** and Pd(II)OETPP **244** were observed to swap in intensity from QIII>QIV to QIV>QIII as shown in figure 5 in the introduction. Broadened Q bands were observed for 5-*n*-butyl Pd(II) OEP **17** as well as for 5-*s*-butyl Pd(II)OEP **299** and were attributed to a higher degree of unsymmetry due to the alkyl substitution and relative to Pd(II)OEP **2**. The Q band shapes of the *meso*

monosubstituted Pd(II)OEPs **12**, **273**, **166**, **299** and **17** are shown in figure 5.7.1.1. 5-Phenyl Pd(II)OEP **273** and 5-(9-phenanthrenyl) Pd(II)OEP **12** displayed a similar Q band shape, whereas the Q_y band decreased for 5-methyl Pd(II)OEP **166** and reached a minimum for 5-*n*-butyl Pd(II)OEP **17** and 5-*s*-butyl Pd(II)OEP **299**.

Figure 5.7.1.2 shows furthermore the Q band area of Zn(II) and Pd(II)TPTNP (**375/375a**), Zn(II) and Pd(II)TPTBP (**360a,360**) relative to Zn(II) and Pd(II)TPP **64a,b** reported by Vinogradov and co-workers. As it can be seen, analogous to the aryl Pd(II)OEPs **12** and **273**, the Q_y band of the TPTNPs and TPTBPs (**375/375a/360a/360**) increased in intensity,⁵² while the Zn(II) and Pd(II)TPP **64a/64b** displayed inversed intensities.

However, the intensities of the Zn(II) complexes were the highest. The UV/vis spectrum of 5,10,15-tris(9-phenanthrenyl) Pd(II)OEP **14** is shown in figure 5.7.1.3 and displayed Q bands with equal intensity, while the Q_x band is slightly broadened relative to the Q_y band. 5,15-Bis(9-phenanthrenyl) Pd(II)OEP **9**, 5,10-bis-(1-naphthyl) Pd(II)OEP **284** and the mixture of 5-(9-phenanthrenyl)-10-*s*-butyl Pd(II)OEP/5-(9-phenanthrenyl)-15-*s*-butyl Pd(II)OEP **278/279** (not shown, compare to the appendix) displayed on the other hand Q_y>Q_x intensities, similar to the *meso* monosubstituted Pd(II) and Pt(II)OEPs.

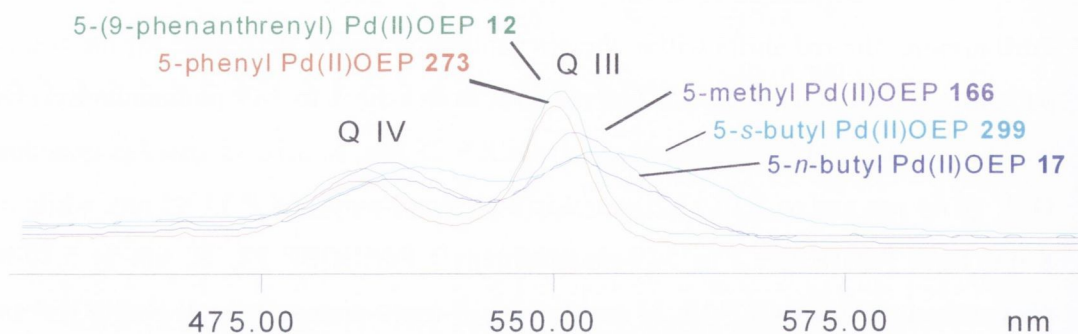


Fig. 5.7.1.1. Q band area of selected *meso* monosubstituted palladium (II) complexes.

The UV/vis spectrum of the Pd(II)TPTBP **360a** is also shown in figure 5.7.1.4 and displayed a Soret band at 444 nm, equal to the for 5,10,15,20-tetrakis(9-phenanthrenyl) Pd(II)OEP **15** observed Soret band and is expected to be similar distorted. The Q_y band of the Pd(II)TPTBP **360a** was furthermore observed at 629 nm and was red shifted

compared to 5,10,15,20-tetrakis(9-phenanthrenyl) Pd(II)OEP **15** (Q_x at 553 nm, Q_y at 590 nm).

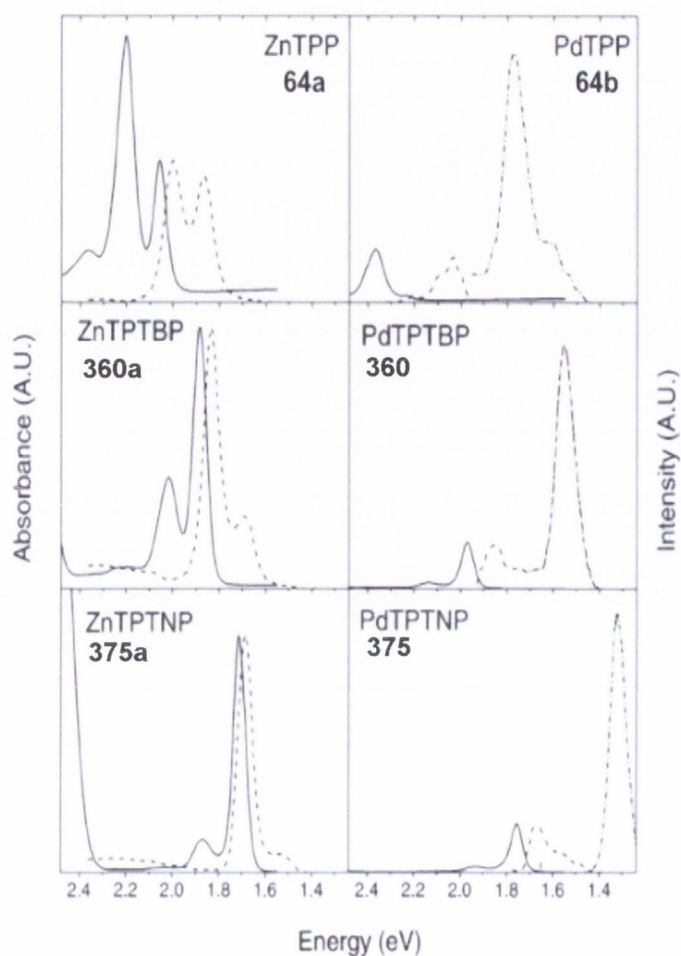


Fig. 5.7.1.2. Q band absorption (plain line) and emission (dashed line) of Pd(II)/Zn(II)TPP **64a/64b**, Zn(II)/Pd(II)TPTBP **360a/360** (tetraphenyltetrabenzoporphyrin) and Zn(II)/Pd(II)TPTNP **375a/375** (tetraphenyltetranaphthoporphyrin).⁵²

The Soret and Q bands of Pd(II)OETPP **18** were furthermore displayed at 433 nm (Soret), 546 nm (Q_x) and 592 nm (Q_y), indicating a smaller degree of overall distortion relative to the Pd(II)TPTBP **360a** and the Pd(II)OEP **15**.

The UV/vis spectrum of 5-phenyl Pt(II)OEP **307** is displayed in figure 5.7.1.5 and has the same shape as the respective Pd(II)OEP **273**, while the overall Q band intensities increased.

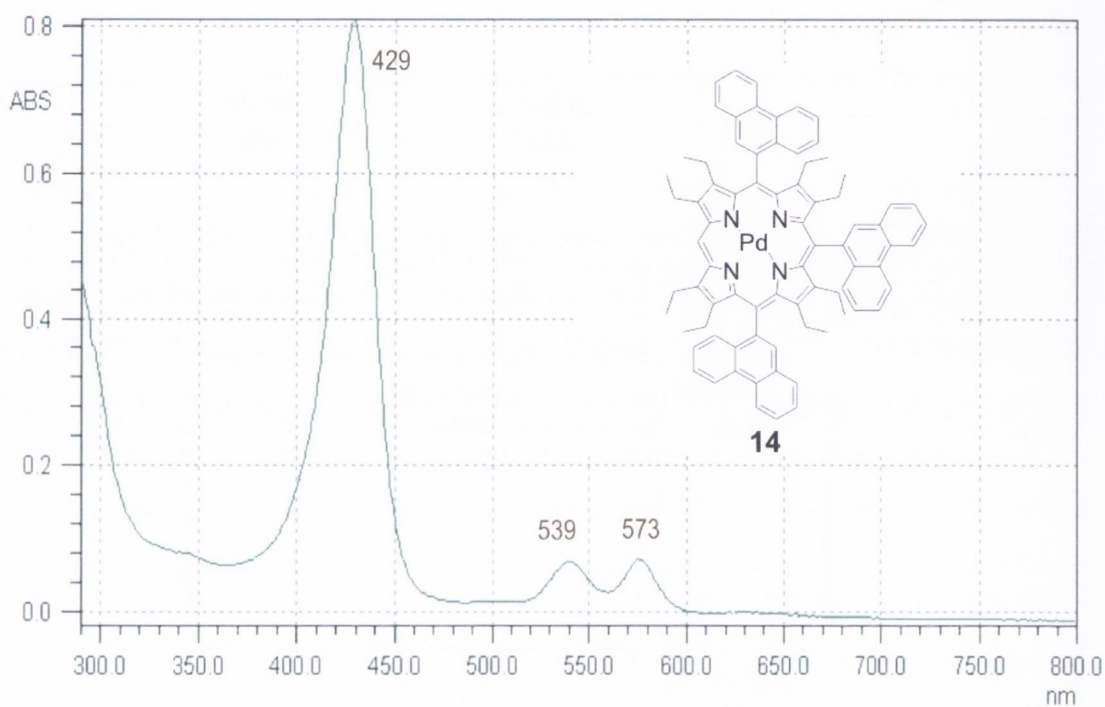


Fig. 5.7.1.3. UV/vis spectrum of 5,10,15-tris(9-phenanthrenyl) Pd(II)OEP **14**

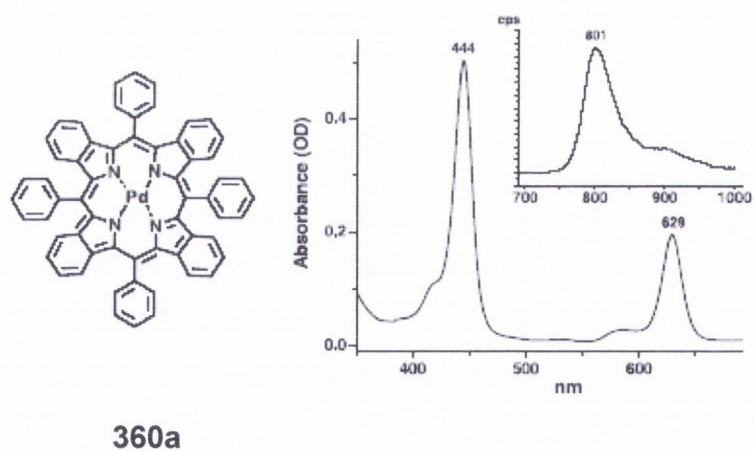


Fig. 5.7.1.4. Structure, absorption and emission spectra of 5,10,15,20-tetrakisphenyl Pd(II)TBP **360a**.²¹

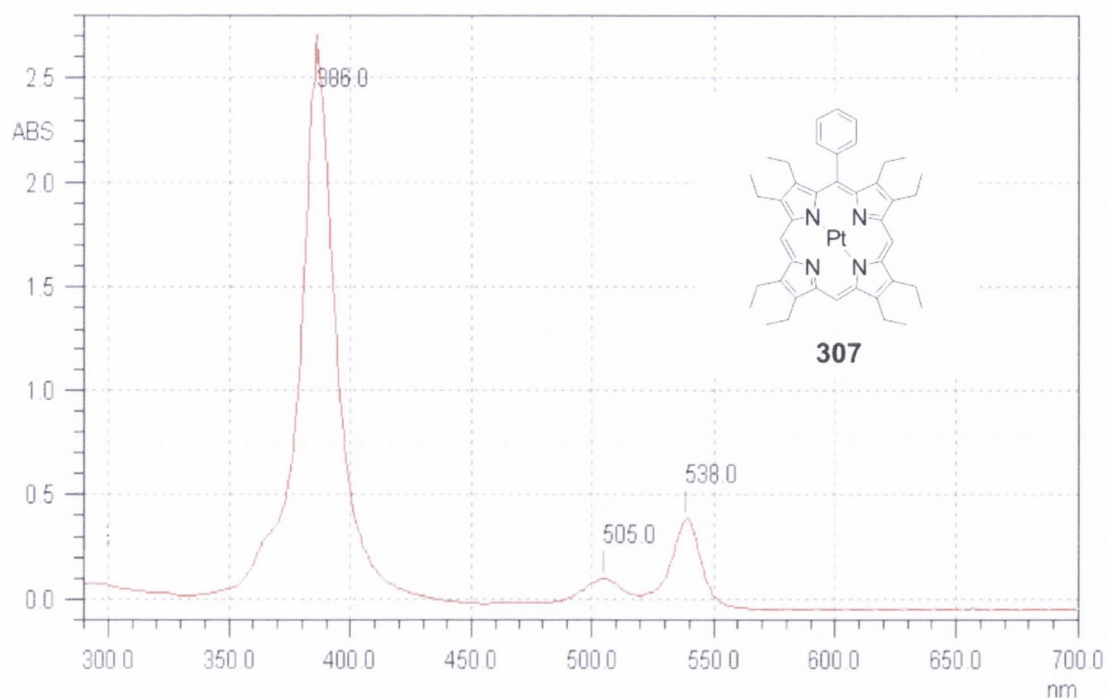


Fig. 5.7.1.5. UV/vis spectrum of 5-phenyl Pt(II)OEP **307**

5.8 Absorption bands of additional chromophores in the UV/vis spectra

Phenanthrenyl, anthracenyl, naphthyl, phenyl, dimethylaminophenyl and methoxyphenyl chromophores were introduced in the prepared OEPs and possess their own absorption maxima. An absorption band appeared for example in the UV/vis spectrum of 5-(9-phenanthrenyl) Pd(II)OEP **12** at 254 nm, while the corresponding free base OEP **8** displayed two absorption bands, located at 254 and 297 nm corresponding to the introduced phenanthrenyl chromophore.²⁷ Absorption maxima in similar areas were furthermore observed for dimethylaminophenyl substituents at 254 nm, whereas aniline absorbs at 280 nm.²⁷ The respective spectra of 5-(9-phenanthrenyl) OEP **8** and 5-(4-dimethylaminophenyl) OEP **230** are shown in figure 5.8.1. In literature the following absorption maxima could be found for anthracene **330**, phenanthrene **328**, acenaphthene, naphthalene **329**, benzene and the bromo chromophore: anthracene: λ_{\max} (ϵ_{\max}) = 252 (199 000), 375 (7900) nm; phenanthrene: λ_{\max} (ϵ_{\max}) = 251 (66 000), 292 (14 000) nm; acenaphthene: λ_{\max} (ϵ_{\max}) = 272 (180 000), 473 (12 500) nm; naphthalene: λ_{\max} (ϵ_{\max}) = 222 (112 000), 275 (5 600) nm; benzene: λ_{\max} (ϵ_{\max}) = 184 (46 700), 204 (6 900), 255 (170) nm and Br: λ_{\max} (ϵ_{\max}) = 208 (300)/ in DMF: λ_{\max} (ϵ_{\max}) = 270 nm.²⁷

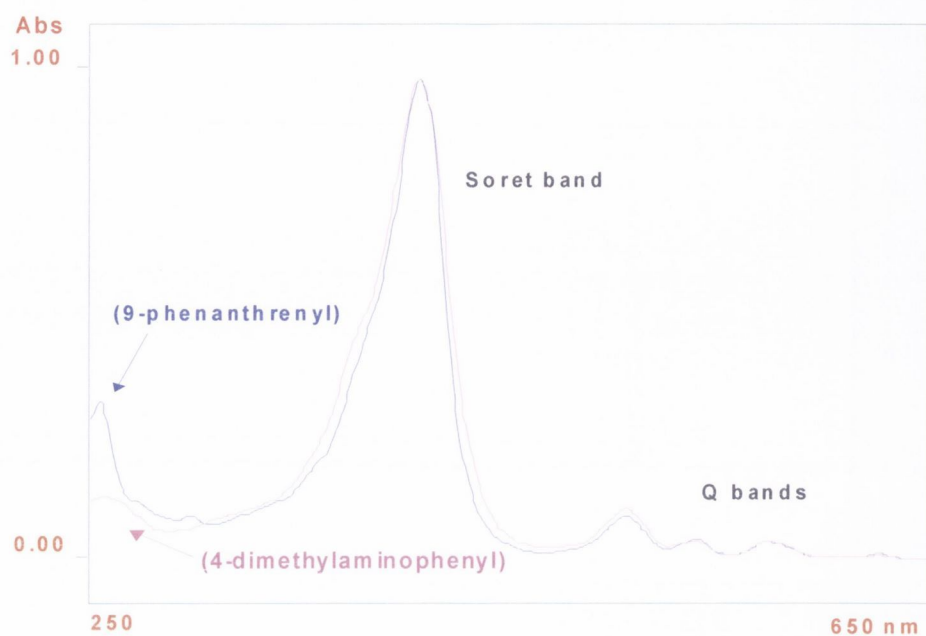


Fig. 5.8.1. UV/vis spectra of 5-(9-phenanthrenyl) OEP **8** (blue) and 5-(4-dimethylaminophenyl) OEP **230** (purple)

REFERENCES

- 1) R. G. George (2002): "Studies on some new meso-aryl substituted porphyrins their bromoderivatives and their metalloderivatives" PhD thesis, Mahatma Gandhi University, Kottayam.
- 2) R. G. George, M. Padmanabhan *Proc. Indian Acad. Sci. (Chem. Sci.)* **2003**, *115*, 4, 263.
- 3) B. Chen, S. Wu, A. Li, F. Liang, X. Zhou, X. Cao, Z. He *Tetrahedron* **2006**, *62*, 5487.
- 4) S. A. Syrbu, L. Lyobumova, A. S. Semeikin *Chem. Heterocyclic Comp.* **2004**, *40*, 10, 1262.
- 5) S. A. Syrbu, T.V. Lyubimova, A.S. Semeikin *Russ. J. Gen. Chem.* **2001**, *71*, 10, 1656.
- 6) X. Z. Song, W. Jentzen, L. Jaquinod, R. G. Khoury, C. J. Medforth, S.-L. Jia; J.-G. Ma, K. M. Smith, J. A. Shelnut *Inorg. Chem.* **1998**, *37*, 2117.
- 7) J. Takeda, M. Sato *Chemistry Lett.* **1994**, 2233.
- 8) J. Takeda, T. Ohya, M. Sato *Chem. Phys. Lett.* **1991**, *183*, 384.
- 9) C. J. Medforth, M. O. Senge, K. M. Smith, L. D. Sparks, J. A. Shelnut *J. Am. Chem. Soc.* **1992**, *114*, 9859.
- 10) J. Takeda, M. Sato *Chem. Pharm. Bull.* **1994**, *42*, 1005.
- 11) K. M. Barkigia, M. W. Renner, L. R. Furenlid, C. J. Medforth, K. M. Smith, J. Faer *J. Am. Chem. Soc.* **1993**, *115*, 3627.
- 12) W. W. Kalisch, M. O. Senge *Tetrahedron Lett.* **1996**, *37*, 8, 1183.
- 13) O. S. Finikova, A. V. Cheprakov, S. A. Vinogradov *J. Org. Chem.* **2005**, *70*, 9562 / P. Bhyrappa, V. Krishnan **1991** *Inorg. Chem.* **30** 239.
- 14) K. M. Barkigia, M. D. Berber, J. Fajer, C. J. Medforth, M. W. Renner, K. M. Smith **1990** *J. Am. Chem. Soc.*, *112*, 885.
- 15) G. A. Spyroulias, A. G. Coutsolelos **1995** *Polyhedron* **14** 2483.
- 16) P. Bhyrappa, P. Bhavana **2001** *Chem. Phys. Lett.* **342** 39.
- 17) A. Rosa, G. Ricciardi, E. J. Baerends, M. Zimin, M. A. J. Rodgers *Inorg. Chem.* **2005**, *44*, 19, 6609.

- 18) A. Rosa, G. Ricciardi, E. J. Baerends, A. Romeo, L. M. Scolaro *J. Phys. Chem. A* **2003**, *107*, 11468.
- 19) X. Zhou, M. K. Tse, T. S. M. Wan, K. S. Chan *J. Org. Chem.* **1996**, *61*, 3590.
- 20) G. Cornejo, G. Ramirez, M. Villagran, J. Costamagna, E. Troll, M J. Aguirre *J. Chil. Chem. Soc.* **2003**, *48*, *1*, 49.
- 21) O. S. Finikova, A. V. Cheprakov, S. A. Vinogradov *J. Org. Chem.* **2005**, *70*, 9562.
- 22) T. E. O. Screen, I. M. Blake, L. H. Rees, W. Clegg, S. J. Borwick, H. L. Anderson *J. Chem. Soc., Perkin Trans. 1* **2002**, 320.
- 23) M. O. Senge, W. W. Kalisch, I. Bischoff *Chem. Eur. J.* **2000**, *6*, 2721.
- 24) K. Jayaraj, A. Gold, L. M. Ball, P. S. White *Inorg. Chem.* **2000**, *39*, 3652.
- 25) V. S.-Y. Lin, S. G. DiMagno, M. J. Therien *Science* **1994**, *264*, 1105.
- 26) A. B. J. Parusel, T. Wondimagegn, A. Ghosh *J. Am. Chem. Soc.* **2000**, *122*, 6371.
- 27) J. A. Dean (1995): „Analytical Chemistry Handbook.“ McGraw-Hill, Inc. (New York).
- 28) H. Kalish, J. E. Camp, M. Stepien, L. Latos-Grazynski, M. M. Olmsted, A. Balch *Inorg. Chem.* **2002**, *41*, 989.
- 29) S. A. Sibia, R. S. Czernuszewicz, M. J. Crossley, T. G. Spiro *Inorg. Chem.* **1997**, *36*, 6450.
- 30) H. Kalish, J. E. Camp, M. Stepien, L. Latos-Grazynski, M. M. Olmsted, A. Balch *J. Am. Chem. Soc.* **2001**, *123*, 11719.
- 31) R. A. Binstead, M. J. Crossley, N. S. Hush *Inorg. Chem.* **1991**, *30*, 1259.
- 32) T. Murashima, Y. Uchihara, N. Wakamori, H. Uno, T. Ogawa, N. Ono *Tetrahedron Lett.* **1996**, *37*, 3133.
- 33) G.-Y. Gao, A. J. Colvin, Y. Chen, X. P. Zhang *Org. Lett.* **2003**, *5*, 3261.
- 34) A. Merz, A. R. Schropp, J. Lex *J. Angew. Chem. Int. Ed.* **1993**, *32*, 291.
- 35) W. Su, T. M. Copper *Chem. Mater.* **1998**, *10*, 1212.
- 36) A. Tsuda, H. Furuta, A. Osuka *J. Am. Chem. Soc.* **2001**, *123*, 10304.
- 37) T. E. O. Screen, K. B. Lawton, G. S. Wilson, N. Dolney, R. Ispasoiu, T. Goodson III, S. J. Martin, D. D. C. Bradley, H. L. Anderson *J. Mater. Chem.* **2001**, *11*, 312.
- 38) M. J. Frampton, H. Akdas, A. R. Cowley, J. E. Rogers, J. E. Slagle, P. A. Fleitz, M. Drobizhev, A. Rebane, H. L. Anderson *Org. Lett.* **2005**, *7*, *25*, 5365.
- 39) Y. Nakamura, I.- W. Hwang, N. Aranti, T. K. Ahn, D. M. Ko, A. Takagi, T. Kawai, T. Matsumo, D. Kim, A. Osuka *J. Am. Chem. Soc.* **2005**, *127*, 236.

- 40) A. Tsuda, A. Nakano, H. Furuta, H. Yamochi, A. Osuka *Angew. Chem. Int. Ed.* **2000**, *39*, 3, 558.
- 41) A. Osuka, N. Aranti *Org. Lett.* **2001**, *3*, 26, 4213.
- 42) A. Tsuda, Y. Nakamura, A. Osuka *Chem. Comm.* **2003**, 1096.
- 43) A. Tsuda, A. Osuka *Adv. Mater.* **2002**, *14*, 1, 75.
- 44) M. Kamo, A. Tsuda, Y. Nakamura, N. Aratani, K. Furukawa, T. Kato, A. Osuka *Org. Lett.* **2003**, *5*, 12, 2079.
- 45) N. Aranti, H. S. Cho, T. K. Ahn, S. Cho, D. Kim, H. Sumi, A. Osuka *J. Chem. Soc.* **2003**, *125*, 32, 9668.
- 46) J.-H. Ha, H. S. Cho, J. K. Song, D. Kim, N. Aranti, A. Osuka *Chem. Phys. Chem.* **2004**, *5*, 57.
- 47) D. Kim, A. Osuka *Acc. Chem. Res.* **2004**, *37*, 10, 735.
- 48) A. Tsuda, Y. Nakamura, A. Osuka *Chem. Comm.* **2003**, 1096
- 49) O. S. Finikova, S. E. Aleshchenkov, R. P. Brinas, A. V. Cheprakov, P. J. Carroll, S. A. Vinogradov *J. Org. Chem.* **2005**, *70*, 12, 4617.
- 50) V. V. Rozhkov, M. Khajepour, S. A. Vinogradov *Inorg. Chem.* **2003**, *42*, 4253.
- 51) J. E. Rogers, K. A. Nguyen, D. C. Hufnagle, D. G. McLean, W. Su, K. M. Gosset, A. R. Burke, S. A. Vinogradov, R. Prachter, P. A. Fleitz *J. Phys. Chem. A* **2003**, *107*, 11331.
- 52) I. B. Rietveld, E. Kim, S. A. Vinogradov *Tetrahedron* **2003**, *59*, 3821.
- 53) N. Hayashi, A. Naoe, K. Miyabayashi, M. Yamada, M. Miyake, H. Higuchi *Tetrahedron Lett.* **2004**, *45*, 8215.
- 54) N. Hayashi, A. Matsuda, E. Chikamatsu, K. Mori, H. Higuchi *Tetrahedron Lett.* **2003**, *44*, 7155.
- 55) H. Higuchi, T. Maeda, K. Miyabayashi, M. Miyake, K. Yamamoto *Tetrahedron Lett.* **2002**, *43*, 3097.
- 56) W. W. Kalisch (1997): "Synthese, Modifizierung und Strukturuntersuchung neuer Tetrapyrrolsysteme mit variabler Konformation als Modellverbindungen natürlicher Pigmente" Dissertation (Berlin).
- 57) Y. Chen, C. J. Medforth, K. M. Smith, J. Alderfer, T. J. Dougherty, R. K. Pandey *J. Org. Chem.* **2001**, *66*, 3930.
- 58) T. Wondimagegn, A. Ghosh. *J. Phys. Chem. A* **2000**, *104*, 4606.

6. Phosphorescence and Distortion of Pd(II) and Pt(II)OEPs

In order to gain a deeper understanding of the influence of the distortion of porphyrins on the triplet state dynamics e.g. the phosphorescence quantum yields and lifetimes, the Pd(II) and Pt(II)OEPs **12**, **17**, **166**, **273**, **300**, **301**, **282**, **304** and **307** were prepared as described in chapter 2.3 and phosphorescence measurements were carried out by Vinogradov and co-workers. The obtained data, was additionally compared to calculated and from X-ray investigation obtained solid state structures and both will be presented in section 6.3, while basic concepts are reported in the chapters 6.1 and 6.2.

6.1 Phosphorescence and fluorescence of porphyrins

Photoluminescence is the emission of visible light by a molecule after or during UV radiation and can be used in spectroscopy and technical applications e.g. the sensing of oxygen in blood. The emitted light can be classified as fluorescence (τ_f) or phosphorescence (τ_p) depending on the electronic excitation state from which it is emitted. The π electrons of a dye propagated to the lowest excited singlet state, 1Q (J, J^*), loose their energy a) quickly and quantum chemically allowed in form of fluorescence ($S_1 \rightarrow S_0$) or b) in form of long lived phosphorescence through the lower situated triplet state, 3T (J, J^*) and $T_1 \rightarrow S_0$, involving slow, quantum chemically forbidden spin flips, as shown in figure 6.1.1.

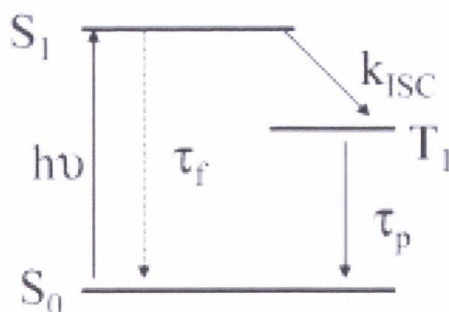


Fig. 6.1.1. Illustration of fluorescence (τ_f) and phosphorescence (τ_p) emission after excitation into S_1 and intersystem crossing (ISC) to T_1 .¹

Furthermore, phosphorescence can become the dominant emission when the singlet and triplet excited states are close to each other. In that case, the to S_1 propagated electron

loses parts of its energy due to rotation, vibrational movements and collisions e.g. so-called annihilation processes or internal conversion, and falls down by intersystem crossing (ISC) into the thermodynamically favored triplet state.

However, the by porphyrins emitted fluorescence is commonly light of shorter, more energetic wavelengths, located around 700 nm (+/- 50 nm), whereas phosphorescence is often observed in the IR area, at longer, less energetic wavelengths (810 +/- 20 nm). As vibrational relaxation competes with both emissions, low phosphorescence and fluorescence quantum yields and lifetimes are observed for highly distorted porphyrins which are loose and floppy due to the high steric strain caused by the substituents.² Phosphorescence is furthermore long lived compared to fluorescence due to prolonged lifetime of the triplet state (τ) and higher phosphorescence lifetimes are encountered. The phosphorescence can last for hours and the respective dyes are known for their "glowing in the dark" capacity and can be used as energy storages. However, the phosphorescence of porphyrins lasts usually only a few micro seconds, whereas the fluorescence is emitted in nano seconds. The phosphorescence can be also prolonged in highly viscous media and at low temperatures, which disfavor annihilation processes. For sensor applications phosphorescence quantum yields and lifetime of $\Phi=0.02-0.5$ and $\tau < 300 \mu\text{s}$ are required in order to ensure exact and repeatable measurements (compare to table 6.4.1). Furthermore, many dyes emit both, phosphorescence and fluorescence and also so-called delayed fluorescence can be found. Delayed fluorescence is the result of the additional recombination of two triplet states to an energetically higher singlet state and causes emission of light typical for fluorescence, but long lived as phosphorescence.^{3,4} Usually free base porphyrins exhibit relative strong fluorescence whereas for palladium and platinum porphyrins the possibility of intersystem crossing into the triplet state T_1 is high due to the influence of the heavy metal atom and results in phosphorescence.^{5,6,7} In figure 6.1.1 the absorption and emission spectrum (inlay) of Pd(II)OEP **2** is shown. The excitation was performed at the wavelength of the QIII band at 546 nm and the recorded phosphorescence appears at longer wavelengths e.g. at 665 nm due to the vibrational loss of energy. A phosphorescence quantum yield of $\Phi=0.087$ and a lifetime (τ) of 459 μs were measured.

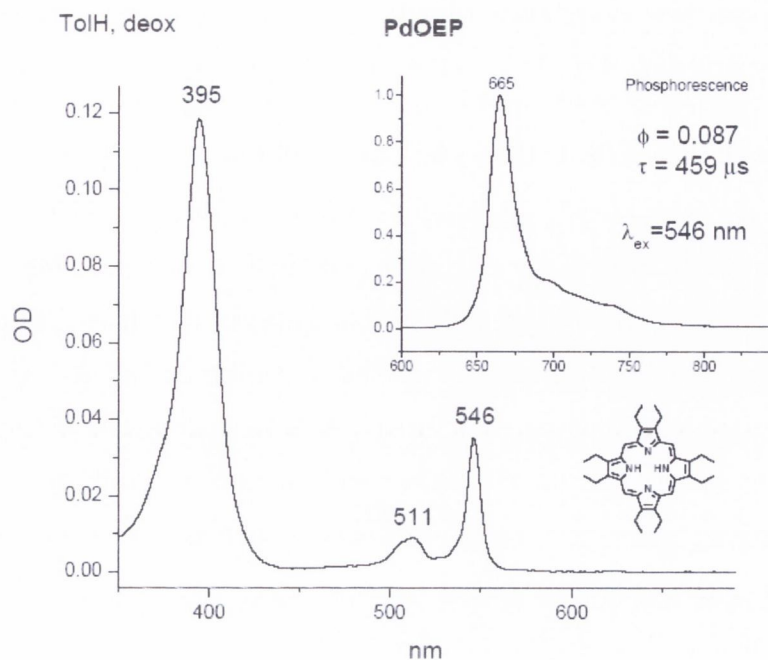


Fig. 6.1.2. Absorption and emission spectrum of Pd(II)OEP **2** recorded by Vinogradov and co-workers with excitation at 546 nm and measured phosphorescence lifetime (τ) and quantum yield (Φ) in deoxygenated toluene.

6.2 The distortion of porphyrins

Porphyrins, that occur in nature are often surrounded by a protein matrix as in heme proteins e.g. hemoglobin or myoglobin. As a consequence, they are deformed due to the steric strain induced by the protein matrix in accordance with their biological functioning.⁸ In laboratory convenience, the distortion can be induced by demanding peripheral substitution, core protonation, metal insertion, axial ligation and by the solvent. *Meso* tetraalkyl porphyrins, nona-, deca-, undeca- and dodecasubstituted porphyrins as well as nickel (II) porphyrins are known to be distorted.⁹

6.2.1 Indicators of distortion

Indicators of the distortion are red shifted UV/vis absorption bands, as was demonstrated for the obtained OEPs in chapter 5, and downfield shifted NH signals in the respective ^1H NMR spectra as shown in chapter 3 and as reported in literature for series of porphyrins.¹⁰⁻¹⁶ A higher signal shift can be roughly related to a higher degree of distortion, whereas exceptions are possible. However, a detailed analysis of the

distortion can be only obtained from model calculations using symmetry criteria or from the crystal structures directly as will be described in the following section.

6.2.2 Calculation of distortions and representation in the NSD model

The interest in distorted dodecasubstituted porphyrins was high in the 1990th when research groups started to investigate the possibilities of mimicking natural systems. C. J. Medforth, K. M. Smith and J. A. Shelnuttt believed that dodecaarylporphyrins (DAPs) show a particular wide range of nonplanar conformations due to a high molecular flexibility and they synthesized a variety of dodecasubstituted porphyrins derived from TPP *via* bromination of the β -positions and subsequent Suzuki-type coupling reactions as reported in chapter 1.5.¹⁷ Dynamic processes such as NH tautomerisation, macrocycle inversion and *meso*- and β -aryl rotation were investigated and correlated to the conformation of the porphyrin. It was found that the rotational barriers of phenyl substituents were smaller when the phenyl substituents were sticking out of the porphyrin plane. Saddle shaped DAPs furthermore moved the respective β substituents out of plane, whereas ruffled conformations pushed the *meso* substituents out of plane.¹⁷ Afterwards, also quantum chemical calculations were used in order to investigate porphyrin distortions and in particular, DFT calculations (density functional theory) furnished a fairly understanding of the factors that controlled the ruffling of porphyrins.¹⁸⁻²⁰ With the knowledge of atom binding, radii and atom interactions, conformers of minimal energy were obtained by molecular mechanistic (MM) calculations, simulating the 3D structure of unknown porphyrins. In 1998, Medforth/Smith/Shelnutt synthesized the in figure 6.2.2.1 shown *tert*-butyl nickel (II) porphyrins and calculated and optimized the respective minimal energy conformers in comparison to the obtained solid state structures of 5-*tert*-butyl Ni (II) and 5,15-di-*tert*-butyl Ni (II) porphyrin **361** and **362**.^{21,22} Furthermore for a better description of the 3D shape of the porphyrins, they introduced the NSD (normal-coordinate structural decomposition) model which was developed in Shelnuttt's group. In the NSD representation from the crystal or from calculations obtained geometric data is translated in a number of defined distortion modes, which built in their sum the observed 3D shape. The crystallographic assignments were kept and saddled, ruffled, domed, wave and propeller distortions were used to describe the observed out-of-plane displacements

(OOPs, figure 6.2.2.2), whereas the used in-plane-displacements are shown in fig. 6.2.2.3.

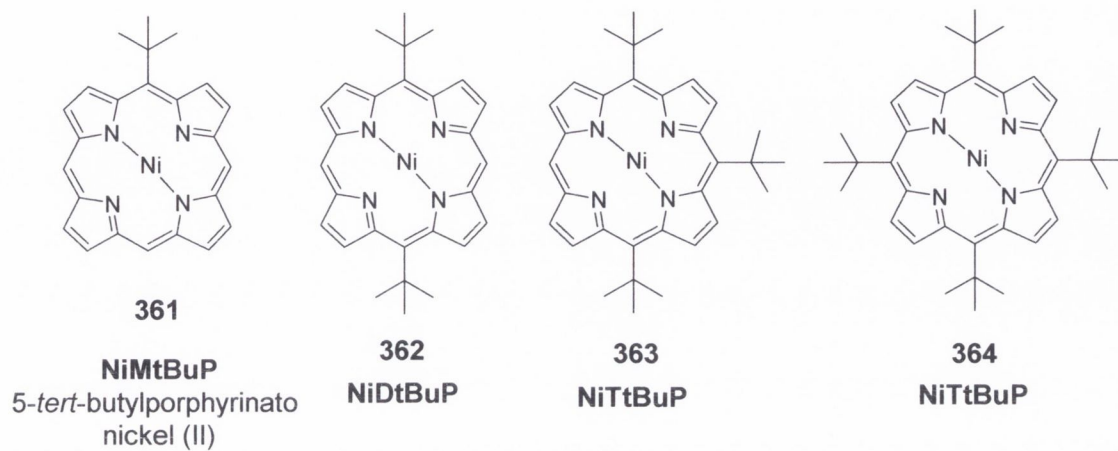


Fig. 6.2.2.1. Investigated porphyrins 416-419 by Smith/Shelnut/Medforth.^{21,22}

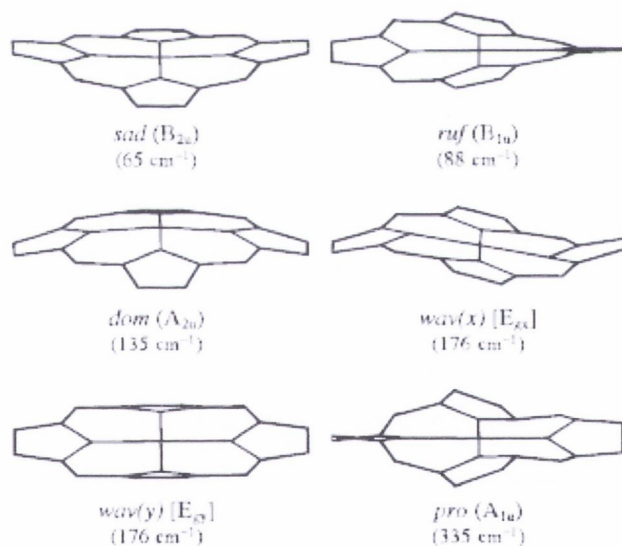


Fig. 6.2.2.2. Out-of-plane distortions used by the NSD model for the description of distinct porphyrin distortions.²¹

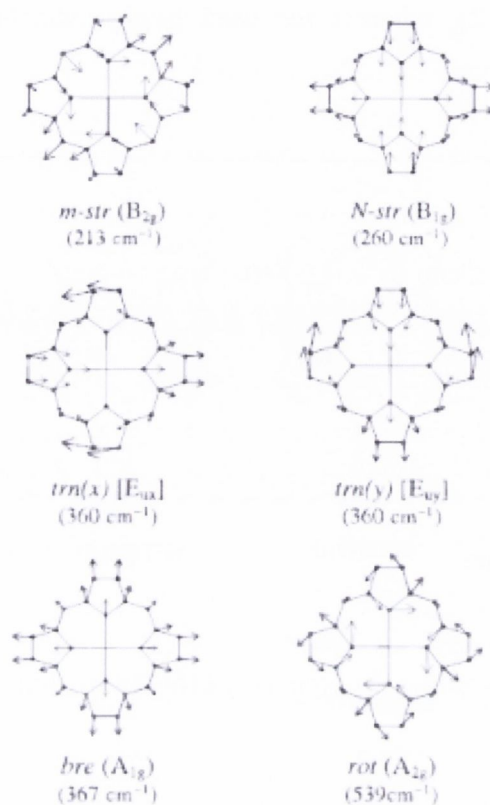


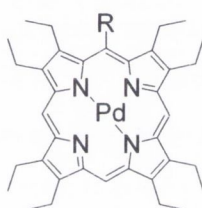
Fig. 6.2.2.3. Illustrations of the in-plane eigenvectors used for the simulation of the porphyrin macrocycle distortions.²¹

The model is today updated as described on the respective internet site and commonly used for the representation of the 3D shape of porphyrins.²³

6.3 Phosphorescence and distortion modes of Pd(II) and Pt(II)OEPs

The phosphorescence of porphyrins is expected to depend on the macrocycle distortion and its flexibility.⁹ Different distortion modes were defined in the NSD model and could have an influence on the phosphorescence quantum yields and lifetimes. An elucidation is of interest as a better knowledge could redefine structural needs which are important for future synthesis and the fine-tuning of photophysical properties. Therefore Pd(II) and Pt(II)OEPs were prepared and phosphorescence quantum yields and lifetimes were measured and compared to the respective calculated 3D shapes and obtained solid state structures (compare to chapter 4). The *ab initio* calculations were performed using the free base models as the calculation of the respective palladium (II) complexes was too demanding in a first attempt. In order to study the influence of the substituent type and

bulk the respective *meso* 5-methyl, 5-*n*-butyl, 5-phenyl, 5-(3-trifluoromethylphenyl), 5-(4-*n*-pentylphenyl), 5-(1-naphthyl), 5-(2-naphthyl), 5-acenaphthyl and 5-(9-phenanthrenyl) Pd(II)OEPs **166**, **17**, **273**, **300**, **301**, **282**, **302**, **303** and **12** as well as the respective platinum (II) complexes, 5-phenyl Pt(II)OEP **307**, 5-(1-naphthyl) Pt(II)OEP **309** and 5-(9-phenanthrenyl) Pt(II)OEP **310**, were prepared as a first generation as reported in chapter 2.3. Phosphorescence lifetimes and quantum yields were measured by Prof. Vinogradov and co-workers and were also determined for the in figure 2.3.1.1 shown *meso* trisubstituted Pd(II)OEP **304** and are displayed in table 6.3.1.



		Phosphorescence			
R	M	Emission λ_{max} , (λ_{ex}), nm	Lifetime τ_0 , μs	Quantum Yield Φ , %	
2	-	Pd	665 (546)	459	15.4
166	methyl	Pd	686 (553)	276	4.7
17	<i>n</i> -butyl	Pd	711 (554)	217	2.04
12	9-phenanthrenyl	Pd	671 (551)	52	1.1
282	1-naphthyl	Pd	672 (551)	-	0.62
273	phenyl	Pd	669 (550)	-	0.09
300	3-trifluoromethylphenyl	Pd	665 (550)	-	0.04
301	4- <i>n</i> -pentylphenyl	Pd	661 (550)	-	0.01
304	n. a.	Pd	651 (539)	-	0.00
307	phenyl	Pt	651 (539)	-	0.08

Table 6.3.1. Phosphorescence of *meso* monosubstituted Pd(II) and Pt(II)OEPs and the trisubstituted Pd(II)OEP **304**. The measurements were performed in toluene which was deoxygenated by prolonged bubbling of argon, until no changes in phosphorescence lifetime were detected.

As it can be seen in table 6.3.1, high phosphorescence lifetimes and high quantum yields were obtained for the alkyl substituted Pd(II)OEP **17** and **166**. On the other hand, the phosphorescence was for those OEPs reduced relative to Pd(II)OEP **2** and could be related to the induced out-of-plane distortion, which was reported in chapter 4. It was assumed that the distortion would result in an increased conformational flexibility of the porphyrins and would therefore give rise to annihilation process and lower phosphorescence quantum yields and lifetimes compared to Pd(II)OEP **2**.^{1,2} The conformational flexibility induced by the methyl substituent, was furthermore expected to be minor relative to the distortion induced by the *n*-butyl substituent, which would explain the observed higher phosphorescence quantum yields and lifetimes for 5-methyl Pd(II)OEP **166** relative to the Pd(II)OEP **17**. The introduction of phenyl substituents had furthermore the strongest impact on the observed phosphorescence e.g. the trisubstituted Pd(II)OEP **304** displayed no phosphorescence, while the *meso* monosubstituted Pd(II)OEPs **273**, **300** and **301** showed compared to the OEP **304** slightly enhanced phosphorescence quantum yields, whereas the phosphorescence lifetimes remained short e.g. couldn't be measured. In literature, it was furthermore described that the rotation of the phenyl substituent could lead to additional internal energy conversion, which would result in the loss of the emission properties by the porphyrin as observed for the OEPs **273**, **300**, **301** and **304** despite of the additional phenanthrenyl substituent in the OEP **304**.¹⁷ On the other hand, as will be described in section 6.4, phenyl substituents had no decreasing effect on the phosphorescence quantum yields and lifetimes of reported TBPs and TNPs.^{1,2,24-27} Furthermore, also the platinum (II) insertion was observed to be ineffective in combination with phenyl substitution. For larger aromatic substituents on the other hand e.g. in the case of the OEPs **12** and **282**, higher phosphorescence quantum yields were observed, while the phosphorescence lifetime of 5-(1-naphthyl) OEP **282** remained still very short. For 5-(9-phenanthrenyl) OEP **12** on the other hand a phosphorescence lifetime of 52 μ s and a quantum yield of $\Phi = 1.1$ was determined and the OEP **12** was suggested for single molecule experiments in order to investigate its qualities as an oxygen sensor.^{1,2} However, it was described in chapter 3, that naphthyl and phenanthrenyl substituents were rotational hindered, remaining in orthogonal orientations relative to the porphyrin plane (compare also to chapter 4 for the respective solid state structures). The hindered rotation could have furthermore circumvented annihilation processes for 5-(9-phenanthrenyl) Pd(II) OEPs **12**, which resulted in the

described increased phosphorescence quantum yield and lifetime. The outstanding position of 5-(9-phenanthrenyl) Pd(II)OEP **12** is furthermore illustrated in figure 6.3.1. The OEP **12** displayed a, as wished, diminished phosphorescence lifetime in combination with a high enough quantum yield relative to Pd(II)OEP **2** and the alkyl Pd(II)OEPs **17** and **166**.

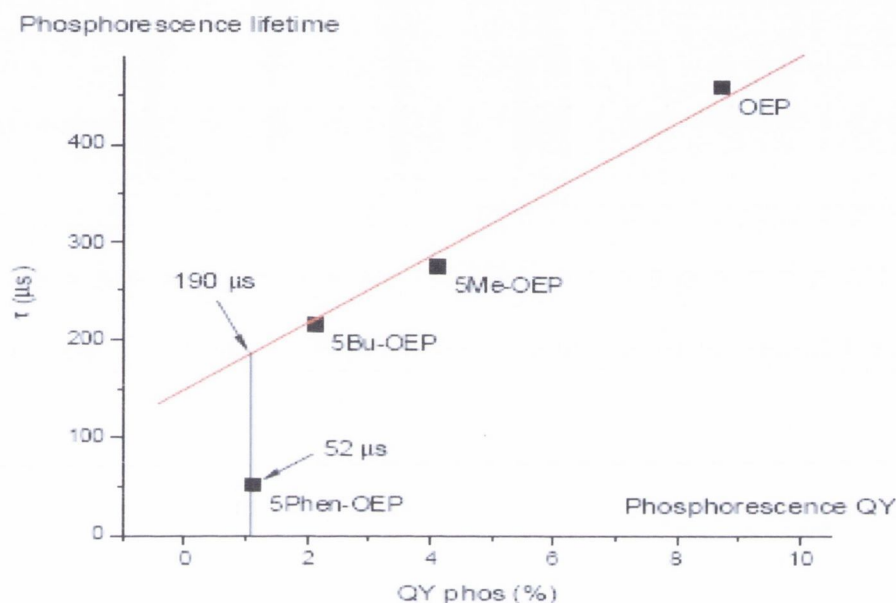


Fig. 6.3.1. Correlation of phosphorescence lifetime and phosphorescence quantum yields (QY) of the in table 6.3.1 shown Pd(II)OEPs; the graphic was obtained from Vinogradov *et al.*

In order to elucidate the relationship between particular distortion modes and aryl and alkyl substitution, Vinogradov and co-worker calculated the respective distortion modes of the investigated Pd(II)OEPs using free base OEPs as model compounds. The obtained data is shown in figure 6.3.2. As it can be seen, the major distortion mode of 5-(9-phenanthrenyl) Pd(II)OEP **12** is a saddling deformation, while also minor amounts of ruffling were calculated. The ruffling conformation was furthermore confirmed by the additionally obtained solid state structure as described in chapter 4. Else wise, 5-phenyl OEP **273** displayed the for aryl substituents common saddled conformation, while the alkyl substituted OEPs **17** and **166** were mainly ruffled.

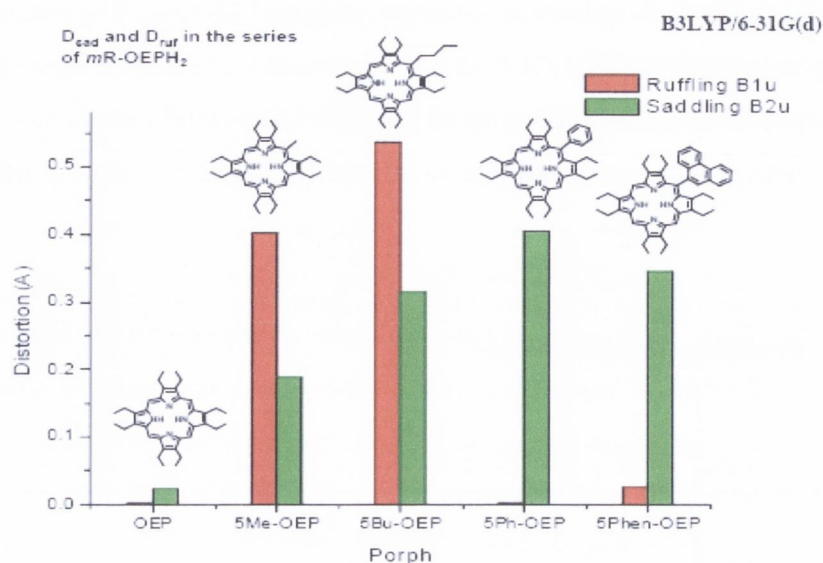


Fig. 6.3.2. Ruffling and saddling distortion modes calculated by Vinogradov *et al.* for the prepared Pd(II)OEPs.

However, the in 5-(9-phenanthrenyl) Pd(II)OEP **12** the induced amount of ruffling might have had an impact on the observed phosphorescence lifetime and quantum yield in similarity to the alkyl substituted Pd(II)OEPs. The saddled conformation on the other hand might correlate to the observed quenching in phenyl substituted OEPs, while it was also shown in chapter 4 for the solid state structures, that 5-phenyl OEP **272** as well as the naphthyl substituted OEP **283** were similarly flat as Pd(II)OEP **2** ($\Delta 24 = 0.05 \text{ \AA}$), while a minor degree of saddling distortion was confirmed by the respective NSD analyses. The largest out-of-plane distortion was found for 5-*n*-butyl Pd(II) OEP **17** ($D_{\text{oop}}=0.64 \text{ \AA}$). A detailed analysis is also shown for 5-*n*-butyl Pd(II)OEP **17** and 5-(9-phenanthrenyl) Pd(II)OEP **12** in figure 6.3.3 and was obtained by Vinogradov *et al.* from the respective *ab initio* calculations. As it can be seen, different amounts of OOPs were calculated for propeller and doomed conformations, while the orientation of the wave conformation was observed to be opposite. The in-plane distortions were similar in their amounts, while a different orientation was found. The amount of saddling distortion is furthermore nearly equal for both Pd(II)OEPs, whereas the amount of ruffling is much higher for the alkyl substituted OEP **17**.

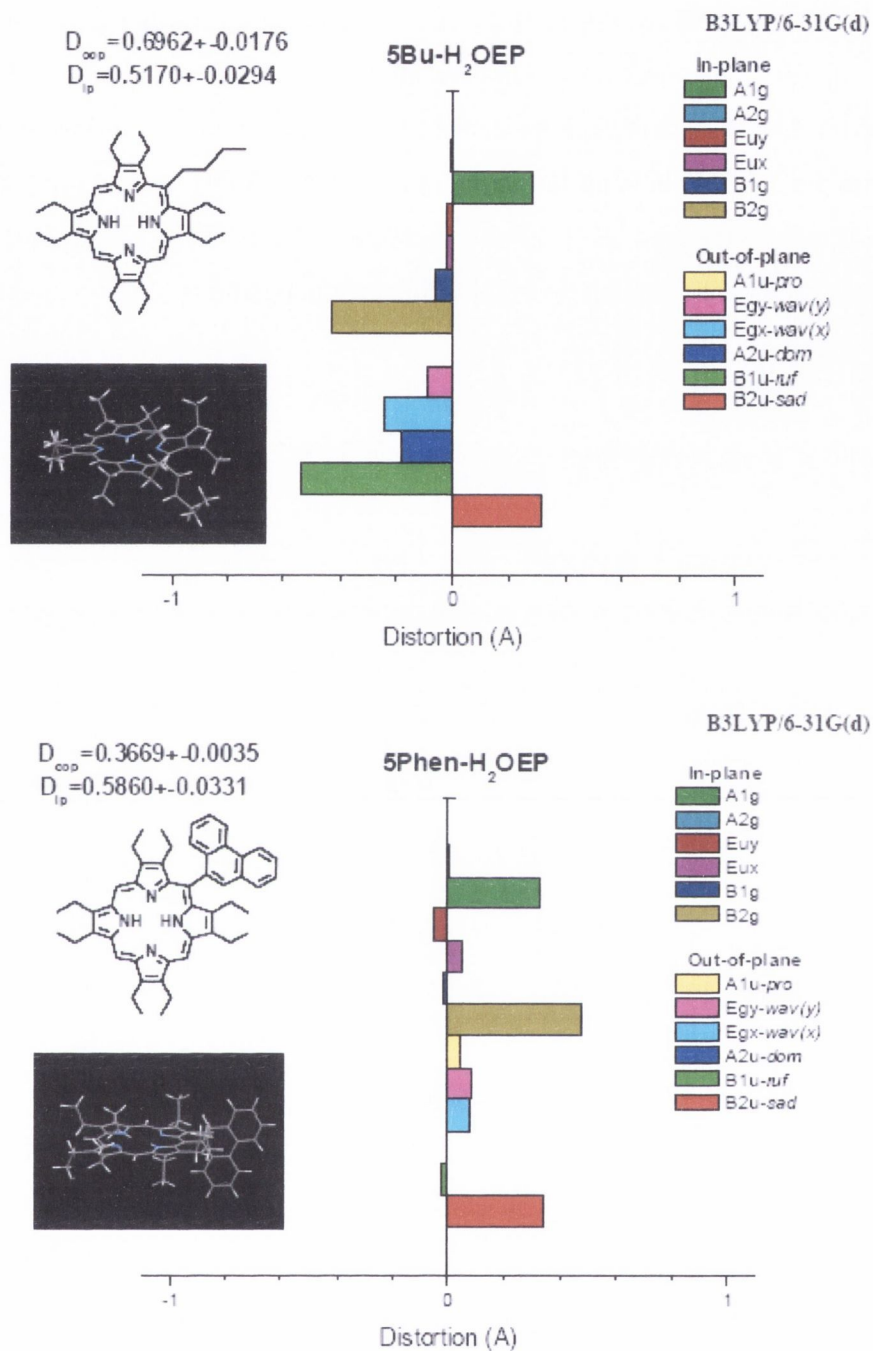


Fig. 6.3.3. Distortion modes in Shelnutz's NSD model, calculated by Vinogradov and co-workers for the prepared Pd(II)OEPs **12** and **17**. Shown are the free base models as the calculation of the metal complexes were too complex, Phen = 9-phenanthrenyl.

However, alkyl and aryl-mixed Pd(II)OEPs, seem to be desirable targets for future synthesis and investigation, as those might be situated between 5-*n*-butyl Pd(II)OEP **17**

and 5-(9-phenanthrenyl) Pd(II)OEP **12**. In figure 6.4.3 furthermore, are shown the crystal structure and the NSD representation of the by Vinogradov and co-workers obtained TNP **365**. The phosphorescence lifetime and quantum yield were not displayed, but from the NSD model can be seen that the TNP **365** displayed a mixture of saddling and ruffling distortions as 5-(9-phenanthrenyl) Pd(II)OEP **12**. It was furthermore emphasized in the article that favorable triplet state dynamics were obtained.²⁴⁻²⁷

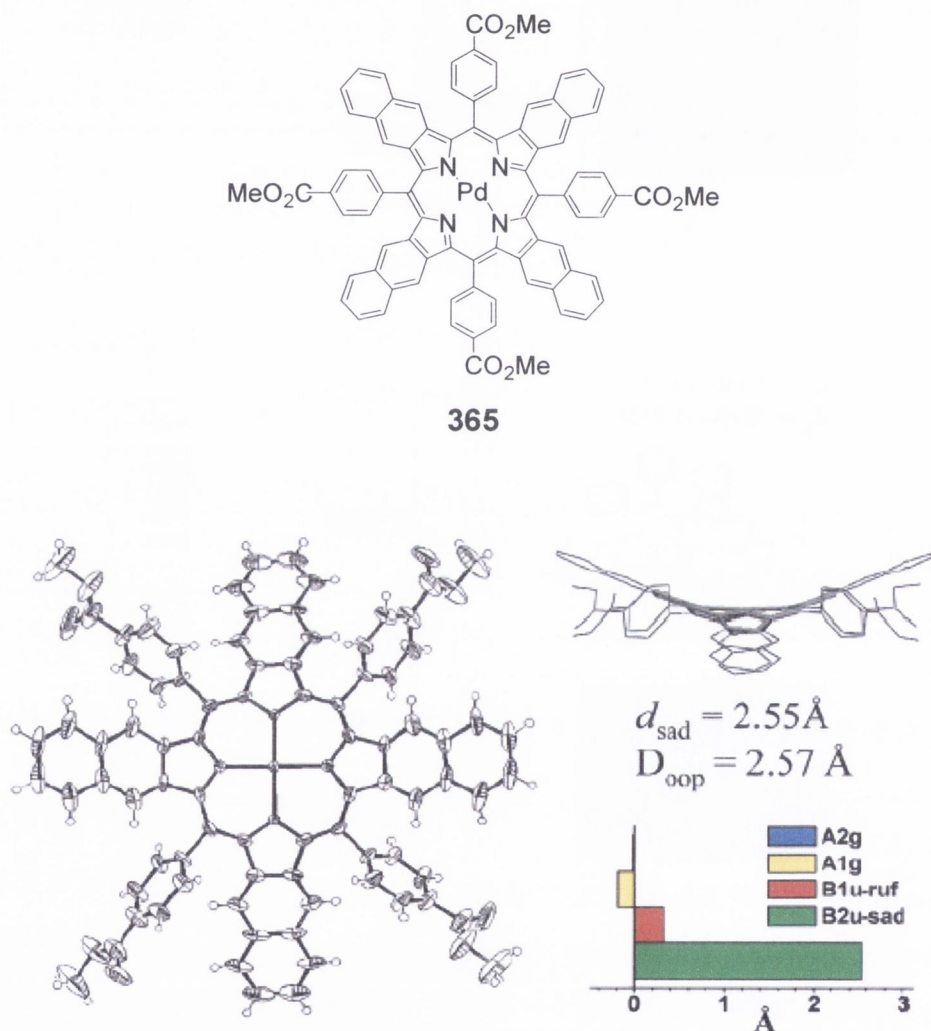


Fig. 6.3.4. Structure, crystal structure and NSD analysis of the tetranaphthoporphyrin **365**, obtained by Vinogradov *et al.*²⁴

6.4 Phosphorescent porphyrins described in literature

First investigations of porphyrins for sensor applications were reported in the 1980th by Chang *et al.* for anthracenyl and bisphenylenyl linked porphyrin dimers.^{28,29,30} After

2000, the synthesis of novel, more rigid cofacial bisporphyrins with variations in the C-C *meso* distances (3.8–6.3 Å) and interplanar angles was investigated by Nocera,³¹⁻³⁵ Guillard and Faure *et al.*³⁶⁻³⁸ The porphyrin sandwich structures shown in figure 6.4.1 and in figure 6.4.4 were prepared and the cofacial etioporphyrin Pd₂DPS for example was obtained in a laborious fourteen step synthesis with an overall yield of 0.3%.³⁰⁻⁴³ Furthermore, S. Vinogradov and co-workers prepared novel TBPs and TNPs (compare to the chapters 1.4.4) for sensor applications with high phosphorescence quantum yields and lifetimes.^{1,2,24-27} However, also Pt(II)OEP **3** was investigated in regard to its qualities as an oxygen sensor,⁴⁴ while Pd(II)TPP is used for the biological probing of oxygen.⁴⁵

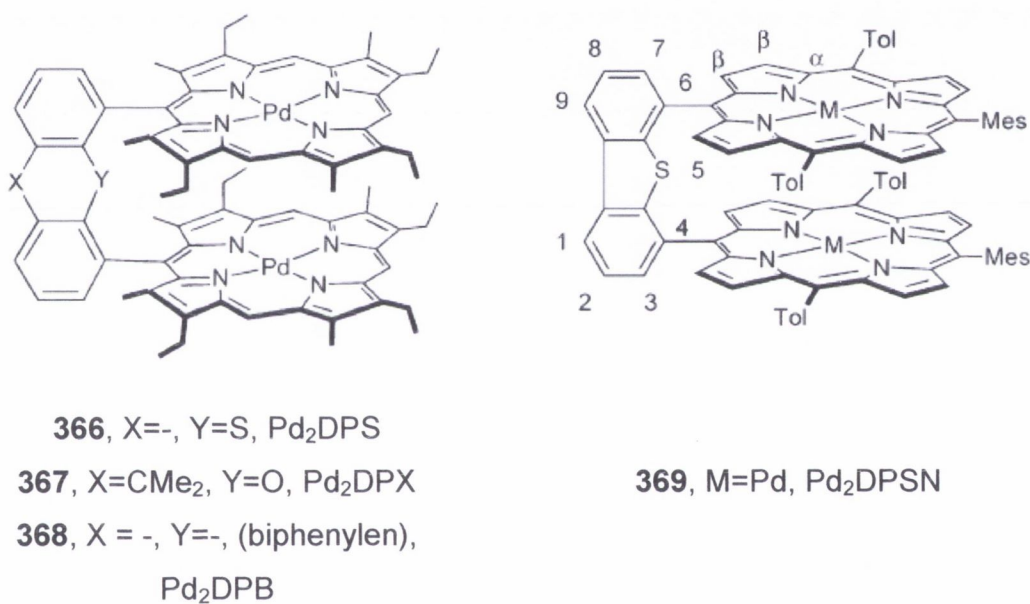


Fig. 6.4.1. Cofacial sandwich porphyrins described and investigated by Nocera, Faure and Guillard *et al.*³⁶

Pd(II) *meso* porphyrin (PdmP) **372** and 5,10,15,20-tetra-(4-carboxyphenyl)porphyrinato palladium (II) (PdTCPP) **374** were also applied due to their appropriate phosphorescence qualities (absorption near the IR window, >600 nm, as tissue absorbs light of shorter wavelengths) in the treatment of cancer by photodynamic therapy (PDT).⁴⁵ The in table 6.4.1 summarized phosphorescence quantum yields and lifetimes were furthermore collected from the respective articles for comparison purpose. The phosphorescence

measurements were performed by the research groups in different solvents depending on the solubility of the porphyrins and were carried out at ambient temperature. As it can be seen in table 6.4.1, the phosphorescence quantum yields decrease in the order Pt(II)OEP **3** > Pd(II)OEP **2** > Pd(II)TBP **65a** > Pd(II)Etio **376** > Pd(II)TPP **64b** (“Pt(II)OEP **3**/Pd(II)TPP **64b** window”). The influence of platinum (II) in the porphyrin core is favourable (enhances the quantum yields), while also substitution with carboxyl and ester groups seems to increase the quantum yields (compare Pd(II)TPP to Pd(II)TCPP and Pd(II)TBP **65a** to PtTBP x CO₂Bu **371**, while also the PdTPTNP **86** is displayed above Pd(II)TBP **65a**). Furthermore phenyl substitution in the *meso* position of OEP and etioporphyrin decreased, as also described in chapter 6.3, the phosphorescence lifetimes and quantum yields.

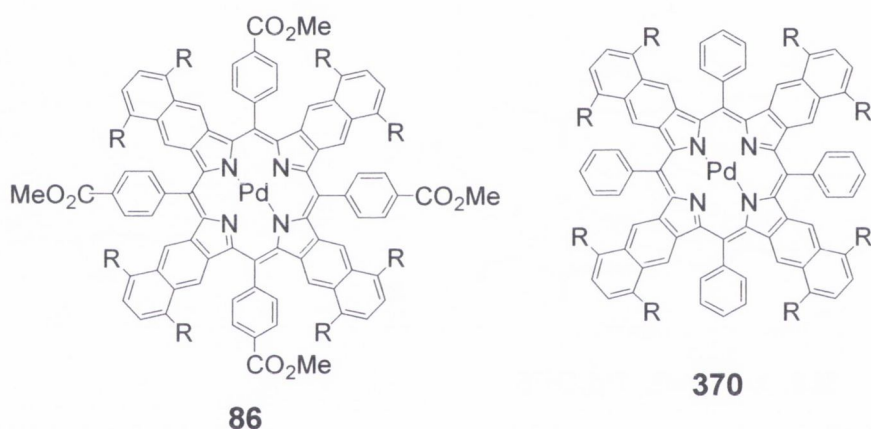


Fig.6.4.2. In table 6.4.1 displayed PdTPTNPs **86**, **370**, R=OMe.^{24,25}

On the other hand, for β -aryl substituted TBPs and TNPs the phosphorescence quantum yields were not affected by the *meso* phenyl substitution.

However, the phosphorescence quantum yield of 5-(9-phenanthrenyl) Pd(II)OEP **12** is low compared to the other Pd(II) and Pt(II) porphyrins and is situated among the cofacial bisporphyrins (red in table 6.4.1), for which, with exception of Pd₂DPSN **329**, lower quantum yields were measured relative to Pd(II)TPP **64b**.

		Phosphorescence			
Name	Emission λ_{\max} , (λ_{ex}), nm	Solvent	Lifetime T_0 , μs	Quantum Yield Φ	
371	PtTBP x CO ₂ Bu ²⁵	770	Py	50	0.51
3	PtOEP ⁴⁴	-	-	≈100	<0.5
371a	PdTBP x CO ₂ Bu ²⁵	-	DMF	400	0.23
372	PdmpP ⁴⁵	-	DMF	670	0.19
2	Pd(II)OEP	665	Toluene	459	0.15
360a	PdTPTBP ⁴⁵	785	DMF	250	0.08
86	PdTPTNP ²⁴	-	-	63	0.079
65a	PdTBP ⁴⁵	767	DMF	260	0.079
374	PdTCPP ⁴⁵	-	DMF	220	0.068
375	PdTPTNP ²⁶	-	DMF	65	0.065
376	PdEtio ⁴³	669	CH ₂ Cl ₂	321	0.064
377	PdTNP x R ²⁵	923	Py	75	0.04
329	Pd ₂ DPSN ³⁶	699	MCH	506	0.037
370	PdTPTNP ²⁵	-	-	38	0.025
64b	PdTTPP ³⁶	-	MCH	258	0.02
367	Pd ₂ DPX ⁴³	678	CH ₂ Cl ₂	102	0.029
12	5-phenPd(II)OEP	671	Toluene	52	0.01
378	Pd ₂ DPD ⁴³	673	CH ₂ Cl ₂	18.2	0.0046
379	Pd(PhEtio) ⁴³	673	CH ₂ Cl ₂	1.14	0.00072

Table 6.4.1. Reported phosphorescence quantum yields and lifetimes of porphyrins;

MCH=methylcyclohexane, PdmpP-Pd *meso* porphyrin,⁴⁵ PdTCPP-Pd (*meso*-tetracarboxyphenyl) porphyrin,⁴⁵ phen=(9-phenanthrenyl).

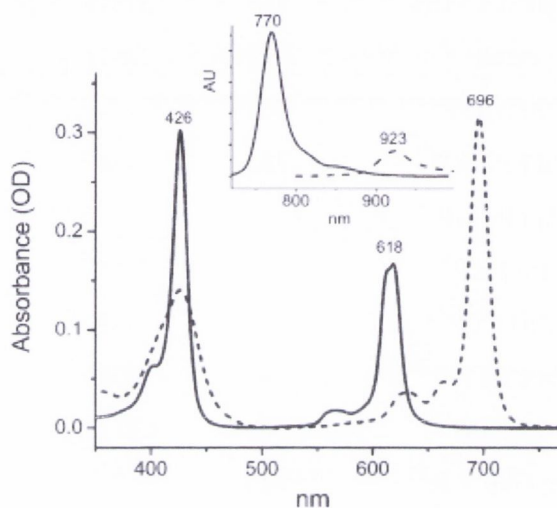
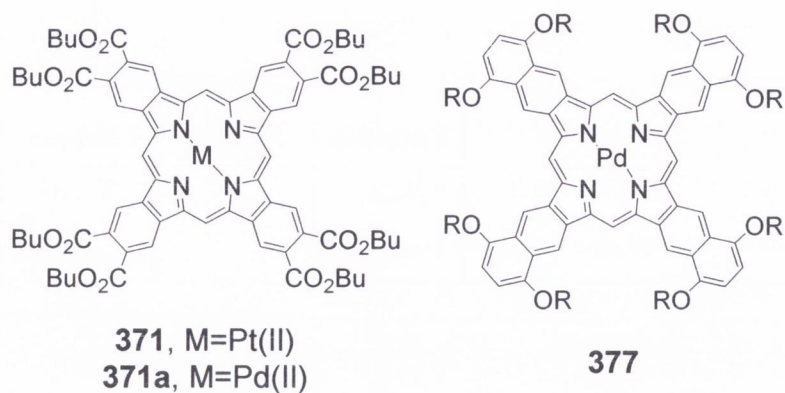


Fig. 6.4.3. Structure of the TNP and TBPs **371** and **377** together with absorption and emission spectra (**371**: plane line, **377**: dashed line); R=(CH₂)₃CO₂Et.²⁵

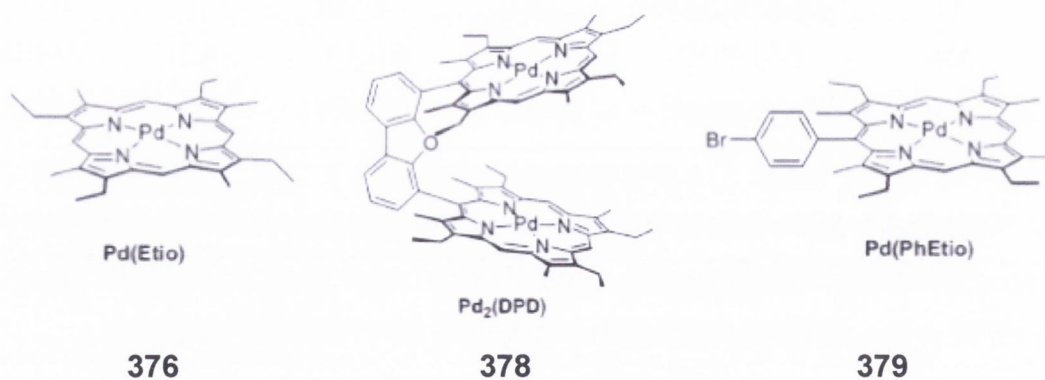


Fig. 6.4.4. By Nocera *et al.* synthesized and investigated pacman etioporphyrin **378** and the etioporphyrin monomers **376** and **379**. The graphic was taken from the respective article in order to keep the 3D geometries.⁴³

The sandwich porphyrins are furthermore described in literature as less flexible than *meso* monosubstituted porphyrins and the lower quantum yields observed for 5-(9-phenanthrenyl) Pd(II)OEP **12** and Pd(II)(PhEtio) **379** can be related to an increased rate of annihilation processes relative to Pd(II)OEP.³¹⁻³⁸ The flexibility of the sandwich porphyrins increased furthermore with a wider angle of the sandwich cavity, while the UV/vis intensities were also higher than for the respective monomers due to the fact that two subunits were emitting.

REFERENCES

- 1) E. Mei, S. Vinogradov, R. M. Hochstrasser *J. Am. Chem. Soc.* **2003**, *125*, 13198.
- 2) J. E. Rogers, K. A. Nguyen, D. C. Hufnagle, D. G. McLean, W. Su, K. M. Gossett, A. R. Burke, S. A. Vinogradov, R. Prachter, P. A. Fleitz *J. Phys. Chem. A* **2003**, *107*, *51*, 11331.
- 3) D. A. McQuarrie, J. D. Simon (1997): "Physical Chemistry, a molecular approach." University Science Books: Sausalito.
- 4) K. Nassau (2001): "The physics and chemistry of colour, the fifteen causes of colour." Wiley: Weinheim.
- 5) H. N. Fonda, J. V. Gilbert, R. A. Cormier, J. R. Sprague, K. Kamioka, J. S. Connolly *J. Phys. Chem.* **1993**, *97*, 7025.
- 6) A. Rosa, G. Ricciardi, J. E. Baerends, A. Romeo, L. M. Scolaro *J. Phys. Chem. A* **2003**, *107*, 11468.
- 7) R. E. Haddad, S. Gazeau, J. Pecault, J. C. Marhon, C. J. Medforth, J. A. Shelnut *J. Am. Chem. Soc.* **2003**, *125*, 1253.
- 8) J. A. Shelnut, X.-Z. Song, J.-G. Ma, S.-L. Jia, W. Jentzen, C. J. Medforth *Chem. Soc. Reviews* **1998**, *27*, 31.
- 9) M. O. Senge. In *The Porphyrin Handbook*; K. M. Kadish, K.M., Smith, R. Guilard (Eds.); Academic Press: San Diego, 2000; Vol. 1, pp 239-347.
- 10) J. Takeda, M. Sato *Chemistry Lett.* **1994**, 2233.
- 11) C. J. Medforth, K. M. Smith *Tetrahedron Lett.* **1990**, *31*, 5583.
- 12) J. Takeda, T. Ohja, M. Sato *Chem. Phys. Lett.* **1991**, *183*, 384.
- 13) J. Takeda, M. Sato *Chem. Pharm. Bull.* **1994**, *42*, 1005.
- 14) C. J. Medforth, M. O. Senge, K. M. Smith, L. D. Sparks, J. A. Shelnut *J. Am. Chem. Soc.* **1992**, *114*, 9859.
- 15) K. M. Barkigia, M. W. Renner, L. R. Furenlid, C. J. Medforth, K. M. Smith, J. Faer *J. Am. Chem. Soc.* **1993**, *115*, 3627.
- 16) J. Takeda, T. Ohja, M. Sato *Inorg. Chem.* **1992**, *31*, 2887.
- 17) C. M. Muzzi, C. J. Medforth, L. Voss, M. Cancilla, C. Lebrilla, J.-G. Ma, J. A. Shelnut, K. M. Smith *Tetrahedron Lett.* **1999**, *40*, 6159.
- 18) A. Ghosh *Acc. Chem. Res.* **1998**, *31*, 189.

- 19) A. Ghosh. In *The Porphyrin Handbook*; Kadish, K. M., Smith, K. M., Guillard, R., Eds.; Academic: New York, 2000; Vol. 7, pp 1-38.
- 20) T. Vangberg, A. Ghosh, *A. J. Am. Chem. Soc.* **1999**, *121*, 12154.
- 21) X. Z. Song, W. Jentzen, L. Jaquinod, R. G. Khoury, C. J. Medforth, S.-L. Jia, J.-G. Ma, K. M. Smith, J. A. Shelnut *Inorg. Chem.* **1998**, *37*, 2117,
- 22) W. Jentzen, X.-Z. Song, J. A. Shelnut *J. Phys. Chem. B* **1997**, *101*, 1684.
- 23) <http://jasheln.unm.edu/>
- 24) O. S. Finikova, A. V. Cheprakov, P. J. Carroll, S. A. Vinogradov *J. Org. Chem.* **2003**, *68*, *19*, 7517.
- 25) O. S. Finikova, A. V. Cheprakov, S. A. Vinogradov *J. Org. Chem.* **2005**, *70*, 9562.
- 26) V. V. Rozhkov, M. Khajehpour, A. A. Vinogradov *Inorg. Chem.* **2003**, *42*, 4253.
- 27) O. Finikova, A. Galkin, V. Rozhkov, M. Cordero, C. Hagerhall, S. Vinogradov *J. Am. Chem. Soc.* **2003**, *125*, 4882.
- 28) C. K. Chang, I. Abdalmuhdi *J. Org. Chem.* **1983**, *48*, 5388.
- 29) C. K. Chang, I. Abdalmuhdi *Angew. Chem. Int. Ed.* **1984**, *23*, 164.
- 30) S. S. Eaton, G. R. Eaton, C. K. Chang *J. Am. Chem. Soc.* **1985**, *107*, 3177.
- 31) C. J. Chang, D. G. Nocera *J. Am. Chem. Soc.* **2000**, *122*, 410.
- 32) C. J. Chang, E. A. Baker, B. J. Pistorio Y. Deng, Z.-H. Loh, S. E. Miller, S. D. Carpenter, D. G. Nocera *Inorg. Chem.* **2002**, *41*, 3102.
- 33) B. J. Pistorio, C. J. Chang, D. G. Nocera *J. Am. Chem. Soc.* **2002**, *124*, 7884.
- 34) C. J. Chang, Y. Deng, A. F. Heyduk, C. K. Chang, D. G. Nocera *Inorg. Chem.* **2000**, *39*, 959.
- 35) C. J. Chang, C.-Y. Yeh, D. G. Nocera *J. Org. Chem.* **2002**, *67*, 403.
- 36) S. Faure, C. Stern, R. Guillard, P. D. Harvey *Inorg. Chem.* **2005**, *44*, 9232.
- 37) S. Faure, C. Stern, E. Espinosa, J. Douville, R. Guillard, P. D. Harvey *Chem. Eur. J.* **2005**, *11*, 3469.
- 38) K. M. Kadish, J. Shao, Z. Ou, L. Fremont, R. Zhan, F. Burdet, J.-M. Barbe, C. P. Gros, R. Guillard *Inorg. Chem.* **2005**, *44*, 6744.
- 39) C. J. Chang, Y. Deng, C. Shi, C. K. Chang, F. C. Anson, D. G. Nocera *Inorg. Chem. Commun.* **2000**, 1355.
- 40) C. J. Chang, Y. Deng, G.-H. Lee, S. M. Peng, C.-Y. Yeh, D. G. Nocera *Inorg. Chem.* **2002**, *41*, 3008.

- 41) F. Bolze, C. P. Gros, M. Drouin, E. Espinosa, P. D. Harvey, R. Guilard *J. Organometal. Chem.* **2002**, *89*, 643.
- 42) S. Faure, C. Stern, R. Guilard, P. D. Harvey *J. Am. Chem. Soc.* **2004**, *126*, 1253.
- 43) Z.-H. Loh, S. E. Miller, C. J. Chang, S. D. Carpenter, D. G. Nocera *J. Phys. Chem. A* **2002**, *106*, 11700.
- 44) Y. Amao, K. Asai, I. Okura H. Shinohara, H. Nishide *Analyst* **2000**, *125*, 1911.
- 45) S. A. Vinogradov, D. F. Wilson *J. Chem. Soc., Perkin Trans. 2* **1995**, 103.

Results of Part II

UV/vis

Meso monosubstituted OEPs showed slightly deviant UV/vis Q band intensities relative to OEP **1**. The phenomenon was explained by the increased unsymmetry, the induced distortion and the increased meso- β interaction. The deviant behavior was previously reported in literature,¹⁻³ while the Q band region of the prepared *meso* di- and trisubstituted OEPs became stronger perturbed. A changed Q band behavior was also reported previously for chlorins,^{4,5} but wasn't identical with the Q band shape of the prepared OEPs. However, split Soret bands were observed for di- and trisubstituted OEPs and additional red shifts occurred for the substitution in *meso* position with 9-phenanthrenyl and 3-methoxyphenyl residues (OEPs **256**, **287** and **291**). The split Soret bands were explained for the porphyrins **9**, **10**, **252**, **259** and **289** by the existence of atropisomers, and for the OEPs **252**, **257**, **258** and the AAB substituted OEPs **293** and **294** by the unsymmetric substitution pattern and the induced distortion. The spectra of the respective palladium (II) complexes **9**, **10** and **304** (with exception of the Pd(II)OEP **284**) displayed furthermore common UV/vis spectra e.g. normal Soret bands were observed. Else wise, 5,10,15,20-tetrakis(9-phenanthrenyl) OEP **11** displayed also a for *meso* tetrasubstituted OEPs common spectrum with a slim Soret, a strong QI and a weak QII band in analogy to the previously reported 5,10,15,20-tetrakisphenyl OEP **244**.¹ Extended Π -conjugation was furthermore not observed for the prepared OEPs as the residues were connected by single bonds and due to perpendicular orientations of the *meso* substituents. Π -Extension is furthermore known to cause broadened absorption bands and to enhance the Q band intensities.^{6,7} However, the spectrum of 5-(4-dimethylaminophenyl)-10-phenyl OEP **249** was slightly and the spectrum of the mini push-pull OEP **253**, 5-(3-trifluoromethylphenyl)-10-(4-dimethylaminophenyl) OEP, was strongly broadened and the broadening was attributed to Π -extension due to the distortion as well as to the influence of the additional chromophores and push-pull effects (NMe₂ and CF₃).⁸

Soret and Q band shifts of 20 nm to 40 nm were observed for subsequent *meso* substitution due to a higher degree of distortion and also respective ¹H NMR NH signal shifts could be reported in accordance to literature.¹⁻³

Phosphorescence

Measurements of phosphorescence quantum yields and lifetimes were carried out by Vinogradov and co-workers and displayed lower quantum yields and lifetimes for *meso* monosubstituted Pd(II)OEPs relative to Pd(II)OEP **2**. *Meso* monosubstituted Pd(II)OEPs were described to be conformational more flexible than Pd(II)OEP **2**, which resulted in an increased rate of annihilation processes and lower phosphorescence quantum yields and lifetimes.^{9,10} Saddling and ruffling distortion modes, induced by the respective alkyl or aryl substituents, were found to have different impacts on the emission from the triplet state. The introduction of phenyl residues, quenched the phosphorescence and it was reported previously that the phenyl rotation might contribute to internal energy conversion processes.¹¹ However, 5-methyl Pd(II)OEP **166** displayed a phosphorescence quantum yield of $\Phi = 4.7$ and a lifetime of 276 μs , while the phosphorescence of 5-*n*-butyl Pd(II)OEP **17** was decreased relative to 5-methyl Pd(II)OEP **166** and could be explained by the stronger distortion induced by the *n*-butyl substituent, which could be again related to a higher degree of conformational flexibility. On the other hand, a desired decreased phosphorescence lifetime, but high enough quantum yield was obtained for 5-(9-phenanthrenyl) Pd(II)OEP **12** ($\Phi = 1.1$, $\tau = 54 \mu\text{s}$) and made the OEP attractive for single molecule experiments in order to investigate its qualities as an oxygen sensor. It was furthermore observed, as described in chapter 3 and 5, that the rotation of the phenanthrenyl substituent was hindered, which might have circumvented additional annihilation process. 5-Phenyl and 5-(1-naphthyl) Pd(II)OEP **271** and **282** were else wise observed to show almost no deviation from the porphyrin zero plane ($\Delta z = 0.05 \text{ \AA}$, compare to chapter 4), while 5-*n*-butyl OEP **17** was described with the largest out-of-plane distortion ($D_{\text{oop}} = 0.64 \text{ \AA}$). *Ab initio* calculations showed furthermore that a minor degree of ruffling should be induced by the 9-phenanthrenyl substituent besides the for aryl substituents common saddle shape conformation and the solid state structure and the NSD analysis carried out for the free base OEP **8**, confirmed the ruffling. However, *meso* mixed alkyl-aryl substituted Pd(II)OEPs might possess phosphorescence properties situated between 5-(9-phenanthrenyl) Pd(II)OEP **12** and the prepared alkyl substituted Pd(II)OEPs **17** and **166** due to a slightly changed degree of ruffling and could be synthesized and investigated in future.

REFERENCES

- 1) S. A. Syrbu, L. Lyobumova, A. S. Semeikin *Chem. Heterocyclic Comp.* **2004**, *40*, 10, 1262.
- 2) J. Takeda, M. Sato *Chemistry Lett.* **1994**, 2233.
- 3) W. W. Kalisch, M. O. Senge *Angew. Chem.* **1998**, *110*, 8, 1156.
- 4) Y. Chen, C. J. Medforth, K. M. Smith, J. Alderfer, T. J. Dougherty, R. K. Pandey *J. Org. Chem.* **2001**, *66*, 3930.
- 5) A. R. Genady, D. Gabel *Tetrahedron Lett.* **2003**, *44*, 2915.
- 6) A. Tsuda, H. Furuta, A. Osuka *J. Am. Chem. Soc.* **2001**, *123*, 10304.
- 7) T. E. O. Screen, I. M. Blake, L. H. Rees, W. Clegg, S. J. Borwick, H. L. Anderson *J. Chem. Soc., Perkin Trans. 1* **2002**, 320.
- 8) H. Higuchi, T. Maeda, K. Miyabayashi, M. Miyake, K. Yamamoto *Tetrahedron Lett.* **2002**, *43*, 3097.
- 9) E. Mei, S. Vinogradov, R. M. Hochstrasser *J. Am. Chem. Soc.* **2003**, *125*, 13198.
- 10) J. E. Rogers, K. A. Nguyen, D. C. Hufnagle, D. G. McLean, W. Su, K. M. Gossett, A. R. Burke, S. A. Vinogradov, R. Prachter, P. A. Fleitz *J. Phys. Chem. A* **2003**, *107*, 51, 11331.
- 11) C. M. Muzzi, C. J. Medforth, L. Voss, M. Cancilla, C. Lebrilla, J.-G. Ma, J. A. Shelnut, K. M. Smith *Tetrahedron Lett.* **1999**, *40*, 6159.

Conclusions and Outlook

The use of organolithium reagents provided convenient access to *meso* monosubstituted and 5,10-disubstituted OEPs and in some cases also tri- and tetrasubstituted OEPs were produced in a one-pot reaction from the *meso* monosubstituted OEPs. Yields and OEPs obtained were furthermore influenced during the disubstitution step by the equivalents and amounts of bromide and *n*-BuLi used and the 9-phenanthrenyl series was prepared as described in chapter 2.2 in a straightforward manner. Further optimisation yielded also successfully in the use of *meso* monosubstituted Pd(II)OEPs in nucleophilic substitution reactions with organolithium reagents and will be available for future synthesis. Additionally, the *meso* AAB-substituted OEPs **292-294**, which were obtained from 5,10-bisphenyl OEP **236**, open the pathway to 5,10-A₂-15,20-B₂ substituted OEPs, targeted for NLO purposes.¹

The triplet state dynamics of the phenanthrenyl series will be furthermore investigated in order to classify novel oxygen sensors and the prepared 5-(9-phenanthrenyl) Pd(II)OEP **12** showed already a prolonged phosphorescence lifetime and a for sensor applications high enough quantum yield ($\Phi = 1.1$, $\tau = 54 \mu\text{s}$). Unfortunately, nitrophenyl substituents, which are of interest for NLO technique,² couldn't be introduced, whereas the mini push-pull OEP **253**, shown in figure I, could be prepared in good yield (48%) and displayed a broadened UV/vis spectrum. Additionally, the AB substituted OEPs **249** and **260** bearing dimethylaminophenyl substituents were prepared in high yields (71-79%) and could have been adequately derived to obtain nitro-phenyl OEPs.

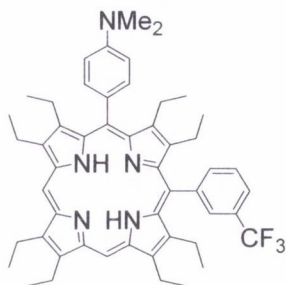
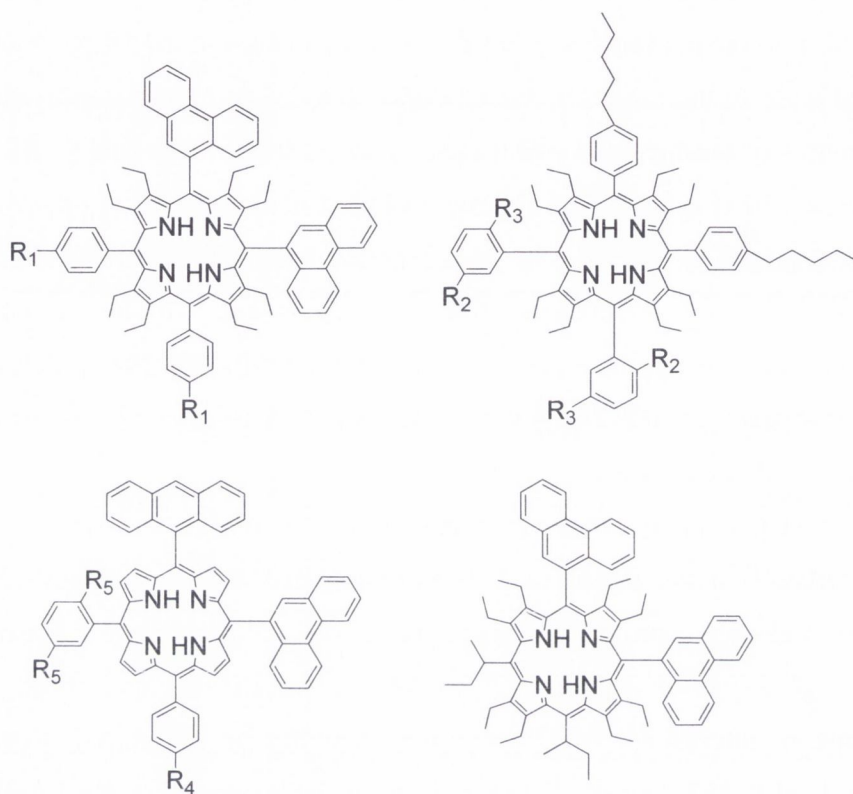


Fig. I. Obtained mini push-pull OEP **253**.

Additionally, a tolyl substituent, which was reported in porphyrins that showed desired NLO qualities,³ could be introduced in the *meso* position of OEP **1** (**229**, 20%) and further synthesis could be carried out in succeeding works as shown in figure II.



$R_1 = \text{Me}, n\text{-pentyl}, \text{NMe}_2, \text{NO}_2$
 $R_2 = \text{OMe}, \text{H}, \text{OH}, R_3 = \text{OMe}, \text{OH}, \text{CF}_3$
 $R_4 = \text{NMe}_2, \text{NO}_2, R_5 = \text{OMe}, \text{OH}$

Fig. II. OEPs aimed for future synthesis.

However, the results of the phosphorescence measurements (chapter 6) suggested an investigation of alkyl-aryl mixed Pd(II)OEPs and the synthesis of those was previously reported by I. Bischoff and W. W. Kalisch and was also attempted during the PhD as described in chapter 2.2.3.^{4,5} The in figure III shown OEPs were also obtained previously by Bischoff and Kalisch and the synthetical knowledge could be used for future synthesis.

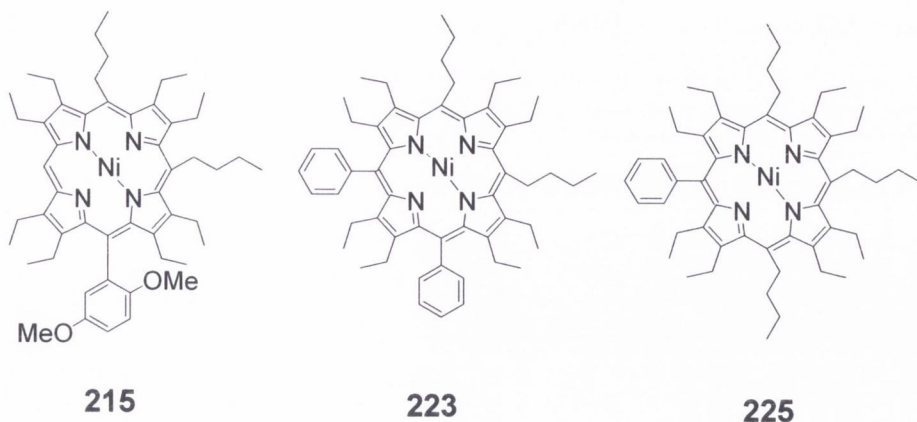


Fig. III. Previously synthesized A_2B , A_3B and A_2B_2 octaethylporphyrins.^{4,5}

However, methoxyphenyl OEPs were also obtained as reported in the chapters 2.1.2 and chapter 2.2 by W. W. Kalisch⁵ and could enlarge the palette of available starting materials. Also OEPs obtained from [2+2] McDonald condensation reactions^{6,7,8} and OEPs prepared by Syrbu *et al.*⁹ (see chapter 1.4.5 and 1.4.6) could be used and *meso* chlorination could be attempted to afford OEPs for subsequent coupling reactions as described in chapter 2.1.¹⁰

Additionally, the *meso* substitution with azulenyl substituents, which was achieved on other porphyrins by Osuka *et al.*¹² could be carried out with OEPs as well as the introduction of perylene and anthenyl residues, which was reported by Gold *et al.*,¹³ Wasielewski and co-workers,¹⁴ Wang¹⁵ and Lindsey¹⁶ *et al.*

Meso-β doubly linked porphyrins, which displayed broadened UV/vis spectra due to the π -extension, could be obtained in future from 5,10,15-tris(9-phenanthrenyl) Pd(II)OEP **10** by the use of $Sc(OTf)_3$ or other Lewis acid and also directly linked, non communicating *meso* linkages seem to be attractive, as the UV/vis intensities could be increased with such linkages, enhancing the triplet state of the respective diporphyrin relative to *meso* monosubstituted porphyrin (compare to chapter 6).¹⁷⁻¹⁹

On the other hand for applications in body fluid, it is necessary to enhance the hydrophilic character of the porphyrin and recent synthesis^{20,21} reported the preparation of carboxylic acids, derived from methyl-substituted triptycene^{22,23} and similar reactions could be carried out with 5-methyl OEP **227** and 5-(4-tolyl) OEP **229**. Also coupling reactions could be performed with the prepared *meso* monosubstituted OEPs

221 and **222** as well as Diels-Alder cycloaddition with the OEPs **246** and **255** and non communicating diporphyrins could be prepared. Additionally the solubility of the porphyrins could be enhanced by the introduction of ester groups with maleic acid, which adds readily to the anthracenyl residue.

REFERENCES

- 1) H. Chou, C.-T. Chen, K. F. Stork, P. W. Bob, K. S. Suslick *J. Phys. Chem.* **1994**, *98*, 383.
- 2) M. Yeung, A. C. H. Ng, M. G. B. Drew, E. Vorpapel, E. M. Breitung, R. J. McMahon, D. K. P. Ng *J. Org. Chem.* **1998**, *63*, 7143.
- 3) M. Pizzotti, R. Ugo, E. Annoni, S. Quici, I. Ledoux-Rak, G. Zerbi, M. Del Zoppo, P. C. Fantucci, I. Invernizzi *Inorg. Chim. Acta* **2002**, *340*, 70.
- 4) I. Bischoff, M. O. Senge *Eur. J. Org. Chem.* **2001**, 1735.
- 5) Kalisch, M. O. Senge, W. W. Kalisch *Angew. Chem. Int. Ed.* **1998**, *110*, 8, 1156.
- 6) J. Tang, J. G. Verkade *J. Org. Chem.* **1994**, *59*, 7793.
- 7) H. Tamiaki, A. Kiyomori, K. Maruyama *Bull. Chem. Soc. Jpn.* **1994**, *67*, 2478.
- 8) T. Tanaka, K. Endo, Y. Aoyama *Tetrahedron Lett.* **1988**, *29*, 41, 5271.
- 9) A. Syrbu, L. Lyobumova, A. S. Semeikin *Chem. Heterocyclic Comp.* **2004**, *40*, 10, 1262.
- 10) Y. Narutam, F. Tani, K. Maruyama *Tetrahedron Lett.* **1992**, *33*, 1069.
- 11) K. Kurotobi, A. Osuka *Org. Lett.* **2005**, *7*, 6, 1055.
- 12) A. Tsuda, H. Furuta, A. Osuka *J. Am. Chem. Soc.* **2001**, *123*, 10304.
- 13) K. Jayaraj, A. Gold, L. M. Ball, P. S. White *Inorg. Chem.* **2000**, *39*, 3652.
- 14) X. G. Yang, J. Z. Sun, M. Wang, H. Z. Chen *Chin. Chem. Lett.* **2003**, *14*, 11, 1105.
- 15) M. P. O. Neil, M. P. Niemczyk, W. A. Svec, D. Gosztola, G. L. Gaines, M. R. Wasielewski *Science* **1992**, *257*, 63.
- 16) S. Prathapan, S. I. Yang, M. A. Miller, D. F. Bocian, D. Holten, J. S. Lindsey *J. Phys. Chem. B* **2001**, *105*, 8237.
- 17) A. Osuka, N. Aranti *Org. Lett.* **2001**, *3*, 26, 4213.
- 18) N. Aranti, H. S. Cho, T. K. Ahn, S. Cho, D. Kim, H. Sumi, A. Osuka *J. Chem. Soc.* **2003**, *125*, 32, 9668.
- 19) H. S. Gill, M. Harmjanz, J. Santamaria, I. Finger, M. J. Scott *Angew. Chem.* **2004**, *116*, 491.
- 20) K. Kurotobi, M. Miyauchi, K. Takakura, T. Murafuji, Y. Sugihara *Eur. J. Org. Chem.* **2003**, 3663.
- 21) F. de Montigny, G. Argouarch, C. Lapinte *Synthesis* **2006**, *2*, 293.

- 22) M. Rybackova, M. Belohradsky, P. Holy, R. Pohl, J. Zavada *Synthesis* **2006**, *12*, 2039.
- 23) G. V. Ambulgekar, S. D. Samant, A. B. Pandit *Ultrason. Sonochem.* **2004**, *11*, 191.

Experimental Part

7. General Methods

^1H NMR and ^{13}C NMR spectra were recorded on a Bruker DPX 400 (400 MHz for ^1H NMR) or a Bruker AV 600 instrument (600 MHz for ^1H NMR and 100 MHz for ^{13}C NMR). High resolution mass spectrometry was carried out on Micromass/Waters Corp. USA liquid chromatography time-of-flight spectrometer equipped with electrospray source (ES+). Low resolution mass spectra were recorded on Micromass/Waters Corp. Quattro *micro*TM LC-MS/MS instrument. UV/vis measurements were performed using a Shimadzu MultiSpec-1501 instrument. Melting points were determined using a Stuart SMP10 melting point apparatus and are uncorrected. Thin layer chromatography (TLC) was performed on silica gel 60F₂₅₄ (Merck) coated aluminium sheets. Column chromatography was performed using a forced flow of the indicated solvent system on Fluka silica gel 60 (230-400 mesh) or aluminium oxide. Diethyl ether (Et₂O) and tetrahydrofuran (THF) were distilled from sodium/benzophenone under argon. *n*-Butyl lithium, 1-bromonaphthalene, 2-bromonaphthalene, 1,4-dibromobenzene and 3-bromobenzotrifluoride were purchased from Aldrich Chem. Co., 1-bromo-4-pentylbenzene was supplied from Maybridge, 9-bromophenanthrene, 3-bromoanisole and 9-bromoanthracene from Acros and 4-bromo-dimethylaniline from Fluka. All named chemicals were used without further purification.

7.1 Synthesis of 2,3,7,8,12,13,17,18-octaethylporphyrin (OEP) (1)

OEP 1 was prepared according to standard procedures as described in chapter 1.4.2.

7.2 General synthetic procedure for the preparation of meso mono-, di-, tri- and tetrasubstituted free base 2,3,7,8,12,13,17,18-octaethylporphyrins

For the preparation of *in situ* generated organo lithium reagents the corresponding bromide (optimized equivalents) was dissolved in 15 mL ether and an excess of *n*-BuLi (optimized equivalents, 2.5 molar in *n*-hexane) was added during 5 to 15 minutes at 0 to $-75\text{ }^\circ\text{C}$ depending on the bromide under an argon atmosphere. The reaction mixture was stirred for an hour at rt and the corresponding octaethylporphyrin, dissolved in 50 mL THF, was added at rt to $-75\text{ }^\circ\text{C}$. The reaction mixtures was allowed to warm up to ambient temperature while stirring was continued for one hour or until TLC monitoring

indicated the formation of the product (red and slightly more polar than OEP for *meso* monosubstituted OEPs and a green-brown, polar spot for di- and higher substituted OEP on silica gel, *n*-hexane/CH₂Cl₂, v/v, 1/1. The reaction was quenched with 1 to 2 mL of water at rt to -50 °C (colour change from reddish brown to dark green for *meso* monosubstituted OEPs), 5 minutes later a solution of DDQ (150–300 mg) in 15 mL CH₂Cl₂ was added quickly for oxidation at the same temperature (colour change to dark red for *meso* monosubstituted OEPs). The stirring was continued for another 15 to 30 minutes at rt. Reaction mixtures affording *meso* monosubstituted OEPs were filtered through a frit with silica gel, eluting with *n*-hexane/CH₂Cl₂, v/v, 1/1 to 1/2 and for complete elution with CH₂Cl₂. For more polar *meso* di- and higher substituted OEPs, it was filtered through aluminium oxide with CH₂Cl₂ and for complete elution ethylacetate was added. The solvent was evaporated and the crude OEPs were dissolved in a small amount of CH₂Cl₂ or in *n*-hexane/CH₂Cl₂, v/v, 1/1.

Further purification was carried out for *meso* monosubstituted OEPs by column chromatography on silica gel eluting slowly with *n*-hexane/CH₂Cl₂, v/v, 2/1 to 1/2 and after the separation of yellow impurities and traces of starting material for complete elution with CH₂Cl₂. Mixtures of di-, tri- and tetrasubstituted OEPs were purified and separated using column chromatography on silica gel eluting with *n*-hexane/CH₂Cl₂, v/v, 4/1 to 2/1 and after the elution of yellow impurities, by addition of 20 mL acetone to 200 mL of the eluent affording the disubstituted OEPs (brown-orange solution, purple solid) and the tri- and tetrasubstituted OEPs (green-brown to green solutions, purple and green solids) by addition of 20 mL ethylacetate to 200 mL of the eluent or of 5 mL of EtOH to 200 mL of the eluent. Alternatively, tetrasubstituted OEPs could be separated from trisubstituted OEPs by column chromatography on aluminium oxide with *n*-hexane/CH₂Cl₂, v/v, from 7/1 to 2/1 to pure CH₂Cl₂ and by addition of acetone or ethylacetate to the eluent (20 mL to 200 mL CH₂Cl₂) for complete elution. Passing through aluminium oxide, avoided also the formation of dications of tri- and tetrasubstituted OEPs (brown solutions instead of dark green solutions), which was necessary for the subsequent palladium (II) insertion described in section 8.3. The *meso* monosubstituted OEPs were precipitated from CH₂Cl₂/CH₃OH whereas higher substituted OEPs couldn't be precipitated.

7.2.1 Octaethylporphyrins with one *meso* substituent

7.2.1.1 2,3,7,8,12,13,17,18-Octaethyl-5-methylporphyrin (227)

OEP (150 mg, 0.28 mmol) was dissolved in 50 mL THF under an argon atmosphere and 1.9 mL of methyllithium (3.08 mmol, 11 equivalents, 1.6 M in diethyl ether) were added slowly at $-70\text{ }^{\circ}\text{C}$. The reaction mixture was stirred for 80 minutes at rt. It was quenched with 1 mL of water quickly at $-50\text{ }^{\circ}\text{C}$ and oxidized with a solution of DDQ (118 mg, 0.50 mmol) in 15 mL dichloromethane at the same temperature 10 minutes later. After 30 minutes of stirring at rt the reaction mixture was filtered through silica gel and the solvent was evaporated. The crude OEP was purified by column chromatography using silica gel and eluting with *n*-hexane/ CH_2Cl_2 , v/v, 1/1. A single, red product fraction was obtained, the solvent was evaporated and the OEP **227** was dissolved in a small amount of dichloromethane and precipitated with methanol to yield 41 mg (0.075 mmol, 27%,) of a purple solid. Mp $> 300\text{ }^{\circ}\text{C}$; R_f 0.88 (*n*-hexane/ CH_2Cl_2 /MeOH, v/v, 3/3/1, silica); ^1H NMR (400 MHz, CDCl_3): $\delta = 10.01$ (s, 2H, *meso* H), 9.81 (s, 1H, *meso* H), 4.58 (s, 3H, 5- CH_3), 4.10 (m, 16H, CH_2), 1.83 (m, 24H, CH_3), -2.88 ppm (br s, 2H, NH); ^{13}C NMR (100 MHz, CDCl_3): $\delta = 17.0, 18.3, 18.4, 19.6, 19.7, 21.5, 22.7, 96.4, 113.8, 140.8, 141.9, 143.8$ ppm; UV/vis (CH_2Cl_2): λ_{max} (lg ϵ) = 406 (5.53), 506 (4.39), 541 (4.07), 575 (3.96), 624 (3.16) nm; MS (ES $^+$): m/z (%): 549 (85) $[\text{M}+\text{H}]^+$; HRMS (ES $^+$) $[\text{C}_{37}\text{H}_{48}\text{N}_4+\text{H}]^+$: calcd 549.3957, found 549.3957.

7.2.1.2 2,3,7,8,12,13,17,18-Octaethyl-5-(*s*-butyl)porphyrin (228)

OEP (150 mg, 0.28 mmol) was dissolved at room temperature in 50 mL THF under an argon atmosphere and during 15 minutes 3.2 mL of *sec*-butyllithium (4.20 mmol, 15 equivalents, 1.3 molar in cyclohexane) were added slowly at $-70\text{ }^{\circ}\text{C}$. The reaction mixture turned from red to green and stirring was continued at $-50\text{ }^{\circ}\text{C}$ for 30 minutes followed by 25 minutes at rt. TLC control indicated a polar orange and a brown-green product (CH_2Cl_2 /*n*-hexane/MeOH, v/v/v, 3/3/1, silica) and it was quenched with 1 mL of water and five minutes later oxidized with DDQ in dichloromethane at the same temperature. The stirring was continued for 10 minutes at $-40\text{ }^{\circ}\text{C}$ and 20 minutes at rt. It was filtered through a fritte filled with aluminium oxide eluting with *n*-hexane/ CH_2Cl_2 /v/v, 1/1 and the solvent was evaporated. The crude OEP **228** was purified using a silica gel column with *n*-hexane/ CH_2Cl_2 , v/v, 1/1 and after yellow and brown fractions, a deep

red product fraction was obtained by adding 2 mL of ethanol to 200 mL of the eluent. The solvent was evaporated, the residue dissolved in dichloromethane and precipitated with MeOH within a month time to yield to 19 mg (0.03 mmol, 11%) of a purple solid. R_f 0.80 (*n*-hexane/CH₂Cl₂/MeOH, v/v, 3/3/1, silica); Mp 278 °C; ¹H NMR (400 MHz, CDCl₃): δ = 10.08 (s, 2H, *meso* H), 9.74 (s, 1H, *meso* H), 5.11 (m, 1H, *s*-butyl CH), 4.03 (m, 16H, CH₂), 2.62 (d, 3H, *J* = 7.3 Hz, *s*-butyl CH₃), 2.48 (m, 2H, *s*-butyl CH₂), 1.95 (m, 18H, CH₃), 1.81 (t, 6H, *J* = 7.0 Hz, CH₃), 0.51 (t, 3H, *J* = 7.3 Hz, *s*-butyl CH₃), –2.30 ppm (s, 2H, NH); ¹³C NMR (100 MHz, CDCl₃): δ = 13.7, 17.4, 17.8, 18.4, 19.7, 20.0, 22.4, 24.4, 29.7, 33.7, 40.1, 95.1, 96.6, 124.4, 140.0, 140.6, 140.7, 141.9, 142.1, 144.4, 145.7, 146.1 ppm; MS (ES⁺): *m/z* (%): 591 (100) [M+H]⁺; HRMS (ES⁺) [C₄₀H₅₄N₄+H]⁺: calcd 591.4425; found 591.4425.

7.2.1.3 2,3,7,8,12,13,17,18-Octaethyl-5-(3-methoxyphenyl)porphyrin (231)

The reaction was performed following the general procedure with 10 equivalents of 3-bromoanisole (0.523 g, 2.8 mmol) and 20 equivalents of *n*-BuLi (2.24 mL, 5.60 mmol). Addition of *n*-BuLi was carried out at –75 °C and the reaction mixture was stirred afterwards without cold bath at ambient temperature. OEP (150 mg, 0.28 mmol) in THF was added after 1 hour at –40 °C and after 24 hours of stirring at rt, it was quenched at 0 °C with water, oxidized and purified to yield 7 mg (0.0109 mmol, 3.5%) of a purple solid. Mp 217 °C; ¹H NMR (400 MHz, CDCl₃): δ = 10.17 (s, 2H, *meso* H), 9.92 (s, 1H, *meso* H), 7.82 (d, 1H, *J* = 7.2 Hz, phenyl H), 7.77 (br s, 1H, 3-OMe-phenyl H), 7.56 (t, 1H, *J* = 7.2 Hz, phenyl H), 7.36 (m, 1H, phenyl H), 4.07 (m, 12H, CH₂), 3.96 (s, 3H, 3-OMe-phenyl H), 2.82 (m, 4H, CH₂), 1.91 (m, 18H, CH₃), 1.21 (m, 6H, CH₃), –3.07 ppm (s, 2H, NH); ¹³C-NMR (100 MHz, CDCl₃): δ = 18.0, 18.4, 19.7, 20.7, 55.4, 95.3, 96.6, 114.5, 118.6, 119.0, 126.5, 127.3, 140.9, 141.3, 141.8, 142.2, 142.7, 143.3, 144.2, 145.6, 157.6 ppm; UV/vis (CH₂Cl₂): λ_{max} (lg ε) = 405 (5.32), 503 (4.26), 537 (3.95), 571 (3.92), 623 (3.41) nm; MS (ES⁺): *m/z* (%): 641 (100) [M+H]⁺; HRMS (ES⁺) [C₄₃H₅₂N₄O+H]⁺: calcd 641.4219, found 641.4244.

7.2.1.4 2,3,7,8,12,13,17,18-Octaethyl-5-(3-trifluoromethylphenyl)porphyrin (229)

The reaction was performed following the general procedure with 20 equivalents of 3-bromobenzotrifluoride (0.77 mL, 5.6 mmol) and 40 equivalents of *n*-BuLi (4.48 mL, 11.2 mmol). Addition of *n*-BuLi was carried out at –30 °C and the reaction mixture was

stirred afterwards without cold bath at ambient temperature. OEP (150 mg, 0.28 mmol) in THF was added after 3 hours at $-30\text{ }^{\circ}\text{C}$ and after 20 minutes of stirring at rt and 20 minutes at $50\text{ }^{\circ}\text{C}$, it was quenched at $-10\text{ }^{\circ}\text{C}$ with water, oxidized and purified to yield 125 mg (0.179 mmol, 64%) of a shiny purple solid. Mp $212\text{ }^{\circ}\text{C}$; ^1H NMR (400 MHz, CDCl_3): $\delta = 10.20$ (s, 2H, *meso* H), 9.67 (s, 1H, *meso* H), 8.61 (s, 1H, phenyl H), 8.36 (d, 1H, $J = 7.6$ Hz, phenyl H), 8.11 (d, 1 H, $J = 7.7$ Hz, phenyl H), 7.81 (t, 1H, $J = 7.8$ Hz, phenyl H), 4.09 (m, 12H, CH_2), 2.81 (m, 2H, CH_2), 2.61 (m, 2H, CH_2), 1.93 (t, 12H, $J = 7.1$ Hz, CH_3), 1.85 (t, 6H, $J = 7.5$ Hz, CH_3), 1.15 (t, 6H, $J = 7.4$ Hz, CH_3), -3.02 (s, 1H, NH), -3.17 ppm (s, 1H, NH); ^{13}C NMR (100 MHz, CDCl_3): $\delta = 17.7, 18.4, 18.50, 18.53, 19.7, 20.7, 95.7, 96.1, 116.5, 125.1, 127.0, 129.5, 136.5, 141.1, 142.0, 142.3, 142.9, 144.5, 145.8$ ppm; UV/vis (CH_2Cl_2): 404 (6.68), 503 (5.44), 537 (4.93), 571 (4.76) nm; MS (ES⁺): m/z (%) = 679 (100) $[\text{M}+\text{H}]^+$; HRMS (ES⁺) $[\text{C}_{43}\text{H}_{49}\text{F}_3\text{N}_4+\text{H}]^+$: calcd 679.3988 found 679.3958.

7.2.1.5 2,3,7,8,12,13,17,18-Octaethyl-5-(4-*n*-pentylphenyl)porphyrin (5)

The reaction was performed following the general procedure with 20 equivalents of 1-bromo-4-pentylbenzene (1 mL, 5.6 mmol) and 40 equivalents of *n*-BuLi (4.48 mL, 11.2 mmol). Addition of *n*-BuLi was carried out at $0\text{ }^{\circ}\text{C}$ and the reaction mixture was stirred afterwards without cold bath at ambient temperature. OEP (150 mg, 0.28 mmol), in THF was added after 4 hours at $0\text{ }^{\circ}\text{C}$ and after 30 minutes of stirring at rt, it was quenched at $0\text{ }^{\circ}\text{C}$ with water, oxidized and purified to afford 160 mg (0.22 mmol, 82%) of a shiny purple solid. Mp $200\text{ }^{\circ}\text{C}$; ^1H NMR (400 MHz, CDCl_3): $\delta = 10.16$ (s, 2H, *meso* H), 9.92 (s, 1H, *meso* H), 8.10 (d, 2H, $J = 7.8$ Hz, phenyl H), 7.47 (d, 2H, $J = 7.8$ Hz, phenyl H), 4.06 (m, 12H, CH_2), 2.98 (t, 2H, $J = 7.2$ Hz, pentyl CH_2), 2.79 (m, 4H, CH_2), 1.91 (t, 12H, $J = 7.7$ Hz, CH_3), 1.85 (t, 6H, $J = 7.7$ Hz, CH_3), 1.51 (m, 6H, pentyl CH_2), 1.15 (t, 6H, $J = 7.7$ Hz, CH_3), 1.04 (t, 3H, $J = 7.3$ Hz, pentyl CH_3), -3.02 (s, 1H, NH), -3.15 ppm (s, 1H, NH); ^{13}C NMR (400 MHz, CDCl_3): $\delta = 14.2, 18.0, 18.4, 18.5, 19.8, 20.7, 22.7, 31.7, 31.5, 72.7, 80.5, 96.6, 153.6, 155.0, 184.9, 191.6$ ppm; UV/vis (CH_2Cl_2): λ_{max} (lg ϵ) = 404 (5.12), 503 (4.99), 537 (4.69), 571 (4.64) nm; MS (ES⁺): m/z (%): 681 (13) $[\text{M}+\text{H}]^+$; HRMS (ES⁺) $[\text{C}_{47}\text{H}_{60}\text{N}_4+\text{H}]^+$: calcd 681.4896, found 681.4871. Also traces of a green product were obtained by addition of EtOH to the eluent as a second fraction but couldn't be identified.

7.2.1.6 2,3,7,8,12,13,17,18-Octaethyl-5-(4-dimethylaminophenyl)porphyrin (230)

The reaction was performed following the general procedure with 20 equivalents of 4-dimethylaniline (1.12 g, 5.6 mmol) and 40 equivalents of *n*-BuLi (4.48 mL, 11.2 mmol). Addition of *n*-BuLi was carried out at $-75\text{ }^{\circ}\text{C}$ and the reaction mixture was stirred afterwards without cold bath at ambient temperature. OEP (150 mg, 0.28 mmol) in THF was added after 1 hour at $-40\text{ }^{\circ}\text{C}$ and after 1 hour of stirring at rt, it was quenched at $-40\text{ }^{\circ}\text{C}$ with water, oxidized and purified to yield 33 mg (0.050 mmol, 17%) of a purple solid. Mp $> 300\text{ }^{\circ}\text{C}$; R_f 0.03 ($\text{CH}_2\text{Cl}_2/n\text{-hexane}$, v/v, 2/1, silica); R_f 0.62 ($\text{CH}_2\text{Cl}_2/n\text{-hexane/MeOH}$, v/v, 3/3/1, silica); $^1\text{H NMR}$ (400 MHz, CDCl_3): $\delta = 10.20$ (s, 2H, *meso* H), 9.95 (s, 1H, *meso* H), 8.04 (d, 1H, $J = 8.7$ Hz, phenyl H), 7.49 (d, 1H, $J = 8.9$ Hz, phenyl H), 7.04 (d, 1H, $J = 8.7$ Hz, phenyl H), 6.83 (d, 1H, $J = 8.9$ Hz, phenyl H), 4.09 (m, 12H, CH_2), 3.24 (s, 3H, NMe_2), 2.99 (s, 3H, NMe_2), 2.94 (m, 4H, CH_2), 1.96 (t, 12H, $J = 7.7$ Hz, CH_3), 1.90 (t, 6H, $J = 7.6$ Hz, CH_3), 1.20 (t, 6H, $J = 7.3$ Hz, CH_3), -2.91 ppm (br. s, 2H, NH); $^{13}\text{C NMR}$ (100 MHz, CDCl_3): $\delta = 18.1, 18.4, 19.7, 19.8, 20.8, 40.7, 40.9, 96.5, 110.4, 113.7, 119.7, 126.5, 133.9, 140.7, 142.0, 143.0, 143.7, 145.5, 150.8, 162.8, 170.5$ ppm; UV/vis (CH_2Cl_2): λ_{max} ($\lg \epsilon$) = 257 (4.41), 406 (5.26), 505 (4.33), 538 (3.97), 572 (3.97), 624 (3.59) nm; MS (ES⁺): m/z (%): 654 (100) [$\text{M}+\text{H}$]⁺; HRMS (ES⁺) [$\text{C}_{44}\text{H}_{55}\text{N}_5+\text{H}$]⁺: calcd 654.4536, found 654.4537.

7.2.1.7 2,3,7,8,12,13,17,18-Octaethyl-5-(3-hydroxyphenyl)porphyrin (232)

The reaction was performed following the general procedure with 20 equivalents of 3-bromophenol (0.968 g, 5.6 mmol) and with 60 equivalents of *n*-BuLi (6.72 mL, 16.8 mmol). Addition of *n*-BuLi was carried out at $-75\text{ }^{\circ}\text{C}$ and the reaction mixture was stirred afterwards without cold bath at ambient temperature. OEP (150 mg, 0.28 mmol) in THF was added after 1 hour at $-40\text{ }^{\circ}\text{C}$ and after 30 minutes at $-20\text{ }^{\circ}\text{C}$ and 30 minutes at rt, it was quenched at $-40\text{ }^{\circ}\text{C}$ with water, oxidized and purified to afford 46 mg (0.073 mmol, 26%) of a red-purple solid. Mp $> 300\text{ }^{\circ}\text{C}$; R_f 0.00 ($\text{CH}_2\text{Cl}_2/n\text{-hexane}$, v/v, 2/1, silica); R_f 0.65 ($\text{CH}_2\text{Cl}_2/n\text{-hexane/MeOH}$, v/v, 3/3/1, silica); $^1\text{H NMR}$ (400 MHz, CDCl_3): $\delta = 10.16$ (s, 2H, *meso* H), 9.92 (s, 1H, *meso* H), 7.78 (m, 1H, phenyl H), 7.59 (m, 1H, phenyl H), 7.49 (t, 1H, $J = 7.9$ Hz, phenyl H), 7.22 (m, 1H, phenyl H), 4.06 (m, 12H, CH_2), 2.83 (q, 4H, $J = 7.4$ Hz, CH_2), 1.91 (t, 12H, $J = 7.5$ Hz, CH_3), 1.85 (t, 6H, $J = 7.5$ Hz, CH_3), 1.18 ppm (t, 6H, $J = 7.4$ Hz, CH_3); $^{13}\text{C NMR}$ (100 MHz, CDCl_3): $\delta =$

21.2, 104.3, 105.4, 107.9, 109.1, 114.1, 115.9, 151.7, 152.5, 155.5, 159.8, 162.4, 172.5, 176.9, 182.5, 183.9, 184.6, 188.1, 195.6, 199.3, 208.5, 212.2 ppm; UV/vis (CH₂Cl₂): λ_{\max} (lg ϵ) = 404 (5.03), 503 (4.02), 537 (3.79), 571 (3.76), 623 (3.45) nm; MS (ES⁺): m/z (%): 627 (100) [M+H]⁺; HRMS (ES⁺) [C₄₂H₅₀N₄O+H]⁺: calcd 627.4063, found 627.4036. Furthermore, as a first red fraction, 33 mg (0.061 mmol, 21 %) of OEP were recovered.

7.2.1.8 2,3,7,8,12,13,17,18-Octaethyl-5-(4-methylphenyl)porphyrin (229)

The reaction was performed following the general procedure with 20 equivalents 4-bromotoluene (0.957 g, 5.6 mmol) and 40 equivalents of *n*-BuLi (4.48 mL, 11.8 mmol). Addition of *n*-BuLi was carried out at -10 °C and the reaction mixture was stirred afterwards without cold bath at ambient temperature. OEP (150 mg, 0.28 mmol) in THF was added after 1 hour at -0 °C and after 2 hours at rt and 1 hour at 60 °C, it was quenched at -0 °C with water, oxidized and purified to afford 35 mg (0.056 mmol, 20%) of a purple solid. Mp 220 °C; ¹H NMR (400 MHz, CDCl₃): δ = 10.23 (s, 2H, *meso* H), 9.98 (s, 1H, *meso* H), 8.14 (d, 2H, *J* = 7.8 Hz, phenyl H), 7.52 (d, 2H, *J* = 7.8 Hz, phenyl H), 4.12 (m, 12H, CH₂), 2.85 (q, 4H, *J* = 7.4 Hz, CH₂), 2.77 (s, 3H, phenyl CH₃), 1.98 (t, 12H, *J* = 7.8 Hz, CH₃), 1.88 (t, 6H, *J* = 7.6 Hz, CH₃), 1.21 (t, 6H, *J* = 7.4 Hz, CH₃), -2.94 ppm (s, 2H, NH); ¹³C NMR (100 MHz, CDCl₃): δ = 11.4, 13.7, 14.1, 18.0, 18.4, 18.5, 19.1, 19.7, 19.8, 20.7, 20.8, 21.7, 22.6, 24.9, 25.2, 26.9, 29.0, 30.7, 31.6, 34.3, 34.6, 36.0, 41.3, 95.2, 96.6, 119.1, 133.2, 138.0, 138.9, 140.8, 141.8, 142.1, 142.6, 142.8, 143.7, 144.0, 145.6, 173.9 ppm; UV/vis (CH₂Cl₂): λ_{\max} (lg ϵ) = 406 (5.09), 505 (3.95), 538 (3.67), 571 (3.66), 624 (3.16) nm; MS (ES⁺): m/z (%): 625 (80) [M+H]⁺; HRMS (ES⁺) [C₄₃H₅₂N₄+H]⁺: calcd 625.4270, found 625.4272. As a first red fraction, also 23 mg (0.042 mmol, 15%) of OEP were recovered.

7.2.1.9 2,3,7,8,12,13,17,18-Octaethyl-5-(1-naphthyl)porphyrin (7)

The reaction was performed following the general procedure, using 31 equivalents of 1-bromonaphthalene (1.2 mL, 8.68 mmol) and 40 equivalents of *n*-BuLi (4.48 mL, 11.2 mmol). Addition of *n*-BuLi was carried out at -30 °C and the reaction mixture was stirred afterwards without cold bath at ambient temperature. OEP (150 mg, 0.28 mmol) in THF was added after 1 hour at -30 °C and after 1 hour rt, it was quenched at -20 °C with water, oxidized and purified to afford 91 mg (0.128 mmol, 46%) of a purple solid.

Mp 200 °C, ¹H NMR (400 MHz, CDCl₃): δ = 10.20 (s, 2H, *meso* H), 9.98 (s, 1H, *meso* H), 8.40 (d, 1H, *J* = 5.8 Hz, naphthyl H), 8.30 (d, 1H, *J* = 7.7 Hz, naphthyl H), 8.12 (d, 1H, *J* = 8.3 Hz, naphthyl H), 7.84 (t, 1H, *J* = 6.9 Hz, naphthyl H), 7.47 (m, 1H, naphthyl H), 7.01 (m, 2H, naphthyl H), 4.12 (m, 8H, CH₂), 3.97 (m, 4H, CH₂), 2.64 (m, 2H, CH₂), 2.29 (m, 2H, CH₂), 1.95 (t, 12H, *J* = 7.8 Hz, CH₃), 1.87 (t, 6H, *J* = 7.6 Hz, CH₃), 0.87 (t, 6H, *J* = 7.6 Hz, CH₃), -2.79 (s, 1H, NH), -3.04 ppm (s, 1H, NH); ¹³C NMR (100 MHz, CDCl₃): δ = 16.6, 18.4, 19.7, 19.8, 20.7, 95.4, 96.6, 116.4, 124.3, 125.9, 127.7, 128.4, 128.8, 131.7, 132.6 ppm; UV/vis (CH₂Cl₂): λ_{max} (lg ε) = 406 (4.13), 504 (4.02), 538 (3.84), 572 (3.85), 625 (-) nm; MS (ES⁺): *m/z* (%): 661 (100) [M+H]⁺; HRMS (ES⁺) [C₄₆H₅₂N₄+H]⁺: calcd 661.4270, found 661.4265. Also traces of the green trisubstituted OEP **235** were obtained in traces and accumulated during several reactions.

7.2.110 2,3,7,8,12,13,17,18-Octaethyl-5-(2-naphthyl)porphyrin (233)

The reaction was performed following the general procedure with 20 equivalents of 2-bromonaphthalene (0.7449 g, 3.6 mmol) and 60 equivalents of *n*-BuLi (4.5 mL, 10.8 mmol). Addition of *n*-BuLi was carried out at -50 °C and the reaction mixture was stirred afterwards without cold bath at ambient temperature. OEP (100 mg, 0.18 mmol) in THF was added after 45 minutes at -45 °C and after 2 hours at rt, it was quenched at rt with water, oxidized and purified to afford 45 mg (0.055 mmol, 31 %) of a purple solid. Mp 198 °C; ¹H NMR (400 MHz, CDCl₃): δ = 10.22 (s, 2H, *meso* H), 9.98 (s, 1H, *meso* H), 8.72 (s, 1H, naphthyl H), 8.39 (d, 1H, *J* = 8.1 Hz, naphthyl H), 8.21 (d, 1H, *J* = 7.6 Hz, naphthyl H), 8.16 (d, 1H, *J* = 8.1 Hz, naphthyl H), 8.04 (d, 1H, *J* = 7.2 Hz, naphthyl H), 7.73 (m, 2H, naphthyl H), 4.12 (m, 8H, CH₂), 4.03 (m, 4H, CH₂), 2.77 (m, 2H, CH₂), 2.57 (m, 2H, CH₂), 1.59 (t, 12H, *J* = 7.6 Hz, CH₃), 1.86 (t, 6H, *J* = 7.5 Hz, CH₃), 1.08 (t, 6H, *J* = 7.2 Hz, CH₃), -2.92 (s, 1H, NH), -3.09 ppm (s, 1H, NH); ¹³C NMR (100 MHz, CDCl₃): δ = 17.7, 18.4, 18.5, 19.7, 19.8, 20.8, 95.3, 96.7, 118.7, 125.5, 126.4, 126.8, 131.6, 132.1, 133.1, 139.2, 140.9, 141.8, 142.2, 142.6, 142.7, 143.6, 144.2, 145.7 ppm; UV/vis (CH₂Cl₂): λ_{max} (lg ε) = 406 (5.61), 505 (4.48), 538 (4.20), 572 (4.20), 624 (3.71) nm; MS (ES⁺): *m/z* (%): 661 (100) [M+H]⁺; HRMS (ES⁺) [C₄₆H₅₂N₄+H]⁺: calcd 661.4270, found 661.4290.

7.2.1.11 2,3,7,8,12,13,17,18-Octaethyl-5-acenaphthylporphyrin (234)

The reaction was performed following the general procedure with 31 equivalents of 1-bromoacenaphthene (2.021 g, 8.68 mmol) and with 40 equivalents of *n*-BuLi (4.48 mL, 11.2 mmol). Addition of *n*-BuLi was carried out at $-60\text{ }^{\circ}\text{C}$ and the reaction mixture was stirred afterwards without cold bath at ambient temperature. OEP (150 mg, 0.28 mmol) in THF was added after 1 hour and 20 minutes at $-20\text{ }^{\circ}\text{C}$ and after 20 minutes at $-20\text{ }^{\circ}\text{C}$ and 1 hour rt, it was quenched at $-20\text{ }^{\circ}\text{C}$ with water, oxidized and purified to afford 51 mg (0.074 mmol, 26%) of a purple solid. Mp $190\text{ }^{\circ}\text{C}$; ^1H NMR (400 MHz, CDCl_3): $\delta = 10.21$ (s, 2H, *meso* H), 9.98 (s, 1H, *meso* H), 8.36 (d, 1H, $J = 6.6$ Hz, acenaphthyl H), 7.65 (d, 1H, $J = 6.8$ Hz, acenaphthyl H), 7.32 (d, 1H, $J = 6.6$ Hz, acenaphthyl H), 7.05 (m, 1H, acenaphthyl H), 6.66 (d, 1H, $J = 8.2$ Hz, acenaphthyl H), 4.12 (m, 8H, CH_2), 3.99 (m, 4H, CH_2), 3.79 (m, 2H, acenaphthyl CH_2), 3.72 (m, 2H, acenaphthyl CH_2), 2.73 (m, 2H, CH_2), 2.35 (m, 2H, CH_2), 1.95 (t, 12H, $J = 7.5$ Hz, CH_3), 1.85 (t, 6H, $J = 7.5$ Hz, CH_3), 0.91 (t, 6H, $J = 7.3$ Hz, CH_3), -2.80 (s, 1H, NH), -3.04 ppm (s, 1H, NH); ^{13}C NMR (100 MHz, CDCl_3): $\delta = 17.1, 18.4, 18.5, 19.73, 19.78, 19.83, 20.8, 95.3, 96.5, 116.3, 117.8, 119.2, 123.0, 127.9, 133.1, 135.5, 138.3, 140.8, 141.8, 142.5, 144.4, 144.3, 145.3, 145.5, 146.8$ ppm; UV/vis (CH_2Cl_2): λ_{max} (lg ϵ) = 407 (5.02), 505 (3.92), 538 (3.66), 574 (3.64), 625 (3.26) nm; MS (ES⁺): m/z (%): 687 (42) $[\text{M}+\text{H}]^+$; HRMS (ES⁺) $[\text{C}_{48}\text{H}_{54}\text{N}_4+\text{H}]^+$: calcd 687.4427 found 687.4450.

7.2.1.12 2,3,7,8,12,13,17,18-Octaethyl-5-(9-phenanthrenyl)porphyrin (8)

The reaction was performed following the general procedure with 31 equivalents of 9-bromophenanthrene (2.23 g, 8.86 mmol) and with 40 equivalents of *n*-BuLi (4.48 mL, 11.2 mmol). Addition of *n*-BuLi was carried out at $-30\text{ }^{\circ}\text{C}$ and the reaction mixture was stirred afterwards without cold bath at ambient temperature. OEP (150 mg, 0.28 mmol) in THF was added after 2 hours at $-20\text{ }^{\circ}\text{C}$ and after 1 hour and 30 minutes at rt, it was quenched at $-0\text{ }^{\circ}\text{C}$ with water, oxidized and purified to afford 147 mg (0.207 mmol, 89%) of a purple solid. Mp $> 300\text{ }^{\circ}\text{C}$, R_f 0.86 ($\text{CH}_2\text{Cl}_2/n$ -hexane/MeOH, v/v, 3/3/1, silica), R_f 0.24 ($\text{CH}_2\text{Cl}_2/n$ -hexane, v/v, 2/1, silica); ^1H NMR (400 MHz, CDCl_3): $\delta = 10.20$ (s, 2H, *meso* H), 9.98 (s, 1H, *meso* H), 9.04 (d, 1H, $J = 8.5$ Hz, phenanthrenyl H), 9.00 (d, 1H, $J = 7.5$ Hz, phenanthrenyl H), 8.71 (s, 1H, phenanthrenyl H), 8.08 (d, 1H, $J = 7.7$ Hz, phenanthrenyl H), 7.92 (m, 1H, phenanthrenyl H), 7.81 (m, 1H, phenanthrenyl H), 7.65 (m, 1H, phenanthrenyl H), 7.27 (m, 1H, phenanthrenyl H), 7.14

(m, 1H, phenanthrenyl H), 4.13 (m, 8H, CH₂), 3.96 (m, 4H, CH₂), 2.79 (m, 2H, CH₂), 2.36 (m, 2H, CH₂), 1.94 (t, 12H, $J = 7.5$ Hz, CH₃), 1.82 (t, 6H, $J = 7.6$ Hz, CH₃), 0.85 (t, 6H, $J = 7.4$ Hz, CH₃), -2.73 (s, 1H, NH), -3.00 ppm (s, 1H, NH); ¹³C NMR (100 MHz, CDCl₃): $\delta = 17.0, 18.6, 18.7, 20.0, 21.1, 21.3, 96.1, 97.1, 116.4, 123.4, 126.9, 127.8, 129.4, 131.2, 137.7, 141.8, 142.9, 143.0, 145.4$ ppm; UV/vis (CH₂Cl₂): λ_{\max} (lg ϵ) = 406 (5.13), 504 (4.13), 538 (3.86), 571 (3.83), 624 (3.52) nm; MS (ES⁺): m/z (%): 711 (49) [M+H]⁺; HRMS (ES⁺) [C₅₀H₅₄N₄+H]⁺: calcd 711.4427, found 711.4426. Also traces of the green tetrasubstituted OEP **11** were obtained and accumulated during several reactions.

7.2.2 Octaethylporphyrins with two *meso* substituents

7.2.2.1 2,3,7,8,12,13,17,18-Octaethyl-5-(9-anthracenyl)-10-phenylporphyrin (**246**)

The reaction was performed following the general procedure with 50 equivalents of 9-bromoanthracene (1.2403 g, 4.90 mmol) and 60 equivalents of *n*-BuLi (2.35 mL, 5.88 mmol). Addition of *n*-BuLi was carried out at -40 °C and the reaction mixture was stirred afterwards without cold bath at ambient temperature. 5-(Phenyl) OEP **4** (60 mg, 0.098 mmol) in THF was added after 1 hour and 20 minutes at -20 °C and after 1h and 20 minutes stirring at rt, it was quenched at -0 °C with water, oxidized and purified to yield 13 mg (0.0165 mmol, 16 %) of a purple solid. Mp 110 °C, ¹H NMR (400 MHz, CDCl₃) $\delta = 9.70$ (s, 1H, *meso* H), 9.67 (s, 1H, *meso* H), 8.89 (s, 1H, anthracenyl H), 8.30 (m, 2H, phenyl), 8.26 (d, 2H, $J = 8.6$ Hz, anthracenyl H), 7.74 (m, 1H, phenyl H), 7.64 (t, 2H, $J = 7.6$ Hz, phenyl H), 7.49 (m, 4 H, anthracenyl), 7.10 (m, 2H, anthracenyl H), 3.96 (m, 4H, CH₂), 3.83 (m, 2H, CH₂), 3.63 (m, 2H, CH₂), 2.66 (m, 2H, CH₂), 2.11 (m, 2H, CH₂), 1.84 (m, 4H, CH₂), 1.59 (m, 6H, CH₃), 1.45 (t, 3H, $J = 7.5$ Hz, CH₃), 0.89 (m, 3H, CH₃), 0.68 (t, 3H, $J = 7.3$ Hz, CH₃), 0.33 (t, 3H, $J = 7.2$ Hz, CH₃), 0.01 (m, 3H, CH₃), -0.08 (t, 3H, $J = 7.3$ Hz, CH₃), -2.50 ppm (br s, 2H, NH); ¹³C NMR (100 MHz, CDCl₃): $\delta = 15.3, 15.9, 17.4, 18.0, 18.2, 19.2, 19.3, 19.6, 20.5, 31.8, 94.9, 95.2, 113.8, 125.3, 126.5, 127.1, 127.9, 128.0, 128.1, 128.6, 130.9, 135.2, 135.4$ ppm; UV/vis (CH₂Cl₂): λ_{\max} (lg ϵ) = 425 (4.54), 520 (3.50), sh, 592 (3.92), sh nm; MS (ES⁺): m/z (%): 787 (20) [M+H]⁺; HRMS (ES⁺) [C₅₆H₅₈N₄+H]⁺: calcd 787.4740, found 787.4703. Furthermore 7 mg (0.0072 mmol, 7 %) of the trisubstituted ABA regio isomer **291** were isolated as a green solid in a second fraction.

7.2.2.2 2,3,7,8,12,13,17,18-Octaethyl-5-(9-phenanthrenyl)-10-phenylporphyrin (**247**)

The reaction was performed following the general procedure with 34 equivalents of 9-bromophenanthrene (1.708 g, 6.64 mmol) and 43 equivalents of *n*-BuLi (3.37 mL, 8.425 mmol). Addition of *n*-BuLi was carried out at $-30\text{ }^{\circ}\text{C}$ and the reaction mixture was stirred afterwards without cold bath at ambient temperature. 5-(Phenyl)-OEP **4** (120 mg, 0.196 mmol) in THF was added after 1 hour at rt and after 40 minutes of stirring it was quenched with water, oxidized and purified to yield 125 mg (0.181 mmol, 92 %) of a purple solid. Mp $168\text{ }^{\circ}\text{C}$; ^1H NMR (400 MHz, CDCl_3): $\delta = 9.69$ (s, 1H, *meso* H), 9.67 (s, 1H, *meso* H), 9.00 (m, 2H, phenanthrenyl H), 8.66 (s, 1H, phenanthrenyl H), 8.33 (br d, 2H, $J = 6.5$ Hz, phenyl H), 8.09 (d, 1H, $J = 7.6$ Hz, phenanthrenyl H), 7.87 (m, 1H, phenanthrenyl H), 7.65–7.80 (m, 3H, phenyl H, 2H, phenanthrenyl H), 7.59 (d, 1H, $J = 7.9$ Hz, phenanthrenyl H), 7.29 (m, 1H, phenanthrenyl H), 3.96 (m, 4H, CH_2), 3.84 (m, 2H, CH_2), 3.70 (m, 2H, CH_2), 2.72–2.53 (m, 4H, CH_2), 2.27–2.09 (m, 4H, CH_2), 1.83 (t, 6H, $J = 7.4$ Hz, CH_3), 1.59 (t, 6H, $J = 7.4$ Hz, CH_3), 0.67 (t, 3H, $J = 7.3$ Hz, CH_3), 0.45 (t, 3H, $J = 7.3$ Hz, CH_3), 0.37 (m, 6H, CH_3), -2.58 ppm (s, 2H, NH); ^{13}C NMR (100 MHz, CDCl_3): $\delta = 16.4, 16.7, 17.3, 18.0, 18.2, 19.2, 19.3, 19.4, 19.5, 19.8, 20.2, 20.6, 29.6, 94.9, 95.1, 116.0, 118.9, 122.5, 122.9, 126.4, 126.6, 127.1, 127.2, 128.2, 129.1, 129.2, 129.4, 130.7, 130.9, 134.1, 135.2, 136.4, 137.3, 141.3$ ppm; UV/vis (CH_2Cl_2): λ_{max} ($\lg \epsilon$) = 430 (sh), 454 (4.76), 587 (3.63), 638 (3.42) nm; MS (ES⁺): m/z (%): 787 (30) $[\text{M}+\text{H}]^+$; HRMS (ES⁺) $[\text{C}_{56}\text{H}_{58}\text{N}_4+\text{H}]^+$: calcd 787.4739, found 787.4702. When the reaction was performed following the general procedure with 30 equivalents of 9-bromophenanthrene (1.865 g, 7.26 mmol), 30 equivalents of *n*-BuLi (2.90 mL, 7.26 mmol) and 150 mg of 5-phenyl OEP **4** (0.24 mmol), 26 mg (0.032 mmol, 13%) of the disubstituted OEP **247** and 25 mg (0.025 mmol, 10%) of the trisubstituted OEP **287** were obtained. Furthermore as a first fraction 34 mg (0.055 mmol, 22%) of 5-phenyl OEP **4** were recovered. When the reaction was performed following the general procedure with 25 equivalents of 9-bromophenanthrene (1.554 g, 6.049 mmol), 32 equivalents of *n*-BuLi (3.22 mL, 7.74 mmol) and 150 mg of 5-phenyl OEP **4** (0.24 mmol), 16 mg (0.02 mmol, 8%) of the disubstituted OEP **247** and 21 mg (0.021 mmol, 8%) of the trisubstituted OEP **287** were obtained. Furthermore as a first fraction 77 mg (0.126 mmol, 52%) of 5-phenyl OEP **4** were recovered. When the reaction was performed following the general procedure with 20 equivalents of 9-bromophenanthrene

and 40 equivalents of *n*-BuLi only (2.90 mL, 7.26 mmol) the in literature reported 5-phenyl-10-(*n*-butyl) OEP (not shown, compare to chapter 2.2.1) was isolated. As described in chapter 2.2.6.2, the use of 24 equivalents of 9-bromophenanthrene and 37 equivalents of *n*-BuLi afforded exclusively 39 mg (0.0404 mmol, 33%) of the trisubstituted OEP **287**.

7.2.2.3 2,3,7,8,12,13,17,18-Octaethyl-5-(1-naphthyl)-10-phenylporphyrin (**248**)

The reaction was performed following the general procedure with 40 equivalents of 1-bromonaphthalene (0.71 mL, 5.24 mmol) and 50 equivalents of *n*-BuLi (2.62 mL, 6.55 mmol). Addition of *n*-BuLi was carried out at $-40\text{ }^{\circ}\text{C}$ and the reaction mixture was stirred afterwards without cold bath at ambient temperature. 5-(Phenyl) OEP **4** (80 mg, 0.131 mmol) in THF was added after 1 hour at $-10\text{ }^{\circ}\text{C}$ and after 30 minutes at rt, it was quenched at rt, oxidized and purified to yield 46 mg (0.062 mmol, 47%) of a purple solid. Mp $155\text{ }^{\circ}\text{C}$; $^1\text{H NMR}$ (400 MHz, CDCl_3): $\delta = 9.69$ (s, 1H, *meso* H), 9.67 (s, 1H, *meso* H), 8.42 (d, 1H, $J = 6.8$ Hz, naphthyl H), 8.33 (d, 2H, $J = 7.0$ Hz, phenyl H), 8.29 (d, 1H, $J = 8.2$ Hz, naphthyl H), 8.11 (d, 1H, $J = 8.0$ Hz, naphthyl H), 7.82 (t, 1H, $J = 7.0$ Hz, phenyl H), 7.75 (m, 1H, naphthyl H), 7.68 (m, 2H, phenyl H), 7.53 (m, 2H, naphthyl H), 7.22 (m, 1H, naphthyl H), 3.97 (m, 4H, CH_2), 3.84 (m, 2H, CH_2), 3.74 (m, 2H, CH_2), 2.69 (m, 2H, CH_2), 2.42 (m, 2H, CH_2), 2.39–2.24 (m, 4H, CH_2), 1.84 (t, 6H, $J = 7.6$ Hz, CH_3), 1.60 (t, 3H, $J = 7.5$ Hz, CH_3), 1.53 (t, 3H, $J = 7.4$ Hz, CH_3), 0.67 (t, 3H, $J = 7.3$ Hz, CH_3), 0.46 (t, 3H, $J = 7.4$ Hz, CH_3), 0.41 (t, 3H, $J = 7.3$ Hz, CH_3), 0.34 (t, 3H, $J = 7.2$ Hz, CH_3), -2.60 ppm (s, 2H, NH); $^{13}\text{C NMR}$ (100 MHz, CDCl_3): $\delta = 16.6$, 16.9, 17.3, 17.4, 18.0, 18.2, 19.2, 19.4, 19.5, 20.4, 20.5, 94.9, 95.0, 116.2, 118.9, 124.4, 125.8, 126.0, 126.6, 127.7, 128.1, 128.2, 128.9, 132.2, 133.4, 135.2, 137.1, 139.1, 141.3 ppm; UV/vis (CH_2Cl_2): λ_{max} ($\lg \epsilon$) = 425 (3.22), 520 (3.01), 592 (sh), 650 (sh) nm; MS (ES⁺): m/z (%): 737 (32) [$\text{M}+\text{H}$]⁺; HRMS (ES⁺) [$\text{C}_{52}\text{H}_{56}\text{N}_4+\text{H}$]⁺: calcd 737.4583, found 737.4572.

7.2.2.4 2,3,7,8,12,13,17,18-Octaethyl-5-(4-dimethylaminophenyl)-10-phenylporphyrin (**249**)

The reaction was performed following the general procedure using 40 equivalents of 1-bromo-4-dimethylaminobenzene (1.048 g, 5.24 mmol) and 50 equivalents of *n*-BuLi (2.62 mL, 6.55 mmol). Addition of *n*-BuLi was carried out at $-45\text{ }^{\circ}\text{C}$ and the reaction

mixture was stirred afterwards without cold bath at ambient temperature. 5-(Phenyl) OEP **4** (80 mg, 0.131 mmol) in THF was added after 1 hour at $-20\text{ }^{\circ}\text{C}$ and after 30 minutes stirring at rt, it was quenched at the same temperature, oxidized and purified to yield 76 mg (0.104 mmol, 79%) of a purple solid. Mp $151\text{ }^{\circ}\text{C}$; ^1H NMR (400 MHz, CDCl_3): $\delta = 9.61$ (s, 1H, *meso* H), 9.60 (s, 1H, *meso* H), 8.33 (d, 2H, $J = 6.9$ Hz, phenyl H), 8.12 (d, 2H, $J = 8.6$ Hz, 4-NMe₂phenyl H), 7.77 (m, 1H, phenyl H), 7.67 (m, 2H, phenyl H), 7.03 (d, 2H, $J = 8.6$ Hz, 4-NMe₂phenyl H), 3.92 (q, 4H, $J = 7.5$ Hz, CH₂), 3.81 (m, 4H, CH₂), 3.23 (s, 6H, NMe₂), 2.83 (m, 2H, CH₂), 2.69 (br s, 2H, CH₂), 2.35 (br s, 2H, CH₂), 2.23 (br s, 2H, CH₂), 1.80 (t, 6H, $J = 7.5$ Hz, CH₃), 1.63 (m, 12H, CH₃), 0.63 (m, 6H, CH₃), 0.42 (m, 6H, CH₃), -2.64 ppm (br s, 2H, NH); ^{13}C NMR (100 MHz, CDCl_3): $\delta = 13.9, 17.3, 17.8, 19.2, 19.5, 24.6, 31.5, 40.6, 40.7, 74.1, 74.2, 94.3, 94.6, 110.5, 112.5, 112.9, 125.2, 126.6, 126.9, 130.0, 130.5, 132.7, 135.3, 136.2, 150.1, 155.5$ ppm; UV/vis (CH_2Cl_2): λ_{max} (lg ϵ) = 427 (4.40), 593 (3.27), 667 (3.30) nm; MS (ES⁺): m/z (%): 730 (100) $[\text{M}+\text{H}]^+$; HRMS (ES⁺) $[\text{C}_{50}\text{H}_{59}\text{N}_5+\text{H}]^+$: calcd 730.4867, found 730.4849.

7.2.2.5 2,3,7,8,12,13,17,18-Octaethyl-5-(4-*n*-pentylphenyl)-10-phenylporphyrin (**250**)

The reaction was performed following the general procedure using 40 equivalents of 1-bromo-4-pentylbenzene (0.93 mL, 5.24 mmol) and 50 equivalents of *n*-BuLi (2.62 mL, 6.55 mmol). Addition of *n*-BuLi was carried out at $0\text{ }^{\circ}\text{C}$ and the reaction mixture was stirred afterwards without cold bath at ambient temperature. 5-(Phenyl) OEP **1** (80 mg, 0.131 mmol) in THF was added after 1 hour and 20 minutes at $0\text{ }^{\circ}\text{C}$. After 30 minutes at rt, it was quenched at $0\text{ }^{\circ}\text{C}$, oxidized and purified to yield 46 mg (0.060 mmol, 45 %) of a purple solid. Mp $110\text{ }^{\circ}\text{C}$; ^1H NMR (400 MHz, CDCl_3): $\delta = 9.68$ (s, 2H, *meso* H), 8.37 (d, 2H, $J = 7.0$ Hz, phenyl H), 8.25 (d, 2H, $J = 7.8$ Hz, pentylphenyl H), 7.80 (t, 1H, $J = 7.4$ Hz, phenyl H), 7.72 (m, 2H, phenyl H), 7.53 (d, 2H, $J = 7.8$ Hz, pentylphenyl H), 3.98 (m, 4H, CH₂), 3.79 (m, 4H, CH₂), 2.99 (t, 2H, $J = 7.4$ Hz, pentyl CH₂), 2.73 (m, 4H, CH₂), 2.32 (m, 4H, CH₂), 1.86 (t, 6H, $J = 7.5$ Hz, CH₃), 1.62 (t, 6H, $J = 7.5$ Hz, CH₃), 1.52 (m, 6H, pentyl CH₂), 1.04 (t, 3H, $J = 6.8$ Hz, pentyl CH₃), 0.69 (m, 6H, CH₃), 0.50 (m, 6H, CH₃), -2.70 ppm (s, 2H, NH); ^{13}C NMR (100 MHz, CDCl_3): $\delta = 14.0, 14.1, 17.3, 17.9, 18.1, 19.3, 19.5, 20.5, 22.5, 22.6, 31.2, 31.4, 35.9, 94.7, 94.8, 119.2, 119.5, 125.7, 126.6, 126.8, 128.2, 135.1, 135.3, 138.7, 141.4, 143.1$ ppm; UV/vis

(CH₂Cl₂): λ_{\max} (lg ϵ) = 425 (5.50), 521 (4.29), 592 (4.13) nm; MS (ES⁺): m/z (%): 556 (39), 757 (38) [M+H]⁺; HRMS (ES⁺) [C₅₃H₆₄N₄+H]⁺: calcd 757.5209, found 757.5180.

7.2.2.6 2,3,7,8,12,13,17,18-Octaethyl-5-(4-bromophenyl)-10-phenylporphyrin (251)

The reaction was performed following the general procedure using 40 equivalents of 1,4-dibromobenzene (1.236 g, 5.24 mmol) and 50 equivalents of *n*-BuLi (2.6 mL, 6.55 mol). Addition of *n*-BuLi was carried out at -30 °C and the reaction mixture was stirred afterwards without cold bath at ambient temperature. 5-(Phenyl) OEP **4** (80 mg, 0.131 mmol) in THF was added after 1 hour 40 minutes at -30 °C and after 30 minutes stirring at rt, it was quenched at -30 °C with water, oxidized and purified to yield 47 mg (0.061 mmol, 46%) of a purple solid. Mp 119 °C; ¹H NMR (400 MHz, CDCl₃): δ = 9.66, 9.65 (each s, each 1H, *meso* H), 8.33 (m, 2H, phenyl H), 8.23 (d, 2H, *J* = 8.1 Hz, 4-bromophenyl H), 7.86 (d, 2H, *J* = 8.1 Hz, 4-bromophenyl H), 7.77 (t, 1H, *J* = 7.4 Hz, phenyl H), 7.69 (t, 2H, *J* = 7.4 Hz, phenyl H), 3.95 (q, 4H, *J* = 7.4 Hz, CH₂), 3.82 (m, 4H, CH₂), 2.71 (m, 4H, CH₂), 2.29 (m, 4H, CH₂), 1.84 (t, 6H, *J* = 7.5 Hz, CH₃), 1.59 (t, 6H, *J* = 7.4 Hz, CH₃), 0.66 (t, 6H, *J* = 7.3 Hz, CH₃), 0.47 (m, 6H, CH₃), -2.72 ppm (s, 2H, NH₂); ¹³C NMR (100 MHz, CDCl₃): δ = 11.2, 13.9, 17.0, 17.8, 18.0, 20.2, 20.4, 22.4, 25.0, 26.7, 28.8, 30.7, 31.4, 34.3, 34.4, 94.8, 94.9, 117.3, 119.3, 122.7, 126.4, 128.1, 129.6, 135.0, 136.5, 140.0, 141.1 ppm; UV/vis (CH₂Cl₂): λ_{\max} (lg ϵ) = 425 (3.99), 521 (3.81), 592 (3.61), sh nm, MS (ES⁺): m/z (%): 765 (48) [M+H]⁺; HRMS (ES⁺) [C₄₈H₅₃N₄Br+H]⁺: calcd 765.3532, found 765.3538.

7.2.2.7 2,3,7,8,12,13,17,18-Octaethyl-5-(3-methoxyphenyl)-10-phenylporphyrin (252)

The reaction was performed following the general procedure using 40 equivalents of 3-bromoanisole (0.66 mL, 5.24 mmol) and 50 equivalents of *n*-BuLi (2.62 mL, 6.55 mmol). Addition of *n*-BuLi was carried out at -60 °C and the reaction mixture was stirred afterwards without cold bath at ambient temperature. 5-(Phenyl) OEP **4** (80 mg, 0.131 mmol) in THF was added after 1 hour and 30 minutes at -50 °C. The reaction mixture was kept at -50 °C for 15 minutes and then stirred for 35 minutes at rt. It was quenched at -20 °C, oxidized and purified to yield 4 mg (0.0054 mmol, 4%) of a purple solid. Mp 133 °C, ¹H NMR (400 MHz, CDCl₃): δ = 9.63 (s, 2H, *meso* H), 8.31 (d, 2H, *J* = 6.8 Hz, phenyl H), 7.92 (d, 1H, *J* = 7.9 Hz, 3-OMe-phenyl), 7.87 (br s, 1H, 3-OMe-phenyl H), 7.76 (t, 1H, *J* = 7.2 Hz, phenyl H), 7.67 (t, 2H, *J* = 7.6 Hz, phenyl H), 7.57 (t, 1H, *J* =

7.6 Hz, 3-OMe-phenyl H), 7.33–7.31 (m, 1H, 3-OMe-phenyl), 3.95 (s, 3H, OMe), 3.92 (q, 4H, $J = 7.4$ Hz, CH₂), 3.81 (m, 4H, CH₂), 2.69–2.63 (m, 4H, CH₂), 2.34–2.25 (m, 4H, CH₂), 1.80 (t, 6H, $J = 7.6$ Hz, CH₃), 0.88 (m, 6H, CH₃), 0.70 (t, 3H, $J = 7.4$ Hz, CH₃), 0.62 (t, 3H, $J = 7.4$ Hz, CH₃), 0.51 (t, 3H, $J = 6.8$ Hz, CH₃), 0.44 (t, 3H, $J = 6.93$ Hz, CH₃), –2.74 ppm (s, 2H, NH); ¹³C NMR (100 MHz, CDCl₃): $\delta = 14.1, 17.35, 17.39, 17.4, 18.0, 18.2, 19.3, 19.5, 20.5, 22.6, 29.6, 55.5, 60.4, 94.9, 114.3, 118.9, 119.2, 120.8, 126.6, 127.5, 128.2, 135.2, 141.3, 142.6$ ppm; UV/vis (CH₂Cl₂): λ_{max} (lg ϵ) = 425 (4.59), 448 (4.36), 521 (3.48), sh, 592 (3.37), 636 (3.57) nm; MS (ES⁺): m/z (%): 717 (45); [M+H]⁺; HRMS (ES⁺) [C₄₉H₅₆N₄O+H]⁺: calcd 717.4523, found 717.4555. Furthermore as a second green fraction, 4 mg (0.0048 mmol, 3%) of the ABA substituted OEP **291** were obtained.

7.2.2.8 2,3,7,8,12,13,17,18-Octaethyl-5-(4-dimethylaminophenyl)-10-(3-trifluoromethylphenyl)-porphyrin (**253**)

The reaction was performed following the general procedure using 60 equivalents of 1-bromodimethylanilin (1.0088 g, 5.04 mmol) and 75 equivalents of *n*-BuLi (2.52 mL, 6.30 mmol). Addition of *n*-BuLi was carried out at –20 °C and the reaction mixture was stirred afterwards without cold bath at ambient temperature. 5-(3-trifluoromethylphenyl) OEP **6** (57 mg, 0.084 mmol) in THF (low solubility) was added after 40 minutes at rt and after 25 minutes, it was quenched at the same temperature with water, oxidized and purified to yield 33 mg (0.041 mmol, 48 %) of a purple solid. Mp 125 °C; ¹H NMR (400 MHz, CDCl₃): $\delta = 9.64, 9.61$ (each s, each 1H, *meso* H), 8.66 (s, 1H, 3-CF₃phenyl H), 8.50 (d, 1H, $J = 7.5$ Hz, 3-CF₃phenyl H), 8.11 (d, 2H, $J = 8.0$ Hz, 4-NMe₂phenyl H), 8.05 (d, 1H, $J = 7.9$ Hz, 3-CF₃phenyl), 7.82 (t, 1H, $J = 7.6$ Hz, 3-CF₃phenyl), 7.04 (d, 2H, $J = 8.7$ Hz, 4-NMe₂phenyl), 3.93 (q, 4H, $J = 7.32$ Hz, CH₂), 3.81 (m, 4H, CH₂), 3.23 (s, 6H, NMe₂), 2.62 (m, 4H, CH₂), 2.35 (m, 4H, CH₂), 1.81 (t, 6H, $J = 7.84$ Hz, CH₃), 0.89 (m, 6H, CH₃), 0.63 (m, 6H, CH₃), 0.45 (t, 3H, $J = 6.33$ Hz, CH₃), 0.39 (t, 3H, $J = 6.71$ Hz, CH₃), –2.68 ppm (s, 2H, NH); ¹³C NMR (100 MHz, CDCl₃): $\delta = 14.0, 14.7, 17.2, 17.3, 17.9, 18.1, 18.3, 19.2, 19.3, 19.4, 19.5, 20.3, 20.4, 20.6, 22.6, 25.2, 26.8, 28.9, 29.6, 31.5, 34.6, 39.8, 40.6, 74.1, 94.5, 95.1, 110.4, 110.5, 110.9, 112.4, 116.7, 120.6, 124.7, 125.0, 126.8, 127.1, 130.1, 136.1, 138.3, 142.1, 150.5, 153.1$ ppm; UV/vis (CH₂Cl₂): λ_{max} (lg ϵ) = 429 (4.72), 513 (sh), 595 (3.67), 663 (3.74) nm; MS

(ES+): m/z (%): 798 (40) $[M+H]^+$; HRMS (ES+) $[C_{51}H_{58}N_5F_3+H]^+$: calcd 798.4723, found 798.4743.

7.2.2.9 2,3,7,8,12,13,17,18-Octaethyl-5,10-bis(4-*n*-pentylphenyl)porphyrin (254)

The reaction was performed following the general procedure, using 40 equivalents of 1-bromo-4-pentylbenzene (0.83 mL, 4.68 mmol) and 50 equivalents of *n*-BuLi (2.34 mL, 5.87 mmol). Addition of *n*-BuLi was carried out at -20 °C and the reaction mixture was stirred afterwards without cold bath at ambient temperature. 5-(4-*N*-pentylphenyl) OEP **5** (80 mg, 0.117 mmol) in THF was added after 1 hour and 20 minutes at rt and after 1 hour stirring at the same temperature, it was quenched with water at 0 °C, oxidized and purified to yield 46 mg (0.055 mmol, 47%) of a purple solid. Mp 60 °C; 1H NMR (400 MHz, $CDCl_3$): δ = 9.62 (s, 2H, *meso* H), 8.19 (d, 4H, J = 7.9 Hz, phenyl H), 7.48 (d, 4H, J = 7.9 Hz, phenyl H), 3.83 (q, 4H, J = 7.4 Hz, CH_2), 3.81 (m, 4H, CH_2), 2.95 (t, 4H, J = 7.4 Hz, pentyl CH_2), 2.70 (br m, 4H, CH_2), 2.28 (br m, 4H, CH_2), 1.88 (m, 4H, pentyl CH_2), 1.81 (t, 6H, J = 7.4 Hz, CH_3), 1.57 (t, 6H, J = 7.4 Hz, CH_3), 1.49 (m, 8H, pentyl CH_2), 1.00 (t, 6H, J = 6.8 Hz, pentyl CH_3), 0.64 (t, 6H, J = 7.35 Hz, CH_3), 0.45 (t, 6H, J = 6.75 Hz, CH_3), -2.71 ppm (s, 2H, NH); ^{13}C NMR (100 MHz, $CDCl_3$): δ = 14.2, 17.3, 18.0, 18.1, 19.5, 19.6, 20.5, 22.6, 29.7, 31.3, 31.4, 35.9, 94.7, 119.4, 135.2, 138.7, 143.1 ppm; UV/vis (CH_2Cl_2): λ_{max} (lg ϵ) = 425 (5.17), 521 (4.00), 592 (3.78), 639 (sh) nm; MS (ES+): m/z (%): 827 (100) $[M+H]^+$; HRMS (ES+) $[C_{58}H_{74}N_4+H]^+$: calcd 827.5992, found 827.5952.

7.2.2.10 2,3,7,8,12,13,17,18-Octaethyl-5-(9-anthracenyl)-10-(4-*n*-pentylphenyl)porphyrin (255)

The reaction was performed following the general procedure using 60 equivalents of 9-bromoanthracene (1.3668 g, 5.40 mmol) and 75 equivalents of *n*-BuLi (2.7 mL, 6.75 mmol). Addition of *n*-BuLi was carried out at -30 °C and the reaction mixture was stirred afterwards without cold bath at ambient temperature. 5-(4-*N*-pentylphenyl) OEP **5** (62 mg, 0.090 mmol) in THF was added after 1 hour at -10 °C and after 4 hours of stirring at rt, it was quenched at 0 °C with water, oxidized and purified to yield 30 mg (0.035 mmol, 38%) of a purple solid. Mp 72 °C; 1H NMR (400 MHz, $CDCl_3$) δ = 9.70 (s, 1H, *meso* H), 9.68 (s, 1H, *meso* H), 8.90 (s, 1H, anthracenyl H), 8.25 (d, 2H, J = 8.1 Hz, anthracenyl H), 8.19 (d, 2H, J = 7.8 Hz, phenyl H), 7.51 (m, 4H, anthracenyl H, 2H

phenyl H), 7.13 (m, 2H, anthracenyl H), 3.98 (m, 4H, CH₂), 3.85 (m, 2H, CH₂), 3.65 (m, 2H, CH₂), 2.93 (t, 2H, *J* = 7.4 Hz, pentyl CH₂), 2.70 (m, 2H, CH₂), 2.16 (m, 2H, CH₂), 1.86 (m, 6H, CH₃, 2H, CH₂), 1.72 (m, 2H, CH₂), 1.60 (t, 3H, *J* = 7.5 Hz, CH₃), 1.47 (m, 6H, pentyl CH₂, 3H, CH₃), 1.00 (m, 3H, pentyl CH₃), 0.71 (t, 3H, *J* = 7.4 Hz, CH₃), 0.36 (t, 3H, *J* = 7.2 Hz, CH₃), 0.02 (t, 3H, *J* = 7.5 Hz, CH₃), -0.07 (t, 3H, *J* = 7.5 Hz, CH₃), -2.48 ppm (s, 2H, NH); ¹³C NMR (100 MHz, CDCl₃): δ = 1.3, 14.1, 15.2, 15.8, 17.3, 17.8, 18.1, 19.3, 19.7, 20.3, 20.8, 22.5, 26.9, 29.0, 31.2, 31.6, 34.6, 35.9, 94.1, 95.1, 113.6, 125.4, 125.8, 126.7, 127.8, 128.0, 128.8, 130.9, 135.1, 135.6 ppm; UV/vis (CH₂Cl₂): λ_{max} (lg ε) = 425 (4.68), 520 (3.63), 592 (3.34), 644 (2.78) nm; MS (ES⁺): *m/z* (%): 578 (60), 857 (20) [M+H]⁺; HRMS (ES⁺) [C₆₁H₆₈N₄+H]⁺: calcd 857.5522, found 857.5541.

7.2.2.11 2,3,7,8,12,13,17,18-Octaethyl-5-(4-*n*-pentylphenyl)-10-(9-phenanthrenyl)porphyrin (256)

The reaction was performed following the general procedure, using 40 equivalents of 1-bromophenanthrene (2.263 g, 8.80 mmol) and 40 equivalents of *n*-BuLi (3.52 mL, 8.80 mmol). Addition of *n*-BuLi was carried out at -50 °C and the reaction mixture was stirred afterwards without cold bath at ambient temperature. 5-(4-Pentylphenyl) OEP **3** (150 mg, 0.220 mmol) in THF was added after 1 hour 30 minutes at -30 °C. After 40 minutes at rt, it was quenched at -30 °C, oxidized and purified to yield 32 mg (0.037 mmol, 16 %) of purple crystals from MeOH / CH₂Cl₂. Mp 165 °C; ¹H NMR (400 MHz, CDCl₃): δ = 9.71 (s, 1H, *meso* H), 9.70 (s, 1H, *meso* H), 9.01 (d, 1H, *J* = 9.6 Hz, phenanthrenyl H), 9.00 (d, 1H, *J* = 9.0 Hz, phenanthrenyl H), 8.70 (s, 1H, phenanthrenyl H), 8.23 (m, 2H, phenyl H), 8.12 (d, 1H, *J* = 7.6 Hz, phenanthrenyl H), 7.89 (t, 1H, *J* = 7.6 Hz, phenanthrenyl H), 7.80 (t, 1H, *J* = 7.5 Hz, phenanthrenyl H), 7.72 (t, 1H, *J* = 7.5 Hz, phenanthrenyl H), 7.63 (d, 1H, *J* = 8.2 Hz, phenanthrenyl H), 7.50 (d, 2H, *J* = 7.6 Hz, phenyl H), 7.32 (t, 1H, *J* = 7.4 Hz, phenanthrenyl H), 3.99 (m, 4H, CH₂), 3.87 (m, 2H, CH₂), 3.74 (m, 2H, CH₂), 2.97 (t, 2H, *J* = 7.3 Hz, pentyl CH₂), 2.74 (m, 2H, CH₂), 2.61 (m, 2H, CH₂), 2.25 (m, 4H, CH₂), 1.86 (t, 6H, *J* = 7.2 Hz, CH₃), 1.62 (t, 3H, *J* = 7.3 Hz, CH₃), 1.52 (m, 3H, CH₃, 6H, pentyl CH₂), 1.01 (m, 3H, pentyl CH₃), 0.70 (t, 3H, *J* = 7.2 Hz, CH₃), 0.42 (t, 3H, *J* = 7.2 Hz, CH₃), 0.40 (m, 6H, CH₃), -2.53 ppm (br s, 2H, NH); ¹³C NMR (100 MHz, CDCl₃): δ = 14.1, 16.4, 16.7, 17.3, 18.0, 18.1, 19.3, 19.4, 19.6, 19.7, 20.6, 20.5, 22.6, 31.2, 31.4, 35.8, 94.8, 95.1, 116.0, 119.2, 119.8, 122.5,

122.9, 126.4, 126.6, 126.7, 127.1, 127.2, 129.1, 129.5, 130.7, 131.0, 134.1, 135.1, 136.5, 137.4, 138.7, 143.1 ppm; UV/vis (CH₂Cl₂): λ_{\max} (lg ϵ) = 460 (5.25), 589 (4.19), 639 (4.07) nm; MS (ES⁺): m/z (%): 857 (48) [M+H]⁺; HRMS (ES⁺) [C₆₁H₆₈N₄+H]⁺: calcd 857.5522, found 857.5526. Furthermore, a second, green fraction was obtained and identified as 58 mg (0.056 mmol, 25%) of the trisubstituted OEP **288** and the last green fraction couldn't be identified.

7.2.2.12 2,3,7,8,12,13,17,18-Octaethyl-5,10-bis(1-naphthyl)porphyrin (**257**)

The reaction was performed following the general procedure using 60 equivalents of 1-bromonaphthalene (1.08 mL, 8.00 mmol) and 75 equivalents of *n*-BuLi (3.99 mL, 9.97 mmol). Addition of *n*-BuLi was carried out at -20 °C and the reaction mixture was stirred afterwards without cold bath at ambient temperature. 5-(1-Naphthyl) OEP **7** (88 mg, 0.133 mmol) in THF was added after 45 minutes at rt and after 25 minutes stirring, it was quenched at rt with water, oxidized and purified to yield 46 mg (0.060 mmol, 44%) of a purple solid. Mp 178 °C; ¹H NMR (400 MHz, CDCl₃): δ = 9.69 (s, 1H, *meso* H), 9.67 (s, 1H, *meso* H), 8.47 (d, 1H, *J* = 6.8 Hz, naphthyl H), 8.40 (d, 1H, *J* = 6.8 Hz, naphthyl H), 8.27 (d, 2H, *J* = 8.2 Hz, naphthyl H), 8.09 (m, 2H, naphthyl H), 7.81 (m, 2H, naphthyl H), 7.50 (m, 4H, naphthyl H), 7.20 (m, 2H, naphthyl H), 3.98 (m, 4H, CH₂), 3.75 (m, 4H, CH₂), 2.60 (m, 2H, CH₂), 2.42 (m, 2H, CH₂), 2.23–2.00 (m, 4H, CH₂), 1.84 (m, 6H, CH₃), 0.89 (m, 6H, CH₃), 0.45 (m, 6H, CH₃), 0.26 (m, 6H, CH₃), -2.44 (s, 1H, NH), -2.52 ppm (s, 1H, NH); ¹³C NMR (100 MHz, CDCl₃): δ = 13.9, 14.0, 14.1, 16.6, 16.7, 16.93, 16.95, 18.01, 18.02, 18.6, 19.4, 19.6, 20.5, 22.4, 22.5, 22.6, 31.2, 31.5, 33.7, 35.2, 35.5, 95.0, 95.1, 116.0, 124.3, 124.4, 125.9, 126.6, 127.7, 127.9, 128.0, 128.2, 129.0, 132.6, 132.7, 133.2, 133.3, 137.2, 137.3, 138.8, 139.1 ppm; UV/vis (CH₂Cl₂): λ_{\max} (lg ϵ) = 426 (4.89), 521 (3.79), 592 (3.53) nm; MS (ES⁺): m/z (%): 787 (90) [M+H]⁺; HRMS (ES⁺) [C₅₆H₅₈N₄+H]⁺: calcd 787.4740, found 787.4733. As it can be seen in the ¹H NMR spectrum and as it has been described in chapter 3, the title compound **257** was afforded in a mixture of two atropisomers due to the at ambient temperature hindered naphthyl rotation.

7.2.2.13 2,3,7,8,12,13,17,18-Octaethyl-5-(1-naphthyl)-10-(4-n-pentylphenyl)porphyrin (258)

The reaction was performed following the general procedure, using 40 equivalents of 1-bromo-4-pentylbenzene (0.85 mL, 4.84 mmol) and 50 equivalents of *n*-BuLi (2.42 mL, 6.05 mmol). Addition of *n*-BuLi was carried out at $-30\text{ }^{\circ}\text{C}$ and the reaction mixture was stirred afterwards without cold bath at ambient temperature. 5-(1-Naphthyl) OEP **7** (80 mg, 0.121 mmol) in THF was added after 1 hour and 20 minutes at $-0\text{ }^{\circ}\text{C}$. After 30 minutes at rt, it was quenched at $0\text{ }^{\circ}\text{C}$, oxidized and purified to yield 46 mg (0.057 mmol, 47%) of a purple solid. Mp $133\text{ }^{\circ}\text{C}$; ^1H NMR (400 MHz, CDCl_3): $\delta = 9.67$ (s, 1H, *meso* H), 9.66 (s, 1H, *meso* H), 8.41 (d, 1H, $J = 6.8$ Hz, naphthyl H), 8.28 (d, 1H, $J = 8.2$ Hz, naphthyl H), 8.20 (d, 2H, $J = 7.8$ Hz, phenyl H), 8.11 (d, 1H, $J = 7.9$ Hz, naphthyl H), 7.81 (m, 1H, naphthyl H), 7.52 (m, 2H, naphthyl H), 7.47 (d, 2H, $J = 7.8$ Hz, phenyl H), 7.20 (m, 1H, naphthyl H), 3.95 (q, 4H, $J = 7.5$ Hz, CH_2), 3.83 (m, 2H, CH_2), 3.73 (m, 2H, CH_2), 2.95 (t, 2H, $J = 7.4$ Hz, pentyl CH_2), 2.70 (m, 2H, CH_2), 2.40 (m, 2H, CH_2), 2.25 (m, 2H, CH_2), 2.11 (m, 2H, CH_2), 1.83 (m, 6H, CH_3), 1.59 (t, 3H, $J = 7.5$ Hz, CH_3), 1.53 (m, 6H, pentyl CH_2 , 3H, CH_3), 0.99 (m, 3H, pentyl CH_3), 0.67 (t, 3H, $J = 7.4$ Hz, CH_3), 0.45 (m, 6H, CH_3), 0.33 (t, 3H, $J = 7.3$ Hz, CH_3), -2.61 ppm (s, 2H, NH); ^{13}C NMR (100 MHz, CDCl_3): $\delta = 14.1, 16.5, 16.9, 17.3, 17.9, 18.1, 19.4, 19.5, 19.6, 20.4, 20.5, 22.6, 26.9, 31.2, 31.4, 35.8, 94.8, 95.0, 116.2, 124.4, 125.8, 126.0, 126.7, 127.7, 128.1, 128.9, 132.7, 133.4, 135.1, 137.2, 139.2, 143.1$ ppm; UV/vis (CH_2Cl_2): λ_{max} (lg ϵ) = 426 (4.88), sh, 519 (3.74), 555 (3.61), 592 (3.72), 643 (3.48) nm; MS (ES⁺): m/z (%): 807 (100) [$\text{M}+\text{H}$]⁺; HRMS (ES⁺) [$\text{C}_{57}\text{H}_{66}\text{N}_4+\text{H}$]⁺: calcd 807.5366, found 807.5374.

7.2.2.14 2,3,7,8,12,13,17,18-Octaethyl-5,10-bis(9-phenanthrenyl)porphyrin (9)

The reaction was performed following the general procedure, using 40 equivalents of 9-bromophenanthrene (2.137 g, 8.44 mmol) and 40 equivalents of *n*-BuLi (3.37 mL, 8.44 mmol). Addition of *n*-BuLi was carried out at $-50\text{ }^{\circ}\text{C}$ and the reaction mixture was stirred afterwards without cold bath at ambient temperature. 5-(9-Phenanthrenyl) OEP **8** (150 mg, 0.221 mmol) in THF was added after 1 hour at $-50\text{ }^{\circ}\text{C}$ and after 45 minutes stirring at rt, it was quenched at $-30\text{ }^{\circ}\text{C}$ with water, oxidized and purified to yield 81 mg (0.093 mmol, 43%) of purple crystals from MeOH/ CH_2Cl_2 . Mp $> 300\text{ }^{\circ}\text{C}$; ^1H NMR (400 MHz, CDCl_3): $\delta = 9.73, 9.70$ (each s, each 1H, *meso* H), 8.98 (d, 2H, $J = 8.4$ Hz, phenanthrenyl H), 8.94 (d, 2H, $J = 7.2$ Hz, phenanthrenyl H), 8.74 (s, 1H, phenanthrenyl

H), 8.65 (s, 1H, phenanthrenyl H), 8.12 (d, 1H, $J = 7.6$ Hz, phenanthrenyl H), 8.08 (d, 1H, $J = 7.6$ Hz, phenanthrenyl H), 7.87 (t, 2H, $J = 7.6$, phenanthrenyl H), 7.78 (m, 2H, phenanthrenyl H), 7.69 (m, 2H, phenanthrenyl H), 7.60 (m, 2H, phenanthrenyl H), 7.31 (m, 2H, phenanthrenyl H), 3.98 (m, 4H, CH₂), 3.74 (m, 4H, CH₂), 2.57 (m, 2H, CH₂), 2.28 (m, 2H, CH₂), 2.02 (m, 4H, CH₂), 1.85 (m, 6H, CH₃), 1.53 (m, 6H, CH₃), 0.49 (m, 6H, CH₃), 0.30 (m, 6H, CH₃), -2.40 (s, 1H, NH), -2.41 ppm (s, 1H, NH); ¹³C NMR (100 MHz, CDCl₃): $\delta = 116.4, 16.7, 17.9, 18.1, 19.4, 19.5, 20.7, 29.6, 32.0, 55.3, 55.5, 95.2, 115.8, 122.3, 122.8, 123.0, 124.3, 125.8, 126.4, 126.5, 127.1, 127.5, 128.5, 128.6, 128.8, 129.0, 129.1, 129.2, 129.4, 133.9, 134.7, 136.4, 137.0, 137.3, 203.3, 205.3$ ppm; UV/vis (CH₂Cl₂): λ_{max} (lg ϵ) = 426 (5.45), 455 (5.03), 519 (4.56), sh, 592 (4.35), sh nm; MS (ES⁺): m/z (%): 887 (14) [M+H]⁺; HRMS (ES⁺) [C₆₄H₆₂N₄+H]⁺: calcd 887.5053, found 887.5009. Furthermore, a second, green fraction was obtained and identified as 57 mg (0.055 mmol, 25%) of the green trisubstituted OEP **10** and the last green fraction contained 21 mg (0.0169 mmol, 7%) of the tetrasubstituted OEP **11**. When 110 mg of 5-(9-phenanthrenyl) OEP **8** were reacted with 31 equivalents of 9-bromophenanthrene (1.213 g, 4.79 mmol) and 40 equivalents of *n*-BuLi (2.46 mL, 6.16 mmol), 14 mg (0.018 mol, 12%) of the *meso* 5,10-disubstituted OEP **9**, 13 mg (0.0135 mmol, 9%) of the trisubstituted OEP **10** and 29 mg (0.0165 mmol, 11%) of the tetrasubstituted OEP **11** were obtained. When 66 mg (0.092 mmol) of 5-(9-phenanthrenyl) OEP **8** were reacted with 60 equivalents of 9-bromophenanthrene (1.431 mg, 5.57 mmol) and 60 equivalents *n*-BuLi (2.2 mL, 5.57 mmol) the yields were shifted to the tetrasubstituted OEP **11**. A mixture of 63 mg crude di- and trisubstituted OEP **9** and **10** was isolated together with 63 mg (0.050 mmol, 54%) of green crystals of the tetrasubstituted OEP **11** precipitated from *n*-hexane/MeOH by addition of perchloric acid and which was deprotonated by passing through aluminium oxide to afforded 48 mg (0.0392 mmol, 42%) pure OEP **11**. The tri- and tetrasubstituted OEPs **10** and **11** are displayed with full details in chapter 8.2.3.10 and 8.2.4.1 As it can be seen in the ¹H NMR spectrum and as it has been described in chapter 3, the title compound **9** was afforded in a statistical mixture (1/1) of atropisomers due to the at ambient temperature hindered phenanthrenyl rotation.

7.2.2.15 2,3,7,8,12,13,17,18-Octaethyl-5-(1-naphthyl)-10-(9-phenanthrenyl)porphyrin (259)

The reaction was performed following the general procedure using 40 equivalents of 9-bromophenanthrene (1.2427 g, 4.84 mmol) and 50 equivalents of *n*-BuLi (2.42 mL, 6.05 mmol). Addition of *n*-BuLi was carried out at $-30\text{ }^{\circ}\text{C}$ and the reaction mixture was stirred afterwards without cold bath at ambient temperature. 5-(1-Naphthyl) OEP **7** (80 mg, 0.121 mmol) in THF was added after 1 hour at $-10\text{ }^{\circ}\text{C}$. After 30 minutes at rt, it was quenched at $-0\text{ }^{\circ}\text{C}$, oxidized and purified to yield 47 mg (0.056 mmol, 46%) of a purple solid. Mp $140\text{ }^{\circ}\text{C}$; ^1H NMR (400 MHz, CDCl_3): $\delta = 9.71$ (s, 1H, *meso* H), 9.68 (s, 1H, *meso* H), 8.99–8.93 (m, 2H, phenanthrenyl H), 8.72 (s, 0.5H, phenanthrenyl H), 8.67 (s, 0.5H, phenanthrenyl H), 8.49 (d, 0.5H, $J = 6.7$ Hz, naphthyl H), 8.39 (d, 0.5H, $J = 6.7$ Hz, naphthyl H), 8.26 (d, 1H, $J = 8.6$ Hz, naphthyl H), 8.09 (m, 1H, phenanthrenyl H, 1 H naphthyl H), 7.88–7.77 (m, 2H, phenanthrenyl H, 1H, naphthyl H), 7.69 (m, 1H, phenanthrenyl H), 7.59–7.48 (m, 2H, naphthyl H, 2H, phenanthrenyl H), 7.32 (m, 1H, phenanthrenyl H), 7.20 (m, 1H, naphthyl H), 3.97 (m, 4H, CH_2), 3.75 (m, 4H, CH_2), 2.57–2.00 (br m, 8H, CH_2), 1.85 (m, 6H, CH_3), 0.89 (m, 6H, CH_3), 0.47 (m, 6H, CH_3), 0.31–0.22 (m, 6H, CH_3), -2.42 (s, 1H, NH), -2.50 ppm (s, 1H, NH); ^{13}C NMR (100 MHz, CDCl_3): $\delta = 11.0, 11.4, 14.1, 16.5, 16.9, 18.0, 18.3, 19.4, 19.5, 19.6, 20.4, 20.6, 20.7, 22.7, 25.2, 26.8, 27.6, 29.0, 31.5, 34.7, 35.9, 41.4, 95.3, 116.0, 122.4, 122.9, 124.4, 125.9, 126.5, 127.0, 127.6, 128.8, 129.1, 129.6, 130.8, 132.5, 133.3, 133.9, 136.5, 137.4$ ppm; UV/vis (CH_2Cl_2): λ_{max} ($\lg \epsilon$) = 430 (5.01), 455 (5.01), 519 (3.90), 591 (4.04), 554 (sh), 643 (3.81) nm; MS (ES⁺): m/z (%): 837 (19) $[\text{M}+\text{H}]^+$; HRMS (ES⁺) $[\text{C}_{60}\text{H}_{60}\text{N}_4+\text{H}]^+$: calcd 837.4896, found 837.4871. Furthermore, a second green fractions was obtained, containing 22 mg (0.0217 mmol, 14%) of the green trisubstituted OEP **289**. As it can be seen in the ^1H NMR spectrum and as it has been described in chapter 3, the title compound **259** was afforded in a statistical mixture of atropisomers due to the at ambient temperature hindered phenanthrenyl and naphthyl rotation.

7.2.2.16 2,3,7,8,12,13,17,18-Octaethyl-5-(4-dimethylaminophenyl)-10-(9-phenanthrenyl)porphyrin (260)

The reaction was performed following the general procedure, using 40 equivalents of 1-bromoanilin (0.942 g, 4.71 mmol) and 50 equivalents of *n*-BuLi (2.35 mL, 5.88 mmol). Addition of *n*-BuLi was carried out at $-30\text{ }^{\circ}\text{C}$ and the reaction mixture was stirred

afterwards without cold bath at ambient temperature. 5-(9-phenanthrenyl) OEP **8** (80 mg, 0.117 mmol) in THF was added after 1 hour at 0 °C and after 30 minutes stirring at rt, it was quenched at the same temperature, oxidized and purified to yield 70 mg (0.084 mmol, 71%) of a purple solid. Mp > 300 °C; ¹H NMR (400 MHz, CDCl₃): δ = 9.64 (s, 1H, *meso* H), 9.61 (s, 1H, *meso* H), 9.00 (d, 1H, *J* = 8.5 Hz, phenanthrenyl H), 8.97 (d, 1H, *J* = 7.2 Hz, phenanthrenyl H), 8.66 (s, 1H, phenanthrenyl H), 8.09 (m, 1H, phenanthrenyl H, 2H phenyl H), 7.85 (m, 1H, phenanthrenyl H), 7.76 (m, 1H, phenanthrenyl H), 7.70 (m, 1H, phenanthrenyl H), 7.63 (m, 1H, phenanthrenyl H), 7.28 (m, 1H, phenanthrenyl H), 7.00 (d, 2H, *J* = 8.6 Hz, phenyl H), 3.93 (m, 4H, CH₂), 3.81 (m, 2H, CH₂), 3.70 (m, 2H, CH₂), 3.19 (s, 6H, NMe₂), 2.83 (m, 2H, CH₂), 2.55 (m, 2H, CH₂), 2.22 (m, 4H, CH₂), 1.80 (m, 6H, CH₃), 1.55 (t, 3H, *J* = 7.6 Hz, CH₃), 1.48 (m, 3H, CH₃), 0.63 (t, 3H, *J* = 7.3 Hz, CH₃), 0.44 (t, 3H, *J* = 7.3 Hz, CH₃), 0.32 (m, 6H, CH₃), –2.55 ppm (s, 2H, NH); ¹³C NMR (100 MHz, CDCl₃): δ = 16.3, 16.6, 17.1, 17.4, 17.9, 18.2, 19.2, 19.4, 19.6, 19.8, 20.5, 26.8, 40.1, 40.8, 94.3, 94.9, 110.6, 115.8, 120.2, 122.2, 122.9, 126.7, 127.1, 129.1, 129.6, 130.2, 130.7, 131.0, 134.2, 136.3, 136.3, 137.4, 150.6 ppm; UV/vis (CH₂Cl₂): λ_{max} (lg ε) = 433 (4.93), 521 (4.04), 596 (3.63), 664 (3.45) nm; MS (ES⁺): *m/z* (%): 578 (60), 830 (60) [M+H]⁺, 831 (20/2) [M+2H]⁺⁺; HRMS (ES⁺) [C₅₈H₆₃N₅+H]⁺: calcd. 830.5162, found 830.5185.

7.2.2.17 (2,3,7,8,12,13,17,18-Octaethyl-5-phenyl-10-*s*-butylporphyrinato)palladium (II) (**276**)

5-Phenyl Pd(II)OEP **273** (80 mg, 0.112 mmol) was dissolved in 35 mL THF under an argon atmosphere and 0.8 mL of *s*-BuLi (1.12 mmol, 10 equivalents, 1.4 M) were added slowly at –60 °C. The reaction mixture turned dark red within 10 minutes of stirring and it was quenched with 1 mL of water at the same temperature after 20 minutes and oxidized with a solution of DDQ (50 mg, 0.224 mmol) in 15 mL dichloromethane subsequently. Purification was carried out on silica gel with H/CH₂Cl₂ = 3/1 to afford a single dark red fraction e.g. 35 mg (0.045 mmol, 37%) of a dark red solid, formed by the title compound and the respective 5,15 regio isomer **277**. Precipitation from CH₂Cl₂/methanol afforded a small amount of red crystals (9 mg) of the 5,15-disubstituted regio isomer **277** as described in chapter 2.2.4 and section 8.2.2.18, while the 5,10 regio isomer remained in solution. ¹H NMR (400 MHz, CDCl₃): 9.58 (s, 1H, *meso* H), 9.50 (s, 1H, *meso* H), 8.12 (d, 2H, *J* = 8.6 Hz, phenyl H), 7.74 (t, 1H, *J* = 7.4

Hz, phenyl H), 7.62 (t, 2H, $J = 7.5$ Hz, phenyl H), 4.49 (m, 1H, *s*-butyl CH), 3.97-3.73 (m, 12H, CH₂), 2.68-2.32 (m, 4H, CH₂), 2.25 (d, 3H, $J = 7.0$ Hz, *s*-butyl CH₃), 1.79 (m, 12H, CH₃), 1.64 (t, 3H, $J = 7.6$ Hz, CH₃), 1.52 (t, 3H, $J = 7.2$ Hz, CH₃), 0.98 (m, 2H, *s*-butyl CH₂), 0.86 (m, 6H, CH₃), 0.48 (t, 3H, $J = 7.3$ Hz, *s*-butyl CH₃) ppm.

7.2.2.18 (2,3,7,8,12,13,17,18-Octaethyl-5-phenyl-15-*s*-butylporphyrinato)palladium
(II) (277)

The OEP **277** was afforded in a mixture with the OEP **276** as described in section 8.2.2.17 and could be separated by precipitation from CH₂Cl₂/MeOH e.g. 9 mg (0.011 mmol, 9%) red crystals were obtained. ¹H NMR (400 MHz, CDCl₃): $\delta = 9.76$ (s, 2H, *meso* H), 8.08 (d, 2H, $J = 7.6$ Hz, phenyl H), 7.43 (t, 1H, $J = 7.4$ Hz, phenyl H), 7.60 (t, 2H, $J = 7.9$ Hz, phenyl H), 4.51 (m, 1H, *s*-butyl CH), 4.16 (m, 2H, CH₂), 3.92-3.83 (m, 12H, CH₂), 2.67 (m, 4H, CH₂, *s*-butyl CH₂), 2.58 (d, 3H, $J = 7.3$, *s*-butyl CH₃), 1.77 (t, 12H, $J = 7.6$ Hz, CH₃), 1.64 (t, 6H, $J = 7.6$ Hz, CH₃), 1.02 (t, 6H, $J = 7.2$ Hz, CH₃), 0.11 ppm (t, 3H, $J = 7.3$ Hz, *s*-butyl CH₃); ¹³C NMR (100 MHz, CDCl₃): $\delta = 13.3, 14.1, 17.9, 18.2, 19.5, 19.7, 21.1, 22.0, 24.5, 29.6, 31.5, 33.3, 40.6, 50.9, 98.6, 126.3, 133.2, 136.8, 137.6, 138.2, 141.4, 142.4, 143.4, 143.6, 144.2$ ppm; UV/vis (CH₂Cl₂): λ_{max} (lg ϵ) = 417 (4.55), 533 (3.53), 563 (3.48) nm.

7.2.2.19 (2,3,7,8,12,13,17,18-Octaethyl-5-phenyl-10-*n*-butylporphyrinato)palladium
(II) (285)

The reaction was performed following the general procedure, using 25 equivalents of 1-bromoaphthalene (0.29 mL, 2.1 mmol) and 95 equivalents of *n*-BuLi (3.46 mL, 7.98 mmol). Addition of *n*-BuLi was carried out at -50 °C and the reaction mixture was stirred afterwards without cold bath at ambient temperature. 5-(1-Phenyl) Pd(II)OEP **273** (60 mg, 0.084 mmol) in 30 mL THF (low solubility) was added after 1 hour and 20 minutes at rt and it was stirred at -40 °C for 20 minutes, while the reaction mixture turned from red to brown to green, and stirring was continued afterwards at rt for 40 minutes. Then it was quenched with water at -10 °C, oxidized and purified to yield 33 mg (0.028 mmol, 50%) of a pink-red solid. ¹H NMR (400 MHz, CDCl₃): $\delta = 9.76$ (s, 2H, *meso* H), 7.69 (s, 1H *meso* H), 7.86-7.49 (br m, 5H, phenyl H), 4.77 (br m, 2H, *n*-butyl CH₂), 3.94 (m, 14H, 12H CH₂, 2H *n*-butyl CH₂), 2.92-2.35 (br m, 4H, CH₂), 2.01 (t, 3H, $J = 7.5$ Hz, CH₃), 1.86 (m, 14H, 12H, CH₃, 2H *n*-butyl CH₂), 1.76 (t, 3H, $J = 7.5$ Hz,

CH₃), 1.12 (m, 6H, CH₃), 0.56 ppm (t, 3H, *J* = 7.2 Hz, *n*-butyl CH₃); ¹³C NMR (100 MHz, CDCl₃): δ = 13.7, 17.8, 18.2, 18.3, 19.5, 19.6, 20.5, 20.9, 21.6, 22.6, 23.3, 29.7, 34.3, 38.1, 53.4, 93.6, 97.6, 118.8, 120.9, 126.4, 128.2, 133.6, 137.2, 137.6, 138.2, 138.6, 138.9, 139.1, 139.5, 141.3, 141.4, 141.6, 141.9, 143.0, 144.0, 145.4 ppm.

7.2.2.20 (2,3,7,8,12,13,17,18-Octaethyl-5,10-bis-*n*-butylporphyrinato)palladium (II) (274)

5-*N*-Butyl Pd(II)OEP **17** (100 mg, 0.143 mmol) was dissolved in 40 mL THF under an argon atmosphere and 0.74 mL of *n*-BuLi (1.87 mmol, 13 equivalents, 2.5 M in hexane) were added slowly at -50 °C. The reaction mixture turned dark brown-green and stirring was continued at the same temperature for 35 minutes. It was quenched with 1 mL of water at -40 °C and oxidized with a solution of DDQ (64 mg, 0.286 mmol) in 15 mL dichloromethane. Purification was carried out on silica gel with H/CH₂Cl₂ = 2/1 to afford a single dark red fraction e.g. 88 mg (0.117 mmol, 82%) of a dark red solid, formed by the title compound, the respective 5,15 regioisomer **275** (3/1 mixture) and 5-*n*-butyl Pd(II)OEP **17**. Further separation was not possible and the OEPs **274**, **275** were identified as shown in figure 2.2.4.2 due to their *meso* proton and CH₂ *n*-butyl signals at 9.63, 9.61 and 4.46 ppm (**274**) and 9.78 and 4.59 (**275**). ¹H NMR (400 MHz, CDCl₃): δ = 9.66 (s, 0.5H, *meso* H), 9.56 (s, 1.5H, *meso* H), 4.78 (m, 1H, *n*-butyl CH₂), 4.68 (m, 3H, *n*-butyl CH₂), 3.90 (m, 20H, 16H, CH₂, 4H, *n*-butyl CH₂), 1.96-1.75 (m, 28H, 24H, CH₃, 4H, *n*-butyl CH₂), 0.92 (m, 3H, *n*-butyl CH₃), 0.65 ppm (m, 3H, *n*-butyl CH₃).

7.2.2.21 (2,3,7,8,12,13,17,18-Octaethyl-5,15-bis-*n*-butylporphyrinato)palladium (II) (275)

The OEP **275** was obtained as described in section 8.2.2.20 in a mixture with its 5,10 regioisomer **274** and was identified due to the ¹H NMR signals at 9.78 and 4.59 ppm (*meso* H and *n*-butyl CH₂).

7.2.2.22 (2,3,7,8,12,13,17,18-Octaethyl-5-(9-phenanthrenyl)-10-*s*-butylporphyrinato)palladium (II) (278)

5-(9-Phenanthrenyl) Pd(II)OEP **9** (49 mg, 0.060 mmol) was dissolved in 30 mL THF under an argon atmosphere and 0.42 mL of *s*-BuLi (0.6 mmol, 10 equivalents, 1.4 M) were added slowly at -60 °C. The reaction mixture was stirred for 20 minutes at the

same temperature, and turned from red to brown and from brown to green. It was quenched with 1 mL of water in the cold and oxidized with a solution of DDQ (27 mg, 0.12 mmol) in 15 mL dichloromethane. Purification on silica gel afforded 7 mg of a red solid (0.008 mmol, 11%), which was identified as a statistical mixture of the OEP **278** and its regioisomer **279** (2/1) as shown in figure 2.2.4.3. Furthermore, the double set of signals in the ^1H NMR spectrum indicated a 1/1 mixture of two atropisomers with a second chiral centre e.g. a pair of diastereoisomers for the OEP **278**. **278/279**: Mp 110 °C; ^1H NMR (400 MHz, CDCl_3): δ = 9.78 (s, 0.7H, *meso* H, 5,15 regioisomer), 9.58, 9.59 (each s, each 0.35H, *meso* H, 5,10 regioisomer), 9.53, 9.52 (each s, each 0.35H, *meso* H, 5,10 regio isomer), 8.98 (m, 1H, phenanthrenyl H), 8.93 (d, 1H, J = 8.4 Hz, phenanthrenyl H), 8.56 (s, 0.33H, 8'-phenanthrenyl H), 8.54 (s, 0.33H, 8'-phenanthrenyl H), 8.52 (s, 0.33H, 8'-phenanthrenyl H), 8.03 (m, 1H, phenanthrenyl H), 7.86 (m, 1H, phenanthrenyl H), 7.76 (m, 1H, phenanthrenyl H), 7.62-7.59 (m, 1H, phenanthrenyl H), 7.22-7.14 (m, 1H, phenanthrenyl H), 7.03 (m, 1H, phenanthrenyl H), 4.54 (m, 0.15H, *s*-butyl CH), 4.40 (m, 0.15H, *s*-butyl CH), 4.19 (m, 0.3H, *s*-butyl CH_2), 4.02 (m, 0.3H, *s*-butyl CH_2), 3.87-3.73 (m, 8H, CH_2), 3.65 (m, 1.3H, *s*-butyl CH_2), 3.47 (m, 0.7H, *s*-butyl CH_2), 2.69-1.95 (m, 8H, CH_2), 2.61 (d, 1H, J = 7.2 Hz, *s*-butyl CH_3), 2.27 (d, 1H, J = 7.0 Hz, *s*-butyl CH_3), 2.19 (d, 1H, J = 6.9 Hz, *s*-butyl CH_3), 1.82-1.68 (m, 15H, CH_3), 1.59 (m, 6H, CH_3), 0.41 (t, 1H, J = 7.2 Hz, *s*-butyl CH_3), 0.35 (t, 3H, J = 7.0 Hz, CH_3), 0.26 (t, 1H, J = 7.2 Hz, *s*-butyl CH_3), 0.13 ppm (t, 1H, J = 7.3 Hz, *s*-butyl CH_3); ^{13}C NMR (100 MHz, CDCl_3): δ = 14.1, 16.8, 18.1, 22.6, 29.7, 122.2, 122.4, 122.9, 126.4, 127.0, 121.1, 129.0, 129.3, 130.6, 132.1, 133.2, 137.0, 137.7, 138.9, 139.9, 141.4, 142.5, 143.4, 143.8, 144.3 ppm; UV/vis (CH_2Cl_2): λ_{max} ($\lg \epsilon$) = 413 (5.16), 527 (3.56), 560 (3.83) nm.

7.2.2.23 (2,3,7,8,12,13,17,18-Octaethyl-5-(9-phenanthrenyl)-15-*s*-butylporphyrinato)palladium (II) (**279**)

The OEP **279** was obtained as reported in section 8.2.2.22 in a 1/2 e.g. the statistical mixture with its regioisomer **278** (7 mg, 0.008 mmol, 11%).

7.2.2.24 (2,3,7,8,12,13,17,18-Octaethyl-5-(1-naphthyl)-10-*n*-butylporphyrinato)palladium (II) (286)

The reaction was performed following the general procedure, using 30 equivalents of 1-bromoaphthalene (0.42 mL, 3.12 mmol) and 80 equivalents of *n*-BuLi (3.32 mL, 8.32 mmol). Addition of *n*-BuLi was carried out at $-60\text{ }^{\circ}\text{C}$ and the reaction mixture was stirred afterwards without cold bath at ambient temperature. 5-(1-Naphthyl) Pd(II)OEP **282** (80 mg, 0.104 mmol) in THF was added after 1 hour at $-50\text{ }^{\circ}\text{C}$ and it was stirred for an additional 50 minutes, then quenched with water at $0\text{ }^{\circ}\text{C}$, oxidized and purified to yield 88 mg (0.107 mmol, >103%) of pink-red crystals from MeOH/dichloromethane. The OEP **286** contained still higher amounts of naphthalene (multiplets at 7.87 and 7.50 ppm) as it could be seen in the respective downfield ^1H NMR area. ^1H NMR (400 MHz, CDCl_3): $\delta = 9.79$ (s, 1H, *meso* H), 9.73 (s, 1H, *meso* H), 8.30 (d, 1H, $J = 8.3$ Hz, naphthyl H), 8.10 (m, 1H, naphthyl H), 7.92-7.34 (m, 4H, naphthyl H), 7.02-6.81 (m, 1H, naphthyl H), 4.81 (m, 2H, *n*-butyl CH_2), 3.96 (m, 10H, CH_2), 3.80 (m, 2H, CH_2 , 2H, *n*-butyl CH_2), 2.66 (m, 2H, CH_2), 2.29 (m, 2H, CH_2), 2.03 (m, 3H, CH_3 , 2H, *n*-butyl CH_2), 1.88 (m, 12H, CH_3), 1.78 (m, 9H, CH_3), 0.64 ppm (m, 3H, *n*-butyl CH_3); ^{13}C NMR (100 MHz, CDCl_3): $\delta = 13.7, 17.8, 18.1, 18.2, 18.3, 19.5, 19.6, 19.7, 21.0, 21.6, 22.6, 34.1, 37.9, 53.4, 96.8, 118.3, 118.6, 124.3, 125.7, 127.6, 127.8, 128.2, 128.7, 131.6, 132.5, 137.4, 137.8, 138.1, 138.5, 138.9, 139.4, 141.5, 142.8, 143.1, 143.4, 144.2$ ppm.

7.2.2.25 (2,3,7,8,12,13,17,18-Octaethyl-5,10-bis(1-naphthyl)porphyrinato)palladium (II) (284)

The reaction was performed following the general procedure, using 60 equivalents of 1-bromoaphthalene (0.80 mL, 5.96 mmol) and 75 equivalents of *n*-BuLi (2.97 mL, 7.42 mmol). Addition of *n*-BuLi was carried out at $-20\text{ }^{\circ}\text{C}$ and the reaction mixture was stirred afterwards without cold bath at ambient temperature. 5-(1-Naphthyl) Pd(II)OEP **282** (76 mg, 0.099 mmol) in THF was added after 1 hour at rt and it was stirred for an additional hour, then quenched with water at $0\text{ }^{\circ}\text{C}$, oxidized and purified to yield 56 mg (0.060 mmol, 61 %) of a pink-red solid. Mp $245\text{ }^{\circ}\text{C}$; ^1H NMR (400 MHz, CDCl_3): $\delta = 9.88$ (s, 1H, *meso* H), 9.87 (s, 1H, *meso* H), 8.40 (m, 2H, naphthyl H), 8.27 (d, 2H, $J = 8.2$ Hz, naphthyl H), 8.08 (m, 2H, naphthyl H), 7.81 (m, 2H, naphthyl H), 7.50 (m, 2H, naphthyl H), 7.34-7.25 (m, 2H, naphthyl H), 7.16 (m, 2H, naphthyl H), 3.98 (m, 4H,

CH₂), 3.77 (m, 4H, CH₂), 2.48–2.21 (m, 2H, CH₂), 2.21–2.20 (m, 6H, CH₂), 1.87 (t, 6H, $J = 7.5$, CH₃), 1.65 (m, 6H, CH₃), 0.55 (t, 6H, $J = 7.2$ Hz, CH₃), 0.39 ppm (m, 6H, CH₃); ¹³C NMR (100 MHz, CDCl₃): $\delta = 14.0, 16.8, 17.2, 18.0, 19.6, 20.2, 20.6, 21.2, 22.5, 25.2, 29.0, 29.7, 31.5, 34.6, 97.6, 117.3, 124.4, 125.9, 127.6, 127.8, 128.1, 128.8, 132.4, 132.7, 137.0, 139.0, 139.2, 140.4, 141.6, 143.3, 144.7$ ppm; UV/vis (CH₂Cl₂): λ_{max} (lg ϵ) = 340 (3.94), 412 (4.98), 527 (3.95), 561 (4.08) nm. As it can be seen in the ¹H NMR spectrum and as it has been described in chapter 3, the title compound **284** was afforded in a 1/1 mixture of two atropisomers due to the at ambient temperature hindered naphthyl rotation.

7.2.3 Octaethylporphyrins with three *meso* substituents

7.2.3.1 2,3,7,8,12,13,17,18-Octaethyl-5,15-bis(9-phenanthrenyl)-10-phenylporphyrin (**287**)

The the reaction was performed following the general procedure with 24 equivalents of 9-bromophenanthrene (0.771 g, 3.00 mmol) and 37 equivalents of *n*-BuLi (1.8 mL, 4.5 mmol). Addition of *n*-BuLi was carried out at -70 °C and the reaction mixture was stirred afterwards without cold bath at ambient temperature. 5-phenyl OEP **4** (74 mg, 0.121 mmol) in THF was added after 1 hour at -40 °C and after 40 minutes at rt, it was quenched at -30 °C with water, oxidized and purified to afford 39 mg (0.0404 mmol, 33 %) of a green solid as the only product. Mp 148 °C; ¹H NMR (400 MHz, CDCl₃): $\delta = 9.52$ (s, 1H, *meso* H), 8.98 (m, 4H, phenanthrenyl H), 8.68 (s, 1H, phenanthrenyl H), 8.67 (s, 1H, phenanthrenyl H), 8.43 (br s, 0.5H, phenyl H), 8.36 (d, 1H, $J = 6.9$ Hz, phenyl H), 8.34 (br s, 0.5H, phenyl H), 8.08 (d, 2H, $J = 7.8$ Hz, phenanthrenyl H), 7.85 (t, 2H, $J = 7.6$ Hz, phenanthrenyl H), 7.76 (t, 2H, $J = 7.2$ Hz, phenyl H), 7.75–7.64 (m, 6H, phenanthrenyl H, 1H, phenyl H), 7.36 (m, 2H, phenanthrenyl H), 3.67 (m, 4H, CH₂), 2.59 (m, 2H, CH₂), 2.37 (m, 2H, CH₂), 2.28–2.01 (m, 8H, CH₂), 1.52 (m, 6H, CH₃), 0.54 (t, 6H, $J = 7.3$ Hz, CH₃), 0.40 (t, 6H, $J = 7.3$ Hz, CH₃), 0.27 (m 6H, CH₃), -1.78 ppm (br s, 2H, NH); ¹³C MR (100 MHz, CDCl₃): $\delta = 16.2, 16.6, 17.1, 17.8, 19.3, 19.5, 20.4, 20.5, 114.6, 122.8, 126.4, 126.6, 127.1, 127.4, 128.1, 128.9, 129.1, 130.9, 131.0$ ppm; UV/vis (CH₂Cl₂): λ_{max} (lg ϵ) = 472 (5.14), 564 (sh), 608 (3.38), 663 (3.70) nm; MS (ES⁺): m/z (%): 963 (100) [M], 964 (10) [M+H]⁺, HRMS (ES⁺) [C₇₀H₆₆N₄]: calcd 963.5375, found 963.5366. The title compound was also isolated in 21 mg (0.021 mmol, 8%) besides 16 mg (0.02 mmol, 8%) of the disubstituted OEP **247** using changed

equivalents as described in chapter 8.2.2.2 and also in 25 mg (0.025 mmol, 10%) besides 26 mg (0.032 mmol, 13%) of the disubstituted OEP **247**. As it can be seen in the ^1H NMR spectrum and as it has been described in chapter 3, the title compound **287** was afforded a mixture of atropisomers due to the at ambient temperature hindered phenanthrenyl rotation.

7.2.3.2 2,3,7,8,12,13,17,18-Octaethyl-5-(4-pentylphenyl)-10,20-bis(9-phenanthrenyl)porphyrin (**288**)

The title compound was isolated in the disubstitution step starting with 5-(4-pentylphenyl) OEP **5** and afforded also 32 mg (0.037 mmol, 16 %) of the disubstituted OEP **256** as described in chapter 8.2.2.11. It was isolated as a second fraction during column chromatography and 58 mg (0.056 mmol, 25%) of a green solid were obtained. Mp 136 °C; ^1H NMR (400 MHz, CDCl_3): δ = 9.50 (s, 0.5H, *meso* H), 9.49 (s, 0.5H, *meso* H), 8.98 (m, 4H, phenanthrenyl H), 8.68 (s, 1H, phenanthrenyl H), 8.67 (s, 1H, phenanthrenyl H), 8.32 (br s, 0.5H, phenyl H), 8.28 (d, 1H, J = 7.8 Hz, phenyl H), 8.15 (br s, 0.5H, phenyl H), 8.12 (d, 2H, J = 7.8 Hz, phenanthrenyl H), 7.87 (t, 2H, J = 7.5 Hz, phenanthrenyl H), 7.80 (t, 2H, J = 7.3 Hz, phenanthrenyl H), 7.72 (m, 4H, phenanthrenyl H), 7.46 (d, 2H, J = 7.7 Hz, phenyl H), 7.34 (m, 2H, phenanthrenyl H), 3.67 (m, 4H, CH_2), 2.90 (t, 2H, J = 7.3 Hz, pentyl CH_2), 2.59 (m, 2H, CH_2), 2.22 (m, 12H, CH_2), 1.84 (m, 2H, pentyl CH_2), 1.51 (m, 4H, pentyl CH_2 , 6H, CH_3), 0.94 (m, 3H, pentyl CH_3), 0.53 (t, 6H, J = 7.3 Hz, CH_3), 0.37 (t, 6H, J = 7.3 Hz, CH_3), 0.29 (m, 6H, CH_3), -1.73 ppm (s, 2H, NH); ^{13}C NMR (100 MHz, CDCl_3): δ = 14.1, 16.3, 16.7, 17.1, 17.9, 19.2, 19.4, 19.5, 20.4, 20.6, 22.5, 29.2, 31.2, 31.3, 31.7, 35.8, 53.7, 114.6, 122.6, 122.9, 126.7, 126.8, 126.5, 127.1, 129.0, 129.1, 129.6, 131.0, 133.6, 133.8, 135.9, 136.2, 136.6, 138.7, 140.2, 142.5, 142.1, 143.0 ppm; UV/vis (CH_2Cl_2): λ_{max} (lg ϵ) = 442 (5.06), 470 (4.76), 537 (3.95), 609 (3.75), 665 (3.72) nm; MS (ES⁺): m/z (%): 1033 (100) $[\text{M}+\text{H}]^+$, HRMS (ES⁺) $[\text{C}_{75}\text{H}_{76}\text{N}_4+\text{H}]^+$: calcd 1033.6148, found 1033.6157. As it can be seen in the ^1H NMR spectrum and as it has been described in chapter 3, the title compound **288** was afforded in a mixture of atropisomers due to the at ambient temperature hindered phenanthrenyl rotation.

7.2.3.3 2,3,7,8,12,13,17,18-Octaethyl-5,10,15-tris(9-phenanthrenyl)porphyrin (**10**)

The title compound **10** was isolated in the disubstitution step affording also 81 mg (0.093 mmol, 43%) of the disubstituted OEP **9** as a first fraction and 21 mg (0.0169 mmol, 7%) of the tetrasubstituted OEP **11** as a third fraction as described in the chapters 8.2.2.14 and 8.2.4.1. It was isolated in 57 mg (0.053 mmol, 25%) as a green solid. Mp 179 °C; ¹H NMR (400 MHz, CDCl₃): δ = 9.54 (s, 0.33 H, *meso* H), 9.50 (s, 0.66 H, *meso* H), 8.99–8.89 (m, 6 H, phenanthrenyl H), 8.84 (s, 0.17H, phenanthrenyl H), 8.78 (s, 0.66H, phenanthrenyl H), 8.77 (s, 0.66H, phenanthrenyl H), 8.73 (s, 0.66H, phenanthrenyl H), 8.65 (s, 0.34H, phenanthrenyl H), 8.63 (s, 0.34H, phenanthrenyl H), 8.61 (s, 0.17H, phenanthrenyl H), 8.15 (d, 2H, *J* = 7.8 Hz, phenanthrenyl H), 8.09 (d, 1H, *J* = 6.9 Hz, phenanthrenyl H), 7.90–7.67 (m, 12H, phenanthrenyl H), 7.46–7.36 (m, 3H, phenanthrenyl H), 3.71 (m, 4H, CH₂), 2.69–2.52 (m, 2H, CH₂), 2.42–2.29 (m, 2 H, CH₂), 2.18–2.05 (m, 4H, CH₂), 1.96–1.84 (m, 4H, CH₂), 1.50 (m, 6H, CH₃), 0.54 (m, 6H, CH₃), 0.25 (m, 6H, CH₃), 0.13 (m, 6H, CH₃), –1.53 ppm (br s, 2H, NH); ¹³C NMR (100 MHz, CDCl₃): δ = 14.1, 16.3, 16.5, 16.7, 17.8, 19.3, 19.5, 20.6, 22.6., 29.3, 29.6, 31.9, 94.1, 114.6,114.7, 116.0, 116.2, 116.3, 122.5, 122.9, 126.5, 127.2, 128.8, 129.2, 129.4, 129.6, 130.7, 130.9, 133.5, 133.6, 133.8, 134.5, 134.7, 136.3, 136.5, 137.9, 137.2, 140.8, 140.9, 141.7 ppm; UV/vis (CH₂Cl₂): λ_{max} (lg ε) = 445 (4.38), 473 (4.14), 539 (3.14), 608 (3.09), 665 (2.95) nm; MS (ES⁺): *m/z* (%): 1063 (5) [M]; HRMS (ES⁺) [C₇₈H₇₀N₄]: calcd 1063.5679, found 1063.5652. With changed equivalents, the OEP **10** was also obtained in lower yields as reported in chapter 8.2.2.14. As it can be seen in the ¹H NMR spectrum and as it has been described in chapter 3, the title compound **10** was afforded in a statistical mixture of the possible atropisomers due to the at ambient temperature hindered phenanthrenyl rotation.

7.2.3.4 2,3,7,8,12,13,17,18-Octaethyl-5-(1-naphthyl)-10,20-bis(9-phenanthrenyl)porphyrin (**289**)

The title compound **289** was isolated in the disubstitution step affording also 47 mg (0.056 mmol, 46%) of the disubstituted OEP **259** as a first fraction as described in chapter 8.2.2.15. It was isolated in 22 mg (0.0217 mmol, 14%) as a green solid. Mp 132 °C; ¹H NMR (400 MHz, CDCl₃): δ = 9.54 (s, 0.25H, *meso* H), 9.49 (s, 0.75H, *meso* H), 8.98 (m, 4H, phenanthrenyl H), 8.74 (s, 0.5H, phenanthrenyl H, α,α',β atropisomer), 8.75 (s, 0.5H phenanthrenyl H, α,α',β atropisomer), 8.65 (s, 0.5H, phenanthrenyl H,

α,α',α or α,β',α atropisomer), 8.64 (s, 0.5H, phenanthrenyl H, α,α',α or α,β',α atropisomer), 8.57 (d, 0.25H, $J = 6.8$ Hz, naphthyl H), 8.48 (d, 0.5H, $J = 7.2$ Hz, naphthyl H), 8.37 (d, 0.25H, $J = 7.2$ Hz, naphthyl H), 8.27–8.22 (m, 1H, naphthyl H), 8.12 (m, 1H, naphthyl H, 1H, phenanthrenyl H), 8.05 (m, 1H, phenanthrenyl H), 7.87 (m, 2H, phenanthrenyl H), 7.81–7.71 (m, 6H, phenanthrenyl H, 1H, naphthyl H), 7.53 (m, 2H, naphthyl H), 7.39 (m, 2H, phenanthrenyl H), 7.30 (m, 1H, naphthyl H), 3.69 (m, 4 H, CH₂), 2.71–2.13 (m, 6 H, CH₂), 1.88 (m, 6H, CH₂), 1.51 (m, 12H, CH₃), 0.53 (m, 6H, CH₃), 0.30 (m, 3H, CH₃), 0.01 (m, 3H, CH₃), –1.51 ppm (s, 2H, NH); ¹³C NMR (100 MHz, CDCl₃): $\delta = 14.1, 16.2, 16.7, 18.7, 19.2, 19.3, 19.4, 22.6, 29.3, 29.6, 31.9, 122.5, 122.9, 125.9, 126.5, 126.9, 127.1, 128.8, 129.2, 130.7, 130.9$ ppm; UV/vis (CH₂Cl₂): λ_{\max} (lg ϵ) = 445 (4.89), 472 (3.65), 538 (3.78), 611 (3.64), 665 (3.51) nm; MS (ES⁺): m/z (%): 1013 (50) [M]; HRMS (ES⁺) [C₇₄H₆₈N₄]: calcd 1013.5522, found 1013.5505. As it can be seen in the ¹H NMR spectrum and as it has been described in chapter 3, the title compound **289** was afforded in a mixture of atropisomers due to the at ambient temperature hindered phenanthrenyl and naphthyl rotation.

7.2.3.5 2,3,7,8,12,13,17,18-Octaethyl-5,15-bis(9-anthracenyl)-10-phenylporphyrin (**290**)

The title compound **290** was isolated in the disubstitution step affording also 13 mg (0.0165 mmol, 16 %) of the disubstituted OEP **246** as a first fraction. It was isolated in 7 mg (0.0072 mmol, 7 %) as a green solid. Mp 145 °C; ¹H NMR (400 MHz, CDCl₃): $\delta = 9.52$ (s, 1H, *meso* H), 8.90 (s, 2H, anthracenyl H), 8.35 (d, 2H, $J = 6.7$ Hz, phenyl H), 8.26 (d, 4H, $J = 8.5$ Hz, anthracenyl H), 7.69 (m, 1H, phenyl H), 7.62 (m, 2H phenyl, 4 H anthracenyl), 7.52 (m, 4H, anthracenyl H), 7.21 (m, 4H, anthracenyl H), 3.56 (m, 6H, CH₂), 3.40 (m, 2H, CH₂), 2.09–1.88 (m, 8H, CH₂), 1.56 (t, 6H, $J = 7.4$ Hz, CH₃), 0.25 (t, 6H, $J = 7.1$ Hz, CH₃), 0.08 (t, 6H, $J = 7.3$, CH₃), –0.06 (t, 6H, $J = 7.2$ Hz, CH₃), –0.25 ppm (s, 2H, NH); ¹³C NMR (100 MHz, CDCl₃): $\delta = 11.4, 14.1, 15.3, 19.3, 20.4, 20.6, 22.65, 22.69, 25.2, 26.9, 29.0, 29.3, 29.6, 31.5, 31.9, 24.6, 41.3, 112.4, 125.3, 128.2, 128.4, 131.0, 135.3$ ppm; UV/Vis (CH₂Cl₂): λ_{\max} (lg ϵ) = 446 (4.59), 538 (3.59), 609 (3.42), 666 (3.31) nm; MS (ES⁺): m/z (%): 578 (80), 963 (15) [M]; HRMS (ES⁺) [C₇₀H₆₆N₄]: calcd 963.5366, found 963.5388.

7.2.3.6 2,3,7,8,12,13,17,18-Octaethyl-5,15-bis(3-methoxyphenyl)-10-phenylporphyrin (291)

The title compound **291** was isolated in the disubstitution step affording also 4 mg (0.0054 mmol, 4%) of the disubstituted OEP **252** as a first fraction. It was also isolated in 4 mg (0.0048 mmol, 3%) as a green solid. Mp 168 °C; ¹H NMR (400 MHz, CDCl₃): δ = 9.38 (s, 0.66 H, *meso* H), 9.24 (s, 0.33 H, *meso* H), 8.60–8.40 (m, 2H, phenyl H), 8.05 (m, 2H, 3-OMe-phenyl H), 7.84 (m, 1H, phenyl, 2H, 3-OMe-phenyl H), 7.68 (m, 2H, phenyl), 7.50 (m, 2H, 3-OMe-phenyl H), 7.37 (m, 2H, 3-OMe-phenyl H), 4.10 (s, (m, 2H, OMe), 4.03 (s, 4H, OMe), 3.66 (m, 4H, CH₂), 2.73–2.67 (m, 12H, CH₂), 1.53 (m, 6H, CH₃), 0.68–0.20 (m, 18H, CH₃), –0.08 ppm (s, 2H, NH); ¹³C NMR (100 MHz, CDCl₃): δ = 15.3, 16.4, 18.1, 19.9, 55.9, 116.0, 121.0, 121.9, 29.1, 129.3, 130.8, 137.3, 139.2, 142.7 ppm; UV/vis (CH₂Cl₂): λ_{max} (lg ε) = 465 (5.23), 569 (3.56), 608 (3.86), 663 (4.01) nm; MS (ES⁺): m/z (%): 578 (29), 823 (22) [M]; HRMS (ES⁺) [C₅₆H₆₂N₄O₂]: calcd 823.4951, found 823.4958. As it can be seen in the ¹H NMR spectrum and as it has been described in chapter 3, the title compound **291** was afforded in a mixture of atropisomers due to the at ambient temperature hindered methoxyphenyl rotation.

7.2.3.7 2,3,7,8,12,13,17,18-Octaethyl-5,10-bisphenyl-15-(4-dimethylaminophenyl)porphyrin (292)

The reaction was performed following the general procedure with 60 equivalents of 1-bromo-4-dimethylanilin (1.048 g, 5.24 mmol) and 75 equivalents of *n*-BuLi (2.60 mL, 6.55 mmol). Addition of *n*-BuLi was carried out at –40 °C and the reaction mixture was stirred afterwards without cold bath at ambient temperature. 5,10-Bisphenyl OEP **236** (60 mg, 0.087 mmol) in THF was added after 1 hour at rt and after 1 hour stirring at the same temperature, it was quenched at –0 °C, oxidized and purified to yield 60 mg (0.074 mmol, 69%) of a purple solid. Mp 90 °C; ¹H NMR (400 MHz, CDCl₃): δ = 9.40 (s, 1H, *meso* H), 8.36 (d, 2H, *J* = 6.8 Hz, phenyl H), 8.25 (d, 2H, *J* = 6.7 Hz, phenyl H), 8.07 (d, 2H, *J* = 8.4 Hz, 4-NMe₂-phenyl H), 7.73 (m, 2H, phenyl H), 7.65 (m, 4H, phenyl H), 7.02 (d, 2H, *J* = 8.4 Hz, 4-NMe₂-phenyl H), 3.72 (m, 4H, CH₂), 3.21 (s, 6H, NMe₂), 2.82 (m, 2H, CH₂), 2.67 (m, 2H, CH₂), 2.34 (m, 2H, CH₂), 2.26–2.17 (m, 6H, CH₂), 1.54 (m, 6H, CH₃), 0.70 (m, 6H, CH₃), 0.43 (m, 6H, CH₃), 0.33 (m, 6H, CH₃), –2.05 ppm (br s, 2H, NH₂); ¹³C NMR (100 MHz, CDCl₃): δ = 14.0, 14.1, 17.1, 17.9, 19.2, 19.5, 20.4,

22.7, 31.9, 29.7, 31.6, 31.9, 40.7, 40.8, 93.4, 110.7, 112.3, 112.5, 125.2, 126.7, 126.9, 128.1, 134.9, 135.7, 136.0, 140.2, 141.5 ppm; UV/vis (CH₂Cl₂): λ_{\max} (lg ϵ) = 446 (4.10), 480 (4.02), 623 (3.09), 682 (3.47) nm; MS (ES⁺): m/z (%): 806 (15) [M]; HRMS (ES⁺) [C₅₆H₆₃N₅]: calcd 806.5162, found 806.5122.

7.2.3.8 2,3,7,8,12,13,17,18-Octaethyl-5,10-bisphenyl-15-(4-bromophenyl)porphyrin
(293)

The reaction was performed following the general procedure with 60 equivalents of 1,4-dibromobenzene (1.8823 g, 8.13 mmol) and 75 equivalents of *n*-BuLi (4.05 mL, 10.12 mmol). Addition of *n*-BuLi was carried out at -30 °C and the reaction mixture was stirred afterwards without cold bath at ambient temperature. 5,10-Bisphenyl OEP **236** (93 mg, 0.135 mmol) in THF was added after 1 hour at rt and after another hour stirring at the same temperature, it was quenched at 0 °C, oxidized and purified to yield 44 mg (0.052 mmol, 38%) of a green solid. Mp < 75 °C; ¹H NMR (400 MHz, CDCl₃): δ = 9.43 (s, 1H, *meso* H), 8.36 (d, 2H, *J* = 7.1 Hz, phenyl H), 8.28 (d, 2H, *J* = 7.0 Hz, phenyl H), 8.17 (d, 2H, *J* = 8.2 Hz, 4-bromophenyl H), 7.84 (d, 2H, *J* = 8.2 Hz, 4-bromophenyl H), 7.73 (m, 2H, phenyl H), 7.67 (m, 4H, phenyl H), 3.73 (m, 4H, CH₂), 2.67 (m, 4H, CH₂), 2.26–2.20 (m, 8H, CH₂), 1.55 (m, 6H, CH₃), 0.71 (m, 6H, CH₃), 0.44 (t, 6H, *J* = 7.3 Hz, CH₃), 0.36 (t, 6H, *J* = 7.3 Hz, CH₃), -2.11 ppm (s, 2H, NH); ¹³C NMR (100 MHz, CDCl₃): δ = 14.0, 16.8, 17.2, 17.7, 19.2, 19.5, 20.5, 22.3, 22.7, 25.2, 26.8, 29.7, 34.5, 93.8, 126.7, 128.3, 130.0, 132.4, 134.9, 136.0, 136.4 ppm; UV/vis (CH₂Cl₂): λ_{\max} (lg ϵ) = 441 (4.35), 465 (4.46), 533 (3.30), sh, 610 (3.20), 676 (3.31) nm; MS (ES⁺): m/z (%): 841 (84) [M], 842 (20) [M+H]⁺, 843 (100/2) [M+2H]²⁺, 844 (6) [M+3H]³⁺; HRMS (ES⁺) [C₅₄H₅₇BrN₄]: calcd 841.845, found 841.3856.

7.2.3.9 2,3,7,8,12,13,17,18-Octaethyl-5,10-bisphenyl-15-(4-*n*-pentylphenyl)porphyrin
(294)

The reaction was performed following the general procedure with 60 equivalents of 1-bromo-4-pentylbenzene (1.63 mL, 9.22 mmol) and 75 equivalents of *n*-BuLi (4.19 mL, 11.5 mmol). Addition of *n*-BuLi was carried out at -30 °C and the reaction mixture was stirred afterwards without cold bath at ambient temperature. 5,10-Bisphenyl OEP **236** (106 mg, 0.1537 mmol) in THF was added after 1 hour at rt and after 3 hours stirring at the same temperature, it was quenched at 0 °C, oxidized and purified to yield 23 mg

(0.027 mmol, 17%) of a green solid. Mp 68°C; ^1H NMR (400 MHz, CDCl_3): δ = 9.43 (s, 1H, *meso* H), 8.35 (d, 2H, J = 7.1 Hz, phenyl H), 8.28 (d, 2H, J = 7.0 Hz, phenyl H), 8.17 (d, 2H, J = 7.7 Hz, 4-*n*-pentylphenyl H), 7.74 (m, 2H, phenyl H), 7.66 (t, 4H, J = 7.1 Hz, phenyl H), 7.46 (d, 2H, J = 7.7 Hz, 4-*n*-pentylphenyl H), 3.73 (m, 4H, CH_2), 2.95 (m, 2H, pentyl CH_2), 2.69 (m, 4H, CH_2), 2.57 (m, 4H, CH_2), 2.24 (m, 4H, CH_2), 1.55 (m, 6H CH_3), 1.47 (m, 6H, pentyl CH_2), 0.99 (m, 3H, pentyl CH_3), 0.70 (t, 6H, J = 7.3 Hz, CH_3), 0.44 (m, 6H, CH_3), 0.35 (m, 6H, CH_3), -2.12 ppm (s, 2H, NH); ^{13}C NMR (100 MHz, CDCl_3): δ = 14.0, 17.1, 17.9, 19.0, 19.2, 19.5, 20.4, 22.4, 27.9, 29.4, 29.5, 30.9, 31.5, 35.3, 35.9, 38.6, 93.4, 125.8, 126.7, 127.0, 127.7, 128.1, 128.5, 134.7, 135.8, 136.1, 140.4, 142.7 ppm; UV/vis (CH_2Cl_2): λ_{max} (lg ϵ) = 438 (4.65), sh, 533 (3.72), 605 (3.43), 673 (3.24) nm; MS (ES+): m/z (%): 578 (70), 833 (25) $[\text{M}+\text{H}]^+$, 834 (10/2) $[\text{M}+2\text{H}]^{2+}$; HRMS (ES+) $[\text{C}_{59}\text{H}_{68}\text{N}_4+\text{H}]^+$: calcd 833.5514, found 833.5522.

7.2.3.10 2,3,7,8,12,13,17,18-Octaethyl-5,10,15-tris(1-naphthyl)porphyrin (235)

The green title compound **235** was obtained repeatedly in traces during the *meso* monosubstitution affording also 91 mg (0.128 mmol, 46%) of the OEP **4** as described in chapter 2.2. It was accumulated by carrying out the reactions several times, purified and identified in milligram amounts. Mp < 75 °C; ^1H NMR (400 MHz, CDCl_3): δ = 9.51 (s, 0.33H, *meso* H), 9.47 (s, 0.66H, *meso* H), 8.59 (d, 0.5H, J = 8.4 Hz, naphthyl H), 8.54 (d, 0.5H, J = 7.0 Hz, naphthyl H), 8.48 (m, 1H, naphthyl H), 8.41 (d, 0.5H, J = 6.9 Hz, naphthyl H), 8.36 (d, 0.5H, J = 6.7 Hz, naphthyl H), 8.27 (d, 2H, J = 8.0 Hz, naphthyl H), 8.22 (d, 1H, J = 8.4 Hz, naphthyl H), 8.12–7.98 (m, 6H, naphthyl H), 7.54–7.47 (m, 6H, naphthyl H), 7.32–7.27 (m, 3H, naphthyl H), 3.67 (m, 6H, CH_2), 2.50–1.80 (m, 10H, CH_2), 1.51 (t, 6H, J = 7.3 Hz, CH_3), 0.51 (m, 6H, CH_3), 0.26 (m, 6H, CH_3), 0.12 (m, 6H, CH_3), -1.64 ppm (s, 2H, NH); ^{13}C NMR (100 MHz, CDCl_3): δ = 13.0, 14.0, 16.4, 16.7, 17.7, 19.1, 19.2, 20.5, 22.6, 25.5, 26.7, 27.4, 29.7, 31.6, 34.6, 38.9, 114.6, 124.4, 125.7, 127.9, 128.9, 132.9, 137.3, 138.3, 140.8, 141.8, 142.9 ppm; UV/vis (CH_2Cl_2): λ_{max} (lg ϵ) = 442 (4.80), 537 (3.78), 609 (3.51), 673 (3.23) nm; MS (ES+): m/z (%): 913 (10) $[\text{M}+\text{H}]^+$; HRMS (ES+) $[\text{C}_{66}\text{H}_{64}\text{N}_4+\text{H}]^+$: calcd 913.5209, found 913.5180.

As it can be seen in the ^1H NMR spectrum and as it has been described in chapter 3, the title compound **235** was afforded in a mixture of atropisomers due to the at ambient temperature hindered naphthyl rotation.

7.2.4 Octaethylporphyrins with four *meso* substituents

7.2.4.1 2,3,7,8,12,13,17,18-Octaethyl-5,10,15,20-tetrakis(9-phenanthrenyl)porphyrin (**11**)

As described in chapter 8.2.2.14, 66 mg (0.092 mmol) of 5-(9-phenanthrenyl) OEP **8** were reacted with 60 equivalents of 9-bromophenanthrene (1.431 mg, 5.57 mmol) and 60 equivalents *n*-BuLi (2.2 mL, 5.57 mmol) following the general procedure to afford the title compound **11** as a last green fraction after elution of the di- and trisubstituted OEPs **9** and **10** in a crude mixture (63 mg). The dication complex of **11** could be precipitated as green crystals from MeOH/*n*-hexane by addition of one drop of perchloric acid and was isolated in 63 mg (0.050 mmol, 54%). It was deprotonated by passing through aluminum oxide with CH₂Cl₂ and addition of ethyl acetate for complete elution and 48 mg (0.0392 mmol, 42 %) of the green-brown free base were obtained. Mp < 86 °C; ¹H NMR (400 MHz, CDCl₃): δ = 8.96 (m, 8H, phenanthrenyl H), 8.86 (s, 1H, 8'-phenanthrenyl H), 8.83 (s, 0.5H, 8'-phenanthrenyl H), 8.82 (s, 0.33H, 8'-phenanthrenyl H), 8.68 (s, 1H, 8'-phenanthrenyl H), 8.67 (s, 0.58H, 8'-phenanthrenyl H), 8.57 (s, 0.25 H, 8'-phenanthrenyl H), 8.54 (s, 0.33H, 8'-phenanthrenyl H), 8.33–8.09 (m, 4H, phenanthrenyl H), 8.02 (m, 2H, phenanthrenyl H), 97.87–7.72 (m, 14H, phenanthrenyl H), 7.62 (m, 2H, phenanthrenyl H), 7.53 (m, 2H, phenanthrenyl H), 2.18 (m, 12H, CH₂), 1.58 (m, 4H, CH₂), 1.24 (m, 24H, CH₃), -1.14 ppm (s, 2H, NH); ¹³C NMR (100 MHz, CDCl₃): δ = 16.1, 16.4, 19.0, 19.9, 122.5, 122.9, 126.6, 127.1, 129.7, 129.8, 130.7, 136.3, 136.4 ppm; UV/vis (CH₂Cl₂): λ_{max} (lg ε) = 493 (5.37), 640 (3.11), 697 (4.13) nm; MS (ES⁺): m/z (%): 1240 (20) [M+H]⁺; HRMS (ES⁺) [C₉₂H₇₈N₄+H]⁺: calcd 1240.6383, found 1240.6368. As it can be seen in the ¹H NMR spectrum and as it has been described in chapter 3, the title compound **11** was afforded in a statistical mixture of four possible atropisomers due to the at ambient temperature hindered phenanthrenyl rotation.

7.3 Palladium(II) insertion

The free base porphyrin was dissolved in chloroform (c = 0.002 molL⁻¹) and two equivalents of palladium acetate in methanol (c = 0.015 molL⁻¹) were added. Tri- and tetrasubstituted OEPs which formed easily dication complexes during elution of silica gel were beforehand neutralized by passing through aluminium oxide (colour change

from green to green-brown). The reaction mixture was stirred under an air atmosphere for 4 hours to 5 days at ambient temperature and under TLC monitoring (silica gel, *n*-hexane/CH₂Cl₂, v/v, 1/1). A colour change from red to pink was observed for *meso* mono- and disubstituted OEPs and from brown-green to blood red for tri- and tetrasubstituted OEPs. The solvent was evaporated afterwards and the residue dissolved in small amount of dichloromethane and purified using column chromatography (silica gel, *n*-hexane/CH₂Cl₂, v/v, 4/1 to 2/1). For further purification the Pd(II) OEPs were precipitated from CH₂Cl₂ with *n*-hexane or methanol. Mass spectra were not obtained due to the technique used (ES+) in accordance with reported difficulties described in the porphyrin handbook. In some cases base e.g. sodium acetate was added in order to speed up the reaction but was avoided later as it decreased the yields. Also DMF was first used as a solvent and will be indicated if so.

7.3.1 Palladium (II) octaethylporphyrins with one *meso* substituent

7.3.1.1 (2,3,7,8,12,13,17,18-Octaethyl-5-methylporphyrinato)palladium(II) (166)

5-Methyl OEP **277** (86 mg, 0.156 mmol) was dissolved in 10 mL DMF and two equivalents of palladium acetate (65 mg, 0.29 mmol) as well as 20 equivalents of sodium acetate (238 mg, 2.90 mmol) were added. It was stirred over night under an argon atmosphere at 50 °C. After column chromatography on aluminium oxide (*n*-hexane/CH₂Cl₂, 1/1, v/v) followed by precipitation from dichloromethane/methanol 39 mg (0.29 mmol, 37 %) red crystals were isolated. The Pd(II)OEP **166** had been prepared before *via* reaction of Pd(II)OEP **2** with methylfluorosulfonate as described in chapter 2.1 and gave similar UV/vis data whereas the melting point was reported as > 300 °C and was measured as: Mp 274 °C; R_f 0.93 (*n*-hexane/CH₂Cl₂/MeOH, 3/3/1, v/v, silica); R_f 0.90 (*n*-hexane/CH₂Cl₂, 1/2, v/v, silica); ¹H NMR (400 MHz, CDCl₃): δ = 9.94 (s, 2H, *meso* H), 9.90 (s, 1H, *meso* H), 4.43 (s, 3H, 5-CH₃), 4.02 (m, 16H, CH₂), 1.85 ppm (m, 24H, CH₃); ¹³C NMR (100 MHz, CDCl₃): δ = 17.2, 18.3, 19.7, 22.8, 29.7, 67.1, 92.9, 98.4, 133.7, 138.0, 141.0, 141.2, 143.6, 157.1, 165.0, 184.5, 185.7, 212.1, 214.2 ppm; UV/Vis (DCM): λ_{max} (lg ε) = 405 (5.18), 520 (4.15), 552 (5.92) nm.

7.3.1.2 (2,3,7,8,12,13,17,18-Octaethyl-5-*n*-butylporphyrinato)palladium(II) (17)

5-*n*-butyl OEP **16** (355 mg, 0.60 mmol) was dissolved in a mixture of 150 mL CHCl₃ and 35 mL MeOH and two equivalents of palladium acetate (275 mg, 1.2 mmol) were added following the general procedure. Stirring at rt during three hours, purification and precipitation afforded 142 mg (0.6 mmol, 100 %) of pink crystals. Mp 216 °C; R_f 0.44 (*n*-hexane/CH₂Cl₂, 5:2, v/v, silica); ¹H NMR (400 MHz, CDCl₃): δ = 9.93 (s, 2H, *meso* H), 9.89 (s, 1H, *meso* H), 4.96 (t, 2H, *J* = 7.8 Hz, *n*-butyl CH₂), 4.13–3.97 (m, 2H, *n*-butyl CH₂, 16H, CH₂), 1.98–1.80 (m, 2H, *n*-butyl CH₂, 24H CH₃), 0.63 ppm (t, 3H, *J* = 7.3 Hz, *n*-butyl CH₃); ¹³C NMR (100 MHz, CDCl₃): δ = 39.5, 42.0, 42.8, 45.2, 45.6, 50.9, 54.4, 58.4, 98.4, 101.9, 124.1, 133.3, 137.0, 138.3, 139.2, 141.1, 143.7, 166.1, 171.8, 174.7, 176.1, 178.2, 179.9, 193.6, 206.2, 209.1, 209.8, 210.5, 211.9, 212.6 ppm; UV/vis (CH₂Cl₂): λ_{max} (lg ε) = 406 (5.79), 521 (4.64), 555 (4.78) nm.

7.3.1.3 (2,3,7,8,12,13,17,18-Octaethyl-5-*s*-butylporphyrinato)palladium(II) (299)

5-*s*-butyl OEP **228** (50 mg, 0.084 mmol) was dissolved in a mixture of 10 mL DMF and 35 mL MeOH and two equivalents of palladium acetate (138 mg, 0.0600 mmol) were added following the general procedure. Stirring at rt during 12 hours, followed by refluxing for two hours, purification and precipitation afforded 37 mg pink crystals. The OEP **299** (0.045 mmol, 53%) was furthermore obtained impure as could be seen in the ¹H NMR spectrum and was contaminated with higher amount of Pd(II)OEP **2** (0.187 mmol, 22%), formed under the drastic conditions and the mixture (1/4 = Pd(II)OEP **2**/5-*s*-butyl Pd(II)OEP **299**) was inseparable. ¹H NMR (400 MHz, CDCl₃): δ = 10.14 (s, 1H, *meso* H Pd(II)OEP **2**), 9.88 (s, 2H, *meso* H), 9.83 (s, 1H, *meso* H), 4.68 (m, 1H, *s*-butyl CH), 4.27 (m, 2H, *s*-butyl CH₂), 3.98 (m, 16H, CH₂, 4H, CH₂ Pd(II)OEP **2**), 2.69 (d, 3H, *J* = 7.2 Hz, *s*-butyl CH₃), 1.88 (m, 24H, CH₃), 1.73 (t, 6H, *J* = 7.4 Hz, CH₃, Pd(II)OEP **2**), 0.00 ppm (t, 3H, *J* = 7.2 Hz, *s*-butyl CH₃); ¹³C NMR (100 MHz, CDCl₃): δ = 18.2, 18.3, 18.4, 19.7, 19.8, 22.0, 22.1, 98.6, 137.1, 138.2, 139.2, 141.1, 141.2, 141.7, 144.0 ppm; UV/vis (CH₂Cl₂): λ_{max} (lg ε) = 409 (6.01), 526 (4.94), 557 (5.04) nm. The UV/vis spectrum was obtained from a single crystal, separated mechanically.

7.3.1.4 (2,3,7,8,12,13,17,18-Octaethyl-5-phenylporphyrinato)palladium(II) (273)

5-phenyl OEP **4** (145 mg, 0.237 mmol) was reacted with 106 mg (0.475 mmol) palladium acetate in a mixture of 120 mL CHCl₃ and 30 mL MeOH following the

general procedure and yielded after stirring for two hours, purification and precipitation in 158 mg (0.22 mmol, 92%) of pink crystals. When 10 equivalents of sodium acetate were added, the yield was reduced to 58%. Mp 236 °C; R_f 0.37 (*n*-hexane/CH₂Cl₂, 5/2, v/v, silica); ¹H NMR (400 MHz, CDCl₃): δ = 10.08 (s, 2H, *meso* H), 10.00 (s, 1H, *meso* H), 8.18 (m, 2H, phenyl H), 8.15 (m, 1H, phenyl H), 7.78 (m, 1H, phenyl H), 7.63 (m, 1H, phenyl H), 4.02 (q, 8H, *J* = 7.6 Hz, CH₂), 3.95 (q, 4H, *J* = 7.5 Hz, CH₂), 2.65 (q, 4H, *J* = 7.4 Hz, CH₂), 1.92–1.81 (m, 18H, CH₃), 1.14 ppm (t, 6 H, *J* = 7.4 Hz, CH₃); ¹³C NMR (100 MHz, CDCl₃): δ = 18.2, 18.4, 19.8, 98.7, 126.3, 133.3, 138.4, 138.7, 139.7, 141.3, 142.1, 143.5, 193.8 ppm; UV/vis (CH₂Cl₂): λ_{max} (lg ε) = 399 (5.14), 515 (3.98), 549 (4.35) nm.

7.3.1.5 (2,3,7,8,12,13,17,18-Octaethyl-5-(3-trifluoromethylphenyl)porphyrinato)palladium(II) (300)

The palladium(II) complex **300** was prepared from the corresponding free base OEP **6** following the general procedure under section 8.3. The reaction afforded 117 mg (0.149 mmol, 93 %) of red-pink crystals. The stirring time was 30 minutes at 40 °C. Mp 236 °C; ¹H NMR (400 MHz, CDCl₃): δ = 10.10 (s, 2H, *meso* H), 10.03 (s, 1H, *meso* H), 8.57 (s, 1H, phenyl H), 8.30 (d, 1H, *J* = 7.5 Hz, phenyl H), 8.08 (d, 1H, *J* = 7.8 Hz, phenyl H), 7.77 (t, 1H, *J* = 7.5 Hz, phenyl H), 4.03 (q, 8H, *J* = 7.6 Hz, CH₂), 3.95 (q, 4H, *J* = 7.3 Hz, CH₂), 2.71 (q, 2H, *J* = 7.3 Hz, CH₂), 2.48 (q, 2H, *J* = 7.3 Hz, CH₂), 1.90 (m, 12H, CH₃), 1.84 (t, 6H, *J* = 7.5 Hz, CH₃), 1.12 ppm (t, 6H, *J* = 7.3 Hz); ¹³C NMR (100 MHz, CDCl₃): δ = 17.8, 18.4, 19.8, 139.9, 141.5, 142.7 ppm; UV/Vis (CH₂Cl₂): λ_{max} (lg ε) = 400 (5.41), 516 (3.89), 550 (4.53) nm.

7.3.1.6 (2,3,7,8,12,13,17,18-Octaethyl-5-(1-naphthyl)porphyrinato)palladium(II) (301)

The palladium(II) complex **301** was prepared from the corresponding free base OEP **7** following the general procedure under section 8.3. The reaction afforded 91 mg (0.116 mmol, 89 %) of red crystals. The stirring time was one hour at rt. Mp 265 °C; ¹H NMR (400 MHz, CDCl₃): δ = 10.12 (s, 2H, *meso* H), 10.59 (s, 1H, *meso* H), 8.42 (d, 1H, *J* = 6.7 Hz, naphthyl H), 8.31 (d, 1H, *J* = 8.1 Hz, naphthyl H), 8.10 (d, 1H, *J* = 8.3 Hz, naphthyl H), 7.82 (t, 1H, *J* = 7.2 Hz, naphthyl H), 7.45 (t, 1H, *J* = 7.8 Hz, naphthyl H), 6.97 (t, 1H, *J* = 6.8 Hz, naphthyl H), 6.86 (d, 1H, *J* = 8.3 Hz, naphthyl H), 4.05 (m, 8H,

CH₂), 3.86 (m, 4H, CH₂), 2.59 (m, 2H, CH₂), 2.16 (m, 2H, CH₂), 1.93 (m, 12H, CH₃), 1.81 (t, 6H, *J* = 7.6 Hz, CH₃), 0.84 ppm (t, 6H, *J* = 7.4 Hz, CH₃); ¹³C NMR (100 MHz, CDCl₃): δ = 17.1, 18.3, 19.7, 21.4, 97.7, 98.7, 117.9, 124.2, 125.9, 127.6, 128.3, 128.8, 138.4, 138.7, 139.7, 141.4, 143.1, 143.9 ppm; UV/vis (CH₂Cl₂): λ_{max} (lg ε) = 401 (5.00), 516 (3.79), 551 (4.18) nm.

7.3.1.7 (2,3,7,8,12,13,17,18-Octaethyl-5-(2-naphthyl)porphyrinato)palladium(II) (302)

The palladium(II) complex **302** was prepared from the corresponding free base OEP **233** following the general procedure under section 8.3. The reaction afforded 10 mg (0.0130 mmol, 20% JR-253-A2) of pink-red crystals. The stirring time was two hours at rt. Mp 253 °C; ¹H NMR (400 MHz, CDCl₃): δ = 10.12 (s, 2H, *meso* H), 10.04 (s, 1H, *meso* H), 8.66 (s, 1H, naphthyl H), 8.33 (d, 1H, *J* = 8.1 Hz, naphthyl H), 8.18 (d, 1H, *J* = 7.9 Hz, naphthyl H), 8.12 (d, 1H, *J* = 8.4 Hz, naphthyl H), 8.01 (d, 1H, *J* = 7.8 Hz, naphthyl H), 7.70 (m, 2H, naphthyl H), 4.05 (q, 8H, *J* = 7.70 Hz, CH₂), 3.94 (q, 4H, *J* = 7.58 Hz, CH₂), 2.68 (m, 2H, CH₂), 2.46 (m, 2H, CH₂), 1.94 (m, 12H, CH₃), 1.84 (t, 6H, *J* = 7.66 Hz, CH₃), 1.03 ppm (t, 6H, *J* = 7.48 Hz, CH₃); ¹³C NMR (100 MHz, CDCl₃): δ = 11.4, 14.0, 17.8, 18.3, 19.8, 21.5, 22.6, 25.3, 26.9, 27.6, 28.9, 31.4, 34.7, 41.4, 53.2, 95.7, 98.7, 125.5, 126.2, 126.7, 128.2, 128.4, 131.6, 131.7, 131.8, 132.0, 133.2, 138.1, 138.4, 139.0, 139.3, 141.4, 143.4, 143.6 ppm; UV/Vis (CH₂Cl₂): λ_{max} (lg ε) = 400 (4.90), 516 (3.80), 550 (4.14) nm.

7.3.1.8 (2,3,7,8,12,13,17,18-Octaethyl(5-acenaphthyl)porphyrinato)palladium(II) (303)

The palladium(II) complex **303** was prepared from the corresponding free base OEP **234** following the general procedure under section 8.3. The reaction afforded 49 mg (0.054 mmol, 72 %) of pink crystals. The stirring time was 24 hours at rt. Mp 288 °C; ¹H NMR (400 MHz, CDCl₃): δ = 10.11 (s, 2H, *meso* H), 10.05 (s, 1H, *meso* H), 8.35 (d, 1H, *J* = 7.1 Hz, acenaphthyl H), 7.62 (d, 1H, *J* = 6.9 Hz, acenaphthyl H), 7.29 (d, 1H, *J* = 6.7 Hz, acenaphthyl H), 7.01 (t, 1H, *J* = 7.2 Hz, acenaphthyl H), 6.52 (d, 1H, *J* = 8.5 Hz, acenaphthyl H), 4.07 (m, 8H, CH₂), 3.91 (m, 4H, CH₂), 3.78 (m, 2H, acenaphthyl CH₂), 3.69 (m, 2H, acenaphthyl CH₂), 2.66 (m, 2H, CH₂), 2.22 (m, 2H, CH₂), 1.93 (m, 12H, CH₃), 1.82 (t, 6H, *J* = 7.6 Hz, CH₃), 0.88 ppm (t, 6H, *J* = 7.5 Hz, CH₃); ¹³C NMR (100 MHz, CDCl₃): δ = 17.1, 18.4, 19.7, 21.8, 30.5 (acenaphthyl C), 30.7 (acenaphthyl C), 95.3, 96.5, 117.2 (acenaphthyl C), 119.8 (acenaphthyl C), 123.0 (acenaphthyl C), 127.9

(acenaphthyl C), 133.1 (acenaphthyl C), 134.9, 135.5, 138.2, 138.3, 138.6, 138.8, 139.6, 141.2, 143.3, 143.6, 145.3, 146.7 ppm; UV/vis (CH₂Cl₂): λ_{max} (lg ϵ) = 399 (5.11), 515 (5.13), 548 (4.36) nm.

7.3.1.9 (2,3,7,8,12,13,17,18-Octaethyl-5-(9-phenanthrenyl)porphyrinato)palladium(II) (**12**)

The palladium(II) complex **12** was prepared from the corresponding free base OEP **8** following the general procedure under section 8.3. The reaction afforded 320 mg (0.448 mmol, 85 %) of red crystals. The stirring time was 3 hours at rt. When sodium acetate was added, the yield was decreased to 60%. Mp 295 °C; R_f 0.93 (*n*-hexane/CH₂Cl₂, 2:1, v/v, silica); R_f 0.50 (*n*-hexane/CH₂Cl₂, 5/2, v/v, silica); ¹H NMR (400 MHz, CDCl₃): δ = 10.10 (s, 2H, *meso* H), 10.04 (s, 1H, *meso* H), 8.98 (d, 1H, *J* = 8.2 Hz, phenanthrenyl H), 8.93 (d, 1H, *J* = 8.0 Hz, phenanthrenyl H), 8.65 (s, 1H, phenanthrenyl H), 8.05–8.02 (m, 1H, phenanthrenyl H), 7.89–7.84 (m, 1H, phenanthrenyl H), 7.80–7.74 (m, 1H, phenanthrenyl H), 7.63–7.58 (m, 1H, phenanthrenyl H), 7.08–7.03 (m, 1H, phenanthrenyl H), 6.96–6.93 (m, 1H, phenanthrenyl H), 4.08–4.00 (m, 8H, CH₂), 3.91–3.82 (m, 4H, CH₂), 2.78–2.66 (m, 2H, CH₂), 2.32–2.20 (m, 2H, CH₂), 1.94–1.87 (m, 12H, CH₃), 1.79 (t, 6H, *J* = 7.5 Hz, CH₃), 0.80 ppm (t, 6H, *J* = 7.3 Hz, CH₃); ¹³C NMR (100 MHz, CDCl₃): δ = 17.3, 18.7, 20.2, 138.8, 139.2, 139.1, 140.1, 141.8, 143.0, 143.4, 144.4, 150.2, 208.0, 209.8 ppm; UV/vis (CH₂Cl₂): λ_{max} (lg ϵ) = 400 (5.86), 516 (4.79), 550 (5.12) nm.

7.3.2 Palladium (II) octaethylporphyrins with two *meso* substituents

7.3.2.1 (2,3,7,8,12,13,17,18-Octaethyl-5,10-bis(1-naphthyl)porphyrinato) palladium (II) (**284**)

The palladium(II) complex **284** was prepared from the corresponding free base OEP **257** following the general procedure under section 8.3. The reaction afforded 34 mg (0.0381 mmol, 65 %) of red crystals. The stirring time was two hours at rt. For NMR and UV/vis data compare to chapter 8.2.2.25.

7.3.2.2 (2,3,7,8,12,13,17,18-Octaethyl-5,10-bis(9-phenanthrenyl)porphyrinato)-palladium (II) (**13**)

The palladium(II) complex **13** was prepared from the corresponding free base OEP **9** following the general procedure under section 8.3. The reaction afforded 26 mg (0.025 mmol, 55 %) of red crystals. The stirring time was 5 hours at rt. Mp 238 °C; ¹H NMR (400 MHz, CDCl₃): δ = 9.88 (s, 1H, *meso* H), 9.86 (s, 1H, *meso* H), 8.96 (d, 2H, *J* = 8.5 Hz, phenanthrenyl H), 8.92 (m, 2H, phenanthrenyl H), 8.64 (s, 1H, phenanthrenyl H), 8.58 (s, 1H, phenanthrenyl H), 8.06 (d, 1H, *J* = 7.8 Hz, phenanthrenyl H), 8.03 (d, 1H, *J* = 7.8 Hz, phenanthrenyl H), 7.85 (m, 2H, phenanthrenyl H), 7.75 (m, 2H, phenanthrenyl H), 7.68 (m, 2H, phenanthrenyl H), 7.43 (d, 1H, *J* = 8.1 Hz, phenanthrenyl H), 7.36 (d, 1H, *J* = 8.1 Hz, phenanthrenyl H), 7.28 (m, 1H, phenanthrenyl H), 7.22 (m, 1H, phenanthrenyl H), 3.97 (m, 4H, CH₂), 3.75 (m, 4H, CH₂), 2.59–2.49 (m, 2H, CH₂), 2.23–1.95 (m, 6H, CH₂), 1.85 (t, 6H, *J* = 7.5 Hz, CH₃), 1.62 (m, 6H, CH₃), 0.54 (m, 6H, CH₃), 0.39 (t, 3H, *J* = 7.3 Hz, CH₃), 0.35 ppm (t, 3H, *J* = 7.3 Hz, CH₃); ¹³C NMR (100 MHz, CDCl₃): δ = 16.6, 16.9, 18.2, 18.1, 18.2, 19.5, 19.6, 20.4, 21.3, 21.9, 97.8, 117.0, 122.5, 122.9, 126.4, 127.1, 127.2, 128.9, 129.12, 129.17, 130.6, 130.82, 130.86, 136.41, 136.45, 137.2, 137.3, 140.0, 140.1, 140.3, 140.4, 141.5, 143.3, 143.4, 143.6, 144.5, 144.6 ppm; UV/vis (CH₂Cl₂): λ_{max} (lg ε) = 414 (5.15), 5.27 (4.09), 5.62 (4.24) nm.

7.3.3 Palladium (II) octaethylporphyrins with three *meso* substituents

7.3.3.1(2,3,7,8,12,13,17,18-Octaethyl-5,15-bis(9-phenanthrenyl)-10-phenylporphyrinato)palladium (II) (**304**)

The palladium(II) complex **304** was prepared from the corresponding free base OEP **287** following the general procedure under section 8.3. The reaction afforded 52 mg (0.047 mmol, 54%) of red crystals. The stirring time was 30 minutes at 40 °C. Mp 257 °C; ¹H NMR (400 MHz, CDCl₃): δ = 9.70 (s, 1H, *meso* H), 8.98 (d, 2H, *J* = 7.8 Hz, phenanthrenyl H), 8.99 (d, 2H, *J* = 7.8 Hz, phenanthrenyl H), 8.64 (s, 1H, phenanthrenyl H), 8.60 (s, 1H, phenanthrenyl H), 8.36 (d, 0.5 H, *J* = 7.7 Hz, phenyl H), 8.33 (d, 1H, *J* = 6.5 Hz, phenyl H), 8.23 (d, 0.5H, *J* = 7.7 Hz, phenyl H), 8.09 (m, 2H, phenanthrenyl H), 7.88 (t, 2H, *J* = 7.1 Hz, phenanthrenyl H), 7.79 (t, 2H, *J* = 7.5 Hz, phenanthrenyl H), 7.73 (m, 2H, phenanthrenyl H, 1H, phenyl H), 7.68–7.63 (m, 2H, phenyl H, 2H, phenanthrenyl H), 7.41–7.34 (m, 2H, phenanthrenyl H), 3.67 (m, 4H,

CH₂), 2.59–2.30 (m, 4H, CH₂), 2.24–2.19 (m, 4H, CH₂), 2.12–2.04 (m, 4H, CH₂), 1.56 (m, 6H, CH₃), 0.51–0.40 ppm (m, 18H, CH₃); ¹³C NMR (100 MHz, CDCl₃): δ = 16.55, 16.90, 16.96, 17.41, 17.52, 17.94, 19.4, 19.7, 20.0, 20.8, 20.9, 122.6, 122.9, 126.5, 126.6, 126.70, 126.74, 127.1, 127.2, 128.2, 128.94, 128.93, 129.1, 129.4, 130.9, 131.0, 133.4, 134.9, 135.0, 136.0, 136.9, 141.1, 141.6, 141.9, 142.1, 142.8, 142.91, 142.95, 142.99, 143.5, 143.70, 143.77 ppm; UV/Vis (CH₂Cl₂): λ_{max} (lg ε) = 427 (4.87), 539 (3.78), 573 (3.72) nm.

7.3.3.2 (2,3,7,8,12,13,17,18-Octaethyl-5,10,15-tris(9-phenanthrenyl)porphyrinato)palladium(II) (**14**)

The palladium(II) complex **14** was prepared from the corresponding free base OEP **10** following the general procedure under section 8.3. The reaction afforded 40 mg (0.033 mmol, 80 %) of red crystals. The stirring time was 30 minutes at 50 °C and the reaction vessel was flooded with argon. Mp 268 °C; ¹H NMR (400 MHz, CDCl₃): δ = 9.70 (s, 0.25H, *meso* H), 9.69 (s, 0.50H, *meso* H), 9.68 (s, 0.25H, *meso* H), 8.99–8.89 (m, 6H, phenanthrenyl H), 8.77 (s, 0.17H, 8'-phenanthrenyl H), 8.73 (s, 0.66H, 8'-phenanthrenyl H), 8.69 (s, 0.66H, 8'-phenanthrenyl H), 8.66 (s, 0.66H, phenanthrenyl H), 8.59 (s, 0.34H, 8'-phenanthrenyl H), 8.55 (s, 0.34H, 8'-phenanthrenyl H), 8.52 (s, 0.17H, 8'-phenanthrenyl H), 8.14–8.03 (m, 3H, phenanthrenyl H), 7.88–7.67 (m, 12H, phenanthrenyl H), 7.54–7.33 (m, 3H, phenanthrenyl H), 3.65 (m, 4H, CH₂), 2.56–2.49 (m, 2H, CH₂), 2.16 (m, 6H, CH₂), 1.97 (m, 4H, CH₂), 1.54 (m, 6H, CH₃), 0.51 (m, 6H, CH₃), 0.31 (t, 6H, *J* = 7.4 Hz, CH₃), 0.24 ppm (m, 6H, CH₃), ¹³C NMR (100 MHz, CDCl₃): δ = 16.5, 16.6, 16.9, 17.9, 19.4, 20.0, 20.9, 29.6, 53.4, 116.2, 117.3, 117.4, 122.6, 122.9, 126.5, 127.1, 127.2, 128.2, 129.2, 129.4, 130.7, 130.9, 133.3, 136.0, 136.5, 136.7, 136.9, 141.0, 141.2, 141.4, 142.3, 142.5, 143.0, 143.8, 144.4, 144.5, 144.6 ppm; UV/vis (CH₂Cl₂): λ_{max} (lg ε) = 429 (4.11), 539 (4.04), 575 (4.06) nm.

7.3.4 Palladium (II) octaethylporphyrins with four *meso* substituents

7.3.4.1 (2,3,7,8,12,13,17,18-Octaethyl-5,10,15,20-tetrakis(9-phenanthrenyl)porphyrinato)palladium (II) (**15**)

The palladium(II) complex **15** was prepared from the corresponding free base OEP **11** following the general procedure under section 8.3. The reaction afforded 12 mg (0.0094 mmol, 12%) of red crystals. The stirring time was 3 days at rt. Mp 290 °C; ¹H NMR (400 MHz, CDCl₃): δ = 8.93 (m, 8H, phenanthrenyl H), 8.84 (s, 0.5 H, 8'-phenanthrenyl H), 8.79 (s, 1.33 H, 8'-phenanthrenyl H), 8.71 (s, 0.58H, 8'-phenanthrenyl H), 8.66 (s, 1H, 8'-phenanthrenyl H), 8.54 (s, 0.33 H, 8'-phenanthrenyl H), 8.50 (s, 0.25H, 8'-phenanthrenyl H), 8.13–7.95 (m, 4H, phenanthrenyl H), 7.86–7.70 (m, 14H, phenanthrenyl H), 7.62–7.42 (m, 6H, phenanthrenyl H), 1.88 (m, 2H, CH₂), 1.72 (m, 4H, CH₂), 1.56 (m, 10H, CH₂), 1.16–1.08 (m, 6H, CH₃), 0.29 ppm (m, 18H, CH₃); ¹³C NMR (100 MHz, CDCl₃): δ = 14.1, 16.5, 19.7, 22.7, 29.8, 31.6, 31.9, 53.4, 116.8, 122.7, 123.0, 126.6, 127.2, 128.3, 129.3, 129.7, 130.8, 131.1, 133.4, 133.6, 133.8, 135.9, 136.4, 136.6, 136.8, 144.1, 144.5 ppm; UV/vis (CH₂Cl₂): λ_{max} (lg ε) = 443 (4.43), 553 (3.89), 590 (3.75) nm.

7.4 Platinum (II) insertion

7.4.1 Platinum (II) octaethylporphyrins with one *meso* substituent

7.4.1.1 (2,3,7,8,12,13,17,18-Octaethyl-5-phenylporphyrinato)platinum (II) (**307**)

5-Phenyl OEP **4** (60 mg, 0.098 mmol) and 52 mg PtCl₂ (0.196 mmol, 2 equivalents) were refluxed at 188 °C in benzonitrile under an argon atmosphere. Heating was continued for 5 days until TLC monitoring showed a single red-brown product spot. The solvent was evaporated under reduced pressure (2 to 4 mbar at 120 °C). The residue was dissolved in a small amount of dichloromethane and filtered through silica gel, eluting with CH₂Cl₂/*n*-hexane, 1/2, v/v. Further purification was achieved by column chromatography using silica gel and CH₂Cl₂/*n*-hexane, 1/3, v/v to yield after precipitation from dichloromethane/methanol 60 mg (0.74 mmol, 76 %) of red-brown crystals. Mp 253 °C; ¹H NMR (400 MHz, CDCl₃): δ = 10.02 (s, 2H, *meso* H), 9.98 (s, 1H, *meso* H), 8.19 (d, 2H, *J* = 6.9 Hz, phenyl H), 7.80 (t, 1H, *J* = 7.7 Hz, phenyl H), 7.67 (t, 2H, *J* = 7.5 Hz, phenyl H), 4.01 (q, 8H, *J* = 7.6 Hz, CH₂), 3.93 (q, 4H, *J* = 7.5

Hz, CH₂), 2.66 (q, 4H, $J = 7.5$ Hz, CH₂), 1.91 (m, 12H, CH₃), 1.86 (t, 6H, $J = 7.6$ Hz, CH₃), 1.13 ppm (t, 6H, $J = 7.5$ Hz, CH₃); ¹³C NMR (100 MHz, CDCl₃): $\delta = 18.2, 19.5, 21.3, 29.6, 97.9, 99.3, 126.3, 128.4, 133.2, 137.0, 138.0, 139.1, 140.7, 141.6, 141.7, 143.0$ ppm; UV/vis (CH₂Cl₂): λ_{max} (lg ϵ) = 386 (6.60), 504 (5.28), 539 (5.78) nm.

7.4.1.2 (2,3,7,8,12,13,17,18-Octaethyl-5-(1-naphthyl)porphyrinato)platinum (II) (308)

The platinum(II) insertion was performed in accordance to Pt(II)OEP **307** described in section 8.4.1. After 6 days of heating, followed by purification *via* column chromatography using silica gel 52 mg (0.060 mmol, 44 %) of brown-red crystals were obtained. Mp 178 °C; ¹H NMR (400 MHz, CDCl₃): $\delta = 10.02$ (s, 2H, *meso* H), 9.99 (s, 1H, *meso* H), 8.40 (d, 1H, $J = 6.6$ Hz, naphthyl H), 8.30 (d, 1H, $J = 6.3$ Hz, naphthyl H), 8.10 (d, 1H, $J = 8.2$ Hz, naphthyl H), 7.82 (t, 1H, $J = 8.2$ Hz, naphthyl H), 7.44 (t, 1H, $J = 7.0$ Hz, naphthyl H), 6.96 (t, 1H, $J = 6.7$ Hz, naphthyl H), 6.89 (d, 1H, $J = 8.4$ Hz, naphthyl H), 4.01 (m, 8H, CH₂), 3.85 (m, 4H, CH₂), 2.55 (m, 2H, CH₂), 2.10 (m, 2H, CH₂), 1.90 (m, 12H, CH₃), 1.80 (t, 6H, $J = 7.5$ Hz, CH₃), 0.82 ppm (t, 6H, $J = 7.2$ Hz, CH₃); ¹³C NMR (100 MHz, CDCl₃): $\delta = 17.1, 18.1, 18.23, 18.28, 19.5, 19.6, 21.3, 98.1, 99.3, 118.4, 124.2, 125.8, 125.9, 127.6, 128.2, 128.8, 131.3, 132.4, 137.1, 137.2, 137.9, 138.1, 139.1, 140.8, 140.9, 142.6, 143.4$ ppm; UV/vis (CH₂Cl₂): λ_{max} (lg ϵ) = 387 (5.79), 504 (4.51), 538 (4.99) nm.

7.4.1.3 (2,3,7,8,12,13,17,18-Octaethyl-5-(9-phenanthrenyl)porphyrinato)platinum (II) (309)

The platinum(II) insertion was performed in accordance to Pt(II)OEP **307** described in section 8.4.1. After 5 days of heating, followed by purification *via* column chromatography using silica gel 103 mg (0.113 mmol, 54 %) of red-brown crystals were obtained. Mp 295 °C; ¹H NMR (400 MHz, CDCl₃): $\delta = 10.05$ (s, 2H, *meso* H), 10.02 (s, 1H, *meso* H), 8.99 (d, 1H, $J = 8.5$ Hz, phenanthrenyl H), 8.94 (d, 1H, $J = 8.1$ Hz, phenanthrenyl H), 8.68 (s, 1H, phenanthrenyl H), 8.07 (m, 1H, phenanthrenyl H), 7.88 (m, 1H, phenanthrenyl H), 7.81 (m, 1H, phenanthrenyl H), 7.62 (m, 1H, phenanthrenyl H), 7.09 (m, 1H, phenanthrenyl H), 7.01 (m, 1H, phenanthrenyl H), 4.05 (m, 8H, CH₂), 3.86 (m, 4H, CH₂), 2.73 (m, 2H, CH₂), 2.27 (m, 2H, CH₂), 1.93 (m, 12H, CH₃), 1.81 (m, 6H, CH₃), 0.84 ppm (m, 6H, CH₃); ¹³C NMR (100 MHz, CDCl₃): $\delta = 16.9, 18.2, 18.3,$

19.5, 19.6, 21.7, 98.2, 99.3, 118.2, 122.5, 122.9, 126.4, 126.6, 127.0, 127.3, 129.0, 129.2, 129.3, 130.6, 132.1, 136.5, 137.1, 137.7, 138.0, 138.2, 139.1, 140.8, 141.0, 142.5, 143.5 ppm; UV/vis (CH₂Cl₂): λ_{max} (lg ϵ) = 387 (6.04), 504 (5.68), 538 (6.20) nm.

APPENDIX

ABBREVIATIONS

Ac - acetyl

AcO - acetate

AIBN - azobis(isobutyronitrile)

BAHA - tris(4-bromophenyl)aminium hexachloroantimonate

Bz - benzoyl

COD - cyclooctadiene

DBU - 1,8-diazabicyclo[5,4,0]undec-7-ene

DDQ - 2,3-dichloro-5,6-dicyano-1,4-benzoquinone

DMF - N,N-dimethylformamide

DMSO - dimethylsulphoxide

etioporphyrin - 2,8,12,17-tetraethyl-3,7,13,18-tetramethylporphyrin

Et₂O - diethyl ether

Et - ethyl

IPA - isopropyl alcohol

Me - methyl

mesityl - 2,4,6-trimethylphenyl

MCH - methylcyclohexane

NBS - N-bromosuccinimide

OMTP - 2,3,7,8,13,14,17,18-octakisethylthioporphyrin

OEP - octaethylporphyrin

P - porphyrin

Ph - phenyl

*p*Me - 2-methoxycarbonyl ethyl

PPA - phosphoric acid

p-TsOH - PTSA - *p*-toluenesulphonic acid

Py - pyridine

EA - ethylacetate

rt - room temperature

s-Bu - *sec*-butyl

TBAF - tetrabutylammonium fluorid

TBP - tetrabenzoporphyrin

TPTBP - tetraphenyltetrabenzoporphyrin

TPTNP - tetraphenyltetranaphthoporphyrin

t-Bu - *tert*-butyl

TFA - trifluoroacetic acid

TfO - trifluoromethanesulfonate

THF - tetrahydrofuran

TMP - 5,10,15,20-tetrakis(2,4,6-trimethylphenyl)porphyrin

TNP - tetranaphthoporphyrin

TPP - tetraphenylporphyrin

CRYSTALLOGRAPHIC DATA

The crystals were immersed in hydrocarbon oil (Paraton N[®]), suitable single crystals selected under the microscope, mounted on a glass fiber and placed in the low-temperature N₂ stream on the diffractometer.¹ Intensity data for all compounds were collected with an Bruker Smart CCD system using graphite monochromated Mo-K_α radiation ($\lambda = 0.71073 \text{ \AA}$) with ϕ and ω scans. The intensities were corrected for Lorentz and polarization effects. Absorption corrections were applied using the program Sadabs,² extinction effects were disregarded. The structures of the OEPs **17**, **273**, **307**, **382** and **8** were solved using Direct Methods.³ OEP **309** was solved using the SIR92 program.⁴ Refinements were carried out by full-matrix least squares on $|F^2|$ with the program SHELXL-97 using all data.⁵ Unless otherwise stated, nonhydrogen atoms were refined with anisotropic thermal parameters. Except for disordered groups, hydrogen atoms were generally placed into geometrically calculated positions and refined using a riding model. Details for the crystal data, data collection and refinement are given in table I.

Complete crystallographic details have been deposited at the Cambridge Crystallographic Data Centre (CCDC), 12 Union road, Cambridge, CB2 1EZ, UK and copies can be obtained on request, free of charge, by quoting the publication citation and the deposition numbers.

Refinement details: **17**: One ethyl side chain showed high thermal libration movement which was discounted. **273**: Some of the ethyl side chains showed high thermal libration movement. **307**: Some of the ethyl side chains showed high thermal libration movement. **382**: The structure contains a disordered methylene chloride of solvation. No hydrogen atoms were included in the refinement and no suitable disorder model was found. The residual electron density is located in the disordered region. **309**: Isostructural to **382** with similar solvent disorder. **8**: The structure is disordered with high thermal motion observed for C13B. The ethyl chain at C17 was refined as disordered over two split positions and refined with a free variable for the occupancy. The crystal showed some degree of twinning. However, attempts to use twin refinements gave no significant improvements in the refinement. Pyrrole hydrogen atoms were added to all four nitrogen atoms and refined with 0.5 occupancy, each.

REFERENCES

- 1) H. Hope *Prog. Inorg. Chem.* **1994**, *41*, 1.
- 2) G. M. Sheldrick, SADABS, Program for Absorption Correction, Universität Göttingen, Germany, **1996**.
- 3) G. M. Sheldrick, SHELXS-97, Program for Crystal Structure Solution, Universität Göttingen, Germany, **1997**.
- 4) A. Altomare, G. Cascarano, C. Giacovazzo, A. Guagliardi, M. C. Burla, G. Polidori, M. Camalli *J. Appl. Cryst.* **1994**, *27*, 435.
- 5) G. M. Sheldrick, SHELXL-97, Program for Crystal Structure Refinement, Universität Göttingen, Germany, **1997**.

Table I. Summary of Crystal Data, Data Collection and Refinement for the Crystal Structure Determinations.

Compound	17	273	307	382	309	8
chemical formula	C ₄₀ H ₅₂ N ₄ Pd	C ₄₂ H ₄₈ N ₄ Pd	C ₄₂ H ₄₈ N ₄ Pt	C ₄₆ H ₅₀ N ₄ Pd• ½CH ₂ Cl ₂	C ₄₆ H ₅₀ N ₄ Pt• ½CH ₂ Cl ₂	C ₅₀ H ₅₄ N ₄
Mol. wt.	695.26	715.24	803.93	807.82	896.45	710.97
Crystallization	CH ₂ Cl ₂ /CH ₃ OH	CH ₂ Cl ₂ /CH ₃ OH	CH ₂ Cl ₂ /CH ₃ OH	CH ₂ Cl ₂ /CH ₃ OH	CH ₂ Cl ₂ /CH ₃ OH	CH ₂ Cl ₂ /CH ₃ OH
color, habit	red plate	red block	red parallelepiped	red parallelepiped	red plate	red parallelepiped
crystal size (mm)	0.4 x 0.3 x 0.1	0.5 x 0.4 x 0.3	0.5 x 0.1 x 0.1	0.5 x 0.12 x 0.12	0.43 x 0.13 x 0.11	0.4 x 0.1 x 0.05
lattice type	Orthorhombic	Monoclinic	monoclinic	triclinic	triclinic	monoclinic
space group	<i>P2₁2₁2₁</i>	<i>P2₁/c</i>	<i>P2₁/c</i>	<i>P 1̄</i>	<i>P 1̄</i>	<i>P2₁/c</i>
<i>a</i> (Å)	12.5820(5)	17.2044(12)	17.1661(6)	11.0936(3)	11.1008(7)	17.7602(4)
<i>b</i> (Å)	13.2552(6)	8.9082(6)	8.9301(3)	13.2346(4)	13.3368(8)	15.6178(3)
<i>c</i> (Å)	20.4236(8)	22.9020(16)	22.8471(8)	13.8443(4)	13.8062(8)	15.0509(3)
α (°)				94.524(1)	94.506(1)	
β (°)		99.532(1)	99.367(1)	99.452(1)	99.442(1)	112.74(2)
γ (°)				105.186(1)	105.601(1)	
<i>V</i> (Å ³)	3406.2(2)	3461.5(4)	3455.6(2)	1919.07(10)	1925.8(2)	3850.29(14)
<i>Z</i>	4	4	4	2	2	4
<i>d</i> _{calc} (Mg m ⁻³)	1.356	1.372	1.545	1.410	1.546	1.227
μ (mm ⁻¹)	0.579	0.572	4.097	0.593	3.752	0.071
<i>T</i> _{max} , <i>T</i> _{min}	0.80, 0.94	0.76, 0.85	0.23, 0.66	0.76, 0.93	0.30, 0.66	0.98, 0.99
<i>T</i> (K)	90	90	90	90	123	90
θ _{max} (°)	27.55	27.55	27.58	27.52	28.19	27.55
collec. Reflections	33209	44563	43758	16158	19486	56381

Table I. Summary of Crystal Data, Data Collection and Refinement for the Crystal Structure Determinations.

Compound	17	273	307	382	309	8
indep. Reflections	7860	7968	7989	8621	9384	12755
reflections with $F > 4.0\sigma(F)$	7215	6990	6809	7628	8877	7961
R_{int}	0.0433	0.0336	0.0368	0.0193	0.0175	0.0488
no. of parameters	415	432	432	485	485	515
S	1.072	1.028	1.057	1.019	1.079	1.047
Δ/ρ_{max} ($\text{e } \text{\AA}^{-3}$)	0.724	0.997	1.150	1.991	1.251	0.924
$R1 [F > 4.0\sigma(F)]$	0.0269	0.0277	0.0205	0.0362	0.0226	0.0757
$wR2 [F > 4.0\sigma(F)]$	0.0590	0.0708	0.0458	0.0861	0.0585	0.1891
$R1$ (all data)	0.0340	0.0347	0.0317	0.0433	0.0244	0.1188
$wR2$ (all data)	0.0629	0.0768	0.0527	0.0917	0.0595	0.2205

Table II. Selected Bond Lengths and Structural Parameters for Some of the Porphyrins Studied [in Å].

Compound	M-N, Å	M-N22	M-N23	M-N24	\otimes ^[a]	Ξ ^[b]	$\Delta 24$ ^[c]	ΔC_m ^[d]	δC_m subst. ^[e]	δC_m unsubst. ^[f]
	<i>M-N21</i>									
17	2.022(2) av. = 2.022(2)	2.013(2)	2.027(2)	2.026(2)	2.022	0.048	0.1062	0.2125	0.37	0.160
273	2.026(2) av. = 2.027(2)	2.024(2)	2.032(2)	2.027(2)	2.027	0.025	0.039	0.043	0.0311	0.047
307	2.019(2) av. = 2.022(2)	2.020(2)	2.023(2)	2.025(2)	2.022	0.076	0.0391	0.046	0.028	0.052
382	2.024(2) 2.025(2)	2.026(2)	2.025(2)	2.025(2)	2.025	0.062	0.050	0.043	0.008	0.054
309	2.013(2) 2.016	2.015(2)	2.018(2)	2.019(2)	2.016	0.063	0.049	0.041	0.002	0.053
8	–	–	–	–	2.075	0.325	0.055	0.078	0.132	0.06

^[a] Core size, average vector length from the geometric center of the four nitrogen atoms to the nitrogen atoms.

^[b] Core elongation parameter defined as the difference between the vector lengths ($|N21-N22|+|N23-N24|$)/2- ($|N22-N23|+|N21-N24|$)/2. ^[c] Average deviation of the 24 macrocycle atoms from their least-squares plane. ^[d]

Average deviation of the C_m carbon atoms from the 4N-plane. ^[e] Average deviation of the substituted C_m carbon atoms from the 4N-plane. ^[f] Average deviation of the unsubstituted C_m carbon atoms from the 4N-plane. ^[g] Two crystallographically independent molecules.

Table III. Normal Structural Decomposition (NSD) Calculations for the Crystal Structure Determinations.

Compound	Out-of-plane distortions							
	D_{oop}	d_{oop}	B2u	B1u	A2u	Eg(x)	Eg(y)	A1u
17	0.6391	0.0287	0.0233	0.5622	0.1723	0.0943	0.2308	0.0051
273	0.2219	0.0152	0.1616	0.0883	0.0859	0.0504	0.0689	0.0259
307	0.2191	0.0157	0.1577	0.0926	0.0799	0.0698	0.0491	0.0298
382	0.2989	0.0115	0.2622	0.0370	0.0273	0.1305	0.0364	0.0087
309	0.2933	0.0111	0.2545	0.0421	0.0374	0.1279	0.0413	0.0046
8	0.3221	0.0136	0.2177	0.2205	0.0343	0.0684	0.0420	0.0111
	In plane distortions							
	D_{ip}	d_{ip}	B2g	B1g	Eu(x)	Eu(y)	A1g	A2g
17	0.1226	0.0138	0.0801	0.0129	0.0065	0.0025	0.0915	0.0050
273	0.1987	0.0165	0.1138	0.0042	0.0490	0.0652	0.1410	0.0002
307	0.1883	0.0169	0.1077	0.0078	0.0639	0.0516	0.1300	0.0018
382	0.1859	0.0180	0.0897	0.0075	0.0805	0.0528	0.1308	0.0085
309	0.1623	0.0175	0.0945	0.0062	0.0846	0.0499	0.0878	0.0057
8	0.5130	0.0304	0.4387	0.0015	0.0576	0.0247	0.2584	0.0030

UV/vis data of synthesized OEPs

OEPs added from literature are display with a yellow background. Prepared Pd(II) and Pt(II)OEPs are shown with a blue background and Q band shoulders are marked by 'sh'.

N ^o	5	10	15	20	Pd	Pt	Soret	sh	QIV	QIII	QII	QI
1	-	-	-	-			398		497	531	566	619
2	-	-	-	-	+		392 (5.41)		511 (4.36)	545 (4.87)		
3	¹	-	-	-		+	380 (5.30)		500 (4.22)	535 (4.62)		
227	methyl	-	-	-			406 (5.53)		506 (4.39)	541 (4.07)	575 (3.96)	624 (3.16)
16	<i>n</i> -butyl						407 (5.48)		506 (4.26)	541 (3.71)	576 (3.75)	622 (2.86)
229	4-tolyl	-	-	-			406 (5.09)		505 (3.95)	538 (3.67)	571 (3.66)	624 (3.16)
5	4-pentylphenyl	-	-	-			404 (5.12)		503 (4.99)	537 (4.69)	571 (4.64)	n. d.
230	4-NMe ₂ -phenyl	-	-	-			406 (5.26)		505 (4.33)	538 (3.97)	572 (3.97)	624 (3.59)
232	3-OH-phenyl	-	-	-			404 (5.03)		503 (4.02)	537 (3.79)	571 (3.76)	623 (3.45)
6	3-CF ₃ -phenyl	-	-	-			404 (6.68)		503 (5.44)	537 (4.93)	571 (4.76)	n. d.
231	3-OMe-phenyl	-	-	-			405 (5.32)		503 (4.26)	537 (3.95)	571 (3.92)	623 (3.41)
7	1-naphthyl	-	-	-			406 (4.13)		504 (4.02)	538 (3.84)	572 (3.85)	625 (n. d.)
233	2-naphthyl	-	-	-			406 (5.61)		505 (4.48)	538 (4.20)	572 (4.20)	624 (3.71)
234	acenaphthyl	-	-	-			407 (5.02)		505 (3.92)	538 (3.66)	574 (3.64)	625 (3.26)
8	9-phenanthrenyl	-	-	-			406 (5.13)		504 (4.13)	538 (3.86)	571 (3.83)	624 (3.52)
166	methyl				+		405 (5.18)			520 (4.15)	552 (5.92)	

¹ R. C. Kwong, S. Sibley, T. Dubovoy, M. Baldo, S. R. Forest, M. E. Thompson *Chem. Mater.* **1999**, *11*, 3709.

N ^o	5	10	15	20	Pd	Pt	Soret	sh	QIV	QIII	QII	QI
17	<i>n</i> -butyl				+		406 (5.79)			521 (4.64)	555 (4.78)	
299	<i>s</i> -butyl				+		409 (6.01)			526 (4.94)	557 (5.04)	
273	phenyl				+		399 (5.14)			515 (3.98)	549 (4.35)	
301	4-pentylphenyl				+		402 (4.47)			516 (3.89)	549 (4.00)	
300	3-CF ₃ -phenyl				+		400 (5.41)			516 (3.89)	550 (4.53)	
282	1-naphthyl				+		401 (5.00)			516 (3.79)	551 (4.18)	
302	2-naphthyl				+		400 (4.90)			516 (3.80)	550 (4.14)	
303	acenaphthyl				+		399 (5.11)			515 (4.03)	548 (4.36)	
12	9-phenanthrenyl				+		400 (5.86)			516 (4.79)	550 (5.12)	
307	phenyl					+	386 (6.60)			504 (5.28)	539 (5.78)	
308	1-naphthyl					+	387 (5.79)			504 (4.51)	538 (4.99)	
309	9-phenanthrenyl					+	387 (6.04)			504 (4.71)	538 (6.20)	
236	phenyl ²	phenyl					413 (5.39)		510 (4.25)	sh	578 (3.89)	sh
216	phenyl ^{2,3}	-	phenyl	-			410 (5.35)		508 (4.25)	542 (3.76)	575 (3.87)	627 (3.30)
254	4-pentylphenyl	4-pentylphenyl					425 (5.17)		521 (4.00)	552 (sh)	592 (3.78)	639 (sh)
257	1-naphthyl	1-naphthyl					426 (4.89)		521 (3.79)	552 (sh)	592 (3.53)	639 (sh)
9	9-phenanthrenyl	9-phenanthrenyl					426 (5.45)	455 (sh)	519 (4.56)	sh	592 (4.35)	sh
250	4-pentylphenyl	phenyl					425 (5.50)		521 (4.29)	sh	592 (4.13)	sh
251	4-bromophenyl	phenyl					425 (3.99)		521 (3.81)	sh	592 (3.61)	sh
248	1-naphthyl	phenyl					425 (3.22)		520 (3.01)	sh	592 (sh)	650 (sh)

² S. A. Syrбу, T.V. Lyubimova, A.S. Semeikin *Russ. J. Gen. Chem.* **2001**, 71, 10, 1656.

³ A. Syrбу, L. Lyobumova, A. S. Semeikin *Chem. Heterocyclic Comp.* **2004**, 40, 10, 1262.

N°	5	10	15	20	Pd	Pt	Soret	sh	QIV	QIII	QII	QI
246	9-anthracenyl	phenyl					425 (4.54)		520 (3.54)	sh	592 (3.92)	sh
255	9-anthracenyl	4-pentylphenyl					425 (4.68)		520 (3.63)	sh	592 (3.34)	644 (2.78)
253	3-CF ₃ -phenyl	4-NMe ₂ -phenyl					429 (4.72)		514 (sh)		595 (3.67)	663 (3.74)
249	4-NMe ₂ -phenyl	phenyl					427 (4.40)		522 (sh)	sh	593 (3.27)	667 (3.30)
260	4-NMe ₂ -phenyl	9-phenanthrenyl					433 (4.93)		521 (4.09)		596 (3.63)	664 (3.45)
258	1-naphthyl	4-pentylphenyl					426 (4.88)	sh	519 (3.74)	555 (3.61)	592 (3.72)	643 (3.48)
252	3-OMe-phenyl	phenyl					425 (4.59)	448 (4.36)	521 (3.48)	sh	592 (3.37)	636 (3.57)
259	1-naphthyl	9-phenanthrenyl					430 (5.01)	455 (5.01)	519 (3.90)	559 (sh)	591 (4.04)	643 (3.81)
247	9-phenanthrenyl	phenyl					430 (sh)	454 (4.76)			587 (3.63)	638 (3.42)
256	4-pentylphenyl	9-phenanthrenyl						460 (5.25)	sh	589 (4.19)	639 (4.07)	sh
277	phenyl		s-butyl		+		417 (4.55)			533 (3.53)	563 (3.48)	
278		9-phenanthrenyl		s-butyl	+		413 (5.16)			527 (3.56)	560 (3.84)	
279												
284	1-naphthyl	1-naphthyl			+		412 (4.98)	486 (sh)		527 (3.95)	561 (4.08)	
9	9-phenanthrenyl	9-phenanthrenyl			+		414 (5.15)			527 (4.09)	562 (4.24)	
217	phenyl	phenyl	phenyl ⁴				438 (5.28)		534 (4.14)	sh	608 (3.91)	667 (3.79)
292	phenyl	phenyl	4-NMe ₂ -phenyl				446 (4.10)		480 (4.02)	sh	623 (3.09)	682 (3.47)
293	phenyl	phenyl	4-bromophenyl				441 (4.35)	465 (4.46)	533 (3.30)	sh	610 (3.20)	676 (3.31)
294	phenyl	phenyl	4-pentylphenyl				438 (4.65)	sh	533 (3.72)	sh	605 (3.43)	673 (3.24)
288	9-phenanthrenyl	4-pentylphenyl	9-phenanthrenyl				442 (5.06)	470 (4.76)	537 (3.95)	sh	609 (3.75)	665 (3.73)

⁴ W. W. Kalisch, Dissertation 1997 (Freie Universität Berlin): „Synthese, Modifizierung und Strukturuntersuchung neuer Tetrapyrrolsysteme mit variabler Konformation als Modelverbindungen natürlicher Pigmente.“, p. 110, 157ff.

N°	5	10	15	20	Pd	Pt	Soret	sh	QIV	QIII	QII	QI
290	9-anthracenyl	phenyl	9-anthracenyl				446 (4.59)		538 (3.59)	sh	609 (3.42)	666 (3.31)
235	1-naphthyl	1-naphthyl	1-naphthyl				442 (4.80)		537 (3.78)		609 (3.51)	673 (3.23)
291	3-OMe-phenyl	phenyl	3-OMe-phenyl					465 (5.32)	569 (3.56)	608 (3.86)	663 (4.01)	sh
289	9-phenanthrenyl	1-naphthyl	9-phenanthrenyl				445 (4.89)	472 (3.65)	538 (3.78)	sh	611 (3.64)	665 (3.51)
10	9-phenanthrenyl	9-phenanthrenyl	9-phenanthrenyl				445 (4.38)	473 (4.14)	539 (3.14)	sh	608 (3.09)	665 (2.95)
287	9-phenanthrenyl	phenyl	9-phenanthrenyl					472 (5.14)		564 (sh)	608 (3.38)	663 (3.70)
304	9-phenanthrenyl	phenyl	9-phenanthrenyl		+		427 (4.87)			539 (3.78)	573 (3.72)	
10	9-phenanthrenyl	9-phenanthrenyl	9-phenanthrenyl		+		429 (4.11)			539 (4.04)	573 (4.06)	
-	1-naphthyl ⁵	1-naphthyl	1-naphthyl	1-naphthyl			472 (5.00)				610 (3.81)	692 (3.82)
							488 (5.08)				636 (3.56)	692 (4.00)
244	phenyl ³	phenyl	phenyl	phenyl			475				sh	697
11	9-phenanthrenyl	9-phenanthrenyl	9-phenanthrenyl	9-phenanthrenyl				493 (5.37)		sh	640 (3.11)	697 (4.13)
244	phenyl	phenyl	phenyl	phenyl	+		433			546	592	
15	9-phenanthrenyl	9-phenanthrenyl	9-phenanthrenyl	9-phenanthrenyl	+			443 (4.43)		553 (3.89)	590 (3.75)	

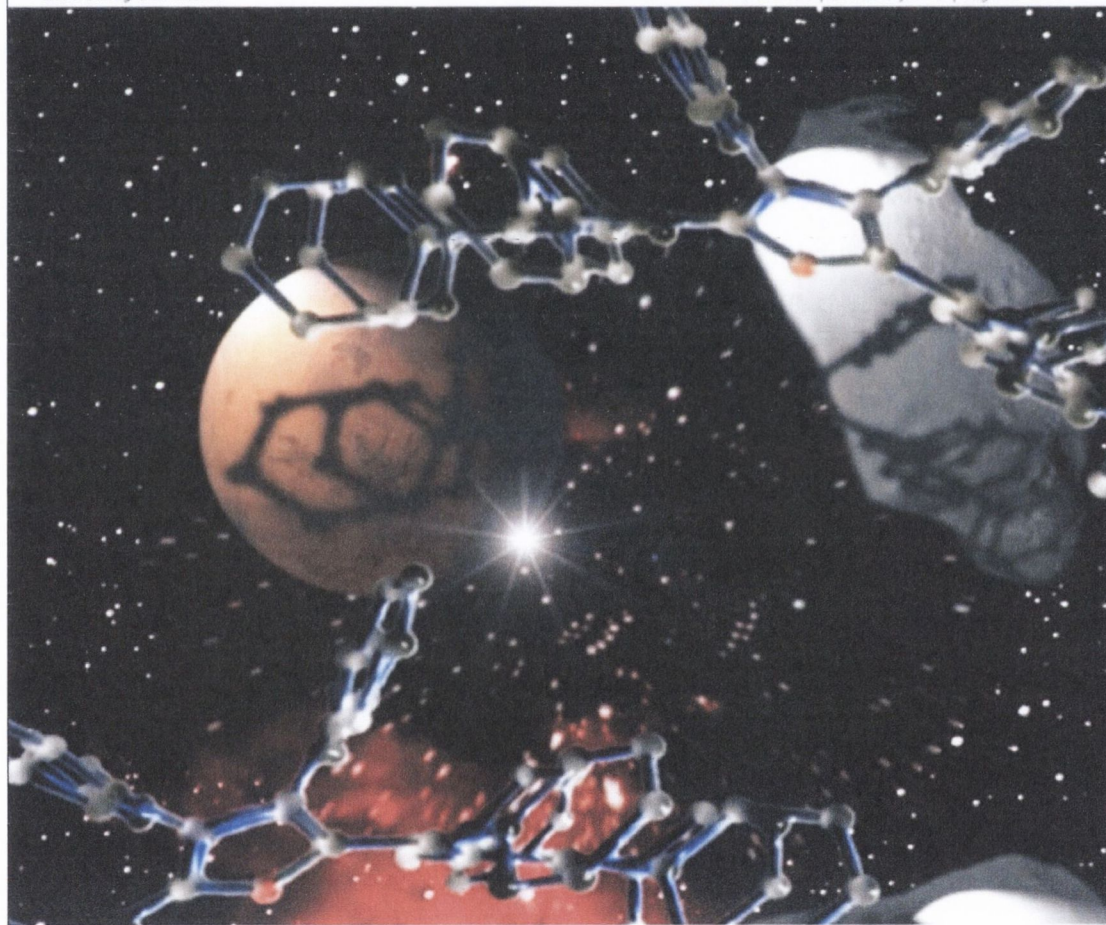
⁵ The existence of the OEP couldn't be proven by mass spectroscopy, two different green fractions were obtained.

ChemComm

Chemical Communications

www.rsc.org/chemcomm

Number 3 | 21 January 2006 | Pages 229–352



ISSN 1359-7345

RSC Publishing

FEATURE ARTICLE

Matthias O. Senge
Exercises in molecular gymnastics
– bending, stretching and twisting
porphyrins

COMMUNICATION

D. Gottlieb, C. Grunwald, C. Nowak, J.
Kuhlmann and H. Waldmann
Intein-mediated *in vitro* synthesis of
lipidated Ras proteins

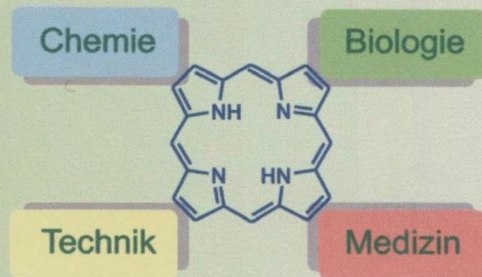


1359-7345(2006)3:1-6

Organische, bioorganische und medizinische Chemie

Motivation

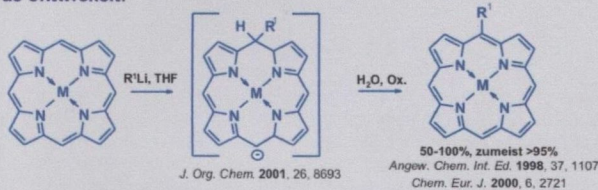
Ziel der Arbeitsgruppe ist die Synthese von Verbindungen basierend auf dem Tetrapyrrolgerüst der Porphyrine, sowie deren technische, bio-technologische und medizinische Anwendung. Ausschnittsweise sollen die Darstellung asymmetrisch substituierter Porphyrine via Kondensation und Reaktion mit Lithiumorganyle (I), die Synthese und Untersuchung von biomimetischen Verbindungen (II), sowie der Einsatz von Porphyrinen in der Photodynamischen Diagnostik und Therapie (PDD und PDT) zur Bekämpfung von Krebszellen (III) vorgestellt werden.



(I) Synthese asymmetrisch substituierter Porphyrine

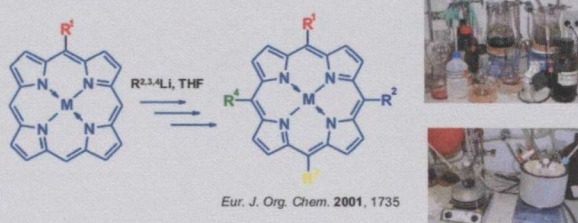
Methodenentwicklung S_NAr an Porphyrinen

Im Rahmen der Arbeitsgruppe wurde die Reaktion von Porphyrinen mit Lithiumorganyle als effektive Funktionalisierungsmethode entwickelt.



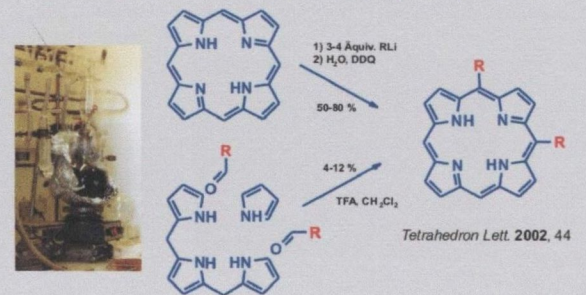
Die Reaktion verläuft nach dem S_NAr Mechanismus unter Bildung des Meisenheimer Komplex. Das monoanionische Porphyrinderivat wird anschließend mit DDQ zum Porphyrin oxidiert.

In einfacher Weise können so mit guten bis sehr guten Ausbeuten Porphyrinderivate mit meso-Substituenten dargestellt werden. Di-, Tri- und Tetrasubstitution führen zu asymmetrisch substituierten Zielverbindungen. Auf diese Weise können Moleküle mit speziellen Eigenschaften wie Amphilie, veränderter Konformation, besonderen Rezeptoreigenschaften, sowie verändertem Redox- und photo-chemischem Verhalten aufgebaut werden.



A₂-Typ Porphyrine

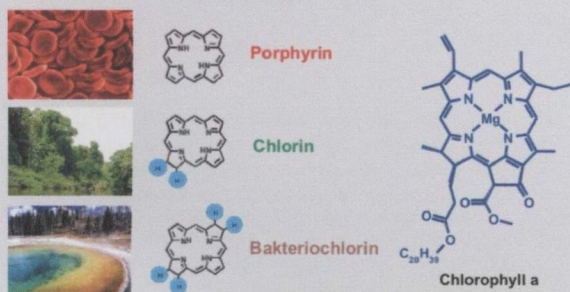
Alternativ sind durch Kondensation oder durch Einsatz von RLi im Überschuss auch A₂-Typ Porphyrine darstellbar. Diese können anschließend mit Lithiumorganyle zu asymmetrisch substituierten Porphyrinen weiter umgesetzt werden.



(II) Synthese biomimetischer Verbindungen

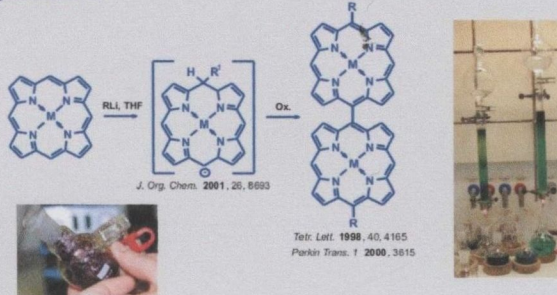
Bausteine des Lebens

Hämoglobin, Chlorophyll und Bakteriochlorophyll erfüllen entscheidende Grundfunktionen des Lebens. Hämoglobin als roter Blutfarbstoff transportiert den zur Zellatmung nötigen Sauerstoff, während die Chlorophylle als lichtabsorbierende Pigmente die Energie zur Verfügung stellen, die zum Aufbau energiereicher Verbindungen benötigt wird. Alle Farbstoffe leiten sich vom Grundgerüst des Porphyrins ab, welches durch Reduktion pyrrolischer Doppelbindungen in seiner Lichtabsorption und somit seinem photo-chemischen Verhalten variabel ist.



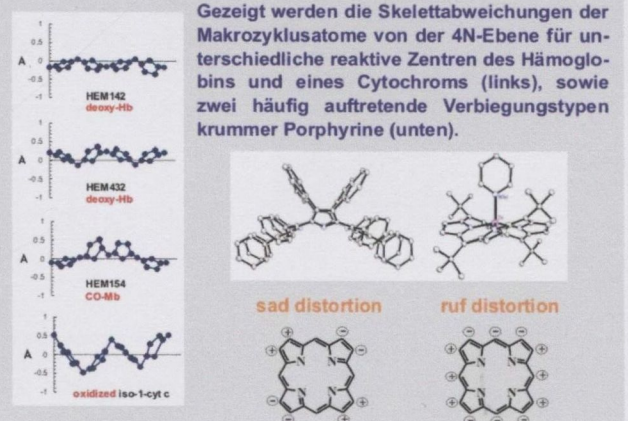
Durch die besonderen Eigenschaften natürlicher Porphyrine, die durch Substitution und Metallierung gezielt beeinflusst werden können, ist die Synthese von Derivaten bzw. biomimetischen Verbindungen mit dem Ziel der Anwendung als Pigmente mit neu modellierten Eigenschaften, als Katalysatoren oder als künstliche Photorezeptoren interessant.

Z. B. können monoanionische Porphyrinintermediate mit DDQ in Abwesenheit von Wasser zu meso-meso-linked Bisporphyrinen umgesetzt werden, die aufgrund ihrer gekoppelten Chromophore als Modellverbindungen für Photosynthesereaktionen herangezogen werden:



Konformation natürlicher Porphyrin Kofaktoren

Durch Metallierung und Einführung sterisch anspruchsvoller Substituenten kann die Konformation der Porphyrine wie bei natürlichen Tetrapyrrolen beeinflusst werden. Man unterscheidet dabei u.a. die Sattel- und gewellte Konformation (sad & ruf distortion).



Gezeigt werden die Skelettabweichungen der Makrozyklusatome von der 4N-Ebene für unterschiedliche reaktive Zentren des Hämoglobins und eines Cytochroms (links), sowie zwei häufig auftretende Verbiegungstypen krummer Porphyrine (unten).

(III) Photodynamische Therapie (PDT)

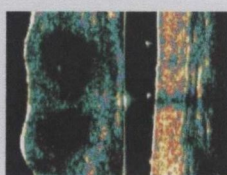
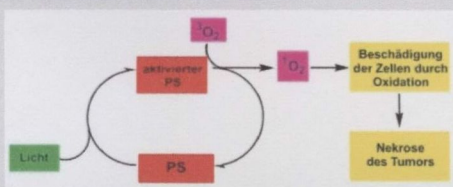
Photodynamische Diagnostik (PDD)

Durch Verabreichung von bestimmten Tetrapyrrolen, den sogenannten Photosensibilisatoren (PS), und anschließender Belichtung (violette Licht) können Tumorzellen, in denen sich die PS bevorzugt anreichern, durch Fluoreszenz sichtbar gemacht werden.



Photodynamische Therapie (PDT)

Werden die verabreichten photosensiblen Verbindungen mit Licht anderer Wellenlänge belichtet (rotes Licht, 600 bis 800 nm), werden angeregte PS generiert, die ihre Energie auf Sauerstoffmoleküle übertragen. Der so gebildete reaktive Singulett-Sauerstoff schädigt oxidativ Zellorganellen und führt damit zum Zelltod.

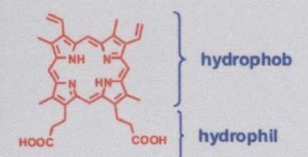
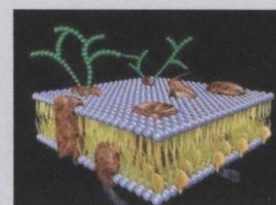


Vorteile der PDT gegenüber anderen Behandlungsmethoden sind der nicht invasive Charakter, der lokal begrenzbare Einsatz der PS und die nicht DNA schädigende Wirkung. Beschränkt ist die Anwendung jedoch auf mit Licht erreichbares Gewebe (in max. 2 bis 3 mm Tiefe) bzw. der endoskopischen Behandlungsmöglichkeit.

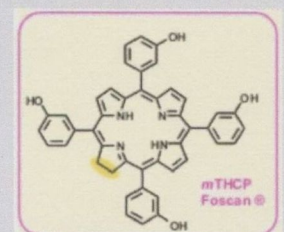
Eigenschaften von Photosensibilisatoren (PS)

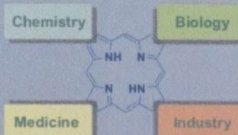
- selektive Anreicherung im Tumorgewebe durch schwach basischen Charakter und Möglichkeit von Photobleaching (Zerstörung des PS) zur Konzentrationsminimierung in nicht zu therapierendem Gewebe
- hohe Absorption im therapeutischen Fenster (600-800 nm, Licht hoher Eindringtiefe)
- effektive Energieübertragung auf Sauerstoff (hohe Quantenausbeute, lange Lebensdauer des angeregten Zustands)
- nicht gewebschädigend in der Dunkelheit bzw. hohe Phototoxizität
- begrenzte Verweildauer im Körper bzw. rascher Abbau und Ausscheidung nach der Behandlung

Amphilie von Photosensibilisatoren (PS)



Um sich in den Zellwänden des Tumorgewebes ideal einlagern zu können, muss der PS ausreichend amphiphil sein. Foscan® ist ein derzeit kommerziell erhältliches Therapeutikum mit entsprechenden Eigenschaften. Es dient im Rahmen unserer Forschung als aktuelle Leitstruktur für die Weiterentwicklung von Photosensibilisatoren.





Porphyrins in NLO

Julia Richter*, Marijana Fazekas*, Sergei Vinogradov**, Mathias O. Senge*

* School of Chemistry - Trinity College Dublin

** Department of Biochemistry and Biophysics - University of Pennsylvania



Molecules with nonlinear (NLO) properties have been extensively investigated due to their potential applications in the area of telecommunication, data storage, computers and display technologies. Over time, materials changed from traditional inorganic solids to organic and organometallic compounds. Phthalocyanines bearing suitable donor-acceptor substituents were proposed more than a decade ago as candidates for NLO applications^[1] while porphyrins were first investigated in the beginning of the 1990's by Suslick and co-workers.^[2] Since then, a substantial number of porphyrin-based NLO chromophores have been synthesized and investigated by different methods for their second and third order NLO properties. Our work focuses on the synthesis of novel porphyrins for NLO measurements using advanced molecular design methods.

The porphyrin system and its second and third order NLO properties

The polarization of a molecule subjected to an electric field E is given by:

$$P = \alpha \cdot E + \beta \cdot E + \gamma \cdot E + \dots$$

α is the linear polarizability and is high in small fields where the polarization is directly proportional to the strength of the applied field (linear optical behaviour). In that case β and γ , the quadratic and the cubic hyperpolarizabilities, are negligible. Once the molecule is subjected to a strong field such as that due to an intense laser pulse a nonlinear optical response is generated with increasing values for the quadratic (β) and cubic (γ) polarizabilities known as second and third order NLO properties. Two dimensional extended conjugated π -electron systems of porphyrins are easily polarised by laser light. Asymmetrical substitution patterns with donor and acceptor groups enhance the second and third order linear responses. Synthesis of porphyrins with high NLO potentials therefore focuses on facile accessible tetra-meso-substituted porphyrins with an unsymmetric substitution pattern and push-pull properties. Typical compounds are related to the following A_2B_2 -porphyrin structure:

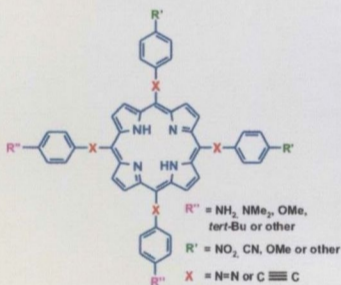


Fig. 1. A typical push-pull porphyrin.

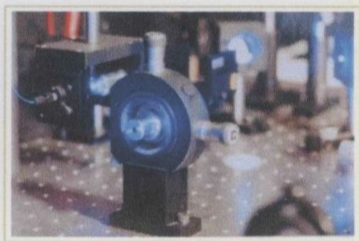


Fig. 2. Z-Scan technique for the determination of optical non-linearities.

Electron releasing groups (donors like NH_2 , NMe_2 , OMe , etc.) are combined with electron withdrawing groups (acceptors, NO_2 , CN) to get the desired properties and often so-called spacers (see X) are introduced between the donor or acceptor moiety and the porphyrin ring, extending the conjugated π -electron system and enhancing the nonlinear response of the molecule. Besides phenyl substituents also heteroaromatics (pyrrole or thiophene derivatives) with donor qualities are desired. Likewise, metal insertion (Pd and Pt) can be used to alter the properties of the molecule.

Synthesis of 5-mono substituted OEP's and PdOEP's for structural and photophysical investigations

Julia Richter

Compound	Absorption λ_{max} , nm	Emission λ_{max} (nm), nm	Phosphorescence lifetime τ_p , ps	Phosphorescence quantum yield ϕ_p , %
PdOEP	546 511 395	665 (546)	459	8.7
5-Me-PdOEP (1b)	553 521 467	686 (553)	276	4.1
5-Bu-PdOEP (2b)	554 523 468	711 (554)	217	2.1
5-Ph-PdOEP (4b)	556 518 462	669 (556)	-	0.09
5-Phen-PdOEP (10b)	551 517 463	671 (551)	52	1.1

Table 1. Photophysical data of 5-mono substituted PdOEP's.^a

^a All measurements were performed in toluene solutions. For the phosphorescence measurements, toluene was deoxygenated by prolonged bubbling of Ar , until no more changes in phosphorescence lifetimes of the dissolved Pd-porphyrins were detected.

Table 2 shows the collected data for the synthesis of some mono-meso-substituted octaethylporphyrins (OEP's). Methyl, *n*-butyl, *s*-butyl and the phenyl substituents (**1a**, **2a**, **3**, **4a**) were introduced by nucleophilic substitution reaction with commercially available MeLi , *n*-BuLi, *s*-BuLi and PhLi .^[6,7] Other substituents were accessible by trans-lithiation of the bromides followed by RLi reaction on OEP (**5** to **10a**). For photophysical investigations a first series of five palladium complexes was synthesized (**1b**, **2b**, **4b** and **10b**) and triplet state and phosphorescence data were studied. As can be seen in Table 1 phosphorescence quantum yields and lifetimes were greatly diminished especially for 5-Ph- and 5-Phen-PdOEP (**4b** and **10b**, phen = phenantrenyl). Surprisingly, 5-Phen-PdOEP (**10b**) showed a longer triplet lifetime and even a higher quantum yield than 5-Ph-PdOEP (**4b**) although carrying a larger substituent and causing therefore probably more distortion. Indeed, the shortened lifetime and not too small quantum yield seem to make 5-Phen-PdOEP(**10b**) a valuable candidate for further single molecule experiments. Furthermore, structure calculations suggest that the saddling distortion mode of the aromatic 5-Ph-PdOEP (**4b**) and 5-Phen-PdOEP (**10b**) is most closely related to the photophysical changes while molecules like 5-Me-PdOEP (**1b**) and 5-Bu-PdOEP (**2b**) with a ruffling distortion do not have similar photophysical properties. The calculations also indicate that for 5-Ph-PdOEP (**4b**) the $D_{3h,d}$ distortion of the molecule is probably larger than that of 5-Phen-PdOEP (**10b**) although expected differently but correlating well with the measured higher lifetime and increased quantum yield of 5-Phen-PdOEP (**10b**).

Table 2. Synthesis of 5-mono-substituted OEP derivatives by reaction with commercially available or *in situ* generated RLi followed by pallidation of the 5-mono-substituted compounds.

R Li	% yield	% yield
1a,b Me	27	37
2a,b	43	87
3	11	-
4a,b	46	58
5	3	-
6	17	-
7	26	-
8	64	-
9	82	-
10a,b	73	60

[1] Li, D. A.; Ratner, M. A.; Marks, T. J. *J. Am. Chem. Soc.* **1988**, *110*, 1707-1710.
 [2] Suslick, K. S.; Chen, C.-T.; Meredith, G. R.; Cheng, L.-T. *J. Am. Chem. Soc.* **1992**, *114*, 6928-6930.
 [3] Hatscher, S.; Senge, M. O. *Tetrahedron Letters* **2003**, *44*, 157-160.
 [4] Pereira, M. M.; Muller, G.; Ordinas, J. I.; Azenha, M. E.; Arnaut, L. G. *J. Chem. Soc., Perkins Trans 2* **2002**, 1583-1588.

[5] Shi, B.; Boyle, R. W. *J. Chem. Soc., Perkins Trans 1* **2002**, 1397-1400.
 [6] Feng, X.; Bischoff, I.; Senge, M. O. *J. Org. Chem.* **2001**, *66*, 26, 8693-8700.
 [7] Senge, M. O.; Bischoff, I. *Tetrahedron Lett.* **2004**, *45*, 1647-1650.
 [8] Senge, M. O.; Kalisch, W. W.; Bischoff, I. *Chem. Eur. J.* **2000**, *6*, 5, 2721-2738.

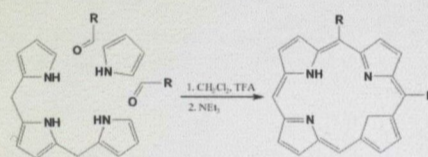
^aThe photophysical measurements were performed by Prof. Sergei Vinogradov, Department of Biochemistry and Biophysics, University of Pennsylvania.

* Special thanks to John Kelly for Fig. 2 and 3.

Synthesis of push-pull porphyrins for nonlinear investigations

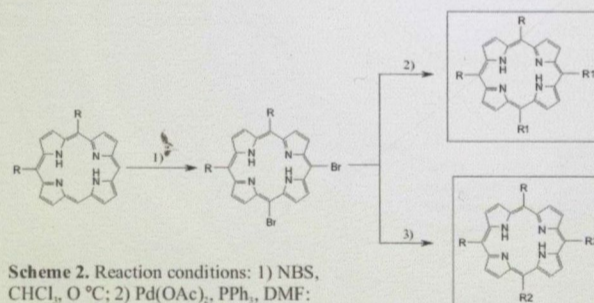
Marijana Fazekas

Unsymmetrically substituted push-pull porphyrins with electron donating groups on one side and electron withdrawing groups on the other side of the macrocycle are the target compounds for NLO (see Fig.1). No rational method to synthesize this type of porphyrins had been described until now in the literature. However, our group has developed a synthetic route to 5,10- A_2B_2 push-pull porphyrins. The first step is the synthesis of 5,10-disubstituted porphyrins bearing electron donating groups by condensation of tripyrrane with different alkyl or aryl aldehydes (Scheme 1).^[1]



Scheme 1

After bromination (**1**) of the free meso positions, the introduction of an electron withdrawing group using Heck reactions (route 2) or Suzuki coupling reactions (route 3) (Scheme 2) is carried out.^[4,5]



Scheme 2. Reaction conditions: 1) NBS, CHCl_3 , 0°C ; 2) $\text{Pd}(\text{OAc})_2$, PPh_3 , DMF ; 3) K_3PO_4 , $\text{Pd}(\text{PPh}_3)_4$, THF, boronic acids or esters.

In the last step, the metal insertion will be performed and then the nonlinear optical properties of the porphyrins will be investigated in collaboration with Prof. Werner Blau and Dr. Eleni G. A. Nataras from the school of physics (TCD).



Fig. 3. Z-Scan set-up using Q switched Nd:YAG nanosecond laser at 532 nm.*



Fig. 4. A condensation reaction.

Julia Richter*, Mathias. O. Senge* and Sergei Vinogradov#

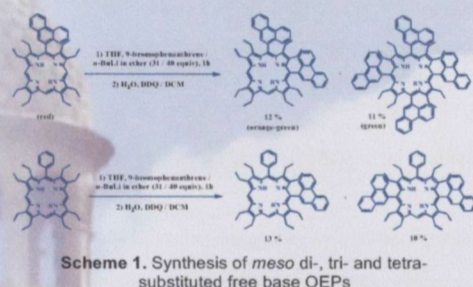
* School of Chemistry, SFI Tetrapyrrole Laboratory, Trinity College Dublin, Dublin 2, Ireland

Department of Biochemistry and Biophysics, University of Pennsylvania, Philadelphia, PA 19104, USA

The synthesis of highly distorted porphyrins and the investigation of their physical and chemical properties is a challenge in porphyrin chemistry.^[1] We are particularly interested in nonplanar Pd²⁺ and Pt porphyrins with future use in photophysical applications (e. g. sensors and NLO (nonlinear optics)). For a deeper insight in the relationship between the 3D structure of the molecule and its chemical and physical properties a series of meso monosubstituted PdOEPs was synthesized for phosphorescence and chemical reactivity investigations.

Synthesis and Reactivity of Meso Monosubstituted OEPs

Several meso monosubstituted free base 2,3,7,8,12,13,17,18-octaethylporphyrins (OEPs)^{[3],[4]} with residues of different steric bulk have been synthesized in good yields with organolithium reagents from free base OEP [Fig.1, a)]. After introduction of the substituent the compounds were palladated^[5] [Fig.1, b)] or platinated^[6] [Fig.1, c)] followed by an investigation of their physical and chemical properties and their potential use in technical applications. A typical ¹H-NMR spectrum is shown in Fig.2. Furthermore, the free base meso monosubstituted OEPs were reacted with organolithium reagents and di-, tri- and even tetrasubstituted compounds were obtained in one step in good yields (Scheme 1). Best results for the preparation of meso disubstituted compounds have been obtained by using the meso monosubstituted Pd complexes as starting material.



Scheme 1. Synthesis of meso di-, tri- and tetra-substituted free base OEPs

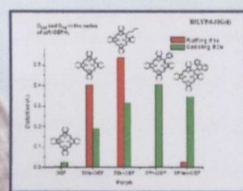
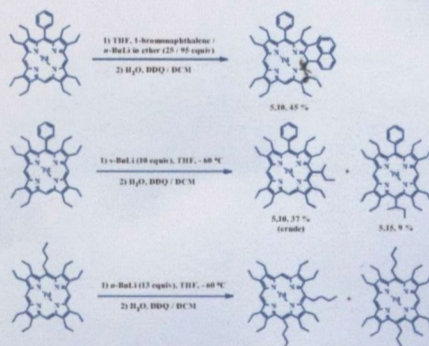


Fig. 4. Ruffling and saddling distortion of selected OEPs



Scheme 2. Synthesis of meso disubstituted PdOEPs

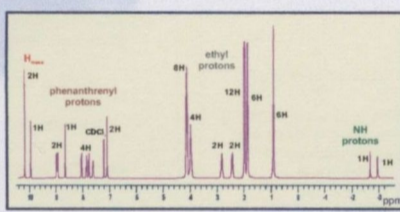


Fig. 2. ¹H-NMR spectrum of 5-phenanthrenyl-OEP

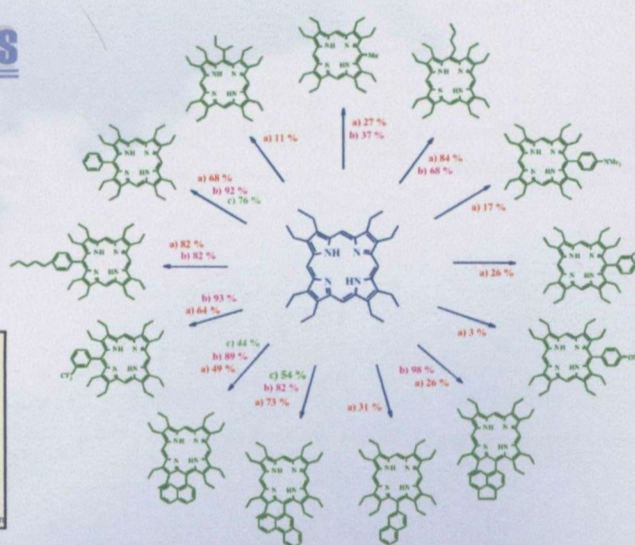


Fig. 1. Synthesized meso monosubstituted free base, Pd- and Pt-OEPs [a], X = 2H; b), X = Pd, c) X = Pt].

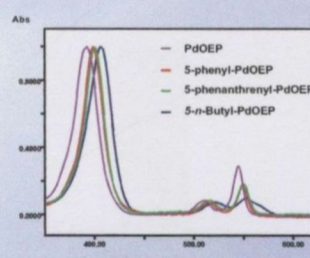


Fig. 3. UV/visible spectra of selected PdOEPs

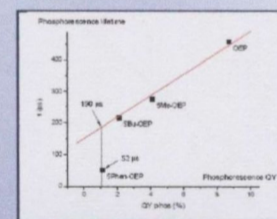


Fig. 5. Correlation of phosphorescence lifetime and phosphorescence quantum yields (QZ)

Macrocycle Distortion, Spectra and Photophysics

The introduction of a substituent in the meso position yielding a nonsubstituted OEP system causes a slight distortion of the planar macrocycle. A bathochromic shift of the Soret band in the UV / visible spectrum (Fig. 3) and a downfield shift of the inner NH protons are known as possible indicators for the increase in distortion (Fig. 3 & Table 1). In general, alkyl substituents distort the macrocycle more than aryl substituents and therefore their Soret bands are shifted farther to the red. Furthermore the NH signals for synthesized mono-, di-, and trisubstituted compounds (Table 1, last three entries) appear between -3 and -1.5 ppm indicating also an increase in the overall distortion.

Ab initio calculations (B3LYP/6-31Gd) on model free base compounds gave the first insight into the 3D structure of the synthesized compounds and are shown in Fig. 4 and Fig. 6 using Shelnutz's NSD representation. Aryl substituents induce a saddle shaped conformation mixed with elements of ruffling while alkyl substituted porphyrins show a predominantly ruffled conformation. For a series of five synthesized Pd compounds (PdOEP, 5-methyl-PdOEP, 5-butyl-PdOEP, 5-phenyl-PdOEP and 5-phenanthrenyl-PdOEP) phosphorescence lifetime and quantum yields have been measured. Surprisingly, for the saddle-shaped 5-phenanthrenyl-PdOEP a short phosphorescence lifetime is combined with an unexpected high quantum yield making the compound a valuable candidate for single molecule experiments and sensor applications (e.g. oxygen sensing *via* quenching of the phosphorescence for clinical applications).

[1] Senge, M.O. in *The Porphyrin Handbook*; Kadish, K.M.; Smith, K.M.; Guillard, R., Eds.; Academic Press: San Diego, 2000; Vol. 1; p. 239. [2] Wiehe, A.; Stollberg, H.; Runge, S.; Paul, A.; Senge, M.O.; Röder, B.J. *Porphyrins Phthalocyanines* 2001, 5, 853. [3] Senge, M.O. *Acc. Chem. Res.* 2005, 38, 9, 733. [4] Senge, M.O. *Chem. Commun.* 2006, 243. [5] Pawlicki, M.; Latos-Grazynski, L. *Chem. Eur. J.* 2003, 9, 4650. [6] Furuta, H.; Youfu, K.; Maeda, H.; Osuka, A. *Angew. Chem., Int. Ed.* 2003, 42, 2186.

Compound	H _{meso} signals / [ppm]	NH signals / [ppm]
OEP	10.12	-3.65
5-methyl-OEP	10.05 / 9.86	-3.02
5-n-butyl-OEP	10.07 / 9.83	-2.78 / -2.80
5-s-butyl-OEP	10.03 / 9.77	-2.31
5-phenyl-OEP	10.17 / 9.93	-3.01 / -3.15
5-phenanthrenyl-OEP	10.24 / 10.02	-2.73 / -3.00
5,10-diphenanthrenyl-OEP	9.73 / 9.70	-2.26
5,15-diphenanthrenyl-10-phenyl-OEP	9.53	-1.75

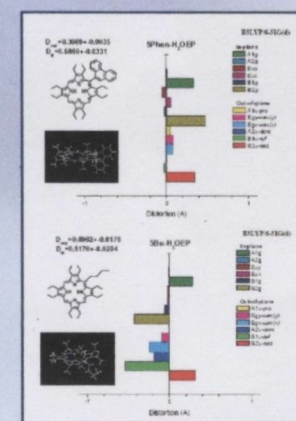


Fig. 6. NSD analysis of the distortion modes



NMR and quantum chemical investigations of conformations, ring current effects, and NH-tautomerism of porphyrins

Philipp Wacker*, Claudia Ryppa**, Katja Dahms**, Julia Richter**,
Mathias O. Senge**, Erich Kleinpeter*

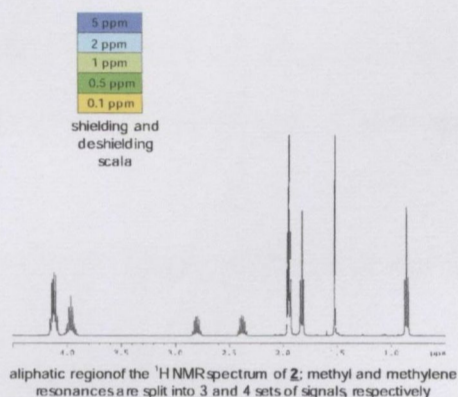
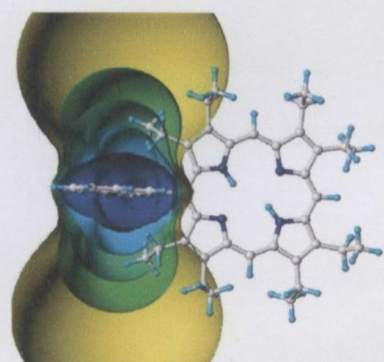
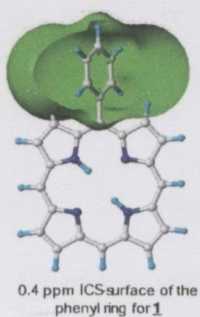
* Department of Chemistry, University of Potsdam
Karl-Liebknecht-Strasse 24-25, D-14476, Golm

** Department of Chemistry, Trinity College Dublin Dublin 2, Ireland



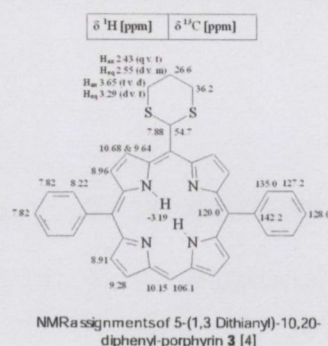
Calculation of substituent ring current effects

- high field shift of the ^1H NMR resonances of adjacent β -protons can be observed for meso aryl substituted porphyrins
- B3LYP/6-31G** optimized geometry of 5-phenylporphyrin [1]; angle between phenyl and porphyrin plane found at 64.8°
- anisotropy cone of benzene [2] applied on 5-phenylporphyrin
- the green iso-chemical-shift-surface (ICSS) represents a shielding of 0.4 ppm.
- adjacent β -protons are located in the shielding region above and below the phenyl plane [3]

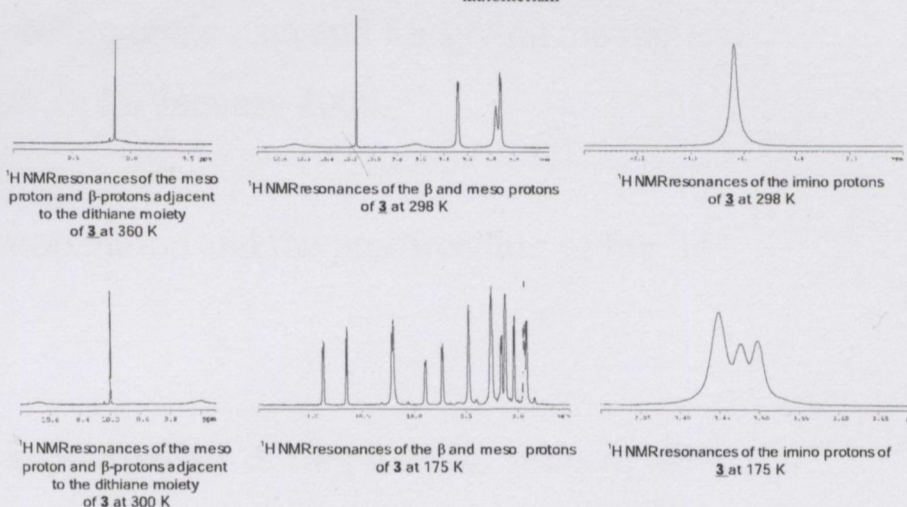


- B3LYP/6-31G** geometry optimization of **2**; angle between phenanthrene and porphyrin plane is 90°
- calculation (thanks to Dr. Sabrina Klod) and application of the ring current effect of phenanthrene to **2**
- different ^1H NMR resonances can be explained by location of the respective protons in different shielding regions of the phenanthrene moiety

Conformational behaviour of 1,3-dithianyl substituted porphyrins

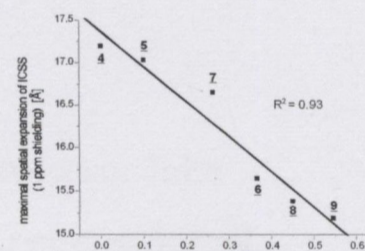
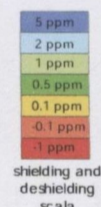


- variable temperature NMR experiments of **3** indicate two conformations at low temperature
- rotation of dithianyl group restricted: splitting of adjacent β -protons resonances at room temperature, coalescence at 332 K, $\Delta G^\ddagger_{\text{exp}} = 44.3$ kJ/mol ($\text{C}_2\text{D}_2\text{Cl}_4$)
- splitting of β - and meso proton resonances in two signal sets below 245 K, $\Delta G^\ddagger = 47.8$ kJ/mol (CD_2Cl_2); the ^1H NMR signals of the dithiane moiety remain unchanged
- Still to do: further NMR spectroscopic investigation of 1,3-dithianyl substituted porphyrins with varying substitution pattern and molecular modelling efforts for conformational search and investigation of NH tautomerism

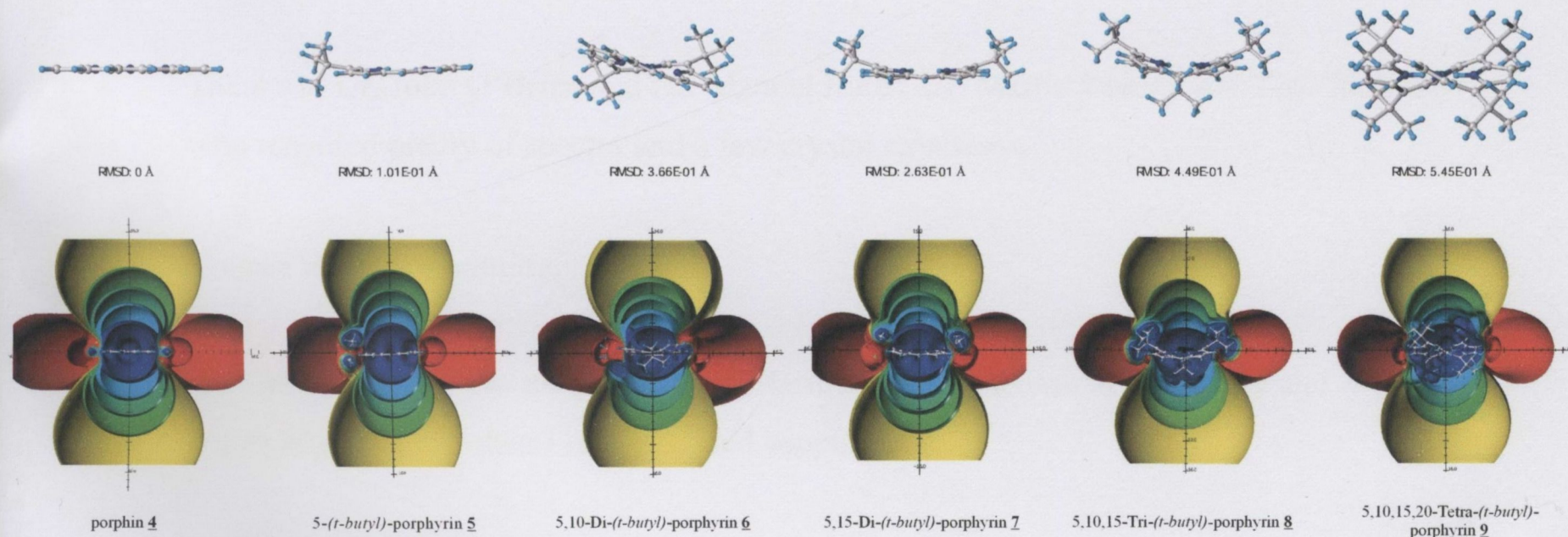


Calculation of porphyrin ring current effect dependent on the distortion of the porphyrin moiety

- B3LYP / 6-31G** geometry optimization of meso substituted porphyrins with increasing number of *t*-butyl substituents
- calculation and visualization of the ring current effect for porphyrins **4-9**; calculation of the chemical shift of ghost atoms in a grid (size $30 \times 30 \times 30$ Å) surrounding the molecule, visualization with Sybyl [5] (thanks to Dr. Bernd Kallies)
- estimation of the root-mean-square distance (RMSD) of all 24 atoms belonging to the porphyrin macrocyclus to the corresponding least-squares plane (NLS) to quantify the macrocyclic distortion for **4-9**
- estimation of the maximal spatial expansion of the 1 ppm shielding ICSS-surface
- good correlation between strength of the ring current effect with distortion of the porphyrin macrocyclus
- 5,10-Di-(*t*-butyl)-porphyrin macrocyclus more distorted than 5,15-Di-(*t*-butyl)-porphyrin



decreasing of the ring current effect with increasing of the distortion of the porphyrin macrocyclus



Literature

- Gaussian 98, Revision A.11.7, M. J. Frisch et al., Gaussian, Inc., Pittsburgh PA, 2002.
- S. Klod, E. Kleinpeter, *J. Chem. Soc., Perkin Trans. 2*, 2001, 1893.
- C. Ryppa, M. O. Senge, S. S. Hatscher, E. Kleinpeter, Ph. Wacker, U. Schilde, A. Wiehe, *Chem. Eur. J.*, 2005, in press.
- M. O. Senge, S. S. Hatscher, A. Wiehe, K. Dahms, A. Kelling, *J. Am. Chem. Soc.*, 2004, **126**, 13624.
- Sybyl 6.9, Tripos Inc., 1699 South Hanley Road, St. Louis, Missouri, USA 2002.
- K. M. Kadish, K. M. Smith, R. Guilard, Eds; *The porphyrin handbook*; Academic Press: New York, 2002.

Acknowledgements

I am most grateful to the Deutsche Forschungsgemeinschaft (DFG) and the Science Foundation Ireland (SFI), who financed this work and gave me an opportunity to study in Germany and Ireland.

I'd like to express thanks to Prof. S. Vinogradov and co-workers for their dedication and for carrying out phosphorescence measurements with utmost cooperation.

I want to thank Prof M. O. Senge for the crystallographic data and for giving me the opportunity to design the *Chem. Commun.* Cover for January 2006.

I also wish to thank Philipp Wacker for his cooperation and the proofreading of the ^1H NMR section.

I want to express gratitude to everyone who supported me during the past years of my busy work schedule and want to thank especially some colleagues who spent their evenings with me in the lab and who proofread parts of this work.

Many thanks to all of you!

I am also extremely honoured to have met Professor John Corish and Professor John Kelly and show appreciation and a big "thank you" to both for their support and final completion advice.

Thanks to Dr. John O'Brien and Dr. Manuel Rüter, Dr. Martin Feeney and Tom McCabe who recorded plenty of spectra and a few crystal structures.

Thanks to Joe for printing.

Furthermore, a big **Thank You** to Ann Marie Keenan who was always there and especially in times when I really needed support.